Related titles

Textile Fibre Composites in Civil Engineering
(ISBN 978-1-78242-446-8)

Biocomposites: Design and Mechanical Performance
(ISBN 978-1-78242-373-7)

Natural Fibre Composites: Materials, Processes and Properties
(ISBN 978-0-85709-524-4)

Woodhead Publishing Series in Composites Science and Engineering: Number 74

Advanced High Strength Natural Fibre Composites in Construction

Edited by

Mizi Fan

Feng Fu

AMSTERDAM • BOSTON • CAMBRIDGE • HEIDELBERG
LONDON • NEW YORK • OXFORD • PARIS • SAN DIEGO
SAN FRANCISCO • SINGAPORE • SYDNEY • TOKYO
Woodhead Publishing is an imprint of Elsevier

Woodhead Publishing is an imprint of Elsevier
The Officers' Mess Business Centre, Royston Road, Duxford, CB22 4QH, United Kingdom
50 Hampshire Street, 5th Floor, Cambridge, MA 02139, United States
The Boulevard, Langford Lane, Kidlington, OX5 1GB, United Kingdom

Notices
Knowledge and best practice in this field are constantly changing. As new research and experience broaden our understanding, changes in research methods, professional practices, or medical treatment may become necessary.

Practitioners and researchers must always rely on their own experience and knowledge in evaluating and using any information, methods, compounds, or experiments described herein. In using such information or methods they should be mindful of their own safety and the safety of others, including parties for whom they have a professional responsibility.

To the fullest extent of the law, neither the Publisher nor the authors, contributors, or editors, assume any liability for any injury and/or damage to persons or property as a matter of products liability, negligence or otherwise, or from any use or operation of any methods, products, instructions, or ideas contained in the material herein.

ISBN: 978-0-08-100411-1 (print)
ISBN: 978-0-08-100430-2 (online)

Library of Congress Cataloging-in-Publication Data
A catalog record for this book is available from the Library of Congress

British Library Cataloguing-in-Publication Data
A catalogue record for this book is available from the British Library

Publisher: Matthew Deans
Acquisition Editor: Gwen Jones
Editorial Project Manager: Charlotte Cockle
Production Project Manager: Omer Mukthar
Designer: Matthew Limbert

Typeset by TNQ Books and Journals

List of contributors

O.S. Abiola Federal University of Agriculture, Abeokuta, Nigeria

M.A. Alam Universiti Tenaga Nasional, Kajang, Selangor, Malaysia

J. Bayer University of Girona, Girona, Spain

J. Bregulla Building Research Establishment, Watford, United Kingdom

C. Cao Green Crane Consulting, Watford, Hertfordshire, United Kingdom

P. Cao Nanjing Forestry University, Nanjing, Jiangsu, China

F. Chen International Centre for Bamboo and Rattan, Beijing, People's Republic of China

S.F. Curling Biocomposites Centre, Bangor, United Kingdom

S.R. Djafari Petroudy Faculty of New Technologies and Energy Engineering, Shahid Beheshti University, Mazandaran, Iran

M. Fan Brunel University London, London, United Kingdom

F. Fu Research Institute of Wood Industry, Chinese Academy of Forestry, Beijing, China

S. Fu Zhejiang A & F University, Linan, Hangzhou, China

S.H. Ghaffar Brunel University London, London, United Kingdom

L.A. Granda University of Girona, Girona, Spain

X. Guo Nanjing Forestry University, Nanjing, Jiangsu, China

L. Hu Research Institute of Wood Industry, Chinese Academy of Forestry, Beijing, China

D. Jones SP Technical Research Institute of Sweden, Stockholm, Sweden

S. Knapic Centro de Estudos Florestais, Instituto Superior de Agronomia, Universidade de Lisboa, Lisboa, Portugal

R. Li Nanjing Forestry University, Nanjing, Jiangsu, China

L. Lin Research Institute of Wood Industry, Chinese Academy of Forestry, Beijing, China

X. Liu Zhejiang A & F University, Linan, Hangzhou, China

J.S. Machado Laboratório Nacional de Engenharia Civil, Lisboa, Portugal

M.R. Mansor Universiti Teknikal Malaysia Melaka, Durian Tunggal, Malacca, Malaysia

J.A. Méndez University of Girona, Girona, Spain

P. Mutjé University of Girona, Girona, Spain

A. Naughton Brunel University London, London, United Kingdom

G.O. Ormondroyd Biocomposites Centre, Bangor, United Kingdom

M.A. Pèlach University of Girona, Girona, Spain

L. Peng Research Institute of Wood Industry, Chinese Academy of Forestry, Beijing, China

C.-M. Popescu Petru Poni Institute of Macromolecular Chemistry, Iasi, Romania

M.-C. Popescu Petru Poni Institute of Macromolecular Chemistry, Iasi, Romania

L. Qin Research Institute of Wood Industry, Chinese Academy of Forestry, Beijing, China

T. Rousakis Democritus University of Thrace, Xanthi, Greece

C. Santulli Università degli Studi di Camerino, Ascoli Piceno, Italy

S.M. Sapuan Universiti Putra Malaysia, Serdang, Selangor, Malaysia

P. Song Zhejiang A & F University, Linan, Hangzhou, China

F. Vilaseca University of Girona, Girona, Spain

G. Wang International Centre for Bamboo and Rattan, Beijing, People's Republic of China

B. Weclawski Brunel University London, London, United Kingdom

E. Xu Research Institute of Wood Industry, Chinese Academy of Forestry, Beijing, China

Q. Yuan Research Institute of Wood Industry, Chinese Academy of Forestry, Beijing, China

Woodhead Publishing Series in Composites Science and Engineering

1 **Thermoplastic aromatic polymer composites**
F. N. Cogswell
2 **Design and manufacture of composite structures**
G. C. Eckold
3 **Handbook of polymer composites for engineers**
Edited by L. C. Hollaway
4 **Optimisation of composite structures design**
A. Miravete
5 **Short-fibre polymer composites**
Edited by S. K. De and J. R. White
6 **Flow-induced alignment in composite materials**
Edited by T. D. Papthanasiou and D. C. Guell
7 **Thermoset resins for composites**
Compiled by Technolex
8 **Microstructural characterisation of fibre-reinforced composites**
Edited by J. Summerscales
9 **Composite materials**
F. L. Matthews and R. D. Rawlings
10 **3-D textile reinforcements in composite materials**
Edited by A. Miravete
11 **Pultrusion for engineers**
Edited by T. Starr
12 **Impact behaviour of fibre-reinforced composite materials and structures**
Edited by S. R. Reid and G. Zhou
13 **Finite element modelling of composite materials and structures**
F. L. Matthews, G. A. O. Davies, D. Hitchings and C. Soutis
14 **Mechanical testing of advanced fibre composites**
Edited by G. M. Hodgkinson
15 **Integrated design and manufacture using fibre-reinforced polymeric composites**
Edited by M. J. Owen and I. A. Jones
16 **Fatigue in composites**
Edited by B. Harris
17 **Green composites**
Edited by C. Baillie
18 **Multi-scale modelling of composite material systems**
Edited by C. Soutis and P. W. R. Beaumont

19 **Lightweight ballistic composites**
Edited by A. Bhatnagar
20 **Polymer nanocomposites**
Y-W. Mai and Z-Z. Yu
21 **Properties and performance of natural-fibre composite**
Edited by K. Pickering
22 **Ageing of composites**
Edited by R. Martin
23 **Tribology of natural fiber polymer composites**
N. Chand and M. Fahim
24 **Wood-polymer composites**
Edited by K. O. Niska and M. Sain
25 **Delamination behaviour of composites**
Edited by S. Sridharan
26 **Science and engineering of short fibre reinforced polymer composites**
S-Y. Fu, B. Lauke and Y-M. Mai
27 **Failure analysis and fractography of polymer composites**
E. S. Greenhalgh
28 **Management, recycling and reuse of waste composites**
Edited by V. Goodship
29 **Materials, design and manufacturing for lightweight vehicles**
Edited by P. K. Mallick
30 **Fatigue life prediction of composites and composite structures**
Edited by A. P. Vassilopoulos
31 **Physical properties and applications of polymer nanocomposites**
Edited by S. C. Tjong and Y-W. Mai
32 **Creep and fatigue in polymer matrix composites**
Edited by R. M. Guedes
33 **Interface engineering of natural fibre composites for maximum performance**
Edited by N. E. Zafeiropoulos
34 **Polymer-carbon nanotube composites**
Edited by T. McNally and P. Pötschke
35 **Non-crimp fabric composites: Manufacturing, properties and applications**
Edited by S. V. Lomov
36 **Composite reinforcements for optimum performance**
Edited by P. Boisse
37 **Polymer matrix composites and technology**
R. Wang, S. Zeng and Y. Zeng
38 **Composite joints and connections**
Edited by P. Camanho and L. Tong
39 **Machining technology for composite materials**
Edited by H. Hocheng
40 **Failure mechanisms in polymer matrix composites**
Edited by P. Robinson, E. S. Greenhalgh and S. Pinho
41 **Advances in polymer nanocomposites: Types and applications**
Edited by F. Gao
42 **Manufacturing techniques for polymer matrix composites (PMCs)**
Edited by S. Advani and K-T. Hsiao

43 **Non-destructive evaluation (NDE) of polymer matrix composites: Techniques and applications**
Edited by V. M. Karbhari
44 **Environmentally friendly polymer nanocomposites: Types, processing and properties**
S. S. Ray
45 **Advances in ceramic matrix composites**
Edited by I. M. Low
46 **Ceramic nanocomposites**
Edited by R. Banerjee and I. Manna
47 **Natural fibre composites: Materials, processes and properties**
Edited by A. Hodzic and R. Shanks
48 **Residual stresses in composite materials**
Edited by M. Shokrieh
49 **Health and environmental safety of nanomaterials: Polymer nanocomposites and other materials containing nanoparticles**
Edited by J. Njuguna, K. Pielichowski and H. Zhu
50 **Polymer composites in the aerospace industry**
Edited by P. E. Irving and C. Soutis
51 **Biofiber reinforcement in composite materials**
Edited by O. Faruk and M. Sain
52 **Fatigue and fracture of adhesively-bonded composite joints: Behaviour, simulation and modelling**
Edited by A. P. Vassilopoulos
53 **Fatigue of textile composites**
Edited by V. Carvelli and S. V. Lomov
54 **Wood composites**
Edited by M. P. Ansell
55 **Toughening mechanisms in composite materials**
Edited by Q. Qin and J. Ye
56 **Advances in composites manufacturing and process design**
Edited by P. Boisse
57 **Structural Integrity and Durability of Advanced Composites: Innovative modelling methods and intelligent design**
Edited by P.W.R. Beaumont, C. Soutis and A. Hodzic
58 **Recent Advances in Smart Self-healing Polymers and Composites**
Edited by G. Li and H. Meng
59 **Manufacturing of Nanocomposites with Engineering Plastics**
Edited by V. Mittal
60 **Fillers and Reinforcements for Advanced Nanocomposites**
Edited by Y. Dong, R. Umer and A. Kin-Tak Lau
61 **Biocomposites: Design and Mechanical Performance**
Edited by M. Misra, J. K. Pandey and A. K. Mohanty
62 **Numerical Modelling of Failure in Advanced Composite Materials**
Edited by P.P. Camanho and S. R. Hallett
63 **Marine Applications of Advanced Fibre-reinforced Composites**
Edited by J. Graham-Jones and J. Summerscales

64 **Smart Composite Coatings and Membranes: Transport, Structural, Environmental and Energy Applications**
Edited by M. F. Montemor
65 **Modelling Damage, Fatigue and Failure of Composite Materials**
Edited by R. Talreja and J. Varna
66 **Advanced Fibrous Composite Materials for Ballistic Protection**
Edited by X. Chen
67 **Lightweight Composite Structures in Transport**
Edited by J. Njuguna
68 **Structural Health Monitoring (SHM) in Aerospace Structures**
Edited by F-G. Yuan
69 **Dynamic Deformation and Fracture in Composite Materials and Structures**
Edited by V. Silberschmidt
70 **Advanced Composite Materials for Aerospace Engineering**
Edited by S. Rana and R. Fangueiro
71 **Lightweight Ballistic Composites: Military and Law-Enforcement Applications, 2nd Edition**
Edited by A. Bhatnagar
72 **Handbook of Advances in Braided Composite Materials: Theory, Production, Testing and Applications**
J. Carey
73 **Novel Fire Retardant Polymers and Composite Materials: Technological Advances and Commercial Applications**
Edited by D.-Y. Wang
74 **Advanced High Strength Natural Fibre Composites in Construction**
Edited by M. Fan and F. Fu

Preface

The modern construction industry is subject to a period of dramatic policy shift and to a priority change from a profit-charged business machine to a socioeconomic and environmentally driven organism. The environmental impact of the construction industry has been the subject of much scrutiny for the past few decades. Energy consumption in use and the construction of buildings account for about 40% of total CO_2 emissions, 15% of which can be attributed to the production of construction materials. The global target of halving CO_2 emissions from industries, along with projections for the demand of materials to double by 2050, means a fourfold reduction in emissions per unit of material used. The expected energy efficiency targets of new buildings will cast the embodied impact of materials into sharp relief. It is therefore crucial that the embodied impact of construction materials is addressed and that new materials in development support the realization of environmental aspirations from the construction industry.

Advanced composite materials are becoming established as a staple in all structures, driving a multibillion dollar market internationally. There has been a growing movement to utilise biomass in the face of climate change, demands for sustainable economic growth and uncertain energy supplies. A typical biomass resource is wood and other natural fibre-based composite products, the raw material of which is a resource that is converted from CO_2 (in the atmosphere) through photosynthesis using solar energy, and can provide a renewable and sustainable raw material source. The first division of biomass-based composites defined as being suitable for construction is particle- or fibre-based composites, known as wood itself as a polymer composite and wood-based composites; the second of these divisions is long natural fibre composites being seen as an alternative to synthetic fibre composites; the third division is the one that is soon likely to have uses in construction, nanocellulose or nanotechnology-enhanced biobased composites; the forth division of these construction composites is laminated composites.

The use of biomass-based products in construction, which facilitates the reduction of environmental impact, for engineering has a direct influence on human life, affecting in many ways the people involved and producing wider ripple effects in many related and non-related fields in the community. The safe and sustainable use of materials in construction necessitates that the natural fibre composites are fit for purpose and that their life-cycle performance can be determined with sufficient accuracy. Ever-changing demands for better products remain a constant challenge, while the facilitation of the market introduction of new products and conformity assessment becomes the foremost difficulty facing the natural fibre composites industry.

The main objective of this book is to provide the basic framework and knowledge required for the efficient and sustainable use of natural fibre composites as a structural and building material, and to improve the efficiency of use and competitiveness of the composites. The book presents vital issues, and is effective and instructive for a mutual understanding of the nature and behaviour of high-strength natural fibre composites in construction. It will serve as a valuable text or reference book challenging academics, research scholars and engineers to think beyond standard practices when designing and creating novel construction materials.

Mizi Fan

Introduction: a perspective – natural fibre composites in construction

1

M. Fan [1], *F. Fu* [2]
[1]Brunel University London, London, United Kingdom; [2]Research Institute of Wood Industry, Chinese Academy of Forestry, Beijing, China

1.1 Introduction

The modern construction industry is subject to a period of dramatic policy shift and priority change from a profit-charged business machine to a socioeconomic and environmentally driven organism. The environmental impact of the construction industry has been the subject of much scrutiny. Energy consumption in the use and the construction of buildings accounts for about 40% of all CO_2 emissions, 15% of which can be attributed to the production of construction materials. Although the embodied impact of materials is relatively low when compared with the operational impact of buildings, the expected energy efficiency targets of new buildings will cast the embodied impact of materials into sharp relief. It is therefore crucial that the embodied impact of construction materials is addressed and that new materials in development support the realisation of the environmental aspirations in the construction industry.

Fibre reinforced polymer composites (FRP) form a multibillion-dollar market internationally. In this market, 95% is comprised of glass reinforced plastics (GRP). The construction industry accounts for one of the largest shares in GRPs, second only to the automotive industry. Polymers in isolation are used extensively in the construction industry, with many applications including electrical fittings, light fittings and design features. GRPs and indeed natural fibre composites, such as glulam, laminate veneer lumber or I-beam composites, are used in structural applications such as beams, columns with self-supporting structures and architectural features such as external cladding.

Natural fibre reinforced polymers (NFCs) have been identified as a potential low-impact alternative to GRPs. Although the replacement of glass fibre with natural fibres for reinforcement in polymer composites appears to be a modern phenomenon, NFCs are not strictly modern by invention. Henry Ford used hemp fibre reinforced plastic to form car panels as early as the 1930s. With the advent of glass fibre technology in 1938, GRPs have, up until recently, been more economically viable than NFCs. However, with the economic viability of materials set to become increasingly influenced by their embodied impact, natural fibres that are less harmful to humans, machinery and the environment are a realistic alternative to the energy intensive production of glass

Advanced High Strength Natural Fibre Composites in Construction. http://dx.doi.org/10.1016/B978-0-08-100411-1.00001-7

fibre. If research and development can resolve the unique technical problems posed by natural fibre reinforcement, NFCs have vast potential as construction materials and as a replacement of GRPs and other structural materials (eg, steel, concrete) in many applications. The assimilation of NFCs into the construction industry will depend on their proven performance in use, their economic viability and the confidence with which structural and architectural components can be designed.

1.2 Basic concept and classification of natural fibre composites for construction

Composite materials combine and maintain two or more discrete phases, each having its own physical and mechanical characteristics. Once formed by the process of combination, as optimised by best practice, the resulting composites have properties that can be markedly superior to their constituent parts. The range of these materials is very diverse, but composites in building construction can be categorised into four main divisions, namely particle/short fibre reinforced, long natural fibre reinforced, nano (cellulose) composites and consolidated composites. Each of these composites has various constituent combinations (Fig. 1.1). Natural fibre itself is a polymer composite with the constituents of cellulose, hemicellulose and lignin.

The first of these three divisions defined as being suitable for construction is that of particle or fibre-based composites, known as wood-based composites. This division of composites can be subdivided into two levels of composites. The first of these is wood itself as a polymer composite. Wood is a low-density, cellular, polymeric composite. The most successful model used to interpret the ultrastructure of timber/composite ascribes the role of 'fibre' to the cellulosic microfibrils, while the lignin and hemicelluloses are considered as separate components of the 'matrix' (Fig. 1.2). There is ample record of the ubiquity of wood as a construction medium. Five thousand years ago, the ancient Egyptians were using it to build boats, to make furniture and coffins and to sculpt statuary. Sophisticated carpentry techniques developed independently from c.1100 AD in England, mainland Europe, China, India and Japan. However, despite some brilliantly innovative exceptions, wood has tended to be usurped for structural and engineering applications by new strong materials. Nevertheless, in defiance of competition from lightweight metals and plastics, whether foamed or reinforced, wood remains the world's most successful natural fibre composite by virtue of its

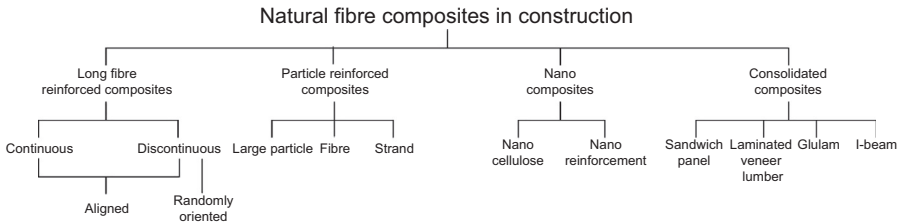

Figure 1.1 A classification of natural fibre composites in construction.

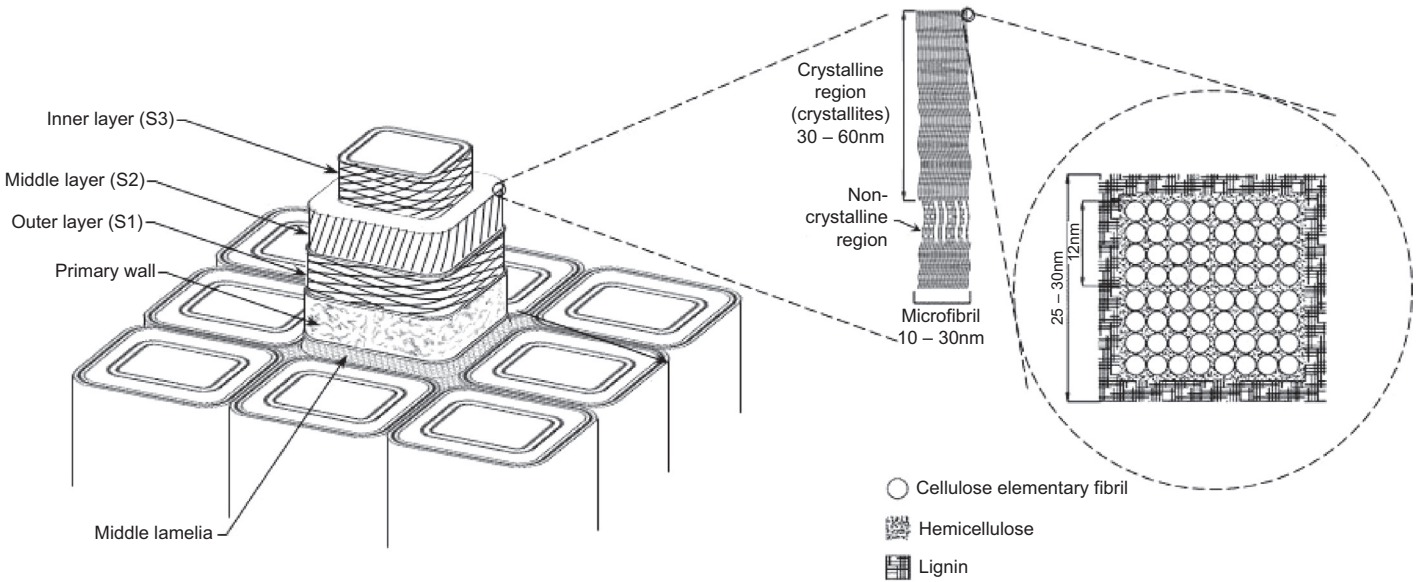

Figure 1.2 Natural fibre as a natural composite of cellulose, hemicellulose and lignin.

Figure 1.3 Various wood-based composites for construction (left = rigid composites and right = insulation mat).

excellent strength-to-weight, ease of formation into complex shapes, ease of jointing, low cost and sustainability.

The second level of the wood-based composites is the reformula of wood particles or fibres, known as particleboard, hardboard, medium density fibreboard (MDF), plywood and oriented strand board (OSB). There has been a surge of interest in these potentially versatile, carbon-capturing and sustainable composites, which has led to a number of new innovations that could succeed in bringing several enhanced natural fibre composites to the building material market (Fig. 1.3). Annual production of wood-based composites has almost reached to 300 million m^3 in 2010, with an annual increase rate of 7%.

One slightly different form of wood used in construction is natural fibre as an insulation material (Fig. 1.3). Natural fibre insulation products can often be used as replacements for mineral fibre or petrochemical-based insulation. Natural fibre insulation materials are not only able to deliver thermal and acoustic insulation comparable to other insulation materials, but also a lower or potentially negative carbon footprint and fewer health issues in using building construction. Natural fibre-based materials are vapour permeable and are able to assist in regulating relative humidity of indoor environments.

The second of these divisions is that of long natural fibre composites. Long natural fibre composites (LNFCs), which are polymers reinforced with cellulosic long fibres, have a potential to be applied into a range of building products. They are often seen as an alternative for glass fibre reinforced plastics in some applications, because of the relatively high strength and low density of long natural fibres (LNF). There are six types of natural fibres used for the long natural fibre composites, which can be classified by botanical type, namely bast, leaf, seed, core, grass and others like wood and root fibres. Flax, hemp, sisal and jute fibres are commonly used reinforcements for LNFC (Fig. 1.4). Various long natural fibre reinforcements, eg, hybrid mats, twisted or nontwisted yarns, hybrid yarns and various fabrics and processing technologies, eg, compression, vacuum bagging, injection, filament winding and pultrusion, could be used for the production of LNFCs for construction. LNFCs have the highest properties in tensile or flexural modes.

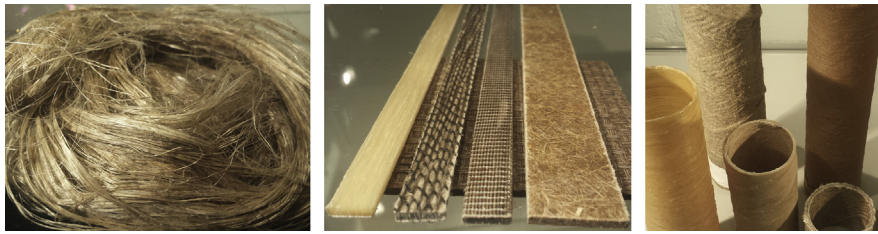

Figure 1.4 Long natural fibre composites for construction (left = long natural fibres, middle and right = long natural fibre composites for construction).

With control over the type and arrangement of reinforcement, LNFCs could be optimised for specific construction components, such as, LNFC rods, panels, tubes and I-beams (Fig. 1.4). The main reasons for the development of LNFCs are their price, performance and low environmental impact. The low price is necessary for the LNFCs to be economically viable, because expensive LNFCs can be substituted by a range of well-established synthetic composites. Low embodied energy is one of the key arguments for NFC competition with glass fibre reinforced plastics.

The third division, one which is soon likely to have uses in construction, is that of nanofibre composites. Nanotechnology is the term used for the manipulation of materials measuring 100 nm or less (ie, the size of a virus) in at least one dimension. Nanotechnology is considered to be one of the most important technological innovations of this century (some are citing it as a second industrial revolution). Research and development (R&D) in nanotechnology is critically important to the new generation of processes and products. New nanomaterials with unique, 'bespoke' properties can now be developed with the aid of nanotechnology. It could enable new techniques of polymerisation to be perfected, which would entail synthesis of fibres augmented either with water or with other organic liquids, with the twin aims of enhancing composite performance and facilitating end-of-life recycling. Nanocomposites in the field of natural fibre composites mainly focus on two directions of research: one is nanocellulose composites and the other nanoparticle-enhanced natural fibre composites (Fig. 1.5).

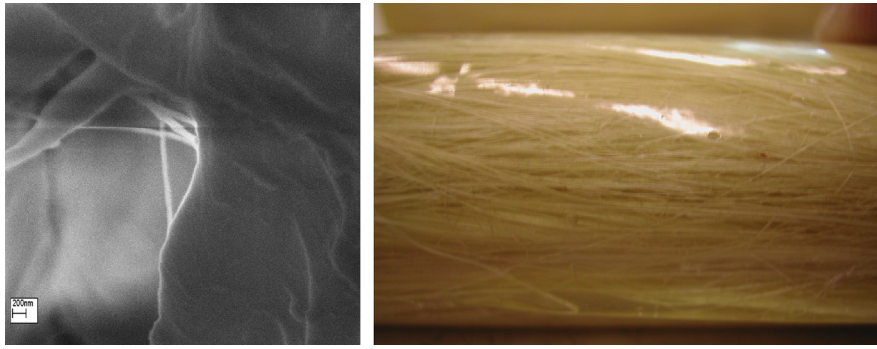

Figure 1.5 Nanocellulose (left) and nanocomposites (right).

Figure 1.6 Consolidated composites: glulam and laminated veneer lumber (left) and cross-laminated lumber (right).

The forth division of these construction composites is that of the consolidated composite, notably, glulam (laminated), laminated veneer lumber (LVL) and cross-laminated lumber (CLT) (Fig. 1.6), which are designed with specialty interfaces to increase the fracture resistance of woo-based composites and to accommodate residual stress in load-bearing building construction. Laminated products are mostly designed and used for structural purposes. The laminates represent a new technology in wood utilisation with currently increasing production and application. The laminates are high-strength engineered wood-based composites and are used for permanent structural applications including beams, lintels, truss chords, formwork and other building components.

Homes and other buildings are getting larger and trending toward more open space. These combined factors mean longer spans and greater loads required for the construction, which can only be realised with the use of steel or advanced natural fibre composites, such as glulam, LVL or their I-beam construction. These reengineered wood composites are often defined as a combination of smaller pieces of wood that together create high-strength structural elements or components.

Reengineered wood composites include a wide range of products manufactured by bonding together wood strands, veneers, lumber, or other forms of wood fibre to produce larger and integral composite units. Structural engineered wood composites are engineered by virtue of possessing design values that are confirmed by methods other than simple visual grading. These products are extremely efficient because they utilise more of the available resources with minimal waste.

1.3 Natural fibre composites in building construction

The construction industry is one of the world's largest consumers of composite materials, with wood-based composites and long natural fibre composites being used as nonload-bearing or semistructural components and consolidated composites for

structural/load-bearing construction. A whole range of advantages of natural fibre composites, such as their light weight, high strength to weight ratio, tremendous fatigue, customised surface finish, high prefabrication profile, nonmagnetic characteristics and the possibility of integrating functions, have made them attractive for innovative structural design. However, the acceptance of new products by the manufacturers and their customers has always been a slow process. A better understanding of the reasons for the acceptance or rejection of structural composites and engineered lumber as raw materials for construction could lead to further expansion of their uses by manufacturers and better sales and marketing by the raw material manufacturers and distributors.

1.3.1 Composites for roofing systems of building construction

Various natural fibre composites have been used for the rafter, purlin, ridge board, and hip or valley members of roofing systems of building construction. The most used components are composite I-joists or solid rectangular structural composites as roof beams, such as glulam, LVL and laminated strand lumber and wood-based composites as blocks. The I-joists are excellent for rafter components, especially where energy-efficient designs require depth in the member for insulation and venting requirements. Wood-based panels, eg, plywood and OSB, are used as blocks, preventing the rotation of the I-joist in the hangers (Fig. 1.7).

Wood-based composites have also been extensively used for the off-site prefabrication of roofing components, eg, stressed skin panels (SSP), to improve the efficiency and waste reduction of building construction. SSPs have a high structural performance on a consistent basis and can be constructed either with joists and/or rigid foam with either a single or two wood-based composites sandwiching the core, which forms the stressed skin. The principle is that the skin and the core act together to provide the structural integrity. Where larger housing developments are being constructed,

Figure 1.7 Natural fibre composites for roofing construction (left = I-joist and right = fibre board blocking).

Figure 1.8 Off-site roofing components in building construction.

significant savings in time can be achieved, for example, a roof can be assembled in two to three hours, which may enable the building to be made watertight more rapidly than traditional methods. This will effectively reduce moisture-related problems of the construction and help the project management of the whole build. This construction could also create a large amount of available roof space, which could be used for additional rooms (Fig. 1.8).

1.3.2 Composite walls of building systems

Using natural fibre composites as a wall system is probably one of the most successful applications (Fig. 1.9). A wall system can be made up of a combination of natural fibre composites, such as MDF and plywood, and linear reengineered wood composites. One of the functions of a wall is to provide in-plane racking and or shear resistance. Walls do not have to be planed in two directions. One-dimensional planar walls allow for curving forms that still have a measurable rigidity (Fig. 1.7). Composites, especially wood-based composites, will continue to be the major materials for the wall construction in meeting the low carbon building construction remit.

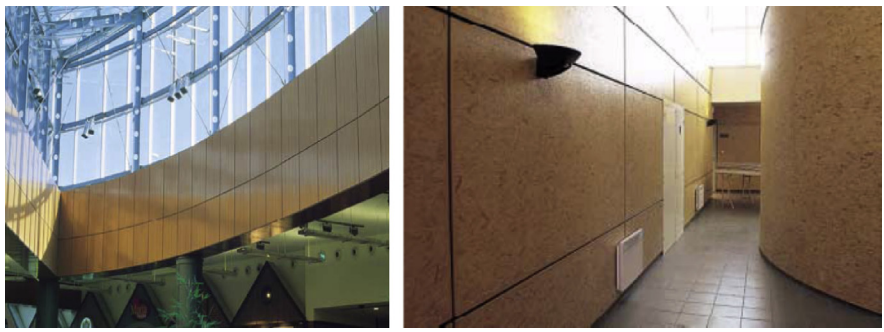

Figure 1.9 Natural fibre composites for wall construction.

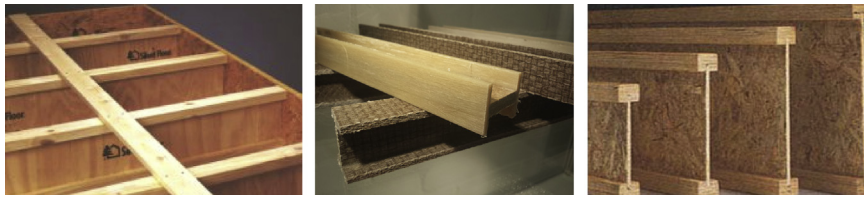

Figure 1.10 Various I-joists made of natural fibre composites (left = plywood flange, middle = long fibre hemp composite flange and right = oriented strand board flange).

1.3.3 Composite flooring and ceiling systems of building construction

Composites for flooring and ceiling systems consist of two main groups: one is the load-bearing composites as joists (Fig. 1.10) and the other is the semistructural composites as floor and ceiling skins. The I-joists are responsible for resisting bending and deflection, which is influenced by their depth. The addition of the subfloor composites gives rise to a measure of T-beam action to help stiffen the system further. The I-shape has been long known for its efficiency in bending strength and deflection control. This has led to a new level of structural, material and environmental efficiency. A number of components have been produced with different materials in the flanges and webs and different connections between the web and the flange. The I-joists can be deep or shallow, usually in sizes that match common dimension lumber depths or other reengineered composites, such as the depth of glulam and LVL.

Another group of ceiling and flooring systems is composites as laminate floors (Fig. 1.11). Composite and laminate floors are growing fast, and most flooring products are laminates of real wood appearance, such as large panels in different patterns, representing the newest designs, different sound reduction and underfloor heating flooring systems.

1.3.4 Natural fibre composite insulation systems

Natural insulation materials, such as hemp, flax and wool, have been the most interesting products for low carbon construction, becoming widely recognised for their sustainability. Natural insulation materials often require a greater thickness of insulation in comparison with standard materials in order to achieve the same U-values, such as

Figure 1.11 Flooring systems for building construction.

Figure 1.12 Natural fibre mats for building insulation system.

Expanded polystyrene (EPS) and Polyurethane (PU) foams. Although this has commonly been considered a barrier to their wide application, much effort has been invested in a greater understanding of their additional benefits in order to minimise these perceived obstacles. For example, some specific characteristics of natural materials are realised: acting as a carbon sink, for example, hemp locks in up to 2 tonnes of CO_2 per tonne of fibre, making it a particularly sustainable choice. It is available in a variety of different insulation forms (Fig. 1.12): semirigid batts for vertical installations and a solid wall solution for the increased thermal mass. Due to the hygroscopic nature of natural fibres, the insulation is able to absorb, store and release moisture, naturally controlling condensation levels within the building and improving internal air quality.

1.3.5 Advanced composite beams and columns

Advanced natural fibre composites are commonly produced for building beams and columns (Fig. 1.13), gradually replacing traditional steel plates or steel jackets, the corrosion of which often causes serious deterioration of bonds at the steel—concrete interface and the construction of which leads to an increase in the overall cross-sectional dimensions and self-weight of structures. The fibres in the composite are placed parallel to the principal stress direction. Various parameters related to the performance of the composite columns and beams have been studied, including the properties of columns, depth-to-width ratio, geometry of and fibre within reinforcements and geometric and loading imperfection. Composite beams and columns have been considered the most beneficial for a long span of building construction.

1.3.6 Full composite building systems

Entire building systems can be formed from a collection of natural fibres acting together and forming hybrid components (Fig. 1.14). System-oriented products for natural house construction are an intelligent way of using natural fibre composites: I-joists, OSB, fibreboard insulation panels and roof and wall panelling for vapour diffusion. Natural fibre composite construction is natural and eco-efficient. Such building and construction systems are cost-effective, thermal and sound insulation solutions that meet all relevant structural, fire protection, soundproofing and environmental requirements. Maximum benefits can thus be expected from sophisticated building

Figure 1.13 Natural fibre composites for beams and columns in building construction.

Figure 1.14 Natural fibre composite hybrid building system (left = wood composites, middle = cross-laminated lumber and right = composite construction).

systems. Hybrid systems can represent a significant savings in time and cost of erection, while producing a high-quality end product.

The composites and their various manufacturing technologies make it feasible to construct complete primary structures. Considerable weight saving presents an excellent opportunity for large-span structures and the architectural freedom of dramatic new construction forms. Full building systems consist of solid interlocking components or cellular components. The system consists of a number of units, which can be brought together by mechanical interlocking with grooved and solid connectors.

Modular construction systems usually consist of several composite panels or elements, which are bonded together to form a membrane structure and provide complete structural integrity without additional framework. Modular building systems are normally installed on site, given that light components make transportation and on-site handling economic and safe. Off-site prefabrication is possible and minimises site assembly and installation time. Modular construction systems have been developed for several application sectors to satisfy the desire for more dramatic features in the construction design of complex forms. However, the design of modular constructions normally requires a great investment in engineering analysis and tooling. Composite structures may be fundamentally different from conventional building structures in both geometric and structural forms. The construction could provide significant savings in production and assembly time on site.

In addition to the development of improved composites or components for the full building systems, connection design, systemic structural optimisation for building geometry, roof configuration, foundation anchorage and building envelop and full system verification tests are much needed. For example, the current joining technology of mechanical interlocking with grooved and solid connectors may work well for metals but would fail when considered from the standpoint of the structure of composites. The alignment and connection between the fibre and matrix of composites are in principle similar to those of wood, indicating an isotropic nature of the composites. Consequently, composites have low bearing and interlaminar shear strengths. Bolts and rivets carry and transfer connection forces to specific points, thus causing high stress concentrations, which threaten the failure of the composite construction at joints.

1.4 Performance in use of natural fibre composites

1.4.1 Long-term performance of natural fibre composites

The long-term performance of construction materials has been an important research subject given the necessity to assure that the materials are able to sustain applied loads without fulfilling ultimate limit states and serviceability limit states. Long-term performance assessment concerns the behaviour of products in service when subject to mechanical (eg, load) (Karbhari et al., 1996; Kumar and GangaRao, 1998; Oh et al., 2005), physical (eg, wetting) and biological (eg, decay) actions. Long-term performance is usually assessed through accelerated short-term laboratory testing capable of simulating static or dynamic actions to which a certain composite is subjected in service. This is normally calibrated to the results of weathering exposure to validate the similar effect between those under the natural environment and under accelerated testing conditions.

Research on long-term behaviour falls conveniently into three aspects: the first relates to the quantification of the time-dependent behaviour of composites of different types and compositions under both natural and artificial climates. Much of the information obtained is subsequently used in the determination of time-dependent factors (the duration of load factor and creep factor) to be incorporated in codes for structural

design. The second aspect relates to the modelling of creep behaviour for both descriptive and predictive purposes, while the third is concerned with the much more academic challenge of trying to understand the basic mechanism underlying rheological behaviour (Fan et al., 2006). The real challenge is how to integrate various parameters (eg, load, air conditions and biological hazards) that can affect the long-term performance of composites by leading to three general types of degradation, mechanical, physical and biological, into testing design and afterwards into a model. What is often followed is to subject specimens to a main variable and in some cases to evaluate the effect of a secondary variable, such as on the effect of dynamic loading on creep deformation.

Composites may not suffer corrosion as steel and concrete. However, the environmental degradation of composites arises from a complex set of processes due to the combined effect of ultraviolet (UV) radiation, heat from the sun and moisture and oxygen from the atmosphere. Natural fibre composites may first be exposed to UV radiation, resulting in photo-oxidative degradation, chain scission, cross-linking and consequent debonding of composites. The resultant products may react with oxygen to form functional groups (secondary oxidative reaction), such as carbonyl (C═O), carboxyl (COOH) or peroxide (O−O). It must be noted that UV exposure usually affects the top few microns of the surface depending on the duration of time, resulting in colour fading or darkening, yellowing, blooming, loss of gloss and chalking. The degradation of polymers may give rise to the exposure of natural fibres, which could respond to the change of the surrounding environments, resulting in the swelling or shrinkage. The swelling or and shrinkage of natural fibres may generate internal stress, which then causes stress concentration and debonding or delamination of the interface between fibres and matrix.

Modelling structural deterioration is difficult due to the inherent complexity of the process and the structure of composites, as well as the multitude of external factors and mechanisms that are responsible for deterioration. The available approaches to model life cycle performance can be classified into network level and structure level methods. The network level methods predict the conditioned deterioration of a group of structures grouped either by locality or type. Markov methods and statistical regression techniques have been widely used in modelling structural deterioration at the network level (Hastak and Halpin, 2002; Mishalini and Madanat, 2002). The structural level modelling should be carried out based on knowledge of the physical and chemical processes that are responsible for material deterioration (Deepak et al., 2007).

1.4.2 Sustainability of construction composites

The ultimate goal of the construction industry would be to develop a material not only possessing the basic requirements of construction, eg, material characteristics such as stiffness, strength, affordability, durability, versatility and ease of use, but also the characteristics of environmentally sustainable profiles. Environmental performance over the whole life cycle is crucial for the success of building materials, from extraction, processing, construction, uses, maintenance, eventual demolition and disposal. Natural fibre composites may offer a solution through various combinations of raw materials and

properties. Life Cycle Assessment (LCA) has been a method of assessing and quantifying the environmental impact of composite products for construction. The use of LCA is to provide a comparison between the use of different materials or manufacturing processes for a given product to determine benefits or disadvantages. The information for LCA can be obtained by calculating and measuring a new set of data for each material or by calculating the data from the constituents of the materials summed together. Natural fibre composites are considered the most sustainable materials; they have negative carbon emission as the tree grows with the photosynthesis of CO_2.

Waste and the disposal of construction materials at the end of life are another major parameter. The construction industry consumes huge amounts of material resources and in turn it is the sector producing the largest quantities of waste. It has been reported that the construction industry may be responsible for more than 50% of the waste arising in the United Kingdom (Hobbs, 2006). The amount of all waste varies considerably from one type of construction to another. In common with other waste, the waste hierarchy for composites is to prioritise the prevention and reduction of wastes, then to reuse and recycle and lastly to optimise final disposal. Composite production waste was generally disposed of since the raw materials used in composite manufacture are considered relatively inexpensive, but the cost for disposing composite waste appears to be relatively low. Natural resources are recognised and have become more and more attractive as the resources of other products, eg, bioenergy. Therefore the by-products of natural fibres are considered invaluable.

The recycling of composites is directly related to the types of composites. Natural fibre composites can be relatively easy to be recycled or composted, as wood or other natural fibres themselves are biopolymers, which can be degraded while there is a little resin content $<10\%$. The biomass, such as wood wastes, has recently been considered as a resource for the biorefinery industry. However, the recycling of polymer-based natural fibre composites are related to the resin systems, ie, thermoplastic or thermoset systems. Thermoplastic natural fibre composites can be recycled by remelting and remoulding, while this is not the case for thermoset composites, which dominate the construction products. Much research work has been carried out to better understand composite wastes and their end-life solutions (Demura et al., 1995; Hobbs and Halliwell, 1999; George and Dillman, 2000).

1.5 New development of natural fibre composites for future engineering

Much of the effort spent on innovation and manufacturing has not only demonstrated the challenges but also significant potentials for natural fibre composites (Fan, 2007, 2015). Plant fibres, such as wood, work across a length scale of more than 10^{10}, therefore this provides an equivalent opportunity for new products, including production and processing innovations (Fig. 1.15). New materials could be developed from biochemistry/bioplastics to nanocellulose composites to natural fibre composites to consolidated structural composites. On the other hand, there has been an expanding search for new materials with a high performance at affordable costs. With growing

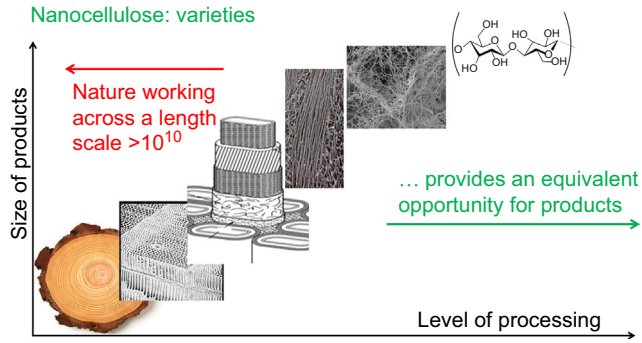

Figure 1.15 Possible new developments from natural resources (wood).

environmental awareness, this search has particularly focused on eco-friendly materials and underscores the emergence of a new type of materials, changing from nonrenewable but difficult to degrade or nondegradable, to renewable and easily degradable materials. The development of such materials has not only been a great motivating factor for material scientists, but also an important provider of opportunities to improve the standard of living of people around the world.

1.5.1 Fundamental research on the structures and related theory

The first of these important researches focuses on the adhesion of matrix and reinforcement (fibre). The internal cohesion of natural fibre composites is mainly determined by bonding quality between elements (particles, fibres) and matrix. The better understanding of the way that adhesion is achieved between the elements (distribution of matrix resin within the contact surface between the elements and variability of that distribution and mechanical resistance of particle/fibre–particle/fibre element), shall support the development of more resistant and durable composites, potentially the specific property of composites. Many studies on mechanical properties of natural fibres incorporated into various thermoplastics (PHA and PLA) and thermosets (polyester, epoxy and phenolformaldehyde) have been attempted. All studies have emphasised that the adhesion between the fibre and matrix plays a significant role in the final mechanical properties of the biocomposites, since the stress transfer between matrix and fibre determines the reinforcement efficiency. However, natural fibres contain large amounts of cellulose, hemicelluloses, lignin and pectins; they tend to be active polar hydrophilic materials, while polymer materials are a polar and exhibit significant hydrophobicity. The weak interfacial bonding between highly polar natural fibre and nonpolar organophilic matrix can lead to a loss of final properties of the biocomposites and ultimately hinder their industrial usage. Different strategies have been applied to eliminate this deficiency in compatibility and interfacial bond strength, including the use of surface modification techniques. Nowadays, various greener methods, such as plasma treatment and treatments using enzymes, fungi and bacteria, have been explored.

The second fundamental aspect of these researches is the deterioration process at the interfaces of matrix and fibres. Scarce information exists to fully understand the degradation processes of the bonding interface. The influence of fibre characteristics and type of polymer resin on this deterioration is most interested as part of the basis for numerical models. These models can be used for advancing the formulation of a new composite, knowing in advance what could be expected in terms of physical and mechanical properties of the composites obtained.

1.5.2 Super lightweight composites

Lightweight advanced natural fibre composites with high mechanical properties and cost effectiveness are highly desired for wood-based composite industries. Lightweight composites are available on the market, such as honeycombs. Currently, a significant investigation has been carried out to further develop the lightweight core facilitated by blowing agents. The process could be executed with a one-step process. For example, foam core particleboards were produced with the newly developed process with either expandable microspheres or polystyrene as a core layer (Shalbafan, 2013). As a recycling option for trimming waste and rejected foam core panels at the industrial scale, flat-pressed wood plastic composites were also made from foam core particleboard residues.

1.5.3 Long-term performance of natural fibre composites

The long-term performance of wood-based composites has been an issue for the safe use of the composites. To perform the research in this area requires considerable efforts and investment. Typical research aspects are considered in the areas of (1) the failure (rupture/deformation) under different stress modes: although safe coefficients can be applied to deal with the uncertainty that still exists about the stress mode with failure (either creep or fatigue), experimental data and numerical models should be available for promoting and optimising the use of composites and allowing the evolution of production standards. (2) The development of characteristic values of new products for engineering design: there is currently no design values for long natural fibre composites, and the design values given in Eurocodes for wood-based composites are for conventional products, although not for all. There are no relevant data or guidance available for new products. (3) Methodology/models to predict the working life of composites: in-service composites may be subject to dynamic actions (variable stress levels and environment conditions). Models that can provide information about the dynamic behaviour of composites can prevent failure in service of the composites. (4) Moisture resistance of composites, such as wood-based panels: moisture resistance of wood-based composites is one of the long-term research areas due to the inherent hygroscopic nature of wood and other natural fibrous materials. More stringent requirements in modern society is another driver for the further development of more moisture-resistant materials. (5) Bioresistance of composites, especially wood-based composites: one of the research areas, which is highly related to the moisture resistance of wood-based composites, is the bioresistance of wood-based composites. Both new

materials with higher bioresistant performance and evaluation methodology, especially the prediction of long-term performance, are required.

Better fire performance of natural fibre composites is another important parameter and crucial property for the success of the development of natural fibre composites. An extensive research on fire and thermal characteristics of natural fibre composites has been carried out at Brunel University London (Naughton et al., 2014; Fan and Naughton, 2016). Documentation of K classes according to the new European procedure in EN 14135 is a great opportunity to demonstrate performance compared with other building panels.

Fire-retardant treated wood-based panels are far from perfect. Research on fire-resistant wood-based panels to fulfil the new/enhanced requirements needs to be initiated in order to achieve reliability and confidence among new users. The effect of fire-retardant products on the quality of the interface of fibre and matrix is another area required for further investigation. The inclusion of fire-retardant products may result in a decrease in the mechanical properties and possible physical deterioration of fibrous elements.

1.5.4 Test methodology for wood-based panel building systems

The appropriate codes and guidelines have to be researched for all prefabricated applications in structural systems to assure their static and seismic resistance. It is obvious that there is also a need for the development of an integral European standard that would cover cyclic testing of such construction parts, where using natural fibre composites represents important segments. The new standard should also include the criteria for determination of deformability limitations, especially of interstory drifts according to the concept of performance based on earthquake engineering design.

1.5.5 Environment and sustainability of natural fibre composites

Due to the concerns about the environment and sustainability, there have been remarkable improvements in green materials in the field of polymer science through the development of biocomposites. These biocomposites can be easily disposed of or composted at the end of their life without harming the environment, which is not possible with synthetic fibre-based polymer composites. The beauty of natural fibre composites is that they are renewable and sustainable. Expectations are that two-thirds of the global industries can eventually be based on renewable resources. Lignocellulosic fibres, such as flax, hemp, kenaf and jute, have drawn considerable attention as substitutes to the synthetic fibres, such as glass and carbon fibres. Natural fibre reinforced biocomposites have been used for many applications, such as automobiles, aerospace, packaging and building industries. However, the timber industry and other natural resources are extremely complex, ie, different raw material types and sources plus considerable interaction between the different processing routes. Obtaining a clear view of all the positive and negative impacts involved in the

environment and sustainability is a difficult task. Much research is being carried out, including the mission of natural fibre composites, the most appropriate environmental assessment of natural fibre composites and the disposal and reuse of natural fibre composites.

The attractive features of natural fibre over the traditional counterparts include relatively high specific strength, free formability, low self-weight and substantial resistance to corrosion and fatigue. In contrast, natural fibre is not a problem-free alternative, and it maintains some shortfall characteristics, such as high moisture absorption and a highly anisotropic nature.

1.5.6 Intelligent and nanotechnology-enhanced natural fibre composites

Advancing nanotechnology research in the forest product industry is highly needed, and research has become a priority in the short-term, medium-term and long-term. Nanomineral and wood composites, along with nanocellulose-based polymers, are intensively studied. The development of nanotechnology seems to be able to bring wood fibre composites to their full potential in the near future. The wood-derived nanocellulose could reach a higher tensile strength than carbon fibres. Since the first report on the superior performance of nanocellulose composites in 1995, the application of nanocellulose has been pushed into a new era and there has emerged extensive research in the application of nanocellulose. Most major governments around the world are investing heavily in nanocellulose. In 2002, the European Commission underpined 'NANOFOREST' to develop a research and development roadmap and to recognise new emerging developments in nanotechnology and related areas suitable for practical application in the forest product sector. In 2004, the United States initiated 'Nanotechnology for the Forest Products Industry-Vision and Technology Roadmap'. In 2011, Innventia opened the world's first pilot plant for the production of nanocellulose, which has a capacity of 100 kg/day. This facility makes it possible to produce nanocellulose on a large scale, which is an important step towards the industrialisation of the technology, promoting the application of nanocellulose in composites and boosting the exploitation of wood resources. In 2012, the forest product laboratory opened a pilot plant for the production of wood-derived cellulosic nanomaterials. Although the large-scale production of wood nanocellulose is still on its way, a boosting development of a new generation of wood fibre composites will come in the future.

Textile engineering and modelling technologies have been used in composite fabrication with a view to develop multifunctionalised composites (Fan and Weclawski, 2016). Textile engineering has provided an opportunity for producing hybrid composites with the flexibility of fibre content, fibre orientation and roving texture of hybrid fabrics, and the options of weave styles, such as plain, twill, satin and leno, to prepare the required form of reinforcements. The addition of textile engineering technologies could also significantly extend the content of the intelligence of natural fibre composites, for example, the weaving of super tough carbon nanotubes with natural fibres could result in a nanocomposite with a special strength and electronic characteristics for making electronic devices such as sensors, connectors and antennas; the

electrospinning of polymeric fibres to produce nanopolymer fibres could give rise to a large surface area useful for various improvements of nanocomposites; the textile engineering can also facilitate the doping of various functional agents for the development of various intelligent composites.

Full biocomposites have also been of great interest and research. The increased attention has been paid to the use of natural polymers and lignocellulosic. It is reported that by 2020, about 10% of the basic chemical building blocks will come from renewable plant resources, which is expected to rise to 50% by 2050 as hurdles to their use are reduced. Work on biodegradable composites started in the 1990s. Different processing techniques and their effect on the properties of biopolymer blends are investigated: of particular interest is the blending of poly(hydroxybutyrate) and poly(hydroxybutyrateco-valerate) through miscibility, poly(lactic acid), poly(glycolic acid) and poly(-caprolactone).

Novel treatment agents, such as nanodye and nanopreservatives, are also interesting subjects for the natural fibre composites industry. Advancing nanotechnology research for natural fibre composites requires cross-disciplinary teams such as material scientists, biological scientists, polymer scientists, paper scientists, wood and plant scientists and chemical and mechanical engineers and a close partnership from industry, government and academia in order to capture synergies.

1.6 Conclusions

Natural fibre composites (NFCs) have been identified as a potential low-impact alternative to other synthetic composites. The replacement of glass fibres with natural fibres for reinforcement in polymer composites appears to be a modern phenomenon. NFCs have vast potential as construction materials and as a replacement of other structural materials (eg, GRP, steel, concrete) in many applications.

Plant fibres, such as wood, work across a length scale of more than 10^{10}; therefore this provides an equivalent opportunity for various innovations, including production and processing innovations. New materials could be developed from biochemistry/bioplastics to nanocellulose composites to natural fibre composites to consolidated structural composites. On the other hand, there has been an expanding search for new materials with high performance at affordable costs, particularly focusing on eco-friendly novel materials changing from nonrenewable.

The range of natural fibre composites is very diverse, but composites in building construction could be categorised into four main divisions: namely, particle/short fibre reinforced, long natural fibre reinforced, nano (cellulose) composites and consolidated composites. Each of these composites has the various constituent combinations. Natural fibre itself is a polymer composite with the constituents of cellulose, hemicellulose and lignin.

The construction industry has been one of the world's largest consumers of composite materials, with wood-based composites and long natural fibre composites being used as nonload-bearing or semistructural components and consolidated composites for structural/load-bearing constructions. A whole range of advantages of natural fibre

composites have made them very attractive for innovative structural design from intelligence insulation building systems to composite roofing, flooring, ceilings, beams and columns and even full hybrid construction systems.

Significant development has been carried out to innovate natural fibre composites for future construction, from the fundamental interface of natural fibre and matrix to super lightweight to long-term durable to full biocomposites with both natural fibres and biopolymers. Intelligent and multifunctional composites have been of particular interest.

References

Deepak, R., Hong, T., Hastak, M., Mirmiran, A., Salem, O., 2007. Life-cycle performance model for composites in construction. Composites 38, 236−246.

Demura, K., Ohama, Y., Satoh, T., 1995. Properties of artificial woods using FRP powder. In: Disposal and Recycling of Organic and Polymeric Construction Materials, Proc Int Rilem Workshop, Tokyo, pp. 26−28.

Fan, M., Naughton, A., 2016. Mechanisms of thermal decomposition of natural fibre composites. Composites Part B Engineering 88, 1−10.

Fan, M., Weclawski, B., 2016. Long natural fibre composites. In: Fan, Fu (Eds.), Advanced Natural Fibre Composites for Construction. Woodhead Publishing.

Fan, M., Bonfield, P., Dinwoodie, J., Enjily, V., 2006. Effect of test piece size on rheological behavior of wood composites. ASCE Journal of Engineering Mechanics 132 (8), 815−822.

Fan, M., 2007. NATCOM (2007), optimally efficient production of high strength natural fibre composites. In: TSB Research Programme.

Fan, M., 2015. Grow2Build, European Centre of Excellence. Brunel University London.

George, S., Dillman, S., 2000. Recycled fibreglass composite as a reinforcing filler in post-consumer recycled HDPE plastic lumber. In: ANTEC Annual Technical Conference.

Hastak, M., Halpin, D.W., 2002. Assessment of life-cycle benefit−cost of composites in construction. ASCE Journal of Composites for Construction 4 (3), 103−111.

Hobbs, G., Halliwell, S., 1999. Recycling of plastics and polymer composites. In: Proc Conf Compos Plastics in Const, Watford, UK, pp. 10−14.

Hobbs, G., 2006. Be-aware-Literature Review. BRE Report. Building Research Establishment.

Karbhari, V.M., Engineer, M., Eckel, D.A., 1996. On the durability of composite rehabilitation schemes for concrete; use of a peel test. Journal of Materials Science 32, 147−156.

Kumar, S.V., GangaRao, H.V.S., 1998. Fatigue response of concrete decks reinforced with FRP rebars. ASCE Journal of Structural Engineering 124 (1), 11−16.

Mishalini, R.G., Madanat, S., 2002. Computation of infrastructure transition probabilities using stochastic duration models. ASCE Journal of Infrastructure Systems 8 (4), 139−148.

Naughton, A., Fan, M., Bregula, J., 2014. Fire resistance characterisation of hemp fibre reinforced polyester composites for use in the construction industry. Composites Part B Engineering 60, 546−554.

Oh, H., Sim, J., Meyer, C., 2005. Fatigue life of damaged bridge deck panels strengthened with carbon fiber sheets. ACI Structural Journal 102 (1), 85−92.

Shalbafan, A., 2013. Investigation of Foam Materials to Be Used in Lightweight Wood-based Composite. University of Hamburg.

Chemical compositions of natural fibres

2

D. Jones [1], G.O. Ormondroyd [2], S.F. Curling [2], C.-M. Popescu [3], M.-C. Popescu [3]
[1]SP Technical Research Institute of Sweden, Stockholm, Sweden; [2]Biocomposites Centre, Bangor, United Kingdom; [3]Petru Poni Institute of Macromolecular Chemistry, Iasi, Romania

2.1 Introduction

The 'bio-based economy' represents an increasing area of global development and covers a wide range of activities incorporating bio-based materials. 'Bio-based' in this context means that the materials and products are derived/made from renewable resources, with the criteria that a renewable resource recovers faster than it is drained, in contrast to many mineral and fossil resources. The processing of the forest biomass into value-adding and durable building materials and products, also taking into account the by-product streams, clearly fulfills these criteria today and, with proactive strategies, will also fulfill the criteria in the future. In addition to this, compared with aluminium, steel and concrete, most such bio-based materials are made with considerable lower energy consumption, and their use acts as a carbon sink, which means that a replacement of materials made from nonrenewable resources directly reduces CO_2 emissions. The future strategies for the world's energy and material supply must consider these facts since some prognoses indicate that the fast growth of the bioenergy sector could result in a higher use than the growth of Europe's forest and agricultural biomass.

The development of building materials incorporating bio-based materials is also an area of rapid development. As well as solid timber, wood fibres and other materials, such as bamboo, miscanthus, phragmites and other gramineae, are now being used for structural purposes as well as for roofing and cladding. In particular the combined use of wood-based and other bio-based materials allows the configuration of diverse composites, such as particle and fibreboards and sandwich panels, or in combinations with polymers, such as extruded profile members and shaped components. Traditional agricultural food plants also have the potential to be used for various building applications, eg, lightweight building boards or insulation wall fillings. Flax, hemp, sisal, coir, corn cobs and rice or wheat straw are just a few of the more commonly used examples of biofibres used in different applications in the building trade. Wood itself is used in its native character, but is also chemically and thermally modified. Finally, the use of classical and new preservatives allows the use of timber products even under severe outdoor exposure conditions.

Advanced High Strength Natural Fibre Composites in Construction. http://dx.doi.org/10.1016/B978-0-08-100411-1.00002-9

2.2 Groups of compounds found in natural fibres

Wood and plant fibres represent highly complex organic matrices comprising three main components: cellulose, hemicellulose and lignin, along with a small percentage of smaller extractable compounds. Due to the nature of growth, the percentage composition of each of these components may vary according to prevailing conditions (Fujita and Harada, 1990). In order to consider the behaviour of wood and agrifibres, it is necessary to take into account the structures of each of the major components present.

2.2.1 Cellulose

Since its isolation by Anselme Payen in 1838, there has been a continual interest into the structure and properties of cellulose. Whilst these original studies were on cellulose from plants, its presence has been shown in fungi, algae, bacteria and in some animals, such as sea squirts (ascidians). Cellulose is the major building block of wood; as in most plants, it makes up between 40% and 50% of the dry mass of timber (Desch and Dinwoodie, 1996) and of plants, as demonstrated in Table 2.1 (Rowell et al., 1997). Glucose ($C_6H_{12}O_6$) is produced in plants and trees by the act of photosynthesis. The glucose units are then transported down to the cambial zone where they bond together linearly to form cellulose. Chemically, cellulose is the polymer of the hexose, ß-D-glucopyranose, with the polymer links being between the fourth and the first carbons on the molecules. This polymer is a crystalline structure (ie, it is made up of repeating units), therefore it is easier to degrade.

The degree of polymerization (DP) of wood cellulose is between 8000 and 10,000, making each cellulose chain approximately 4−5 μm and the molecular weight in the order of 1.5×10^6 (Wilson and White, 1986).

Until recently, it was assumed there were six polymorphic forms of cellulose (O'Sullivan, 1997), these being I, II, III_I, III_{II}, IV_I and IV_{II}. Cellulose I represents the native material present in plants, and it is this polymorph that has been found to be present in two forms, I_α and I_β, respectively (Vanderhart and Atalla, 1984; Sugiyama et al., 1991). Further work has shown that cellulose III_I can be converted to I_β by heating at temperatures in excess of 200°C (Wada, 2002).

Within wood, cellulose molecules over most of their length lay parallel to one another to form a crystalline structure. There have been many attempts to model the crystalline structure of cellulose I; however, it was the model proposed by Gardner and Blackwell (1974) that has gained worldwide acceptance. Gardner and Blackwell proposed an eight-chain structure with all the chains running in the same direction. There are many variants of this model; however, this was the first model proposed.

Both primary and secondary bonding is present in the formation of cellulose I, with the primary, or covalent, bonding located in the glucose rings and in the joining of these rings together. The secondary bonding is comprised of both hydrogen bonds, and Van de Waal forces are present in specific areas. The hydrogen bonds are present within the cellulose molecule and between the molecules, linking them into sheets within a single plane, and Van de Waals forces link the sheets together in the opposite plane.

Table 2.1 Chemical composition of various plant-based fibres (Rowell et al., 1997)

	Cellulose	Hemicellulose	Lignin	Ash	Starch/ Protein/Fat	References
Straw						
Wheat	32.1–48.6	27.1–38.7	5.3–17.0	1.8–6.7		Buranov and Mazza (2008)
Wheat	37.1	23.5	15.8	8.0		Merali et al. (2016)
Flax	53.8	17.1	23.3	3.6		Bray and Peterson (1927)
Barley	37.8	26.3	8.9	8.1		Satpathy et al. (2014)
Corn	44.5	19.7	25.5	1.4	8.9	Yuan et al. (2015)
Rice	30.4–44.0	20.1–32.3	8.6–19.0	6.3–12.0		Buranov and Mazza (2008)
Cane						
Bamboo	41.7–46.0	20.6–24.5	19.6–24.2	1.0–1.8		Cheng et al. (2015)
Grass/Reed						
Miscanthus	31.0–31.5	29.2–35.4	25.3–26.7			Si et al. (2015)
Giant reed	21–42	7–23	8–34	3–8		Faix et al. (1989)
Phragmites communis	44–46	20	22–24	3		Rowell et al. (1997)
Esparto	33–38	27–32	17–19	6–8		Rowell et al. (1997)
Husk						
Wheat	36	18	16		20	Bledzki et al. (2010)
Rye	26	16	13		34	Bledzki et al. (2010)
Oat	32.0–37.3	31.0–36.4	2.3–9.8	4.8–9.3	2.6–7.0	Welch et al. (1983)
Stover						
Corn	31.3–38.6	20.6–28.0	15.0–21.4	6.5–7.1		Buranov and Mazza (2008)

As noted earlier the length of a cellulose molecule is approximately 5 μm or 5000 nm. This length is a great deal larger than the length of the areas of crystallinity, which are approximately 60 nm in length (Desch and Dinwoodie, 1996). This means that a molecule will pass through areas of high crystallinity as well as regions of low crystallinity, in which molecules are only loosely associated with each other. It has been noted (Desch and Dinwoodie, 1996) that the molecules that pass from one area of crystallinity will pass to another and therefore generate a high degree of longitudinal association to form a unit of undefined length known as a microfibril. The degree of crystallinity will vary, but on average, 70% of cellulose in wood is crystalline.

Although cellulose I is produced in nature, it is the cellulose II allomorph that is more thermodynamically stable. Cellulose I allomorphs can be converted to cellulose II as a result of acid regeneration or mercerization, realizing a form that can be more readily hydrolyzed. Cellulose III_I and III_{II} can be produced by ammoniacal treatment of cellulose I and II, respectively (Marrinan and Mann, 1956; Hayashi et al., 1975), whilst these cellulose III allomorphs can be converted to their respective IV allomorphs by heating in glycerol to 206°C (Hess and Kissig, 1941; Gardiner and Sarko, 1985).

2.2.2 Hemicellulose

Hemicellulose, second to cellulose in abundance, differs greatly from cellulose. The molecules are shorter with a DP of between 150 and 200 and are built up of different heteroglycan sugar units, depending upon the species from which they are obtained, ie, hardwood, softwood or agrifibres. As well as glucose, hemicellulose can contain primarily the mannose and galactose, but they can also contain the pentosesxylose and arabinose. The hydroxyl groups in the ring structure can also be replaced by methoxyl and acetoxyl groups. The differing sugars may also be present in their uronic acid forms.

In softwoods the majority of the hemicelluloses are known as Galactoglucomannans; these are one to four polymers of glucose and mannose, in which the mannose predominate, while the galactose units are borne laterally on this main chain.

It has been noted (Wilson and White, 1986) that hemicellulose make up 25−40% of dry wood mass. Typical components of hemicelluloses are a group of compounds called aldoses and may be linked together either in a linear or branched arrangement. Typical components present within hemicelluloses include D-xylose, D-mannose, D-glucose, D-galactose, L-arabinose, L-rhamnose, 4-O-methyl-D-glucuronic acid, D-glucuronic acid and D-galacturonic acid. It is not uncommon for such aldoses to undergo redox reactions, where ring opening and closing occurs, thus changing the stereoconformity. Similarly, some compounds may occur through reactions of other molecules; for example, L-arabinose may be obtained from the decarboxylation of D-galacturonic acid (Crawford and Crawford, 1980).

2.2.3 Phenolics and lignin

Lignin is a highly complex noncrystalline molecule comprised of a large number of phenyl-propane units (Desch and Dinwoodie, 1996). It may be described as a

polymeric material obtained from the enzymatic dehydrogenation of phenylpropane units (syringyl, guaiacyl and *p*-hydroxyphenyl units, respectively, depending on the species in question), which then couple together via aryl ether interunit linkages and carbon−carbon bonds. Unlike cellulose, lignin is a three-dimensional polymer. Unlike cellulose, lignin is not susceptible to hydrolysis; however, other forms of chemical breakdown give a range of products, which have a common carbon skeletal structure. The molecular weight of lignin after it is extracted from wood has been estimated at 1100, which means that it contains approximately 60 of the monomer units; however, this is the extracted size and is undoubtedly larger within the wood (Wilson and White, 1986). The large number of bond types in lignin means that the structure is hard to break down.

About 25% of all the lignin in wood is found in the middle lamella (Dinwoodie, 2000), an intercellular layer that is made of lignin and pectin. The middle lamella is very thin and therefore the concentration of lignin is very high (approximately 70%). The other 75% of lignin is found in the secondary cell wall and is deposited following the completion of the cellulosic frame work. The lignification of the cell wall begins when the middle lamella is about half formed and it begins to extend across the secondary cell wall (Saka and Thomas, 1982).

Lignin composition differs among different plant species and also among different tissues from the same individual plant. The concentration of the three phenyl-propane units vary between the lignin types (botanical origin), as well as with differences in the amount to type of linkages and chemical functional groups (Gabov et al., 2014). The lignin in hardwoods is composed of syringyl and guaicyl units in varying ratios; lignin in softwoods is composed of mostly guaiacyl units (more than 95%) and small amounts of *p*-hydroxyphenyl units, whereas the lignin from agroplants contain all three units (H, G, S) in significant amounts with different ratios, making its structure more complex (del Río et al., 2012). Also, lignin presents different cross-linking degrees and structure rigidity, depending on the type and the substitution degree.

Over the years, there have been a range of methods developed for the extraction of lignin from bio-based materials. The extraction of lignin, typically from hardwoods with aqueous ethanol at high pressures and temperatures is known as the Alcell process or organosolv process, which produces low molecular weight lignin fractions (Aronovsky and Gortner, 1936; Kleinert, 1974; Pye and Lora, 1991; Pan et al., 2006). The acidic depolymerization and fragmentation of lignin is commonly referred to as Klason lignin, first developed by the Swedish scientist Johan Peter Klason in 1893 for the preparation of pure lignin from spruce, through prehydrolysis with sulphuric acid. If, instead of using sulphuric acid, hydrochloric acid was used, the process would be known as the Willstatter method (Horst et al., 2014). Another extraction method was developed by Björkman (1954), the so-called milled wood lignin. For agrifeedstocks, an alternative method using a combination of formic acid and hydrogen peroxide in order to generate peroxyformic acid in situ has been reported (Siegle, 2001); this method is referred to as being similar to the Milox process.

In order to improve the lignin yield, different isolation methods have been proposed, obtaining cellulolytic enzyme lignin (Pew, 1957); enzymatic mild acidolysis lignin, though a procedure which combine enzymatic and mild acidolysis (Wu and

Argyropoulos, 2003); and swollen residual enzyme lignin, obtained by a combined mild alkaline treatment and subsequent in situ enzymatic hydrolysis (Wen et al., 2015).

Significant efforts have been put into assessing methods for using transition metal catalysts for obtaining lignin fractions. A thorough review (Deuss and Barta, 2016) considered chemical pathways for acid or base cleavage, oxidative cleavage and reductive cleavage (via hydrogen gas or silanes, hydrogen gas under neutral conditions or hydrogen transfer from alcohols). These improvements in process methods have been applied into sequential extraction methods as part of the bio-based economy, particularly for second generation liquid biofuels. Since lignin is not fermentable, these improvements have allowed efficient separation not only for the synthesis of pure lignin fractions but for cleaner biofuel production and hence efficient biorefinery concepts (Zhang, 2008).

2.2.4 Terpenes, waxes, acids and alcohols

Due to the biosynthetic pathways of plants, each species is capable of producing its own individual range of chemical components. Many of the fragrances recognizable for wood and plant species are due to the combination of these compounds, often referred to as volatile organic compounds (VOCs). Among the range of compounds that comprise VOCs are terpenes, waxes, acids and alcohols.

Terpenoids are a range of compounds based on isoprene units, a C_5-building unit derived naturally from mevalonic acid. Full details on the biosynthesis of terpenoids can be found in a variety of publications (eg, Breitmaier, 2006). The presence of terpenoids within a plant has been attributed as a protective system against biological attack or stress during growth, with the diverse needs of plant protection being demonstrated by the fact that more than 20,000 terpenoids are known and classified. They are produced in cellular organelles, to be stored within a structure until needed. The degree of variation is a result of the polymeric properties of the C_5 units. Typically, monoterperoids (C_{10} compounds) and sesquiterpenoids (C_{15} compounds) are known as essential oils, whilst diterpenes (C_{20} compounds), because of their higher molecular weights, are known as resins. The triterpenoids (C_{30} compounds) are typically attributed to steroids, whilst larger compounds such as tetraterpenoids (C_{40}) and polyterpenoids ($\geq C_{50}$) tend to be less common polymeric products.

In order to maintain an external protective layer, plants use cuticles. These are lipophilic structures deposited onto the outer side of epidermal cell walls. Two major components of plant cuticles are recognized through their levels of solubility: cuticular wax, comprising lipophilic components soluble in organic solvents, and cutin, which comprises nonextractable components. The waxes present on plants and tree materials represent a water-repellent barrier to aid in the bioprotection of the plant. Depending on its position within a plant, there are cuticular waxes formed on the cutin (leaves, fruits and primary shoots), suberin (secondary shoots and roots), and other associated waxes. Cuticular wax contains a wide range of hydrocarbons from fatty acids, including medium to long chain alkanes such as undecane and eicosane. Alternative biochemical pathways allow for the reduction of fatty acids to alcohols, aldehydes and ketones, as well as esters from the reaction of aldehydes

and alcohols (Samuels et al., 2008). Cuticular waxes also include pentacyclic triterpenoids and a limited amount of aromatic components. The cuticular waxes can also include hydroxy fatty acids, hydroxy fatty acid methylesters and alkanols, all with alkyl chains up to C_{32} (Racovita et al., 2015). A cutin biopolymer is formed by cross-linking hydroxylated fatty acids (often C_{16} and C_{18}) via intermolecular ester bonds, leading to a three-dimensional structure. Suberin consists of a polyaliphatic component and a polyaromatic component. The polyaliphatic components have similar biosynthetic pathways as the cuticular wax compounds, whilst the polyaromatic compounds have similar metabolic pathways to the aromatic moieties in lignin.

2.2.5 Proteins

Mature wood (both hard and soft types) contains only small amounts of proteins (up to max 0.5% of dry matter). These are of the elastin type and are important for cell wall growth. They have negligible effects on the mechanical properties of mature wood (Bao et al., 1992).

'Lignocellulosic' materials (fibres and fibre bundles/chips) sourced from annual crops contain more protein than wood but again the proteins have little influence on fibre/chip mechanical properties. An example is cereal straws such as wheat straw. In wheat straw dry matter, there is c. 4% protein, which is mainly cuticular protein located on the outer leaf parts and outer surface of the stem cells (Sun, 2010). This has little influence on fibre or fibre bundle strength and/or mechanical properties but can, when coated with cuticular wax (which it interfaces to the more hydrophilic lignocellulose components), inhibit gluing with water-based adhesives (eg, urea-formaldehyde, etc.) and contribute to poor bonding in straw-based chips and fibreboards. This can be rectified by switching to other binders (eg, PMDI type), which are more hydrophobic in nature.

Bast fibres, such as those derived from hemp and flax, contain less than 2% crude protein (Crônier et al., 2005), and their strengths and mechanical properties are mainly derived from cellulose.

There are of course a whole range of natural fibres that are of high (>90%) protein content (Lilholt and Lawther, 2000), whose mechanical properties are entirely due to the properties of constituent proteins, but these are outside of the range of this chapter.

2.2.6 Inorganic material

The inorganic content of natural fibres is usually defined only as silica; these levels are often determined by thermal degradative processes. A range of metallic species may also be found in low concentrations, often linked to local growing conditions. Hence certain species, such as giant reed (*Arundo donax* L.), have been used for the remediation of contaminated lands and water courses (Papazoglou, 2007). Among other species that have attracted research are various members of the cress family (McGrath et al., 2006).

2.3 Major differences in chemical composition of fibres

Natural fibres can be classified into a number of categories based on their source, with the first separation based on whether the fibre is plant or animal (protein) based. Plant-based fibres are further classified by the type of plant and location of the fibre as follows: wood, seed (eg, cotton), fruit (eg, Coir), bast (eg, flax and hemp), leaf (eg, sisal), stalk (eg, wheat and barley) and cane, grass or reed fibres (eg, bamboo, bagasse) (Bismark et al., 2005).

2.3.1 Plant-based fibres

Because a wide variety of plants can be used as sources of plant-based fibres, it is not surprising that the obtained fibres have different chemical compositions and properties. Some examples of differences between fibre types and the numerical values of some chemical compositions are shown in Table 2.1, which is a revision of a previously published table (Rowell, 1991).

2.3.2 Wood-based fibres

Wood-based fibres are derived from trees with a lignin-rich, woody trunk that is formed by secondary growth. Wood fibres are generally richer in lignin than nonwood fibres. There are physical and chemical differences between the wood fibres from softwood (coniferous) and hardwood (deciduous) trees; for example, softwood fibres have an average length of 3−3.6 mm, while for hardwoods the average length is only 0.9−1.5 mm long. Differences are identified in the chemical composition too, with softwood hemicelluloses having a higher proportion of galactoglucomannans (20−25%) compared to hardwoods (2−5%). Hardwoods subsequently have a higher proportion of arabinoxylans (15−30%) than softwoods (5−10%). Differences in the lignin composition are also apparent with softwoods having a majority of guaiacyl units from *trans*-coniferyl alcohol, while hardwoods also have syringyl units, which are not found in softwoods.

2.3.3 Bast fibres

Bast fibres may be defined as those obtained from the outer cell layers of the stems of various plants. Among the main plants used for the supply of bast fibres are flax, jute, hemp, ramie and kenaf. Since these are annual crops, there is a significant supply of materials, and they are gaining increasing interest in a variety of nonwood composite manufacturing processes. Bast fibres are comprised of a bundle of tube-like cell walls. Each cell wall contains primary, secondary S1, S2 and S3 layers (Burgert and Dunlop, 2011). The fibres can be much longer than wood fibres with lengths of 20 mm for hemp for example. These types of fibres have a lower lignin content than wood fibres; consequently, the cellulose content is higher (as shown in Table 2.1). The cellulose in bast fibres also tends to be more crystalline (80−90%) than that of wood fibres (50−70%) (Madsen and Gamstedt, 2013).

2.3.4 Stalk fibres

The straw of annual crops such as rice, wheat and barley produces fibres of 0.5−2.5 mm in length that are also low in lignin and have a cellulose level broadly similar to wood. The crystallinity of straw fibre is also similar to that of wood at 55−65%. The hemicelluloses of straws consist mainly of arabino-xylan units. Cereal straws can have a high silica content that can make processing more complicated.

2.3.5 Cane, grass and reed fibres

Canes such as sugar cane (bagasse) or bamboo, grasses such as Esparto and reeds are also common fibre sources. The canes and reeds have lignin contents higher than bast or straw fibres and, in the case of bamboo, as high as wood fibres. The lignin of these fibres contains *p*-hydroxyphenyl units, from *trans-p*-coumaryl alcohol, which is a type not found in wood fibres to any great extent. They also contain guaiacyl and syringyl units.

2.3.6 Leaf

Leaf fibre (also known as hard fibre) is normally obtained by scraping away the non-fibrous material, and the fibre produced can be coarser than other fibres. When obtained from sources such as sisal (agave) and abaca, some of the longest fibre lengths can be obtained (1−4 m). Leaf fibre can have cellulose contents as high as 70% (Smole et al., 2013), though they also have low lignin contents compared to wood. Due to their length, the properties of the fibres may change over the course of the fibre (Smole et al., 2013). However, pineapple and banana leaves give fibres of much shorter length that are also high in cellulose and low in lignin content.

2.3.7 Seed and fruit

One of the most ubiquitous of plants fibres in use is cotton derived from the seed of plants of the cotton (*Gossypium*) family. Cotton has a three-walled structure consisting of a wax and pectin cuticle, a crystalline cellulose primary wall, a three-layer cellulosic secondary wall and a tertiary wall surrounding the lumen. The fibre produced is almost pure cellulose at 85−91% with a crystallinity of 60−65% (Ioelovich and Leykin, 2008). In contrast, the fibre derived from the husk of the coconut has a very high lignin content at 40−45% (Bismark et al., 2005).

2.3.8 Protein-based fibres

Wool is the generic term for the fibre obtained from sheep (*Ovisaries*) as well as other animals such as mohair from goats (*Capra aegagrushircus*), qiviut from muskoxen (*Ovibosmoschatus*) and angora from rabbits (*Leporidae* spp.) (Braaten, 2005). Wool differs from hair in several ways: it is crimped, it is elastic in nature and it grows in staples (clusters) (D'Arcy, 1990). The term wool has also been used to describe other

materials that have a similar gross appearance as sheep's wool, and these include glass wool, mineral wool and cotton wool. However, the similarity ends at their gross appearance, and they will not be discussed further here.

The composition of wool is complex and has been studied for some time. Wool is composed of cortical cells, surrounded by a cuticular made up of a scale-like structure (Bones and Sikorski, 1967; Rogers, 1959). Each cortical cell contains several macrofibrils, which are a collection of microfibrils surrounded by a sulphur-rich cementing matrix. Within the microfibrils, there are two types of cortical cells: *ortho* and *para*. *Para*-cortical cells have a more uniform/fused keratin structure and are more resistant to chemical attack and swelling than the *ortho*-cortex, which explains why wool crimps. Different wool types will vary in their ability to crimp, which is attributed to the difference between cortical cells: finer wool fibres have two distinct halves in which the *ortho*- and *para*-cortical cells are distributed. When the fibre is exposed to moisture, the cortical cells swell at different rates and to different degrees, making the fibre bend.

The whole bundle of macrofibrils is encapsulated by the cuticle, which unlike the cortex is amorphous but is composed of cells of similar interlocking extensions as the cortex. The outermost membrane on the fibre is the epicuticle, about 13 nm thick (Swift and Smith, 2001) and resistant to chemical attack, with 12% of its protein component being keratin (Negri et al., 1993; Ward et al., 1993). Keratin is a fibrous protein that maintains its rigid structure via disulphide bridges, characteristic of the amino acid cystine, in addition to intra- and intermolecular hydrogen bonds. The epicuticle is highly insoluble due to isodipeptide cross-links of 1-amino-(γ-glutamyl)-lysine (Folk, 1977). It is longitudinally striated with ridges about 350 nm long, which face away from the root; this helps dirt and water droplets to drop away in one direction. The striation is what gives wool fibres a great frictional force and allows felting. Below the epicuticle is the A-layer, 35% of it being cystine (Negri et al., 1993). The underlying exocuticle is stabilized by disulphide bonds, which indicate the presence of keratin. In contrast, the layer below that, the endocuticle, does not contain keratin. In between cuticle cells is a cell membrane complex, which in turn is divided into β and δ layers.

In the case of raw wool, the fibre is covered by about a 0.9 nm thick layer of lipids that comprises one-fourth of the epicuticle (Negri et al., 1993). These lipids, which are mainly 18-methyleicosanoic acid (18-MEA), are covalently bonded to the keratin protein (Evans et al., 1985). Evans et al. (1985) proposed that the bond occurs as a thioester linkage with the amino acid cysteine; the amino acid cysteine is not to be confused with cystine, the latter being formed by the oxidation of two cysteine molecules. Breakspear et al. (2005) conclude that the lipid layer is homogenous and not disordered. However, this explanation does not account for two observations: the good stability of the thioester bond (Bizzozero, 1995) and that the surface is solid and ionizable when present in an aqueous solution (Evans et al., 2002). To overcome these observations, Swift and Smith (2001) hypothesize that the lipid layer is disordered and dynamic, changing its position when the surrounding environment changes from wet to dry; when placed in a hydrophobic environment the hydrophobic chains of the lipid layer face outwards but 'reorients itself upon exposure to an aqueous

environment so that the protein (amide) and polar side chain groups of the proteolipid are oriented outwards' (Maxwell and Hudson, 2005).

These lipids are removed by extraction with potassium *tert*-butoxide in *tert*-butanol or methanoic potassium hydroxide solutions (Ward et al., 1993). Five minutes of treatment oxidizes the surface of cysteine and thus decreases the fatty acid content by about half and significantly increases the wettability of the fibres. It is interesting to note that similar treatments are used to scour wool (clean the wool and remove the natural coatings). However, there are claims that this layer cannot be physically or chemically removed uniformly and without damaging the underlying protein, suggesting that it is an integral part of the structure (Maxwell and Huson, 2005). On the other hand, Swift and Smith (2001) observed 'with no alteration to the visual appearance of the surface of the fibres as viewed by SEM and SPM' after successive treatments, but agree that the removal is 'patchy'. That being said, the surface structure of wool is complex, and the chemical functionalities are not all fully understood.

Lanolin, whose name originates from the Latin 'lana' (wool) and 'oleum' (oil) is a combination of unattached sterols, sterol esters, and other lipids secreted by sebaceous glands that coat wool fibres as they grow.

2.4 Effects of modification on natural fibre composition

The inherent properties of many natural materials are in of themselves valuable characteristics useful in modern products. Conversely, however, some of these properties, such as poor fibre−polymer compatibility and reduction in physical properties with moisture sorption, are disadvantageous when developing materials. In order to alleviate these disadvantages, research has been targeted at altering these properties via modification of the material. These modification methods can be separated into the broad categories of chemical, thermal or enzymatic modifications.

2.4.1 Chemical modification

Chemical modification of lignocellulosic materials has been mainly aimed at wood, and there has been considerable research over a number of years that has been previously reviewed (Rowell, 1977; Hill, 2006, 2011). Most chemical modification methods of timber have been utilized in reactions with the hydroxyl (−OH) groups of the wood cell wall polymers. This has the potential to change the characteristics of the polymers and may impart beneficial properties to the wood itself. The chemical wood modification method that has seen the most research is acetylation following a reaction with acetic anhydride. Acetylation of wood has been shown to have beneficial effects on durability, dimensional stability and some mechanical properties of the timber (Rowell, 1984; Hill and Jones, 1996; Dinwoodie, 2000). This process has been commercialized by Accsys Technologies to produce acetylated Radiata Pine (*Pinus radiata*), which is marketed as Accoya. Acetylation may also be carried out using other reagents, including isopropenyl acetate (Nagarajappa and Pandey, 2016), vinyl acetate

(Jebrane et al., 2011), ketene gas (Karlsons et al., 1976b) and diketene liquid (Karlsons et al., 1976a). Other chemical modifications have been researched, eg, using noncyclic and cyclic anhydrides, acid chlorides isocyanates and aldehydes (reviewed in Hill, 2006).

An alternative to cell wall modification is a modification of the surface of the material. These methods generally aim to improve compatibility with other materials or to improve UV stability and moisture interactions. Indeed when moving away from solid wood to the use of other natural fibres, it is surface treatments that appear to be the most used. This is especially the case when the fibres are being used in fibre reinforced composites (John and Anandjiwala, 2008). There are a number of chemical modifications used for this purpose, and these are briefly discussed in the next section.

2.4.1.1 Mercerization *(alkali treatment)*

Alkaline treatment is one of the more common methods employed. Initially this treatment breaks down the fibre bundles of plant fibres to release the individual fibres. This results in smaller particles with a higher aspect ratio and a rougher topography that enhances fibre/matrix interactions (Kalia et al., 2009). The process also affects the chemical nature of the fibre, removing hemicelluloses, pectins and wax. The cellulose of the cell wall causes an apparent increase in the degree of crystallinity at lower concentrations and at higher concentrations. Both conditions can have aid fibre/matrix interactions dependent on the nature of the matrix (Mwaikambo and Ansell, 2001; Ray et al., 2009; Mokaloba and Batane, 2014; Pickering et al., 2016). However, at high alkali concentrations, the damage done to the fibre can exceed any advantage gained from the method.

2.4.1.2 *Acetylation*

Acetylation has also been used with nonwood fibres such as sisal (Mishra et al., 2003; Tserki et al., 2005; Mokolaba and Batane, 2014). The result is similar to solid wood with increased stability and durability.

2.4.1.3 *Graft copolymerization*

Active monomers can be grafted on the polymeric structure of the fibres, with examples including:

- Benzyl chloride can improve thermal stability of the resultant composite (Joseph et al., 2000).
- Maleic anhydride can reduce moisture uptake of sisal fibres (Mishra et al., 2000). Improved tensile properties for jute have also been reported (Bera et al., 2010).
- Acrylonitrile reduced moisture uptake and improved mechanical properties of sisal fibres when used at low concentrations (Mishra et al., 2001), although these improvements were not observed using acrylonitrile with oil palm fibre (Sreekala et al., 2002).

2.4.1.4 Coupling agents

Silanes have been used as coupling agents to increase the cross-linking between fibres. The most commonly reported silanes used are amino, methacryl, glycidoxy and alkyl silanes (Pickering et al., 2016). These silanes are able to interact with hydrophilic groups on the fibre and with hydrophobic groups in the matrix. Increases in fibre hydrophobicity and some strength increases have been reported (Pickering et al., 2003; Rachini et al., 2012).

2.4.1.5 Permanganate

Potassium permanganate/acetone has been used to treat fibres and improve the fibre/matrix compatibility (Sreekala et al., 2000).

2.4.1.6 Nanocellulose treatment

A novel approach of modifying hemp fibres with nanocellulose has been investigated (Dai and Fan, 2013), which led to increased interfacial properties and an increase in the modulus and other mechanical properties of the hemp fibre.

2.4.2 Thermal modification

As with chemical modification, the idea behind thermal modification is to alter the internal chemical composition of the material. Instead of adding reagents capable of interacting with reactive sites (as in chemical modification), thermal modification uses the internal reactivity of a material and the removal of active sites. In order to prevent oxidative combustion of materials, thermal modifications are undertaken under inert conditions (typically nitrogen, in vacuo, or under steam). Among the key reactions in thermal modification are the conversions of the polysaccharides present within the hemicelluloses, often following similar pathways to those observed in the caramelization of sugars (hence the increase in colour of the thermally modified materials).

The concept of thermally modifying wood has gained popularity due to the increased dimensional stability and inferred natural durability compared to the untreated material. There have been numerous examples of different species undergoing thermal modification, as shown in Table 2.2.

As a result of the wide range of scientific study in this area, there have been several commercial processes. Such commercial activity is not new. Among the first noted examples of thermally modified wood was Lignostone (Kollman, 1936), closely followed by Staypack (Seborg et al., 1945) and Staybwood (Stamm et al., 1946). After a period of approximately 40 years, commercial activity has re-emerged across Europe, with several companies now producing thermally modified wood (Esteves and Pereira, 2009).

Work has not been solely concerned with solid wood. There have been investigations into heat-treating rice straw, willow (*Salix alba*), cymbopogon grass and pine

Table 2.2 Examples of thermal modifications of various wood and plant species

Species	Thermal treatment applied	References
Oak (*Quercus petraea* Lieb.)	$T = 130, 180, 230°C$; $t = 2, 8$ h	Akyildiz and Ates (2008)
Oak (*Quercus robur*)	$T = 160°C$; steam	Wikberg and Maunu (2004)
	$T = 160, 180, 210, 240°C$	Barcík et al. (2015a,b)
Silver oak (*Grevillea robusta*)	$T = 210–240°C$; $t = 1–8$ h	Srinivas and Pandey (2012)
Beech (*Fagus sylvatica* L.)	$T = 180, 200, 220°C$; $t = 4$ h	Bächle et al. (2010)
	$T = 160, 190°C$	Boruszewski et al. (2011)
	$T = 125–130°C$; $t = 6.5$ h; steam	Dzurenda (2013)
	$T = 170, 180, 190, 212°C$; $t = 2$ h	Kol and Sefil (2011)
Beech (*Fagus moesica* C.)	$T = 170, 190, 210°C$; $t = 4$ h	Todorović et al. (2015)
Beech (*Fagus Orientalis*)	$T = 150, 160, 170°C$; $t = 1, 3, 5, 7$ h	Charani et al. (2007)
	$T = 130, 150, 180, 200°C$; $t = 2, 6, 10$ h	Yildiz et al. (2005)
Aspen (*Populus tremula*)	$T = 195°C$	Wikberg and Maunu (2004)
	$T = 170°C$; $t = 1$ h, pressure = 0.6 MPa; water vapour medium	Cirule et al. (2016)
	$T = 160–170°C$; $t = 1, 3$ h; pressure = 6.5–7.6 bar; steam	Grinins et al. (2013)
Poplar (*Populus cathayaha*)	$T = 180–220°C$; $t = 4$ h	Ling et al. (2016)
	$T = 160, 180, 200, 220, 240°C$; $t = 4$ h	Wang et al. (2015)
Lime (*Tilia cordata*)	$T = 140°C$; RH = 10%; $t = 0–504$ h	Popescu et al. (2013a,b), Popescu and Popescu (2013)
Birch (*Betula pendula*)	$T = 195°C$	Wikberg and Maunu (2004)
	$T = 160, 180, 210, 240°C$	Barcík et al. (2015a)
	$T = 140, 160, 180°C$; $t = 1$ h	Biziks et al. (2013)
	$T = 160–170°C$; $t = 1, 3$ h; pressure = 6.5–7.6 bar; steam	Grinins et al. (2013)

Birch (*Betula pubescens* Ehrh.)	$T = 160, 190°C$	Boruszewski et al. (2011)
Pear (*Pyrus elaeagnifolia* Pall.)	$T = 160, 180, 200°C$; $t = 3, 5, 7$ h	Gunduz et al. (2009)
Hazelnut (*Corylus colurna* L.)	$T = 120, 150, 180°C$; $t = 2, 6, 10$ h	Korkut and Hiziroglu (2009)
Chestnut (*Castanea sativa* Mill.)	$T = 130, 180, 230°C$; $t = 2, 8$ h	Akyildiz and Ates (2008)
	$T = 160, 180°C$; $t = 2, 4$ h	Korkut et al. (2012)
Alder (*Alnus glutinosa* L.)	$T = 150, 180, 200°C$; $t = 2, 6, 10$ h	Yildiz et al. (2011)
Grey alder (*Alnus incana*)	$T = 160–170°C$; $t = 1, 3$ h; pressure = 6.5–7.6 bar; steam	Grinins et al. (2013)
Red-bud maple (*Acer trautvetteri* Medw.)	$T = 120, 150, 180°C$; $t = 2, 6, 10$ h	Korkut et al. (2008a,b), Korkut and Guller (2008)
Narrow-leaved ash (*Fraxinus angustifolia* Vahl.)	$T = 160, 180°C$; $t = 2, 4$ h	Korkut et al. (2012)
	$T = 140, 180, 200, 220°C$; $t = 2, 4, 6$ h; steam	Yalcin and Sahin (2015)
Paulownia (*Paulownia elongata*)	$T = 150, 170°C$; pressure = 20, 22.5 bar; $t = 45$ min	Candan et al. (2013)
	$T = 160, 180, 200°C$; $t = 3, 5, 7$ h	Kaygin et al. (2009)
Gympie messmate (*Eucaliptus cloeziana*)	$T = 180, 200, 220, 240°C$; $t = 4$ h	de Cademartori et al. (2013a)
Eucalyptus grandis	$T = 180, 200, 220, 240°C$; $t = 4, 8$ h	de Cademartori et al. (2013b)
Rubberwood (*Hevea brasiliensis*)	$T = 210–240°C$; $t = 1–8$ h	Srinivas and Pandey (2012)
Acacia hybrid (*Acacia mangium* × *auriculiformis*) sapwood	$T = 210–230°C$; $t = 2–6$ h; nitrogen	Tuong and Li (2011)
Western red cedar (*Thuja plicata*)	$T = 220°C$; $t = 1, 2$ h	Awoyemi and Jones (2011)
Norway spruce (*Picea abies* L.)	$T = 200°C$; $t = 5, 30, 60$ min	Follrich et al. (2006)
	$T = 113, 134, 158, 187, 221, 237, 253, 271°C$; $t = 90$ min	Kačíková et al. (2013)
	RH = 50, 65, 80, 95%; $T = 200°C$; $t = 2, 4, 8, 10, 24$ h; $T = 100, 150°C$; $t = 24$ h	Bekhta and Niemz (2005)

Continued

Table 2.2 Continued

Species	Thermal treatment applied	References
	$T = 195°C$	Wikberg and Maunu (2004)
	$T = 180, 200, 220°C$; $t = 4$ h	Bächle et al. (2010)
	TERMOVUOTO® technology $T = 160, 220°C$; vacuum	Allegretti et al. (2012)
	$T = 160–260°C$; $t = 2–8$ h	Kotilainen et al. (2000)
Black spruce (*Picea mariana*)	$T = 190, 200, 210°C$	Lekounougou and Kocaefe (2014)
Fir (*Abies alba* Mill.)	TERMOVUOTO® technology $T = 160, 220°C$; vacuum	Allegretti et al. (2012)
	$T = 170, 180, 190, 212°C$; $t = 2$ h	Kol and Sefil (2011)
Calabrian pine (*Pinus brutia* Ten.)	$T = 130, 180, 230°C$; $t = 2, 8$ h	Ates et al. (2009); Akyildiz and Ates (2008)
Black pine (*Pinus nigra* Arnold.)	$T = 130, 180, 230°C$; $t = 2, 8$ h	Akyildiz and Ates (2008)
Scots pine (*Pinus sylvestris* L.)	$T = 120, 150, 180°C$; $t = 2, 6, 10$ h	Korkut et al. (2008a,b)
	$T = 180, 200, 240°C$	Kekkonen et al. (2010)
	$T = 160–260°C$; $t = 2–8$ h;	Kotilainen et al. (2000)
	$T = 160, 180, 210, 240°C$	Barcík et al. (2015a)
Maritime pine (*Pinus pinaster*)	$T = 170–200°C$; $t = 2–24$ h	Esteves et al. (2008)
Oil palm mesocarp fibre	$T = 190–230°C$; $t = 1, 2, 3$ h	Nordin et al. (2013)
Bamboo (*Dendrocalamus barbatus* and *Dendrocalamus asper*)	$T = 130, 180°C$; $t = 2, 5$ h	Nguyen et al. (2012)
	$T = 130, 220°C$; $t = 2, 5$ h	Bremer et al. (2013)
Bamboo (*Dendrocalamus asper*)	$T = 140–200°C$; $t = 30–120$ min − coconut oil medium	Manalo and Garcia (2012)

needles (Negi and Chawla, 1993) over a range of temperatures and treatment times. These treated fibres were then used in the manufacture of fibreboard.

Earlier investigations (Chawla and Sharma, 1972) suggested that during heat treatment, crosslinking between polysaccharide chains could occur. This would exert a stabilizing effect on the sample and increase its resistance to swelling and water absorption. In addition, some of the hydrolysis and/or oxidation products produced during thermal treatment may recombine with some of the partly degraded compounds present. Once temperatures exceed 160°C, sufficient flow of lignin occurred to produce some blocking of the pores, further improving the water resistivity. This flow in the lignin also accompanied a slight increase in the crystallinity of cellulose. It was observed (Negi and Chawla, 1993) that results, as would be expected, followed those of solid wood, with the improvement in strength following the order willow > rice straw > cymbopogon grass > pine needles on testing relevant fibreboards. Thus the use of lower-temperature treatments was found to be more favourable for nonwood lignocellulose fibreboards with respect to the dry mechanical strength properties. Typically, it was found that increases in MOR and tensile strength were in the ranges 19−42% and 23−28%, respectively.

2.4.3 Enzymatic modification and oxidative and hydrothermal modification

Whilst the main theme of the uses of enzymes, oxidative and hydrothermal processes for natural fibres are mainly reported in the literature to date in second generation bioprocesses such as the production of bioethanol, base chemicals or saccharific products. There are a few examples of how natural biochemical processes can be applied in an advantageous way for enhancing the properties of natural materials.

Bio-based materials in their natural environment are affected by the presence of enzymes into activating certain processes, whether it is biochemical transformations for the benefit of the plant or as a direct result of degradative processes. The interactions of natural fibres either within their natural environment or in a secondary (as in the case of composite materials) environment require varying degrees of mechanical entanglement and covalent cross-linking. A method for increasing the degree of bonding, particularly through auto-adhesion is the use of oxidoreductases. These enzymatic treatments, such as the use of laccase and peroxidase, have been used to activate the surfaces of fibres in composite manufacture for several years (Felby et al., 2002), whereby the enzymes activate phenoxy radicals in the plant cell wall, specifically within lignin components. The use of a range of different enzymatic treatments (laccase, pectinases and xylanases) have been shown to improve the separation of alfa (*Stipa tenacissima* L.) fibres from leaves (Hanana et al., 2015), providing high-quality fibres suitable for use within the composite materials.

The biodegradative process can prove beneficial in the treatment of refractory wood species. Work during the 1990s focused on the use of either wood colonizing moulds such as *Trichoderma* or weakly degradative *basidiomycetes* fungi (Messner et al., 1999). The resulting materials were found to be more susceptible to a range of

treatments to further enhance the inferred durability of the refractory species under investigation (Messner et al., 2003).

2.5 Analysis of chemical components

Chemical composition of the components from wood or natural fibres varies from species to species and within different parts of the same species. Moreover, after different modification procedures, the chemical composition is changed considerably. There are several classes of methods through which one can evaluate the chemical composition of the materials before or after their modification.

2.5.1 Extraction and isolation methods

The classical methods of chemical wood and natural fibres analysis include the determination of the quantity of the components by isolating, purifying and quantifying them by weight: holocellulose (cellulose and hemicelluloses), lignin, extractives and ash. In a wet chemical analysis, the various components need to be separated, although there are serious difficulties in achieving selective isolation. There is an array of classical wet-chemical procedures for these purposes, which in some cases have been officially standardized (Browning, 1967; Łucejko et al., 2012).

Several different solvents (water, toluene or ethanol, or combinations of them, different ethers or sodium hydroxide) may be used for the extraction treatments in order to obtain fractions of different soluble solvents *extractive compounds*. The extractives are classified by the solvent used to extract them: for example, water-soluble or toluene ethanol-soluble or ether-soluble extractives.

The pretreatment and dissolution of lignocellulosic biomass with various types of solvents is followed by fractionation into its major components.

Hemicellulose isolation involves alkaline hydrolysis of ester bonds. A gradient elution at varying alkali concentrations can be used for the fractionation of the hemicelluloses from wood, followed by precipitation from the alkaline solution by acidification (using acetic acid). Further treatment of the neutralized solution with a neutral organic solvent (like ethyl alcohol) results in a more complete precipitation (Rowell et al., 2005). The extraction of hemicelluloses from the annual plants is easier than that of wood xylan due to the lower amounts and different structure of lignin. However, different hemicelluloses exhibit different solubility properties. This forces us to use specially designed separation processes, depending on the particular wood or natural fibres we have (Gabrielii et al., 2000). More recently, the ultrasonic treatment is widely used for the processing of plant materials, especially to extract low molecular substances. It has been reported to improve pectin technology and to increase the amount of xylans from corn hulls and cobs without changing the structural and molecular properties (Sun and Tomkinson, 2002).

Traditionally, *cellulose* is extracted from wood through the Kraft pulping process, which involves the semichemical degradation of the lignin/hemicellulose matrix by treatment with solutions of sodium hydroxide and sodium sulfide at high temperatures

and pressures. Another extraction procedure is the nitration isolation that attempts to maximize the yield while minimizing the depolymerization of the cellulose. Other methods for cellulose extraction include modifications of the Jayme-Wise (Loader et al., 1997), Brendel (Brendel et al., 2000) and diglyme-HCl methods (Macfarlane et al., 1999). The last method involves a single processing step that removes most extractives, hemicellulose and lignin, takes less than 24 h to complete and does not require specialized glassware (Cullen and Macfarlane, 2005).

Lignin extraction from lignocellulosic biomass involves several methods. Klason lignin is obtained after hydrolyzing the polysaccharides with sulphuric acid; it is highly condensed and does not truly represent the lignin in its native state in the wood. Björkman (1954) has a major contribution in advancing the extraction of lignin using solvents and a vibratory ball mill. This technique has been widely studied and improvised with other methods such as enzyme treatments and enzymatic hydrolysis, focussing on obtaining a higher yield and less degradation of lignin content (Wu and Argyropoulos, 2003). Other common methods used to extract lignin from wood generally involve the use of alkaline solutions (eg, soda and alkali hydrogen peroxide) and organic solvent (eg, alcohols and organic acids) treatments.

A new approach is the extraction of lignin by dissolution in ionic liquids. It was reported that it was possible to extract lignin from the raw material via the ionic liquids dissolution technique due to the destruction of the cell wall structure, cellulose crystallinity and cellulose sheathing with the hemicelluloses−lignin network (Lan et al., 2011; Mohtar et al., 2015).

Subcritical water (pressurized below its critical point) can be also involved in lignin extraction methods. These physical−chemical modifications enable water to easily solubilize hydrophobic chemical moieties, such as lignin or hydrophobic compounds. Subcritical water has already been successfully applied to agricultural biomass to obtain phenolic antioxidants or phenol-formaldehyde adhesives. Both organic solvents and catalysts are often mixed with subcritical water in order to enhance extraction yields (Savy et al., 2015; Qu et al., 2015).

One of the drawbacks of these procedures is the partial loss of material; the overall determined amount of wood components, expressed in relative terms and referring to the oven-dry material, generally does not reach 100%. Extensive chemical modifications are required in order to obtain soluble fractions of the various components, and consequently the results appear method-dependent to some extent. Moreover, wet chemical treatments are reagent and time-consuming and require substantial amounts of samples (Łucejko et al., 2012).

2.5.2 Chromatographic analysis

Several chromatographic techniques may be involved in the wood and natural fibres analysis, namely: gas chromatography−mass spectrometry (GC−MS), gas chromatography-flame ionization detection, liquid-phase chromatography−mass spectrometry, multidimensional liquid chromatography, multidimensional gas chromatography or high performance liquid chromatography. Sample preparation, especially for complex samples containing a large number of components, is the crucial

first step in the chromatographic analysis (Romanik et al., 2007). The samples are degraded to their constituent building blocks, and the resulting products are further analyzed. For example, acid hydrolysis has been used to estimate the sugar components and content of uronic acids. Indirectly, it may be used to derive information about the composition of the original polymer of hemicelluloses or for the evaluation of the chemical composition of extractives in thermally modified wood. Alkaline nitrobenzene oxidation has been used to estimate the extent of uncondensed units in lignins based on the yield of vanillin, syringaldehyde and *p*-hydroxybenzaldehyde, resulting from the three constitutive monomeric lignin units guaiacyl, syringyl and *p*-hydroxyphenyl, respectively (Sun and Tomkinson, 2002). The separation and quantitation of hydrolyzed carbohydrate components of woods and wood pulps by high performance liquid chromatography is fast and efficient. The carbohydrate moieties in the lignin and hemicellulose fractions can also be determined by high performance anion exchange chromatography (HPAEC).

The most common and fast method is the coupling of the GC and GC−MS with analytical pyrolysis or thermodesorption. These hyphenated techniques represent promising approaches for obtaining quantitative information on the chemical composition of wood or/and natural fibres, avoiding any pretreatment by allowing the online thermal scission of the macromolecule. Through pyrolysis or thermodesorption the macromolecules of wood or natural fibres are fragmented (Faix et al., 1991; Nonier et al., 2006; Candelier et al., 2011), and the pool of fragments observed provides a fingerprint that characterizes the sample chemical composition in terms of both fragment nature and relative distribution. Analytical pyrolysis and thermodesorption techniques have been proven to be very useful for gaining information on the structure of lignocellulosic polymers including wood, cellulose, lignin isolated from softwoods, hardwoods and grasses (Yokoi et al., 1999; Nonier et al., 2006), as well as residual lignin from paper pulping (Galletti and Bocchini, 1995) or to give information on the particular treatment intensity.

Inverse gas chromatography (IGC) is a useful technique for providing information on the surface thermodynamic characteristics of particles including surface free energy, acid−base interactions, enthalpy and entropy. All these aspects are important when it is necessary to obtain specified properties of wood or wood-based products, which strongly depend on the intermolecular forces and binding energies between the constituents. The operation of this technique is similar to gas chromatography. While in conventional gas chromatography the sample (mobile phase) is injected into a specific column (stationary phase) and the sample components are separated and quantified, in inverse gas chromatography the column is typically packed with the solid sample under investigation, and a single gas (vapour) is injected into the column. This technique is based on the physical adsorption of well-known probes by the sample's solid surface. The time it takes a known gas to pass through the IGC column relative to a reference gas is the parameter used in determining the free energy, enthalpy, entropy of adsorption and the acid−base surface properties. Cellulose and lignocellulosic materials have been intensively studied using IGC, because of the importance of their physicochemical surface properties in the context of papermaking,

textile area and, particularly, in the production of composites with polymeric matrices or for gluability and coatability of the solid products (Gamelas, 2013).

2.5.3 Spectroscopic analysis

Spectroscopic methods, such as Fourier transform infrared spectroscopy (FTIR), near infrared spectroscopy (NIR), Raman spectroscopy (Raman), X-ray photoelectron spectroscopy (XPS), X-ray diffraction and nuclear magnetic resonance (NMR) spectroscopy, are widely used to analyze the chemical composition of the wood and natural fibres by measuring their functional groups and chemical bonds. These methods are fast and require little or no sample preparation, as they are more convenient than most conventional chemical methods used for biomass characterization. Besides, since there is no degradative chemical treatment used during analysis, the information gained is more representative of the chemical structures in the original compound.

The infrared (IR) domain consists of three regions according to wavelength range: near infrared (780−2500 nm or 12,800−4000 cm^{-1}), mid-infrared (2500−25,000 nm or 4000−400 cm^{-1}) and far-infrared (25,000−1,000,000 nm or 400−10 cm^{-1}). Upon an interaction of the IR radiation with an oscillating dipole moment associated with a vibrating bond, the absorption of the radiation corresponds to a change of the dipole moment. Generally, different functional groups correspond to different components of the IR spectrum; therefore the spectral features can be used for structural analysis.

Mid-infrared spectroscopy or *Fourier transform infrared spectroscopy* (FTIR) provides information about certain components in the plant cell wall through absorbance bands. This technique has been extensively used to analyze the structure of wood constituents (Pandey, 1999; Popescu et al., 2011a; Xu et al., 2013) to determine the lignin content in pulp, paper and wood (Rodrigues et al., 1998; Popescu et al., 2007) and to investigate the changes in composition and structure occurring during weathering, decay or natural ageing (Faix et al., 1993; Popescu et al., 2010a; Ganne-Chédeville et al., 2012). It is also commonly used to analyze the structural changes occurring during different chemical (Eranna and Pandey, 2012; Lang et al., 2013) or thermal, hydrothermal, and thermohydromechanical (Tjeerdsma and Militz, 2005; Windeisen and Wegener, 2008; Popescu et al., 2013a) modifications.

FTIR coupled with *chemometric analysis* may be involved in the characterization of the spectral features whenever these contain robust information about chemical bonds. Sometimes compositional information is not directly available from their results, or online calibration models for product processing are required. In order to get more details on the structural features, chemometric methods, such as multivariate models, are necessary for spectra analysis. By reducing the large amount of spectral data in several latent variables, the statistical methods/models could build a relationship between spectral features and chemical components/bonds. For example, PLS and FTIR were used to predict glucan, hemicellulose, lignin and extractives from a calibration model consisting on spectral data and reference values (Meder et al., 1999).

Near infrared spectroscopy (NIR) has shown a great potential for the biomass analysis. As in mid-infrared spectroscopy, NIR offers a unique combination of speed, simplicity of sample preparation, easy usage, nondestructiveness and good

reproducibility (Schwaninger et al., 2011; Lupoi et al., 2014). It has been applied in the pulp and paper industry to monitor the moisture content or basic weight under online conditions (Tsuchikawa, 2007), or to evaluate the structure of thermally modified wood (Schwanninger et al., 2004; Popescu and Popescu, 2013). But one of the main applications of NIR has been the development of the composition prediction models of the biomass. Generally, standard extraction techniques are coupled with NIR spectral data, producing robust calibration matrices capable of predicting future sample metrics, eliminating the need to perform laborious wet chemical techniques on all samples. Therefore NIR coupled with chemometrics has proved to be an invaluable tool for screening biomass for optimal traits that will translate to higher fuel yields, for monitoring processes in real time, such that analysts can quickly identify complications during reactions rather than upon completion, and for determining useful structural parameters such as lignin S/G ratios. The straightforward, economic instrumentation and simplicity of sample handling should generate further NIR research, allowing researchers to catalogue higher numbers of plants than with solely standard/wet chemical techniques.

Another method used for the evaluation of the characteristic spectral variables is *two-dimensional correlation spectroscopy*, which may be applied whenever an external perturbation appears in the time of the measurement. This technique has been applied both for FT-IR and NIR spectroscopy to evaluate the modifications appearing in wood after thermal or hydrothermal treatments of wood or to discriminate between plants from the same species but with different origins (Chen et al., 2009; Popescu et al., 2013a; Popescu and Popescu, 2013).

Raman spectroscopy measures the light scattered from a molecule when irradiated with a light source (laser) (Lupoi et al., 2014). When the laser interacts with the sample, the electron cloud is perturbed and excites the molecule to a short-lived 'virtual state' as there is insufficient energy to promote the molecule to a higher energy level. A key experimental parameter when developing Raman applications is the selection of excitation wavelength. The use of Raman spectroscopy for studying lignocellulosic biomass has become widespread in the literature, with the majority of research exploring the applicability of Fourier transform (FT) Raman spectroscopy for woody feedstock analysis (Ona et al., 1997). It was found that band positions were similar between the hard and softwoods, but they also revealed separated unique bands. Also the band characteristic to vibrational mode of aliphatic C—H bonds was more intense in hardwoods due to a higher degree of aromatic methoxy groups from syringyl moieties. FT-Raman spectroscopy was used to explore the phenomenon known as 'self-absorption', which refers to the absorption of scattered photons by the analyte, leading to decreases in spectral intensities. It was evidenced that cellulose, not lignin, is the cause (Agarwal and Kawai, 2005).

Raman spectroscopy has been developed with new techniques and instruments, which may elucidate the key attributes for biomass analysis. Some of these techniques are (i) N*ear-Infrared Dispersive Raman Spectroscopy* (Agarwal et al., 2013); (ii) S*urface Enhanced Raman Spectroscopy* (Smith and Dent, 2005); (iii) *Resonance Raman Spectroscopy* (Barsberg et al., 2005); (iv) *Ultraviolet Resonance Raman spectroscopy* (Pandey and Vuorinen, 2008) or (v) *Raman microscopy* (Gierlinger and Schwanninger, 2006).

Another interesting technique for the characterization of the material surface is *X-ray Photoelectron Spectroscopy* (XPS) (also known as ESCA, Electron

Spectroscopy for Chemical Analysis). The method is considered nondestructive and gives information on surface chemistry, surface reactivity and surface passivation of nature-derived interphases of complex organic materials. The studies focus attention on the surface chemical composition of lignocellulosic materials, wood, pulp and cellulose (Johansson et al., 1999, 2012; Sinn et al., 2001), surface analysis of wood chemical composition after heat treatment (Inari et al., 2006; Källbom et al., 2015), natural degradation and the weathering of wood and wood-plastic composites (Matuana and Kamdem, 2002; Popescu et al., 2009).

Fluorescence spectroscopy measures the emission of electromagnetic radiation after a molecule has been excited to higher energy levels. Although this technique is more sensitive than some analytical instruments, fluorescence spectroscopy requires the presence of a fluorophore, whether intrinsic to the molecule, or through analyte labelling with a highly fluorescing species (Lupoi et al., 2014). The viability of fluorescence spectroscopy has been explored for studying biomass nondestructively (Liukko et al., 2007; Nkansah and Dawson-Andoh, 2010), as there is relatively little sample preparation required and the instrumentation is inexpensive, capable of on- or offline methodology and can be field portable.

UV microspectrophotometry is an established analytical technique to evaluate the direct imaging of lignin distribution and lignin modification (biodegradation, delignification) within individual cell wall layers (Koch and Kleist, 2001; Rehbein and Koch, 2011).

In *Nuclear Magnetic Resonance Spectroscopy*, nuclei absorb radiation in the radio frequency range of the electromagnetic spectrum (Smith and Webb, 2000). Analytes are inserted into intense magnetic fields to create the splitting of electronic states necessary for absorption. NMR is described as a nondestructive, noninvasive technique, since the low radiofrequency excitation energy cannot induce molecular physical/chemical changes, and therefore provides an excellent tool for determining unaltered molecular structures (Lupoi et al., 2014). The most widespread usage of NMR is for lignin molecular structure elucidation (Rencoret et al., 2011; del Rio et al., 2012). In a solid state, 13C NMR has been used in the structural analysis of cellulose (Atalla and VanderHart, 1999; Hult et al., 2000) and for the determination of cellulose crystallinity (Hult et al., 2001). This technique has also been involved for the structural elucidation of whole biomass (Maunu, 2002; Nuopponen et al., 2006) and detection of various chemical changes (increasing crystallinity of cellulose, deacetylation of hemicelluloses and degradation of amorphous carbohydrates and demethoxylation and cross-linking reactions in lignin) during thermal treatments of wood (Tjeerdsma et al., 1998; Brosse et al., 2010) or biodegradation and natural ageing (Popescu et al., 2011b, 2013b).

The arrangement of the cellulose molecules into ordered domains or cellulose crystallites may be studied by means of diffraction techniques. In particular, *X-ray diffraction* has been widely used to resolve the crystalline configuration of cellulose microfibrils, ie, to estimate the crystallite size and the cellulose crystalline fraction (Ciolacu et al., 2011; Popescu et al., 2011b).

Small angle X-ray scattering techniques provide an efficient approach to study the structure of plant cell walls in their native state, ie, partially hydrated, preventing structural alterations and covering a relatively wide size range (Martínez-Sanz et al., 2015).

2.5.4 Emerging technologies

Apart from the extraction and fractionation, chromatographic and spectral techniques, there are several other methods, which may be used alone or in correlation with other methods in order to evaluate the chemical structure of wood and natural fibres.

X-ray computed tomography is a new method applied for both descriptive and quantitative identification of wood anatomy, and to solve details on a three-dimensional representation of the composition and morphology (Van den Bulcke et al., 2009; Biziks et al., 2015). The 3-D object under study is reconstructed based on a set of two-dimensional projections (radiographies) taken from different angles by rotating the sample around a defined axis. Due to the nondestructive nature of the scanning process, it can be used to monitor and quantify structural changes occurring during modification, fungal growth, water movement or weathering. Such a technique can therefore play an important role in the characterization of modified wood products (Van den Bulcke et al., 2009; Biziks et al., 2015).

Time-of-flight secondary-ion mass spectrometry (ToF-SIMS) is a powerful technique to reveal the chemical distribution in plant tissue. It provides detailed chemical information via identification of intact molecular ions or characteristic molecular fragments that are emitted from the wood surface; therefore they can be used to identify lignin, carbohydrates (polysaccharides), extractives and inorganic ions. It is capable to provide information on the spatial distribution of these components on the surface of wood, providing information about the composition across cell walls (Jung et al., 2010; Mahajan et al., 2012). The *cryo-TOF-SIMS* can be used for the analysis of the frozen-hydrated plant tissues; therefore additional to the distribution of the elements, the relationship between the water and the chemicals in frozen-hydrated samples can be evaluated (Kuroda et al., 2013).

Electron spin resonance spectroscopy (ESR) is a technique, which enables the detection and characterization of chemical species that possess unpaired electrons. It is based on the measurement of microwave resonance absorbance in the presence of an applied magnetic field. ESR signals are very stable, and a high correlation between the ESR signal intensity and the mass loss or durability of the thermal treated wood has been observed; therefore this technique may be correlated with the treatment severity induced by temperature and treatment time (Willems et al., 2010; Altgen et al., 2012).

Thermogravimetry/differential thermogravimetry (TG/DTG) describes physical and chemical changes of materials as a function of temperature. Wood as a whole material undergoes a complex degradation scheme, which is greatly affected by its physical and chemical nature. During the thermal decomposition process of wood, small molecules are eliminated, and eventually a charred mass is left. Noncombustible products, such as carbon dioxide, traces of inorganic compounds and water vapour are produced up to 130°C. At about 150°C, some components begin to break down chemically; low temperature degradation at a low rate occurs in lignin and hemicelluloses. The mass loss between 300 and 500°C corresponds to the degradation of cellulose and has also been associated to the pyrolitic degradation of lignin involving fragmentation of interunit linkages decomposition and condensation of the aromatic rings (Beall, 1986; Popescu et al., 2010b). It is a well-established technique for the evaluation of

the mass loss of samples during thermal degradation or of the kinetic parameters, but TG/DTG has been applied for the quantification of the chemical components in wood and biodegraded wood (Popescu et al., 2010b, 2011a; Alfredsen et al., 2012), as well as to determine the severity of the thermal modification (Korosec et al., 2009). This technique may also be coupled with infrared spectroscopy or GC−MS; therefore the evolved gases can be analyzed online.

References

Agarwal, U.P., Kawai, N., 2005. "Self-absorption" phenomenon in near-infrared fourier transform Raman spectroscopy of cellulosic and lignocellulosic materials. Applied Spectroscopy 59 (3), 385−388.

Agarwal, U.P., Reiner, R.R., Ralph, S.A., 2013. Estimation of cellulose crystallinity of lignocelluloses using near-IR FT-Raman spectroscopy and comparison of the Raman and segal-WAXS methods. Journal of Agricultural and Food Chemistry 61 (1), 103−113.

Akyildiz, M.H., Ates, S., 2008. Effect of heat treatment on equilibrium moisture content (EMC) of some wood species in Turkey. Research Journal of Agriculture and Biological Sciences 4 (6), 660−665.

Alfredsen, G., Bader, T.K., Dibdiakova, J., Filbakk, T., Bollmus, S., Hofstetter, K., 2012. Thermogravimetric analysis for wood decay characterization. European Journal of Wood and Wood Products 70, 527−530.

Allegretti, O., Brunetti, M., Cuccui, I., Ferrari, S., Nocetti, M., Terziev, N., 2012. Thermo-vacuum modification of spruce (picea abies karst.) and fir (abies alba mill.) wood. BioResources 7 (3), 3656−3669.

Altgen, M., Welzbacher, C., Humar, M., Militz, H., 2012. ESR-spectroscopy as a potential method for the quality control of thermally modified wood. In: COST Action FP 0904 Conference on Current and Future Trends of Thermo Hydro-mechanical Modification of Wood. Opportunities for New Markets? Nancy, p. 132.

Aronovsky, S.I., Gortner, R.A., 1936. The Cooking Process. IX. Pulping Wood with Alcohols and Other Organic Reagents. Industrial & Engineering Chemistry 28 (11), 1270−1276.

Atalla, R.H., VanderHart, D.L., 1999. The role of solid-state carbon-13 NMR spectroscopy in studies of the nature of native celluloses. Solid State Nuclear Magnetic Resonance 15 (1), 1−19.

Ates, S., Akyildiz, M.H., Ozdemir, H., 2009. Effects of heat treatment on calabrian pine (*Pinus brutia* ten.) wood. BioResources 4 (3), 1032−1043.

Awoyemi, L., Jones, I.P., 2011. Anatomical explanations for the changes in properties of western red cedar (*Thuja plicata*) wood during heat treatment. Wood Science and Technology 45, 261−267.

Bao, W., O'Malley, D.M., Sederroth, R.R., 1992. Wood contains a cell-wall structural protein. In: Proceedings of the National Academy of Sciences USA, 89, pp. 6604−6608.

Barcík, Š., Gašparík, M., Razumov, E.Y., 2015a. Effect of temperature on the color changes of wood during thermal modification. Cellulose Chemistry and Technology 49 (9−10), 789−798.

Barcík, Š., Gašparík, M., Razumov, E.Y., 2015b. Effect of thermal modification on the colour changes of oak wood. Woods Research 60 (3), 385−396.

Barsberg, S., Matousek, P., Towrie, M., 2005. Structural analysis of lignin by resonance Raman spectroscopy. Macromolecular Bioscience 5 (8), 743−752.

Beall, F.C., 1986. Thermal degradation of wood. In: Bever, M.B. (Ed.), Enciclopedia of Materials Science and Engineering. Pergamon Press, Oxford, p. 4933.

Bekhta, P., Niemz, P., 2005. Effect of high temperature on the change in color, dimensional stability and mechanical properties of spruce wood. Holzforschung 57 (5), 539–546.

Bera, M., Alagirusamy, R., Das, A., 2010. A study on interfacial properties of jute-PP composites. Journal of Reinforced Plastics and Composites 29 (20), 3155–3161.

Bismark, A., Mishra, S., Lampke, T., 2005. In: Mohanty, A.K., Misra, M., Drzal, L. (Eds.), Plant Fibers as Reinforcement for Green Composites. In Natural Fibres, Biopolymers and Biocomposites. Taylor and Francis, Boca Raton, USA.

Biziks, V., Andersons, B., Beçkova, L., Kapača, E., Militz, H., 2013. Changes in the microstructure of birch wood after hydrothermal treatment. Wood Science and Technology 47 (4), 717–735.

Biziks, V., Van den Bulcke, J., Grīniņš, J., Militz, H., Andersons, B., Andersone, I., Dhaene, J., Van Acker, J., 2015. Study on the microstructural changes of thermo-hydro treated wood using x-ray computed tomography. In: The Eighth European Conference on Wood Modification, Helsinki, p. 297.

Bizzozero, O.A., 1995. Chemical analysis of acylation sites and species. Methods in Enzymology 250, 361–379.

Björkman, A., 1954. Isolation of lignin from finely divided wood with neutral solvents. Nature 174, 1057–1058.

Bledzki, A.K., Mamun, A.A., Bolk, J., 2010. Physical, chemical and surface properties of wheat husk, rye husk and soft wood and their polypropylene composites. Composites: Part A 41, 480–488.

Bonès, R.M., Sikorski, J., 1967. The histological structure of wool fibres and their plasticity. The Journal of the Textile Institute 58, 521–532.

Boruszewski, P., Borysiuk, P., Mamiński, M., Grześkiewicz, M., 2011. Gluability of thermally modified beech (*Fagus silvatica* L.) and birch (*Betula pubescens* Ehrh.) wood. Wood Material Science & Engineering 6 (4), 185–189.

Braaten, A.W., 2005. Wool. In: Encyclopedia of Clothing and Fashion 3. Thomson Gale.

Bray, M.W., Peterson, C.E., 1927. Chemistry of pulping flax straw. Hydrolysis with sodium sulfite. Industrial & Engineering Chemistry 19 (3), 371–372.

Breakspear, S., Smith, J.R., Luengo, G., 2005. Effect of the covalently linked fatty acid 18-MEA on the nanotribology of hair's outermost surface. Journal of Structural Biology 149, 235–242.

Breitmaier, E., 2006. Terpenes. Wiley-Verlag GmbH, Weinham.

Bremer, M., Fischer, S., Nguyen, T.C., Wagenfuhr, A., Phuong, L.X., Dai, V.H., 2013. Effects of thermal modification on the properties of two Vietnamese bamboo species. Part II: effects on chemical composition. BioResources 8 (1), 981–993.

Brendel, O., Iannetta, P.P.M., Stewart, D., 2000. A rapid and simple method to isolate pure alpha-cellulose. Phytochemical Analysis 11, 7–10.

Brosse, N., El Hage, R., Chaouch, M., Petrissans, M., Dumarcay, S., Gerardin, P., 2010. Investigation of the chemical modifications of beech wood lignin during heat treatment. Polymer Degradation and Stability 95, 1721–1726.

Browning, B.L., 1967. Methods of Wood Chemistry. Interscience Publishers, New York.

Buranov, A.U., Mazza, G., 2008. Lignin in straw of herbaceous crops. Industrial Crops and Products 28, 237–259.

Burgert, I., Dunlop, J.W.C., 2011. Micromechanics of Cell Walls, Mechanical Integration of Plant Cells and Plants. Springer-Verlag, Berlin, Heidelberg.

Bächle, H., Zimmer, B., Windeisen, E., Wegener, G., 2010. Evaluation of thermally modified beech and spruce wood and their properties by FT-NIR spectroscopy. Wood Science and Technology 44, 421–433.

Candan, Z., Korkut, S., Unsal, O., 2013. Effect of thermal modification by hot pressing on performance properties of paulownia wood boards. Industrial Crops and Products 45, 461–464.

Candelier, K., Chaouch, M., Dumarçay, S., Pétrissans, A., Pétrissans, M., Gérardin, P., 2011. Utilization of thermodesorption coupled to GC-MS to study stability of different wood species to thermodegradation. Journal of Analytical and Applied Pyrolysis 92 (2), 376−383.

Charani, P.R., Rovshandeh, J.M., Mohebby, B., Ramezani, O., 2007. Influence of hydrothermal treatment on the dimensional stability of beech wood. Caspian Journal of Environmental Sciences 5 (2), 125−131.

Chawla, J.S., Sharma, A.N., 1972. Experiments on tempering of fibreboards. Indian Academy of Wood Science 2, 70−73.

Chen, J., Zhou, Q., Noda, I., Sun, S., 2009. Discrimination of different genera Astragalus samples via quantitative symmetry analysis of two-dimensional hetero correlation spectra. Analytica Chimica Acta 649 (1), 106−110.

Cheng, L., Adhikari, S., Wang, Z., Ding, Y., 2015. Characterization of bamboo species at different ages and bio-oil production. Journal of Analytical and Applied Pyrolysis 116, 215−222.

Ciolacu, D., Gorgieva, S., Tampu, D., Kokol, V., 2011. Enzymatic hydrolysis of different allomorphic forms of microcrystalline cellulose. Cellulose 18 (6), 1527−1541.

Cirule, D., Meija-Feldmane, A., Kuka, E., Andersons, B., Kurnosova, N., Antons, A., Tuherm, H., 2016. Spectral sensitivity of thermally modified and unmodified wood. BioResources 11 (1), 324−335.

Crawford, T.C., Crawford, S.A., 1980. Synthesis of L-ascorbic acid. Advances in Carbohydrate Chemistry and Biochemistry 37, 79−155.

Crônier, D., Monties, B., Chabbert, B., 2005. Structure and Chemical Composition of Bast Fibers Isolated from Developing Hemp Stem. Journal of Agricultural Food Chemistry 53 (21), 8279−8289.

Cullen, L.E., Macfarlane, C., 2005. Comparison of cellulose extraction methods for analysis of stable isotope ratios of carbon and oxygen in plant material. Tree Physiology 25, 563−569.

Dai, D., Fan, M., 2013. Green modification of natural fibres with nanocellulose. RSC Advances 3, 4659.

D'Arcy, J.B., 1990. Sheep Management and Wool Technology. NSW University Press, Kensington.

de Cademartori, P.H.G., dos Santos, P.S.B., Serrano, L., Labidi, J., Gatto, D.A., 2013a. Effect of thermal treatment on physicochemical properties of Gympie messmate wood. Industrial Crops and Products 45, 360−366.

de Cademartori, P.H.G., Schneid, E., Gatto, D.A., Stangerlin, D.M., Beltrame, R., 2013b. Thermal modification of *Eucalyptus grandis* wood: variation of colorimetric parameters. Maderas: Ciencia y Tecnología 15 (1), 57−64.

del Río, J.C., Rencoret, J., Prinsen, P., Martinez, A.T., Ralph, J., Gutierrez, A., 2012. Structural characterization of wheat straw lignin as revealed by analytical pyrolysis, 2D-NMR, and reductive cleavage methods. Journal of Agricultural and Food Chemistry 60 (23), 5922−5935.

Desch, H.E., Dinwoodie, J.M., 1996. Timber: Structure, Properties, Conversion and Use. MacMillan Press Ltd, London.

Deuss, P.J., Barta, K., 2016. From models to lignin: transition metal catalysis for selective bond cleavage reactions. Coordination Chemistry Reviews 306, 510−532.

Dinwoodie, J.M., 2000. Timber: Its Nature and Behaviour, second ed. E. and F.N. Spon, London.

Dzurenda, L., 2013. Modification of wood colour of *Fagus sylvatica* L. to a brown-pink shade caused by thermal treatment. Woods Research 58 (3), 475−482.

Eranna, P.B., Pandey, K.K., 2012. Solvent-free chemical modification of wood by acetic and butyric anhydride with iodine as catalyst. Holzforschung 66 (8), 967−971.

Esteves, B.M., Pereira, H.M., 2009. Heat treatment of wood. BioResources 4 (1), 370−404.
Esteves, B.M., Domingos, I.J., Pereira, H.M., 2008. Pine wood modification by heat treatment in air. BioResources 3 (1), 142−154.
Evans, D.J., Leeder, J.D., Rippon, J.A., Rivett, D.E., 1985. Separation and analysis of the surface lipids of the wool fiber. International Wool Textile Research Conference Proceedings 135−142.
Evans, D.J., Denning, R.J., Church, J.S., 2002. Interface of keratin fibres with their environment. In: Encyclopedia of Surface and Colloid Science, pp. 2628−2642.
Faix, O., Meier, D., Beinhoff, O., 1989. Analysis of lignocelluloses and lignins from *Arundo donax* L. and *Miscanthus sinensis* Anderss., and hydroliquefaction of *Miscanthus*. Biomass 18 (2), 109−126.
Faix, O., Fortmann, I., Bremer, J., Meier, D., 1991. Thermal degradation products of wood. Holz als Roh und Werkstoff 49, 213−219.
Faix, O., Bremer, J., Schmidit, O., Stevanovic, T., 1993. Monitoring of chemical changes in white-rot degraded beech wood by pyrolysis-gas chromatography and fourier transform infrared spectroscopy. Journal of Analytical and Applied Pyrolysis 21, 147−162.
Felby, C., Hassingboe, J., Lund, M., 2002. Pilot-scale production of fiberboards made by laccase oxidized wood fibers: board properties and evidence for cross-linking of lignin. Enzyme and Microbial Technology 31, 736−741.
Folk, J.E., 1977. The epsilon-(gamma-glutamyl) lysine crosslink and the catalytic role of transglutaminase. In: Advances in Protein Chemistry, pp. 1−120.
Follrich, J., Müller, U., Gindl, W., 2006. Effects of thermal modification on the adhesion between spruce wood (picea abies karst.) and a thermoplastic polymer. Holz als Roh und Werkstoff 64, 373−376.
Fujita, M., Harada, H., 1990. Ultrastructure and Formation of Wood Cell Wall. In: Hon, D.N.-S., Shiraishi, N. (Eds.), Wood and Cellulosic Chemistry. Marcel Dekker Inc.
Gabov, K., Gosselink, R.J.A., Smeds, A.I., Fardim, P., 2014. Characterization of lignin extracted from birch wood by a modified hydrotropic process. Journal of Agricultural and Food Chemistry 62, 10759−10767.
Gabrielii, I., Gatenholm, P., Glasser, W.G., Jain, R.K., Kenn, L., 2000. Separation, characterization and hydrogel-formation of hemicellulose from aspen wood. Carbohydrate Polymers 43, 367−374.
Galletti, G.C., Bocchini, P., 1995. Pyrolysis/gas chromatography/mass spectrometry of lignocellulose. Rapid Communications in Mass Spectrometry 9, 815−826.
Gamelas, J.A.F., 2013. The surface properties of cellulose and lignocellulosic materials assessed by inverse gas chromatography: a review. Cellulose 20, 2675−2693.
Ganne-Chédeville, C., Jääskeläinen, A.S., Froidevaux, J., Hughes, M., Navi, P., 2012. Natural and artificial ageing of spruce wood as observed by FTIR-ATR and UVRR spectroscopy. Holzforschung 66, 163−170.
Gardiner, E.S., Sarko, A., 1985. Packing analysis of carbohydrates and polysaccharides. 16. The crystal structures of celluloses IV_I and IV_{II}. Canadian Journal of Chemistry 63, 173−180.
Gardner, K.H., Blackwell, J., 1974. The structure of native cellulose. Biopolymers 13, 1975−2001.
Gierlinger, N., Schwanninger, M., 2006. Chemical imaging of poplar wood cell walls by confocal Raman microscopy. Plant Physiology 140 (4), 1246−1254.
Grinins, J., Andersons, B., Biziks, V., Andersone, I., Dobele, G., 2013. Analytical pyrolysis as an instrument to study the chemical transformations of hydrothermally modified wood. Journal of Analytical and Applied Pyrolysis 103, 36−41.

Gunduz, G., Aydemir, D., Karakas, G., 2009. The effects of thermal treatment on the mechanical properties of wild pear (*Pyrus elaeagnifolia* Pall.) wood and changes in physical properties. Materials & Design 30, 4391−4395.

Hanana, S., Elloumi, A., Placet, V., Tounsi, H., Belghith, H., Bradai, C., 2015. An efficient enzymatic-based process for the extraction of high-mechanical properties alfa fibres. Industrial Crops and Products 70, 190−200.

Hayashi, J., Sufoka, A., Ohkita, J., Watanabe, S., 1975. The confirmation of existence of cellulose III_I, III_{II}, IV_I and IV_{II} by X-ray method. Journal of Polymer Science Part C Polymer Letters 13, 23−27.

Hess, K., Kissig, H., 1941. ZurKenntnis der hochtemperatur-modifikation der cellulose (cellulose IV). Zietschrift Physikalische Chemie *B*49, 235−239.

Hill, C.A.S., Jones, D., 1996. The dimensional stabilisation of corsican pine sapwood by reaction with carboxylic acid anhydrides. Holzforschung 50 (5), 457−462.

Hill, C.A.S., 2006. Wood Modification: Chemical, Thermal and Other Processes. John Wiley and Sons, Chichester.

Hill, C.A.S., 2011. Wood modification: an update. BioResources 6 (2), 918−919.

Horst, D.J., Behainne, J.J.R., de Andrade Júnior, P., Kovaleski, J.L., 2014. An experimental comparison of lignin yield from the Klason and Willstatter extraction methods. Energy for Sustainable Development 23, 78−84.

Hult, E.-L., Larsson, P.T., Iversen, T., 2000. Comparative CP/MAS ^{13}C-NMR study of cellulose structure in spruce wood and kraft pulp. Cellulose 7 (1), 35−55.

Hult, E.-L., Larsson, P.T., Iversen, T., 2001. A CP/MAS ^{13}C-NMR study of supermolecular changes in the cellulose and hemicellulose structure during kraft pulping. Nordic Pulp & Paper Research Journal 16 (1), 33−39.

Inari, G.N., Petrissans, M., Lambert, J., Ehrhardt, J.J., Gerardin, P., 2006. XPS characterization of wood chemical composition after heat-treatment. Surface and Interface Analysis 38, 1336−1342.

Ioelovich, M., Leykin, A., 2008. Structural Investigations of various cotton fibers and cotton celluloses. BioResources 3 (1), 170−177.

Jebrane, M., Pichavant, F., Sèbe, G., 2011. A comparative study on the acetylation of wood by reaction with vinyl acetate and acetic anhydride. Carbohydrate Polymers 83, 339−345.

Johansson, L.-S., Campbell, J.M., Koljonen, K., Stenius, P., 1999. Evaluation of surface lignin on cellulose fibers with XPS. Applied Surface Science 144−145, 92−95.

Johansson, L.-S., Campbell, J.M., Ganne-Chedeville, C., Hänninen, T., Hughes, M., Vuorinen, T., Laine, J., 2012. XPS and the medium-dependent surface adaptation of cellulose in wood. Surface and Interface Analysis 44, 899−903.

John, M.J., Anandjiwala, R.D., 2008. Recent developments in chemical modification and characterization of natural fiber-reinforced composites. Polymer Composites 29 (2), 187−207.

Joseph, K., Mattoso, L.H.C., Toledo, R.D., Thomas, S., de Carvalho, L.H., Pothen, L., Kala, S., James, B., 2000. Natural fiber reinforced thermoplastic composites. In: Frollini, E., Leao, A.L., Mattoso, L.H.C. (Eds.), Natural Polymers and Agrofibers Composites. Embrapa, USP-IQSC, UNESP, San Carlos, Brazil, p. 159.

Jung, S., Foston, M., Sullards, C.M., Ragauskas, A.J., 2010. Surface characterization of dilute acid pretreated populus deltoides by ToFSIMS. Energy Fuel 24, 1347−1357.

Kačíková, D., Kačík, F., Čabalová, I., Ďurkovič, J., 2013. Effects of thermal treatment on chemical, mechanical and colour traits in Norway spruce wood. Bioresource Technology 144, 669−674.

Kalia, S., Kaith, B.S., Kaura, I., 2009. Pretreatments of natural fibers and their application as reinforcing material in polymer composites − a review. Polymer Engineering & Science 49, 1253−1272.

Källbom, S., Rautkari, L., Johansson, L.-S., Wålinder, M., Segerholm, K., Jones, D., Laine, K., 2015. Surface chemical analysis and water vapour sorption of thermally modified wood exposed to increased relative humidity. In: The Eighth European Conference on Wood Modification, Helsinki, p. 241.

Karlsons, I., Svalbe, K., Neimanis, E., Ozolina, I., Sterns, S., 1976a. Modified wood. USSR Patent 532 525, published in Otkrytiia, Izobreteniia, Promyshlennye Obraztsy. Tovarnye Znaki 53 (32), 47.

Karlsons, I., Svalbe, K., Neimanis, E., Ozolina, I., Sterns, S., 1976b. Modified wood by evacuation and subsequent acetylation with ketene. USSR Patent 526 508, published in Otkrytiia, Izobreteniia, Promyshlennye Obraztsy. Tovarnye Znaki 53 (39), 43.

Kaygin, B., Gunduz, G., Aydemir, D., 2009. Some physical properties of heat-treated paulownia (*Paulownia elongata*) wood. Drying Technology: An International Journal 27 (1), 89−93.

Kekkonen, P.M., Telkki, V.-V., Jokisaari, J., 2010. Effect of thermal modification on wood cell structures observed by pulsed-field-gradient stimulated-echo NMR. The Journal of Physical Chemistry C 114 (43), 18693−18697.

Kleinert, T.N., 1974. Organosolv Pulping with Aqueous Alcohol. Tappi Journal 57 (8), 99−102.

Koch, G., Kleist, G., 2001. Application of scanning UV microspectrophotometry to localise lignins and phenolic extractives in plant cell walls. Holzforschung 55 (6), 563−567.

Kol, H.Ş., Sefil, Y., 2011. The thermal conductivity of fir and beech wood heat treated at 170, 180, 190, 200, and 212°C. Journal of Applied Polymer Science 121 (4), 2473−2480.

Kollmann, F., 1936. Technologie des Holzes und der Holzwerkstoffe. Springer verlag, Berlin.

Korkut, D.S., Guller, B., 2008. The effects of heat treatment on physical properties and surface roughness of red-bud maple (*Acer trautvetteri* Medw.) wood. Bioresource Technology 99, 2846−2851.

Korkut, S., Hiziroglu, S., 2009. Effect of heat treatment on mechanical properties of hazelnut wood (*Corylus colurna* L.). Materials & Design 30, 1853−1858.

Korkut, S., Kök, M.S., Korkut, D.S., Gürleyen, T., 2008a. The effects of heat treatment on technological properties in red-bud maple (*Acer trautvetteri* Medw.) wood. Bioresource Technology 99, 1538−1543.

Korkut, S., Akgüla, M., Dündar, T., 2008b. The effects of heat treatment on some technological properties of Scots pine (*Pinus sylvestris* L.) wood. Bioresource Technology 99, 1861−1868.

Korkut, S., Korkut, D.S., Kocaefe, D., Elustondo, D., Bajraktari, A., Çakicier, N., 2012. Effect of thermal modification on the properties of narrow-leaved ash and chestnut. Industrial Crops and Products 35 (1), 287−294.

Korosec, R.C., Lavric, B., Rep, G., Pohleven, F., Bukovec, P., 2009. Thermogravimetry as a possible tool for determining modification degree of thermally Norway spruce wood. Journal of Thermal Analysis and Calorimetry 98, 189−195.

Kotilainen, R.A., Toivanen, T.-J., Alén, R.J., 2000. FTIR monitoring of chemical changes in softwood during heating. Journal of Wood Chemistry and Technology 20 (3), 307−320.

Kuroda, K., Fujiwara, T., Imai, T., Takama, R., Saito, K., Matsushita, Y., Fukushima, K., 2013. The cryo-TOF-SIMS/SEM system for the analysis of the chemical distribution in freeze-fixed *Cryptomeria japonica* wood. Surface and Interface Analysis 45, 215−219.

Lan, W., Liu, C.F., Sun, R.C., 2011. Fractionation of bagasse into cellulose, hemicellulose and lignin with ionic liquid treatment followed by alkaline extraction. Journal of Agricultural and Food Chemistry 59, 8691−8701.

Lang, Q., Chen, H.-Y., Pu, J.-W., 2013. Wood modification using a urea-formaldehyde prepolymer. Wood and Fiber Science 45 (2), 162−169.

Lekounougou, S., Kocaefe, D., 2014. Effect of thermal modification temperature on the mechanical properties, dimensional stability, and biological durability of black spruce (*Picea mariana*). Wood Material Science & Engineering 9 (2), 59−66.

Lilholt, H., Lawther, J.M., 2000. Natural Organic Fibres. In: Chou, T.-W. (Ed.), Comprehensive Composite Materials. Elsevier Science.

Ling, Z., Ji, Z., Ding, D., Cao, J., Xu, F., 2016. Microstructural and topochemical characterization of thermally modified poplar (*Populus cathayaha*) cell wall. BioResources 11 (1), 786−799.

Liukko, S., Tasapuro, V., Liitia, T., 2007. Fluorescence spectroscopy for chromophore studies on bleached kraft pulps. Holzforschung 61 (5), 509−515.

Loader, N.J., Robertson, I., Barker, A.C., Switsur, V.R., Waterhouse, J.S., 1997. An improved technique for the batch processing of small whole wood samples to α-cellulose. Chemical Geology 136, 313−317.

Łucejko, J.J., Zborowska, M., Modugno, F., Colombini, M.P., Prądzy'nski, W., 2012. Analytical pyrolysis vs. classical wet chemical analysis to assess the decay of archaeological waterlogged wood. Analytica Chimica Acta 745, 70−77.

Lupoi, J.S., Singh, S., Simmons, B.A., Henry, R.J., 2014. Assessment of lignocellulosic biomass using analytical spectroscopy: an evolution to high-throughput techniques. BioEnergy Research 7, 1−23.

Macfarlane, C., Warren, C.M., White, D.A., Adams, M.A., 1999. A rapid and simple method for processing wood to crude cellulose for analysis of stable carbon isotopes in tree-rings. Tree Physiology 19, 831−835.

Madsen, B., Gamstedt, K.E., 2013. Wood versus plant fibers: similarities and differences in composite applications. Advances in Materials Science and Engineering 2013, 564346.

Mahajan, S., Jeremic, D., Goacher, R.E., Master, E.R., 2012. Mode of coniferous wood decay by the white rot fungus *Phanerochaete carnosa* as elucidated by FTIR and ToF-SIMS. Applied Microbiology and Biotechnology 94, 1303−1311.

Manalo, R.D., Garcia, C.M., 2012. Termite resistance of thermally-modified *Dendrocalamus asper* (Schultes f.) Backer ex Heyne. Insects 3, 390−395.

Marrinan, M., Mann, J., 1956. Infrared spectra of the crystalline modifications of cellulose. Journal of Polymer Science 21, 301−311.

Martínez-Sanz, M., Gidley, M.J., Gilbert, E.P., 2015. Application of X-ray and neutron small angle scattering techniques to study the hierarchical structure of plant cell walls: a review. Carbohydrate Polymers 125, 120−134.

Matuana, L.M., Kamdem, D.P., 2002. Accelerated ultraviolet weathering of PVC/wood-flour composites. Polymer Engineering & Science 42, 1657−1666.

Maunu, S.L., 2002. NMR studies of wood and wood products. Progress in Nuclear Magnetic Resonance Spectroscopy 40 (2), 151−174.

Maxwell, J.M., Huson, M.G., 2005. Scanning probe microscopy examination of the surface properties of keratin fibres. Micron 36, 127−136.

McGrath, S.P., Lombi, E., Gray, C.W., Caille, N., Dunham, S.J., Zhao, F.J., 2006. Field evaluation of Cd and Zn phytoextraction potential by the hyperaccumulators *Thlaspi caerulescens* and *Arabidopsis halleri*. Environmental Pollution 141, 115−125.

Meder, R., Gallagher, S., Mackie, K.L., Bohler, H., Meglen, R.R., 1999. Rapid determination of the chemical composition and density of *Pinus radiata* by PLS modeling of transmission and diffuse reflectance FTIR spectra. Holzforschung 53 (3), 261−266.

Merali, Z., Marjamaa, K., Käsper, A., Kruus, K., Gunning, A.P., Morris, V.J., Waldron, K.W., 2016. Chemical characterization of hydrothermally pretreated and enzyme-digested wheat straw: an evaluation of recalcitrance. Food Chemistry 198, 132−140.

Messner, K., Fleck, V., Bruce, A., Rosner, B., 1999. Process for Improving the Impregnability of Wood by Pre-treatment With Fungi. Patent EP1015199 B1.

Messner, K., Bruce, A., Bongers, H.P.M., 2003. Treatability of refractory wood species after fungal pre-treatment. In: Proceedings European Conference on Wood Modification, pp. 389–401.

Mishra, S., Naik, J.B., Patil, Y.P., 2000. The compatibilising effect of maleic anhydride on swelling and mechanical properties of plant-fiber-reinforced novolac composites. Composites Science and Technology 60 (9), 1729–1735.

Mishra, S., Misra, M., Tripathy, S.S., Nayak, S.K., Mohanty, A.K., 2001. Graft copolymerization of acrylonitrile on chemically modified sisal fibers. Macromolecular Materials and Engineering 286, 107–113.

Mishra, S., Mohanty, A.K., Drzal, L.T., Misra, M., Parija, S., Nayak, S.K., Tripathy, S.S., 2003. Studies on mechanical performance of biofibre/glass reinforced polyester hybrid composites. Composites Science and Technology 63 (10), 1377–1385.

Mohtar, S.S., Tengku Malim Busu, T.N.Z., Md Noor, A.M., Shaari, N., Yusoff, N.A., Bustam Khalil, M.A., Abdul Mutalib, M.I., Mat, H.B., 2015. Extraction and characterization of lignin from oil palm biomass via ionic liquid dissolution and non-toxic aluminium potassium sulfate dodecahydrate precipitation processes. Bioresource Technology 192, 212–218.

Mokaloba, N., Batane, R., 2014. The effects of mercerization and acetylation treatments on the properties of sisal fiber and its interfacial adhesion characteristics on polypropylene. International Journal of Engineering. Science and Technology 6 (4), 83–97.

Mwaikambo, L., Ansell, M.P., 2002. Chemical modification of hemp, sisal, jute, and kapok fibers by alkalization. Journal of Applied Polymer Science 84, 2222–2234.

Nagarajappa, G.B., Pandey, K.K., 2016. UV resistance and dimensional stability of wood modified with isopropenyl acetate. Journal of Photochemistry and Photobiology B 155, 20–27.

Negi, J.S., Chawla, J.S., 1993. Heat Treatment of Fibreboards. Research and Industry (New Delhi) 38 (4), 248–253.

Negri, A.P., Cornell, H.J., Rivett, D.E., 1993. A model for the surface of keratin fibers. Textile Research Journal 63, 109–115.

Nguyen, C.T., Wagenfuhr, A., Phuong, L.X., Dai, V.H., Bremer, M., Fischer, S., 2012. The effects of thermal modification on the properties of two Vietnamese bamboo species, Part I: effects on physical properties. BioResources 7 (4), 5355–5366.

Nkansah, K., Dawson-Andoh, B., 2010. Rapid characterization of biomass using fluorescence spectroscopy coupled with multivariate data analysis. I. Yellow poplar (*Liriodendron tulipifera* L.). Journal of Renewable and Sustainable Energy 2 (2), 023103.

Nonier, M.F., Vivas, N., Vivas de Gaulejaca, N., Absalon, C., Soulié, P., Fouquet, E., 2006. Pyrolysis–gas chromatography/mass spectrometry of *Quercus* sp. wood. Application to structural elucidation of macromolecules and aromatic profiles of different species. Journal of Analytical and Applied Pyrolysis 75, 181–193.

Nordin, N.I.A.A., Ariffin, H., Andou, Y., Hassan, M.A., Shirai, Y., Nishida, H., Yunus, W.M.Z.W., Karuppuchamy, S., Ibrahim, N.A., 2013. Modification of oil palm mesocarp fiber characteristics using superheated steam treatment. Molecules 18, 9132–9146.

Nuopponen, M.H., Wikberg, H.I., Birch, G.M., Jääskeläinen, A.-S., Maunu, S.L., Vuorinen, T., Stewart, D., 2006. Characterization of 25 tropical hardwoods with fourier transform infrared, ultraviolet resonance Raman, and 13C-NMR cross-polarization/magic-angle spinning spectroscopy. Journal of Applied Polymer Science 102 (1), 810–819.

O'Sullivan, A., 1997. Cellulose: the structure slowly unravels. Cellulose 4, 173–207.

Ona, T., Sonoda, T., Ito, K., Shibata, M., Kato, T., Ootake, Y., 1997. Nondestructive determination of wood constituents by fourier transform Raman spectroscopy. Journal of Wood Chemistry and Technology 17 (4), 399–417.

Pan, X., Kadla, J.F., Ehara, K., Gilkes, N., Saddler, J.N., 2006. Organosolv ethanol lignin from hybrid poplar as a radical scavenger: Relationship between lignin structure, extraction conditions, and antioxidant activity. Journal of Agricultural Food Chemistry 54, 5806−5813.

Pandey, K.K., Vuorinen, T., 2008. UV resonance Raman spectroscopic study of photodegradation of hardwood and softwood lignins by UV laser. Holzforschung 62 (2), 183−188.

Pandey, K.K., 1999. A study of chemical structure of soft and hardwood polymers by FTIR spectroscopy. Journal of Applied Polymer Science 71, 1969−1975.

Papazoglou, E.G., 2007. *Arundo donax* L. stress tolerance under irrigation with heavy metal aqueous solutions. Desalination 211 (1−3), 304−313.

Pew, J.C., 1957. Properties of powered wood and isolation of lignin by cellulytic enzymes. Tappi 40 (7), 553−558.

Pickering, K.L., Abdalla, A., Ji, C., McDonald, A.G., Franich, R.A., 2003. The effect of silane coupling agents on radiata pine fibre for use in thermoplastic matrix composites. Composites Part A 34 (10), 915−926.

Pickering, K.L., Aruan Efendy, M.G., Le, T.M., 2016. A review of recent developments in natural fibre composites and their mechanical performance. Composites: Part A Applied Science and Manufacturing 83, 98−112.

Popescu, C.-M., Popescu, M.-C., 2013. A near infrared spectroscopic study of the structural modifications of lime (*Tilia cordata* Mill.) wood during hydro-thermal treatment. Spectrochimica Acta Part A: Molecular and Biomolecular Spectroscopy 115, 227−233.

Popescu, C.-M., Popescu, M.-C., Singurel, G., Vasile, C., Argyropoulos, D.S., Willfor, S., 2007. Spectral characterization of eucalyptus wood. Applied Spectroscopy 61, 168−1177.

Popescu, C.-M., Tibirna, C.M., Vasile, C., 2009. XPS characterization of naturally aged wood. Applied Surface Science 256 (5), 1355−1360.

Popescu, C.-M., Popescu, M.-C., Vasile, C., 2010a. Structural changes in biodegraded lime wood. Carbohydrate Polymers 79, 362−372.

Popescu, C.-M., Lisa, G., Manoliu, A., Gradinariu, P., Vasile, C., 2010b. Thermogravimetric analysis of fungus-degraded lime wood. Carbohydrate Polymers 80 (1), 78−83.

Popescu, C.-M., Larsson, P.T., Vasile, C., 2011. Carbon-13 CP/MAS solid state NMR and X-ray diffraction spectroscopy studies on lime wood decayed by *Chaetomium globosum*. Carbohydrate Polymers 83 (2), 808−812.

Popescu, M.-C., Popescu, C.-M., Lisa, G., Sakata, Y., 2011a. Evaluation of morphological and chemical aspects of different wood species by spectroscopy and thermal methods. Journal of Molecular Structure 988, 65−72.

Popescu, M.-C., Froidevaux, J., Navi, P., Popescu, C.-M., 2013a. Structural modifications of *Tilia cordata* wood during heat treatment investigated by FT-IR and 2D IR correlation spectroscopy. Journal of Molecular Structure 1033, 176−186.

Popescu, C.−M., Demco, D.E., Möller, M., 2013b. Solid state ^{13}C CP/MAS NMR spectroscopy assessment of historic lime wood. Polymer Degradation and Stability 98 (12), 2730−2734.

Pye, E.K., Lora, J.H., 1991. The ALCELL Process: A Proven Alternative to Kraft Pulping. Tappi Journal 74 (3), 113−118.

Qu, Y., Luo, H., Li, H., Xu, J., 2015. Comparison on structural modification of industrial lignin by wet ball milling and ionic liquid pretreatment. Biotechnology Reports 6, 1−7.

Rachini, A., Le Troedec, M., Peyratout, C., Smith, A., 2012. Chemical modification of hemp fibres by silane coupling agents. Journal of Applied Polymer Science 123 (1), 601−610.

Racovita, R.C., Peng, C., Awakawa, T., Abe, I., Jetter, R., 2015. Very-long-chain 3-hydroxy fatty acids, 3-hydroxy fatty acid methyl esters and 2-alkanols from cuticular waxes of *Aloe arborescens* leaves. Phytochemistry 113, 183−194.

Ray, D., Das, M., Mitra, D., 2009. Influence of alkali treatment on creep properties and crystallinity of jute fibres. Bioresources 4 (2), 730−739.

Rehbein, M., Koch, G., 2011. Topochemical investigation of early stages of lignin modification within individual cell wall layers of Scots pine (*Pinus sylvestris* L.) sapwood infected by the brown-rot fungus *Antrodia vaillantii* (DC.: Fr.) Ryv. International Biodeterioration & Biodegradation 65, 913−920.

Rencoret, J., Gutierrez, A., Nieto, L., Jimenez-Barbero, J., Faulds, C.B., Kim, H., Ralph, J., Martinez, A.T., del Rio, J.C., 2011. Lignin composition and structure in young versus adult *Eucalyptus globulus* plants. Plant Physiology 155 (2), 667−682.

Rodrigues, J., Faix, O., Pereira, H., 1998. Determination of lignin content of *Eucalyptus globulus* wood using FTIR spectroscopy. Holzforschung 52, 46−50.

Rogers, G.E., 1959. Electron microscope studies of hair and wool. Annals of the New York Academy of Sciences 83, 378−399.

Romanik, G., Gilgenast, E., Przyjazny, A., Kamiński, M., 2007. Techniques of preparing plant material for chromatographic separation and analysis. Journal of Biochemical and Biophysical Methods 70, 253−261.

Rowell, R.M., Young, R.A., Rowell, J.K., 1997. Paper and Composites From Agro-based Resources. CRC Press Inc., New York.

Rowell, R.M., Pettersen, R., Han, J.S., Rowell, J.S., Tshabalala, M.A., 2005. Cell wall chemistry. In: Rowell, R.M. (Ed.), Handbook of Wood Chemistry and Wood Composites. CRC Press, Boca Raton.

Rowell, R.M., 1977. Nonconventional wood preservation methods. In: Goldstein, I.S. (Ed.), Wood Technology Chemical Aspects, ACS Symposium Series, 43, pp. 47−56.

Rowell, R.M., 1984. Penetration and reactivity of cell wall components. In: Rowell, R.M. (Ed.), The Chemistry of Solid Wood, Advances in Chemistry Series, 207. American Chemical Society, pp. 175−210.

Rowell, R.M., 1991. Chemical Modification of Non-wood Lignocellulosics. In: Hon, D.N.-S. (Ed.), Chemical Modification of Lignocellulosic Materials. Marcel Dekker inc, ISBN 9780824794729.

Saka, S., Thomas, R.J., 1982. A study of lignification in loblolly pine tracheids by the SEM-EDAX technique. Wood Science and Technology 12, 51−62.

Samuels, A.L., Kunst, L., Jetter, R., 2008. Sealing plant surfaces: cuticular wax formation by epidermal cells. Annual Review of Plant Biology 59, 683−707.

Satpathy, S.K., Tabil, L.G., Meda, V., Naik, S.N., Prasad, R., 2014. Torrefaction of wheat and barley straw after microwave heating. Fuel 124, 269−278.

Savy, D., Mazzei, P., Roque, R., Nuzzo, A., Bowra, S., Santos, R., 2015. Structural recognition of lignin isolated from bioenergy crops by subcritical water: ethanol extraction. Fuel Processing Technology 138, 637−644.

Schwanininger, M., Rodrigues, J.C., Fackler, K., 2011. A review of band assignment in near infrared spectra of wood and wood components. Journal of Near Infrared Spectroscopy 19, 287−308.

Schwanninger, M., Hinterstoisser, B., Gierlinger, N., Wimmer, R., Hanger, J., 2004. Application of fourier transform near infrared spectroscopy (FT-NIR) to thermally modified wood. Holz als Roh und Werkstoff 62, 483−485.

Seborg, R., Millet, M., Stamm, A., 1945. Heat-stabilized compressed wood (staypak). Mechanical Engineering 67, 25−31.

Si, S., Chen, Y., Fan, C., Hu, H., Li, Y., Huang, J., Liao, H., Hao, B., Li, Q., Peng, L., Tu, Y., 2015. Lignin extraction distinctively enhances biomass enzymatic saccharification in

hemicelluloses-rich *Miscanthus* species under various alkali and acid pretreatments. Bioresource Technology 183, 248−254.
Siegle, S., 2001. Method of Producing a Pulp From Cellulosic Material Using Formic Acid and Hydrogen Peroxide. Patent US6183597.
Sinn, G., Reiterer, G.S., Stanzl-Tschegg, S.E., 2001. Surface analysis of different wood species using X-ray photoelectron spectroscopy (XPS). Journal of Materials Science 36, 4673−4680.
Smith, W., Dent, G., 2005. Modern Raman Spectroscopy. Wiley, Chichester.
Smith, M.E., Webb, G.A., 2000. Solid state NMR. Nuclear Magnetic Resonance 29, 251−315.
Smole, M.S., Hribernik, S., Kleinschek, K.S., Kreže, T., 2013. Plant fibres for textile and technical applications. In: Grundas, S. (Ed.), Advances in Agrophysical Research, ISBN 978-953-51-1184-9.
Sreekala, M.S., Kumaran, M.G., Joseph, S., Jacob, M., Thomas, S., 2000. Oil palm fibre reinforced phenol formaldehyde composites: influence of fibre surface modifications on the mechanical performance. Applied Composite Materials 7, 295.
Sreekala, M.S., Kumaran, M.G., Thomas, S., 2002. Water sorption in oil palm fiber reinforced phenol formaldehyde composites. Composites Part A 33 (6), 763−777.
Srinivas, K., Pandey, K.K., 2012. Effect of heat treatment on color changes, dimensional stability, and mechanical properties of wood. Journal of Wood Chemistry and Technology 32 (4), 304−316.
Stamm, A., Burr, H., Kline, A., 1946. Staybwood—A heat-stabilized wood. Industrial & Engineering Chemistry 38 (6), 630−634.
Sugiyama, J., Persson, J., Chanzy, H., 1991. Combined IR and electron diffraction study of the polymorphism of native cellulose. Macromolecules 24, 2461−2466.
Sun, R.C., Tomkinson, J., 2002. Characterisation of hemicelluloses obtained by classical and ultrasonically assisted extractions from wheat straw. Carbohydrate Polymers 50, 263−271.
Sun, R., 2010. Cereal Straw as a Resource for Sustainable Biomaterials and Biofuels. 1st Edition: Chemistry, Extractives, Lignins, Hemicelluloses and Cellulose. Elsevier, ISBN 9780444532343.
Swift, J.A., Smith, J.R., 2001. Microscopical investigations on the epicuticle of mammalian keratin fibres. Journal of Microscopy 204, 203−211.
Tjeerdsma, B., Militz, H., 2005. Chemical changes in hydrothermal treated wood: FTIR analysis of combined hydrothermal and dry heat treated wood. Holz als Roh und Werkstoff 63, 102−111.
Tjeerdsma, B.F., Boonstra, M., Pizzi, A., Tekely, P., Militz, H., 1998. Characterisation of thermelly modified wood: molecular reasons for wood performance improvement. Holz als Roh und Werkstoff 56, 149−153.
Todorović, N., Popović, Z., Milić, G., 2015. Estimation of quality of thermally modified beech wood with red heartwood by FT-NIR spectroscopy. Wood Science and Technology 49 (3), 527−549.
Tserki, V., Zafeiropoulos, N.E., Simon, F., Panayiotou, C., 2005. A study of the effect of acetylation and propionylation surface treatments on natural fibres. Composites: Part A 36, 1110−1118.
Tsuchikawa, S., 2007. A review of recent near infrared research for wood and paper. Applied Spectroscopy Reviews 42, 43−71.
Tuong, V.M., Li, J., 2011. Changes caused by heat treatment in chemical composition and some physical properties of acacia hybrid sapwood. Holzforschung 65 (1), 67−72.
Van den Bulcke, J., Boone, M., Van Acker, J., Stevens, M., Van Hoorebeke, L., 2009. X-ray tomography as a tool for detailed anatomical analysis. Annals of Forest Science 66, 508.

VanderHart, D.L., Atalla, R.H., 1984. Studies of microstructure in native celluloses using solid state C-13 NMR. Macromolecules 17, 1465−1472.

Wada, M., 2002. Lateral thermal expansion of cellulose I_β and III_I polymorphs. Journal of Polymer Science Part B 40 (11), 1095−1102.

Wang, W., Zhu, Y., Cao, J., Sun, W., 2015. Correlation between dynamic wetting behavior and chemical components of thermally modified wood. Applied Surface Science 324 (1), 332−338.

Ward, R.J., Willis, H.A., George, G.A., Guise, G.B., Denning, R.J., Evans, D.J., Short, R.D., 1993. Surface analysis of wool by x-ray photoelectron spectroscopy and static secondary ion mass spectrometry. Textile Research Journal 63, 362−368.

Welch, R.W., Hayward, M.V., Jones, D.I.H., 1983. The composition of oat husk and its variation due to genetic and other factors. Journal of the Science of Food and Agriculture 34, 417−426.

Wen, J.L., Sun, S.L., Yuan, T.Q., Sun, R.C., 2015. Structural elucidation of whole lignin from eucalyptus based on preswelling and enzymatic hydrolysis. Green Chemistry 17 (3), 1589−1596.

Wikberg, H., Maunu, S.L., 2004. Characterisation of thermally modified hard- and softwoods by ^{13}C CPMAS NMR. Carbohydrate Polymers 58 (4), 461−466.

Willems, W., Tausch, A., Militz, H., 2010. Direct estimation of the durability of high-pressure steam modified wood by ESR spectroscopy. The International Research Group on Wood Protection. IRG/WP 10−40508.

Wilson, K., White, D.J.B., 1986. The Anatomy of Wood: Its Diversity and Variability. Stobart& Sons Ltd, London.

Windeisen, E., Wegener, G., 2008. Behaviour of lignin during thermal treatments of wood. Industrial Crops and Products 27, 157−162.

Wu, S., Argyropoulos, D., 2003. An improved method for isolating lignin in high yield and purity. Journal of Pulp and Paper Science 29, 235−239.

Xu, F., Yu, J., Tesso, T., Dowell, F., Wang, D., 2013. Qualitative and quantitative analysis of lignocellulosic biomass using infrared techniques: a mini-review. Applied Energy 104, 801−809.

Yalcin, M., Sahin, H.I., 2015. Changes in the chemical structure and decay resistance of heat-treated narrow-leaved ash wood. Maderas: Ciencia y Tecnologia 17 (2), 435−446.

Yildiz, U.C., Yildiz, S., Gezer, E.D., 2005. Mechanical and chemical behavior of beech wood modified by heat. Wood and Fiber Science 37 (3), 456−461.

Yildiz, S., Yildiz, U.C., Tomak, E.D., 2011. The effects of natural weathering on the properties of heat-treated alder wood. BioResources 6 (3), 2504−2521.

Yokoi, H., Ishida, Y., Ohtani, H., Tsuge, S., Sonoda, T., Ona, T., 1999. Characterization of within-tree variation of lignin components in eucalyptus camaldulensis by pyrolysis−gas chromatography. Analyst 124, 669−674.

Yuan, Z., Long, J., Wang, T., Shu, R., Zhang, Q., Ma, L., 2015. Process intensification effect of ball milling on the hydrothermal pretreatment for corn straw enzymolysis. Energy Conversion and Management 101, 481−488.

Zhang, Y.-H.P., 2008. Reviving the carbohydrate economy via multi-product lignocellulose biorefineries. Journal of Industrial Microbiology & Biotechnology 35, 367−375.

Physical and mechanical properties of natural fibers

3

S.R. Djafari Petroudy
Faculty of New Technologies and Energy Engineering, Shahid Beheshti University, Mazandaran, Iran

3.1 Introduction

Technology development is aimed at creating a better standard of living for the benefit of mankind. Nowadays, the natural plant fiber form is an interesting option for the most widely applied fiber in the composite technology. Natural fibers have a good potential as a substitute for petroleum or nonrenewable source material in many applications. The development of environmentally friendly green composites is because of natural fiber's biodegradability, light weight, relative cheapness, high specific strength, natural abundance, plentiful supply, and swift replenishing ability (compared to nonrenewable products), and these characteristics are the strongest arguments to utilize them in the composites. Composites, the wonder material with lightweight, high strength-to-weight ratio and stiffness properties have come a long way in replacing conventional materials like metals, glass, plastics, etc. Since 1995, natural plant fiber (mainly from wood and nonwood materials) has emerged as the most acceptable alternative reinforcement for fiber composite products. The combination of interesting mechanical and physical properties of natural fibers and their environmental benefits have been the main drivers for their application as alternatives for conventional reinforcements in composites (Asasutjarit et al., 2007). For these reasons, much research has been conducted to study the exploitation of natural fibers as load-bearing constituents in composite materials (Asasutjarit et al., 2007). From an economic development and sustainability perspective, natural fiber reinforced composites provide an opportunity to develop forestry and an agriculture-based economy (nonfood sector). Furthermore, in comparison with the most common synthetic reinforcing fibers, natural fibers require less energy to produce and are the ultimate green products (Mobasher, 2012). The global natural fiber composite market reached $2.1 billion in 2010, with a compound annual growth rate of 15% in the last five years. The automotive and construction industries were the largest segment among all natural fiber composite applications. The North American natural fiber composite market was the largest for wood plastic division, whereas the European region was the leader in automotive segments, driven by government support, environmental regulations, and customer acceptance. By 2016, the natural fiber composite market is expected to reach $3.8 billion (Lucintel, 2011).

Advanced High Strength Natural Fibre Composites in Construction. http://dx.doi.org/10.1016/B978-0-08-100411-1.00003-0

3.2 Natural plant fiber

The cells of plants are surrounded by a rigid cell wall, and this is the main characteristic distinguishing them from cells in animals. In some types of cells, the cell walls are enlarged to have superior mechanical properties, which provide the required structural performance of the plants. The dimensions of these so-called fibers vary between different plants, but their overall shape is most often elongated with lengths in the range 1−35 mm and diameters in the range 15−30 μm. In the perspective of composite reinforcement, it is better to group the fibers by their lengths:

1. Short fibers (1−5 mm), originating typically from wood and nonwood species and typically used for making composites with in-plane isotropic properties, that is, composites with a nonspecific (random) fiber orientation.
2. Long fibers (5−50 mm), originating typically from nonwood annual plants species (eg, flax, hemp, jute) and typically used for making composites with anisotropic properties, that is, composites with a specific fiber orientation. Also, natural plant fiber consists of:
   - **a.** Seed hairs; fibers collected from seeds or seed cases i.e. cotton, kapok, coir and poplar seed. The most important seed fiber is cotton which have properties that permit them to be spun into thread or stuffing.
   - **b.** Bast fibers—fibers derived from the bark of dicotyledons, which include herbaceous plants, shrubs, and trees (hardwood, softwood, and recycled wood);
   - **c.** Leaf fibers, fibers derived from the vascular bundles of very long leaves of some monocotyledons. Leaf fibers are also known as "hard" fibers because they are more lignified than bast fibers;
   - **d.** Grass fibers, these are another group of monocotyledonous fibers, where the entire stem together with the leaves are pulped and used in papermaking. Such pulps are composed not only of fibers, but of other cellular elements as well (Bismarck et al., 2005) (Fig. 3.1).

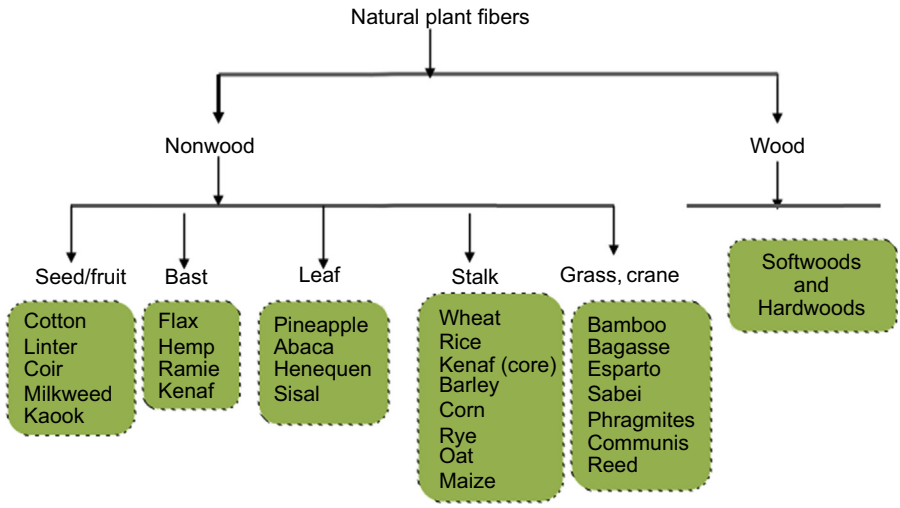

Figure 3.1 Hierarchy graph for natural plant fiber classification.

The chemical constituents and the plant fiber structure are fairly complicated. Plant fibers are a well-designed composite material by nature. The fibers are basically a rigid, crystalline cellulose microfibril-reinforced amorphous lignin and/or hemicelluloses matrix. Most plant fibers, except for cotton, are composed of cellulose, hemicelluloses, lignin, waxes, and some water-soluble compounds, where cellulose, hemicelluloses, and lignin are the major constituents (Bledzki and Gassen, 1999).

The major component of most natural plant fibers is cellulose. Cellulose is made up of thousands of glucose molecular units joined in long chains and represents 40—45% of plants. It contains 44.4% carbon, 6.2% hydrogen, and 49.4% oxygen and is relatively unaffected by alkalis and dilute acids. A framework substance as cellulose is a linear macromolecule consisting of D-anhydroglucose ($C_6H_{11}O_5$) repeating units joined by β-1,4-glycosidic linkages with a degree of polymerization (DP) of around 10,000 (Bismarck et al., 2005). Each repeating unit contains three hydroxyl groups (Sjöström, 1981). These hydroxyl groups and their ability to bond hydrogen play a major role in directing the crystalline packing and also govern the physical properties of cellulose materials (Sjöström, 1981).

Wood cellulose is about 60−70% crystalline, and solid cellulose has a semicrystalline structure, ie, consists of highly crystalline and amorphous regions (Williams, 2005). Cellulose forms slender rod-like crystalline microfibrils, whereas hemicelluloses are the matrix substances present between cellulose microfibrils. Lignin, on the other hand, is the encrusting substance solidifying the cell wall associated with the matrix substances. The significance of lignin as the encrusting substance can be demonstrated by examination of the lignin skeleton created by the acid removal of carbohydrates (Bismarck et al., 2005).

The roles of these three chemical substances in the cell wall are compared to those of the constructing materials in the structures made from the reinforced concrete in which cellulose, lignin, and hemicelluloses correspond, respectively, to the iron core, cement, and buffering material to improve their bonding (Fujita and Herada, 2001). The plant fibers comprise different hierarchical microstructures. The cell wall in a fiber is not a homogeneous membrane. It is built up of several layers; as can be seen from the SEM image of a natural plant fiber cross section (Fig. 3.2), the primary cell wall is the first layer deposited during cell growth, and the secondary cell wall (S) again consists of three layers (S1, S2, and S3). The cell walls are formed from oriented-reinforcing semicrystalline cellulose microfibrils embedded in a hemicelluloses/lignin matrix of varying composition (Bismarck et al., 2005).

Cellulose microfibrils with a diameter of about 10−50 nm provide mechanical strength to the natural plant fibers (Djafari Petroudy et al., 2015). In most natural plant fibers the cellulose microfibrils, as can be seen from Fig. 3.3(a,b) and Fig. 3.4, are oriented at an angle to the normal fiber axis called the Microfibrillar Angle (MFA). The structure, MFA, cell dimensions, defects, and the chemical composition of the plant fibers are the most important variables that determine the overall properties of the fibers (Mukherjee and Satyanarayana, 1986; Satyanarayana et al., 1986).

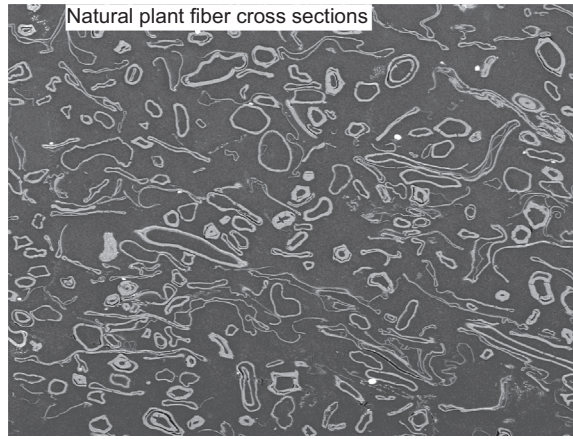

Figure 3.2 SEM image of natural plant fiber cross section.

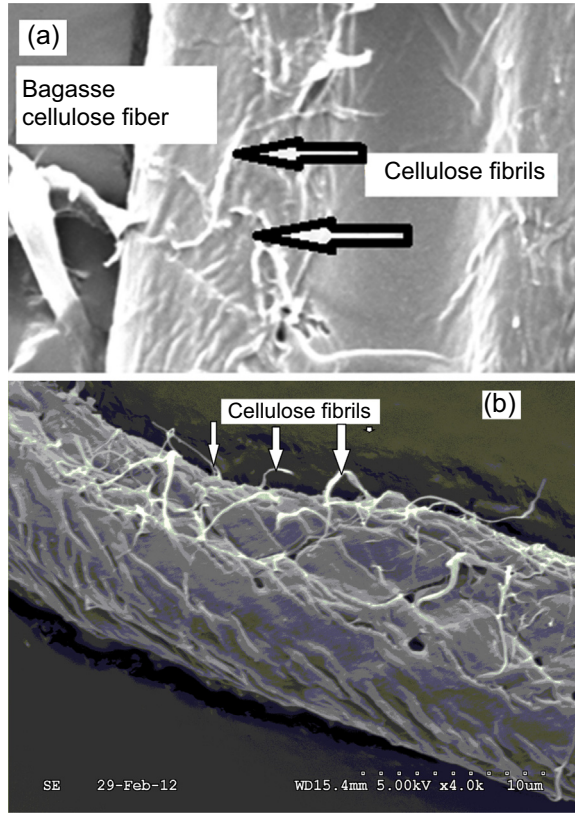

Figure 3.3 (a) SEM image of bagasse cellulose fiber. (b) SEM image of cellulose fibril features on a fiber surface.

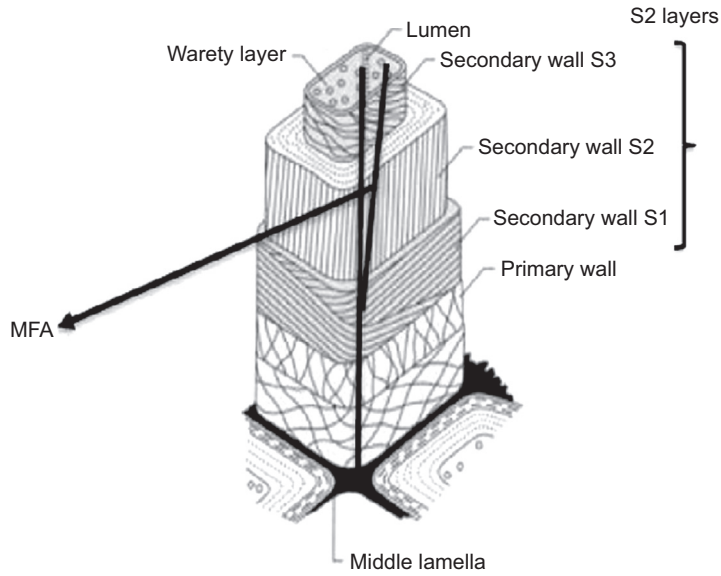

Fig. 3.4 MFA definition in the microstructure of plant cell wall together with cell wall sub-layers.

3.3 Physical properties of natural plant fiber

3.3.1 Ultrastructure

The hierarchical structure of natural plant fibers gives the fibrous material excellent performance properties, ie, high strength to weight ratio. The fibers can be obtained from woody and nonwoody plants by chemical, mechanical, and biological processes, as well as many combined processes. At the macroscopic level (normally 0.1−1 m), wood fibers mainly exist within the layer of xylem. Fig. 3.5 illustrates bagasse cell wall structure through top-down approach including its macrostructure as well as ultrastructure. In this figure a natural fiber is itself a composite material by nature because it consists of cellulose fibrils embedded in a hemicellulose/lignin matrix (Bismarck et al., 2005). The hemicellulose molecules are hydrogen bonded to cellulose and act as a cementing matrix between the cellulose microfibrils, forming the cellulose/hemicellulose network, which is thought to be the main structural component of the fiber cell (Bismarck et al., 2005). The mechanical properties of the fibers vary depending on their constitution and the amount of cellulose and the crystallinity. They are also influenced by the DP of the cellulose and microfibrillar orientation (Netravali, 2001). The MFA as microfibrillar orientation indicator especially affects the axial strength properties of a fiber. The fiber stiffness (and strength) is thus very sensitive to the microfibril angle, even if the mechanical properties in the microfibril direction are constant. The low microfibril angle of plant fibers makes them highly anisotropic (which also is the case for the synthetic carbon fibers but

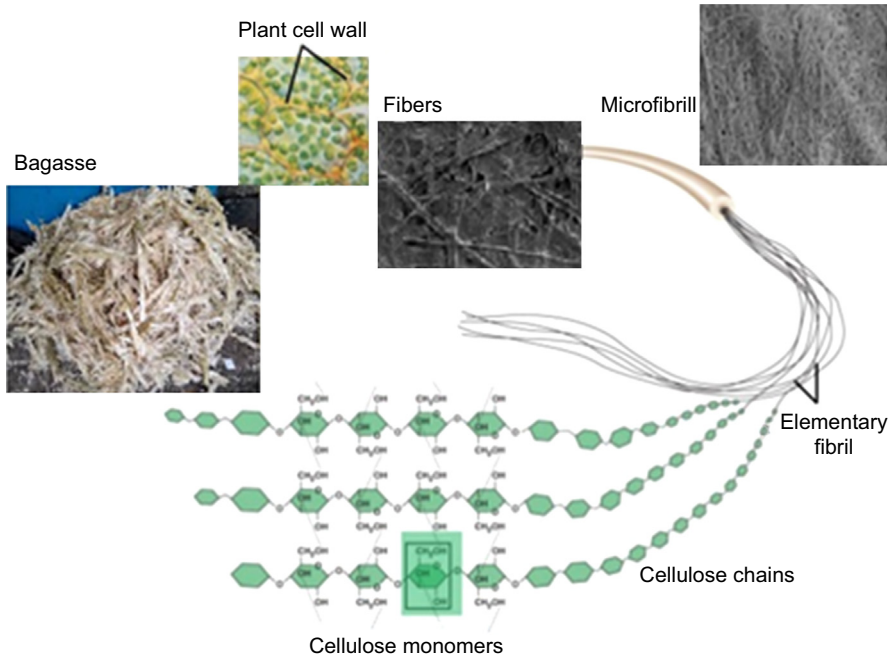

Fig. 3.5 The ultrastructure of bagasse cell wall.

not for glass fibers), and this leads to relatively low transverse mechanical properties, and as a result, cell wall structure dictates the physical properties of natural plant fiber.

3.3.2 Geometric features including fiber length, width, and aspect ratio

The mechanical properties of plant fibers are much lower when compared to those of the most widely used competing reinforcing glass fibers (Bismarck et al., 2005). However, because of their low density, the specific properties (property to density ratio), strength, and stiffness of plant fibers are comparable to the values of glass fibers (Wambua et al., 2003). Common natural fiber geometric diameter properties, comprising their length, width, and corresponding aspect ratio, are presented in Table 3.1. In this section, geometric diameter properties of common natural fibers are compared to each other.

Natural plant individualization includes two main methods: physical separation, such as the pulverizing process, and chemical separation, such as the pulping process. Pulverizing is the process by which the natural plant fibers are reduced into small particles (180−425 μm). It is the main step for the production of wood flour, which

Table 3.1 Geometric characterizations of common technically natural plant fibers

Fiber types	Mean length (mm)	Mean width (μm)	Aspect ratio	References
Softwoods	2–6	20–40	50–200	Da and Fan (2014)
Hardwoods	1–2	10–50	28–86	Da and Fan (2014)
Wheat straw	1.5	15	100	Mohanty et al. (2005a,b)
Rice straw	0.65–3.48	5–14	170	Mohanty et al. (2005a,b)
Flax	33	19	1737	Mohanty et al. (2005a,b)
Hemp	25	25	1000	Mohanty et al. (2005a,b)
Kenaf	5	21	238	Mohanty et al. (2005a,b)
Sisal	3	20	150	Mohanty et al. (2005a,b)
Jute	2	20	100	Mohanty et al. (2005a,b)
Cotton	25	20	1250	Mohanty et al. (2005a,b)
Ramie	12–15	20–75	2000–6000	Berglund (2012)
Abaca	6	24	250	Mohanty et al. (2005a,b)
Bamboo	2.7	14	193	Mohanty et al. (2005a,b)
Esparto	1.9	13	146	Mohanty et al. (2005a,b)
Bagasse	0.68–1.7	22.8–20	29.8–85	Mohanty et al. (2005a,b)
				Djafari Petroudy et al. (2015)
Sunflower stalk	1.18	22	55	Ashori and Nourbakssh (2010)
Oil palm fiber	6	15–50	12–40	Shinoj and Visvanathan (2015)
Cereal straw	1.5	23	65	Mohanty et al. (2005a,b)
Coir	0.7	20	35	Mohanty et al. (2005a,b)
Cellulose fibril	>10,000	2–10	>10,000	Siro and Plackett (2010)
Microfibrillated cellulose (MFC)	>10,000	10–40	100–150	Siro and Plackett (2010)
Cellulose whisker	100–600	2–20	10–100	Siro and Plackett (2010)

is mainly used as filler in different composites. For dry mechanical processing, the final products typically have low aspect ratios (only 1−5). These low aspect ratios allow wood flour to be more easily metered and fed than individual natural plant fibers, which tend to bridge. Aspect ratio is one of the most important parameters governing mechanical properties, which can be obtained from geometric characterizations. However, the low aspect ratio limits the reinforcing ability. For maximum reinforcement, the fiber aspect ratio of any composite system should be above its critical value to ensure maximum stress transfer to the fiber before composite failure. Fiber aspect ratio lower than the critical value results in insufficient stress transfer to fiber and thus the reinforcement is improper, and in some cases, fiber just acts as fillers (Hull and Clyne, 1996; De and White, 1996; Mallik, 2007). In contrast, if the fiber aspect ratio is too high the fibers may get entangled during processing, leading to poor mechanical properties due to poor dispersion, since cellulosic fibers are flexible and are less prone to breakage during processing. This ensures that the input fiber length distribution remains the same even after processing. Thus it is important to know fiber length/fiber length distribution (in the case of natural/short fibers) in order to determine the efficacy of reinforcement material. High aspect ratio means that only small proportions of the fiber ends carry lower stress (Berglund, 2012). The very high aspect ratio of the seed fibers makes them suitable for spinning technologies. For natural plant fiber with a short aspect ratio, ie, coir, cereal straw, and bagasse, the stress in the fiber never reaches the fiber strength, and when the composite fails, intact fibers are pulled out of the matrix. Some minimum fiber length is therefore needed in order to utilize the fiber strength. This gives a definition for the critical fiber length (l_{crit}). l_{crit} is the shortest length of fibers in a given composite that allows the fibers to be loaded maximally so that they start failing (Berglund, 2012). Mohanty et al. (2005a,b) reported that when the fiber aspect ratio is in the range 10−50, moduli ratios of 10^2−10^3 can be achieved if there is good adhesion between the fiber and the matrix. It can be concluded that improved tensile and flexural strength and impact performance can be achieved by increasing both the aspect ratio and the fiber volume fraction, as it provides more space for interaction with the matrix (Yilmaz, 2015). However, partial fibrillation of short natural fibers is the most important way to increase the aspect ratio and surface area per unit volume of the fiber bundles (Djafari Petroudy et al., 2014). The fibers will be a filler rather than reinforcement below at a critical aspect ratio.

3.3.3 Microfibrillar angle (MFA)

Microfibrillar angle is defined as the angle microfibrils make with respect to the fiber axis (Fig. 3.4). The MFA of some natural plant fibers are presented in Table 3.2. It is concluded that microfibrillar angle is the main parameter that affects the inherent fiber strength properties. Also, it is reported that higher cellulosic content and lower MFA are essential for high fiber strength (Mohanty et al., 2005a,b). In this connection, Mukherjee and Satyanarayana (1986) have shown that fibers with higher cellulosic content and lower MFA when pulled in tension possess higher ultimate tensile strength and initial modulus with intracellular fracture. Mohanty et al. (2005a,b) reported that a

Table 3.2 The Microfibril angle (MFA), C_I, and cellulose content values in some natural plant fibers

Fiber	MFA (degrees)	Cellulose crystallinity	Cellulose content (%)	References
Hemp	6	50–90	70–74	Gassan et al. (2001)
Flax	6–10	50–90	64–71	Gassan et al. (2001)
Jute	8	50–80	61–72	Gassan et al. (2001)
Sisal	10–25	50–70	66–78	Gassan et al. (2001)
Banana	11	45–55	44–64	Gassan et al. (2001)
Coir	30–49	27–33	32–43	Gassan et al. (2001)
Sisal	10–25	50–70	66–78	Gassan et al. (2001)
Ramie	8	64	76	Gassan et al. (2001)
Abaca	22.5	52	62	John and Sabu (2012)
Cornstalk	10.9	52–59		John and Sabu (2012)
Soybean straw	12	47	85	John and Sabu (2012)
Oil palm	46	20–30	40–50	Mohanty et al. (2005a,b)
Bagasse	14–15	51.1	52	John and Sabu (2012)
Pineapple leaf fibers	12–14	44–60	70–82	Mohanty and Fatima (2015)
Bamboo	2–10	40–60	26–60	Mohanty and Fatima (2015)
Softwood fiber	3–45	52–62	40–45	John and Sabu (2012)
Eucalyptus	3–44	68	40–50	John and Sabu (2012)
Pine (kraft pulp)	N.D	68	76	John and Sabu (2012)

N.D, No data available

higher MFA and lower cellulose content impart ductility to the fibers, as in the case of a coir fiber. It is reported that the larger the MFA, the higher the failure strain, since the fibrils will be able to twist when stretched (Hu and Hsieh, 1996; Mwaikambo and ansell, 2002). This is not true for all natural plant fibers, as cotton and bamboo fibers possess several MFA.

The small angle of the MFA dictates the overall anisotropic properties of the fibers. The Young's modulus of the cell wall will then depend on the volume fraction of cellulose and the average MFA with respect to the loading direction. Such a model clarifies the effect of MFA on a wood modulus (Wainwright et al., 1982). The effect of MFA on a modulus is also clear from data on sisal fiber specimens and modulus differences between different bast fibers.

Generally, it can be noted that the MFA in wood fibers varies in the range from 3−45 degrees depending on the type and location of the fibers in the wood (eg, early and late wood), whereas MFA in plant fibers is more constant in the range from 6−10 degrees (Anagnost et al., 2002). In terms of strength, the MFA is a very important property, and the MFA is inversely proportional to fiber stiffness. As Page et al. (1977) reported, the stiffness of wood fibers is well correlated with the MFA, ie, at small angles (<5 degrees), stiffness is in the range 50−80 GPa, and at large angles (40−50 degrees), stiffness is reduced to about 20 GPa. From Table 3.2, it can be concluded that nonwood fibers have higher stiffness in comparison to wood fibers. Higher stiffness and strength of the fiber can be obtained when the MFA is found to be small, but higher MFA leads to higher ductility in the fiber. The ductility of the fiber also depends upon the orientation of the microfibrils. If the microfibrils are spirally oriented to the fiber axis, the ductility of the plant fibers is found to be more. But if the microfibrils have a parallel orientation to the fiber axis, the fiber characteristics will be rigid and inflexible with high tensile strength. In addition the failure strain is smaller for lower MFA. The MFA also dictates the nonlinear stress-strain behavior of plant fibers. While the elastic range is smaller for higher MFA, the plastic range increases with increasing MFA.

Satyanarayana et al. (1986) established a semiempirical relationship to correlate the fiber elongation and the MFA:

$$\varepsilon = 2.78 + 7.28 \times 10^{-2}\theta + 7.7 \times 10^{-3}\theta^2 \tag{3.1}$$

where ε = elongation percentage and θ = MFA and also the tensile strength and MFA with the cellulose content

$$\sigma = 334.005 - 2.830\theta + 12.22W \tag{3.2}$$

where σ = tensile strength and W = cellulose content.

From the aforementioned equations, it can be concluded that the smaller the MFA, the stiffer and stronger the fiber and the superior mechanical properties of natural plant fibers are associated with its high cellulose content and comparatively low MFA.

3.3.4 Cellulose content and its crystallinity index (C_rI)

Cellulose includes crystalline and amorphous regions. Cellulose content and cellulose crystallinity are two critical microstructural parameters that affect the mechanical properties of natural plant fibers. Crystalline cellulose has significantly better stiffness than all other constituents. Hence when selecting plant fibers for use as reinforcement in structural applications, high cellulose content and high cellulose crystallinity are desirable. Table 3.2 presents typical values for the cellulose content and its crystallinity of various plant fibers. As it can be seen from Table 3.2, wood fibers show lower cellulose crystallinity than natural plant fibers, with typical values in the ranges of 55−70% and 60−70%, respectively. Also, the crystallinity values increased upon partial delignification of natural plant fiber and alkaline peroxide bleaching. Moreover, physical and chemical treatments of plant fibers are known to change the cellulose content as well as degree of crystallinity. The rigidity of cellulose fibers increases and their flexibility decreases with increasing the ratio of crystalline to amorphous regions. While increasing crystallinity means greater strength, decreasing crystallinity means increasing elongation, higher water intake, and sites available for chemical reactions. Reddy and Yang (2005), reported a crystallinity degree of 48−50% and crystal size of 3.2 nm for corn husk fibers compared to those of flax and jute, which are 65−70% and 2.8 nm, for degree of crystallinity and crystal size, respectively. The crystallinity also has an effect on moisture absorption of the fibers, since amorphous regions can absorb more water. Poletto et al. (2014), concluded that the thermal decomposition of natural fibers is shifted to higher temperatures with an increase in the cellulose crystallinity and crystallite size. These results indicated that the cellulose crystallite size affects the thermal degradation temperature of natural fibers.

3.3.5 Density

The biodegradable plant-based "lignocellulosic" fibers are nonabrasive and hence do not cause much damage. They have a hollow and cellular nature and thus perform well as acoustic and thermal insulators. The hollow tubular structure also reduces their bulk density and makes them lighter in weight. An advantage of natural plant fiber over E-glass fiber for reinforcement is their 40−50% lower density. Different natural plant fibers have varying density values. The density and some corresponding strength properties of natural plant fiber are shown in Table 3.3.

It is to be noted that from Table 3.3, most natural fibers have a maximum density of about 1600 kg/m^3 and are heavier than water. Though some natural fibers, such as wood, are hollow and have low densities in their native state, they are often densified during processing. Nevertheless, even the maximum density of these fibers is considerably less than that of inorganic fibers such as glass fibers. As such, their low density makes them attractive as reinforcements in applications where weight is a consideration. Natural fibers are added to plastics to improve mechanical performance, such as stiffness and strength, without increasing the density too much (Mohanty and Fatima, 2015). The generally low-impact performance of natural fiber composites tends to limit their use, and addressing this issue is an active area of research. The

Table 3.3 Density and properties of some synthetic organic and inorganic fibers are added for comparison

Fiber	Fiber type	Density (Kg/m^3)	Tensile strength (MPa)	Elongation at break (%)	Young's modulus (GPa)	References
Flax		1380	343–1035	1.2–3	27.6	Mohanty et al. (2005a,b)
Jute		1230	187–773	1.5–3.1	13–26.5	Mohanty et al. (2005a,b)
Hemp	Bast	1350	580–1110	1.6–4.5	70	Mohanty et al. (2005a,b)
Kenaf (bast)		1200	295–930	2.7–6.9	53	Mohanty et al. (2005a,b)
Ramie		1440	400–938	2–4	61.4–128	Mohanty et al. (2005a,b)
Sisal		1200	507–885	1.9–3	9.4–22	Mohanty et al. (2005a,b)
Pineapple	Leaf	1500	170–1627	1–3	34.5–82.5	Mohanty et al. (2005a,b)
Banana		1350	529–914	3–10	8–32	Mohanty et al. (2005a,b)
Cotton		1500–1600	287–587	7–8	5–13	Mwaikambo (2006)
Coir	Seed	1200	175	30	4–6	Mwaikambo (2006)
Oil palm		700–1550	248	14	3.2	Mwaikambo (2006)
Kenaf (core)		310	N.D	N.D	N.D	Thakur and Singha (2013)

Bamboo	Stalk/grass/wood	800–1400	391–1000	2	11–30	Thakur and Singha (2013)
Bagasse		1200	20–290	1–3		Thakur and Singha (2013)
Softwood kraft pulp		1500	1000	N.D	40	Thakur and Singha (2013)
Hardwood kraft pulp		1200	950	N.D	37.9	Thakur and Singha (2013)
Wheat straw		1600	273	2.7	4.76–6.58	O'Dogherty et al. (1995)
Rice straw		1650	449	2.2	1.21–1.25	Tavakoli et al. (2010)
E-glass		2500	2000–3500	2.5	73	Mohanty et al. (2005a,b)
S-glass Synthetic fiber		2500	4570	2.8	86	Mohanty et al. (2005a,b)
Aramide		1400	3000–3150	3.3–3.7	63–67	Mohanty et al. (2005a,b)
Carbon		1400	4000	1.4–1.8	240–425	Mohanty et al. (2005a,b)

OPEFB, oil palm empty fruit bunch; *N.D*, No data available

low density of natural fibers offers more flexibility in composite structure design (Mohanty and Fatima, 2015). Since density plays a significant role in biocomposite weight reduction, Madsen and Gamstedt (2013), have stated that due to the low density of lignocellulosic fibers, the specific mechanical properties of cellulose fiber composites is particularly competitive compared with glass fiber composites. Joseph et al. (1996), have concluded that the addition of 10% short sisal fibers into low density polyethylene increases the storage moduli and loss moduli of the composites, which then become steady at a higher volume fraction. An advantage of natural plant fibers over glass fibers for reinforcement is their 40−50% lower density. This becomes particularly important where the weight of the structure needs to be reduced. Hence the specific properties of composites are of interest, particularly as specific tensile modulus and tensile strength. It is to be noted that the natural fiber density of approximately 1500 kg m^{-3} higher fiber content at the same structural weight can be incorporated into biocomposites, resulting in a higher reinforcement. Owing to the excellent mechanical and low-density properties of natural plant fibers, these high-performance fibers and derived composites became very popular in aerospace, marine, automotive, and construction industries (Kandola, 2012).

3.3.6 Water, moisture absorption, and swelling thickness

High moisture content, or a water absorption characteristic, is one of the natural plant fiber obstacles for different applications. This is an intrinsic property of natural plant fibers due to free hydroxyl and other polar groups existing therein and leads to a decrease of the mechanical properties and the dimensional stability, whereas it may play a positive role in the biodegradability of biocomposites (Mukhopadhyay and Fangueiro, 2009). In the lignocellulosic fibers, hemicelluloses are the main contributor to water absorption, although the noncrystalline cellulose regions and lignin also take part in the process. Hemicellulose consists of highly hydrophilic polysaccharide chains, which are the main contributor to water absorption by lignocellulosic fibers as they are more accessible than the cellulose chains in crystalline regions (Djafari Petroudy et al., 2015). In the water absorption process, water saturates the cell walls of the natural plant fiber. Next, water occupies void spaces; this “free” water does not lead to additional swelling such as thickness swelling. Water absorption in a fibrous composite is dependent on many factors such as temperature, fiber loading, fiber orientation, fiber permeability, surface protection, area of the exposed surfaces, diffusivity, void content, and hydrophilicity of the individual components. ASTM D 5708 was used to measure the water and moisture absorption of natural plant fiber biocomposites. Mohanty and Fatima (2015), have stated that this test is carried out to determine the amount of water absorbed and performance of the materials in water environments. This is very similar to the moisture absorption test. Three square-shaped samples of 3.0 cm × 3.0 cm of 5% natural rubber-based jute composite were kept in an oven at a temperature of 100°C. Then weights of the three samples were measured. After that, these samples were kept in a Petri dish full of distilled water. Then after

24 h and 48 h, the weights of the samples were taken, and the water absorption was calculated using Eq. (3.3).

$$\text{Water absorption } (\%), \quad W_a = (W_1 - W_2)/W_1 \times 100 \tag{3.3}$$

Where W_1 is original weight of the sample and W_2 is final weight of the sample after 24, 48, and 120 h.

Mohanty and Fatima (2015), have also concluded that the percentage of the water and moisture absorption gradually increases with time, and then it reaches a saturation point where an average of 114% of water and 10.05% of moisture are absorbed at the end of 120 h. Thickness swelling can be introduced as an important indicator for water absorption performance. In this connection, ASTM D570 standard covers a method for the determination of swelling in water of natural plant composites. Based on this standard, the hydrophilic nature of 3 cm× 2.7 cm× 0.4 cm natural plant fiber composite can be investigated. The average of the three values obtained for the change in thickness expressed as a percentage of the original average thickness is reported as the swelling value. The thickness of swelling in water was measured as per Eq. (3.4),

$$\text{Thickness swelling } (\%), \quad T_S = \frac{T_2 - T_1}{T_1} \times 100 \tag{3.4}$$

Where T_1 is initial thickness and T_2 is the final thickness after water absorption.

Mohanty and Fatima (2015), have reported that the jute composite saturation point occurred at 24 h, and thickness swelling was approximately 100%.

3.3.7 Water repellent treatment

One of the major weaknesses of the natural plant fibers as a matrix is their water absorption and swelling thickness. As the fibers absorb water they expand, and when the earth is drying they lose water and their dimensions change to original size. Therefore they lose the bonding with the filler material. Generally the water absorption of the natural fiber composites increased with the increase in natural fiber contents in composites. Fickian diffusion is normally used to study the water absorption of natural fiber composites (Mohanty et al., 2005a,b). When the water absorption curve fits the linear Fickian diffusion curve the water absorption process is considered a Fickian diffusion. In a typical linear Fickian diffusion curve the water absorption of natural fiber composites increased linearly as a function of the time of water soaking during the early period of immersion; then it reached a plateau region and finally the curve became constant. Water absorption in natural fiber composites can be reduced by the use of a coupling agent in the fiber matrix interface. It is distributed on the surface of the fiber (Mohanty et al., 2005a,b). The coupling agent blocked the water permeation into the fiber. Zabihzadeh (2010a,b) has reported that inclusion of Maleated Polyethylene (MAPE) into the composite formulation is routinely conducted for water

repellent. Although in some cases, the inclusion of MAPE in the formulation actually resulted in greater water absorption than that from composites without MAPE. Also, several investigators have reported that incorporation of maleate olefins with the composite blend considerably reduces water absorption when using biofillers such as with Paulownia wood, loblolly wood, pine wood, sisal fiber, and wheat straw (Joseph et al., 2002; Ayrilmis and Kaymakci, 2013). Rozman et al. (1998), concluded that treating oil plam empty fruit bunches (EFB) with Maleic Anhydride (MAH) would result in the OH groups being converted to a more hydrophobic ester group, and as a result, water absorption and thickness swelling of the composites with MAH-treated EFB were lower than those without treated EFB.

Bisanda and Ansell (1991), concluded that the water absorption of the sisal−epoxy composites could be remarkably reduced by the treatment of the fibers with a pure silane. The effects of various chemical modifications ie, dewaxing, alkali treatment, cyanoethylation, and Acrylonitrile (AN) grafting of Pineapple leaf fiber (PALF) on its mechanical properties and water absorption have been studied. All types of chemical modifications of the fiber improved the mechanical strength of the resultant composites as well as reduced the percentage of water absorption (Ray and Rout. 2005). The addition of polyvinyl alcohol and fast curing agents for cement could improve bending strength and dimensional stability and significantly reduce water absorption and swelling thickness (Mo et al., 2005). Linoleic acid was more effective than oleic acid in reducing the water absorption of sheets, possibly due to the filling up of the pores and gaps in the structure and preventing it from swelling (Santosa and Pauda, 1999).

Hybridization also has a profound effect on the water absorption property of composites. An attempt to study the moisture uptake characteristics of hybrid systems was performed by Mishra et al. (2003). The composite systems chosen were sisal/glass and pineapple/glass fiber reinforced polyester composites. Composites were prepared by varying the concentration of glass fiber and by subjecting the biofibers to different chemical treatments. The authors observed that water uptake of hybrid composites was less than that of unhybridized composites. A comparative study of the water absorption of the glass fiber (7 wt%)/natural biofiber (13 wt%) with that of nonhybrid composites shows lower water absorption (Rout et al., 2001).

3.4 Mechanical properties of natural plant fiber

3.4.1 Tensile strength and Young's modulus

Natural plant fibers possess high strength and stiffness. Cellulose fibrils in all natural plant fibers have typically a diameter of about 10−30 nm, are made up of 30−100 cellulose molecules in an extended chain conformation, and provide mechanical strength to the fiber. The structure, microfibrillar angle, cell dimensions and defects, and the chemical composition of the plant fibers are the most important variables that determine the overall properties of the fibers (Mohanty et al., 2005a,b). Generally the tensile strength and Young's modulus of plant fibers increase with increasing cellulose content of the fibers. The natural fiber can be considered as a composite material

consisting of cellulose, hemicelluoses, pectin, lignin, and waxes. The reinforcing elements of natural fibers are cellulose microfibrils; the microfibrils are surrounded by the matrix elements hemicelluloses and lignin. When a load is applied, the microfibrils become aligned with fiber axis. The failure of fiber takes place when a matrix element losses its bonding with the reinforcing fibrils, and the hydrogen bonding in the cellulose microfibrils is broken. Hence, the smaller the content of cellulose, the lower the tensile strength (Komuraiah et al., 2014). From chemical composition viewpoint, it can be concluded that an increase in the content of hemicelluloses decreases the tensile strength since hemicelluloses are amorphous in nature and nonhomogeneous in their properties (Park et al., 2006). The orientation of the cellulose fibrils with respect to the fiber axis determines stiffness of the fibers. Plant fibers are more ductile if the fibrils have a spiral orientation to the fiber axis. Fibers are inflexible, rigid, and have a high tensile strength if the fibrils are oriented parallel to the fiber axis. They serve as reinforcement by giving strength and stiffness to the matrix structure. Table 3.3 shows the broad classification of natural plant fibers (nonwood and wood fibers) over synthetic fibers with their reinforcement potential. As can be seen from this classification the tensile strengths, as well as Young's modulus of natural fibers like kenaf, hemp, flax, jute, and sisal, are lower than that of E-glass fibers commonly used in composites. However, the density of E-glass is high, $\sim$2.5 g/cm^3, while that of natural fibers is much lower ($\sim$1.4 g/cm^3). The specific strength and specific moduli of some of these natural fibers are quite comparable to glass fibers (Mohanty et al., 2000, 2002). This becomes particularly important where the weight of the structure needs to be reduced. However, the origin place and climatic conditions affect the physical-mechanical properties of natural plant fibers. Researchers are going to produce a new generation of cellulose-rich biofibers for wide-scale industrial applications due to the important role of natural plant fibers in the composite industries (Mohanty et al., 2005a,b). Table 3.3 presents that the tensile and Young's modulus of natural plant fibers are in the following order: bast fiber > leaf fiber > seed fiber. In fact, only bast fibers have tensile strength and Young's modulus comparable to inorganic fibers such as glass and carbon. It is also important to note that natural plant fibers with poor mechanical properties may be suitable for nonstructural applications.

3.4.2 Elongation at break (%)

Elongation at break, also known as fracture strain, is the ratio between changed length and initial length after breakage of the test specimen. It expresses the capability of natural plant fiber to resist changes of shape without crack formation. The elongation at break can be determined by tensile testing in accordance with EN ISO 527. In general, synthetic fibers show better mechanical and physical properties compared to the natural fiber, whereas the specific modulus and elongation at break are better in natural fibers than the synthetic fibers, which is considered as an important factor in polymer engineering composites. Bast and leaf fibers have lower elongation at break compared to industrially man-made fiber as well as seed or stalk fibers. This statement can clearly be seen from Table 3.3, where fibers with high elongation values show lower strength and Young's modulus values. Generally the inclusion of natural plant fibers into

thermoplastics, such as polyethylene or other thermoplastic polymers, results in a decrease in elongation at break but an increase in Young's modulus. Surface chemical treatment, such as NaOH treatment, improved the elongation of the fiber almost twofold, but no improvement in tensile strength was observed (Du et al., 2015). Yu et al. (2010), concluded that the NaOH treatment was shown to be more effective than the silane treatment. Increasing concentrations of natural plant fiber resulted in increased tensile strength and water vapor permeability but decreased elongation at break. In contrast to this finding, Tewari et al. (2012), have shown that the decrease in ultimate tensile strength with an increase in bagasse fiber content is due to voids present in the material. As bagasse content increased, the modulus of elasticity and ultimate compressive strength decreased. On the other hand, percentage elongation and impact strength increased with the increase of bagasse content in the composite, due to the more elastic nature of natural fibers in comparison to resin. The addition of bagasse fiber reduced the bending strength and hardness of the composite. The stress–strain curve of natural fibers is nonlinear. Cellulose corresponds to high stresses and hemicelluloses to low ones. When hemicelluloses fail, the stresses are transferred to microfibrils (Komuraiah et al., 2014). These authors have concluded that the regression graph of failure strain lignin content shows that an increase in lignin content increases the failure strain. Also, this result is supported by the observation made by Agu et al., which concluded that a high content of lignin increases the extension ability of natural fibers (Agu et al., 2012). A similar observation is also made by Mortazavi and Moghaddam 2010 which found that leafiran fibers (with 26% lignin) had a greater elongation than kenaf (17% lignin), jute (9% lignin), and pineapple (8.3% lignin) fibers.

3.4.3 Impact strength

Natural plant fiber capability to withstand a suddenly applied load is defined as impact strength and is expressed in terms of energy. In other words, the impact strength is defined as the ability of a material to resist the fracture under stress applied at a high speed. The impact properties of composite materials are directly related to their overall toughness (Ndiyae et al., 2015). They are often measured with the Izod impact strength test or Charpy impact test, both of which measure the impact energy required to fracture a sample. Volume, modulus of elasticity, distribution of forces, and yield strength affect the impact strength of a material. In the Izod standard test, the only measured variable is the total energy required to break a notched sample. This test can be determined by tensile testing in accordance with ASTM D256. Like other mechanical properties, the impact strength of biocomposites is highly affected by the fiber, ie, the impact strength of biocomposites increase with increasing fiber content. Muller and Krobjilowski (2004), have concluded that flax fibers offer the highest reinforcing potential over different natural fibers (hemp, kenaf, and E–glass). This superiority is most distinctive regarding the tensile and impact strength of the composites. They have also stated that composites with fine reinforcing natural fibers offer the highest impact strength. At the same time, high fiber elongation capabilities lead to high impact strength. Impact strength increases with the number of fiber layers but decreases with fiber spacing. For coir/polyester concrete, low fiber content and

fiber length improve the impact strength. From a large number of studies on biocomposites, it has been understood that the impact strength may be enhanced by appropriate chemical and physical treatments of natural fibers (Cho et al., 2014). Ray et al. (2014), observed that in composites with weak interfacial bonding, the crack propagated along the fiber−matrix interface caused debonding, which could lead to a significant increase of the energy absorption ability of the composites.

3.4.4 Flexural strength

Flexural strength is the ability of a material to withstand bending forces perpendicular to its longitudinal axis. The resulting stresses are a combination of compressive and tensile stresses. If a composite component is a beam subject to bending, a flexural test is more appropriate. Test methods are reported in ASTM D790 and ISO 178 (Shanks, 2015). The flexural strength and modulus have an increasing trend with increased fiber loading and fiber content. Long natural fibers such as bast and leaf fibers have the highest efficiency among the lignocellulosic reinforcements. In this connection the composites reinforced with kenaf bast fibers are found to have higher strength than kenaf core fiber composites (Ishak et al., 2010). Bogoeva-Gaceva et al. (2007), reported that theoretically, tensile and flexural moduli of composites are strongly dependent on the modulus of the components and display slight sensitivity to interfacial adhesions. In natural fiber reinforced biocomposites, the inclusion of a rigid phase, such as cellulose fibers, contributes to increase the polymer matrix stiffness. They have also concluded that flexural strengths are sensitive of the fiber/matrix interfacial adhesion, and the interface is a determining factor in transferring the stress from the matrix to the fibrous phase. For obtaining the best results from this statement and optimization of a strong fiber/matrix interfacial adhesion, generally two approaches are considered as effective: the fiber surface modification and the use of an appropriate compatible agent. In fact, composites whose surfaces are smoother and more homogeneous exhibit the greatest flexural modulus. Dash et al. (2000), concluded that the much higher flexural properties of the bleached fiber composites compared to the untreated fiber composites were attributed to a greater interfacial adhesion in bleached fiber composites. Fiber length plays a major role in the development of flexural strength and fracture toughness of a fiber reinforced composite. As the length increases, both properties improve over a range of fiber contents. Reis (2006), reported that the effectiveness of coir fiber on the flexural properties (eg, flexural toughness) of cementitious composites was even better than synthetic glass or carbon fibers. He also stated an increment of 25.1% and 3.5% and a decrease of 21% are the result of coconut fiber, bagasse, and banana pseudostem reinforcement for flexural strength, respectively compared to unreinforced polymer concrete, and concluded that coconut fiber proves to be an excellent reinforcement for polymer concrete, increasing the fracture and flexural results. Also, it can be mentioned that all types of fiber chemical modifications improve the mechanical properties such as tensile strength, flexural strength, and impact strength. In this context, alkalized and long fiber composites give higher flexural modulus and flexural strength compared with composites made from as-received and short fibers.

Table 3.4 Stiffness and tensile properties of different plant fibers

Natural fiber	Fiber type	Stiffness (GPa)	Ultimate stress (MPa)	References
Hemp	Bast	30–60	300–800	Lilholt and Lawther (2000)
Flax	Bast	50–70	500–900	Lilholt and Lawther (2000)
Jute	Bast	20–55	200–500	Lilholt and Lawther (2000)
Sisal	Leaf	9–22	100–800	Lilholt and Lawther (2000)
Softwood	Stem	10–50	100–170	Anagnost et al. (2002)

3.4.5 Stiffness

There has been research in biocomposites that has demonstrated the advantages of lignocellulosic fibers as excellent stiffness and strength (Faruk and Saine, 2015). In general, the strength and stiffness of plant fibers depend on the cellulose content and spiral angle, which the bands of microfibrils in the inner secondary cell wall make with the fiber axis. The amount of cellulose is closely associated with the crystallinity index of the fiber and the MFA with respect to the main fiber axis. Fibers with high crystallinity index and/or cellulose content have been found to possess superior mechanical properties, ie, the MFA determines the stiffness of the fibers, which in turn governs the mechanical properties of the composite. Low MFA makes the fiber more rigid, inflexible, and mechanically more strong (Faruk and Saine, 2015). Lignin plays an important role in the physical properties of the fibers. Also, the hardness and stiffness of lignocellulosic fibers depend on the lignin content and how it is embedded in cell structure. Incorporation of the reinforcing filler into the matrix improved the stiffness of the composites due to lignocellulosic excellent stiffness properties. Taj et al. (2007), concluded because of the low density of natural plant fibers, the specific properties (property-to-density ratio), strength, and stiffness of plant fibers are comparable to the values for glass fibers. Table 3.4 presents typical reported stiffness and ultimate stress of different types of natural plant fibers.

Page et al. (1977), reported that the stiffness of wood fibers is well-correlated with the MFA. At small angles (<5 degrees), stiffness is in the range 50–80 GPa, and at large angles (40–50 degrees), stiffness is reduced to about 20 GPa. Consequently, the MFA is a key parameter that can define the stiffness of the fibers.

3.5 Conclusion and future perspectives

There has been an increasing interest in the manufacture and use of ecologically friendly natural plant fiber composites since 1995. This is due to excellent specific properties, multiscaled structure, environmental advantages, relatively low cost, and abundant availability. Recently, Natural Polymer Matrix Composites (NPMC) are

emerging as viable alternatives to traditional materials in a wide range of fields, such as automotive, construction, marine, and aerospace applications. Requirements for lighter weight products and strict environmental rules and regulations have led to the development of natural-based fiber reinforced composites, but there are some challenges to be solved, including the lack of good interfacial adhesion between the fibers and polymers, high water absorption, and thermal stability. Consequently, research has been focused on the reactive surface treatment, the chemical modification of natural fibers, and the formation of the polymer interlayer on the fiber surface to improve their mechanical, thermal, and physical properties, as well as their interfacial properties. Therefore designing desirable biocomposite materials through optimal surface treatment or modification of natural fibers is a necessity from an engineering viewpoint. Finally, biobased nanoscale fibers are unique with respect to their high aspect ratio, remarkable strength, renewability, and biodegradability, which make them excellent candidates as reinforcements in producing nanocomposites. The interfacial area of the reinforcing particles is very large due to the small size of the particles, and the reinforcing particle will thus, to a great extent, interact with the polymer, further enhancing the effectiveness of the reinforcement.

Acknowledgments

Many thanks go to cellulose and paper technology department members at Shahid Beheshti University (SBU) for their valuable guidance.

References

Agu, C.V., Njoku, O.U., Chilaka, F.C., Okorie, S.A., Agbiogwn, D., 2012. Physico-chemical characterization of lignocellulosic fibre from Ampelocissus cavicaulis. International Journal of Basic and Applied Sciences 12 (3), 68−77.

Anagnost, S.E., Mark, R.E., Hanna, R.B., 2002. Variation of microfibril angle within individual tracheids. Wood and Fiber Science 34 (2), 337−349.

Asasutjarit, C., Hirunlabh, J., Khedari, J., Charoenvai, S., Zeghmati, B., Shin, U.C., 2007. Development of coconut coir-based lightweight cement board. Construction and Building Materials 21 (2), 277−278.

Ashori, A., Nourbakhsh, A., 2010. Bio-based composites from waste agricultural residues. Waste Management 30, 680−684.

Ayrilmis, N., Kaymakci, A., 2013. Fast growing biomass as reinforcing filler in thermoplastic composites: *Paulownia elongata* wood. Industrial Crops and Products 43, 457−464.

Berglund, L., 2012. Wood biocomposites − extending the property range of paper products. In: Niskanen, K. (Ed.), Mechanics of Paper Products, first ed. Walter de Gruyter, Berlin. Germany, pp. 231−254.

Bisanda, E.T.N., Ansell, M.P., 1991. The effect of silane treatment on the mechanical and physical properties of sisal-epoxy composites. Composites Science and Technology 41, 165.

Bismarck, A., Mishra, S., Lampke, T., 2005. Plant fibers as reinforcement for green composites. Chapter 2. In: Mohanty, A.K., Misra, M., Drzal, T. (Eds.), Natural Fibers, Biopolymers, Biocomposites. CRC Press, New York, USA.

Bledzki, A.K., Gassan, J., 1999. Composites reinforced with cellulose-based fibres. Progress in Polymer Science 24, 221.

Bogoeva-Gaceva, G., Avella, M., Malinconico, M., Buzarovska, A., Grozdanov, A., Gentile, G., Errico, M.E., 2007. Natural fiber eco-composites. Polymer Composites 28 (1), 98−107.

Cho, D., Kim, H.J., Drzal, T.L., 2014. Surface treatment and characterization of natural fibers: effects on the properties of biocomposites. In: Sabu, T., Kuruvilla, J., Malhotra, S.K., Goda, K., Sreekala, M.S. (Eds.), Polymer Composites, Biocomposites, vol. 3. Wiley-VCH, pp. 133−178.

Da, D., Fan, M., 2014. Wood fibres as reinforcements in natural fibre composites: structure, properties, processing and applications. In: Hodzic, A., Shanks, R. (Eds.), Natural Fibre Composites, Materials, Processes and Properties. Woodhead Publishing Limited, Cambridge, UK, pp. 3−65.

Dash, B.N., Rana, A.K., Mishra, H.K., Nayak, S.K., Tripathy, S.S., 2000. Novel, Low-cost jute-polyester composites II: SEM observation of the fractured surfaces. Polymer-Plastics Technology and Engineering 39, 333−350.

De, S.K., White, J.R., 1996. Short Fibre Polymer Composites. Woodhead Publishing, Cambidge, UK.

Djafari Petroudy, S.R., Syverud, K., Chinga-Carrasco, G., Ghasemian, A., Resalati, H., 2014. Effects of bagasse microfibrillated cellulose and cationic polyacrylamide on key properties of bagasse paper. Carbohydrate Polymers 99 (2), 311−318.

Djafari Petroudy, S.R., Ghasemian, A., Resalati, H., Syverud, K., Chinga-Carrasco, G., 2015. The effect of xylan on the fibrillation efficiency of DED bleached soda bagasse pulp and on nanopaper Characteristics. Cellulose 22, 385−395.

Du, Y., Yan, N., Kortschot, M.T., 2015. The use of ramie fibers as reinforcements in composites. In: Faruk, O., Sain, M. (Eds.), Biofiber Reinforcement in Composite Materials, Woodhead Publishing Series in Composites Science and Engineering, vol. 5, pp. 104−137.

Faruk, O., Sain, M., 2015. Biofiber Reinforcement in Composite Materials. Woodhead Publishing, Cambridge, UK.

Fujita, M., Harada, H., 2001. Ultrastructure and formation of wood cell wall. In: Hon, D.N.S., Shiraishi, N. (Eds.), Wood and Cellulosic Chemistry, second ed. Marcel Dekker, Inc., New York, USA, pp. 1−49.

Gassan, J., Chate, A., Bledzki, A.K., 2001. Calculation of elastic properties of natural fibers. Journal of Material Sciences 36, 3715−3720.

Hu, X., Hsieh, Y.J., 1996. Crystalline structure of developing cotton fibers. Journal of Polymer Science Part B: Polymer Physics 34, 1451.

Hull, D., Clyne, T.W., 1996. In: Introduction to Composite Materials, second ed. University of Cambidge.

Ishak, M.R., Leman, Z., Sapuan, S.M., Edeerozey, A.M.M., Othman, I.S., 2010. Mechanical properties of kenaf bast and core fibre reinforced unsaturated polyester composites. Materials Science and Engineering 11 (1), 1−6. http://dx.doi.org/10.1088/1757-899X/11/1/012006.

John, M., Sabu, T., 2012. Natural Polymers. In: Composites, vol. 1. The Royal Society of Chemistry, Cambridge, UK.

Joseph, K., Thomas, S., Pavithran, C., 1996. Effect of chemical treatment on the tensile properties of short sisal fibre-reinforced polyethylene composites. Polymer 37, 5139−5149.

Joseph, P.V., Rabello, M.S., Mattoso, L.H.C., Joseph, K., Thomas, S., 2002. Environmental effects on the degradation behavior of sisal fiber reinforced polypropylene composites. Composites Science and Technology 62 (10−11), 1357−1372.

Kandola, B.K., 2012. Flame retardant characteristics of natural fibre composites. In: John, M., Sabu, T. (Eds.), Natural Polymers, Composites, vol. 1. The Royal Society of Chemistry, Cambridge, UK, pp. 117−186.

Komuraiah, A., ShyamKumar, N., DurgaPrasad, B., 2014. Chemical composition of natural fibers and its influence of their mechanical properties. Mechanics of Composite Materials 50 (3), 359−376.

Lilholt, H., Lawther, J.M., 2000. Natural organic fibres. Chapter 10. In: Kelly, A., Zweben, C. (Eds.), Comprehensive Composite Materials. Elsevier Science, pp. 303−325.

Lucintel, 2011. www.lucintel.com/lucintelbrief/potentialofnaturalfibercomposites-final.pdf.

Madsen, B., Gamstedt, E.K., 2013. Wood versus plant fibers: similarities and differences in composite applications. Advances in Materials Science and Engineering. http://dx.doi.org/10.1155/2013/564346.

Mallick, P.K., 2007. Fiber Reinforced Composites: Materials, Manufacturing and Design, third ed. CRC Press.

Mishra, S., Mohanty, A.K., Drzal, L.T., Misra, M., Parija, S., Nayak, S.K., Tripathy, S.S., 2003. Studies on mechanical performance of biofibre/glass reinforced polyester hybrid composites. Composites Science and Technology 63 (10), 1377−1385.

Mobasher, B., 2012. Mechanics of Fiber and Textile Reinforced Cement Composites. CRC Press, New York, USA.

Mohanty, A.R., Fatima, S., 2015. Biocomposites for industrial noise control. In: Thakur, V.J., Kessler, M. (Eds.), Green Biorenewable Biocomposites: From Knowledge to Industrial Applications. CRC Press, Boca Raton FL, USA.

Mohanty, A.K., Misra, M., Hinrichsen, G., 2000. Biofibers, biodegradable polymers and biocomposites: an overview. Macromolecular Materials and Engineering 276/277, 1−25.

Mohanty, A.K., Misra, M., Drzal, L.T., 2002. Sustainable bio-composites from renewable resources: opportunities and challenges in the green materials world. Journal of Polymers and the Environment 10 (1−2), 19−26.

Mohanty, A.K., Misra, M., Drzal, L.T., Selke, S.E., Harte, R.B., Hinrichsen, G., 2005a. Natural fibers, biopolymers, and biocomposites: an introduction. Chapter 1. In: Mohanty, A.K., Misra, M., Drzal, T. (Eds.), Natural Fibers, Biopolymers, Biocomposites. CRC Press, New York. USA.

Mohanty, A.K., Misra, M., Drzal, T., 2005b. Natural Fibers, Biopolymers, Biocomposites. CRC Press, New York, USA.

Mo, X., Wang, D., Sun, S.X., 2005. Straw-based biomass and biocomposites. Chapter 14. In: Mohanty, A.K., Misra, M., Drzal, T. (Eds.), Natural Fibers, Biopolymers, Biocomposites. CRC Press, New York. USA.

Mortazavi, S.M., Kamali Moghaddam, M., 2010. An analysis of structure and properties of a natural cellulosic fiber (Leafiran). Fibers and Polymers 11 (6), 877−882.

Mueller, D.H., Krobjilowski, A., 2004. Improving the impact strength of natural fiber reinforced composites by specifically designed material and process parameters. International Nonwovens Journal 13 (4).

Mukherjee, P.S., Satyanarayana, K.G., 1986. Structure and properties of some vegetable fibers. 2. pineapple fiber (Anannus-Comosus). Journal of Materials Science 21, 51.

Mukhopadhyay, S., Fangueiro, R., 2009. Physical modification of natural fibers and thermoplastic films for composites−a review. Journal of Thermoplastic Composite Materials 22, 135−162.

Mwaikambo, L.Y., Ansell, M.P., 2002. Chemical modification of hemp, sisal, jute, and kapok fibers by alkalization. Journal of Applied Polymer Science 84, 2222.

Mwaikambo, L.Y., 2006. Review of the history, properties and application of plant fibres. African Journal of Science and Technology (AJST), Science and Engineering Series 7, 120–133.

Ndiyae, D., Gueye, M., Thiandoume, C., Badji, A.M., Tidjani, A., 2015. Reinforcing fillers and coupling agents' effects for performing wood polymer composites. Chapter 12. In: Thakur, V.J., Kessler, M. (Eds.), Green biorenewable Biocomposites: From Knowledge to Industrial Applications. CRC Press, Boca Raton, FL, USA.

Netravali, A.N., 2001. Biodegradable natural fiber composites. In: Blackburn, R.S. (Ed.), Biodegradable and Sustainable Fibres. CRC Press. Woodhead Publishing Limited, Cambridge, England, pp. 271–309.

O'Dogherty, M.J., Huber, J.A., Dyson, J., Marshall, C.J., 1995. A study of the physical and mechanical properties of wheat straw. Journal of Agricultural Engineering Research 62 (2), 133–142.

Page, D.H., El-Hosseiny, F., Winkler, K., Lancaster, A.P.S., 1977. Elastic modulus of single wood pulp fibers. Tappi 60, 114–117.

Park, J.M., Quang, S.T., Hwang, B.S., Lawrence DeVries, K., 2006. Interfacial evaluation of modified jute and hemp fibers/polypropylene (PP)-maleic anhydride polypropylene copolymers (PP-MAPP) composites using micromechanical technique and nondestructive acoustic emission. Composites Science and Technology 66, 2686–2699.

Poletto, M., Ornaghi, J., Zattera, Z., 2014. Native cellulose: structure, characterization and thermal properties. Materials 7, 6105–6119.

Ray, D., Rout, J., 2005. Thermoset biocomposites. Chapter 9. In: Mohanty, A.K., Misra, M., Drzal, T. (Eds.), Natural Fibers, Biopolymers, Biocomposites. CRC Press, New York, USA.

Ray, D., Sarkar, B.K., Rana, A.K., Bose, N.R., 2014. The mechanical properties of vinylester resin matrix composites reinforced with alkali-treated jute fibres. Composites Part A: Applied Science and Manufacturing 32 (1), 119–127.

Reddy, N., Yang, Y., 2005. Biofibers from Agricultural Byproducts for Industrial Applications. Faculty Publications–Textiles, Merchandising and Fashion Design. http://digitalcommons.unl.edu/textiles_facpub/28.

Reis, J.M.L., 2006. Fracture and flexural characterization of natural fiber-reinforced polymer concrete. Construction and Building Materials 20 (9), 673–678.

Rout, J., Misra, J.M., Tripathy, S.S., Nayak, S.K., Mohanty, A.K., 2001. The influence of fibre treatment on the performance of coir-polyester composites. Composites Science and Technology 61 (9), 1303–1310.

Rozman, H.D., Peng, G.B., Mohd. Ishak, Z.A., 1998. The effect of compounding techniques on the mechanical properties of oil palm empty fruit bunch–polypropylene composites. Journal of Applied Polymer Science 70, 2647.

Santosa, F., Padua, G.W., 1999. Tensile properties and water absorption of zein sheets plasticized with oleic and linoleic acids. Journal of Agricultural and Food Chemistry 47, 2070.

Satyanarayana, K.G., Ravikumar, K.K., Sukumaran, K., Mukherjee, P.S., Pillai, S.G.K., Kulkarni, A.K., 1986. Structure and properties of some vegetable fibers. Journal of Materials Science 21, 57.

Shanks, R.A., 2015. Isolation and application of cellulosic fibres in composites. Chapter18. In: Faruk, O., Sain, M. (Eds.), Biofiber Reinforcement in Composite Materials. Woodhead Publishing, Cambridge, UK, pp. 553–570. http://dx.doi.org/10.1533/9781782421276.5.553.

Shinoj, S., Visvanathan, R., 2015. Oil palm fiber polymer composites: processing, characterization and properties. In: Thakur, V.J. (Ed.), Lignocellulosic Polymer Composites Processing, Characterization, and Properties. Scrivener Publishing, MA, USA.

Siro, I., Plackett, D., 2010. Microfibrillated cellulose and new nanocomposite materials: a review. Cellulose 17 (3), 459−494.

Sjöström, E., 1981. Wood Chemistry Fundamentals and Applications. Academic Press, New York.

Taj, S., Munawar, M.A., Khan, S., 2007. Natural fibre-reinforced polymer composites. Proceedings − Pakistan Academy of Sciences 44, 129.

Tavakoli, M., Tavakoli, H., Azizi, M.H., Haghayegh, G.H., 2010. Comparison of mechanical properties between two varieties of rice straw. Advance Journal of Food Science and Technology 2 (1), 50−54.

Tewari, M., Singh, V., Gope, P., Chaudhary, A.K., 2012. Evaluation of mechanical properties of bagasse−glass fibre reinforced composite. Journal of Materials and Environmental Science 3 (1), 171−184.

Thakur, V.K., Singha, A.S., 2013. Biomass-Based Biocomposites. Smithers Rapra Technology Ltd, Shropshire, UK.

Wambua, P., Ivens, J., Verpoest, I., 2003. Natural fibre: Can they replace glass in fibre reinforced plastic? Composites Science and Technology 63, 259−1264.

Williams, A.C., Timmins, P., Lu, M., Forbes, R., 2005. Disorder and dissolution enhancement: Deposition of ibuprofen on to insoluble polymers, European Journal of Pharmaceutical Sciences 26, 288−294.

Wainwright, S.A., Biggs, W.D., Currey, J.D., Gosline, J.M., 1982. Mechanical Design in Organisms. Princeton University Press; Princeton, NJ, USA.

Yilmaz, N.D., 2015. Agro-residual fibers as potential reinforcement elements for biocomposites. In: Thakur, V.J. (Ed.), Lignocellulosic Polymer Composites Processing, Characterization, and Properties. Scrivener Publishing, MA. USA, pp. 233−270.

Yu, T., Ren, J., Li, S., Yuan, H., Li, Y., 2010. Effect of fiber surface-treatments on the properties of poly(lactic acid)/ramie composites. Composites Part A: Applied Science and Manufacturing 41 (4), 499−505.

Zabihzabeh, S.M., 2010a. Water uptake and flexural properties of natural filler/HDPE composites. BioResources 5 (1), 316−323.

Zabihzadeh, S.M., 2010b. Flexural properties and orthotropic swelling behavior of bagasse/thermoplastic composites. BioResources 5 (2), 650−660.

Functional pretreatments of natural raw materials

4

F. Fu, L. Lin, E. Xu
Research Institute of Wood Industry, Chinese Academy of Forestry, Beijing, China

4.1 Introduction

Wood itself is a natural fibre composite. The excellent performance of wood is widely recognized by human beings, including excellent visual, tactile and smell characteristics, such as characteristics of hearing, easy processing, high strength to weight ratio, thermal insulation, renewability, degradation and recycling, less environmental pollution and other characteristics. However, the flammability, easy fungal attack, shrinkage and natural defects limit its application. Moving from oil-based to bio-based economy leads to further development and consumption of wood and other natural fibre composites. Meanwhile the scope of application is also becoming more and more wide. Scarce natural resources coupled with the intrinsic properties of wood and other natural fibres make it difficult to meet the increasing market demand.

Functionalization is an important way of improving the performance of wood, enabling the utilization of low grade wood resources, enhancing the technological content of products and expanding the field of application of wood materials. The current technologies of functionalizing wood materials are mainly to inject function modifiers into wood to achieve the specific functionalities, such as adding flame retardant agents or preservatives into wood to prepare wood products with a flame-retarding effect or anticorrosive properties. The infiltration of these functional modifiers is dependent on the structural characteristics of the wood itself. Nevertheless, due to some particular structures of wood, some of the functional treatment agents are difficult to penetrate into the wood, affecting the efficiency or ineffectiveness of the treatments. The impregnation volume, depth and uniformity of functional fillers are the most important parameters for the treatment, but the functionality of the end products depends on the leaching performance or permeability of wood.

4.2 Functionalization of natural raw materials

4.2.1 Wood colour treatment

As a natural material, wood is widely used in building construction, refurbishment and furniture industries. The supply of raw materials for the global timber industry is gradually shifting from rain forest to plantation forest. The amount of high quality wood

Advanced High Strength Natural Fibre Composites in Construction. http://dx.doi.org/10.1016/B978-0-08-100411-1.00004-2

from rain forest, natural precious wood, is becoming less and less. On the other hand, the colour of most plantation wood is not uniform and light, combined with colour changed and polluted in the storage and processing stage, which limits the use of wood in the furniture, refurbishments or other value-added applications. In some cases, wood colour, texture, strength and density are important indexes to evaluate the quality of wood and determine its value.

Wood bleaching is a process that makes the colour of wood light, uniform and pollution abatement using the chemical reagent. Bleach treatment can eliminate colour difference and remove contaminations from the wood surface to get a lighter colour without destroying the original texture of the wood. Bleach treatment is commonly used for upgrading low value wood to simulate precious wood species in order to obtain an improved performance. Bleaching is very important in wood processing and can increase the value of wood in use and satisfy the requirements of the elegant colour of wood. The factors that affect wood bleaching are tree species, pH value, reaction temperature, reaction time and additives.

Wood dyeing is a technology using physical or chemical methods to adjust or change the colour of wood, preventing and controlling wood discolouration. Wood dyeing can improve the visual, decorative properties and the value of wood. There are typically two kinds of wood dyeing processes: one is that in accordance with dyeing objects can be subdivided for standing tree dyeing, wood dyeing and veneer dyeing. The other is that in accordance with the impregnating method and includes the atmospheric pressure immersion, vacuum impregnation and pressure impregnation. The former is more common.

Commonly used dyes for wood dyeing are the acid dyes, basic dyes, direct dyes and reactive dyes. The dyeing principle of these dyes is not the same. Acid dyes, direct dyes and basic dyes work mainly through intermolecular and hydrogen bond forces with wood. The dyeing principle of reactive dyes is the chemical reaction between the dye and wood to produce a chemical bond, so it is more secured and widely used than other dyes.

The dyeing result is influenced by the physical and chemical properties of wood and the dyes used in the dyeing process. The effectiveness of wood dyeing is evaluated by the index of dye uptake, dyeing fastness, washing fastness and light fastness. Accessibility is the ability of a chemical reagent or dye penetration into the wood internally. Enhancing the permeability of the wood is a way to improve the accessibility of the reaction reagent, so as to make the distribution better in wood structures.

4.2.2 Dimensional stabilization of wood

The water in wood or other natural fibres can be divided into free water and bound water. Free water exists in the capillary system of wood, which has no effect on the dimensional stability of the wood when it increases or decreases. Bound water exists in the microcapillary system between the microfibrils and fibrils in the cell wall. Wood is mainly composed of cellulose, hemicellulose and lignin, and there are a large number of hydroxyls (−OH) on cellulose and hemicellulose molecules. The hydroxyl

group is hydrophilic. With the change of environmental temperature and humidity, natural fibres, such as wood, shrink or swell due to the absorption or desorption of water on to the hydroxyl groups of cellulose and hemicellulose.

The method of improving the dimensional stability of wood can be divided into five categories: mechanical inhibition by cross-lamination, internal or external finishing with waterproof agents, high temperature steam treatment, reducing the hygroscopicity and chemical cross-linking with wood cell wall. This classification does not signify whether the chemical treatment is used or not, but whether the chemical reaction is related to the cell wall composition. Therefore it can also be divided into two categories: physical and chemical processing methods. Chemical reactions of wood with the low molecular crosslinking reagent is the effective method to increase the stability, reduce moisture absorption capability and improve the acoustic properties and durability of other natural textures. The degree of cross-linking of low molecular reagents with wood depends on the impregnating depth and uniform distribution in the structure of wood.

In practical applications, a combined method is often used, or one method which can play a variety of roles. The advance of science and technology leads to the development of a number of new methods, such as metallization or ceramic processing of wood, and not only increases the dimensional stability but also increases the number of other excellent properties.

4.2.3 Wood strengthening

Wood strengthening is a method for improving density (or surface density), mechanical strength or overall mechanics of low quality wood by physical, chemical or mechanical ways. Wood strengthening, such as impregnation wood, compression wood and plastic wood, can improve the strength and functionality of the low quality wood, realize the optimal utilization of inferior and small diameter wood, and improve wood utilization and value (Fang, 2008).

Wood impregnation is impregnating the low molecular weight resin into wood to produce an insoluble polymer in cell walls with low molecular resin bonding to each other and reacting with the carboxyl of wood under high temperature. Therefore the amount of hydroxyl groups is reduced, inhibiting water sorption of cell walls. A cell wall expanded by resin polymer can inhibit the cell wall's shrinkage and increase the density of the wood. The size stability, moisture resistance and mechanical strength of the impregnated wood are significantly improved. Commonly used resins are low molecular weight melamine formaldehyde resin, phenolic resin, urea formaldehyde resin and isocyanate.

The methods of pressure leaching, vacuum impregnation, ultrasonic, pre-extraction and high temperature drying were used to improve the permeability of the wood, reduce the cost and improve the quality of wood products. These methods have the disadvantages of long soaking time, low dipping depth and uneven distribution. Therefore new methods are needed to improve the permeability of wood to solve the above problems.

4.2.4 Flame retardant treatment of wood

Wood flame retardant treatment is a kind of technology, which can convert combustible wood into flame retardant materials. The main method of this kind of transformation is adding chemical substances to wood. The flame retardant wood not only has the fire retardant performance, but also retains the original excellent properties of wood. The ideal wood flame retardant should have the following characteristics: high potency, nontoxic, no environmental effect during use, durable, without heat and light decomposition, not easy to hydrolysis and breach, good dimensional stability of wood after fire retardant treatment, not affected by wood physical and mechanical properties, low cost, rich source and easy to use. The flame retardants can be divided into two types of nonbulgy and intumescent, including, specifically, phosphorus, borate, phenolic, halogenated, nitrogen, halogen-phenolic and FRW flame retardant.

The efficacy of fire retardant treatment depends not only on the flame retardant performance and usage, but is also related to the distribution of flame retardant in wood. Therefore it is important to select a suitable processing technology, which can improve the flame retardant performance and does not damage the physical and mechanical properties of wood.

Flame retardant treatment used to coat a wood surface or penetrate it into the wood to achieve specific properties mainly include dipping, coating, spray, cover, hot pressing, ultrasonic wave assistance and a high energy injection method. The most common treatment is infusion that injects flame retardant solution into wood at atmospheric pressure, vacuum pressure or the combination of several pressure conditions. The pressure impregnation has a good effect; first the wood is placed in a high pressure tank and is vacuumed to pull out the gas inside the wood, then flame retardant liquid is released under the vacuum and pressurized into the wood interior.

Treating wood with flame retardant solution is a complex process, which is due to the complicated structure of the wood, especially the heterogeneity and anisotropy of the structure. The efficacy of the treatment depends on the absorption of the reagent, depth of injection and distribution of the flame retardant in the wood. For a particular flame retardant, usually the more uniform distribution of flame retardant, the better the treatment effect. The depth of the flame retardant into the wood depends on the actual situation of requirements; the general penetration depth of $5 \sim 7$ mm can meet the requirements of the flame retardant performance in most cases. The key is to solve the problem of how to make flame retardant uniformly and get a certain depth distributed in the wood-based material.

4.2.5 Wood preservative treatment

Wood is a natural organic material with obvious biological characteristics. In addition to its flammability, vulnerability to bacteria and insects limit its application. Preservative treatment is required in many cases. Wood preservation treatment is impregnation of anticorrosive, mothproof or mildew-proof chemicals into wood products at atmospheric pressure or pressure. After preservative treatment, the service life of the wood product is much longer than untreated wood.

At present the most common method to prevent wood decay is to use chemical wood preservatives to impregnate wood. The chemical agents used can be divided into three types, including oil-borne preservative, oil-type preservative and water-borne chemicals.

Oil-borne preservatives include pentachlorophenol and copper naphthenate. Pentachlorophenol is a kind of widely used oil-borne preservative, mainly used for processing telegraph poles and pile wood, but it has great toxicity to humans and animals and a bad influence on the environment.

An oil-type preservative is coal tar and its fractions, such as coal tar creosote, anthracene oil and coal tar creosote and oil mixed liquid. It has some disadvantages limiting its application, except toxicity to humans and animals; another major disadvantage of coal tar is exudation phenomenon from treated products. At present this kind preservative is only used for industrial timber processing such as railway sleepers and telegraph poles and cannot be used in civil fields.

Due to the better surface characteristics and the superior performance of water-borne preservatives, oil-borne preservatives are gradually replaced by water-borne preservatives. Common water-borne preservatives are arsenic or chromium preservatives, such as chromated copper arsenate, acid copper chromate, ammoniacal copper arsenate, ammonia soluble zinc copper arsenate and chromium copper borate. In addition to arsenic and chromium, there are some other metals that can be used for wood preservation, including copper, zinc, iron and aluminum. Many kinds of wood preservatives can be produced by the combination of different organic biological killing agents with these metal oxides or salts.

The wood preservative treatment process includes nonpressure and pressure treatments. The treatment of atmospheric pressure mainly includes the diffusion, hot cold tank and vacuum methods. The basic method of pressure processing is full cell process and empty cell methods. Because of the long processing time and low productivity, the pressure treatment method was adopted in most of the wood preservative treatments in the industry.

The main factors affecting the penetration of the preservatives are preservative permeability, preservative retention, replacement, water solubility, pH value and erosion. The preservative retention is one of the most important factors affecting the service life of the wood products, and the distribution types of preservatives in wood can significantly influence the antiseptic performance in order to improve the permeability of preservatives; many new processing technologies are being studied, such as supercritical fluid processing and microwave methods. It must be noted that many water-borne preservatives have also been banned due to their toxicity.

4.2.6 Wood–metal composite materials

A wood–metal composite is a kind of material combining a wooden material with metal through special technology. Wooden material can be solid wood or natural fibre; the composite form can be metalized wood, metal cladding board, wood–metal composite pipe and metal surface coat wood.

Metalized wood refers to the use of a low melting point alloy in the molten state into the wood cell and composite solidification together with wood. Using the different types of wood to composite with metal can result in different composite materials with various properties. In general, metallization, due to filling metal elements to the wood cell, results in an increase in density. Meanwhile, because the metal can play a role of reinforcement, the compressive strength, hardness, wear-resisting property an impact toughness greatly increase, and durability and dimensional stability also improve. As the electrical conductivity and thermal conductivity of the metal itself are good, the thermal conductivity and electrical conductivity of the metalized wood are also greatly improved. In addition the immersed metal will separate wood with an oxidizing medium, so the metalized wood in the fire will be carbonized instead of burning.

With these unique properties, the metalized wood can be used for a wide range of special applications, such as antistatic material, conductive material and electromagnetic shielding materials. For example the wood−metal composite material containing lead has the function of X-ray absorption. Therefore this kind of composite material can be used in the area with ray radiation, such as the floor, the shed board and the wall board, in order to protect human health.

The impregnation volume, depth and uniformity of treatment agents inside the wood are the most important in wood functional modification. The leaching of functional modifiers is closely related to the flow of fluid in the wood cells. Due to the special structure of wood, some of the functional modifiers are too difficult to be impregnated into the wood, which has given rise to some difficulties to the modification of the wood. An in-depth study on the method of improving the permeability of wood and its influence mechanisms has been regarded as a frontier subject in the field of wood−fluid relations. How to improve the performance of the wood and the permeability of the wood is the key to the functional modification of wood. Functional pretreatment is a powerful tool for improving the impregnation and penetration performance of wood, and the efficiency of the impregnation volume, depth and uniformity of modified agents in the wood.

4.3 The main process and mechanism of pretreatments

4.3.1 Mechanical treatment

4.3.1.1 Indentation method

Laser or mechanical incising is carving a certain size crack dent on the surface of wood by a cutting tool or laser; the permeability of wood increased after the surface longitudinal fibres of wood were cut off, which can be applied to wood preservative treatment (Morrell and Morris, 2002). At the same time, the internal stress of the wood was eliminated and cracking was reduced after incising. Incising can significantly increase the permeability of wood. Laser scribing can improve its effectiveness. Different perforation systems using needles, drills, slit discs, lasers and water jets have been reported (Richter, 1989). However, visible marks on the wood surface and strength losses are considered to be disadvantages for certain wood products.

4.3.1.2 Compression method

Transverse compression method is mainly used to compress wood transversely. With the differential pressure formed by wood compression spring back, the treatment reagent was impregnated into wood. The compression method can be divided into flat pressing and rolling methods.

The flat pressing method compresses wood by flat press. After flat pressing the materials are immersed into the liquid, and then the liquid is permeated into wood with different pressures when wood recovers. The research shows that the liquid is injected uniformly (Iida et al., 1995).

The principle of the rolling method uses two pairs of rollers pressuring a transverse direction of wood. The treatment reagent was taken in wood that may be attributed to the rebound of wood texture when rollers leave the wood surface. In the rolling process, the pit membrane of wood cell walls may be damaged, and the weak parts of cell walls may generate fissure. All of these will improve the wood permeability. The rolling method is more effective than the flat pressing method for improving the permeability of wood (Adachi et al., 2003).

Compared to the traditional pressure method, the rolling method can skilfully use 'negative pressure suction' with the advantage of short time, high efficiency and continuous production, processing wet and green wood directly, eliminating the wood drying process and saving energy and time. The wood drying efficiency can be significantly improved due to the damage of the wood pit membrane after rolling and the increase of permeability. The treatment can be conducted under atmospheric pressure without the need of an expensive vacuum and high pressure equipment, with less energy consumption and low cost.

Adjusting the compression ratio, reagent concentration, timber moisture, soaking time and the number of rollers is able to meet the demand of different loading and immersion depth of reagents. After continuous rolling, the reagent distributed in the wood uniformly and the extrusion of the reagent can also be recycled. For industrial production, this technology has the characteristics of a good working environment, simple equipment and high efficiency of comprehensive treatment. In short, the transverse compression method can improve the permeability of wood effectively and is generally suitable for fast growing wood, but this method is not suitable for the treatment of hardwood and wood with low permeability.

4.3.2 Physical method

Physical functional pretreatments include freezing, steam explosion and microwave treatment.

4.3.2.1 Freezing

Frozen processing is to freeze the free water of wood into ice under low temperature conditions, and the wood permeability is improved due to the damage of the bordered pit membranes, which are due to the squeezing of the wood cell wall by the volume

expansion of free water. With the increase of freezing time, the number of fractured pit membranes on vessels and cracks on cell walls of parenchyma cells and wood fibres is gradually increased. The pit membranes between vessels and wood rays collapse, and the individual pit membrane cracks after 24 h of freezing. Freezing for 36 h could result in a rupture of most of the pit membranes between vessels and transverse cracks of parenchyma cell walls. More than 70% of the pit membrane may crack, and cell walls may also seriously rupture after frozen for 48 h (Wang et al., 2003). After 48 h of freezing, the majority ray cells of *Eucalyptus urophylla* damaged and cracked were also observed on the pit membrane of part of the wood fibre-bordered pits. The destruction of the microstructure can expand the water seepage path of the processing material, so as to improve the liquid permeability of the wood (Zhang et al., 2011, 2006b). If the freezing time is too long, after building the water channel the cell wall will be squeezed and damaged. The frozen time and temperature should be adjusted for each frozen treatment, depending on the load-bearing capacity of different species of wood cell walls.

4.3.2.2 Steam explosion method

The steam explosion method uses high temperature steam to soften wood. The weakest pit membrane and the parenchyma of wood are damaged by the steam pressure difference between the internal and external wood through instantaneous controlled pressure drop; thereby wood permeability is improved (Li et al., 2011). The steam explosion treatment not only resets aspirated pits and destroys the pit membrane, but it also can destroy the wood cell wall. However, the treatment effect is not uniform (Zhang and Cai, 2006; Zhang et al., 2006a).

The research of steam explosion treatment on *Abies lasiocarpa* wet heart wood found that five kinds of changes occurred in the aspirated pit of treated wood, including the reset of aspirated pit, the distortion of pit membrane and lateral deviation of pit torus, pit torus partly broken away from the pit aperture, depression of pit membrane and cracks of pit border and cell wall and pit border partly broken away from the cell wall. These changes can enhance the fluid permeability of the wood, which is beneficial to wood drying and functional agent impregnation.

After steam explosion treatment, the wood dehydration occurred and the appearance of the wood colour changed. Wood colour changes more obviously and dehydration more seriously with the increase of pressure and the number of blasting cycles. The radial and tangential gas permeability of *A. lasiocarpa* was improved after steam explosion treatment and increased with the increase of the blasting pressure, temperature and cycle index. Compared to the control, the uniformity of moisture distribution of *A. lasiocarpa* was improved and the modulus of elasticity (MOE) and modulus of rupture (MOR) decreased slightly. Fig. 4.1 is the crack of cross-field pitting (left) and cell wall cracking of steam explosion (right).

4.3.2.3 Microwave treatment

With the same principle as the steam explosion, microwave treatment also improves the permeability through destroying the microstructure of wood by the pressure of

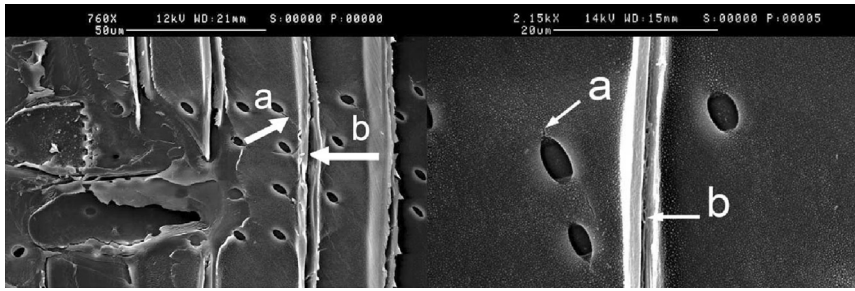

Figure 4.1 Crack of cross-field pitting and cell wall cracking of steam explosion (Zhang and Cai, 2006).

steam. The effectiveness was related to the wood moisture, the microwave power and the processing time. The microwave treatment improves wood permeability, which is one of the most interesting issues in the research field (He et al., 2014a; Torgovnikov and Vinden, 2009, 2010; Li et al., 2007). The improvement of wood permeability is mainly caused by destroying partially weak cells in wood under the steam pressure produced by microwaves, such as ray parenchyma cells and part of the pit membrane of the sclerenchyma cell.

Under the microwave power of 20 kW, the moisture of six kinds of plantation forest wood was treated from 100% to 20%. After microwave treatment, the microstructure of the wood was destroyed, which was mainly reflected in the ray parenchyma, tracheid pit, inclusions in the vessels and the wall of sclerenchyma cell. Fig. 4.2–4.5 showed that the ray parenchyma appeared to fall off (Fig. 4.2), ray parenchyma cells separated from tracheid (Fig. 4.3), part of aspirated pit and pit membrane of larch and Scots pine were destroyed by the steam pressure (Fig. 4.4), the reunited inclusions in Eucalyptus vessels were separated, the size became smaller and more uniformly distributed and the perforation connecting vessels is also destroyed (Fig. 4.5). The destruction of

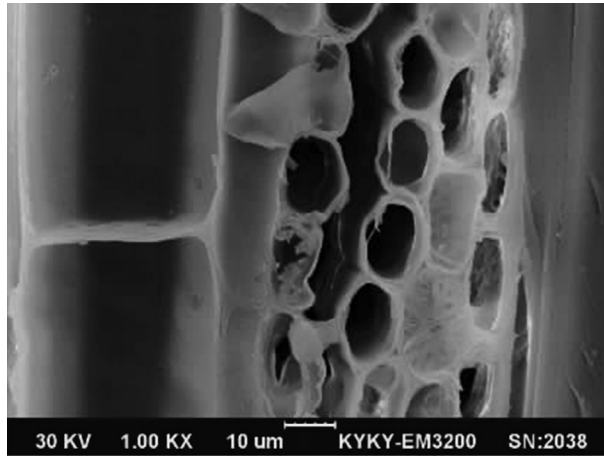

Figure 4.2 Detachment between ray parenchyma cell (*paulownia*).

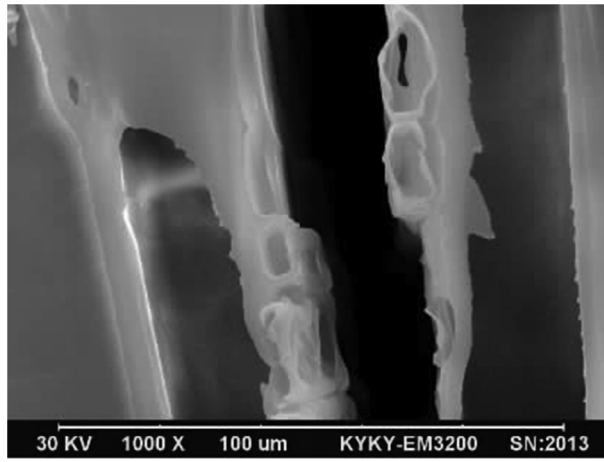

Figure 4.3 Ray parenchyma cells separated from tracheid (*pinus sylvestris*).

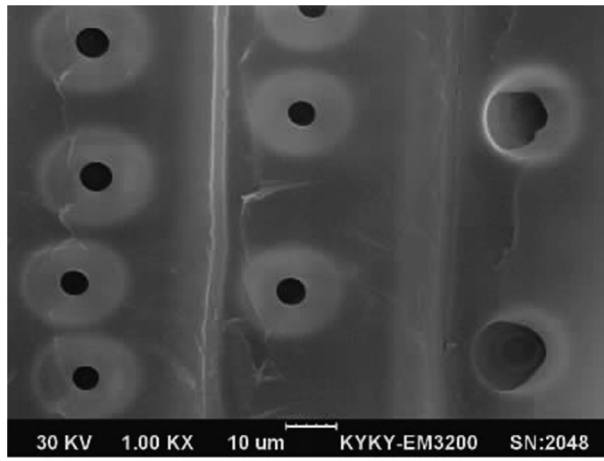

Figure 4.4 Pit torus destroyed by microwave treatment.

wood tissue resulted in a decrease of the resistance fluid flow and an increase in the water absorption rate. The process has also resulted in the reduction in the flexural elastic modulus and bending strength (He et al., 2014b).

4.3.3 Chemical method

The basic principle of the chemical treatment method is replacing an extraction in the pit membrane or degrading the pit membrane by chemical reagents. The process expands the voids between the pit membranes, enlarges the cell flow passageway and improves the permeability of wood (Zhang et al., 2011).

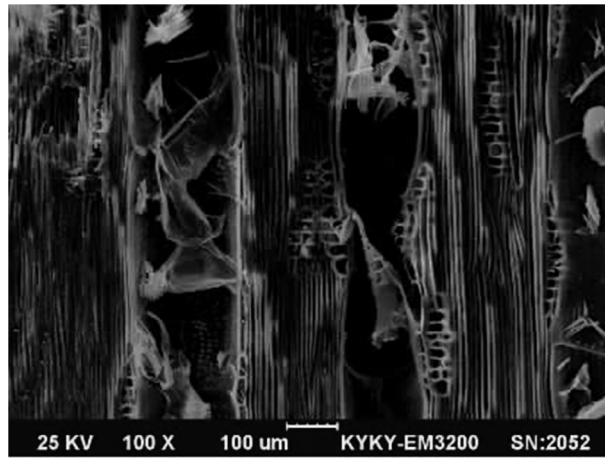

Figure 4.5 Redistribution of inclusions in vessels after microwave treatment.

The application of the supercritical CO_2 fluid treatment of wood is currently the most used technology. The permeability is improved due to the dissolving of extractives by the high diffusion and solubility of the supercritical fluid. Douglas fir was attempted by supercritical CO_2 fluid. The aspirated pit was damaged by the rapidly changed pressure of supercritical CO_2 fluid, wood extractives were dissolved at the same time and the permeability of the treated wood was significantly improved. At the same time the research results showed that an improved effectiveness can be achieved after adding the solvent in the supercritical CO_2 fluid (Demessie et al., 1995). The influence of supercritical CO_2 fluid added with methanol, ethanol and benzene ethanol on the permeability of Chinese fir, *Pinus massoniana* and *Sassafras* was investigated (Xiao et al., 2009; Xiao and Lu, 2009). The extractives can be removed from the wood. The pit membrane also produced a certain degree of damage, and the fluid permeability of the treated material was improved. Compared to air drying treatment, the gas permeability of *Picea jezoensis* var. *komarovii* can be significantly increased with the replacement of air with alcohol (Lv and Bao, 2000). This is mainly because after ethanol exchange and evaporation, the aspirated pits of the treated wood are basically the same as those of the green wood. The vast majority of the pit is still in the middle position, which is beneficial to the fluid permeability.

The permeability improvement of *Picea jezoensis* var. *komarovii* is mainly due to the reduction of extractives in the pores of pit membranes after extraction with a benzene-ethanol solution (Bao et al., 2001). It is effective to extract extractives in the pit membrane, but it is difficult to apply it to the processing industry because of the expense of benzene, toluene and ethanol.

4.3.4 Biological treatment method

The biological treatment method is the erosion of wood parenchyma or pit membrane using enzymes, bacteria and fungi, expanding the passageway of wood fluid and improving the wood permeability (Zhang et al., 2011).

The enzyme treatment of wood is the use of a variety of enzymes to break down ray parenchyma cells or bordered pit of the wood, improving the wood permeability (Militz, 1993).

Loblolly pine was treated by pectinase, cellulose and hemicellulose separately. The results showed that pit torus on pit membranes were degraded at different levels by pectinase, cellulose and hemicellulose, meanwhile, they were only slightly changed in the pit membrane structure. Pectinase treatment had the greatest impact on the permeability of the loblolly pine sapwood. However, various enzymes had no effect on the permeability of loblolly pine heartwood.

It was found that the spruce (*Picea abies* L. Karst.) microfibrils of the pit border have different degrees of degradation or are partially destroyed after they are treated with enzyme preparation, alkali and oxalic acid (Militz, 1993). The structure and ultrastructure of wood pits were studied after treated with an enzyme. The results indicated that the pit torus and pit margo of the treated wood had a certain degree of degradation or part of damage, which can increase the pit membrane pore volume and pore size and improve the permeability of the wood (Meyer, 1974; De Groot and Sachs, 1976).

There are two ways of bacterial treatments: one is to store wood in water, and such ray parenchyma cells or wood pit membrane are decomposed or degraded by bacteria in the pool; the other is to directly inoculate bacteria in the wood, expanding a wood cell liquid flow path through the bacterial erosion of a pit membrane (Pánek et al., 2013).

The treatment on Norway spruce sapwood showed that the permeability was significantly improved without significant reduction of strength after treatment with Trichoderma fungi. Only parts of the pits of the sapwood were damaged, and the cell wall of sapwood tracheid and heartwood was not damaged either, so the method is generally only suitable to improve the permeability of sapwood.

In bacterial growth season, *Picea jezoensis* was treated in a pond for 10 weeks. The water temperature was maintained at 23−28°C and was not changed during the storage period to ensure that there were enough bacteria in the water (Bao and Lv, 1991). It was found that the permeability of *Picea jezoensis* sapwood treated in the pond increased by an average of 29 times, and heartwood increased 1.52 times. The permeability increased unevenly and only 50% of the heartwood samples eroded by bacteria. The main reason sapwood permeability increased significantly is because the cavity formatted with the degradation of most bordered pits of sapwood by bacteria. This is basically consistent with the results of Dunleavy et al., who found that the bacterial treatment improved the permeability of sapwood more significantly and the treatment effect of the heartwood is not significant (Dunleavy et al., 1973).

The degradation of an aspirated pit of *A. lasiocarpa* wet heartwood by bacterium was also studied. The results showed that bacterial activities can make part of ray parenchyma of wet heartwood cells degraded, but the fracture of micofibrils on a pit membrane degraded by bacteria was only observed occasionally. The effect of planting the bacteria directly on the wood is better than that of using water treatment (Zhang et al., 2006a).

The nutrient solution containing the mixed bacteria was sprayed on the new green radiation pine sapwood for a period of time before drying, and the water absorption of

the wood was measured. The change of the wood moisture content was tracked by the neutron detection technology. After inoculation for two days, the water absorption of the board increased significantly, and the water absorption capacity was increased by two times after 14 days (Nijdam et al., 2004). Scanning electron microscopy showed that the bacteria gathered on the surface of the wood pit inoculated for two days, and the wood moisture flow channel opened with the degradation of pit torus and margo of sapwood by the enzyme secreted by bacteria. Relevant research data indicated that bacteria stored in the pool and inoculated usually can only increase the permeability of sapwood, which is not useful for heartwood.

Fungal treatment mainly refers to the inoculation of fungal spores on wood. Fungi removes deposits within the wood cell cavity and the pit of the cell wall, and the pit membrane of the wood cell wall is degraded by enzymes secreted from fungi. The permeability of the wood is improved by damaging the pit membrane or increasing the size of the micropores of pit margo.

Fungi mainly contain wood decay fungi, bacteria and fungi. The pit membrane was destroyed, and the degradation of the cell wall was also very significant after eroded by the wood rot fungus, which affects the strength of the wood directly. Therefore it is appropriate to inoculate mold or stain fungi using fungal treatment methods to improve the permeability of the wood (Zhang et al., 2011). The small specimen of green Douglas fir and the sapwood of loblolly pine inoculated with wood rot fungus was investigated. The results showed that ray parenchyma cells and the half bordered pit of Loblolly pine were destroyed by mold, and the radial permeability of Loblolly pine was improved. However, there is no effect on the permeability of the heartwood and sapwood of Douglas fir (Wan et al., 2006).

Aspen, yellow birch and sugar maple samples were treated with four different fungi for two, four and eight weeks, for biological incising to improve wood permeability. Microscopic examination of aspen samples treated with Trichoderma viride showed that fungal hyphae had moved from cell to cell through the pits. The application of a bioincising treatment is related to the wood species, fungal type and incising time. The pit membrane was damaged, and the cell wall was also seriously destroyed by wood rot fungi, which directly affected the strength of wood. Therefore it is suitable to use mold or the bacteria of fungi for improving wood permeability (Johnson and Gjovik, 1970).

4.4 Evaluation method of pretreatment effect

4.4.1 Fluid permeability

Fluid permeability is an important property of wood and also a parameter for the processing and utilization of wood. The discharge of water and liquid leaching is related to the permeability of the wood. Wood permeability is related to density, moisture, osmotic pressure and permeability media. Because there is no uniform standard, a variety of devices for testing the permeability of wood were designed by scholars, such as the water rising gas flow method (Bao et al., 2001).

4.4.2 Water absorption rate

The water absorption is the percentage of the increased weight of the wood after water absorption. Because of the structural characteristics of the wood, the extent of wood cell pathways can be evaluated by the weight gain rate. The water absorption of six microwave-treated wood and untreated wood were tested. It was found that the water absorption of wood improved after microwave treatment. The change of water absorption is related to the damage of microstructure. The opening of the aspirated pit and the damages of the pit membrane can enhance the liquidity of wood in transverse and longitudinal directions and can increase the diffusion rate of the fluids. A new capillary system is formed with the damage of the intercellular layer between ray cells and the axial thickness of the cell wall, which increased the amount of free water sorption. The destruction of the cell wall can shorten the flow of fluid in the wood cells and increase the specific surface area of the cell wall and the water's ability to cross-flow. The failure of the perforation and the redistribution of the inclusions in the vessel can provide favourable conditions for the longitudinal direction of the moisture migration, but the capillary effect is reduced and the water is easy to lose. The different water absorptions are caused by different damage types of tree species (He et al., 2014b).

4.4.3 Nitrogen adsorption method

The gas adsorption method is a common method to measure the specific surface area and pore size distribution of materials. The principle is based on the absorption characteristic of gas on solid surfaces. Equilibrium adsorption capacity was measured under a certain pressure; the specific surface area, pore size distribution and the amount of physical related with physical adsorption of a tested sample were obtained through the theoretical model.

The nitrogen adsorption at a low temperature is a mature and widely used method to measure the specific surface area and pore size distribution of materials. The surface adsorption capacity of nitrogen in a solid surface depends on the nitrogen-relative pressure (P/P_0), where P is the partial pressure of nitrogen and P_0 is the saturated vapour pressure of nitrogen under temperature of liquid nitrogen. When P/P_0 is in the range of 0.05−0.35, the adsorption and relative pressure P/P_0 are fit for brunauer, emmett and teller (BET) equations. This is the basis of measuring specific surface area by nitrogen adsorption method. When the P/P_0 is equal to or larger than 0.4, nitrogen begins to condense in the micropores due to capillary condensation. The pore volume and pore size can be tested through theoretical analysis and experiments. Mercury intrusion porosimetry can be used to analyze the change of microwave-treated wood; microscopic pore structure in larger pore sizes ranges from 2 to 400,000 nm, but this method is more accurate in macropore analysis (more than 50 nm). The method of nitrogen adsorption can examine the concentration analysis of the pore structure with smaller pore size, and the accurate analysis of the material mesopores (2−50 nm) and some macropores (50 nm).

Fig. 4.6 shows the relationship between the cumulative pore volume and the pore size of the Chinese fir before and after microwave treatment using the method of nitrogen adsorption. It can be seen that the cumulative pore volume of the control sample

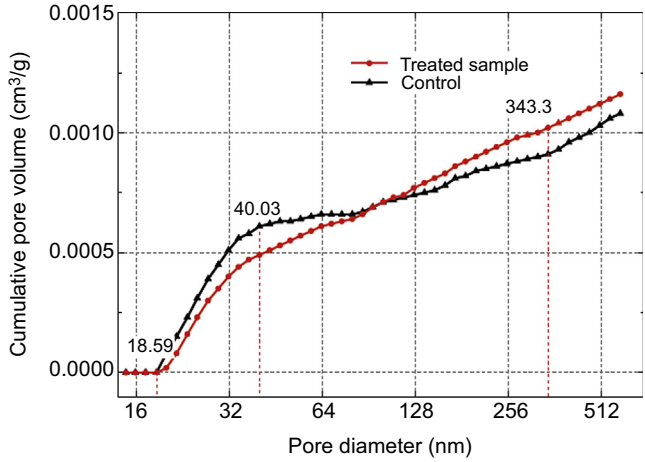

Figure 4.6 Cumulative pore area versus pore diameter of Chinese fir microwave treated and control sample (nitrogen absorption method).

increases greater than that of the treated wood in the pore size distribution range from 18.59 to 40.03 nm, which indicated that the number of pores of the control sample is more than that of the treated sample, but in pore size distribution range from 40.03 to 343.3 nm, the result is just the opposite. It can be speculated that the size of the pore increases from 18.59 to 40.03 nm to 40.03 to 343.31 nm after microwave treatment.

Fig. 4.7 shows the relationship between the differential pore volume and the pore size of the Chinese fir before and after microwave treatment, which is similar to that of Fig. 4.6; that is, the growth rate of the pore volume of the control sample increases greater than that of the treated wood in the pore size distribution ranging from 18.59 to

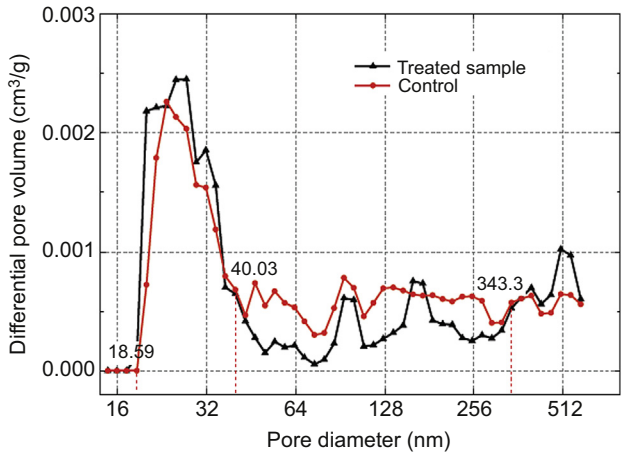

Figure 4.7 Differential pore volume versus pore diameter of Chinese fir microwave treated and control sample (nitrogen absorption method).

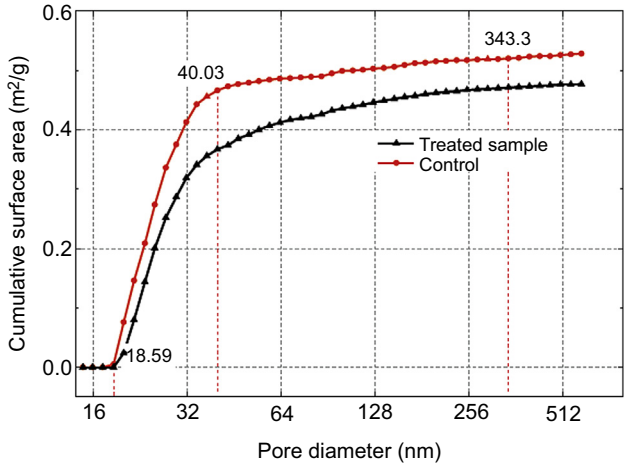

Figure 4.8 Cumulative surface area versus pore diameter of Chinese fir microwave treated and control sample (nitrogen absorption method).

40.03 nm, but the result is the opposite in the pore size distribution ranging from 40.03 to 343.3 nm.

The variation of pore size distribution results in the change of the specific surface area. Fig. 4.8 shows the relationship between the accumulated specific surface area and the pore size of the Chinese fir before and after microwave treatment. It can be seen that the number of pores and accumulated pore volume of the control sample is more than that of treated wood in the pore size distribution ranging from 18.59 to 40.03 nm. The accumulated pore volume of the treated sample is much higher than that of the control one due to the large contribution to specific surface area for small pore size. For the pore size distribution ranging from 40.03 to 343.3 nm, the difference of cumulative pore size between treated wood and the control is reducing. This is mainly because the number of pores of the treated sample is more than that of the control one.

When the pore size is greater than 343.3 nm, the difference of cumulative pore size between treated wood and the control is basically unchanged, and the number of pores is basically the same. This result differs from that obtained by mercury intrusion porosimetry. This difference may be related to the inaccurate analysis of the large pore with nitrogen adsorption.

4.4.4 Mercury intrusion porosimetry

The gas adsorption method is mainly used in the testing of microporous and mesoporous materials, but the method cannot be used to measure the pore with the larger size. Mercury intrusion porosimetry (MIP) can measure the pore structure size of 4−7500 nm and can make up the deficiency of the adsorption method. The testing of macroporous materials generally uses MIP.

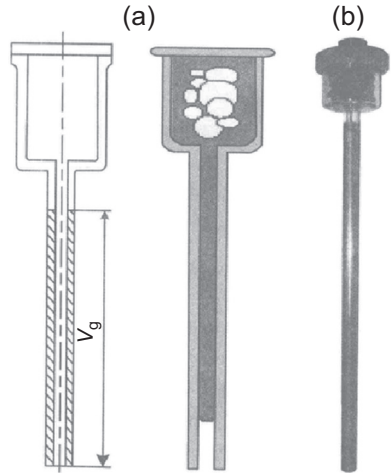

Figure 4.9 Schematic diagram (a) and practical picture (b).

The popularity of mercury injection apparatus makes MIP widely used in the analysis of pore size distribution and specific surface area of the porous materials (Fig. 4.9). Due to the presence of surface tension, the mercury is nonwetting to most solids and the contact angle between mercury and solid is more than 90 degrees. Pressure is needed to make mercury enter into the solid pore. The mercury can enter into the material pore when the pressure increased constantly. The size of the pore is inversely proportional to the pressure. The relationship between the pressure and the volume of mercury can be measured and the data of the pore size distribution be calculated by the mathematical model.

Most of the porous structure of porous materials is irregular. There is a type of pore, whose inlet and outlet are smaller than the pore structure itself, called ink bottle pore. When the pressure is increased to the value corresponding to the pore structure itself, the pore cannot be filled with mercury through the narrow inlet until the pressure is increased to the value corresponding to the narrow inlet. Therefore the pore volume of experimental data corresponding to the pressure is higher, and when the pressure decreases gradually, all the mercury in the ink bottle pore is retained, which will lead to a lag effect of step−down curve, and all of the ink bottle pore volume can be calculated by the end of the step−down curve.

Chinese fir was treated with microwave. Microchecks can be observed at the intercellular layer of ray cells and longitudinal tracheid in microwave-treated samples (Fig. 4.10 left). Parts of the pit membranes in microwave-treated samples were intensively damaged (Fig. 4.10 right). The damage to cell walls was also confirmed with SEM examination (Fig. 4.11). Microstructural changes resulted in the improvement of the liquid permeability of microwave-treated Chinese fir in both the longitudinal and transverse directions. However, because the flow in the longitudinal direction is much faster than that in the transverse direction, the improvement is relatively more significant in the transverse direction.

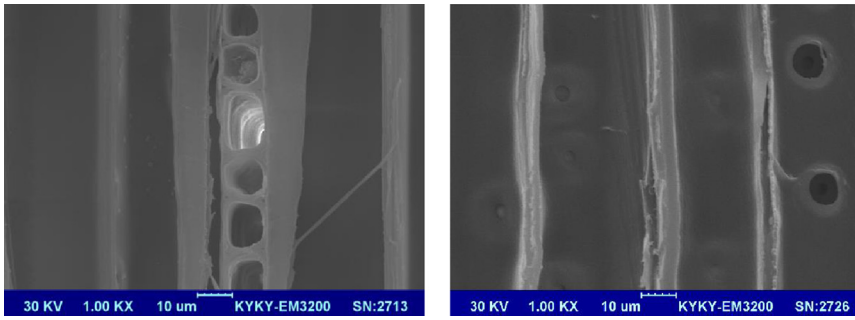

Figure 4.10 Microchecks located at the intercellular layer of ray cells and longitudinal tracheid in microwave-treated samples (20 kW, 40−60%, 60 s) (×1000) (left); Pit membranes in microwave-treated samples (×1000) (right).

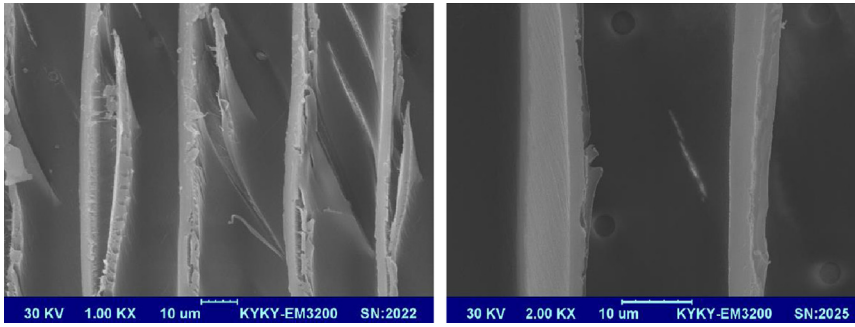

Figure 4.11 Checks in the cell wall of tracheid in microwave-treated samples (×1000) (left) and microchecks in the cell wall of microwave-treated samples (×2000) (right).

Apart from the improvement of permeability, a decrease in mechanical properties caused by microstructural changes was also observed due to the microchecks located at the intercellular layer of ray cells, longitudinal tracheid and tracheid cell walls. Similar results were reported that the reduction of mechanical properties is caused by the fact that checks or voids occur in the radial−longitudinal planes (Torgovnikov and Vinden, 2009). The destruction of pit membranes on the cell walls of tracheid has a negligibly negative effect on the mechanical properties (Pánek et al., 2013).

Microstructural changes in microwave-treated lumbers created additional porosity and altered the pore size distribution, which are important parameters influencing permeability. Table 4.1 shows the results of the MIP measurements for samples before and after microwave treatment. Parameters such as the median pore diameter (volume), median pore diameter (area) and average pore diameter (4V/A) are different, even though the bulk density of control and microwave-treated samples taken for the MIP test were almost the same (0.241 and 0.246 g/cm^3, respectively).

Fig. 4.12 indicates that the primary increase in cumulative pore volume after microwave treatment occurs in the pore diameter ranging from 8039.7 to 36,320.8 nm, and a

Table 4.1 Mercury Intrusion Porosimetry test results before and after microwave treatment

	Total intrusion volume (mL/g)	Total pore area (m^2/g)	Median pore diameter (volume) (nm)	Median pore diameter (area) (nm)	Average pore diameter (nm)	Bulk density at 0.56psia (g/cm^3)	Porosity (%)
Microwave-treated	3.60	34.05	1336.5	20.0	422.5	0.241	86.65
control	3.28	22.37	780.4	436.5	585.6	0.246	80.50

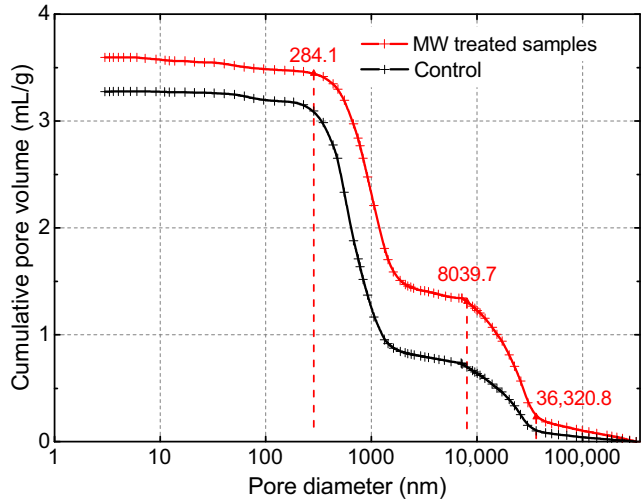

Figure 4.12 Cumulative pore volume versus pore diameter.

similar phenomenon is observed in Fig. 4.13 for the increase of percentage of intrusion volume.

The investigation of the pore size distribution of 30 different wood species with MIP showed that the pore radius in wood could be classified in the range of <0.1 μm for microvoids or cell wall capillaries, 0.1−5 μm for some small tracheid openings (diameter of margo capillaries is 0.1−0.7 μm) and >5 μm for large lumens. Thus the pores with diameters ranging from 8039.7 to 36,320.8 nm are mainly from the tracheid lumens or checks caused by microwave treatment, which still needs to

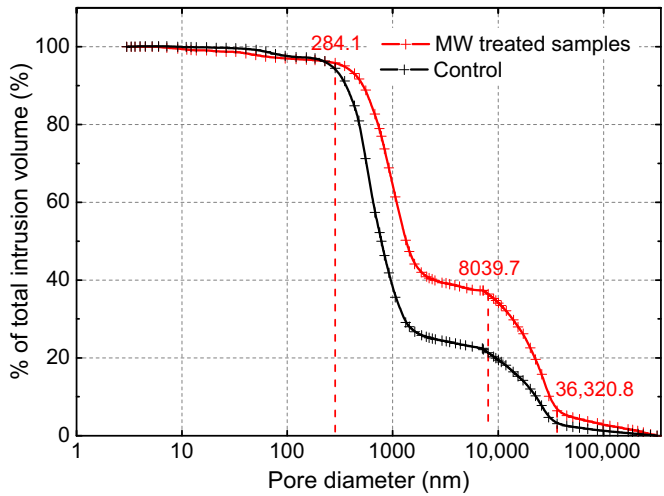

Figure 4.13 Percentage of intrusion volume versus pore diameter.

be confirmed. Because microstructural changes such as the damage of pit membranes could accelerate the flow of liquid through tracheid, it is reasonable to assume that the increase in cumulative pore volume or intrusion volume results from increases in the liquid permeability of tracheid lumens. Checks caused by microwave treatment may also contribute to the increase in cumulative pore volume. As the pore diameter decreased to below 284.1 nm, the cumulative pore volume remained almost unchanged, which indicates that pores with diameters below 284.1 nm made no significant contribution to the pore volume.

The main difference observed in Figs. 4.12 and 4.13 between microwave treatment and control samples occurs in the pore diameter range from 8039.7 to 36,320.8 nm. However, the pore diameter distribution is also different. Fig. 4.14 refers to the pore volumes calculated using the log of the differential pore diameters between microwave-treated samples and control samples. It is apparent that the diameter distribution of macropores includes tracheid lumen as well as some smaller tracheid openings that remain almost unchanged (peak value of a control sample: 25,908.4 nm and that of a microwave-treated sample: 25,918.2 nm). This means hardly any damage was caused by enlarging the diameter of the tracheid lumen, and no checks with a diameter larger than the lumen diameter were produced. As for the pores of pit openings that occur in the mesopore (500−80 nm) as well as in the macropore range (>0.5 μm), the pore diameter turned out to be larger after microwave treatment (peak value of the control sample: 553.7 nm and that of microwave-treated sample: 921.1 nm) (Fig. 4.14). This trend was also confirmed in SEM examinations. The pit membranes can be destroyed to make the pores of pit openings larger and facilitate the intercellular liquid flow. The intensity variation of the curve can be explained by the improvement in permeability of the tracheid lumen diameter range, which results from larger pit openings. Because the bordered pit is the prime factor affecting the liquid flow through tracheid, larger pit openings after microwave treatment resulted in an increase of the intrusion volume dramatically in the tracheid lumen diameter range, which is reflected

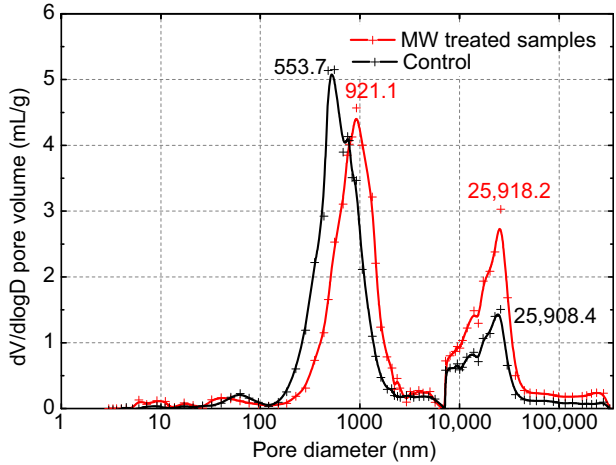

Figure 4.14 Log differential intrusions versus pore diameter.

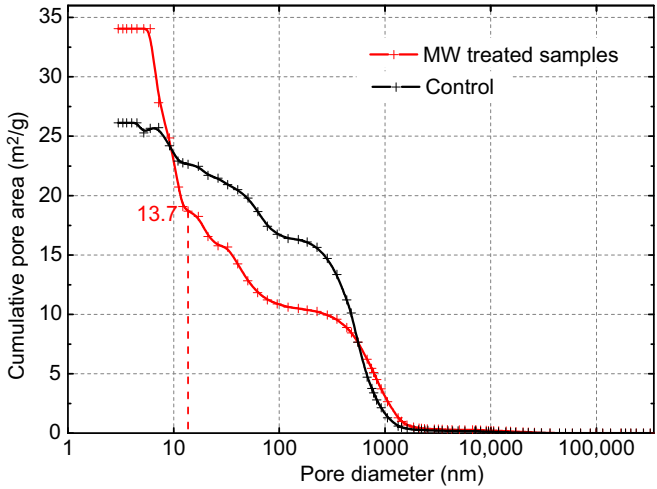

Figure 4.15 Cumulative pore area versus pore diameter.

in the higher intensity in the tracheid lumen diameter range (Fig. 4.14). Moreover, the intensity of the curve in the pit opening diameter range somewhat weakened because most of the intrusion volume had already been occupied in the tracheid lumen diameter range.

Fig. 4.15 shows the cumulative pore area changes before and after microwave treatment. It is evident that the pores with diameters below 1000 nm contributed to 90% of the total pore area for both microwave-treated and control samples. Because the pore diameter is inversely proportional to the specific area, the cumulative pore area is smaller for microwave-treated samples, as the pore diameter increased in the pit opening diameter range after microwave treatment. However, there was a dramatic increase when the pore diameter was below 13.7 nm (Fig. 4.15). It can be inferred that there are more micropores found after microwave treatment and that these micropores contribute to an increase in the pore area, but not to the pore volume (Fig. 4.12). These pores could be located at the interfibril spaces of the margo in the bordered pit. Since liquid permeability is determined by the interfibril space of the margo in the bordered pit, the micropores could be an important parameter in improving the liquid permeability of microwave-treated Chinese fir.

4.4.5 Image processing method

Image processing method can determine the crack area and statistically analyze the crack characteristics. This method has been applied to many materials. The information of crack length and area is obtained by analyzing the surface crack of the wood using the method of image processing (Mekhtiev and Torgovnikov, 2004). In order to identify and analyze the crack in scanning an image, Matlab software was used to process the type conversion, enhancement, segmentation and morphological processing of the original image and obtain the statistical results, including crack number and length, width and area of each crack, which can be used to calculate

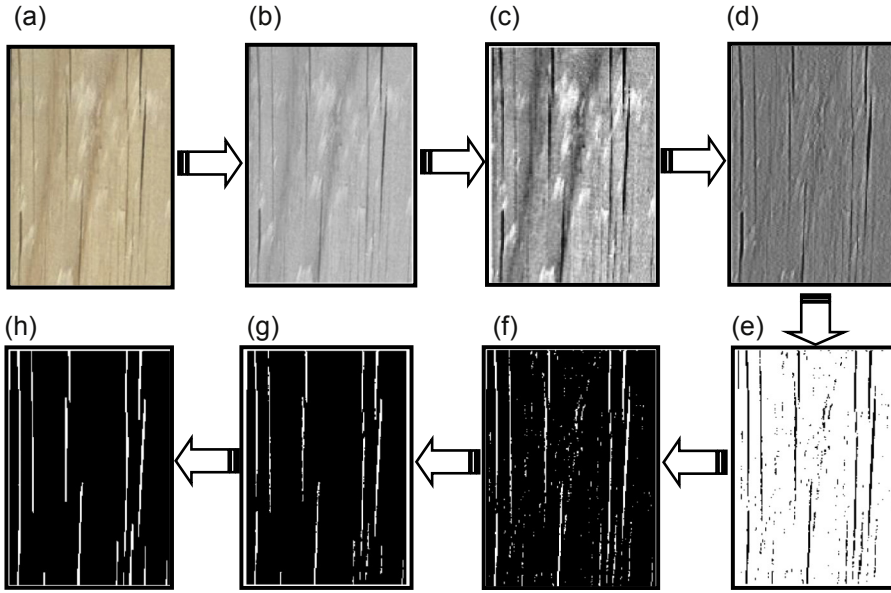

Figure 4.16 The flow chart of crack analysis for the microwave-treated wood. (a) original image, (b) gray image, (c) contrast enhancing processing, (d) spatial filter processing, (e) sharpening processing, (f) image segmentation, (g) denoise processing and (h) the final result of wood crack image.

the percentage the total crack area to image area, average width and total length of cracks in the image.

The crack is produced in the wood after high intensity microwave treatment. The orientation of the crack is the radial direction of the wood, which is the most obvious in the tangential section. The scanning image of the tangential section was used to analyze the crack state of the microwave-treated wood. Image processing is used to analyze the image. The original image is a colour-scanning image of a tangential section of treated wood, and the image resolution is 600 dpi (Fig. 4.16(a)). In Matlab software, the conversion of colour images to grayscale images can be achieved by using the RGB to grey function. The grayscale image after the transformation is shown in Fig. 4.16(b). The microwave-treated wood surface crack is separated from the background image through the following steps: contrast enhancement (c), filter processing (d), sharpening processing (e), image segmentation (f), binary image noise reduction processing (g) and fracture crack closure (h). The software then calculated the proportion of crack region according to the number, length, width and area of cracks on the surface of microwave-treated wood.

4.4.6 X-ray computed tomography

The X-ray computed tomography (CT) technique is a modern imaging technique based on measuring the attenuation coefficient of penetrating rays in a sample. Using a

certain physical technology and mathematical method calculates the two-dimensional distribution matrix of attenuation coefficients in a section of the object by computer processing. The two-dimensional distribution matrix is transformed into grey distribution of the image, so as to re-establish the cross section image.

The CT system mainly includes X-ray equipment, detectors and data acquisition devices, computer systems, image displays, storage devices and auxiliary devices. In order to make the acquired images more clear, the convolution back projection method is used. As the image begins reconstruction, each data convolutes the operation with a convolution kernel before back projection, selection and design of a different convolution kernel, enhancing the reconstructed image edge, which makes the CT image contrast increase and become clear. The application of CT in wood science is mainly focused on the defect detection of wood inner, log 3-D reconstruction and virtual machining, the wood density variation analysis and wood moisture distribution measurement. The process of fungal erosion and the division of fungi in wood can be observed by CT scanning (Van den Bulcke et al., 2009) (Figs. 4.17 and 4.18). The distribution of function modifier in the timber can also be observed by three-dimensional reconstruction (Fig. 4.19) (De Vetter et al., 2006).

4.5 Future trends

With the reduction of rain forest resources and the increased consumption of wood materials, more attention is paid to use plantation forest wood. However, the application of plantation forest wood is limited by defects and low strength. Therefore it is currently a vital research field in order to increase the value-added application of plantation forests by functional modifications.

The volume, depth and uniformity of functional modification in wood are the most important aspects in the wood functional modification process. Therefore how to improve the impregnating performance or permeability of the plantation forest wood is the key.

The microwave has the features of quick, uniform, and internal and external heating. Wood absorbed the microwave and then transformed into heat, and wood temperature rises rapidly. At the same time, microwave penetrates into the wood due to its strong penetrating ability, so that the temperature of the treated material is uniformly distributed. In addition, with the temperature of the treated material increased, the water vapour pressure rapidly increased. When the steam pressure is greater than the strength of the weaker wood tissue, such as pit, pit torus, intercellular layer and ray parenchyma cells, the microstructure of the treated wood produces a certain degree of damage, and even develops into macrocracks. A new fluid channel is formed to improve the permeability of the wood effectively, which is conducive to the impregnation of the functional filler. Microwave radiation improves the permeability of wood and dries the wood at the same time. It is a promising method and worth promoting.

Further enhancement of functionalization may include comprehensive new technology, such as the combination of the extraction, microwave, compression and supercritical methods.

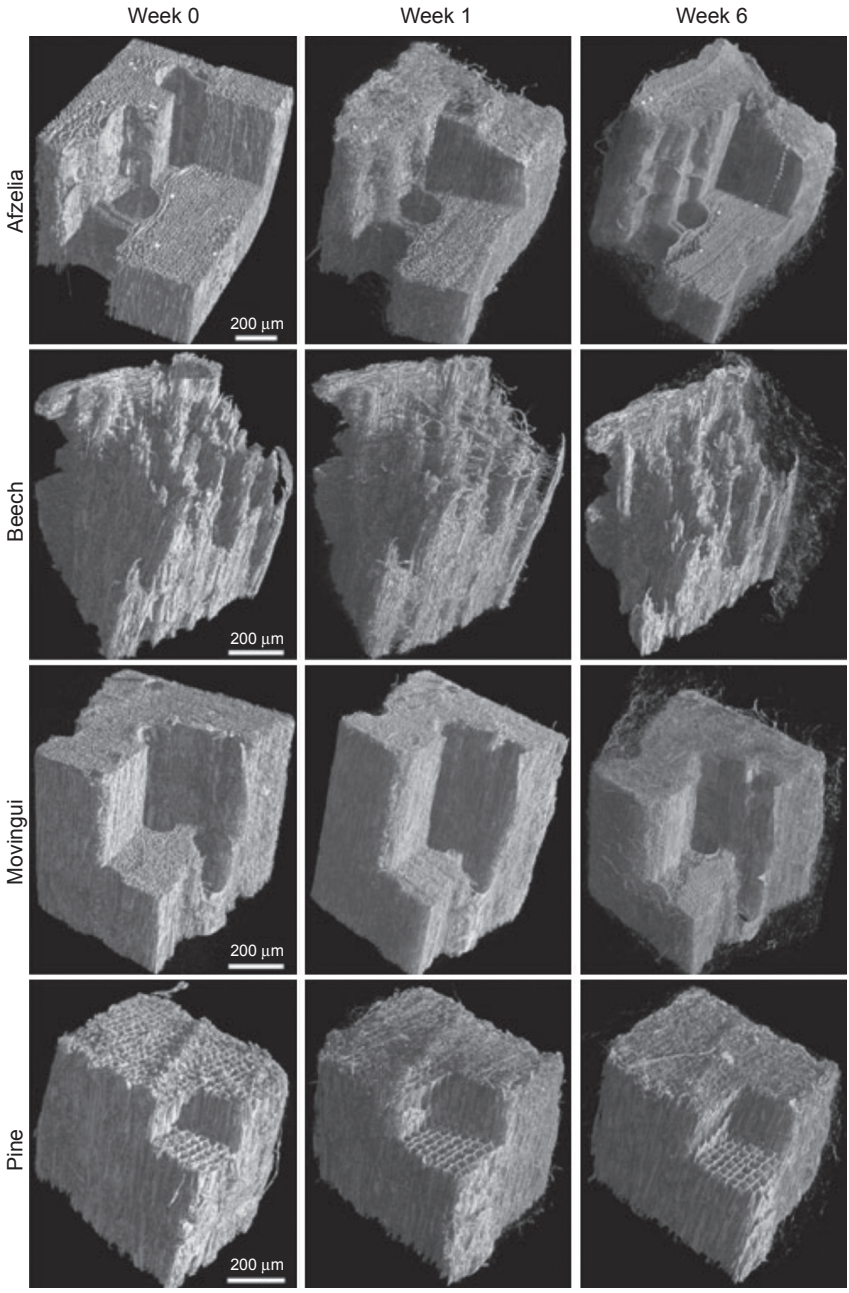

Figure 4.17 Time series scanning of the four wood samples under study: reconstruction before exposure to the fungi and after one and six weeks of incubation.

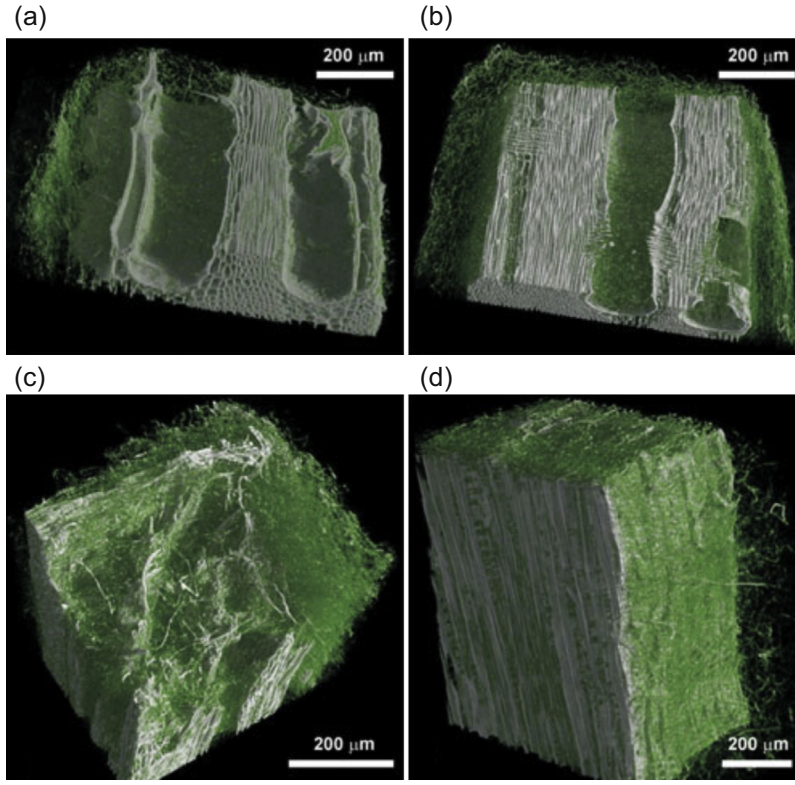

Figure 4.18 Segmentation of hyphae (green) on the (a) afzelia, (b) movingui, (c) beech and (d) pine volumes.

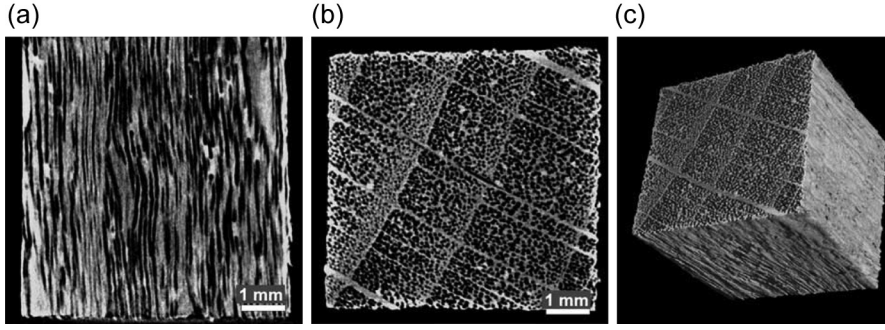

Figure 4.19 Reconstruction of siloxane/silane impregnated beech: (a) longitudinal image, (b) transverse view and (c) 3-D view.

Acknowledgments

This work was financially supported by the Special Fund for Forest Scientific Research in the Public Welfare (No. 201404516), and the National Science and Technology Pillar Program during the Twelfth Five-year Plan Period of China (No. 2015BAD14B04).

References

Adachi, K., Inoue, M., Kanayama, K., Rowell, R.M., Kawai, S., 2003. Drying of wood by roller pressing. In: Proceedings of 8th Int. IUFRO Wood Drying Conference, Brasov-Romania.

Bao, F.C., Lv, J.X., 1991. The influence of microorganism on permeability of *Picea jezoensis* var. *komarovii*. Scientia Silvae Sinicae 27 (6), 615−621.

Bao, F.C., Lv, J.X., Zhao, Y., 2001. Effect of bordered pit torus position on permeability in Chinese yezo spruce. Wood and Fiber Science 33 (2), 193−199.

De Vetter, L., Cnudde, V., Masschaele, B., Jacobs, P.J.S., Van Acker, J., 2006. Detection and distribution analysis of organosilicon compounds in wood by means of SEM-EDX and micro-CT. Materials Characterization 56 (1), 39−48.

Degroot, R.C., Sachs, I.B., 1976. Permeability, enzyme-activity, and pit membrane structure of stored southern pines. Wood Science 9 (2), 89−96.

Demessie, E.S., Hassan, A., Levien, K.L., Kumar, S., Morrell, J.J., 1995. Supercritical carbon dioxide treatment: effect on permeability of Douglas-fir heartwood. Wood and Fiber Science 27 (3), 296−300.

Dunleavy, J.A., Moroney, J.P., Rossell, S.E., 1973. The association of bacteria with the increased permeability of water-stored spruce wood. British Wood Preserving Association 127−148.

Fang, G., 2008. Functional Improvement of Wood. Chemical Industry Press, Beijing, pp. 1−29.

He, S., Lin, L.Y., Fu, F., Zhou, Y.D., Fan, M.Z., 2014a. Microwave treatment for enhancing the liquid permeability of Chinese fir. BioResources 9 (2), 1924−1938.

He, S., Lin, L.Y., Fu, F., Zhou, Y.D., 2014b. Experimental study of six species of wood treated by microwave. Journal of Microwaves 4 (4), 90−96.

Iida, I., Ikeuchi, A., Imamura, Y., 1995. Liquid penetration of precompressed woods III: effects of moisture contents of specimens and ambient temperatures while compression on liquid uptakes of softwoods and hardwoods. Journal of the Japan Wood Research Society 41 (9), 811−819.

Johnson, B.R., Gjovik, L.R., 1970. Effect of Trichoderma viride and a contaminating bacterium on microstructure and permeability of loblolly pine and Douglas fir. American Wood Preservers Association Proceedings 66, 234−240.

Li, X.J., Fu, F., Zhou, Y.D., Chen, Z.L., 2007. Advances in the research of wood microwave modification. Materials Review 21 (11), 295−297.

Li, Y., Liu, Y., Yu, H., Liu, Z., 2011. Theory and research method for the study of wood fluid penetration. Scientia Silvae Sinicae 47 (2), 134−144.

Lv, J.X., Bao, F.C., 2000. Studies on the effect of three different treatments on wood permeability. Scientia Silvae Sinicae 36 (4), 67−76.

Mekhtiev, M.A., Torgovnikov, G.I., 2004. Method of check analysis of microwave-modified wood. Wood Science and Technology 38 (7), 507−519.

Meyer, R.W., 1974. Effect of enzyme treatment on bordered-pit ultrastructure, permeability, and toughness of sapwood of three western conifers. Wood Science 6 (3), 220−230.

Militz, H., 1993. Changes in the micro structure of sprucewood (*Picea abies* L. Karst) through treatment with enzyme preparations, alkali and oxalate. Holzforschung 45 (3), 50–53.

Morrell, J.J., Morris, P.I., 2002. Methods for Improving Preservative Penetration into Wood: A Review. International research group on wood preservation (IRG/WP 02–40227), Stockholm.

Nijdam, J.J., Lehmann, E., Keey, R.B., 2004. Application of neutron radiography to investigate changes in permeability in bacteria treated pinus radiata timber. Maderas Ciencia Y Tecnología 6 (1), 19–31.

Pánek, M., Reinprecht, L., Mamoňová, M., 2013. Trichoderma viride for improving spruce wood impregnability. BioResources 8 (2), 1731–1746.

Richter, K., 1989. Perforation and impregnation methods to improve weather resistance of structural timber. Empa Research and Working Report 115 (19), 1–44.

Torgovnikov, G., Vinden, P., 2009. High-intensity microwave wood modification for increasing permeability. Forest Products Journal 59 (4), 84–92.

Torgovnikov, G., Vinden, P., 2010. Microwave wood modification technology and its applications. Forest Products Journal 60 (2), 173–182.

Van den Bulcke, J., Boone, M., Van Acker, J., Van Hoorebeke, L., 2009. Three-dimensional X-ray imaging and analysis of fungi on and in wood. Microscopy and Microanalysis 15 (5), 395–402.

Wan, H., Yang, D., Zhang, C., 2006. Impact of biological incising to improve phenolic resin retention and hardness of various wood species. Forest Products Journal 56 (4), 61–67.

Wang, X., Zhao, G., Liu, X., Zhen, H., 2003. Study on mechanism of decreasing wood collapse by pre-freezing. Scientia Silvae Sinicae 39 (5), 95–99.

Xiao, Z., Lu, J., 2009. The effects of treatment technology of supercritical CO_2 fluid on wood permeability. Fujian Forestry Science and Technology 36 (03), 24–27.

Xiao, Z., Lu, X., Lu, J., 2009. Effects of co-solvent in supercritical CO_2 treatment on wood permeability. Journal of Fujian Forestry College 29 (2), 178–182.

Zhang, Y., Cai, L., 2006. Effects of steam explosion on wood appearance and structure of sub-alpine fir. Wood Science and Technology 40 (5), 427–436.

Zhang, Y., Cai, L., Xu, Y., 2006a. Aspirated pits in wetwood and micromorphology of microbial degradation of sub-alpine fir. Journal of Nanjing Forestry University 30 (1), 53–56.

Zhang, Y., Miao, P., Zhuang, S., Wang, X., Xia, J., Wu, L., 2006b. Improving the dry-ability of Eucalyptus by pre-microwave or pre-freezing treatment. Journal of Nanjing Forestry University 35 (2), 61–64.

Zhang, Y., Xia, J., Wang, J., 2011. A review of methods of opening wood cell pathways. Journal of Anhui Agriculture University 38 (6), 867–871.

Cellulose polymer composites (WPC)

5

J. Bayer, L.A. Granda, J.A. Méndez, M.A. Pèlach, F. Vilaseca, P. Mutjé
University of Girona, Girona, Spain

5.1 Introduction

Composite materials are frequently classified by the matrix material into Ceramic Matrix Composite, Metallic Matrix Composite and Polymeric Matrix Composite (PMC). The main objective of combining those matrices with fillers is to obtain materials with the combined properties for their constituents. In the last 50 years, there has been an exponential use and research in the field of PMCs as they allow easy and versatile transformation processes. Aerospace or automotive sectors have led the new developments in order to find materials with higher specific properties and better dimensional stability in comparison to standard plastics. Other sectors, such as the building industry, have started to use wood plastic composites (WPC) as a substitute for natural wood, because of the lower water absorption, new designing possibilities and price reduction when compared with high quality wood.

In addition, the ever growing environmental concerns have prompted renewed interest in the study of more environmentally friendly materials. Consequently, concepts such as biodegradability and environmental safety became crucial topics when considering new materials. New products are often designed with the perspective of sustainable development or eco-design, a philosophy that is increasingly being applied in most research fields. Common fillers, such as glass fibre, present some important drawbacks in that field.

In the market of polymer composites, 95% is nowadays led by polypropylene reinforced with glass fibre (Gent et al., 2010). Developed initially to improve the tensile strength, stiffness and lack of dimensional stability from the original polymer matrix, but preserving the easy processing characteristics of polypropylene, it can be processed by injection or extrusion as a main manufacturing technology. The use of standard plastic transformation technologies allows a fast, easy and cheap production, and it can obtain a wide range of geometries and applications.

Since 1965, the market has been led by the composites reinforced with synthetic reinforcement (glass fibre, carbon fibre, aramid fibres), and one of the most commonly used synthetic fibres is the glass fibre. It confers a high tensile strength and stiffness to the composite material.

The values of Fig. 5.1 represent the total amount of production, including all available technologies for transforming fibreglass into composites. The figure of 1100 kt can be considered as the last five years' flat tendency. Germany, Italy and East Europe stay in the front of production.

Advanced High Strength Natural Fibre Composites in Construction. http://dx.doi.org/10.1016/B978-0-08-100411-1.00005-4

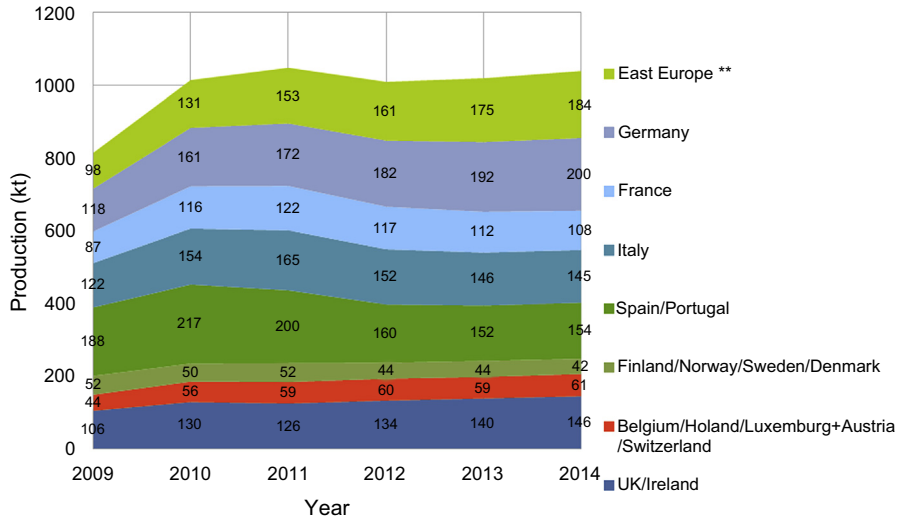

Figure 5.1 Production of glass fibre composites in Europe.
Adaptation of figures from Witten, E.(AVK), Kraus, T.(CCeV), Kühnel, M.(CCeV), 2014. Composites-marktbericht 2014.

A large amount of fibreglass is used in construction and transportation sectors when applied to big surfaces of resins reinforced with fibreglass. However, its high fragility reduces its recyclability drastically. Furthermore, dermatitis and health problems were diagnosed as a consequence of being in contact with that fibre (Donaldson and Tran, 2004; Greenberg et al., 2007; Wang et al., 1993). Another great disadvantage is the high abrasive effect of glass fibre against the tooling, increasing the maintenance cost of the equipment.

The use of natural reinforcements coming from sawdust or agroforest is considered as a healthier and more recyclable way of producing composite materials. Cellulose fibres do not confer as good mechanical improvements as glass fibres do, but their low density leads to reasonable specific properties.

Polypropylene (PP) is the most often used matrix. The nonrenewable tag of PP, as is derived from petrol as well as its difficult disposal when the product arrives to the end of its life, has driven researchers and industry to find more renewable, environmentally friendly, sustainable and low cost polymers. The main reason of the low acceptance of those biodegradable polymers is their high price when compared with conventional polymers. Nevertheless, researchers are nowadays focused on studying the possibilities of using biopolymers as matrices in composite materials, in order to achieve a 100% biodegradable composite with a good relationship of mechanical properties, density and price (Bax and Mussig, 2008; Bledzki and Jaszkiewicz, 2010; Graupner et al., 2009).

The market stays now in the middle point of using petrol-based polymers reinforced with wood fibres or particles. Wood plastic composites are widely used in construction as decking and siding profiles for outdoor performance, which imitates the wood

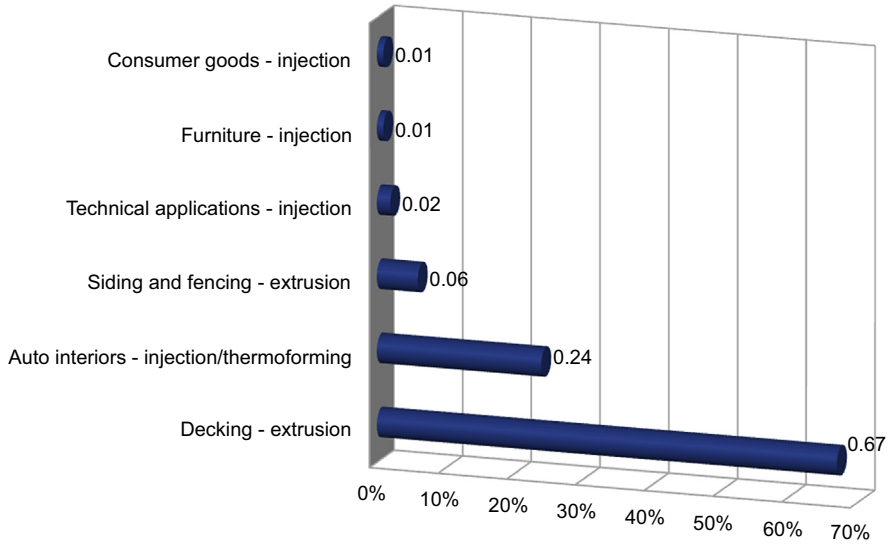

Figure 5.2 Application fields of wood plastic composites and NFC in Europe 2012. Adaptation of figures from Witten, E.(AVK), Kraus, T.(CCeV), Kühnel, M.(CCeV), 2014. Composites-marktbericht 2014.

colour and aspect while reduces its maintenance cost for the consumers. In Fig. 5.2, the main consumption of natural/wood fibres composites in 2012 and their main applications can be seen. Following the same trend, currently the principal WPC-consuming sector is the building industry. It can be seen that decking and siding are manufactured with an extrusion process.

In comparison to tropical wood, wood plastic composites exhibit the improved properties in water absorption and aspect durability and lower cost. On the other hand, they perform lower impact and tensile strength.

5.2 Formulation of wood plastic composites

The correct selection of the matrix, reinforcement and additives that will be mixed is absolutely important for assuring that the properties of the obtained composite material are adequate to the expected performance.

5.2.1 Polymer matrix

The degradation temperature around 200°C of natural fibre limits the selection of polymers to formulate a natural fibre composite. Only those polymers that can be correctly processed under this limited temperature can be considered as possible matrices for natural fibre composites.

These drawbacks are due to the limited thermal stability of wood components, especially the lignin fraction, which is the most temperature-sensitive component. The removal of lignin may enhance the thermal stability of the reinforcement. Although several papers refer to this option (Lopez et al., 2012; Reixach et al., 2013), in practice, fibres or sawdust are not commonly processed before extrusion or injection.

Another interesting debate is whether to use virgin or recycled plastics. The mechanical properties using virgin materials are usually higher in impact and tensile strength. On the other hand, the price per kilo increases when using the virgin matrix. Depending on the use, the balance between price and properties should define which material fits better. For instance, when external timber decking is considered, which is supported by base profiles, the main property is the flexural deflection. Considering that the deck product is usually installed by a third part of workers with a standard distance of 30−35 cm between base profiles, the use of the recycled instead of virgin plastics could be enough for its final requirement under such conditions. If PP matrix decking is considered, this distance could be increased to 40−45 cm with the same deflection. However, the reduction of base profiles quantity and time for installation do not compensate the price difference.

5.2.1.1 Polyolefins

Polyolefins are polymers formed by unsaturated hydrocarbons with double bonds between carbon molecules. The two main olefins used for obtaining plastics are ethylene and propylene. The low cost of polyethylene and polypropylene has led those polymers to be the most used, especially by the packaging industry.

In the wood plastic composite industrial sector, especially in deck production, high density polyethylene (HDPE) is the most used matrix polymer, due to two key factors: price per kg of raw material and speed in extrusion process, around three times quicker than PP (with 60% reinforcement).

Although HDPE shows lower mechanical properties in tensile strength than PP, the addition of 40% or 50% in weight of natural fibre with a good interphase quality can increase the ultimate tensile strength by a factor of two, from 14 MPa (virgin HDPE without reinforcement) to values around 25−30 MPa (composite).

PP and PVC are the other two principal polymers used as matrices. However, PVC has a bad image as a halogenated compound, and consequently, hydrogen chloride generation when burns. Nevertheless, it is used worldwide for window profiles and interior decking.

In the next section the main properties of the principal polyolefins are described (Lukkassen and Meidell, 2006).

Low density polyethylene

Low density polyethylene (LDPE) is a high branched PE. Its high ramification confers a low density to the molecule as well as a lower hardness, stiffness and strength than high density polyethylene, but with higher ductility. It is semitransparent, and only thin foils can be transparent. That strong ramification hinders the packing of the molecules, diminishing the crystallinity of the material.

LDPE is widely used in packaging like foils, trays and plastic bags for both food and nonfood purposes. It is also used as protective film on paper, textiles and other plastics. For instance, one of the most famous applications is in milk cartons, where it forms part of a system of different plastic layers. Other applications are wrapping foil for packaging, plastic bags (the soft type that does not crackle), garbage bags, tubes or ice cube plastic bags.

High density polyethylene

HDPE is a low branched PE. That lower ramification leads to a higher packing capacity, and consequently, an enhanced crystallinity than LDPE. This confers HDPE a higher working temperature than LDPE, but it is also harder, stronger and slightly heavier (but less ductile). It has a wax-like, lustreless and opaque appearance.

It can be moulded, machined and joined together using welding. Some industrial formulations of HDPE can be used in contact with food. Applications can be found in milestones, bottles for motor oil, bottles for organic solvents, street bollards, gasoline tanks, milk bottles, plastic bags, children's toys, lids for honey pots, beer crates and dolphin bicycle trailers.

Polypropylene

PP has a light, soft, wax-like texture and is a white and opaque polymer, although it can be dyed in different colours. It has reasonable chemical stability, which makes it a good candidate for outdoor performance. Despite its low resistance to nitrous gasses, halogens and oxidizing acids, it performs a high resistance to most minerals, strong acids and bases.

PP is a semicrystalline polymer with a glass transition temperature around $-5°C$ and a melting temperature between $160°C$ and $170°C$. Its chemical structure drives it to perform a high crystallinity (60%).

It is a ductile material with higher tensile strength, stiffness and working temperatures than other polyolefins, such as HDPE. Although it performs good properties, they are lower than most polymers. However, they can be improved by adding glass fibre, chalk, talc and other fibres or particles.

Some of the common applications of those plastics are children's toy bins, transport boxes, fuel tanks, suitcases, garbage bins, ropes, shavers (rechargeable), air intake tubes, packing material and auto parts. PP is extensively used in the packaging industry because of its cheap price.

Biodegradable polymers

Biodegradable polymers are polymers that can be degraded by microorganisms. The use of those polymers as matrices would give the 100% green label to the wood plastic composites when used in a massive way. Literature reviews in that field have increased (John and Thomas, 2008).

Fig. 5.3 shows a classification of the biodegradable polymers regarding their respective resource.

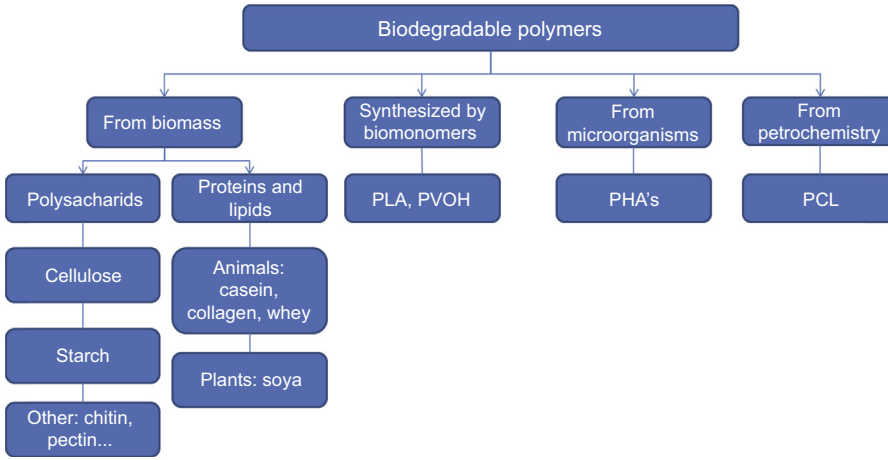

Figure 5.3 Biodegradable polymer classification.

From the biodegradable polymers shown, the most extensively studied for WPC are starch, polylactic acid (PLA) and polyhydroxyalkanoates (PHAs).

Starch biocomposites perform a very good interface quality with wood fibres. However, low mechanical properties of starch make it difficult to substitute polyolefin-based composites.

Polyhydroxyalkanoates have a similar mechanical behaviour to polyolefins, although nowadays the interface quality obtained is lower than using polyethylene or polypropylene (Pérez Amaro, 2015).

Polylactic acid presents higher tensile strength and stiffness than PP. However, as polyhydroxyalkanoates, the low interface quality impedes the increasing strength (Bledzki and Jaszkiewicz, 2010; Ochi, 2008). Although the high tensile strength of those wood composites can be similar to PP wood composites, it is not competitive in the market because of the high price of the matrix.

5.2.2 Natural fibres

One primary classification of natural fibres is to subdivide them by their origin: mineral fibres (glass, carbon, asbestos, basalt), animal fibres (silk, spider silk, wool) and vegetable fibres from plants. The cellulose-rich cultivated plants are used as reinforcement or filler in plastics. Some tropical plants have also been considered, such as sisal, cotton and sugarcane. The main classification of the vegetable plants is based on the origin and the part of the plant they come from (Vallejos, 2006):

- *stalks*: fibres from the straws of cultivated plants like wheat, oat, maize, barley or rape;
- *canes, grasses and reeds*: for instance, the stalks of bamboo or sugar cane;
- *leaf fibres*: fibres from the leaf ribs of sisal, pineapple, banana;
- *bast fibres*: fibres from the inner barks of the stalks like flax, hemp, jute and kenaf;
- *seed and fruit hairs*: flosses of the seed or the husk, for example, cotton and coir;

- *husk:* the by-products of the crop processing, like maize hull and rice hull; and
- *wood fibres*: fibres from hardwood and softwood trees. Examples include pine, maple and spruce.

5.2.2.1 Chemical composition

Chemical composition of the fibre will be strongly bonded to the properties that those fibres and particles will perform as fillers. The composition determinates how good or bad the bonding could be. Hence the selection of the fibre is an important matter.

Wood is mainly formed by cellulose and hemicellulose, lignin and extractives (Koljonen et al., 2003). Despite different defibration and treatment techniques, the chemical percentage of carbohydrates and lignin of the whole pulps were approximately equal (Koljonen et al., 2003). However, differences were observed, both in the chemical composition and morphology on the fibre surfaces (Börás and Gatenholm, 2005). Cellulose is a homopolysaccharide, which is formed by monomer β-glucose. Fig. 5.4 shows its chemical structure. It has a lineal structure. Its chemical structure allows establishing lots of hydrogen bonds between chains that will confer them high mechanical properties. The result becomes a high strong union between chains and, as consequence, a nonwater-soluble molecule, which, despite the linear characteristics, is impossible to melt. It has a structural function in plants, forming part of the cell wall of vegetal cells.

The polymerization number depends on the origin of the fibre, as well as the part of the plant that it comes from, but usually is around 200. However, it can be reduced during shredding processes.

Cellulose forms a microcrystalline structure with very high packing regions. However, they coexist with another cellulose component called hemicellulose. The main differences between these fibres are that hemicelluloses are constituted by different monosaccharides; they have a high ramification degree and a lower polymerization ratio. Furthermore, the composition of hemicellulose differs depending on the origin of the plant, while cellulose is always formed by the same constituents.

The higher microcrystalline structure of the cellulose is the principal structure responsible of the strengthening effect of the reinforcement in wood plastic composites.

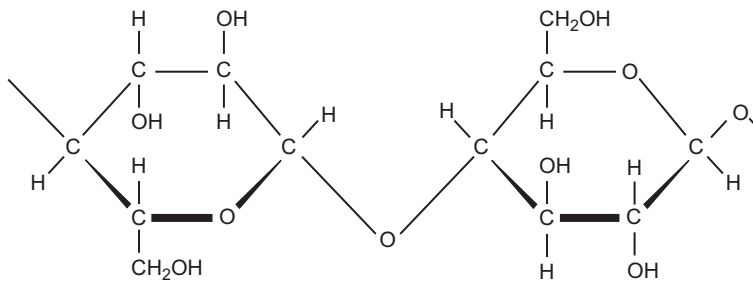

Figure 5.4 Cellulose chemical structure.

Lignin is formed by both aromatic and aliphatic components resulting from the union between different acids and phenylpropylic alcohols, resulting in an amorphous polymer. It has a matrix function in plants, keeping the cellulose fibres united, as well as protecting the cell from the attack of other microorganisms.

Lignin content is also strongly related with the stiffness of the reinforcement. Some studies show that the stiffness increases with increasing lignin contents to a maximum. Higher lignin contents will cause the diminution of the stiffness of the fibre (Neagu et al., 2006). However, lignin will hinder the interaction between the polymeric matrix and cellulose fibre. That fact will have, as a consequence, a reduction of the tensile strength of the polymer.

Beside the described components, wood is also composed by other components such as resin, fatty acids, triglycerides, sterols, waxes and steryl esters. These components are grouped under the name of extractives. They are strongly bonded to the plant where it comes from, as well as the area.

In Table 5.1, some fibre compositions are described according to their origin (Abdul Khalil et al., 2010; Bledzki and Gassan, 1999; Cordeiro et al., 2004; Uma Devi et al., 1996; John and Anandjiwala, 2008; Reddy and Yang, 2005; Tsoumis, 1968; Yueping et al., 2010).

The elemental fibres are formed by crystalline cellulose microfibrils connected by a hemicellulose and lignin complex. The fibre wall structure is formed by different cellulose layers of cellulose, lignin and hemicellulose that form a primary wall (P) and three secondary walls (S). Fig. 5.5 shows the fibre wall structure.

Those walls differ in their composition and the orientation of the microfibrils. The intermediate secondary wall is the one which presents higher cellulose content and more oriented microfibrils.

The traditional mechanical, thermal and chemical treatments that the paper industry developed are useful for a good preparation of reinforcement with increased properties.

5.2.3 Reinforcement treatments

There are different treatments that can be used for increasing the disposable fibrils of the reinforcement, as well as to modify the composition of the reinforcement. Those treatments are grinding, refining, thermomechanical treatment and chemical treatment.

5.2.3.1 Grinding

Grinding consists of shredding the wood through abrasion with different kind of mills. Water is permanently added in order to extract the generated heat during the grinding. Neither lignin nor extractives are removed during this process.

This methodology can be executed either at higher or lower temperatures than the lignin softening temperature (between 50°C and 80°C depending on the composition), being named hot or cold pulp preparation, respectively.

Working at higher temperatures may cause important structural damages on the fibre. The high abrasion forces that those fibres are subjected during the shredding

Table 5.1 Examples of the chemical composition of different fibres

Fibre	Cellulose	Hemicellulose	Lignin	Extractives
Cotton	82.7	5.7	–	6.3
Jute	64.4	12.0	11.8	0.7
Flax	64.1	16.7	2.0	1.5–3.3
Ramie	68.6	13.1	0.6	1.9–2.2
Sisal	65.8	12.0	9.9	0.8–0.11
Oil palm EFB	65.0	–	19.0	–
Oil palm frond	56.0	27.5	20.5	4.4
Abaca	56–63	20–25	7.0–9.0	3.0
Hemp	74.4	17.9	3.7	0.9–1.7
Coir	32.0–43.0	0.15–0.25	40.0–45.0	–
Banana	60.0–65.0	19.0	5.0–10.0	4.6
PALF	81.5	–	12.7	–
Sun hemp	41.0–48.0	8.3–13.0	22.7	–
Bamboo	73.8	12.5	10.2	3.2
Hardwood	31.0–64.0	25.0–40.0	14.0–34.0	0.1–7.7
Softwood	30.0–60.0	20.0–30.0	21.0–37.0	0.2–8.5
Bagasse	55.2	16.8	25.3	–
Kenaf	72.0	20.3	9.0	–
Pinapple	81.0	–	12.7	–
Curaua	73.6	9.9	7.5	–
Wheat straw	35.0–45.0	15.0–31.0	12.0–20.0	–
Rice husk	35.0–45.0	19.0–25.0	20.0	14.0–17.0
Rice straw	41.0–57.0	33.0	8.0–19.0	8.0–38.0

cause a high shear stress, which reduces the fibre length. This is why it is preferred to work with long fibres, usually obtained from resinous woods like pine.

The main advantages of this kind of production are its low cost and that no wide spaces are needed for the installations. However, they do not process hardwoods.

5.2.3.2 Refining

Refining offers a less abrasive shredding process than grinding, allowing the treatment of hardwoods. This method uses sawdust as raw material that is introduced between two discs that rotate in opposite senses, or one rotates and the other remains still.

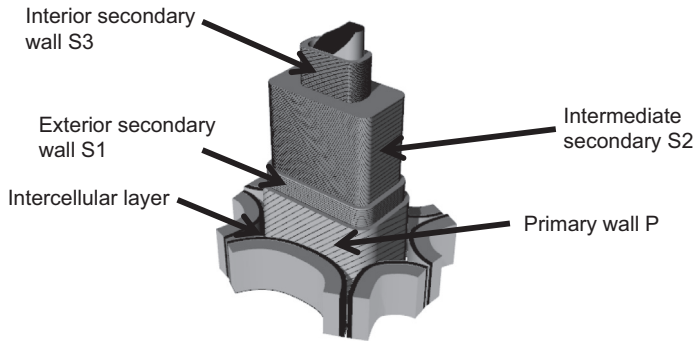

Figure 5.5 Cell wall structure.

Lignin suffers the same softening effect as in grinding, but the sawdust is transformed into intermediate products before being completely shred in the refining process.

It allows working with hardwoods, but a greater inversion and a higher consuming energy is needed.

5.2.3.3 Thermomechanical treatment

It consists of impregnating sawdust with water vapour. Afterwards, sawdust is refined following the same process explained earlier. The water vapour softens the lignin and allows a better fibre separation, without damaging the fibre.

The fibres will be longer and stronger than those obtained through only mechanical treatments. Usually, the refining is performed at higher pressures than atmospheric ones. The process has a higher energy consumption than both explained earlier.

5.2.3.4 Chemical treatment

A chemical treatment can be executed for extracting hemicellulose, lignin and extractives, favouring hydrogen bonds between fibres and with polymeric matrices. Usually, sodium hydroxide, sulfuric acid, anthraquinone or diglyme are used in those treatments. Other systems, like silanes, can be considered by improving the matrix-fibre linkage.

Chemical treatment will not be able by itself to shred the fibre. A mechanical treatment will be needed, but it will allow producing reinforcement with a desired composition.

However, the surface composition could not be predicted from the bulk composition of the pulps (Börás and Gatenholm, 2005; Koljonen et al., 2003). The surface of the fibres were covered by lignin and extractives. Fig. 5.6, based on Sundholm (1999), shows that the mean chemical bulk composition at the middle lamella level (middle lamella + primary wall) is essentially 19% cellulose and 23% hemicellulose, representing 42% of carbohydrates and 58% lignin. These data are consistent with results of Koljonen et al., 2003, who found that 50−75% of the surface of the mechanical

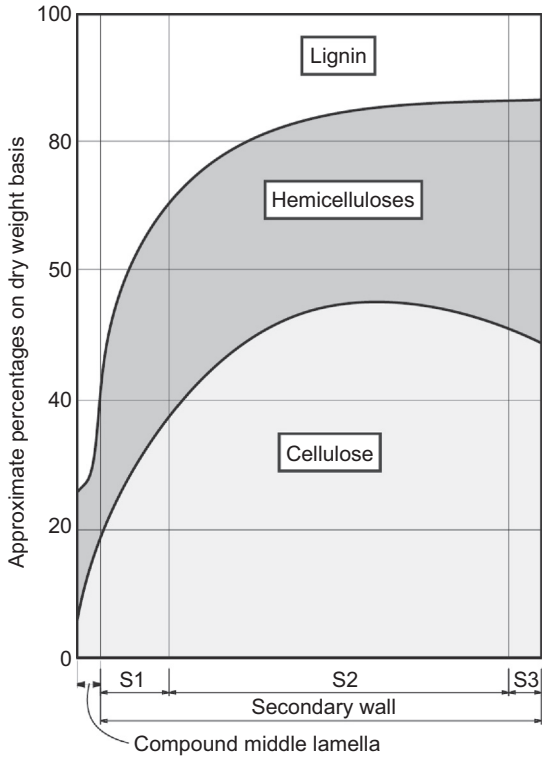

Figure 5.6 Cellulose, hemicellulose and lignin content regarding the cell wall.

pulps was covered by lignin and extractives. This is also consistent with the model of (Börás and Gatenholm, 2005), with 50−55% of the surface covered by extractives and lignin and 49−45% by carbohydrates. The presence of lignin was also observed in the case of high temperature mechanical pulp (Bhattacharya et al., 2014).

5.2.4 Geometry of natural fibres

Aspect ratio determines the difference between a particle and a fibre. It is just a concept of geometrical modelling defined by length/diameter, considering the fibre as a perfect cylinder, which could not always be the best approximation. In case the quotient value is over three, it is considered a fibre, and in the other way around, a particle.

5.2.4.1 Fibre length and diameter distribution

Considering the natural character of wood fibres, the fibres that form the reinforcement in wood plastic composites do not have the same length, neither diameter nor straightness. If the fibre length and diameter are measured, complex distribution of dimensions are rendered. Figs 5.7 and 5.8 offer a length and diameter distribution of sisal fibres.

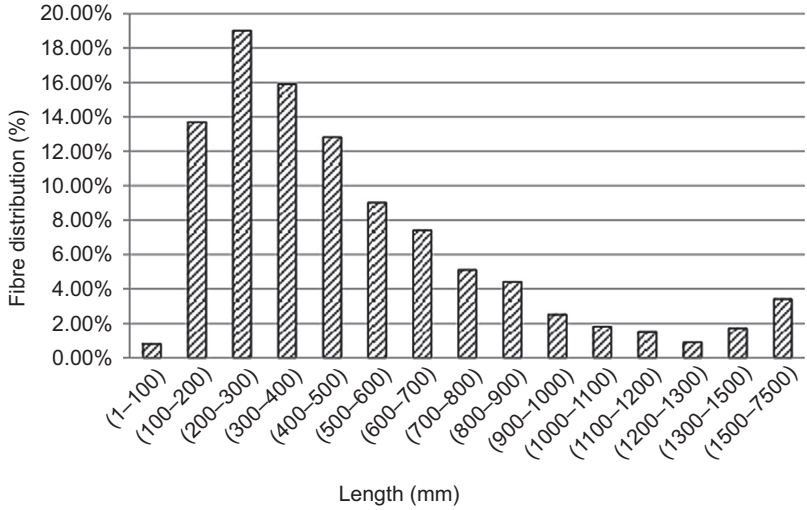

Figure 5.7 Sisal fibre length distribution obtained with MORFI equipment.

Therefore the aspect ratio is statistically obtained from that fibre length and width distribution.

Any transformation process, like extrusion or injection, will subject the fibres to attrition. The high shear stresses to which the fibres are subjected during those processes have a special incidence on the fibre length, shortening the fibres. Moreover, the high working pressures of the transformation processes will also compress the reinforcement. In Fig. 5.9, an SEM image of the section of a composite is shown, offering the disposition of the fibres inside the matrix.

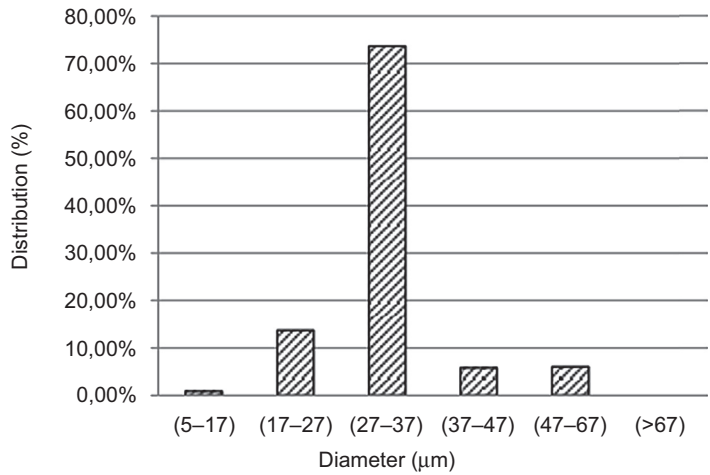

Figure 5.8 Sisal fibre diameter distribution obtained with MORFI equipment.

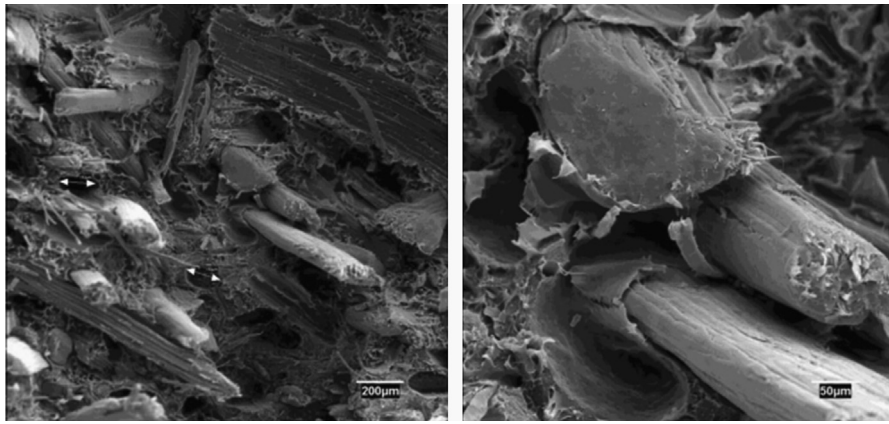

Figure 5.9 Sisal fibre disposition in a composite material after tensile strength test (Bayer Resplandis, 2013).

Hence the length and diameter distribution that must be considered for modelling results are the ones after processing. Nowadays, there exist some automatic and very useful fibre analyzers that optically measure the fibre length and width and render a fibre distribution of the reinforcement analyzed, as well as some statistically treated results.

MORFI equipment was used for obtaining fibre length and diameter distribution of sisal fibres from Figs 5.7 and 5.8. The methodology consists on placing the fibres inside a water tank. Afterwards, the equipment blows air into the water in order to create a turbulent system. Then fibres pass the front of a camera that projects the fibre geometry on a plane as a square. The device measures the projection's width and length, considering width as diameter and square length as cylinder length. It can quickly count from 100 to 20,000 fibres, and the result is a good fibre distribution representation without consuming much time.

A microscope can also be used for this aim, but the main drawback of this technique is that the number of the measured fibres is much lower than the MORFI analysis, as it infrequently analyzes more than 100 fibres, due to the time-consuming nature of the methodology and software.

X-ray microtomography rendered promising results in the composite analysis and could be a future way to analyze aspect ratio in depth with high resolution. The main advantage is that it offers the real fibre distribution inside a composite. Moreover, no extraction is needed to recover the fibre, and the swelling that the cellulose suffers when introduced into water (with MORFI analysis) is avoided with this methodology.

5.2.4.2 Geometrical considerations

While glass fibres and other man-made reinforcements have a controlled length and geometry, natural fibres show irregular lengths and section geometry. Fig. 5.10 shows

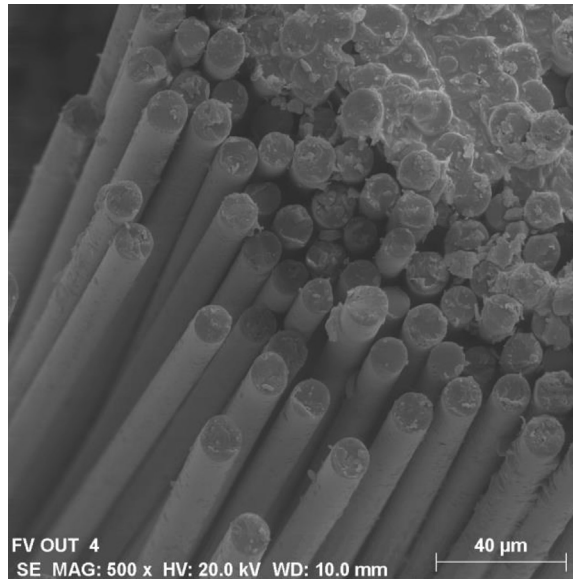

Figure 5.10 Glass fibre SEM photography (Bayer Resplandis, 2013).

a glass fibre bunch. It can be seen as a very regular section shape, with a straight and smooth surface.

On the other hand, in Fig. 5.11 the irregularities of a sisal fibre can be seen, together with the section geometry variability.

The modelling explained in the next sections considers cellulose fibres as a perfect cylinder. Although it is uncertain, it allows predicting and calculating some composite properties with enough accuracy to keep the model as simple as possible.

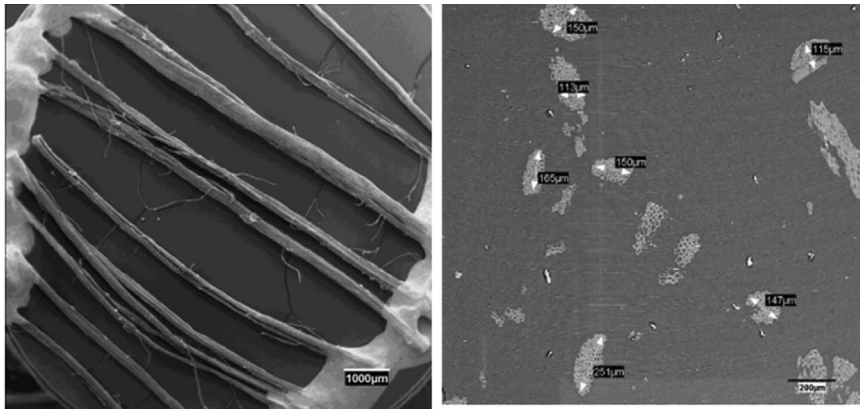

Figure 5.11 Sisal fibre SEM images. Longitudinal view (left) and cross-sectional view (right) (Bayer Resplandis, 2013).

5.2.5 Interface

The interface is the space formed between the matrix and reinforcement. The success on the mechanical properties will be linked to the possibility of the matrix of transferring stresses to the fibre. Hence the correct interaction between both phases is important.

The mechanisms of adhesion matrix reinforcement are:

5.2.5.1 Wetting

The wetting mechanism is a physical interaction that happens when two neutral surfaces are close enough to suffer a physical attraction. It makes it necessary to have a melt matrix to cover the roughness of the reinforcement.

This physical bonding is difficult to achieve because the surface might be contaminated, and the different polarity between some polymers with wood fibres might hinder the spontaneous interactions between matrix and reinforcement.

5.2.5.2 Interdiffusion adhesion

It consists of treating the reinforcement with a polymer that correctly diffuses in the matrix. The bonding strength will depend on the entanglement degree between molecules and the number of molecules involved in the process. The mechanism has been also named autoadhesion.

A clear example can be found in the preparation of PP−nanoclay composites (Hajir Bahrami and Mirzaie, 2011), where montmorillonite is treated with an organic molecule to favour the interactions with PP.

5.2.5.3 Electrostatic attraction

When electrically active polymers are used, it is possible to establish interactions with electrically active reinforcements. The charges must be of opposed polarity in order to generate attraction. The interface strength will depend on the charge density. Although the electrostatic attraction does not contribute strongly in the matrix-reinforcement bonding, it has an important role on fixing the agents that get fixed over the glass fibre reinforcement.

5.2.5.4 Mechanical adhesion

It consists of the interaction between two solids due to the interpenetration of their surfaces. The bonding effectiveness will depend on the roughness of the fibre, but a wide range of internal stresses exist inside the material that may affect the bonding capacity.

5.2.5.5 Chemical bonding

It consists of the formation of chemical bonds between disposable chemical groups on the surface of the reinforcement and the matrix. The bonding strength will depend on the type and quantity of chemical bonds.

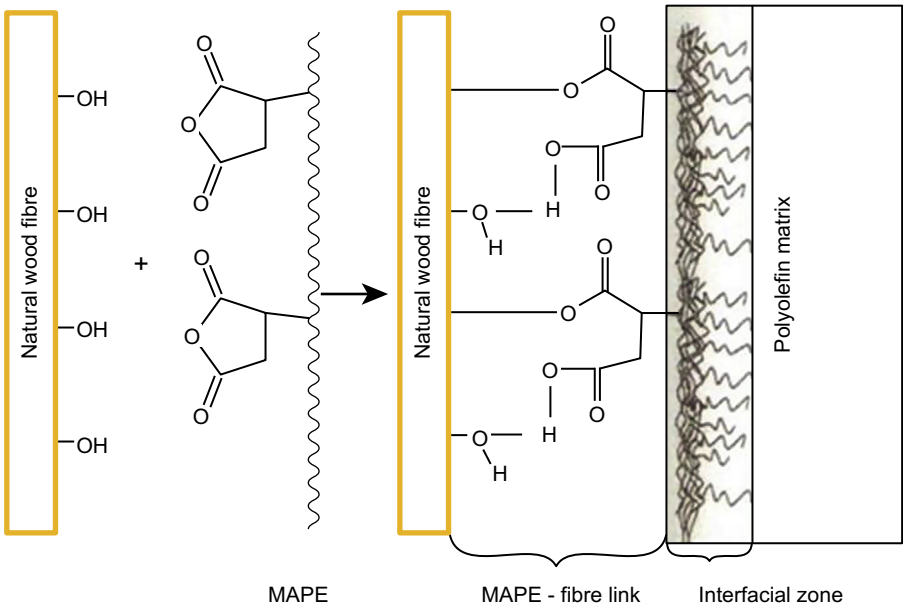

Figure 5.12 Actuation system of maleic anhydride (MAPE) in a wood plastic composite with polyolefin matrix.

The different chemical structure of polyolefins and fibres drive them to a very different polarity. The hydroxyl groups in cellulose fibres confer them a hydrophilic nature, while the hydrocarbon structure of polyolefins confer them hydrophobicity. That different nature hinders spontaneous interactions between cellulose fibres and polyolefins, making it difficult to achieve any strength improvement by the addition of cellulose fibres.

The use of maleic anhydride grafted PE or PP, called MAPE (for PE) and MAPP (for PP), increases the interactions between polar fibres and polyolefins. Maleic anhydride is able to chemically react with the hydroxyl groups present in the fibre surface. The polymeric chain of the MAPE or MAPP is able to diffuse in the polyethylene or polypropylene matrix, creating extraordinary bonds between the fibre and matrix. In Fig. 5.12, either the MAPE or MAPP bonding process is shown.

The optimum amount of coupling agent will depend on the reinforcement that will be used. However, the tensile strength evolution regarding the MAPP quantity has been widely reported. The tensile strength increases with increasing quantities of MAPP to a maximum that is often find between 4% and 8% w/w_{fibre}. Higher values will cause a self-entanglement between the MAPP molecules (Beg and Pickering, 2008; López et al., 2011; Sain et al., 2005; Sanadi et al., 1993) and its corresponding tensile strength shrinkage due to a reduction in the interface quality.

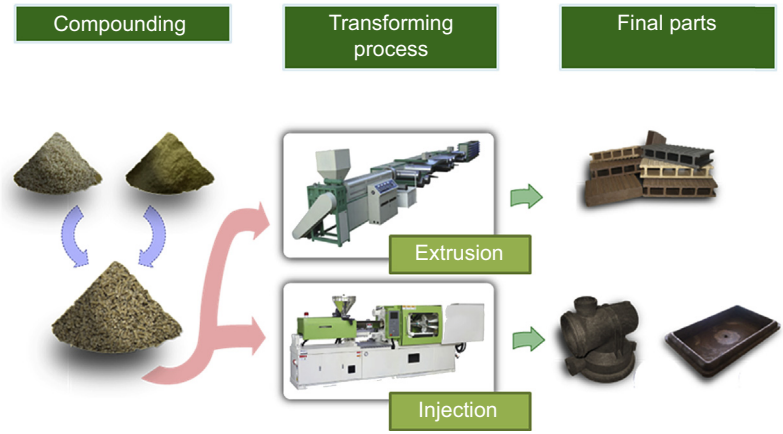

Figure 5.13 Composite producing chart.

5.2.6 Modelling

To sum up, the final properties of the composite will depend on the matrix properties, the reinforcement properties (both geometric aspects and intrinsic mechanical properties), the quality of the interface and the orientation of the fibres inside the matrix, as the fibres tend to orientate in the flow direction during the transformation process (Fig. 5.13). Furthermore, the evolution of the mechanical properties follows a lineal regression.

Hence the properties of a composite material might be expressed with a lineal model as the rule of mixtures (RoM) equation:

$$\sigma_t^c = f_c \cdot \sigma_t^F \cdot V^F + \left(1 - V^F\right) \cdot \sigma_t^{m^*} \tag{5.1}$$

where, σ_t^c and σ_t^F are the maximum tensile strength of the composite and the fibre, respectively, $\sigma_t^{m^*}$ is the tensile strength of the matrix in the breaking point of the composite, V^F is the volumetric fraction of the fibre and f_c is the compatibility factor. $f_c \cdot \sigma_t^F \cdot V^F$ is the fibre contribution, while $(1 - V^F) \cdot \sigma_t^{m^*}$ is the matrix contribution.

At the same time, the compatibility factor is the product of the orientation factor (χ_1) and the longitudinal factor (χ_2):

$$f_c = \chi_1 \cdot \chi_2 \tag{5.2}$$

The orientation factor will depend on the transformation process used, as well as the parameters of it. The longitudinal factor corresponds to the length of the fibre, regarding the critical length of a fibre.

The critical length of a fibre (L_c^F) is the minimum length to completely load a fibre, in other words, the necessary length for the fibre to perform its maximum strength, and it is defined as follows (Vilaseca et al., 2010):

$$L_c^F = \frac{d^F \cdot \sigma_t^F}{2 \cdot \tau} \tag{5.3}$$

where, τ is the interface shear strength of the fibre, the actual parameter that will express the quality of the interface. Greater bonds between fibre and matrix will drive to high values of τ; at the same time, this will produce a shorter critical length. Hence the needed length for the fibre to completely load will be lower, increasing the number of fibres that can be fully loaded.

The longitudinal factor for fibres longer than the critical length will be expressed in a different way than the ones which have a lower length (Vilaseca et al., 2010):

$$\chi_2 = \frac{L^{\mathrm{F}}}{2 \cdot L_{\mathrm{c}}^{\mathrm{F}}} \quad \text{for} \quad L^{\mathrm{F}} < L_{\mathrm{c}}^{\mathrm{F}} \tag{5.4}$$

$$\chi_2 = 1 - \frac{L_{\mathrm{c}}^{\mathrm{F}}}{2 \cdot L^{\mathrm{F}}} \quad \text{for} \quad L^{\mathrm{F}} \geq L_{\mathrm{c}}^{\mathrm{F}} \tag{5.5}$$

If substituting all these expressions in the RoM, the expression, proposed by Kelly and Tyson, is (Kelly and Tyson, 1965):

$$\sigma_{\mathrm{t}}^{\mathrm{c}} = \chi_1 \left(\sum_i \left[\frac{\tau \cdot l_i^{\mathrm{F}} \cdot V_i^{\mathrm{F}}}{d^{\mathrm{F}}} \right] + \sum_j \left[\sigma_{\mathrm{t}}^{\mathrm{F}} \cdot V_j^{\mathrm{F}} \cdot \left(1 - \frac{\sigma_{\mathrm{t}}^{\mathrm{F}} \cdot d^{\mathrm{F}}}{4 \cdot \tau \cdot l_j^{\mathrm{F}}} \right) \right] + \left(1 - V^{\mathrm{F}}\right) \cdot \sigma_{\mathrm{t}}^{\mathrm{m}^*} \right) \tag{5.6}$$

In that equation the subcritic and hypercritic fibres are separated in two summations. A clear influence of the aspect ratio in the fibre contribution can be seen. Increasing aspect ratios will result in greater composite tensile strength. The contribution of the interfacial shear strength is also visible.

However, Eq. (5.6) shows three unknowns: χ_1, $\sigma_{\mathrm{t}}^{\mathrm{F}}$ and τ. Therefore iterative calculation must be performed to solve the equation. Bowyer and Bader (1972) proposed a method in order to solve the equation. It works on the stress–strain curve and consists on determining $\sigma_{\mathrm{t}}^{\mathrm{F}}$ by assimilating that value to the product between the fibre's Young Modulus and the tensile strain of the composite in two different points of the stress–strain curve, generating two expressions and allowing one to solve Eq. (5.6). Once τ and χ_1 are determined, it is possible to calculate $\sigma_{\mathrm{t}}^{\mathrm{F}}$ using Eq. (5.6).

There are several criteria to compare the calculated τ. Von Mises (1913) criteria allow a fine theoretical value, which should be approximate for correctly coupled composite materials. Von Mises Criteria says:

$$\tau = \frac{\sigma_{\mathrm{t}}^{\mathrm{m}}}{\sqrt{3}} \tag{5.7}$$

where, $\sigma_{\mathrm{t}}^{\mathrm{m}}$ is the maximum tensile strength of the fibre.

Table 5.2 shows different τ calculated values from both correctly coupled and uncoupled PP composites produced and calculated by the LEPAMAP research group.

Table 5.2 Interfacial shear strength (τ) of polypropylene composites calculated by Kelly and Tyson and Bowyer and Bader calculation methodology

Matrix	Fibre content (%)	Type of fibre	MAPP (% over fibre content)	Tau min	Tau max
PP	40	Stone groundwood fibres from softwood	0	3.7	
PP	40	CornStark fibre pulp	0	7.9	
PP	40	MP softwoods	0	7.6	
PP	40	DINP	0	9.7	
PP	40	Jute	0	9.9	
PP	40	ONF	6	15.42	
PP	40	Kraft fibre	6	19.26	21.35
PP	40	Stone groundwood fibres from softwood	6	15.95	
PP	40	CornStark fibre pulp	6	15.5	15.5
PP	40	MP softwoods	6	16.86	
PP	40	DINP	6	14.16	
PP	40	Jute	6	14.5	
PP	30	Abaca strands	4–8	14.2	17.6
PP	40	Hemp strands	4–8	14.25	14.25

For a PP with a mean tensile strength value of 28.5 MPa, the expected interfacial shear strength calculated by the Von Mises criteria results in 16.45 MPa.

Uncoupled composites rendered interfacial shear strengths between 3.7 and 10 MPa, while composites that incorporated MAPP as coupling agent increased their interfacial shear strength up to 14.16–19.26 MPa. This increasing effect of the interfacial shear strength may be translated as an improvement on the interface quality.

Later, a method to calculate the intrinsic Young's modulus of the fibre, needed for applying the Bowyer and Bader model, is explained.

Hirsch (1962) proposed a model in order to determine the intrinsic Young's modulus of a fibre, when the matrix and composite material Young's modulus are known. The model is shown in Eq. (5.8):

$$E_t^c = \beta \cdot \left(E_t^F \cdot V^F + E_t^m \cdot \left(1 - V^F\right)\right) + (1 - \beta) \frac{E_t^F \cdot E_t^m}{E_t^m \cdot V^F + E_t^F (1 - V^F)} \tag{5.8}$$

where, E_t^c, E_t^F and E_t^m are the Young's modulus of the composite, fibre and matrix, respectively, and β is a parameter that determines the stress transmission efficiency from the matrix to the reinforcement. That value is the function of the fibre disposition in the matrix, the fibre length and the stress amplification effect at the end of the fibre (Li et al., 2000). Literature agrees that a value of $\beta = 0.4$ agrees with a standard mechanical behaviour (Kalaprasad et al., 1997). E_t^c, E_t^m and V^F can be obtained from experimental data.

5.3 Manufacturing technologies for wood plastic composites

The market chapter defined the main technologies for production in extrusion and injection. In all cases it is necessary to make a mixture of the material that will be processed. This process is called 'compounding'. In order to have a primary vision of these technologies, a short description will be given for this chapter.

5.3.1 Compounding

Compounding refers to the process of mixing the matrix, reinforcements and additives in a single granulate material, which can be processed by the post technologies. Some industries only carry out this production and then sell the material to other customers who will transform the material into profiles and final products.

Compounding usually consists in extruding the mixture in 1−3 mm of diameter pellets, which are automatically cut after die into pellets of around 2−5 mm in length. This process is continuous and has a very good productivity level for the manufacturers. The material is then stored to be used afterwards for the profile extrusion process. Keeping the humidity rate in levels under 5% would be desirable for the best results in the final process.

The use of natural fibres offers difficulties when feeding the equipment, due to the low apparent density of the fibres in comparison to polymers.

Another possibility for compounding used for industry is the kinetic mixer, where material is mixed in batches instead of a continuous process (Fig. 5.14).

Kinetic mixers melt the matrix by subjecting the mixture to high kinetic energy. The friction that the materials will suffer in the mixing chamber will heat and melt the matrix, obtaining a correctly mixed composite.

5.3.2 Extrusion

Decking profiles are manufactured though the extrusion process. The process consists of obtaining long products with a constant section. It is a continuous process. The pieces are cut in the same line to the desired length; for example, for decking it is common to produce decking pieces between 2 and 3 m. After extrusion, the material appears in a brilliant surface, with a plastic aspect. Then the pieces are sent to the finishing

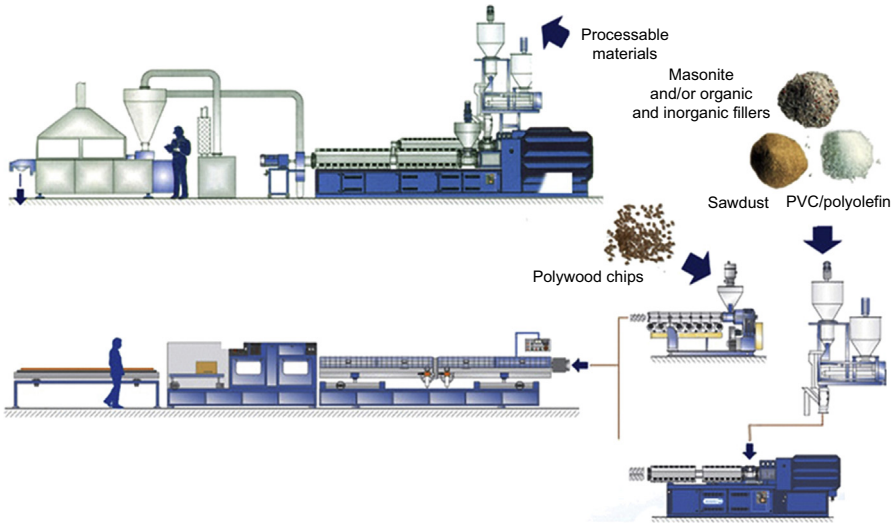

Figure 5.14 Compounding process and extrusion process. Image provided courtesy of Rajoobausano.

section. The finishing process consists of thermoforming wood grain, brushing or sanding on the desired surface of the profile in order to give a perfect wood appearance to the market (Fig. 5.15). Although there is wood inside, the external face of the extrusion process is mainly plastic. The heated metallic roll burns the surface of the matrix to make wood particles visible and give a similar texture to the wood.

Figure 5.15 Wood grain thermoforming over an extrusion profile.

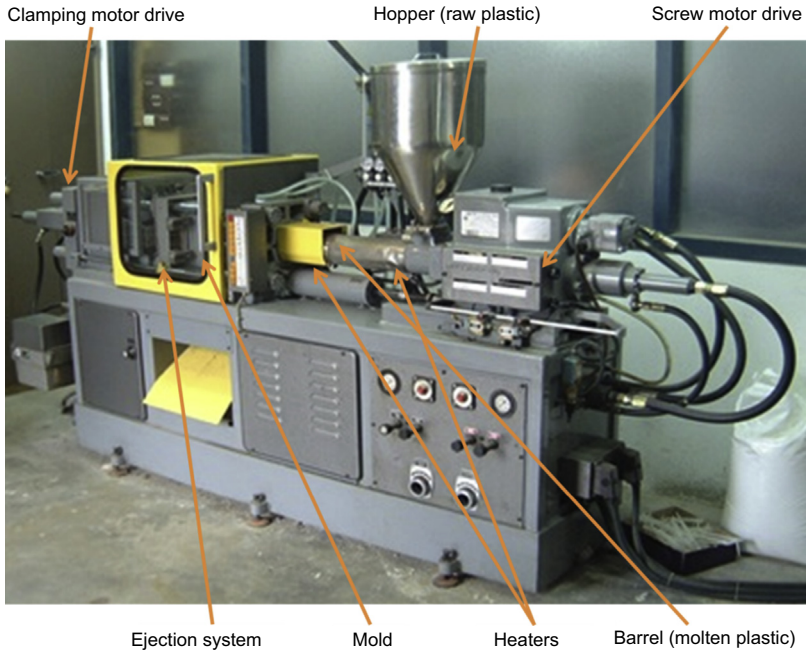

Figure 5.16 Injection process scheme.

5.3.3 *Injection*

The injection process refers to making products with complex geometries. It is a batch process where the composite material is melted and introduced into a mould at high pressure.

When reinforcing plastics with natural fibres, it is necessary to pay special attention to the temperature, which has to be lower than 200°C in order to not result in any major damage to the fibre, as cellulose reinforcements degrades around 220−250°C.

Fig. 5.16 shows a scheme of the injection process (Bayer Resplandis, 2013).

5.4 Future remarks

Cellulose polymer composites stay around us as manufactured products, which can be considered green label substitutes of natural wood in most cases. The similar wood aspect and low maintenance make them great competitors to standard wood.

The future of these compounds follow two main lines:

- The addition of a third rejection material to provide new properties to the final mixture.
- In biocomposites, the substitution of polyolefins by other biodegradable matrices like PLA or PHA.

In the first line, there are initiatives in the frame of Eco-innovation European programmes, such as the RubWPC project (Rubber Fusion of Wood Plastic Composite to Make Functional Composites for Building Applications), which started in 2013 and finishes in 2016. The project is achieving quite satisfactory results, adding up to 35% recycled tire rubber in the composite and manufacturing extruded profiles for outdoor building applications.

In the second line, several academic projects have been carried out (Faruk et al., 2012; John and Thomas, 2008). Although complete green reinforced composites can be produced, the high prices of the matrices compared to standard polyolefins (PP and HDPE); and the low long-term stability for outdoor applications, due to bad results in UV radiation, make them difficult to be manufactured at a large scale for market acceptance.

The new and emerging 3-D printing manufacturing process started to be a good place where these materials could really grow in the market. All fused deposition modelling machines use PLA as a main printing material. Composites of PLA and wood can be found already in the market with 1.75 or 3 mm filament thickness and up to 40% wood filling. It is expected that these technologies will increase in the future and may become one of the biggest markets in the following years.

References

Abdul Khalil, H.P.S., Yusra, A.F.I., Bhat, A.H., Jawaid, M., 2010. Cell wall ultrastructure, anatomy, lignin distribution, and chemical composition of Malaysian cultivated kenaf fiber. Industrial Crops and Products 31, 113–121.

Bax, B., Mussig, J., 2008. Impact and tensile properties of PLA/cordenka and PLA/flax composites. Composites Science and Technology 68, 1601–1607. http://dx.doi.org/10.1016/j.compscitech.2008.01.004.

Bayer Resplandis, J., 2013. Valoración de Materiales Compuestos de HDPE Reforzados con Fibras de Agave Sisalana. Aproximación a un Paradigma de Geometría Fractal Para las Fibras. Universitat de Girona.

Beg, M.D.H., Pickering, K.L., 2008. Mechanical performance of kraft fibre reinforced polypropylene composites: influence of fibre length, fibre beating and hygrothermal ageing. Composites Part A: Applied Science and Manufacturing 39, 1748–1755. http://dx.doi.org/10.1016/j.compositesa.2008.08.003.

Bhattacharya, S., Nayak, S., Dutta, S.C., 2014. A critical review of retrofitting methods for unreinforced masonry structures. International Journal of Disaster Risk Reduction 7, 51–67. http://dx.doi.org/10.1016/j.ijdrr.2013.12.004.

Bledzki, A.K., Gassan, J., 1999. Composites reinforced with cellulose based fibres. Progress in Polymer Science 24, 221–274.

Bledzki, A.K., Jaszkiewicz, A., 2010. Mechanical performance of biocomposites based on PLA and PHBV reinforced with natural fibres – a comparative study to PP. Composites Science and Technology 70, 1687–1696. http://dx.doi.org/10.1016/j.compscitech.2010.06.005.

Börás, L., Gatenholm, P., 2005. Surface composition and morphology of CTMP Fibers. Holzforschung 53, 188–194.

Bowyer, W.H., Bader, M.G., 1972. On the reinforcement of thermoplastics by perfectly aligned discontinuous fibres. Materials Science and Engineering: A 7, 1315−1321.

Cordeiro, N., Belgacem, M., Torres, I., Moura, J.C.V., 2004. Chemical composition and pulping of banana pseudo-stems. Industrial Crops and Products 19, 147−154. http://dx.doi.org/10.1016/j.indcrop.2003.09.001.

Donaldson, K., Tran, C.L., 2004. An introduction to the short-term toxicology of respirable industrial fibres. Mutation Research. Fundamental and Molecular Mechanisms of Mutagenesis 553, 5−9. http://dx.doi.org/10.1016/j.mrfmmm.2004.06.011.

Faruk, O., Bledzki, A.K., Fink, H.P., Sain, M., 2012. Biocomposites reinforced with natural fibers: 2000−2010. Progress in Polymer Science 37, 1552−1596. http://dx.doi.org/10.1016/j.progpolymsci.2012.04.003.

Gent, B.C., Leuven, H., Rue, S.P., Saint-jean, B., 2010. Les Composites : Des Matériaux d' Avenir. Partie 8 : Les composites Biosourcés, pp. 1−10.

Graupner, N., Herrmann, A.S., Mussig, J., 2009. Natural and man-made cellulose fibre-reinforced poly(lactic acid) (PLA) composites: an overview about mechanical characteristics and application areas. Composites Part A: Applied Science and Manufacturing 40, 810−821. http://dx.doi.org/10.1016/j.compositesa.2009.04.003.

Greenberg, M.I., Waksman, J., Curtis, J., 2007. Silicosis: a review. Disease-a-month: DM 53, 394−416. http://dx.doi.org/10.1016/j.disamonth.2007.09.020.

Hajir Bahrami, S., Mirzaie, Z., 2011. Polypropylene/modified nanoclay composite-processing and dyeability properties. World Applied Sciences Journal 13, 493−501.

Hirsch, T.J., 1962. Modulus of elasticity of concrete affected by elastic moduli of cement paste matrix and aggregate. Journal of the American Concrete Institute 59, 427−451.

John, M.J., Anandjiwala, R.D., 2008. Recent developments in chemical modification and characterization of natural fiber-reinforced composites. Polymer Composites 29, 187−207. http://dx.doi.org/10.1002/pc.

John, M.J., Thomas, S., 2008. Biofibres and biocomposites. Carbohydrate Polymers 71, 343−364. http://dx.doi.org/10.1016/j.carbpol.2007.05.040.

Kalaprasad, G., Joseph, K., Thomas, S., Pavithran, C., 1997. Theoretical modelling of tensile properties of short sisal fibre-reinforced low-density polyethylene composites. Journal of Materials Science 32, 4261−4267. http://dx.doi.org/10.1023/a:1018651218515.

Kelly, A., Tyson, W.R., 1965. Tensile properties of fibre-reinforced metals − copper/tungsten and copper/molybdenum. Journal of the Mechanics and Physics of Solids 13, 329. http://dx.doi.org/10.1016/0022-5096(65)90035-9.

Koljonen, K., Österberg, M., Johansson, L.-S., Stenius, P., 2003. Surface chemistry and morphology of different mechanical pulps determined by ESCA and AFM. Colloids and Surfaces A: Physicochemical and Engineering Aspects 228, 143−158. http://dx.doi.org/10.1016/S0927-7757(03)00305-4.

Li, Y., Mai, Y.W., Ye, L., 2000. Sisal fibre and its composites: a review of recent developments. Composites Science and Technology 60, 2037−2055. http://dx.doi.org/10.1016/s0266-3538(00)00101-9.

López, J.P., Méndez, J.A., Mansouri, N.E.El, Mutjé, P., Vilaseca, F., 2011. Mean intrinsic tensile properties of stone groundwood fibers from softwood. BioResources 6, 5037−5049.

Lopez, J.P., Mendez, J.A., Espinach, F.X., Julian, F., Mutjé, P., Vilaseca, F., 2012. Tensile strength characteristics of polypropylene composites reinforced with stone groundwood fibres from softwood. BioResources 7, 3188−3200.

Lukkassen, D., Meidell, A., 2006. Advanced Materials and Structures and Their Fabrication Processes. Narvik University College.

Neagu, R.C., Gamstedt, E.K., Berthold, F., 2006. Stiffness contribution of various wood fibers to composite materials. Journal of Composite Materials 40, 663−699. http://dx.doi.org/10.1177/0021998305055276.

Ochi, S., 2008. Mechanical properties of kenaf fibers and kenaf/PLA composites. Mechanics of Materials 40, 446−452. http://dx.doi.org/10.1016/j.mechmat.2007.10.006.

Pérez Amaro, L., 2015. High performance compostable biocomposites based on bacterial polyesters suitable for injection molding and blow extrusion. Chemical and Biochemical Engineering Quarterly 29, 261−274. http://dx.doi.org/10.15255/CABEQ.2014.2259.

Reddy, N., Yang, Y., 2005. Biofibers from agricultural byproducts for industrial applications. Trends in Biotechnology 23, 22−27. http://dx.doi.org/10.1016/j.tibtech.2004.11.002.

Reixach, R., Franco-Marques, E., El Mansouri, N.E., de Cartagena, F.R., Arbat, G., Espinach, F.X., Mutje, P., 2013. Micromechanics of mechanical, thermomechanical, and chemi-thermomechanical pulp from orange tree pruning as polypropylene reinforcement: a comparative study. BioResources 8, 3231−3246.

Sain, M., Suhara, P., Law, S., Bouilloux, A., 2005. Interface modification and mechanical properties of natural fiber-polyolefin composite products. Journal of Reinforced Plastics and Composites 24, 121−130. http://dx.doi.org/10.1177/0731684405041717.

Sanadi, A.R., Rowell, R.M., Young, R.A., 1993. Evaluation of wood-thermoplastic-interphase shear strengths. Journal of Materials Science 28, 6347−6352.

Sundholm, J., 1999. Mechanical Pulping, Papermaking Science and Technology. Published in Cooperation With the Finnish Paper Engineers' Association and TAPPI.

Tsoumis, G., 1968. Wood as Raw Material. Elsevier. http://dx.doi.org/10.1016/B978-0-08-012378-3.50009-4.

Uma Devi, L., Bhagawan, S.S., Thomas, S., 1996. Mechanical properties of pineapple leaf fiber-reinforced. Journal of Applied Sciences 64, 1739−1748. http://dx.doi.org/10.1002/(SICI)1097-4628(19970531)64:9<1739::AID-APP10>3.0.CO;2-T.

Vallejos, E., 2006. Aprovechamiento Integral del *Cannabis sativa* Como Material de Refuerzo/Carga Del Polipropileno Aprovechamiento Integral del *Cannabis sativa* Como Material de Refuerzo/Carga. Universitat de Girona.

Vilaseca, F., Valadez-Gonzalez, A., Herrera-Franco, P.J., Pelach, M.A., Lopez, J.P., Mutje, P., 2010. Biocomposites from abaca strands and polypropylene. Part I: evaluation of the tensile properties. Bioresource Technology 101, 387−395. http://dx.doi.org/10.1016/j.biortech.2009.07.066.

Von Mises, R., 1913. Mechanik der festen Körper im plastisch deformablen Zustand. Nachrichten von der Gesellschaft der Wissenschaften zu Göttingen, Mathematisch-Physikalische Klasse 1, 582−592.

Wang, B.J., Lee, J.Y., Wang, R.C., 1993. Fiberglass dermatitis: report of two cases. Journal of the Formosan Medical Association 92, 755−758.

Witten, E.(A.V.K.), Kraus, T.(CCeV), Kühnel, M.(CCeV), 2014. Composites-marktbericht 2014.

Yueping, W., Ge, W., Haitao, C., Genlin, T., Zheng, L., Qun Feng, X., Xiangqi, Z., Xiaojun, H., Xushan, G., 2010. Structures of bamboo fiber for textiles. Textile Research Journal 80, 334−343. http://dx.doi.org/10.1177/0040517509337633.

Long natural fibre composites

6

M. Fan, B. Weclawski
Brunel University London, London, United Kingdom

6.1 Introduction

Long natural fibre composites (LNFCs), which are polymers reinforced with cellulosic long fibres, have a potential to be applied into a range of building products. They are often seen as an alternative for glass fibre reinforced plastics in some applications, because of the relatively high strength and low density of long length natural fibres (LNF). Moreover, LNF have a set of beneficial traits, such as thermal insulation, thermal stability, biodegradability and inherently renewability. Those characteristics are of importance when LNF are used as reinforcements in polymer composites, but developments in mechanical performance, reliability and economic viability are still required to be adopted fully by industry.

There are six types of natural fibres classified by botanical type, namely bast, leaf, seed, core, grass and others like wood and roots fibres (Pickering, 2008). Flax, hemp, sisal and jute fibres are commonly used reinforcements for LNFC, especially hemp and flax used in European and Asian countries. Hemp and flax fibres are considered to be the oldest cultivated fibres in the world (Kvavadze et al., 2009; Lawrence, 1951; Joseph, 1986). Hemp and flax fibres, in common with other plant fibres, as opposed to man-made fibres, have inconsistent properties, which are affected by factors such as plant type and species, region of cultivation, weather conditions, fibre position in the plant and fibre extraction techniques (Charlet et al., 2007). From the material point of view, the mechanical properties of cellulosic bast fibres are determined by the chemical composition, ie, cellulose, hemicellulose and lignin. Cellulose, an organic polymer, is the primary structural component of the plant fibre cell wall. The ratio between the main constituents affects fibre mechanical properties. The consistent quality of LNFs may be achieved by controlling growth conditions or optimizing the harvesting and fibre extraction process (Hepworth et al., 2000; Summerscales et al., 2010; Struik et al., 2000; Dai et al., 2013; Graupner et al., 2009). Another approach is to chemically treat fibres to improve their mechanical properties or compatibility with the polymeric matrix, which may dissolve components other than cellulose, thus changing the composition and properties (Bledzki et al., 2004; Aziz and Ansell, 2004; Kalia et al., 2009). In addition, the surface morphology of the LNF reinforcements may be changed, which allows a better mechanical interlocking between fibre surface and matrix (Yuan et al., 1999; Awaja al. 2009) and hence the interface between the matrix and reinforcement.

The main reasons for the development of LNFC are their price, performance and low environmental impact. The low price is necessary for the LNFC to be

Advanced High Strength Natural Fibre Composites in Construction. http://dx.doi.org/10.1016/B978-0-08-100411-1.00006-6

economically viable, because expensive LNFCs can be substituted by a range of well-established synthetic composites. Low embodied energy is one of the key arguments for NFC competition with glass fibre reinforced plastics (La Rosa et al., 2014). Additional treatments and procedures may result in an increase of the NFC embodied energy. Low cost and high volume processing procedures are being considered. Improving the properties of LNFCs has been a great challenge for the full exploitation of NFCs. The performance of LNFCs may be improved by optimizing the reinforcement microstructure and its arrangement within a composite.

6.2 Long length natural fibres and natural fibre reinforcements

Long length natural fibres used for reinforcement are similar to the fibres that are used in the textile industry, which include bast fibres, leaf fibres, seed fibres and animal fibres, but differ in the level of processing and pretreatments. Flax and hemp bast fibres have been considered the most promising reinforcements for composites; in particular, they were recently incorporated into the production of automotive components, as a substitute for a glass fibre, and now are being considered for their uses in the production of civil engineering materials.

6.2.1 Long length natural fibres

6.2.1.1 Extraction and production of long natural fibres

Various processing technologies have been developed to produce LNF depending on raw materials. For example, hemp and flax fibres are extracted from the stem by extracting other components like shiv, lignin and pectin. A traditional fibre separation method is called ‘retting’ and is based on soaking hemp in water tanks, where bacteria enzymes degrade lignin and other tissues, thus freeing bast fibres (Mohanty et al., 2005). During field retting, stalks are chopped into 30−45 cm lengths, immersed and consecutively turned over in two-day intervals. The procedure lasts from 14 to 21 days, and speed depends on environmental factors. Retting usually produces good quality fibres with high uniformity. The mechanical separation process called ‘green retting’ or just decortication has recently been used without the field retting stage (Fig. 6.1). Hemp stems are driven through a series of rollers, which squeeze the material, separating fibres from shiv. The advantage is that there is no need for time and area consuming retting, but the decortication process induces mechanical degradation of the fibre produced (Hepworth et al., 2000).

Decortication removes nonfibrous parts of the plants by mechanical means. Hackling is done by combing of the fibres, which is used to separate long fibres from short fibres and other parts of the plant. Carding produces a sliver by disentangling the fibres between two moving surfaces. Often a combination of mechanical and chemical methods is used to create ‘cottonized’ short hemp fibres, which remove most of the lignin and pectin from the fibres (Munder et al., 2005; Van de Weyenberg et al., 2003).

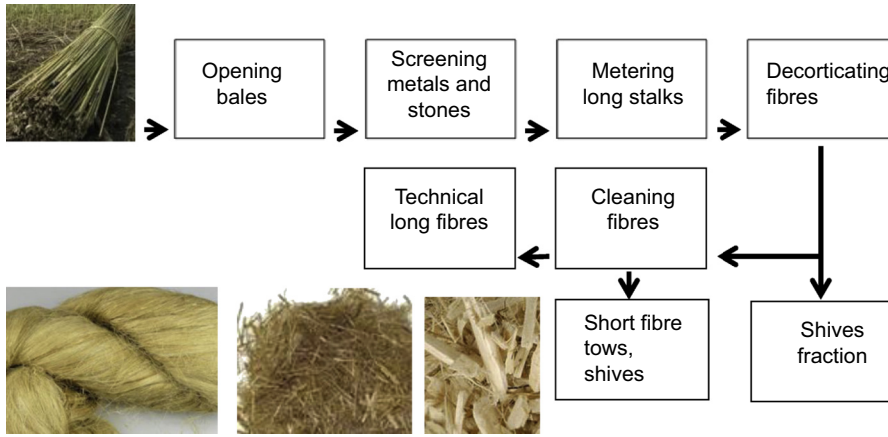

Figure 6.1 A natural fibre processing flow chart.

Other approaches of fibre separation, aiming at improving the efficiency of the process, involve the use of bacterial enzymes or fungi (Wang et al., 2003; Akin et al., 2001; Li et al., 2009), ultrasound (Wielage et al., 1999), steam explosion (Dupeyre and Vignon, 1998), chemical retting (Wang et al., 2003; Sharma, 1988) or their combinations.

The process of hemp and flax normally results in the loss of shives, dust and fibres, about 62−68% of total mass. Typical hemp processing yields about 32% of the fibres, of which 23−27% are considered as long fibres (>20 mm). Flax processing yields about 37% of the fibres, of which 29% are long fibres (Munder et al., 2005).

After processing, fibres can go through various treatments, namely acetylation, bleaching, grafting, mercerization and scouring. Acetylation increases hydrophobic properties of the fibres by the introduction of acetyl radical to an organic molecule. This is usually done with acetic acid (Tserki et al., 2005). To reduce lignin and pectin levels, fibres can be bleached with hydrogen peroxide, sodium hydroxide, sodium sulphite or other alkalines. The process using caustic soda is called mercerization (Khristova et al., 2003). Grafting changes the surface property of the fibre by the incorporation of monomers or oligomers (Ouajai et al., 2004). Scouring removes proteins, waxes, fats, oils and impurities with treatment in aqueous or other solvents (Wang et al., 2003). Treatments are used in the textile industry in order to create a fibre with desired properties. Moreover, they can increase wettability of the fibre and improve interface quality between the matrix and the reinforcement for composite production (Sawpan et al., 2011).

There are three centres for hemp cultivation, namely, Canada, China and Europe. Europe was one of the biggest hemp producers in the world. Since 1995 the production of hemp in Asia has grown. The world production of hemp began to fall in 1966, from almost 370,000 tonnes/year to reach a minimum in 1994 of 51,500 tonnes/year. This decline was the outcome of the revolution in the field of synthetic fibre production, as well as hemp regulatory laws introduced in the United States as the Marijuana Tax Act

of 1937 (Musto, 1972), which later influenced global hemp production and trade. European hemp fibre is mainly used in the processing of paper and specialty paper, technical filters, cigarette paper, NFCs, insulation material, cultivation fleeces, animal bedding and mulch.

In terms of the production of flax fibre and tow, despite almost a 90% decrease in area dedicated to flax cultivation from 2 MHa to 231 kHa during the last 50 years, on average the global production rates have fluctuated around 716 k tonnes/year. This is a result of the increased production efficiency due to the development of cultivation techniques, fertilization, processing machinery and pest control. The highest improvement in efficiency is visible in the European Union, with 734% more flax harvested from the same area in 2009, compared with the 1960's (FAO, 2012).

6.2.1.2 *Structure and composition of long natural fibres*

LNFs, eg, bast fibres, are made up of similar elements as wood fibres, namely, cellulose, hemicellulose, lignin and other minor elements (Table 6.1). It is apparent that all of the presented fibres, except cotton, have around 65% cellulose, which is the reinforcing element of the plant.

The fibres of the stalk normally have a hierarchical structure composed of several distinguishable layers (Fig. 6.2). Each layer has its own substructure. The middle lamella, composed mainly of pectin with macrofibrils, is located in the outer layer and binds the fibres together. This is followed by a thin cellulose network making up the primary wall (Schbib_Schäfer_and_Hon, 2006). The secondary wall consists of the outer layer (S1), middle layer (S2) and inner layer (S3). The middle layer of the bast fibre is of importance for the plant reinforcement due to its cellulose content and arrangement. It makes up to 70−80% of the fibre wall. The arrangement of cellulose fibrils in the middle layer (S2) is almost longitudinal, thus it is the most responsible for plant stiffness and fibre strength. This is considered most important

Table 6.1 Composition of natural fibre cellulose fibres (Summerscales et al., 2010; Bledzki and Gassan, 1999; Krassig, 1985)

	Hemp	Flax	Jute	Sisal	Ramie	Cotton
Cellulose	67.0	62.1−64.1	64.4	65.8	68.8	82.7−92.7
Hemicellulose	16.1	16.7	12.0	12.0	13.1	5.7
Pectin	0.8	1.8	0.2	0.8	1.9	0.0
Lignin	3.3	2.0	11.8	9.9	0.6	0.0
Water soluble	2.1	3.9	1.1	1.2	5.5	1.0
Wax	0.7	1.5	0.5	0.3	0.3	0.6
Water	10	10	10	10	10	10
Microfibril angle	6.2	10.0	8.0	–	7.5	–

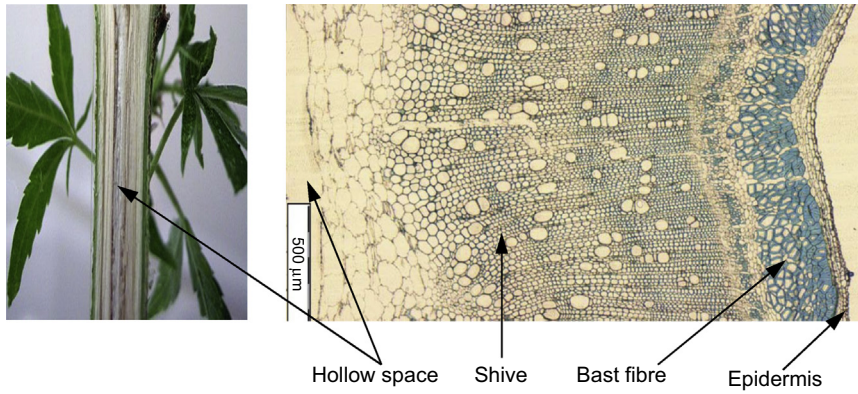

Figure 6.2 Structure of hemp straw stalk and bast fibre.

for producing long length fibres for high strength composites. The elementary cellulose fibrils of the S2 layer are bound together with hemicellulose and amorphous lignin. The inner fibre lumen consists of proteins and pectin (Fan, 2009; Hughes, 2012).

6.2.1.3 *Mechanical properties of long natural fibres*

The mechanical properties of fibres are usually measured with direct tensile tests by stretching fibres or by ring tests, which combine tensile and compression deformations (Bos et al., 2002; Bos and Donald, 1999). However, in many cases, bundles of technical fibres are measured, since single fibres are difficult to separate. In addition, natural fibre bundles have nonuniform cross sections and accurate measurements, which are very challenging. Therefore a consistent way of fibre cross section measurement needs to be implemented (Munawar et al., 2007). This is usually done by testing multiple fibres and performing Weibull analysis (Pickering et al., 2007; Placet, 2009; Zafeiropoulos, andBaillie, 2007; Andersons et al., 2005).

The properties of LNFs vary throughout different parts of the plant. Fibres in the stem have higher mechanical properties in comparison to those of the leaf. Additionally, the position within the stem affects mechanical properties. The strongest fibres are found in the middle of the stem and the weakest at the top (Charlet et al., 2007). This finding led to the development of the harvesting machines, which automatically alter the point at which the stem is cut. Moreover the type of fibre separation from the stem has a significant influence on fibre performance (Gratton and Chen, 2004; Chen et al., 2004).

Strength and stiffness distributions for natural fibres vary considerably (Table 6.2). This might be related to the procedure with which fibres were tested, the treatment of the fibres, and other aforementioned factors. Short fibres can be converted into mats and used as randomly distributed reinforcement in composite production, such as compression moulding. The density of natural fibres is very similar among various species, ranging from 1.20 to 1.52 g/cm^3, which is about one-half of the density of

Table 6.2 Tensile strength of cellulosic fibres and man-made fibres

	Density ρ (g/cm^3)	Fibre length L (mm)	Diameter Ø (μm)	Elong. (%)	Young's modulus E_L (GPa)	Tensile strength σ_L (MPa)	References
Hemp (*Cannabis sativa*)	1.35−1.50	5.6−110	10−51	1.6−4.2	5.5−70	690−1040	Summerscales et al. (2010), Mueller and Krobjilowski (2003), Pickering (2008), Shahzad (2012)
Flax (*Linum usitatissium*)	1.38−1.52	10−70	5−38	1.5−3.2	12−100	345−1100	Summerscales et al. (2010), Pickering (2008), Hagstrand and Oksman (2001)
Wool	1.20−1.32	38−150	12−45		3.9−5.2	40−200	Morton and Hearle (1993)
Jute (*Corchorus capsularis*)	1.23−1.45	0.8−6.0	5−25	1.5−1.8	13.0−55.0	393−773	Summerscales et al. (2010), Pickering (2008)
Soft wood kraft	1.50				40.0	1000	Bledzki and Gassan (1999), Summerscales et al., 2010
E-glass	2.50			2.5	70.0−72.0	2000−3500	Summerscales et al. (2010)
Aramid	1.40			3.3−3.7	63.0−67.0	3000−3150	Bledzki and Gassan (1999), Summerscales et al. (2010)
Carbon	1.40			1.4−1.8	230−240	4000	Bledzki and Gassan (1999), Summerscales et al. (2010)

glass fibres. The Young's modulus of natural fibres also ranges widely from 5.5 to 100 MPa, which exceeds that of glass fibres. The tensile strength ranges from 40 to 100 MPa, which is comparable with that of soft wood kraft fibres and up to three times lower than that of E-glass or aramid fibres. This information can be used when selecting LNFs and predicting the mechanical properties of the composite laminate element, although it is wise to test the raw materials to have reliable mechanical performance data due to the wide range of the properties.

Variations in mechanical properties on the macroscopic level of natural fibres are an outcome of the hierarchical structure of plant fibres. Refinement of the natural fibres leads to an improvement of mechanical properties. Taking wood fibres as an example, the bulk Young's modulus of wood is around 10 GPa. After the pulping process, single pulp fibre stiffness is around 40 GPa. When pulp fibres are hydrolyzed and mechanically disintegrated, microfibrils are exposed, which have a stiffness of about 70 GPa. There is no existing technology that can break down and test microfibrils into crystallites, which have a stiffness value near the level of 250 GPa (Bledzki and Gassan, 1999).

6.2.2 Long natural fibre reinforcements

LNF reinforcements can be categorized by the form. Filaments can be continuous and used directly or processed into various forms of fabrics. Discontinuous, shorter fibres can be used in the form of mats or weaved into continuous yarns. Multiple factors, related with a composite reinforcement, have influences on the properties of LNFCs. Those factors may include type, shape, orientation, volume fraction, mechanical performance, thermal and electrical conductivity and surface/interface properties. The type of reinforcement, when used, can restrict processing routes. For instance, randomly oriented fibres in a mat will yield composites with lower volume fractions, when compared with oriented fibres. The volume fraction has a direct correlation with mechanical properties like the tensile stiffness and strength.

6.2.2.1 Mats

The term mat refers to a nonwoven material, which is made from fibres by chemical, thermal, mechanical or other processes, but is not involved in knitting or weaving of the fibres. Examples of nonwoven materials include felts, insulation mats, packaging materials and reinforcement fibre mats. Natural fibre reinforcement mats can be produced to the specified forms and dimensions. The mat is defined by an average fibre length and level of processing. Mats are prepared with a whole range of fibre lengths. Short fibres are usually not incorporated into composite reinforcement mats but can be used to produce mats for other applications, with the use of binders or technique like hydroentanglement. Processes involving combing or water jets can create the preferred direction of the majority of fibre lengths (Umer et al., 2007).

The processing of mats usually includes chopping the fibres and separating them into specific lengths. Then fibres with the selected lengths are used to create mats with various properties. This is done by a flat or a continuous process with forming

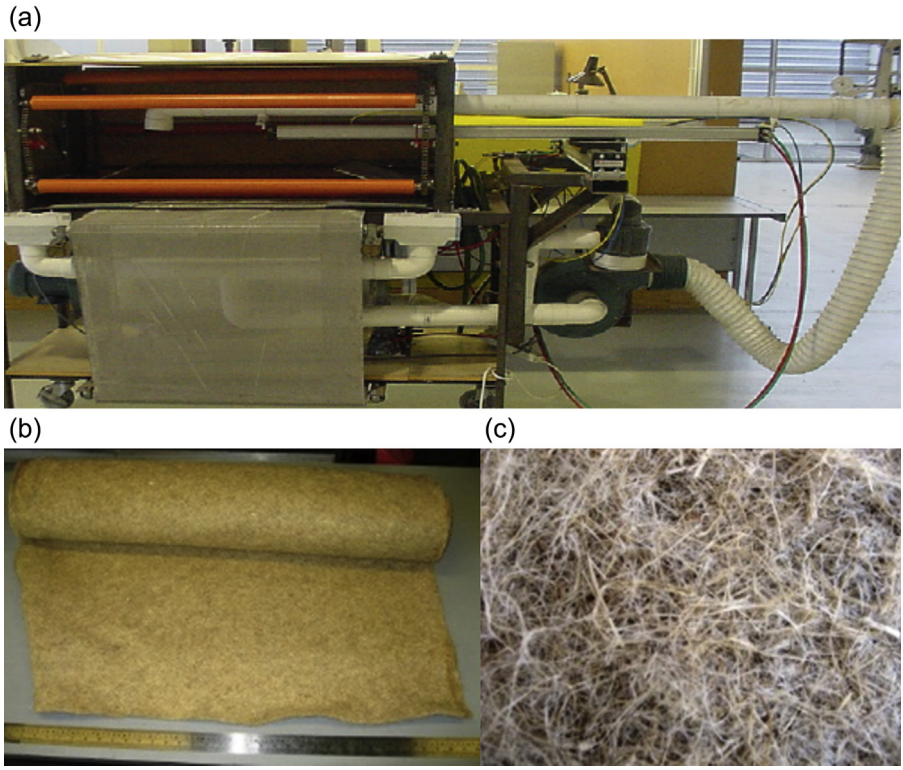

Figure 6.3 (a) Mat forming, (b) hemp mat roll and (c) hemp mat fibres and fibre bundles.

machines (Fig. 6.3). Most of the mats have randomly oriented fibres, which are mainly within the x-y plane of the mat. Fibres are spread over the moving belt and pressed on the continuous forming belt. The process involves in the use of mechanical force, chemical pretreatments, heat or binders to create fibre−fibre bonds.

In order to increase a mechanical interlocking between fibres, the hydroentanglement process can be used. It is a continuous process, which uses high pressure water jets to induce the interlocking of the fibres. A web of fibres is entering the jet area and the water passes through it. The outcome is a thinner layer of nonwoven mat with the increased mechanical properties. Similarly to the pressed mats, hydroentangled mats can be used for composite laminate impregnation, since they do not include binders (Acar and Harper, 2000; Ghassemieh et al., 2001).

6.2.2.2 Hybrid long natural fibre mats

Hybrid mats, eg, hemp−wool mats could be made for LNFC. In this case, wool fibres in the mat can be clipped and washed with a mixture of water and detergent under pressure. This type of mat is processed with the hydroentanglement process. Fibres are mixed together in the desired ratio and spread over a conveyor belt, which

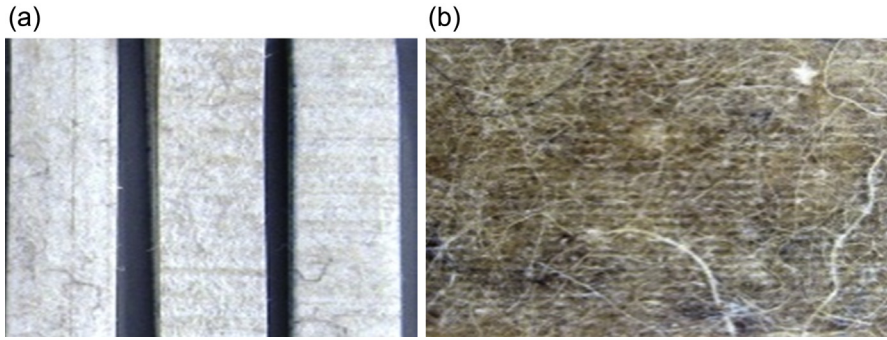

Figure 6.4 (a) Hemp−wool mat stripes: visible surface parallel lines are created by water jet nozzles during processing and (b) impregnated hemp−wool mat in polyester resin with black and white wool fibres and light brown hemp fibres.

transports them under high pressure water jets. Pressure from small nozzles is used to interlock the fibres together, compact and process a uniform mat. Fig. 6.4 presents wool−hemp paper mat stripes and a close up of the mat surface impregnated with polyester resin. The colour of the mat is lightly brown with a distinctive pattern in the form of lines created by water jet nozzles. Additionally, wool dark fibres are visible on the surface. The hemp−wool mat is compact and due to the high fibre entanglement, single fibres cannot be separated as in the previously described hemp mat.

6.2.2.3 *Twisted and nontwisted yarns*

A yarn is composed of short or long fibres, which are held together by means of a mechanical interlocking (Needles, 1986). The main processes of yarns include fabric processing, weaving and rope processing. Natural fibre yarns can be used as the LNFC reinforcement. Using the yarn, instead of the mat to reinforce the composites, allows a better control of fibre orientation, an increase in fibre loading and a continuous production process (Pan et al., 2001). There are two types of natural fibre yarns, which can be used as LNFC reinforcement, namely twisted fibres and nontwisted fibres (Fig. 6.5).

For the twisted yarns, fibres are held together by shear forces created by fibre twisting (Fig. 6.6), such as those in conventional textile yarn or rope. The fibres are aligned at an angle to main direction of the yarn. This type of yarn is produced in the spinning process and is mainly used in the textile industry (Needles, 1986). The bales of technical fibres are opened mechanically or manually and transferred to a picker, which loosens and cleans the fibres. The fibres are then carded, aligned and passed through a funnel to generate the parallel strand of fibres called sliver. Then a set of rollers elongate and slightly twist the sliver, which is then transferred to a container. The spinning of hemp fibres differs from the spinning processes of other fibres, due to the mechanical properties of hemp. Spinning machines, which are used to process cotton yarns, can be used for the processing of short fibre hemp yarns,

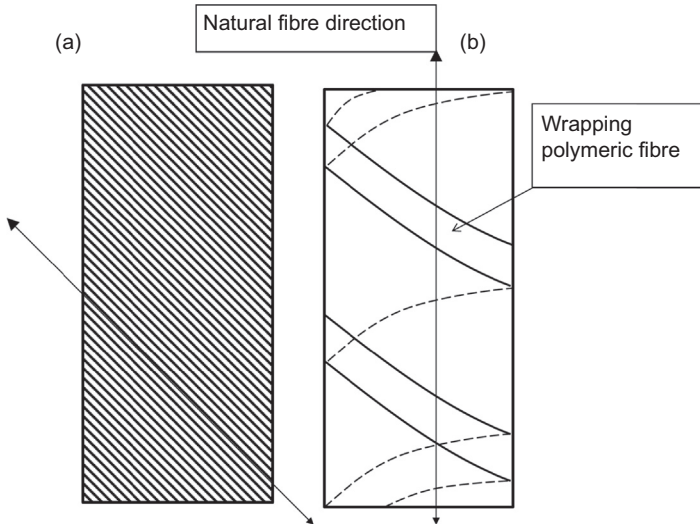

Figure 6.5 Diagrams comparing ring spun yarns with the twisted fibres (a) and wrapped yarns without twist and fibres aligned in the main yarn direction (b).

when hemps go through the 'cottonizing' process (Tang et al., 2011). Slivers are spun into yarns composed of one or multiple twisted slivers. Yarns can be produced continuously in S or Z arrangements, which correspond to two opposite twist directions (Fig. 6.6).

Nontwisted yarns (Fig. 6.6d, e) have been designed as LNFC reinforcement. The fibres are without twist and aligned in the main direction of the yarn. They are held together with friction forces created with the polymeric wrapping wire, which is made out of a continuous synthetic polymer fibre (Fig. 6.6d). The first stage of processing of this type of yarn is the same as processing the twisted yarn. After the creation of sliver, fibres are not twisted. The sliver is divided into multiple strands of slivers with the required linear density. The slivers are then wrapped with polymeric filament, which gives rise to a pressure on the fibres and creates friction forces and holds fibres together. This type of yarn has no application in the textile industry, due to its dry tenacity and low load-bearing capacities. It is possible to produce yarns with various linear densities from 200Tex to over 2000Tex. Lower values of the linear densities (Tex) are usually not practical, since the ratio of artificial yarn and natural fibres becomes too high. Higher Tex values are more practical, but the compaction of the fibres in the high linear density yarn may obstruct the impregnation with resin (Needles, 1986).

6.2.2.4 Hybrid (nontwisted) yarns

Hybrid yarns can also be developed, eg, hemp−wool, nontwisted 1000Tex yarns (Fig. 6.7). This hybrid yarn has significantly higher linear density in comparison with aforementioned hemp yarns. Fibres within the yarn are parallel, not twisted

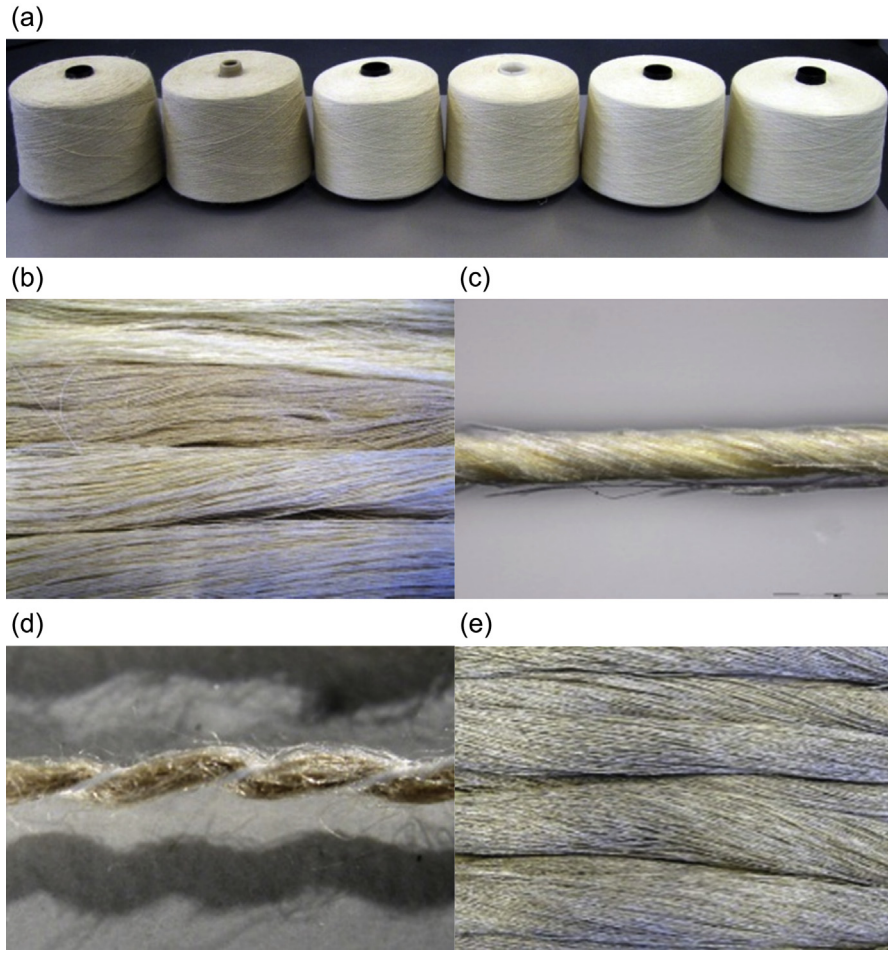

Figure 6.6 (a) Six grades of hemp yarns on spools, (b) bundles of hemp yarns, (c) a single yarn with a distinguishable surface fibre pattern, (d) flax 250Tex nontwisted fibre yarn and (e) flax yarn bundles.

and are held together with wrapping polymeric wire. Fig. 6.7a presents hemp-wool yarn with distinguishable black wrapping yarn. Fig. 6.7b presents a layer of aligned hybrid yarns in preparation to impregnation.

The hemp included in the yarn was mechanically decorticated, by passing hemp stalks through a series of gearwheels. This procedure crumbles up a shive material from the plant and releases the fibres. The wool used for the processing of the yarn is clipped and washed under pressure with mixture of water and detergent. In the next step, hemp and wool fibres are mixed together and aligned by brushing them on the rotating drum. The yarn with no twist is processed by separating narrow slivers of aligned fibres and subsequent wrapping with continuous synthetic fibre.

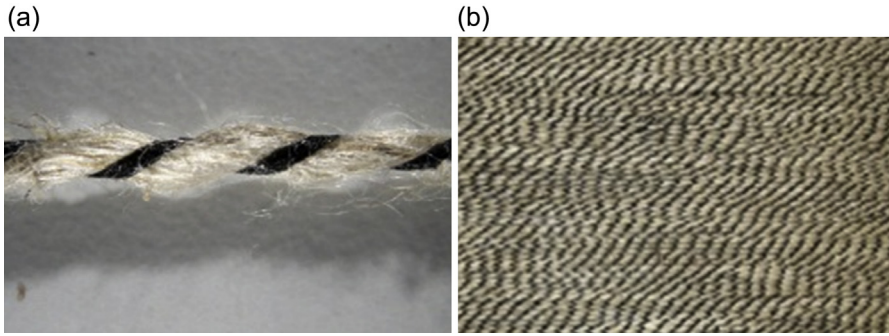

Figure 6.7 (a) A single hybrid hemp−wool yarn and (b) aligned hemp−wool yarns.

Hybrid yarn allows the development of specific property of LNFC by taking advantage of the specific property of constituents. For example, the inclusion of wool fibres into LNFC laminate can enhance vibration damping properties, as well as a sound attenuation of the laminate due to their elastic properties and thermal insulation. Moreover, the inclusion of wool fibres gives the possibility to increase biocontent (animal protein) from alternative sources in the composite. However, the wool presents lower tensile stiffness and strength. Additionally, there might be some issues of interface compatibility between a polyester matrix and the wool fibres. The wool fibre surface is hydrophobic and hydrophilic interior if treated with lanoline, which is a waxy blend (wax, esters, alcohols, acids and hydrocarbons) created by animal glands, becomes water resistant.

6.2.2.5 Fabrics

Yarns may be further processed to form fabrics; after spinning or wrapping, yarns can be weaved to form fabrics. There are various types of fabrics, which vary in the type of weave, as well as the reinforcement direction (Fig. 6.8). Fabric can have yarns aligned in two, three and even four directions. 2-D preforms normally include the weaved, braided and knitted fabrics, and 3-D preforms include the weaved, braided, stitched and knitted fabrics (Ko, 2004). The most commonly used fabrics for the composite reinforcement are the ones with two-dimensional biaxial patterns (Buet-Gautier and Boisse, 2001). Fabrics with plane and twill arrangements are one of the examples.

Using fabrics allows the close packing of the composite, and the fabrics can be easily arranged when processing laminates. Processing techniques like laying-up depend mainly on the use of woven reinforcement fabrics. Various laminate shapes can be processed such as curvatures. The drawback is the waviness, which changes the axial filament arrangement, thus influencing the mechanical properties of the composite. Mechanical properties of the laminates may vary with the change in the form of waved fabrics (Luo and Verpoest, 2002; Hivet and Boisse, 2008).

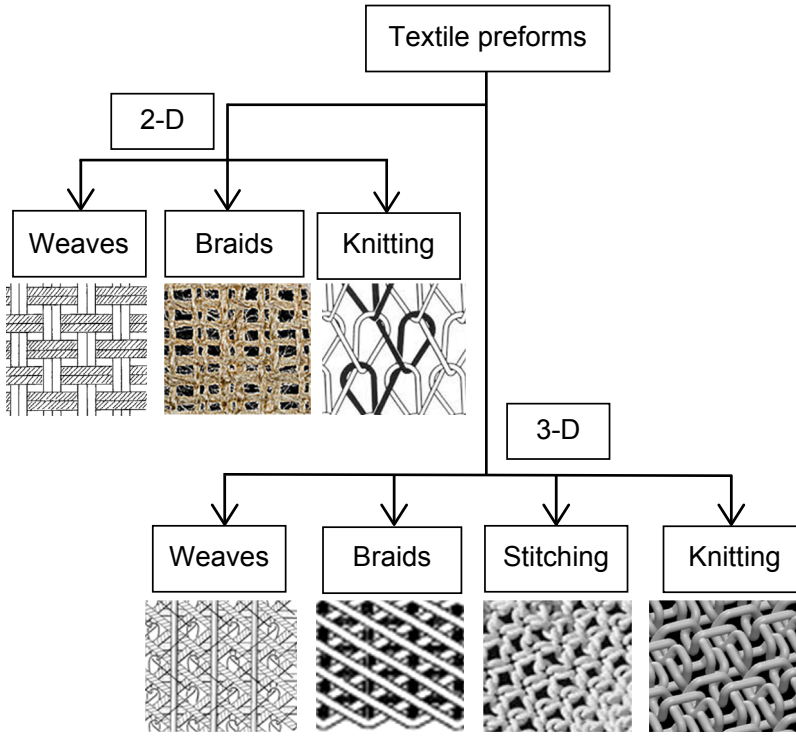

Figure 6.8 Composite fabric reinforcements and preforms.

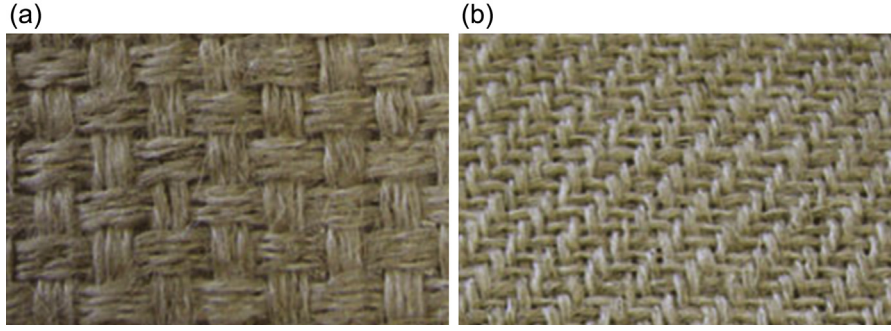

Figure 6.9 (a) Hopsack 4 × 4 flax biaxial fabric with a distinctive plane wave arrangement of yarns and (b) twill 2 × 2 flax biaxial fabric with distinctive twill surface diagonal pattern.

1. Biaxial fabrics

Biaxial fabrics have the reinforcement aligned in two directions. Fabrics are normally composed of certain Tex yarns, which are processed without twist. Yarns are interweaved to compose fabrics with distinctive patterns. For example, Fig. 6.9a illustrates the hopsack 4 x 4 fabric, which is composed of bundles of four yarns interweaved in a plane pattern,

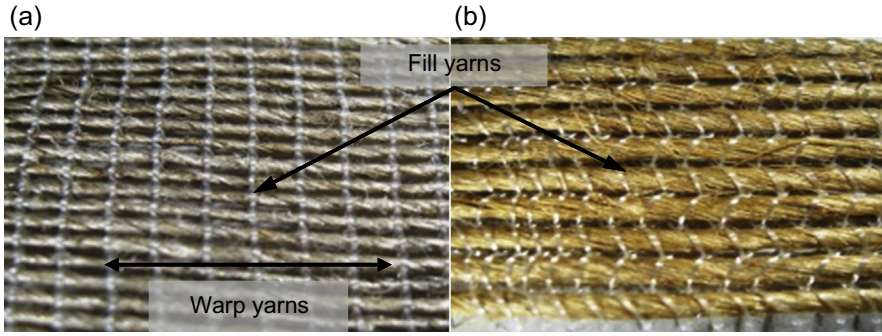

Figure 6.10 (a) Flax unidirectional rowing made out of aligned 240Tex twisted fibre yarns and (b) flax unidirectional rowing made out of 590Tex twisted fibre yarns.

and Fig. 6.9b illustrates the twill 2 x 2 fabric type, which is processed by interweaving single yarns. Both fabrics have two distinctive weaving patterns; they therefore differ in waviness of individual yarns. In synthetic fabric reinforcements, the waviness of the fabric has a significant influence on the mechanical properties of the processed laminate. LNFC yarns are not uniform, in terms of mechanical properties, and are composted out of short fibres, which may result in the reduced effect of the waviness on mechanical properties. Both fabrics have light brown colour. Yarns in both fabrics are not strongly compacted; this allows for easy single yarn separation. Both fabrics can be cut to the desired length with a steel guillotine.

2. Unidirectional fabrics

   Unidirectional fabrics could be the most effective for the development of LNFCs. This type of unidirectional fabric allows easy processing of the laminate of LNFCs by the lay-up technique, compression moulding or vacuum bagging. The desired quantity of fibres can be easily selected. Moreover, this type of fabric allows the processing of the laminates with a high volume fraction of the reinforcement. Since the distances between parallel yarns are fixed, fabrics can be aligned and arranged in a hexagonal packing arrangement, thus increasing volume fraction of the reinforcement.

   Fig. 6.10 presents two flax unidirectional rowing fabrics. Fabrics can differ in the Tex value of the yarns and transverse synthetic fibre interweaving pattern. In Fig. 6.10, the first fabric is processed with 240Tex yarns and is interwoven with a straight transverse pattern, which is compact. Single yarns can be pulled out from the fabric by applying force along the yarn. The second flax fabric is processed with 590Tex yarns and is interwoven with a crisscross pattern, which is relatively loose. This allows for the yarn to be pulled out without any damage. Both yarns are traditional yarns, which hold fibres together with a twist. Polyester interweaving yarn is used.

6.3 Resin systems for long natural fibre composites

LNFCs mainly use thermoset and thermoplastic polymeric matrices, which are classified by the curing mechanisms. The curing mechanism influences the use of the processing techniques and is related to the mechanical performance of the cured composites. Thermoset matrix is of interest in construction due to the thermal stability.

6.3.1 Thermoset resin systems

Thermoset resins for LNFCs mainly include phenolics, polyesters, melamines, silicones, epoxies and polyurethanes. During the curing process, the resin undergoes cross-linking reactions until almost all of the molecules are cross-linked to form three-dimensional networks. After setting, thermoset resins cannot be melted again, and the shape cannot be changed. The thermoset resins are usually supplied in partially polymerized or monomer−polymer mixtures. The cross-linking reaction can be started by the application of heat, oxidizers or UV radiation. The most frequently used thermosetting resins in composite processing are epoxy (Muralidhar et al., 2012; Santulli et al., 2013; Masseteau et al., 2014; Leman et al., 2008) and polyester (Conzatti et al., 2012; Peng et al., 2012; Sawpan et al., 2012; Thiruchitrambalam et al., 2010). Some of thermoset resins can also be cured at room temperature, which makes it popular. Resin mix is normally prepared by mixing resin with the catalyst, which starts an exothermic curing reaction. Additionally, other substances may also be added, such as accelerator, fillers, pigments and solvents. The required pressure and heat can then be applied to accelerate the curing reaction.

Additives can affect the cross-linking process. Additives, which can slow down the reaction, may include inhibitors absorbing free radicals, styrene, fillers, oxygen, flame retardants and reinforcement. Additives, which can accelerate the process, may include initiator content, external heat, UV radiation, accelerators content, waxes and films preventing the access of oxygen. An increase in the thickness of the format composites indirectly accelerates the process by reducing heat dissipation. Factors like resin grade and type, water, pigments and contaminants can affect the cross-linking process speed in either way (Yang and Lee, 1988; Ton-That et al., 2000).

The advantages of using a thermoset matrix system include the availability of lamination techniques, the possibility of room curing or low curing temperature with relatively low cost, superior mechanical properties in comparison with thermoplastic matrices and higher temperature stability in comparison with thermoplastic matrices. However, the volatile organic compound emissions, difficult recycling or reclaiming procedures, short pot and shelf life may become challenging parameters in some cases. Moreover, it is more difficult to achieve a good surface finish compared to the thermoplastics, depending on techniques used (Gay et al., 2002).

6.3.2 Biobased resin systems

The biobased polymers or biobased plastics are a group of materials derived from bioresources, as opposed to fossil fuel-based polymers. Source materials for the biobased composites can come from food industrial waste (Yu et al., 1998). Biobased plastics can be biodegradable under weathering conditions and degraded by microorganisms (Domenek et al., 2004). Biobased origin may not be equivalent with biodegradability. Therefore, NFC fibre reinforcement is intrinsically biodegradable, but the biobased resin may not be (Zini and Scandola, 2011). Bioplastics can be synthesized by microorganisms and have increased biocompatibility (Witholt and Kessler, 1999; Luengo et al., 2003).

Existing biobased polymer systems have relatively poor mechanical properties, such as polylactic acid (PLA), polyhydroxyaldehyde, polyhydroxybutyrate, polyester TP, furan resin and epoxy resins (Wool and Sun, 2005). The main applications for the biobased polymers are in the packaging industry and insulation, which are mainly thermoplastic polymers.

The development of new thermoset biopolymers with the enhanced mechanical properties, such as phenolics, epoxy, polyester and polyurethane resins, makes other applications possible (Raquez et al., 2010). Thermoset biopolymers can be reinforced with natural fibres to create a fully bioresourced composite (Mehta et al., 2004). Plant-based polymers, including proteins (Domenek et al., 2004), oils, carbohydrates, starch (van Soest et al., 1996) and a cellulose, have all been attempted.

In order to improve mechanical properties, partially biobased resin systems have been developed. They combine two or more resin systems where at least one is biobased, such as triglyceride acrylate (Cogins, Tribest S531), epoxidized pine oil waste (Amroy, EPOBIOX™), unsaturated polyester resins from renewable and recycled resources (DSM Palapreg® ECO P55-01, Ashland Envirez®) and soy oil unsaturated polyester (Reichhold, POLYLITE 31,325-00) (Shoseyov et al., 2011). Processing techniques used for biopolymers are usually similar to those for synthetic polymers.

An increase in global fossil fuel prices led to an increased interest in biosources of polymers. Nevertheless, the cost of biobased resin systems is still relatively high. In some cultivation areas the production of plant oils for industrial applications can compete with food production. Cultivation area shortages, together with the increasing global population, led to the increased research in a sea plant and microorganism sources for biopolymers (Mironescu and Mironescu, 2006; Kakita et al., 2003).

6.4 Production of long natural fibre composites

6.4.1 Mat and fabric-reinforced laminates

Flat laminates can be produced with compression moulding, which requires pressure and heat to shape the laminate. Textile or mat reinforcements are cut to the size corresponding to the mould cavity. Resin is mixed with an accelerator or catalyst and degassed in the vacuum chamber. Reinforcements are placed in the mould and subsequently wetted out with resin mix manually or mechanically. Mould with wetted reinforcements is covered with polystyrene release film.

The production can be room or hot pressed, eg, the hot press cycle for several minutes at 100°C with pressure of 10 MPa and cooled under pressure for 20 min down to 30°C. Products can be post-cured for 16 h at 80°C in accordance with BS ISO 3597−1:2003. Fig. 6.11 presents a diagram of the processing methodology, where layers of reinforcement are stacked between aluminium mould plates.

Production can also be carried out with the vacuum bagging aided hot press process. Fig. 6.12 presents a schematic and image of vacuum impregnation set-up. Laminate layers are impregnated one by one in resin using the lay-up technique.

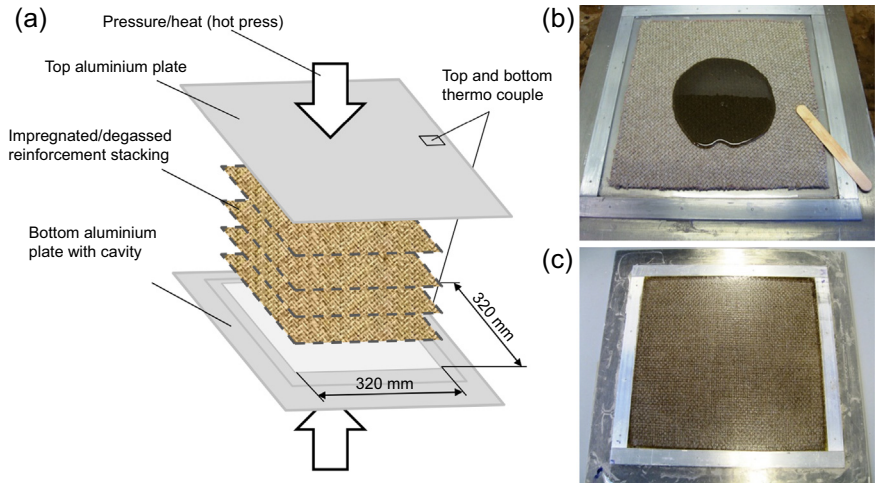

Figure 6.11 (a) Arrangement of reinforcements during compression moulding, (b) fabric reinforcement in a mould during impregnation and (c) Palapreg ECO laminate reinforced with flax 4 × 4 hopsack fabric.

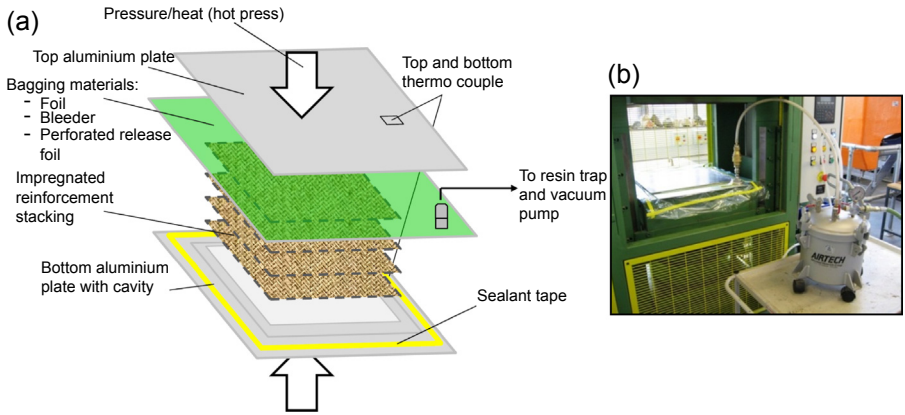

Figure 6.12 (a) Set-up for vacuum impregnation and (b) prepared set-up.

The impregnated stacking is then covered with perforated release and bleed-out film (eg, RF-242RP) and medium-weight breather and absorption fabric (eg, NW153). This is covered with bagging nylon film (eg, NBF-200BT) and connected to the bottom plate with sealant tape (eg, AT-200Y). The lay-up is connected with the resin trap chamber (eg, RB-451) through the nylon bag with a quick release connector (eg, Tygavac-440) and polyethylene tubing. Pressure is controlled with a pressure gauge installed on the resin trap, which is connected to the vacuum pump. After the pumping stage, all materials are checked for leaks in the vacuum bag with an ultrasonic leak detector (eg, LEQ-70).

Laminates can be produced with varying reinforcement stacking arrangements, type of reinforcement, volume fractions and alignment. Volume fraction was controlled by changing the number of layers.

6.4.2 Unidirectional long natural fibre composites

To maximize the tensile properties of the LNFCs, unidirectional composites have to be prepared. Multiple techniques were tested to find the most convenient and easy way to process unidirectional LNFCs. For example, the techniques involve either U-shaped aluminium mould (Fig. 6.13a) or square frame (Fig. 6.13b). Both allow for precise alignment of the yarns and subsequent impregnation by pressing or a vacuum-assisted process.

Composites with parallel yarns are winded onto mandrels. This procedure allows for control over reinforcement content and orientation. Volume fraction is controlled by changing an amount of yarn in the mould cavity. Fig. 6.14 presents a diagram of unidirectional composite preparation. U-shaped aluminium moulds with 'male' and 'female' parts were prepared. Samples are prepared in three steps. In the first step the selected number of yarns is winded onto a cavity of the mould. Fibres are clamped

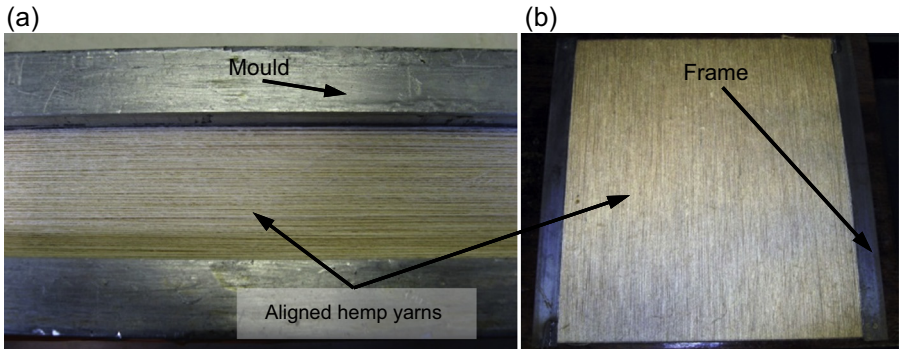

Figure 6.13 (a) Unidirectionally aligned hemp yarns in the rectangular mould and (b) unidirectionally aligned yarns placed in a square mould.

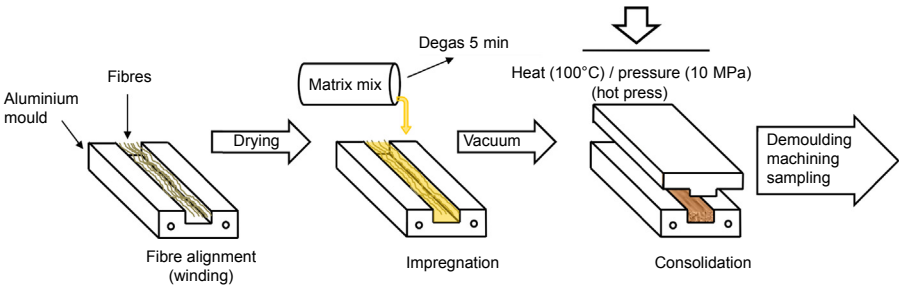

Figure 6.14 Unidirectional yarn long natural fibre composite formatting.

at the end in order to maintain tension and then dried with the mould and cooled down in a decorticator. In the next step, resin mix was introduced and mould was exposed to negative pressure of 1 atm for a duration of five minutes in a vacuum chamber. Samples are then cured with the same hot press cycle, which is used for square laminates.

The square LNFCs can be produced with a similar process as that of the U-shaped mould. Filament winder, described in the next section, is used to wind the yarns onto the frame. This type of sample preparation allows for the uniform distribution of the reinforcement throughout the panel. The impregnation and curing procedures are the same as those of U-shaped moulding.

6.4.3 Tubed long natural fibre composites

Brunel University London has developed the pin winding technique, which is most applicable to control processing parameters during tube preparation (Weclawski, 2015). It allows for control over a whole range of fibre orientations, from 0° to 90° in relation to the mould length. First, aluminium collapsible tubular moulds (Fig. 6.15(c)) and pinned end cups (Fig. 6.15(a)) were prepared. Yarns or filaments are winded onto the core tube and subsequently impregnated. In order to assure easy sample removal the core tube mould was cut diagonally (Fig. 6.15(c)).

Pins attached to the end cups (Fig. 6.15(a)) allow the change in the winding direction for aligning yarns at the 0° direction, parallel to the tube length, which differentiates this technique from conventional filament winding of a tube. Winding of the reinforcement at specific angles and interweaving patterns is possible (Fig. 6.15(b)).

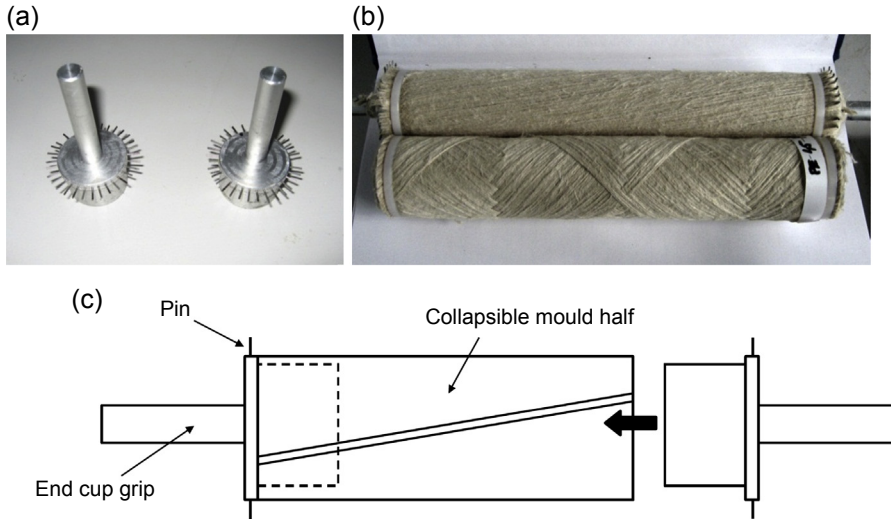

Figure 6.15 (a) Aluminium end cups with pins, (b) moulds with wrapped yarns and (c) collapsible mould with pinned end cups assembly.

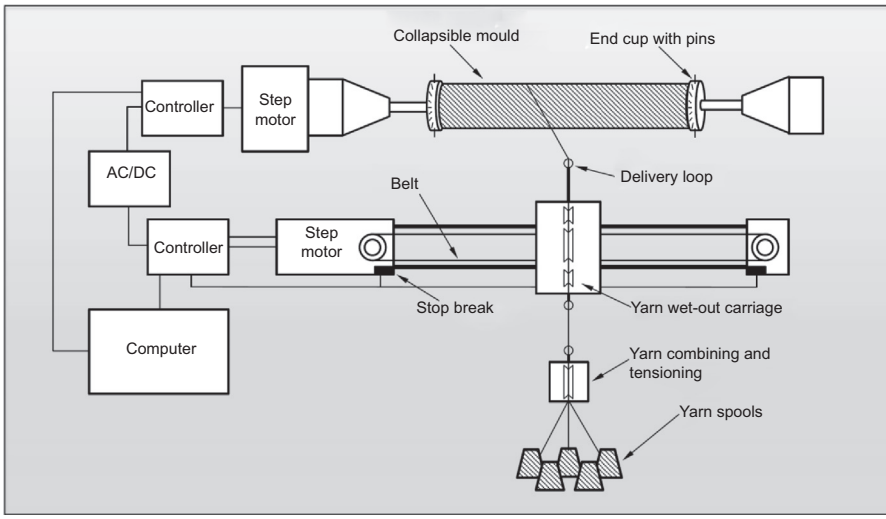

Figure 6.16 Set-up for the natural fibre yarn tube filament winding.

The full filament winding set-up has been prepared in order to facilitate faster and more precise LNFC tube processing (Fig. 6.16). The mould is attached to the end cups, which are connected with the step motor with the end cup grips. This step motor creates the rotation of the mould, thus pulling the yarn onto it. The rotation speed is altered with a controller, which is connected to the computer. Next to the rotating tube mould is the carriage, which is placed on the rails and connected with a step motor with a belt. The carriage has a set of three plastic pulleys, which redirect the yarn to the resin reservoir and apply tension. A delivery loop is connected to the carriage, which allows more precise control over yarn placement onto the rotating mould. The step motor responsible for the carriage movement and the step motor responsible for the rotation of the tube mould are synchronized together with a Q Drive supplied by 'Applied Motion Products'. Synchronization allows the control over winding angle, pattern and processing speed. It is possible to wind multiple yarns at the same time. Multiple yarns are secured in their position and fed through the combining and tensioning tool. Consistent yarn tension was facilitated by friction and adjusted not to exceed the tenacity of the yarn, which was used. The software used allows writing a simple command-based program to create desired tube design in one procedure.

The tubed LNFCs have then been produced. Using the design machine, yarns are fed through the series of loops and attached to the tube mould. The yarns are then winded according to selected program (Fig. 6.17). A rotational speed of the mould and a feeding speed of the fibre carriage are altered, in order to accommodate a change in the thickness, which was measured experimentally. In order to maintain the same wind angle, changes in speed were designed in accordance with Eq. (6.1).

$$\frac{N}{V} = \frac{\theta}{2\pi r} \tag{6.1}$$

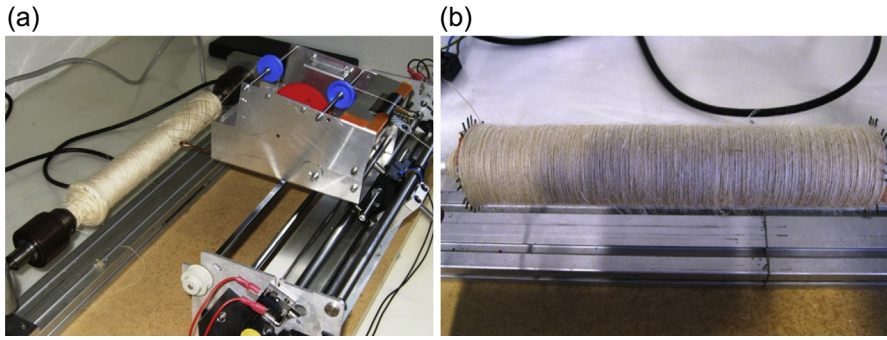

Figure 6.17 (a) Natural fibre winder and (b) tubular mould with surface yarns winded at 90 degree.

where, N denotes the constant rotational speed of the mandrel in revolutions per minute, V is the constant carriage feed, θ is wind angle in relation to the tube main axis and r represents the radius of the mandrel. After the winding procedure of the designated number of layers, yarns are impregnated with resin mix. Two procedures are used, namely compression moulding or vacuum bagging.

Compression moulded samples are first impregnated with resin manually after the winding procedure or with use of the carriage. Next the mould is covered with NV153 perforated release fabric and wrapped with HST400 thermoshrinking tape. Then samples are placed on a prepared stand, which constantly rotates the prepared sample throughout the gelling and curing process (Fig. 6.18). Rotation is used to prevent resin agglomeration due to gravity. After placing the sample in the oven, a pressure is applied by shrinkage of the tape, which is induced by heat. The sample stays in the oven for 15 min. Tubes are postcured at 100°C for 24 h in a vacuum oven. The sample is removed by collapsing the tubular mould. This prevents from inflicting damage to the thin walled tubes prepared.

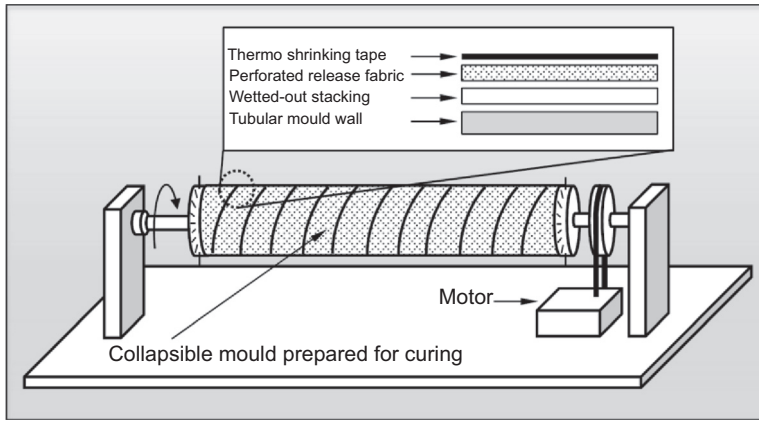

Figure 6.18 Rotating stand used during gelling and curing.

Samples, which were impregnated by vacuum bagging, were sealed with the same sealant materials described in a previous section. The vacuum was created under the bag, and after checking for leaks, valves were opened to introduce the degassed resin mix. Negative pressure created by the vacuum pump creates suction, which transfers the resin through the reinforcement.

6.4.4 Pultrusion of long natural fibre composites

Great efforts are being made at Brunel University, UK in attempt to develop natural fibre composites with a desired structure and good overall properties for construction. Pultrusion has been adapted for the production of LNFCs, and a commercial production has been demonstrated (Fig. 6.19). First, the LNF was made as yarns in the form of continuous roving filaments, and the yarns are then pulled and extruded though a liquid resin, which saturates the LNF reinforcements. Resins used are polyester, vinyl ester, polyurethane and epoxy. Second, the combination of resin and LNF reinforcements is then pulled through a special heated and shaped die for the polymerization using a continuous pulling device. Third, the reinforcement with resin material hardened to formulate the shape of the die and heat set into permanently rigid structurally components. Lastly, the resulting high-strength LNFCs were cut to length as required. The major challenge for the pultrusion of LNFCs is the requirements of LNF, such as the tensile strength of LNF, the wettability of LNF surface and penetration of resin into LNF yarns.

Figure 6.19 Long natural fibre composite pultrusion (Brunel University).

6.5 Properties of long natural fibre composites

LNFCs as construction materials deem to satisfy design characteristics. The properties, such as the tensile, compression and flexural strength, stiffness and durability, shall be achieved. LNFCs, like other unidirectional synthetic composites, have the highest properties in the direction parallel to the fibres in tensile mode. Therefore the engineering designs of the aligned fibrous LNFC laminates should consider the applied stresses in tensile and flexural modes.

6.5.1 Tensile and flexural properties of long natural fibre composites

An extensive programme carried out at the Brunel University London, UK, showed that when using unsaturated polyester resins, the laminates reinforced with hemp randomly oriented mats achieved 50 MPa and 6.8 GPa for tensile strength and tensile modulus, respectively (Weclawski, 2015). Flexural strength and modulus were at 67 MPa and 4.5 GPa, respectively (Fig. 6.20). Most reported laminates reinforced with randomly oriented hemp or flax mat with Vf of fibres between 10% and 45% had ultimate tensile strength ranging between 19 and 65MPa, although a higher value of 90 MPa may be achieved with the partial alignment of the fibres (Hepworth et al., 2000). The reported values for tensile stiffness in composites reinforced with mats in thermoset resin systems range between 0.6 and 10 GPa for hemp and between 2.9 and 9.8 GPa for flax (Dhakal et al., 2007; Rouison et al., 2006; Yuanjian and Isaac, 2007; Mwaikambo et al., 2007; van den Oever et al., 2000).

The tensile properties may be improved if LNF is converted to yarns before fabric formulation. This allows a precise alignment and achievement of an increased volume fraction and hence mechanical properties. Yarns can be processed by a conventional ring spinning process used in the textile industry or by wrapping aligned short fibres with polymeric wire. The reinforcement produced in this way can be handled like most conventional filaments for winding or pultrusion processes. The results again from Brunel University London, by using two flax fabrics (Twill and Hopsack), show that the flax laminates had 6.7 GPa tensile modulus and 63.3 MPa tensile strength, with the flexural stiffness between 5.1 and 6.3 GPa and flexural strength between 140 and 214 MPa with the reinforcement of 45% Vf. Muralidhar et al. (2012) also reported a range of from 31 to 106 MPa flexural strength and from 0.8 to 2.9 GPa flexural stiffness for a flax fabric laminate with the Vf ranging from 18% to 34%.

The team at Brunel University has also investigated the axially aligned laminates in order to find maximum tensile properties. They arranged various hemp and flax aligned yarns in the testing direction. The influence of volume fraction, Tex value, yarn type, yarn twist on tensile properties and fracture pattern of LNFCs was investigated. It was found that the twisted hemp fibre reinforced composites had the highest tensile stress and stiffness properties. The optimal Vf was found at 50% for ECO 39Tex. A further increase in volume fraction led to a decrease in stiffness properties. This is caused by deterioration in wet-out properties, which further leads to the creation of dry spots at the interface. The highest tensile modulus measured for composite

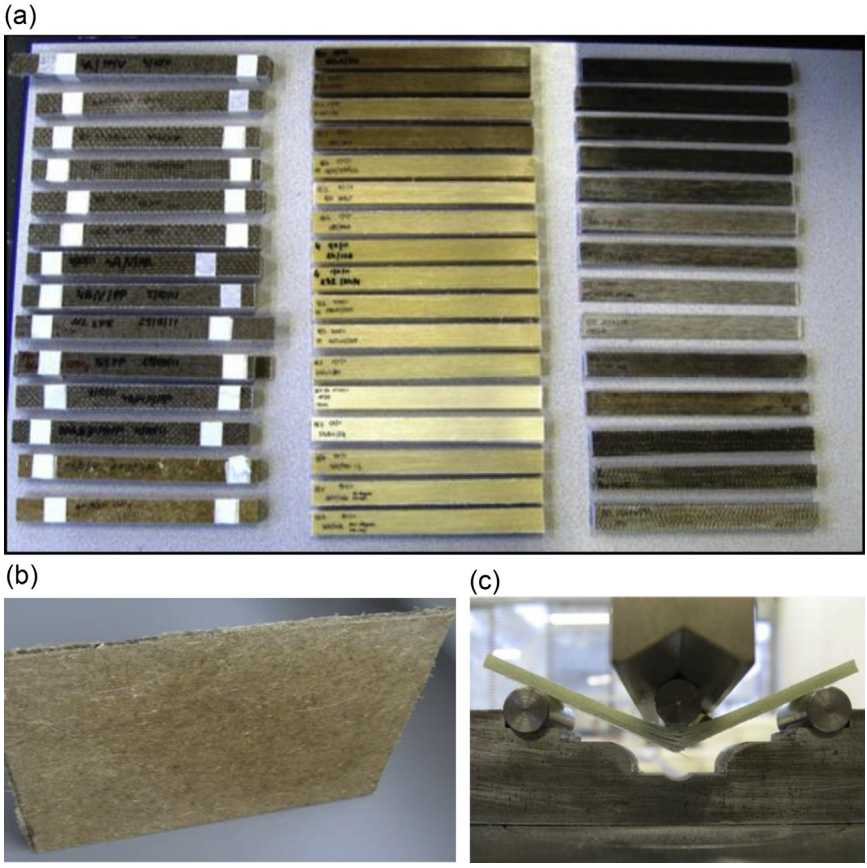

Figure 6.20 (a) Batch of various laminate stripe samples (left = flax, middle = hemp and right = hybrid samples), (b) long natural fibre composite panel and (c) long natural fibre composite flexural loading.

with 39Tex was at the level of 12 GPa, and for 130Tex, composite type was equal to 14 GPa. Tensile strength of the tested composites grew almost linearly throughout whole range of Vf of 23−75%: the tensile strength increased from 180 MPa at 23% Vf to 411 MPa for 75% Vf 39 Tex.

The optimal flexural properties were achieved at 32 GPa for flexural stiffness for 39 Tex yarn, 320 MPa for 130 Tex yarn and up to 330 MPa for 39 Tex yarn for the flexural strength for the composite made with 76% Vf of fibres.

Using the same Vf, it was found that the yarn size, from 25 Tex to 130 Tex yarn, had an influence on the tensile properties, with the tensile modulus increasing with the decrease in yarn size to reach maximum of 14 GPa for 60 Tex and 51 Tex laminate. There was an almost linear relationship between Tex value and tensile stress. The tensile strength of the composite improved from 190 to 337 MPa for the finest 25 Tex type composite.

The flexural properties found declined linearly with the increase of yarn Tex. The flexural stiffness ranged from 15.6 to 22.4 GPa and ultimate flexural strength from 227 to 304 MPa. The use of fine grades of yarns allows for a 44% increase in flexural modulus and a 34% increase in ultimate flexural strength (Weclawski et al., 2014).

An overview of other researchers on the flexural strength and modulus of hemp and flax NFCs, together with the volume fraction and processing methods, showed that with the volume fraction of reinforcement ranging from 10% to 70%, the flexural modulus of NFCs ranged between 0.8 and 25 GPa and the flexural strength between 31 and 219 MPa (Table 6.3). The large variation reported from the literature is due to the dependency of NFC properties on multiple factors, namely fibre aspect ratio, fibre type, surface morphology, fibre treatment, structure, arrangement, resin type and processing route.

Fibre misalignment in the nontwisted yarn could result in a significant effect on the properties of LNFCs due to the different average fibre orientation. Moreover, the polymeric yarn wrapping unidirectional flax fibres can result in the sinusoidal pattern of fibres for the nontwisted yarn due to the tension induced during fibre alignment, wrapping wire shrinkage or processing settings. The main reason for processing nontwisted yarns is to maximize alignment of the fibres in the desired direction. Misalignments can deteriorate the properties of processed material. However, the tensioned polyester wrapping wire induces bending stresses in natural fibres, causing fibres to slide and bend against one another to accommodate the stresses, giving rise to stress concentrations within composite reinforced with nontwisted yarns. Additionally, these results can impair resin impregnation.

6.5.2 Compressive properties of long natural fibre composites

Compressive properties have been thoroughly investigated by using the LNFC tubes (Weclawski et al., 2014) (Fig. 6.21). The correlation between the reinforcement arrangement, material compressive strength and a fracture mode was observed. Fracture modes under compressive loading were observed for LNFC tubes, namely microbuckling, diamond shape buckling, concertina shape buckling and progressive crushing.

It was concluded that the fracture modes were related to the orientations of LNFs and the wall thickness. Thin walled LNFC tubes, with $t/D < 0.04$ and winding angles 30 and 45 degrees, failed with the formation of lobes, and tubes reinforced at 10 degree resulted in the dominated failure of microbuckling, which is characterized by higher compressive stiffness and compressive strength along with catastrophic fracture throughout the sample length. The short and thick tubes ($t/D > 0.04$) had crushing fracture.

The maximum load capacity of LNFC tubes was related to the failure modes, ie, the orientation of NFs (Table 6.4). The compressive modulus and the ultimate compressive strength decreased with the increase of the fibre orientation angle. The maximum strength and stiffness of LNFC tubes reinforced at 0 degree is approximately four times higher than that in comparison with those reinforced at 90 degree.

Table 6.3 Flexural properties of the composites reinforced with aligned hemp or flax fibres

Materials	Vf (%)	MOR (MPa)	MOE (GPa)	Processing	References
Rand Flax hackled-PP/MAPP	20	70	4.0	HP 200° 40 bar	Van den Oever et al. (2000)
Rand Flax hackled-PP/MAPP	40	90	7.0	HP 200° 40 bar	
Rand Flax scutched-PP/MAPP	40	80	6.0	HP 200° 40 bar	
UD Hemp Epoxy	35	148−219	5.9−12.4	FW	Bledzki et al. (2004)
UD Flax PP	35	77−149	−	FW	
UD Flax non hackled UP	25	168	19.4	PU(lab.)	Goutianos et al. (2006)
UD Flax hackled UP	25	182	19.5	PU(lab.)	
0/90Fabric Flax UP	31	198	17.0	RTM	
0/90 Fabric Flax EP	28	190	16.0	Hand lay-Up	
Fabric Flax EP	18−34	*31−106	*0.8−2.9	Hand lay-Up	Muralidhar et al. (2012)
Treated Hemp UP	56	101	10.0	HP 6 MPa	Aziz and Ansell (2004)
Hemp mat Rand UP	10−40	40−110	4.0−7.0	RTM	Sèbe et al. (2000)
Alcali UD Hemp long PLA	10−40	90−68	6.4−5.7	HP 5 MPa	Sawpan et al. (2012)
Alcali and Silane UD Hemp UP	10−50	97−88	4.9−6.8	HP 5 MPa	Sawpan et al. (2011)

HP, Hot press; *Rand*, Random mat reinforcement; *MAPP/PP*, polypropylene; *FW*, Filament winding; *UD*, unidirectional; *PU*, pultrusion; *EP*, epoxy; *UP*, unsaturated polyester; *RTM*, Resin transfer moulding; *, values in MPa/g cm^3; *STBR*, Starch biodegradable resin.

6.5.3 Mechanical property of hybrid long natural fibre composites

NF yarns can be hybridized in order to improve or achieve specific properties. The flexural modulus of the hybrid hemp−wool yarns at a ratio of 0.25 increased with the increase of fibre volume fraction, from 11 to 16 GPa for Vf from 23% to 75%, although this is significantly lower than results of flax or hemp composites

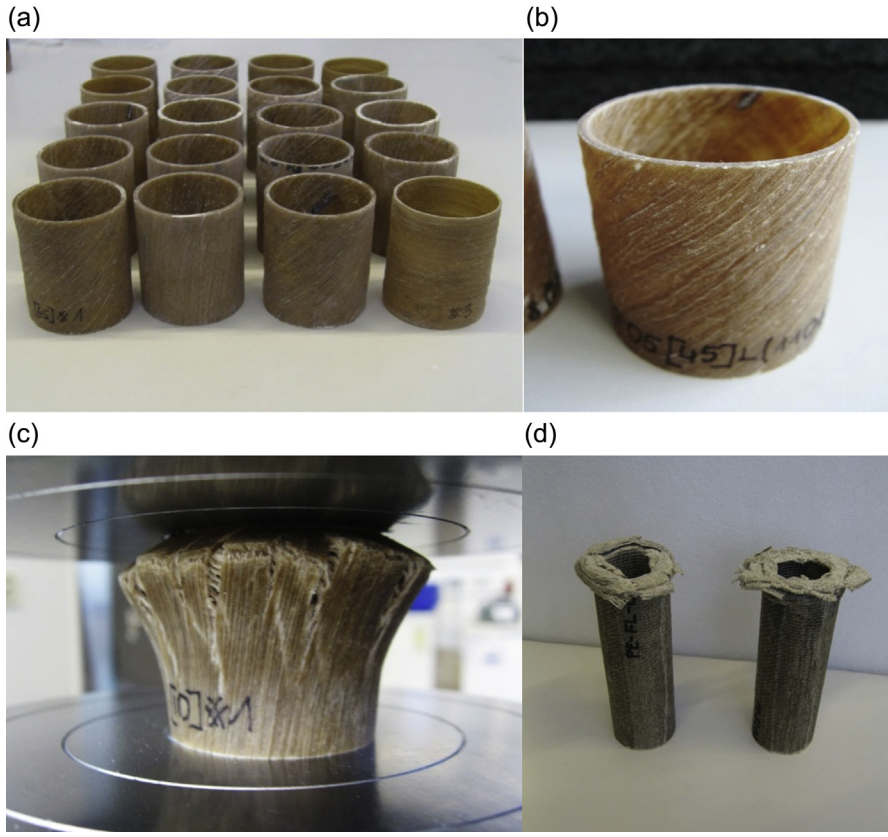

Figure 6.21 (a) One batch of samples trimmed and prepared for the compression test, (b) macro image of the 130Tex hemp twisted ±45 degree yarn long natural fibre composite, (c) tubed long natural fibre composite under compression with a specific fracture pattern and (d) two progressive collapse fracture.

(Weclawski, 2015). The interesting result was found for the ultimate flexural strength of the hybrid LNFCs, which showed an inverse relationship between volume fraction tested and ultimate strength. This was explained by increasing wool percentage, which has lower adhesion properties in comparison with hemp fibre.

6.6 Long natural fibre composites as building components

NFCs used for building elements can be divided into four types depending on their compositions, namely, long fibre structural biocomposites, inorganic shiv composites, organic shiv composites and nonstructural insulation materials. The focus of this chapter is on the use of long fibre structural biocomposites (LNFC) for building

Table 6.4 **Influence of yarn orientation on compressive properties (Weclawski et al., 2002)**

Wind angle [θ]	Σ_{max} [MPa]	CoV (%)	$\sigma_{0.02}$ [MPa]	CoV (%)	Strain at failure [mm/mm]	CoV (%)	E [MPa]	CoV (%)	MoR [MJ/m^3]	CoV (%)
10	76.2	5.5	69.0	11.7	0.0243	3.3	5580.0	11.3	0.63	14.3
30	63.4	9.6	52.4	6.5	0.0313	14.1	3083.7	12.5	0.59	15.5
45	53.9	3.9	40.4	3.2	0.0321	10.3	3585.3	8.1	0.32	12.2
60	33.2	10.2	28.5	10.9	0.0316	17.7	1804.6	12.0	0.30	18.5
90	30.1	8.0	26.5	2.3	0.0360	9.7	1488.0	5.8	0.30	10.9

constructions. As of today, such applications are not fully commercially available. Most existing research has been focused mainly on nonload or semiload bearing applications, such as roof panels or cladding. Hybrid composition panels with sisal and glass fibres can also be processed by compression moulding with epoxy resin; however, the tensile properties of these panels, with 57 MPa and 2.6 GPa, reported for the strength and modulus, respectively, are relatively low (Gupta and Velmurugan, 2000).

Various sandwich structures have been proposed to compensate the insufficiencies of LNFCs for structural applications; for example, Dweib et al. (2004) presented an idea for LNFC sandwich roof construction. It is supposed to be a light and low-cost solution for the roofing in the hurricane-affected areas. The whole roof can be processed with the resin transfer moulding technique. The recycled paper sheets, layered with chicken feathers, corrugated paper or glass fibre, were used as reinforcements. The reported flexural rigidity and strength were 12−20 and 24−26 GPa, respectively, which are similar to the stiffness and two times the strength of wood beams.

Doors made out of sandwich panels have also been reported, with the door skins made with hybrid short natural fibre mats or fabrics and the core formed with various types of foams. LNFC skins are made by compression moulding or pultrusion. LNFC door frames were formed with fabric-reinforced LNFC. The C-shape frame is also filled with foam. Frames happily passed the minimum requirements in accordance with Indian standards (Wool and Sun, 2005).

A team from the Brunel University London, led by Professor Mizi Fan, has undertaken a complex project to investigate the LNFC materials as nonstructural and structural components in construction. Some of the major developments are given below.

6.6.1 One-dimensional long natural fibre composite rods

Circular and square rods made from LNFC have been developed for the possible application to sustain compression or tensile loads (Fig. 6.22). This has been further commercialized at the industrial scale by the pultrusion process. Peng et al. (2012) described a series of mechanical tests used to evaluate and optimize LNFC reinforced with coarse hemp nontwisted yarns. Aligned fibres are tensioned along the axis of the rod, which allows for a higher volume fraction of reinforcement and increased mechanical properties. These type of elements can work as elements of indoor and outdoor furniture.

6.6.2 Two-dimensional long natural fibre composite panels

Most existing NFCs are the laminated panels reinforced with fabrics or rovings and are the most successful in the automotive industry. Flat NFC panels have also been considered most appropriate for building construction, such as wall partitions, roofing elements, flooring or elements of furniture. Properties can be controlled by the use of fabric reinforcements, and panels can be moulded into various shapes (Fig. 6.23). The natural appearance and fibrous texture are appealing and perfectly fit into the current sustainable design trend of low carbon construction.

Figure 6.22 Long natural fibre composite rods.

Figure 6.23 Long natural fibre composite panels.

6.6.3 Three-dimensional long natural fibre composite building components

An extensive programme has been carried out, led by Professor Mizi Fan at Brunel University, to produce square or circular 3-D LNFC tubes by filament winding or by pull winding techniques (Fig. 6.24a). Many important outcomes have been achieved. Tensile and shear properties are controlled by winding or stacking sequences of the composite.

3-D tubes can be loaded in tensile and flexural modes. With a specific design, tubes can be applied to load-bearing applications like household staircases or furniture. The properties of the tubed LNFCs control reinforcement direction, arrangement, tube size and wall thickness. The test showed that the thin walled tubes went through similar collapse mechanisms as glass fibre reinforced tubes.

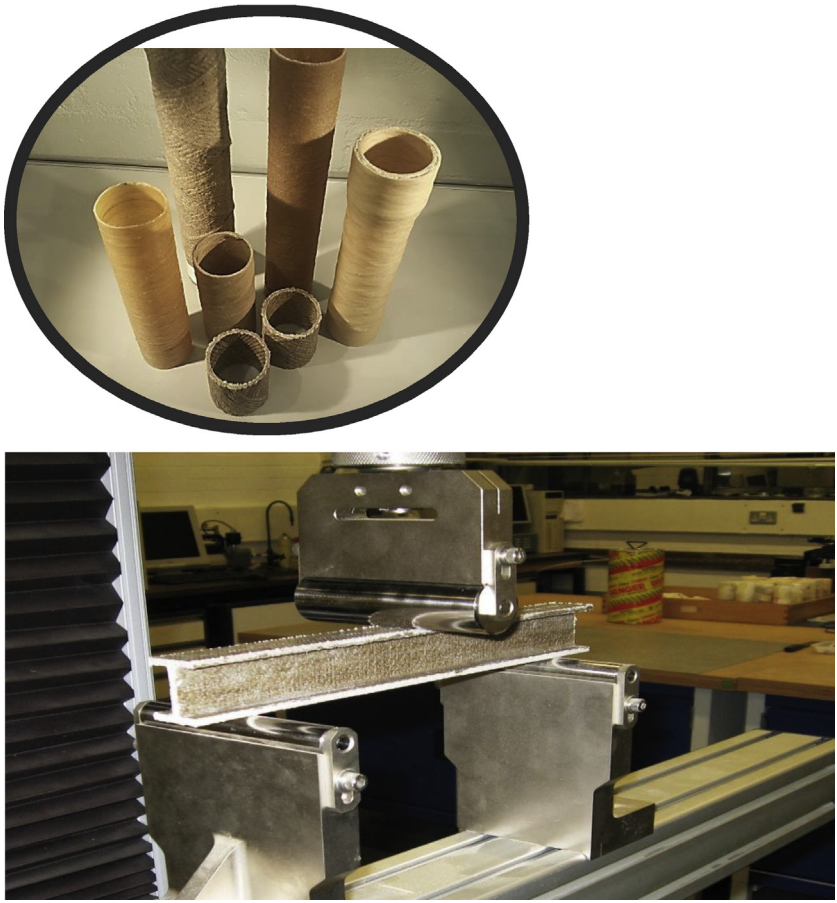

Figure 6.24 Three-dimensional long natural fibre composite tubes and I-beams.

I-section and T-section beams have also been developed at Brunel University, led by Professor Mizi Fan (Fig. 6.24b). The products have been formulated for load-bearing applications out of LNFC, by compression moulding or pultrusion processes. Reinforcement can be arranged with use for fabrics and single yarns in order to maximize mechanical properties and ensure correct fracture mode. Optimized design with regard to shear properties within the web gives the highest result. Those elements can be applied as elements of roofing, door frames and windows elements, among others.

6.7 Conclusions

Long length natural fibre composites have been intensively studied and continue to be a major research topic. Recent improvements in fibre extraction, treatments and resin systems and successful application in the automotive industry have created a positive future trend for LNFCs in construction. Critics have recalled a long history of development, a high price of material, inconsistencies in properties and weathering performance and competitive substitute materials, but most of those challenges have already been answered by the research community. Therefore LNFCs shall move towards commercialization and meanwhile address the bottlenecks in the supply chain.

Various LNF reinforcements, eg, hybrid LNF mats, twisted or nontwisted yarns, hybrid yarns and various fabrics, and processing technologies, eg, compression, vacuum bagging, injection, filament winding and pultrusion, have been discussed for possible applications for the production of LNFCs for construction. LNFCs have the highest properties in tensile or flexural modes. With control over type and arrangement of reinforcement, LNFCs could be optimized for specific construction components, such as LNFC rods, panels, tubes and I-beams.

References

Acar, M., Harper, J.F., 2000. Textile composites from hydro-entangled non-woven fabrics. Computers & Structures 76 (1−3), 105−114.

Akin, D.E., Foulk, J.A., Dodd, R.B., Mcalister III, D.D., 2001. Enzyme-retting of flax and characterization of processed fibers. Journal of Biotechnology 89 (2), 193−203.

Andersons, J., Spārniņš, E., Joffe, R., Wallström, L., 2005. Strength distribution of elementary flax fibres. Composites Science and Technology 65 (3), 693−702.

Awaja, F., Gilbert, M., Kelly, G., Fox, B., Pigram, P.J., 2009. Adhesion of polymers. Progress in Polymer Science 34 (9), 948−968.

Aziz, S.H., Ansell, M.P., 2004. The effect of alkalization and fibre alignment on the mechanical and thermal properties of kenaf and hemp bast fibre composites: Part 1 − polyester resin matrix. Composites Science and Technology 64 (9), 1219−1230.

Bledzki, A.K., Gassan, J., 1999. Composites reinforced with cellulose based fibres. Progress in Polymer Science 24 (2), 221−274.

Bledzki, A., Fink, H., Specht, K., 2004. Unidirectional hemp and flax EP-and PP-composites: influence of defined fiber treatments. Journal of Applied Polymer Science 93 (5), 2150−2156.

Bos, H.L., Donald, A.M., 1999. In situ ESEM study of the deformation of elementary flax fibres. Journal of Materials Science 34 (13), 3029−3034.

Bos, H.L., Van, D.O., Peters, O.C.J.J., 2002. Tensile and compressive properties of flax fibres for natural fibre reinforced composites. Journal of Materials Science 37 (8), 1683−1692.

Buet-Gautier, K., Boisse, P., 2001. Experimental analysis and modeling of biaxial mechanical behavior of woven composite reinforcements. Experimental Mechanics 41 (3), 260−269.

Charlet, K., Baley, C., Morvan, C., Jernot, J.P., Gomina, M., Bréard, J., 2007. Characteristics of Hermès flax fibres as a function of their location in the stem and properties of the derived unidirectional composites. Composites Part A: Applied Science and Manufacturing 38 (8), 1912−1921.

Chen, Y., Gratton, J.L., Liu, J., 2004. Power requirements of hemp cutting and conditioning. Biosystems Engineering 87 (4), 417−424.

Conzatti, L., Giunco, F., Stagnaro, P., Capobianco, M., Castellano, M., Marsano, E., 2012. Polyester-based biocomposites containing wool fibres. Composites Part A: Applied Science and Manufacturing 43 (7), 1113−1119.

Dai, D., Fan, M., Collins, P., 2013. Fabrication of nanocelluloses from hemp fibers and their application for the reinforcement of hemp fibers. Industrial Crops and Products 44, 192−199.

Dhakal, H.N., Zhang, Z.Y., Richardson, M.O.W., 2007. Effect of water absorption on the mechanical properties of hemp fibre reinforced unsaturated polyester composites. Composites Science and Technology 67, 1674−1683.

Domenek, S., Feuilloley, P., Gratraud, J., Morel, M., Guilbert, S., 2004. Biodegradability of wheat gluten based bioplastics. Chemosphere 54 (4), 551−559.

Dupeyre, D., Vignon, M., 1998. Fibres from semi-retted hemp bundles by steam explosion treatment. Biomass and Bioenergy 14 (3), 251−260.

Dweib, M.A., Hu, B., O'donnell, A., Shenton, H.W., Wool, R.P., 2004. All natural composite sandwich beams for structural applications. Composite Structures 63 (2), 147−157.

Fan, M., 2009. Sustainable fibre-reinforced polymer composites in construction. In: Goodship, V. (Ed.), Management, Recycling and Reuse of Waste Composites, 1st ed. Woodhead Publishing, Cambridge, p. 518.

FAO, 2012. *Flax Fibre and Tow Production Data*. Food and Agriculture Organisation of the UN, Available from: http://faostat3.fao.org/home/index.html. SEARCH_DATA.

Gay, D., Hoa, S.V., Tsai, S.W., 2002. Composite Materials: Design and Applications. CRC press.

Ghassemieh, E., Acar, M., Versteeg, H.K., 2001. Improvement of the efficiency of energy transfer in the hydro-entanglement process. Composites Science and Technology 61 (12), 1681−1694.

Goutianos, S., Peijs, T., Nystrom, B., Skrifvars, M., 2006. Development of flax fibre based textile reinforcements for composite applications. Applied Composite Materials 13 (4), 199−215.

Gratton, J., Chen, Y., 2004. Development of a field-going unit to separate fiber from hemp (*Cannabis sativa*) stalk. Applied Engineering in Agriculture 20 (2), 139−145.

Graupner, N., Herrmann, A.S., Müssig, J., 2009. Natural and man-made cellulose fibre-reinforced poly(lactic acid) (PLA) composites: an overview about mechanical characteristics and application areas. Composites Part A: Applied Science and Manufacturing 40 (6−7), 810−821.

Gupta, N.K., Velmurugan, R., 2000. Analysis of polyester and epoxy composite shells subjected to axial crushing. International Journal of Crashworthiness 5 (3).

Hagstrand, P., oksman, K., 2001. Mechanical properties and morphology of flax fiber reinforced melamine-formaldehyde composites. Polymer Composites 22 (4), 568−578.

Hepworth, D.G., Hobson, R.N., Bruce, D.M., Farrent, J.W., 2000. The use of unretted hemp fibre in composite manufacture. Composites Part A: Applied Science and Manufaturing 31, 1279−1283.

Hivet, G., Boisse, P., 2008. Consistent mesoscopic mechanical behaviour model for woven composite reinforcements in biaxial tension. Composites Part B: Engineering 39 (2), 345−361.

Hughes, M., 2012. Defects in natural fibres: their origin, characteristics and implications for natural fibre-reinforced composites. Journal of Materials Science 47 (2), 599−609.

Joseph, M.L., 1986. Introductory Textile Science. Holt, Rinehart and Winston, New York, p. 1.

Kakita, H., Kamishima, H., Ohno, M., Chirapart, A., 2003. Marine biopolymers from the red algae, *Gracilaria* spp. Recent Advances in Marine Biotechnology 9, 79−109.

Kalia, S., Kaith, B.S., Kaur, I., 2009. Pretreatments of natural fibers and their application as reinforcing material in polymer composites? A review. Polymer Engineering & Science 49 (7), 1253−1272.

Khristova, P., Tomkinson, J., Lloyd Jones, G., 2003. Multistage peroxide bleaching of French hemp. Industrial Crops and Products 18 (2), 101−110.

Ko, F.K., 2004. From textile to geotextiles. In: Seminar in Honour of Professor Robert Koerner 2004.

Krassig, H., 1985. Structure of cellulose and its relation to properties of cellulose fibers. In: Kennedy, J.F., et al. (Eds.), Cellulose and its Derivatives: Chemistry, Biochemistry and Applications.

Kvavadze, E., Bar-Yosef, O., Belfer-Cohen, A., Boaretto, E., Jakeli, N., Matskevich, Z., Meshveliani, T., 2009. 30,000-year-old wild flax fibers. Science 325 (5946), 1359.

La Rosa, A.D., Recca, G., Summerscales, J., Latteri, A., Cozzo, G., Cicala, G., 2014. Bio-based versus traditional polymer composites. A life cycle assessment perspective. Journal of Cleaner Production 74, 135−144.

Lawrence, G.H., 1951. Taxonomy of Vascular Plants. New York, 9.

Leman, Z., Sapuan, S.M., Saifol, A.M., Maleque, M.A., Ahmad, M.M.H.M., 2008. Moisture absorption behavior of sugar palm fiber reinforced epoxy composites. Materials & Design 29 (8), 1666−1670.

Li, Y., Pickering, K., Farrell, R., 2009. Analysis of green hemp fibre reinforced composites using bag retting and white rot fungal treatments. Industrial Crops and Products 29 (2), 420−426.

Luengo, J.M., Garcia, B., Sandoval, A., Naharro, G., Olivera, E.R., 2003. Bioplastics from microorganisms. Current Opinion in Microbiology 6 (3), 251−260.

Luo, Y., Verpoest, I., 2002. Biaxial tension and ultimate deformation of knitted fabric reinforcements. Composites Part A: Applied Science and Manufacturing 33 (2), 197−203.

Masseteau, B., Michaud, F., Irle, M., Roy, A., Alise, G., 2014. An evaluation of the effects of moisture content on the modulus of elasticity of a unidirectional flax fiber composite. Composites Part A: Applied Science and Manufacturing 60, 32−37.

Mehta, G., Mohanty, A.K., Misra, M., Drzal, L.T., 2004. Effect of novel sizing on the mechanical and morphological characteristics of natural fiber reinforced unsaturated polyester resin based bio-composites. Journal of Materials Science 39 (8), 2961−2964.

Mironescu, M., Mironescu, V., 2006. New concept for the obtention of biopolymers-based food biofilms. Journal of Agroalimentary Processes and Technologies 12 (1), 216−219.

Mohanty, A.K., Misra, M., Drzal, L.T., 2005. Natural Fibres, Biopolymers, and Biocomposites. CRC Press.

Morton, W.E., Hearle, J.W., 1993. Physical Properties of Textile Fibres. Textile institute.
Mueller, D.H., Krobjilowski, A., 2003. New discovery in the properties of composites reinforced with natural fibers. Journal of Industrial Textiles 33 (2), 111−130.
Munawar, S.S., Umemura, K., Kawai, S., 2007. Characterization of the morphological, physical, and mechanical properties of seven nonwood plant fiber bundles. Journal of Wood Science 53 (2), 108−113.
Munder, F., Furll, C., Hempel, H., 2005. Processing of bast fiber plants for industrial application. Natural Fibers, Biopolymers and Biocomposites 109−140.
Muralidhar, B., Giridev, V., Raghunathan, K., 2012. Flexural and impact properties of flax woven, knitted and sequentially stacked knitted/woven preform reinforced epoxy composites. Journal of Reinforced Plastics and Composites 31 (6).
Musto, D.F., 1972. The 1937 Marijuana Tax Act. Archives of General Psychiatry 26 (2), 101−108.
Mwaikambo, L.Y., Tucker, N., Clark, A.J., 2007. Mechanical properties of hemp-fibre-reinforced euphorbia composites. Macromolecular Materials and Engineering 292, 993−1000.
Needles, H.L., 1986. Textile Fibers, Dyes, Finishes, and Processes: A Concise Guide. Noyes Publications.
Ouajai, S., Hodzic, A., Shanks, R., 2004. Morphological and grafting modification of natural cellulose fibers. Journal of Applied Polymer Science 94 (6), 2456−2465.
Pan, N., Hua, T., Qiu, Y., 2001. Relationship between fiber and yarn strength. Textile Research Journal 71 (11), 960−964.
Peng, X., Fan, M., Hartley, J., Al-Zubaidy, M., 2012. Properties of natural fiber composites made by pultrusion process. Journal of Composite Materials 46 (2), 237−246.
Pickering, K.L., Beckermann, G.W., Alam, S.N., Foreman, N.J., 2007. Optimising industrial hemp fibre for composites. Composites Part A: Applied Science and Manufacturing 38 (2), 461−468.
Pickering, K.L., 2008. Properties and Performance of Natural-fibre Composites. Woodhead Pub.
Placet, V., 2009. Characterization of the thermo-mechanical behaviour of Hemp fibres intended for the manufacturing of high performance composites. Composites Part A: Applied Science and Manufacturing 40 (8), 1111−1118.
Raquez, J., Deléglise, M., Lacrampe, M., Krawczak, P., 2010. Thermosetting (bio) materials derived from renewable resources: a critical review. Progress in Polymer Science 35 (4), 487−509.
Rouison, D., Sain, M., Couturier, M., 2006. Resin transfer molding of hemp fiber composites: optimization of the process and mechanical properties of the materials. Composites Science and Technology 66, 895−906.
Sèbe, G., Cetin, N., Hill, C.S., Hughes, M., 2000. RTM hemp fibre-reinforced polyester composites. Applied Composite Materials 7 (5−6), 341−349.
Santulli, C., Sarasini, F., Tirillò, J., Valente, T., Valente, M., Caruso, A.P., Infantino, M., Nisini, E., Minak, G., 2013. Mechanical behaviour of jute cloth/wool felts hybrid laminates. Materials & Design 50, 309−321.
Sawpan, M.A., Pickering, K.L., Fernyhough, A., 2011. Effect of fibre treatments on interfacial shear strength of hemp fibre reinforced polylactide and unsaturated polyester composites. Composites Part A: Applied Science and Manufacturing 42 (9), 1189−1196.
Sawpan, M.A., Pickering, K.L., Fernyhough, A., 2012. Flexural properties of hemp fibre reinforced polylactide and unsaturated polyester composites. Composites Part A: Applied Science and Manufacturing 43 (3), 519−526.
Schäfer, T., Honermeier, B., 2006. Effect of sowing date and plant density on the cell morphology of hemp (*Cannabis sativa* L.). Industrial Crops and Products 23 (1), 88−98.

Shahzad, A., 2012. Hemp fiber and its composites—a review. Journal of Composite Materials 46 (8), 973–986.

Sharma, H.S., 1988. Chemical retting of flax using chelating compounds. Annals of Applied Biology 113 (1), 159–165.

Shoseyov, O., Heyman, A., Lapidot, S., Meirovitch, S., Nevo, Y., Gustafsson, T., 2011. Cellulose-based Composite Materials.

Struik, P.C., Amaducci, S., Bullard, M.J., Stutterheim, N.C., Venturi, G., Cromack, H.T.H., 2000. Agronomy of fibre hemp (*Cannabis sativa* L.) in Europe. Industrial Crops and Products 11 (2–3), 107–118.

Summerscales, J., Dissanayake, N.P.J., Virk, A.S., Hall, W., 2010. A review of bast fibres and their composites. Part 1 – fibres as reinforcements. Composites Part A: Applied Science and Manufacturing 41 (10), 1329–1335.

Tang, H.B., Xu, B.G., Tao, X.M., Feng, J., 2011. Mathematical modeling and numerical simulation of yarn behavior in a modified ring spinning system. Applied Mathematical Modelling 35 (1), 139–151.

Thiruchitrambalam, M., Athijayamani, A., Sathiyamurthy, S., Thaheer, A.S., 2010. A review on the natural fiber-reinforced polymer composites for the development of Roselle fiber-reinforced polyester composite. Journal of Natural Fibers 7 (4), 307–323.

Ton-That, M., Cole, K.C., Jen, C., França, D.R., 2000. Polyester cure monitoring by means of different techniques. Polymer Composites 21 (4), 605–618.

Tserki, V., Zafeiropoulos, N., Simon, F., Panayiotou, C., 2005. A study of the effect of acetylation and propionylation surface treatments on natural fibres. Composites Part A: Applied Science and Manufacturing 36 (8), 1110–1118.

Umer, R., Bickerton, S., Fernyhough, A., 2007. Characterising wood fibre mats as reinforcements for liquid composite moulding processes. Composites Part A: Applied Science and Manufacturing 38 (2), 434–448.

Van de Weyenberg, I., Ivens, J., De coster, A., Kino, B., Baetens, E., Verpoest, I., 2003. Influence of processing and chemical treatment of flax fibres on their composites. Composites Science and Technology 63 (9), 1241–1246.

Van den Oever, M., Bos, H., Van kemenade, M., 2000. Influence of the physical structure of flax fibres on the mechanical properties of flax fibre reinforced polypropylene composites. Applied Composite Materials 7 (5–6), 387–402.

van Soest, J.J., Hulleman, S., de Wit, D., Vliegenthart, J., 1996. Crystallinity in starch bioplastics. Industrial Crops and Products 5 (1), 11–22.

Wang, H., Postle, R., Kessler, R., Kessler, W., 2003. Removing pectin and lignin during chemical processing of hemp for textile applications. Textile Research Journal 73 (8), 664–669.

Weclawski, B., Fan, M., Hui, D., 2002. Compressive behaviour of natural fibre composite. Composites Part B: Engineering 2014 (67), 183–191.

Weclawski, B., Fan, M., Hui, D., 2014. Compressive behaviour of natural fibre composite. Composites Part B Engineering 67, 183–191.

Weclawski, B., 2015. The Potential of Best Natural Fibres as Reinforcement for Composites in Civil Engineering. Library, Brunel University London.

Wielage, B., Lampke, T., Marx, G., Nestler, K., Starke, D., 1999. Thermogravimetric and differential scanning calorimetric analysis of natural fibres and polypropylene. Thermochimica Acta 337 (1), 169–177.

Witholt, B., Kessler, B., 1999. Perspectives of medium chain length poly (hydroxyalkanoates), a versatile set of bacterial bioplastics. Current Opinion in Biotechnology 10 (3), 279–285.

Wool, R., Sun, X.S., 2005. Bio-based Polymers and Composites. Academic Press.

Yang, Y., Lee, L.J., 1988. Microstructure formation in the cure of unsaturated polyester resins. Polymer 29 (10), 1793−1800.

Yu, P., Huang, A., Lo, W., Chua, H., Chen, G., 1998. Conversion of Food Industrial Wastes into Bioplastics. Biotechnology for Fuels and Chemicals. Springer, pp. 603−614.

Yuan, X., Zhang, Y., Zhang, X., 1999. Maleated polypropylene as a coupling agent for polypropylene−waste newspaper flour composites. Journal of Applied Polymer Science 71 (2), 333−337.

Yuanjian, T., Isaac, D.H., 2007. Impact and fatigue behaviour of hemp fibre composites. Composites Science and Technology 67, 3300−3307.

Zafeiropoulos, N., Baillie, C., 2007. A study of the effect of surface treatments on the tensile strength of flax fibres: Part II. Application of Weibull statistics. Composites Part A: Applied Science and Manufacturing 38 (2), 629−638.

Zini, E., Scandola, M., 2011. Green composites: an overview. Polymer Composites 32 (12), 1905−1915.

Cellulose fiber-based high strength composites

7

L. Lin, F. Fu, L. Qin
Research Institute of Wood Industry, Chinese Academy of Forestry, Beijing, China

7.1 Introduction

Cellulose fiber-based composites, such as wood, are biodegradable and renewable native polymeric composites made up mainly of cellulose, hemicellulose, and lignin, which is widely used in various fields due to many specific merits different from other materials, such as metal, cement, and synthetic polymer. In addition, aesthetical characters and low processing cost make these composites the most preferred materials for building construction.

While wood is a super natural composite material, some inherent properties, such as dimension instability, relatively low strength, easy degradation due to insect attack, and poor perception of fire resistance (Schneider and Brebner, 1985; Norimoto et al., 1992; Rowell, 2006a), prevent its wider utilizations. To overcome such disadvantageous characteristics, many studies have been devoted to modify wood to improve its quality, enlarge its utilization, and add more value to the materials, especially for fast-grown wood.

Wood or natural fiber-based reinforced composites are one of the outcomes of these modification developments, which bring about novel wood or natural fiber composites and hence new applications within reach. This chapter introduces one of the novel developments, namely wood-based reinforced composites. Wood-based reinforced composites can be split into three main categories: thermal, chemical, and mechanical reinforced composites.

7.2 Production of reinforced composites

7.2.1 Thermal induced reinforcement

Thermal treatment is one of the most common modifications of wood and has in fact been used for more than 50 years. Thermal treatments are the controlled pyrolysis of wood being heated to temperatures of more than 200°C without the presence of oxygen. The increasing worldwide environmental pressure has led to an important change in the field of wood preservation, particularly in relation to the biocide toxicity, leading to the development of nonbiocidal alternatives. Among these alternatives, thermal treatment of wood, by mild pyrolysis, has been considered the most promising technology and has been intensively investigated.

Advanced High Strength Natural Fibre Composites in Construction. http://dx.doi.org/10.1016/B978-0-08-100411-1.00007-8

The main targets of thermal treatments are to improve some of the characteristics of final wood products, such as the improved dimensional stability, increased biological durability, enhanced weather resistance, and reduced shrinking and swelling (Bourgeois and Guyonnet, 1988). In particular the improved dimensional stability and durability can be achieved without the use of external chemicals, which enable the treated wood to remain as an environmentally friendly alternative to impregnated chemically wood materials. This thermal treatment process only uses steam and heat, and no chemicals or agents are applied to the material during the process. However, this form of modification does affect the strength of the wood, making it unsuitable for structural applications (Shi et al., 2007a,b).

The first pilot studies of the thermal treatment process were reported by Stamm and Buro (Turner et al., 2010) after a variety of different nonindustrial studies were reported (Scheffer and Eslyn, 1961; Lipska and Parker, 1965; Kollmann and Topf, 1971). Various thermal treatments have been developed in France, Finland, and some other European countries. All the thermal treatment processes have in common that wood was heated at temperatures ranging from 160°C to 260°C in the absence of oxygen at the controlled pyrolysis rate to modify the chemical structure of lumber. The main differences between the different processes are their processing conditions, such as furnace design, process steps, treatment schedules, and different media including nitrogen, steam, and hot oil. Four processes are available at the industrial scale, including Finnish ThermoWood process, Dutch Plato process, French Retification Process, and German OHT process (Militz, 2002).

7.2.1.1 ThermoWood process

The ThermoWood process was developed at VTT Technical Research Center of Finland in the early 1990s. In the ThermoWood process the wood is heated in the presence of hot water steam, and low oxygen contents prevent the wood from burning at high temperatures. Generally, the ThermoWood process consists of three steps: warming up, drying, and cooling and conditioning. The warming up step is to heat and predry lumber. The temperature in the kiln is raised rapidly, and a large amount of steam is generated. At the beginning of the drying step, the temperature is increased steadily and the timber is dried intensively. At a certain point of the drying step, when the moisture content of the lumber reaches nearly 0, the temperature is raised rapidly to a range of 150−240°C, depending on the applications of the treated wood. Wood is kept at this temperature for 0.5 ~ 4 h. In the cooling and conditioning step, the temperature of the wood is cooled to 80−90°C using a water spray system. Conditioning is carried out to moisten the treated wood and bring its moisture content to 4−7%.

7.2.1.2 Plato process

The Plato process was invented by Shell and executed by the Plato Company in the Netherlands (Homan and Jorissen, 2004). The Plato process consists of three steps. The first step is a hydrothermolysis. The wood is heated to between 160°C and 190°C under steam pressure and a low oxygen atmosphere. In this step, it is believed

that aldehydes and phenols are released from hemicellulose and the lignin. The second step is a drying process, which is required for the execution of the third step, that is, the curing is executed at the dry condition of temperatures between 170°C and 190°C, so the aldehydes and phenols react with each other and form new polymers in the cell wall. Finally, conditioning is also carried out for two to three days after the curing step.

7.2.1.3 Retification process

The Retification process developed in France, which is a mild pyrolysis and considerably improves dimensional stability and the durability to resist biodegradation of wood. The Retification process starts with relatively dry wood (below 12%) and slowly heats up wood up to 210−240°C in an inert atmosphere (mostly in the nitrogen atmosphere) with less than 2% oxygen content. Usually temperature was increased by 20°C/min from ambient to the operating temperature. After heating treatment, the temperature decreases automatically until 20°C (Militz, 2002).

7.2.1.4 OHT process

The OHT process started in a German company, which applied hot vegetable oils as the heating medium to the desired temperature, and thus hot oils provide good heat transfer and separate the oxygen from the wood (Welzbacher and Rapp, 2007; Wang and Cooper, 2005). The advantages of oil heat treatment are the absence of oxygen, uniform and fast heat transfer rate to wood, and surface protection by the absorbed oil (Sailer et al., 2000). To obtain a maximum durability and minimum oil consumption, the process is operated at 220°C. However, to obtain a maximum durability at acceptable strength reductions, temperatures between 180°C and 200°C are used. It is proven to be necessary to keep the desired process temperature (for example 220°C) for in the middle of the wooden pieces to be treated for two to four hours. Additional time for heating up and cooling down is necessary, depending on the dimension of the wood (Militz, 2002).

7.2.2 Chemical modification

The term "chemical modification of wood" was first used in 1946, which was defined as a chemical reaction between some reactive parts of wood and a simple single chemical reagent, with or without catalyst, to form a covalent bond between them. This excludes all simple chemical impregnation treatments, which do not form covalent bonds, and monomer impregnations that polymerize in situ but do not bond with the cell wall. The main purpose of chemical modifications of wood was focused on improving strength, dimensional stability, resistance to biological degradation, fire retardants, and resistance to ultraviolet radiation.

Chemical agent modification techniques are becoming increasingly popular and have been proven to be a promising way to improve wood properties. Many chemical reaction systems have been published for the modification of wood, and these systems have been reviewed in the literature several times in the past (Rowell and Gutzmer,

1975; Rowell, 2006a). Reaction systems of chemical agent modification can be split into two main categories: impregnation and sol−gel-derived precursors.

7.2.2.1 Impregnation with organic compounds

Impregnating the void volume of wood with organic compounds is a method that has been developed since the 1960s. Many methods have been devised to improve properties of wood by treating with various etherifying and esterifying agents, acetals, alkylene oxides, alkoxysilane coupling agents, resins, etc (Rowell and Gutzmer, 1975; Rowell et al., 1976; Guevara and Mostemi, 1984; Schneider and Brebner, 1985; Chen, 1994). Thermosetting resin modification and acetylation with acetic anhydride are the most successful two organic compounds treatments.

Resin impregnation treatment is one of the oldest and most effective methods to modify wood, by which wood properties can be improved considerably. The common resins used are phenol formaldehyde resin (Keiko et al., 1999; Wu et al., 2003), urea formaldehyde resin (Deka and Saikia, 2003), melamine formaldehyde resin (Chen, 1994), polyethylene glycol (Makoto, 2002), and isocyanate (Gao et al., 2005; Williams and Hale, 1999; Engonga et al., 1999). The commercial materials known as "Impreg" and "Compreg" are known to have great mechanical strength and high dimensional stability.

Among all the chemical modification reactions studied, acetylation with acetic anhydride is the most promising technology. Acetylation transforms the free hydroxyls in the wood into acetyl groups, reducing the ability to absorb water, thereby making it more dimensionally stable and more durable. Acetylation has been approved to improve the durability, resistance to swelling and shrinkage, hardness, and UV resistance (Rowell, 2006a). Acetylation reaction has been extensively commercialized. Titan Wood is the first company to produce acetylated wood with acetic anhydride on a commercial scale, and now many companies are currently involved in the commercialization of wood acetylation.

7.2.2.2 Impregnation with inorganic compounds

Recent environmental concerns about the toxicity of modified products lead to the development of nontoxic wood products (Mahltig et al., 2008). Silicon is an abundant nontoxic element that can form a variety of inorganic and organic compounds (Mai and Militz, 2004a,b). According to the natural forming of petrified wood, which is a particular transformation of the original material into a form of organic−inorganic composite, the SiO_2 wood composites have been prepared. In the first instance, the SiO_2 wood composites have been prepared by double diffusion process, which is one of the earlier methods to enhance the wood properties, particularly for the fire and decay resistances of wood (Furuno et al., 1991, 1992, 1993; Yamaguchi, 1994a,b). Water glass (sodium silicate) is the popular treating agent reacting with metallic salts and forms the inorganic deposits. Furuno et al. (1991) treated Japanese cedar wood with water glass, and then aluminum sulfate ($Al_2(SO_4)_3$) and calcium chloride ($CaCl_2$) were introduced into the chemical compounds to precipitate the

silicate within the wood structure by replacing the sodium ions in water glass. Further improvement was manipulated by treating similar wood with water glass, plus various salts such as barium chloride ($BaCl_2$), boric acid (H_3BO_3), borax ($Na_2B_4O_7$), boron trioxide (B_2O_3), and potassium borate ($K_2B_4O_7$) (Furuno et al., 1992, 1993). All resulting treated wood displayed a high resistance of fungus and fire but with strong water absorbency because of the high hygroscopicity of both the water glass and the unreacted salts in the lumina of the cells. Leaching experiments revealed that considerable amounts of chemicals were washed out from the specimen (Furuno et al., 1992).

As nanoscale sol solutions have been widely produced, the size of sol becomes smaller and smaller. Nanosols (nanoparticulate inorganic sols) are transparent and stable and form nanosized dispersions of inorganic particles in either water or a mixture of organic liquids. The diameter of the inorganic particles is less than 50 nm, and the solid content of the dispersion is usually between 4% and 20% by weight (Mahltig et al., 2008). However, they did not find a broader use until the 1950s. Nano silica sols are produced by the controlled removal of alkali from water glass through ion exchange techniques. This causes the silicic sol to polymerize and to form particles of amorphous silicon dioxide. To obtain a sol of polysilicic acid molecules, this polycondensation process is stopped at a certain stage by the addition of alkali. Therefore unmodified silica sols are alkaline. Today, there are many commercially available and inexpensive neutral or acidic nanoaqueous silica sols with different types of surface modifications (Mahltig et al., 2008; Greenwood and Gevert, 2011), and they are used in an extensive range of industrial applications covering papermaking, ceramics, catalyst, abrasive, and solid state electrochemical devices. Furthermore, silica sols are used in a vast number of coating applications to improve mechanical properties as well as antiblocking, adhesion, and wetting properties (Greenwood, 2010). Due to their high surface-to-value ratio (in the range of 200 m^2/g and upwards) and extremely small particle size, nanosilica sols have been used to impregnate wood (Pries and Mai, 2013a,b) in order to enhance resistance to fire, fungi, and thermal and mechanical performances.

7.2.2.3 Sol–gel process

To reduce leaching of inorganic salts, the sol–gel process has been applied to prepare the inorganic wood composites, and it was once supposed to be a promising and environmentally friendly method of enhancing the properties of wood (Mai and Militz, 2004a,b). The application of the sol–gel process was most intensively studied by Saka and his research group. They prepared SiO_2 wood composites, from moisture-conditioned wood, by the sol–gel process with tetraethoxysilane (TEOS), 2-heptadecafluorooctylethyltrimethoxysilane (HFOETMOS), and methyltrimethoxysilane (MTMOS). They aimed at using the bound water in the cell wall to initiate the sol–gel process directly and to achieve deposition of the silicate therein (Saka et al., 1992; Ogiso and Saka, 1993, 1994; Saka and Yakake, 1993; Miyafuji and Saka, 1996; Saka and Ueno, 1997). The resulting composites exhibited an improved dimensional stability, fire resistance, and antileachability and retained the porous structure characteristic of wood. This research has been followed up by many other

researchers with other reagents as precursors, such as silicon alkoxides, silicon alkoxides derivatives, titanium alkoxides, and titanium alkoxides derivatives (Donath et al., 2004, 2006, 2007; Qin and Zhang, 2012; Mahr et al., 2012a,b, 2013; Unger et al., 2013; Lu et al., 2014). The modified wood shows improved properties such as enhanced dimensional stability, flame retardancy, and resistance to biological deterioration. These improvements are due to a stable incorporation of the inorganic component in the wood host as a result of internal cross-linking in the treated material. However, a practical application of the sol−gel for treatments of solid woods is hardly feasible, since they require a costly monomer of chemicals, moisture-conditioned wood, and a highly regulated technological process.

7.2.3 Densification treatments

Wood densification is also an environmental friendly modification method in which the porous structure of wood is compressed. Poor mechanical properties of low density wood can be improved to obtain a higher density material (Inoue et al., 1993; Dwianto et al., 1998, 1999, 2000; Navi and Girardet, 2000; Blomberg and Persson, 2004). Most of these improved properties are directly related to density and its profile, which is affected by the temperature, moisture gradients, and their relationship to the glass transition temperature (T_g) of the wood cell wall. Mechanical properties of the densified wood are strongly affected by the process parameters, such as temperature and press closing speed (Laine et al., 2013a,b; Kutnar et al., 2009). According to the degree of densification, densification treatment is divided into bulk densification and surface densification.

7.2.3.1 Bulk densification

Bulk densification, that is, a process in which wood is compressed throughout its entire thickness, is a well-known procedure (Navi and Girardet, 2000; Boonstra and Blomberg, 2007; Kutnar et al., 2009). The CaLignum process is a novel method for semi-isostatic densification of wood using a Quintus press, a kind of press that is widely used for forming sheet metal. Wood is compressed under a flexible oil-filled rubber diaphragm, whereby structures with low density are allowed to deform more than denser wood. Crushing and checking can then be lowered, and the structure may be less disturbed than that when wood is densified uniaxially between steel plates (Blomberg and Persson, 2004; Blomberg et al., 2005).

7.2.3.2 Surface densification

Rather than compressing solid wood throughout, the surface densification targets on the surface only (Inoue et al., 1990, 1993; Rautkari et al., 2011a,b, 2013). In surface densification, only the first few millimeters beneath the wood surface are compressed, just the first few cell layers. For many applications, it is desirable to improve the surface properties and maintain the low bulk density of wood. For example, flooring may only need the densification of the surface alone. Surface densification has some distinct advantages over bulk densification. The process can be short, only a few minutes, less

energy is needed for the modification, and most importantly, the densification process has a significantly lower loss of wood volume (Rautkari et al., 2011b).

Due to the low thermal conductivity, high temperature, moisture, and compression are required. With this method, property improvements, such as increased hardness, are obtained on the wood surface, while property on most of the overall thickness is retained (Rautkari et al., 2013; Laine et al., 2013b). The surface densification process generally has three steps. First, a relatively dry wood specimen is heated and compressed. After the loading plate contacts the stops (target thickness), the press remains closed and the heating continues, usually performed at temperatures exceeding the glass transition temperature (T_g) of the cell wall components, which is highly dependent on its moisture content (Olsson and Salmn , 1997), to prevent the wood cell walls from breaking. Furthermore, a cooling system is turned on, while the load is maintained, to stabilize the densified wood surface.

7.3 Properties of reinforced composites

It is not possible to describe all of the properties of wood-based reinforced composites within the scope of this chapter. Since most of the research in reinforced composites has focused on the mechanical properties, dimensional stability, microstructure, thermal properties, and wettability, this chapter discusses these selected property parameters.

7.3.1 Mechanical properties

7.3.1.1 Mechanical properties of heat-treated wood

For heat-treated wood, the mechanical properties were found to be dependent on the applied processing conditions and wood species and affected predominantly by the process temperature. The average strength loss of 5−18% has been found under mild conditions (Rapp and Sailer, 2000). The high tensions can occur in the wood exposed to high temperatures and rapid evaporation of water. Some softwood wood species were found difficult to treat and showed a comparative higher strength loss because of a number of defects (mainly cracks) if not treated carefully. The MOR of wood, which was heat-treated at 220°C, was about 70% of the value of untreated controls, but there was no reduction in the values for the MOE. The dynamic bending strength is most negatively affected and can be reduced to about 50% of its original values under nonoptimum process conditions (Rapp and Sailer, 2000; Militz and Tjeerdsma, 2000; Antonio, 2000; Gunduz et al., 2009).

7.3.1.2 Mechanical properties of chemically modified wood

Wood is a three-dimensional polymeric composite, and its constituents are responsible for most of the physical and mechanical properties. Mechanical properties are modified as a result of chemical modifications. For example, shear strength parallel to the grain of acetylated wood is significantly decreased, the modulus of elasticity is slightly decreased

but no change in impact strength, while the wet and dry compressive strength, hardness, and fiber stress are increased (Dreher et al., 1964). The modulus of rupture is generally increased in softwoods but decreased for hardwoods (Dreher et al., 1964; Minato et al., 2003). For silica-impregnated wood, the modulus of elasticity and bending strength of composite with 30% WPG can be increased by about 50% and 15%, respectively, and the hardness of composites increased with WPG increasing. It should also be noted that mechanical properties of wood are very dependent on the moisture content of the cell wall. Strength properties, such as fiber stress and maximum crushing strength, are affected by changing moisture content below FSP (Rowell, 2006b).

7.3.1.3 Mechanical properties of densified wood

It is well-known that the density of wood correlates with its mechanical properties; the higher the density, the higher the appropriate property value (Rautkari et al., 2013). In general, the increase of the densified wood in density is in the range of 25−500%, though preferably within the range of 100−200%. Therefore the increased density in the surface layer was expected to increase the hardness of the surface of the densified wood. Boonstra and Blomberg (2007) measured the Brinell hardness of the densified wood by a semi-isostatic densification process and found that the Brinell hardness of radiata pine was increased by 271% after densification. Fang et al. (2012) also reported that the Brinell hardness of densified veneers, using heat, steam, and pressure, was about two to three times that of the control for both aspen and hybrid poplar. However, the degree of densification did not significantly affect the Brinell hardness. This means that the Brinell hardness was approximately the same when the same process parameters for surface modification were used.

7.3.2 Dimensional stability

Wood as a natural composite is very sensitive for moisture. Instability under changing moisture is considered as a major disadvantage of wood compared to other materials. Wood dimensional stability can be improved considerably by altering the molecular structure of the cell wall components, that is, by converting hydrophilic OH-groups into larger, more hydrophobic groups. Dimensionally stable reinforced wood could be created by thermal and chemical treatments or making the cell wall itself in a permanently swollen state that will attract no or very little water.

7.3.2.1 Dimensional stability of heat-treated wood

The changed wood composition results in a lower hygroscopicity of heat-treated wood. The hygroscopicity of the heat-treated wood can vary considerably with processing time and temperature in the second step of the treatment (Tjeerdsma et al., 1998). It can clearly be seen that the swelling percentage of heat-treated wood at different relative humidity was reduced substantially compared with nontreated wood. The reduction in swelling was found independent of the relative humidity. The reduction in swelling (or shrinking) antiswelling efficacy (ASE) can reach up to

about 50%. In general the reduction of swelling in tangential direction was found to be higher compared to the reduction in radial direction. A decreased difference between the absolute swelling in radial and tangential directions may result in less tensions in the wood when exposed to changeable climate conditions.

7.3.2.2 Dimensional stability of chemically modified wood

The dimensional changes due to atmospheric moisture can be minimized either by reducing water absorption and swelling, bulking the fibers to reduce the water holding capacity, or by cross-linking the cellulose chains of the component fibers. These can be achieved by the appropriate chemical modification of wood (Deka and Saikia, 1999). Many methods have been devised to reduce the free swelling and shrinkage of wood by treating with various etherifying and esterifying agents, acetals, alkylene oxides, and alkoxysilane coupling agents (Rowell and Gutzmer, 1975; Rowell et al., 1976; Guevara and Mostemi, 1984; Schneider and Brebner, 1985). The use of thermosetting resin for the modification of wood properties is one of such methods by which wood dimensional stability can be improved considerably. For example, both the rate and extent of swelling are greatly reduced as a result of silica impregnating. At the end of 5 days of water soaking, control wood samples swelled 10%, whereas treated wood samples made from silica sol swelled less than 5%. Drying the wood samples at the end of the test showed that control samples exhibit a greater degree of irreversible swelling as compared to the samples made from silica sol.

7.3.2.3 Dimensional stability of densified wood

High density and an unfractured cellular structure result in high strength; however, the increased density increases the instability potential upon exposure to moisture or water. Therefore it is known that exclusively densified wood undergoes a relaxation process under humid or wet conditions, caused by the release of internal stresses. Certainly, the spring-back effect and hygroscopicity of the densified specimens were significantly ameliorated by implementation of steam posttreatment, which contributed to the swelling behavior, especially in the radial direction (the direction of compression). Steam posttreatment contributes to the fixation of compression set at lower temperatures and shorter treatment durations (Tabarsa and Chui, 2000; Welzbacher and Rapp, 2007). The mechanism, by which the steam treatment stabilizes the compressive set, is thought to be due to the softening of lignin and the degradation of amorphous polysaccharide content and such increasing cross-linkage and relaxation of stored stresses by partial hydrolysis of hemicelluloses and degradation of lignin at elevated temperatures (Norimoto et al., 1993; Navi and Heger, 2004).

7.3.3 Microstructure

7.3.3.1 Microstructure of heat-treated wood

There is limited information on the microscopic characterization of thermal-treated wood. Based on the microstructure, the effect of heat treatment can be seen in the

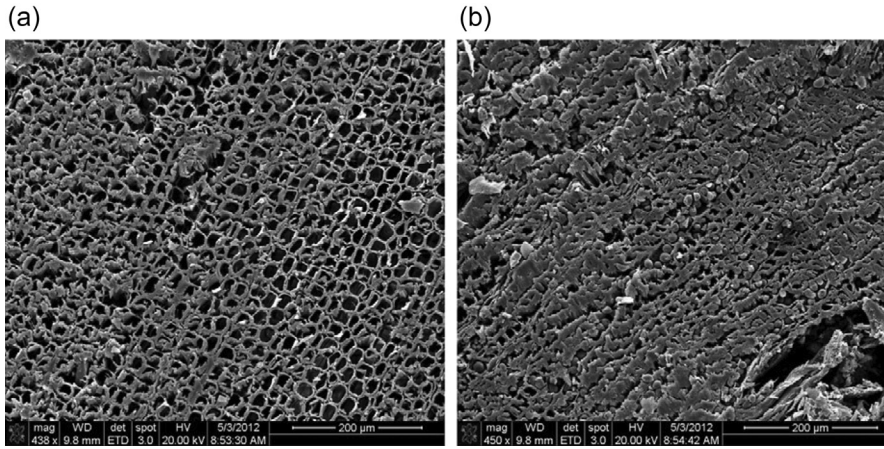

Figure 7.1 Microstructures of (a) red cedar control sample and (b) red cedar sample treated at 190°C for eight hours (Bakar et al., 2013).

form of existence of a compressed cell. Ozcan et al. (2012) indicated that nontreated wood samples did not have any deformation or compression (Fig. 7.1(a)); most of the cells in thermal-treated samples had some deformation, such as collapse (Fig. 7.1(b)). It is known that high temperature influences the structure of the cell wall, consisting of cellulose, hemicellulose, and lignin by thermoplasticization. Any heat treatments above 150°C result in modification of the cell wall and its chemical structure. Such plasticization can also be observed from the surface modification, the difference between control and thermal treatment samples. It appears that high temperature showed some extent of softening of the cell wall and losing its strength, causing closing of the lumens.

7.3.3.2 Microstructure of chemically modified wood

The properties and performance of chemically modified wood depends on adequate distribution of reacted chemicals in water-accessible regions of the cell wall. It is important, therefore, to determine the distribution of bonded chemicals, as this information may lead to a better understanding of how the chemical modification of wood changes the physicochemical properties of the wood. Taking the modification of wood by impregnating MUF resin as an example, the cell wall and vessel of natural wood exhibited a highly voided structure (Fig. 7.2(a)). After low resin concentration modification, a few scattered cells with resin filling their lumina were observed (Fig. 7.2(b)). Resin could be detected in the walls. It is evident from nanomechanical properties that the elastic modulus and hardness of cell walls modified by resin increased by more than 90%. Nanomechanical properties became much greater, evidently indicating an increase of resin concentration. Judging from these observations, the low molecular weight resin may penetrate easily into the cell walls, and almost all of it was located in the walls, and little or no presence of resin was shown

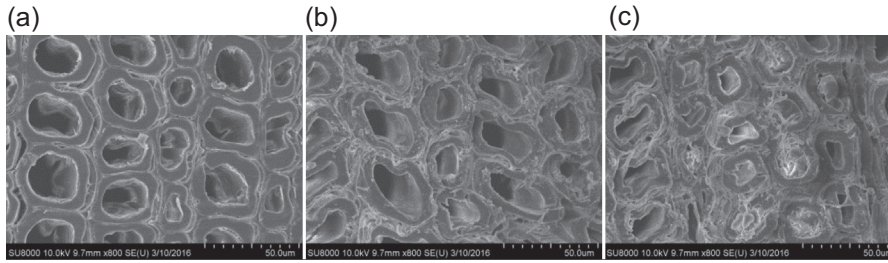

Figure 7.2 SEM pictures of MUF-treated wood: (a) untreated, (b) treated at low resin concentration, and (c) treated at higher resin concentration.

in the cell lumina. When increasing the concentration of resin, excess resins that cannot enter the walls remain in the lumina, coating and/or filling them. The cells containing resin in their lumina were distributed sporadically (Fig. 7.2(c)). Therefore the penetration of resin into the cell walls proved to be very much related to the dimensional stability and the decay resistance of wood. With more resin penetration, the cell walls will be bulked more and absorb less water, resulting in higher ASE values.

7.3.3.3 Microstructure of densified wood

Fig. 7.3 shows microstructures of cross sections exhibiting undeformed, slightly deformed, and highly deformed sections of the same densified sample performed at 200°C and 30 mm/min. During compression, the deformation started at the weakest parts of the sample, that is, earlywood with thinner cell walls, especially close to the abrupt earlywood−latewood border (Fig. 7.3(b and c)). The microscopic analysis of the cross section of the densified samples suggests that there were no major fractures in the tracheid cell walls. Change in the process parameters, ie, increased closing speed and decreased temperature, did not appear to cause any cell wall damage visible in the sampled cross sections. Even with a fast closing speed, the manner of cell wall deformation did not seem to change. It is also worth noting that the deformation started from where the sample was softened due to heat. At lower temperatures, the sample deformed more through the whole thickness, whereas, with the temperature increasing,

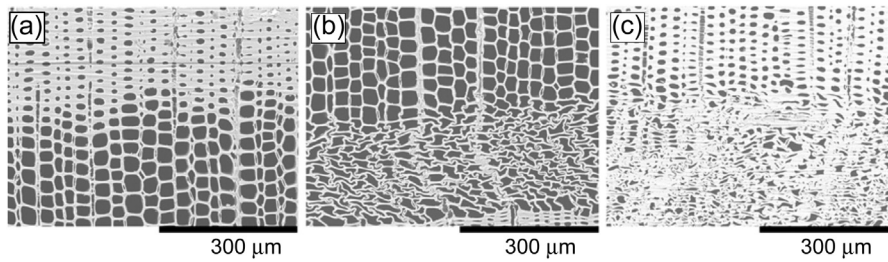

Figure 7.3 Micrographs of differently deformed earlywood performed at 200°C and 30 mm/min: (a) undeformed, (b) slightly deformed, and (c) highly deformed (Laine et al., 2014).

the deformation was concentrated more on the heated surface. This is because at lower temperatures, the heat is not transferred effectively inside the sample, and the wood constituents might not even be in a softened state (Rautkari et al., 2011b).

7.3.4 Thermal properties

7.3.4.1 Thermal properties of heat-treated wood

In general, thermal properties of the heat-treated wood are similar, without significant differences with the control wood. Four regions were characterized, and four peaks of thermogram were observed (Cademartori et al., 2013). The first region (between 0°C and 125°C) showed the moisture loss of the samples. The second region (225−320°C) referred to the hemicellulose degradation. The maximum value of control wood was around 290°C, higher than treatments. Therefore it is possible to affirm that thermal treatments at high temperatures presented a more intensive degradation of hemicellulose. The cellulose degradation started in the same band as hemicellulose degradation. The band of highest intensity and total degradation of cellulose was between 310°C and 400°C, with the maximum peak at approximately 350°C for control and heat-treated woods. After 400°C, a similar peak with low intensity referred to the lignin was observed. However, the lignin degradation is more intensive and occurs fully after 400°C. Therefore the thermal treatments did not modify the lignin content significantly.

7.3.4.2 Thermal properties of chemically modified wood

Wood is usually modified with fire retardants, mostly inorganic salts, to improve its thermal properties. Fire retardants can increase charring of wood at lower temperatures and thus form an insulating layer of nonflammable charcoal. In addition, they often have the side effect of diluting the flammable gases with noncombustible gases and increasing the amount of resulting charcoal. The latter results a diminished formation of combustible gases.

Silicon materials have long been used as fire retardants. Water glass coating protects wood against fire by melting and forming an insulating foam layer on the surface of wood. Unfortunately, the water glass coating is not stable long-term due to neutralization in contact with air. Other silicon compounds have also been used to improve the fire resistance of wood (Saka et al., 1992; Miyafuji and Saka, 1996). Silica sols are another group of inorganic silicon compounds. They are produced by the controlled removal of alkali from water glass through ion exchange techniques. Silica sols have previously been used to impregnate wood (Götze et al., 2008) in order to enhance the resistance to fungi and water-related properties. The influence on fire resistance has not been examined.

Fig. 7.4 shows the results of thermogravimetric analysis of wood chemically modified by silica sol. It is evident that the TG curves of composites and untreated wood had two main steps of decomposition, so-called flaming and glowing. Compared with untreated wood samples, the TG curves of composites are shifted to the upper

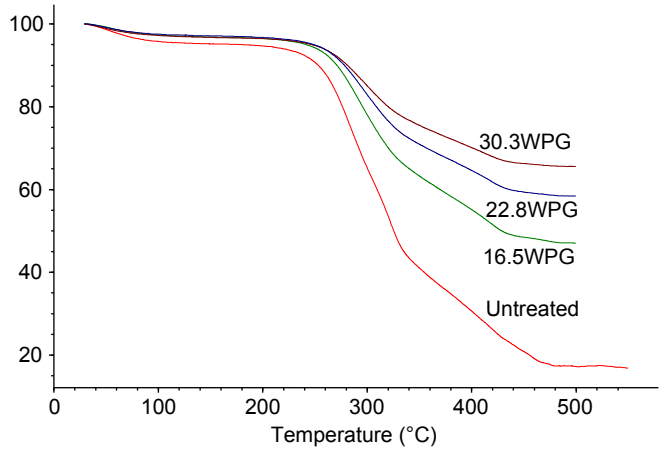

Figure 7.4 TG curves of untreated wood and composites with different WPG.

temperature. The obvious weight loss of composites occurred at temperature between 240°C and 320°C. The weight loss was mainly ascribed to the release of combustible gases of the wood. The weight loss slowed down when the temperature was higher than 320°C. When the temperature was 435°C, the total weight loss of composites was 50%, 40%, and 34% for 16.5% WPG, 22.8% WPG, and 30.3% WPG, respectively. This indicated that SiO_2 impregnated into the wood can endure a higher temperature and can improve the thermal property.

7.3.5 Wettability of reinforced composites

7.3.5.1 Wettability of heat-treated wood

It seems that overall wettability of heat-treated samples had some enhancement as compared to that of control samples. This might be due to the rough surface, which provides higher surface area compared to the smooth wood surface of untreated wood. Additionally, the contact angle had a reverse relationship with the average surface roughness. The surface of wood becomes smoother with increasing temperature of heat treatment, having better wettability due to larger contact angle value.

The coating performance of heat-treated wood is almost not changed, making a surface treatment with oils or paints necessary. Due to its UV degradability, water borne acrylic or solvent borne alkyds are recommended. Meanwhile, due to higher dimensional stability, less flaking, and cracking, the heat-treated wood performs considerably better than nontreated wood after outside exposure (Tjeerdsma et al., 1998).

The ability to glue different heat-treated wood was evaluated following different standards on its bonding strength and moisture performance (Tjeerdsma et al., 1998). The studies showed that, in principle, the heat-treated wood can be glued with many industrial glues (PVAc, PU, EPI, and RF). Due to the lowered shear

strength, a higher wood failure is reported with heat-treated timber. Furthermore, the hydrophobic wood surface causes a slower penetration of the solvents from the glue to the surrounding wood, which makes it necessary to adapt the glue process.

7.3.5.2 Wettability of chemical modified wood

The wettability of a modified wood surface, which is a prerequisite for the adhesion between substrate and adhesive/coating, depends on a number of factors, such as wood species, roughness and age of the surface, anatomical growth direction, penetration behavior, porosity, moisture content, hygroscopicity, and chemical composition, as well as the pH of the wood surface. A strongly modified wood surface may affect wettability and adhesion in coating and gluing processes. The wetting properties, surface energetics, surface composition, and acid−base properties can provide important information relevant to the understanding of the wettability of wood by various liquids, such as coatings and glues. Furthermore, information about the surface properties can be used to assess changes in the chemical composition of the surface following various treatments. Acetylated wood is more hydrophobic than natural wood, so studies have been carried out to determine which adhesives might work best to make composites (Youngquist et al., 1988; Youngquist and Rowell, 1990; Englund et al., 2009; Rowell, 2006b). Shear strength and wood failure were measured using acetylated wood with different WPG and adhesives. In all cases, adhesive strength was reduced by the level of acetylation because of the limited availability of hydroxyl groups in the acetylated wood.

7.3.5.3 Wettability of densified wood

High temperature, moisture, and compression are used to make stable densified wood, which has become a common wood product with the decreased subsequent springback in the presence of moisture (Navi and Girardet, 2000; Gong et al., 2010). Hygrothermal treatment significantly reduced the surface energy. Densified wood exhibits a very slight decrease in surface energy when compared to hygrothermally treated wood. However, the average contact angle found for the densified wood was not statistically different from the angle found for hygrothermally treated wood. This leads to the conclusion that the major cause of surface energy reduction of densified wood is due to the hygrothermal conditioning during the densification process. Densified yellow poplar wood could be a viable raw material for making a reinforced composite, and depending on adhesive type, might be considered a superior material in some cases. It was found that total surface energy of densified yellow poplar (37.7 mJ/m^2) was reduced considerably, from 53.8 mJ/m^2. Therefore no clear relationship was found between surface energy and bond performance for the densified wood. Surface energy results suggest that the bond performance would decrease for the densified samples, but performance was actually found to be the same as or better than the performance for control yellow poplar. It appears, therefore, that the densification treatment did not substantially reduce wetting and bonding performances (Jennings et al., 2005, 2006).

7.4 Mechanism of property changes due to treatments of reinforced composites

7.4.1 Mechanism of thermal treatments

The thermal decomposition of the chemical components occurs via a series of chemical reactions coupled with heat and mass transfer. The high temperature initiates a certain chemical conversion in the wood, called thermos-transformation. This thermo-transformation results in the conversion of hydrophilic groups (−OH) to ether cross-links (C−O−C) between wood fibers, the decrease in volatile and hemicellulose contents of wood, as well as the reduction of the degree of polymerization of wood fibers. The transformation of −OH to C−O−C has a positive impact in terms of the reduction of water penetration into the wood structure and thus prevents swelling and shrinking (Poncsák et al., 2007).

Compared with the influence of cross-linking reactions known to occur during thermal treatment of wood, Tjeerdsma et al. (1998) investigated relatively mild thermal-treated wood to understand the mechanism for the improvements at the molecular level. All the occurrences described appear to be the consequence of reactions, which are well-known in wood chemistry. Cleavage of acetyl groups (CH_3−C═O−) of the hemicellulose has been found to occur in the first treatment step under moist conditions and elevated temperature. This results in the formation of carbonic acids, mainly acetic acid. Most of the CH_3−C═O− were found to be cleaved during the treatment at a high temperature, whereas only partial deacetylation was found to occur at moderate treatment temperature. Esterification reactions were found to occur at an elevated temperature in the curing step. The formed esters mainly linked to the lignin complex, considering that the newly formed carbonyl groups (C═O) were found. Esterification contributes to a decrease of hygroscopicity of wood and consequently improvements of its dimensional stability and durability (Tjeerdsma and Militz, 2005).

In general, when thermal treatment is applied, the cell wall components of thermal-treated wood are modified. By applying thermal treatment, some polymers of wood are broken down, the bending strength of the treated wood showed the reduction from 5% to 40%, and some new water insoluble polymers are formed under high temperature and low oxygen atmosphere. Consequently, several favorable changes in its physical properties, including the reduced shrinkage and swelling, improved biological durability, low equilibrium moisture content, enhanced weather resistance, a decorative dark colour, improved thermal insulation properties, and better decay resistance (Shi et al., 2007a,b; Kocaefe et al., 2007; Sivonen et al., 2002; Alen et al., 2002; Kamdem et al., 2002).The degree of modification changes is very dependent on the wood species, the maximum temperature, and the holding time at that temperature.

7.4.2 Mechanism of chemical modification

There are two major mechanisms to chemically modifying the wood cell wall polymers: hydroxyl reactivity and chemical bond. The most abundant single site for reactivity in cell wall components is the hydroxyl group. Most reaction schemes have been

based on the reaction of hydroxyl groups. If hydroxyl reactivity is selected as the preferred modification site, the chemical must contain functional groups, which can react with the hydroxyl groups of the wood components. The chemical bond formed between the reagent and the wood components is of another major reaction. A chemical bond will occur when the reagent contains more than one reactive group or results in a group that can further react with a hydroxyl group.

As stated before, because the properties of wood are mainly determined from the chemistry of the cell wall components, the basic properties of wood can be changed by modifying the basic chemistry of the cell wall polymers. In summary the broad range of possible wood chemical modification treatments can be divided into three categories related to the mode of action of the chemicals:

1. Lumen filling with a substance, usually resin impregnation. These treatments might increase strength and slow down the process of water or vapor uptake, but they do not change the sorption behavior of the wood over a longer period of time.
2. Bulking to fill the cavities in the cell wall as well as the cell lumen. This is a more general approach. The cell wall can be bulked with nonbonded or bonded chemicals. For the nonbonded chemicals, such as polyethylene glycol, the obtained products could only be used for dry applications; otherwise the chemical will leach. For the bonded chemicals, such as acetic anhydride, which can occupy space in the cell wall and further react with cell wall hydroxyl groups to form stable bonds, the obtained products can be used in highly humid conditions. Bulking treatments tend to reduce the swelling and shrinkage of the wood. They might even have a beneficial effect on the long-term sorption behavior.
3. Modifying treatments are usually the most effective. The chemical structures of cell wall components are altered and covalent bonds are formed. When wood is reacted with chemicals, such as formaldehyde, cross-linking takes place between two hydroxyl groups in the cell wall polymers. Because of the short cross-linking distance, the two polymers are locked in a rigid structure. The locking of the polymers does not allow the cell wall to expand when it gets wet. Many properties can be improved permanently, in particular, durability, dimensional stability, and reduced equilibrium moisture content.

7.4.3 Mechanism of densification treatments

Wood densification is a process combining heat, moisture, and mechanical action to improve the density of wood without changing the characteristics of wood. Densification of wood is due to the porous structure of wood and the ability of wood components to soften in the presence of heat and moisture (Navi and Girardet, 2000; Blomberg and Persson, 2004). Process parameters, such as the temperature and conditions of the steam during densification, all affect the properties of the resulting densified material (Kutnar and Kamke, 2012; Kutnar et al., 2012).

In the process of densification, the alteration of the lignocellulosic structure by combined action with heat and moisture was evident: the carboxyl groups in hemicellulose were destroyed; a portion of the hemicellulose was hydrolyzed or removed; ester linkages of carboxylic groups from lignin and/or hemicellulose were formed; and higher relative peak intensities of higher quantity of lignin were present. Due to the temperature and moisture gradients formed during the densification process and their relationship to the glass transition of the wood cell wall at the time that the compression stress

is applied, a through thickness density profile is created in the densified wood, which varies with the degree of densification (Kutnar et al., 2009; Rautkari et al., 2010, 2011b). While deformations in the densification process are largely the result of the viscous buckling of cell walls without major fracture taking place, the strength and stiffness of the wood material are increased approximately in proportion to the increase in density (Kutnar et al., 2008; Fang et al., 2012).

7.5 Application and future trends

7.5.1 Application prospects

The commercialization of wood-based reinforced composites has become realistic, and the production of wood-based reinforced composites is widely used for non- or semi-structural products. The main characteristics of the thermal-treated wood are its improved durability and dimensional stability. Presently, main commercial products include claddings, windows, doors (Fig. 7.5), garden products, flooring, and other specialty products. The main characteristics of chemical modification lie in the property enhancement of end-products. Permanently bonded chemicals provide fire retardancy, ultraviolet stabilization, colour changes, dimensional stability, and resistance to biological attack to wood products. Main commercial products include flooring (Fig. 7.6), wooden roads, alcoves, frames (Fig. 7.7), and guardrails.

7.5.2 Future trends

7.5.2.1 New reaction system

The screening of potential chemicals and optimizing properties are the major worldwide research work in this relatively new area. As the modification agents in modifying wood for property improvement, one must consider several basic principles when selecting a reagent and a reaction system. In summary the chemicals must be

Figure 7.5 Door by thermal-treated wood.

Figure 7.6 Floors by impregnating silica sol wood.

Figure 7.7 Park landscape by hydrophobic wood.

capable of reacting with wood hydroxyls under neutral, mildly alkaline, or acidic conditions at temperatures below 170°C. The chemical system should be simple and capable to facilitate penetration. The chemicals should react quickly with wood components yielding stable chemical bonds, and the treated wood must still possess the desirable properties of untreated wood.

7.5.2.2 Combination of various techniques

Although many studies have evaluated the single technique for wood-based reinforced composites, few studies have investigated the combined effects of the thermal,

Figure 7.8 Combination of thermal and chemical treatments.

chemical, and mechanical treatment of wood. A combination of thermal, chemical, and mechanical treatments could lead to numerous complex chemical, thermal, thermochemical, and thermomechanical changes in wood. Take the case of the combination of thermal and chemical treatments (Fig. 7.8): due to its reduced mechanical properties, producing highly durable (high temperature needed) and at the same time strong (lower temperatures are needed) thermal-treated wood is the biggest technological challenge. However, thermal treatment of chemical impregnated wood can improve the properties of natural wood, such as the density, the bending strength, and the compressive strength; at the same time, the hygroscopicity was reduced significantly.

7.5.2.3 Functionalization

Functionalization has become an important developmental direction for wood materials, which is driven by an increase in market demand as well as competition from other materials. Fire-retardant and preservative-treated wood are the most traditional wood functional materials, which have been widely used. Many novel wood materials with special functionalities have been developed by chemical or physical modifications. These materials would greatly broaden the areas of application for wood and increase the value of wood products.

7.5.2.4 Industrialization of new technology

Many efforts have been undertaken by industry and research institutes to scale up some of the promising processes from the laboratory to practical, marketable processes. There are many challenges to overcome when developing new technology and introducing new materials to the market. The experiences in Europe have shown that joint efforts in basic and applied research and in process development will help overcome

these challenges and hopefully lead to a successful future for wood modification for the advanced reinforced composites.

Acknowledgements

This work was financially supported by the National Natural Science Foundation of China (No. 31370012 and No. 31000272) and the Fundamental Research Funds of the Institute of Forestry New Technology, Chinese Academy of Forestry (No. CAFINT2013C07).

References

Alen, R., Kotilainen, R., Zaman, A., 2002. Thermochemical behaviour of Norway spruce (*Picea abies*) at 180−225°C. Wood Science and Technology 36, 163−171.

Antonio, J.S., 2000. Mechanical behavior of eucalyptus wood modified by heat. Wood Science and Technology 34, 39−43.

Bakar, B.A., Hiziroglu, S., Tahir, P.M., 2013. Properties of some thermally modified wood species. Materials and Design 43, 348−355.

Blomberg, J., Persson, B., 2004. Plastic deformation in small clear pieces of Scots pine (*Pinus sylvestris*) during densification with the CaLignum process. Journal of Wood Science 50, 307−314.

Blomberg, J., Persson, B., Blomberg, A., 2005. Effects of semi-isostatic densification of wood on the variation in strength properties with density. Wood Science and Technology 39, 339−350.

Boonstra, M.J., Blomberg, J., 2007. Semi-isostatic densification of heat-treated radiata pine. Wood Science and Technology 41, 607−617.

Bourgeois, J., Guyonnet, R., 1988. Characterisation and analysis of torrefied wood. Wood Science and Technology 22, 143−155.

Cademartori, P., Santos, P., Serrano, L., Labidi, J., Gatto, D., 2013. Effect of thermal treatment on physicochemical properties of gympie messmate wood. Industrial Grops and Products 45, 360−366.

Chen, G.C., 1994. Fungal decay resistance of wood reacted with chlorosulfonyl isocyanate or epichlorohydrin. Holzforschung 48, 181−185.

Deka, M., Saikia, C.N., 1999. Effect of amino resin treatment on dimensional stability and strength property of wood. Indian Journal of Chemical Technology 6 (2), 75−78.

Deka, M., Saikia, C.N., 2003. Chemical modification of wood with thermosetting resin: effect on dimensional stability and strength property. Bioresource Technology 73, 179−181.

Donath, S., Militz, H., Mai, C., 2004. Wood modification with alkoxysilanes. Wood Science and Technology 38 (12), 555−566.

Donath, S., Militz, H., Mai, C., 2006. Treatment of wood with aminofunctional silanes for protection against wood destroying fungi. Holzforschung 60 (2), 210−216.

Donath, S., Militz, H., Mai, C., 2007. Weathering of silane treated wood. Holz als Roh-und Werkstoff 65 (1), 35−42.

Dreher, W.A., Goldstein, I.S., Cramer, G.R., 1964. Mechanical properties of acetylated wood. Forest Products Journal 14 (2), 66−68.

Dwianto, T., Norimoto, M., Morooka, T., Tanaka, F., Inoue, M., Liu, Y., 1998. Radial compression of sugi wood (*Cryptomeria japonica* D. Don). Holz als Roh-und Werkstoff 56, 403−411.

Dwianto, T., Morooka, T., Norimoto, M., Kitajima, T., 1999. Stress relaxation of sugi (*Cryptomeria japonica* D. Don) wood in radial compression under high temperature steam. Holzforschung 53 (5), 541−546.

Dwianto, T., Morooka, T., Norimoto, M., 2000. Compressive creep of wood under high temperature steam. Holzforschung 54, 104−108.

Englund, F., Elof Bryne, L., Ernstsson, M., Lausmaa, J., Walinder, M., 2009. Spectroscopic studies of surface chemical composition and wettability of modified wood. Wood Material Science & Engineering 4, 80−85.

Engonga, P.E., Schneider, R., Gerardin, P., Loubinoux, B., 1999. Chemical modification of wood with perfluoralkyl ethanol and 4,4′-diphenylmethane diisocyanate. Holzforschung 53, 272−276.

Fang, C.H., Mariotti, N., Cloutier, A., Koubaa, A., Blanchet, P., 2012. Densification of wood veneers by compression combined with heat and steam. European Journal of Wood and Wood Products 70, 155−163.

Furuno, T., Uehara, T., Jodai, S., 1991. Combination of wood and silicate (I). Impregnation by water glass and application of aluminum sulfate and calcium chloride as reactants. Mokuzai Gakkaishi 37 (5), 462−472.

Furuno, T., Shimada, K., Uehara, T., Jodai, S., 1992. Combinations of wood and silicate (II). Wood-mineral composites using water glass and reactance of barium chloride, boric acid, and borax and their properties. Mokuzai Gakkaishi 38 (5), 448−457.

Furuno, T., Uehara, T., Jodai, S., 1993. Combination of wood and silicate (III). Some properties of wood-mineral composites using the water glass-boron compound system. Mokuzai Gakkaishi 39 (5), 561−570.

Gao, Z.H., Gu, J.Y., Wang, X.M., Li, Z.G., Bai, X.D., 2005. FTIR and XPS study of the reaction of phenyl isocyanate and cellulose with different moisture contents. Pigment & Resin Technology 34, 282−289.

Gong, M., Lamason, C., Li, L., 2010. Interactive effect of surface densification and post-heat-treatment on aspen wood. Journal of Materials Processing Technology 210, 293−296.

Götze, J., Möckel, R., Langhof, N., Hengst, M., Klinger, M., 2008. Silicification of wood in the laboratory. Ceramics-Silikáty 52 (4), 268−277.

Greenwood, P., Gevert, B., 2011. Aqueous silane modified silica sols: theory and preparation. Pigment and Resin Technology 40 (5), 275−284.

Greenwood, P., 2010. Surface Modifications and Applications of Aqueous Silica Sols (dissertation). Department of Chemical and Biological Engineering, Chalmers University of Technology, Gothenburg, Sweden.

Guevara, R., Mostemi, A.A., 1984. The effect of alkylene oxides, furan resin and vinyl-pyrrolidinone on wood dimensional stability. Wood Science and Technology 18, 225−240.

Gunduz, G., Aydemir, D., Karakas, G., 2009. The effects of thermal treatment on the mechanical properties of wild pear (*Pyrus elaeagnifolia* Pall.) wood and changes in physical properties. Materials & Design 30, 4391−4395.

Homan, W.J., Jorissen, A., 2004. Wood modification developments. Heron 49 (4), 361−386.

Inoue, M., Norimoto, M., Otsuka, Y., Yamada, T., 1990. Surface compression of coniferous wood lumber. 1. A new technique to compress the surface-layer. Mokuzai Gakkaishi 36 (11), 969−975.

Inoue, M., Norimoto, M., Tanahashi, M., Rowell, R.M., 1993. Steam or heat fixation of compressed wood. Wood and Fiber Science 25 (3), 224−235.

Jennings, J.D., Zink-sharp, A., Kamke, F.A., Frazier, C.E., 2005. Properties of compression densified wood. Part I: bond performance. Journal of Adhesion Science and Technology 19 (13−14), 1249−1261.

Jennings, J.D., Zink-sharp, A., Frazier, C.E., Kamke, F.A., 2006. Properties of compression densified wood. Part I: surface energy. Journal of Adhesion Science and Technology 20 (4), 335−344.

Kamdem, D., Pizzi, A., Jermannaud, A., 2002. Durability of heat-treated wood. Holz als Roh- und Werkstoff 60 (1), 1−6.

Keiko, S., Masahiro, M., Kazuya, M., 1999. Effects of impregnation of simple phenolic and natural polycyclic compounds on physical properties of wood. Journal of Wood Science 45, 227−232.

Kocaefe, D., Chaudry, B., Ponscak, S., Bouazara, M., Pichette, A., 2007. Thermogravimetric study of high temperature treatment of Aspen: effect of treatment parameters on weight loss and mechanical properties. Journal of Material Sciences 42 (3), 854−866.

Kollmann, F., Topf, P., 1971. Exothermic reactions of wood at elevated temperatures. The Journal of Fire & Flammability 2, 231−239.

Kutnar, A., Kamke, F.A., 2012. Compression of wood under saturated steam, superheated steam, and transient conditions at 150°C, 160°C, and 170°C. Wood Science and Technology 46, 73−88.

Kutnar, A., Kamke, F.A., Sernek, M., 2008. The mechanical properties of densified VTC wood relevant for structural composites. Holz als Roh-und Werkstoff 66, 439−446.

Kutnar, A., Kamke, F.A., Sernek, M., 2009. Density profile and morphology of viscoelastic thermal compressed wood. Wood Science and Technology 43, 57−68.

Kutnar, A., Laine, K., Rautkari, L., Hughes, M., 2012. Thermodynamic characteristics of surface densified solid Scots pine wood. European Journal of Wood and Wood Products 70, 727−734.

Laine, K., Rautkari, R., Hughes, M., 2013a. The effect of process parameters on the hardness of surface densified Scots pine solid wood. European Journal of Wood and Wood Products 71, 13−16.

Laine, K., Rautkari, L., Hughes, M., Kutnar, A., 2013b. Reducing the set-recovery of surface densified solid Scots pine wood by hydrothermal post-treatment. European Journal of Wood and Wood Products 71 (1), 17−23.

Laine, K., Segerholm, K., Walinder, M., Rautkari, L., Ormondroyd, G., Hughes, M., Jones, D., 2014. Micromorphological studies of surface densified wood. Journal of Materials Science 49, 2027−2034.

Lipska, A.E., Parker, W.J., 1965. Kinetics of the pyrolysis of cellulose in the temperature range 250−300°C. Journal of Applied Polymer Science 10, 139−153.

Lu, Y., Feng, M., Zhan, H., 2014. Preparation of SiO_2-wood composites by an ultrasonic-assisted sol-gel technique. Cellulose 21, 4393−4403.

Mahltig, B., Swaboda, C., Roessler, A., Böttcher, H., 2008. Functional wood by nanosol application. Journal of Materials Chemistry 18, 3180−3192.

Mahr, M.S., Hübert, T., Sabel, M., Schartel, B., Bahr, H., Militz, H., 2012a. Fire retardancy of sol-gel derived titania wood-inorganic composites. Journal of Materials Science 47 (19), 6849−6861.

Mahr, M.S., Hübert, T., Schartel, B., Bahr, H., Sabel, M., Militz, H., 2012b. Fire retardancy effects in single and double layered sol-gel derived TiO2 and SiO2-wood composites. Journal of Sol-Gel Science and Technology 64 (2), 452−464.

Mahr, M.S., Hübert, T., Stephan, I., Militz, H., 2013. Decay protection of wood against brown-rot fungi by titanium alkoxide impregnations. International Biodeterioration & Biodegradation 77, 56−62.

Mai, C., Militz, H., 2004a. Modification of wood with silicon compounds. Inorganic silicon compounds and sol-gel systems: a review. Wood Science and Technology 37 (5), 339−348.

Mai, C., Militz, H., 2004b. Modification of wood with silicon compounds. Treatment systems based on organic silicon compounds: a review. Wood Science and Technology 37 (6), 453–461.

Makoto, O., 2002. FTIR-PAS study of light-induced changes in the surface of acetylated or polyethylene glycol-impregnated wood. Journal of Wood Science 48, 394–401.

Militz, H., Tjeerdsma, B., 2000. Heat treatment of wood by the plato-process (Helsinki, Finland). In: Proceedings of Seminar "Production and Development of Heat Treated Wood in Europe".

Militz, H., 2002. Heat treatment technologies in Europe: scientific background and technological state-of-art. In: Proceedings of Conference on "Enhancing the Durability of Lumber and Engineered Wood Products" Kissimmee, Orlando. FPS, Madison, US.

Minato, K., Takazawa, R., Ogura, K., 2003. Dependence of reaction kinetics and physical and mechanical properties on the reaction systems of acetylation. II: physical and mechanical properties. Journal of Wood Science 49, 519–524.

Miyafuji, H., Saka, S., 1996. Wood-inorganic composites prepared by sol-gel process (V). Fire-resisting properties of the SiO_2-P_2O_5-B_2O_3 wood-inorganic composites. Mokuzai Gakkaishi 42 (1), 74–80.

Navi, P., Girardet, F., 2000. Effects of thermo-hydro-mechanical treatment on the structure and properties of wood. Holzforschung 54 (3), 287–293.

Navi, P., Heger, F., 2004. Combined densification and thermo-hydro-mechanical processing of wood. MRS Bulletin 29 (5), 332–336.

Norimoto, M., Grill, J., Rowell, R.M., 1992. Rheological properties of chemically modified wood: relationship between dimensional and creep stability. Wood and Fiber Science 24 (1), 25–35.

Norimoto, M., Ohta, C., Akitsu, H., Yamada, T., 1993. Permanent fixation of bending deformation in wood by heat treatment. Wood Research 79, 23–33.

Ogiso, K., Saka, S., 1993. Wood-inorganic composites prepared by sol-gels process (V). Effect of ultrasonic treatments on preparation of wood-inorganic composites. Mokuzai Gakkaishi 39 (3), 301–307.

Ogiso, K., Saka, S., 1994. Wood-inorganic composites prepared by sol-gel process (IV). Effects of chemical bonds between wood and inorganic substances on property enhancement. Mokuzai Gakkaishi 40 (10), 1100–1106.

Olsson, A.M., Salmén, L., 1997. The effect of lignin composition on the viscoelastic properties of wood. Nordic Pulp & Paper Research Journal 12, 140–143.

Ozcan, S., Ozcifci, A., Hiziroglu, S., Toker, H., 2012. Effects of heat treatment and surface roughness on bonding strength. Construction and Building Materials 33, 7–13.

Poncsák, S., Shi, S., Kocaefe, D., Miller, G., 2007. Effect of thermal treatment of wood lumbers on their adhesive bond strength and durability. Journal of Adhesion Science and Technology 21 (8), 745–754.

Pries, M., Mai, C., 2013a. Treatment of wood with silica sols against attack by wood-decaying fungi and blue stain. Holzforschung 67 (6), 697–705.

Pries, M., Mai, C., 2013b. Fire resistance of wood treated with a cationic silica sol. European Journal of Wood and Wood Products 71, 237–244.

Qin, C., Zhang, W.B., 2012. Antibacterial property of titanium alkoxide/poplar wood composite prepared by sol-gel process. Materials Letters 89, 101–103.

Rapp, A.O., Sailer, M., 2000. Heat treatment in Germany (Helsinki, Finland). In: Proceedings of Seminar "Production and Development of Heat Treated Wood in Europe".

Rautkari, L., Properzi, M., Pichelin, F., Hughes, M., 2010. Properties and set-recovery of surface densified Norway spruce and European beech. Wood Science and Technology 44, 679–691.

Rautkari, L., Kamke, F.A., Hughes, M., 2011a. Density profile relation to hardness of viscoelastic thermal compressed (VTC) wood composite. Wood Science and Technology 45, 693−705.

Rautkari, L., Laine, K., Laflin, N., Hughes, M., 2011b. Surface modification of Scots pine: the effect of process parameters on the through thickness density profile. Journal of Materials Science 46, 4780−4786.

Rautkari, L., Laine, K., Kutnar, A., Medved, S., Hughes, M., 2013. Hardness and density profile of surface densified and thermally modified scots pine in relation to degree of densification. Journal of Materials Science 48, 2370−2375.

Rowell, R.M., Gutzmer, D.I., 1975. Chemical modification of wood: reaction of alkylene oxide with southern yellow pine. Journal of Wood Science 7 (3), 240−246.

Rowell, R.M., Gutzmer, D.I., Sacks, I.B., Kenney, R.E., 1976. Effect of alkylene oxide treatment on dimensional stability of wood. Journal of Wood Science 9 (1), 51−54.

Rowell, R.M., 2006a. Acetylation of wood. Forest Products Journal 56 (9), 4−12.

Rowell, R.M., 2006b. Chemical modification of wood: a short review. Wood Material Science and Engineering 1 (1), 29−33.

Sailer, M., Rapp, A.O., Leithoff, H., 2000. Improved Resistance of Scots Pine and Spruce by Application of an Oil-heat Treatment. The International Research Group on Wood Preservation IRG/WP.

Saka, S., Ueno, T., 1997. Several SiO2 wood-inorganic composites and their fire-resisting properties. Wood Science and Technology 31 (6), 457−466.

Saka, S., Yakake, Y., 1993. Wood-inorganic composites prepared by sol-gel process (III). Chemically-modified wood-inorganic composites. Mokuzai Gakkaishi 39 (3), 308−314.

Saka, S., Sasaki, M., Tanahashi, M., 1992. Wood-inorganic composites prepared by the sol-gel process (I). Wood-inorganic composites with porous structure. Mokuzai Gakkaishi 38 (11), 1043−1049.

Scheffer, T.C., Eslyn, W.E., 1961. Effect of heat on the decay resistance of wood. Forest Products Journal 46, 485−490.

Schneider, M.H., Brebner, K.I., 1985. Wood polymer combination: the chemical modification of wood by alkoxysilane coupling agents. Wood Science and Technology 19, 67−73.

Shi, J.L., Kocaefe, D., Zhang, J., 2007a. Mechanical behaviour of Quebec wood species heat-treated using ThermoWood process. Holz als Roh-und Werkstoff 65 (4), 255−259.

Shi, J.L., Kocaefe, D., Amburgey, T., Zhang, J., 2007b. A comparative study on brown-rot fungus decay and subterranean termite resistance of thermally-modified and ACQ-C-treated wood. Holz als Roh-und Werkstoff 65 (5), 353−358.

Sivonen, H., Maunu, S.L., Sundhohn, F., Jamsa, S., Viitaniemi, P., 2002. Magnetic resonance studies of thermally modified wood. Holzforschung 56, 648−654.

Tabarsa, T., Chui, Y., 2000. Stress-strain response of wood under radial compression. Part I. Test method and influences of cellular properties. Wood and Fiber Science 32 (2), 144−152.

Tjeerdsma, B.F., Militz, H., 2005. Chemical changes in hydrothermal treated wood: FTIR analysis of combined hydrothermal and dry heat-treated wood. Holz als Roh-und Werkstoff 63, 102−111.

Tjeerdsma, B.F., Boonstra, M., Pizzi, A., Tekely, P., Militz, H., 1998. Characterisation of thermal modified wood: molecular reasons for wood performance improvement. Holz als Roh-und Werkstoff 56, 149−153.

Turner, I., Rousset, P., Rémond, R., Perré, P., 2010. An experimental and theoretical investigation of the thermal treatment of wood (*Fagus sylvatica* L.) in the range 200−260°C. International Journal of Heat and Mass Transfer 53, 715−725.

Unger, B., Bücker, M., Reinsch, S., Hübert, T., 2013. Chemical aspects of wood modification by sol-gel-derived silica. Wood Science and Technology 47 (1), 83−104.

Wang, J.Y., Cooper, P.A., 2005. Effect of oil type, temperature and time on moisture properties of hot oil-treated wood. Holz als Roh-und Werkstoff 63, 417−422.

Welzbacher, C., Rapp, A., 2007. Durability of thermally modified timber from industrial-scale process in different use classes: results from laboratory and field tests. Wood Material Science and Engineering 2 (1), 4−14.

Williams, F.C., Hale, M.D., 1999. The resistance of wood chemically modified with isocyanates. Part 1. brown rot, white rot and acid chlorite delignification. Holzforschung 53, 230−236.

Wu, Y.Z., Hiroaki, M., Yutaka, K., 2003. Study on the impregnation of phenol resin in Chinese fir and its improvement. Scientia Silvae Sinicae 39, 136−140.

Yamaguchi, H., 1994a. Properties of solicit acid compounds as chemical agents for impregnation and fixation of wood. Mokuzai Gakkaishi 40 (8), 830−837.

Yamaguchi, H., 1994b. Preparation and physical properties of wood fixed with silicic acid compounds. Mokuzai Gakkaishi 40 (8), 838−845.

Youngquist, J.A., Rowell, R.M., 1990. Adhesive bonding of acetylated aspen flakes. Part 3: adhesion with isocyanates. International Journal of Adhesion and Adhesives 10 (4), 273−276.

Youngquist, J.A., Sachs, I.B., Rowell, R.M., 1988. Adhesive bonding of acetylated aspen flakes. Part 2: effects of emulsifiers on phenolic resin bonding. International Journal of Adhesion and Adhesives 8 (4), 197−200.

Natural fibre cement composites

8

O.S. Abiola
Federal University of Agriculture, Abeokuta, Nigeria

8.1 Introduction

Natural fibre encompasses all forms of fibres from woody plants, grasses, fruits, agricultural crops, seeds, water plants, palms, wild plants, leaves, animal feathers and animal skins. By-products of pineapple, banana, rice, sugarcane, coconut, oil palm, kenaf, hemp, cotton, abaca, sugar palm, sisal, jute and bamboo are among the fibres known to be used to make composites. The ancient Egyptians had been reported to have used natural fibre composites, made from straw and clay or mud around 3000 years ago. This chapter is restricted only to plant-based fibres. The introduction of natural fibres from annual renewable resources is now a popular occurrence or phenomenon in the reinforcement of polymer matrices. They have the properties, composition, structures and features that are suitable to be used as reinforcements or fillers in polymer composites.

The plant-based natural fibres contain cellulose and noncellulose material such as hemicelluloses, pectin and lignin; thus they are known as lignocellulosic or cellulosic fibres. Cellulosic is a semicrystalline polysaccharide found in natural fibres, and it is the reason for the natural fibres to demonstrate hydrophilic behaviour. It provides strength and rigidity to the fibres. Hemicellulose is an amorphous polysaccharide, and its molecular weight is lower than cellulose. Fibres are held together by means of pectin. Pectin is a class of plant cell wall polysaccharide that can be found in a plant's cell wall. Lignin acts as a binder for the cellulose fibres and adds strength and stiffness to the cell walls. Holocellulose contains mainly cellulose and hemicelluloses, and it is the total polysaccharide of natural fibres. A lumen is a cavity inside fibre cells. Ash and wax are normally contained in the fibres. The structural composition and chemical structure of fibres are presented in Table 8.1 and Fig. 8.1, while Fig. 8.2 shows a schematic structure of a natural fibre. Fig. 8.3 presents the model of the structural organization of the three components of the fibre cell wall. Table 8.2 summaries the mechanical properties of natural and man-made fibres.

The advantages of natural lignocellulosic fibres over traditional reinforcing materials, such as glass fibres, talc and mica are as follows (Abiola et al., 2014):

- low density
- low cost
- nonabrasivity
- good thermal properties
- enhanced energy recovery
- biodegradability

Advanced High Strength Natural Fibre Composites in Construction. http://dx.doi.org/10.1016/B978-0-08-100411-1.00008-X

Table 8.1 **Structural composition of natural fibres** (Fakirov and Bhattacharyya, 2007; Mohanty et al., 2000)

Name of the fibres	Cellulose (wt.%)	Lignin (wt.%)	Hemicellulose (wt.%)	Pectin (wt.%)	Wax (wt.%)	Microfibrillar/spiral angle (degree)	Moisture content (wt.%)
Bast fibres							
Jute	61–71.5	12–13	13.6–20.4	0.2	0.5	8.0	12.6
Flax	71	2.2	18.6–20.6	2.3	1.7	10.0	10.0
Hemp	70.2–74.4	3.7–5.7	17.9–22.4	0.9	0.8	6.2	10.8
Ramie	68.6–76.2	0.6–0.7	13.1–16.7	1.9	0.3	7.5	8.0
Leaf fibres							
Sisal	67–78	8.0–11.0	10.0–14.2	10.0	2.0	20.0	11.0
Pineapple leaf fibre	70–82	5–12	–	–	–	14.0	11.8
Seed fibres							
Cotton	82.7	0.7–1.6	5.7	–	0.6	–	33–34

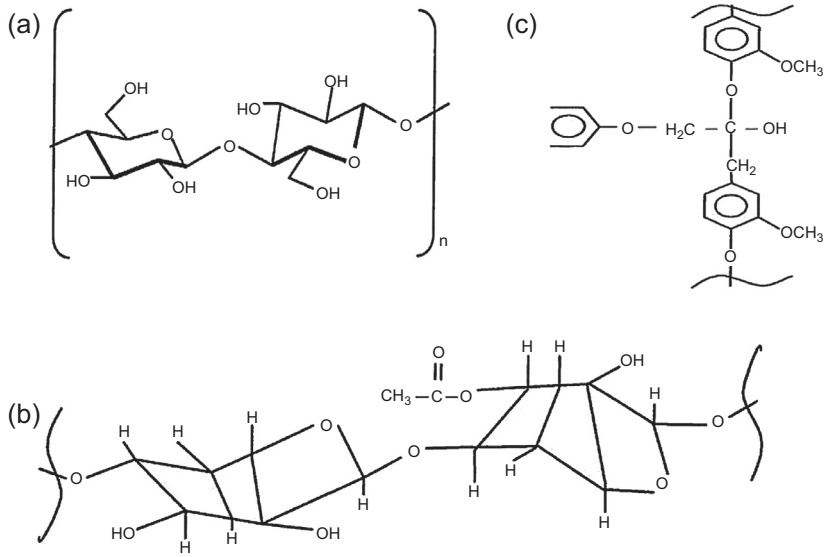

Figure 8.1 Chemical structure of (a) cellulose, (b) hemicelluloses and (c) lignin (Bledzki and Gassan, 1999).

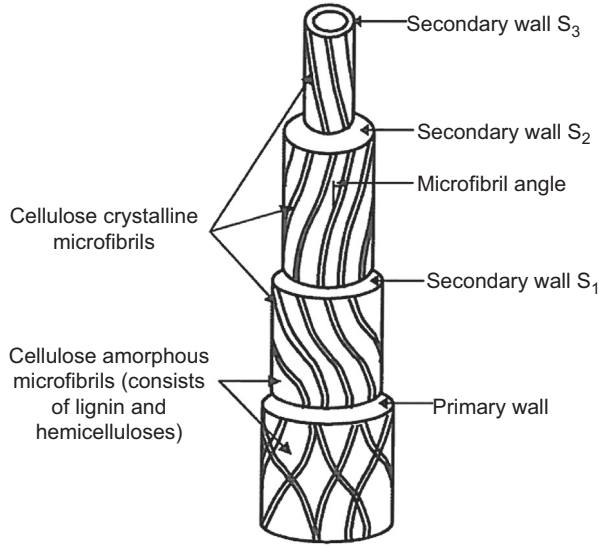

Figure 8.2 Structure of natural fibre (Kabir et al., 2012).

Figure 8.3 Structure organization of the three major constituents in the fibre cell wall (Kabir et al., 2012).

Table 8.2 Natural fibre properties (Natural Fibres, 2009)

Plant fibre	Tensile strength (MPa)	Young's modulus (GPa)	Specific modulus (GPa)	Failure strain (%)	Length of ultimate l (mm)	Diameter of ultimate (μm)	Aspect ratio, *l*/*d*	Microfilb, θ (degree)	Density (kg/m^3)	Moisture content (eq.) (%)
Cotton	300–700	6–10	4–6.5	6–8	20–64	11.5–17	2752	20–30	1550	8.5
Kapok	93.3	4	12.9	1.2	8–32	15–35	724	–	311–384	10.9
Bamboo	575	27	18	–	2.7	10–40	9259	–	1500	–
Flax	500–900	50–70	34–48	1.3–3.3	27–36	17.8–21.6	1258	5	1400–1500	12
Hemp	310–750	30–60	20–41	2–4	8.3–14	17–23	549	6.2	1400–1500	12
Jute	200–450	20–55	14–39	2–3	1.9–3.2	15.9–20.7	157	8.1	1300–1500	12
Kenaf	295–1191	22–60	–	–	2–61	17.7–21.9	119	–	1220–1400	17
Ramie	915	23	15	3.7	60–250	28.1–35	4639	–	1550	8.5
Abaca	12	41	–	3.4	4.6–5.2	17–21.4	257	–	1500	14
Banana	529–914	27–32	20–24	1–3	2–3.8	–	–	11–12	1300–1350	–
Pineapple	413–1627	60–82	42–57	0–1.6	–	20–80	–	6–14	1440–1560	–
Sisal	80–840	9–22	6–15	2–14	1.8–3.1	18.3–23.7	115	10–22	1300–1500	11
Coir	106–175	6	5.2	15–40	0.9–1.2	16.2–19.5	64	39–49	1150–1250	13

- nontoxic
- easy to handle
- renewable, abundant and continuous supply of raw materials

The main bottlenecks in the broad use of these natural fibres in various polymer matrices are the poor compatibility between the fibres and the matrix and the inherent high moisture absorption, which brings about dimensional changes in lignocellulosic-based fibres. The efficiency of a fibre reinforced composite depends on the fibre/matrix interface and the ability to transfer stress from the matrix to the fibre. This stress transfer efficiency plays a dominant role in determining the mechanical properties of the composite.

Cement-based materials suffer from one common shortcoming; they fail in a brittle manner under tensile stresses or impact loads, ie, they lack resistance to the propagation of cracks. The use of short, randomly distributed fibres is an effective method of strengthening brittle materials against cracking under stress. Generally, the reason why weak, brittle materials are made tougher by little additions of fibres is that cracks are deflected in the presence of fibres, and thus the toughness or ductility is dramatically increased. Moreover, fibres give the cement composite material a very good plasticity in its fresh state after mixing the cement with water, making it possible to cast the material into different varying forms such as roofing sheets, floor tiles, etc.

8.2 Natural fibres as reinforcement

The fibres used as reinforcements were in the form of meshes. The fibre content was represented by the number of mesh layers and varied in three different cases. The scientific study of natural fibre reinforcement has followed the developments with synthetic fibres. The reasons for the putting fibres into cement-based materials are generally agreed to be as follows:

- improvement of flexure (bending strength),
- improvement of impact toughness,
- control of cracking and change in failure behaviour to give post-crack load-bearing capacity and
- change in the flow characteristics of the fresh material.

8.3 Reinforcement of cement composites

The use of natural fibres in cement-based matrices can be divided into two categories: unprocessed natural fibres and processed natural fibres. The unprocessed natural fibres are available in many different countries and represent a continuously renewable resource. These fibres are obtained at low cost and energy consumption through the use of locally available manpower and technology. Generally these fibres are used in low cost housing projects in developing countries. Processed natural fibres, such

as kraft pulp fibres using sophisticated manufacturing processes to extract the fibres, have been used in commercial production since the 1960s for manufacturing thin sheet fibre reinforced cement products.

Fibre–cement composite products for residential housing have been generally limited to exterior applications, such as siding and roofing. The exterior use has been limited in the industry due to degradation to ambient wetting and drying. Thus these components must be currently maintained by painting to avoid moisture problems. Furthermore, the applications of these composite products are nonstructural in nature.

In cement-based composites the two major roles played by the fibres are to improve the toughness and the post-cracking performance of the matrices. There are also some changes created to the pre-cracking behaviour of the hardened matrix, which help to define the composite action. Fibre content (% by volume), ratio of fibre modulus to matrix modulus and the ratio of fibre strength to the matrix strength all influence the performance of the composite before and after cracking. In a well-designed composite, the fibres can serve two functions in the post-cracking zone: (1) to increase the strength of the composites over that of the matrix by providing a means of transferring stresses and loads across the cracks and (2) to increase the toughness of the composite by providing energy absorbing mechanisms related to the debonding and pull-out processes of the fibres bridging the cracks. Knowledge of the fibre properties is important for design purposes. Fibre tensile strength is usually higher than the matrix strength and becomes influential in post-cracking behaviour only when long fibres are sued or when the matrix is of high strength and a small volume fraction of fibres is used. A high ratio of fibre modulus to matrix modulus facilitates stress transfer from the matrix to the fibre. Fibres having large values of failure strain give high extensibility in composites. Problems associated with fibre debonding at the fibre–matrix interface are prevented by having a lower Poisson's ratio.

8.4 Application of natural fibre cement composites in construction

Fibre reinforced cements and concretes are today established as construction materials. Since the early 1960s, extensive research and development have been carried out with fibre reinforced composite materials, leading to a wide range of practical applications. Considerable research has gone on in the field of fibre reinforced, cement-based materials, and there is now an abundance of literature on the subject. Fibres such as sisal and coconut fibres used as reinforcement in the form of short fibres in cement matrices were explored. Other natural fibres like coir, jute and hibiscus cannebinus in cement-mortar slabs were also investigated and the results obtained have shown that the addition of these fibres has increased the impact resistance of the plain mortar slab. The major advantage of fibre reinforcement is to impart additional energy-absorbing capability and to transform a brittle material into a pseudo ductile material. Fibres in cement or in concrete serve as crack arrestors, which can create a stage of slow crack

propagation and gradual failure. The application of natural fibres to replace asbestos because of their availability in the tropical and subtropical parts of the world has been explored. The performance of mortar roofing tiles reinforced with natural fibres was studied. Sisal fibre was used as reinforcement in cement-based composites and has shown that the composites are reliable materials to be used for structural materials. It has also been found that this material could be a substitute for asbestos−cement composites. Another work was done to analyse mechanical, physical and thermal performance of roofing tiles produced from cement-based matrices reinforced with sisal and eucalyptus fibres. The study found that vegetable fibres are acceptable as substitutes for asbestos as reinforcements in cement-based sheets. Natural cellulose fibres have been produced either as a full or partial substitute for asbestos because they have similar characteristics such as high aspect ratio, high tensile strength, toughness, flexibility and above all, the buoyancy of the fibre in cement. Cellulose fibre reinforced cement can provide the highest performance-to-cost ratio among fibrous cement composites for the replacement of asbestos.

The wall panels of a house were produced using binder, sand and water by mass mortar reinforced with 2% coconut fibres by volume. After 12 years of construction the fibres were examined, and no significant difference was found in the lignin content of fibres removed from external walls and those removed from internal walls.

8.5 Natural fibre in concrete

Normal concrete is a brittle material, which possesses a high compressive strength, but on the other side has a low tensile strength. On the other hand, reinforced steel is a high cost material, has high energy consumption and comes from nonrenewable resources. Natural fibres are a renewable resource and are available almost all over the world. One of the disadvantages of using fibres is that they have a high variation on their properties, which could lead to unpredictable concrete properties. The pretreatment of natural fibres was found to increase concrete performance. Pulping is one of the fibre treatments that improve fibre adhesion to the cement matrix and also resistance to alkaline attack. Pulping can be obtained by a chemical way or a mechanical way. The latter has a lower cost and does not need effluent treatments. Some authors argue that the Interfacial Transition Zone (ITZ) between concrete and natural fibres is porous, cracked and rich in calcium hydroxide crystal. Fig. 8.4 shows a concrete sample where fibre imprints are visible as an example for low adhesion between the cement matrix and natural fibres.

On the contrary, others reported that using vacuum dewatering and high pressure applied after moulding lead to a dense ITZ. The uses of water repellents also lead to a good bond between natural fibres and concrete. The mechanical treatments of the fibres also improve the bonding between the fibre and cement. Some authors have reported that the alkaline treatment of fibres do improve their strength and also fibre−matrix adhesion (Sedan et al., 2008). The use of 0.2% volume fraction of 25 mm sisal fibres leads to free plastic shrinkage reduction; the combination of coconut

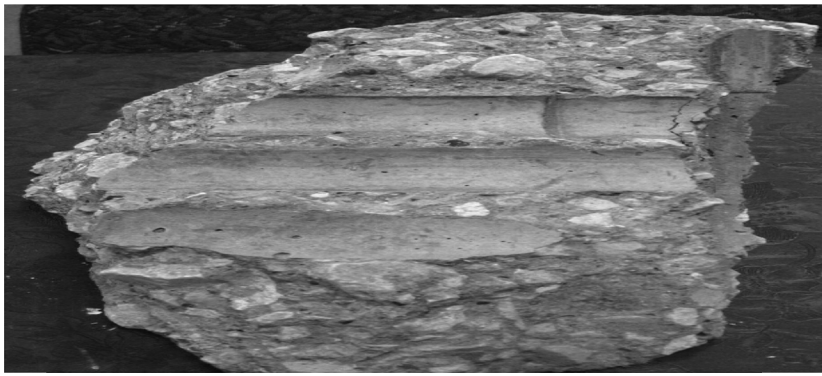

Figure 8.4 Concrete samples with fibre imprints.

and sisal short fibres seems to delay restrained plastic shrinkage, controlling crack development at early ages. As for the mechanical performance of natural fibre concrete, using a low percentage of natural fibres improved the mechanical properties and the impact resistance of concrete and had similar performance when compared to synthetic fibre concrete. Other authors reported that fibre inclusion increases impact resistance 3−18 times higher than when no fibres were used (Ramakrishna and Sundararajan, 2005). Studies have shown that mechanical performance of fibre concrete depends on the type of fibre. Coconut and sugar cane bagasse fibre increases concrete fracture toughness while banana pseudo stem fibre does not. The use of coconut fibres shows better flexural than synthetic fibre (glass and carbon) concrete. The addition of sisal fibres to concrete, as reported, result in lower compressive strength compared with the control. The explanation for that behaviour seems to be related to concrete workability.

The durability of natural fibre reinforced concrete is related to the ability to resist both external (temperature and humidity variations, sulphate or chloride attack, etc.) and internal damage (compatibility between fibres and cement matrix, volumetric changes, etc.). Degradation of natural fibres immersed in Portland cement is due to the high alkaline environment, which dissolves the lignin and hemicellulose phases, thus weakening the fibre structure. The fibre degradation was evaluated by exposing them to alkaline solutions and then measuring the variations in tensile strength. A deleterious effect of Ca^{2+} elements on fibre degradation was reported. It was also stated that fibres were able to preserve their flexibility and strength in areas with carbonated concrete with a pH of nine or less. Filho et al. (2000) investigated the durability of sisal and coconut fibres when immersed in alkaline solutions. Sisal and coconut fibres conditioned in a sodium hydroxide solution retained respectively 72.7% and 60.9% of their initial strength after 420 days. While immersed in calcium hydroxide solution, it was noticed that the original strength was completely lost after 300 days. The explanation according to the authors for higher attack by calcium hydroxide can be related to a crystallization of lime in the fibre pores. The capacity of natural fibres to absorb water is another path to decrease the durability of fibre reinforced concrete. Water

absorption leads to volume changes that can induce concrete cracks. When improving the durability of fibre reinforced concrete, two paths could be used:

1. Matrix modification
   Using low alkaline concrete: adding pozzolanic by-products such as rice husk ash, blast furnace slag or fly ash to Portland cement. Results show that the use of ternary blends containing slag/metakolin and silica fume are effective in preventing degradation. But in some cases the low alkalinity is not enough to prevent lignin from being decomposed. Other authors have reported that fast carbonation can induce lower alkalinity (Agopyan et al., 2005).
2. Fibre modification
   Coating natural fibres prevents water absorption and free alkalis. Use water-repellent agents or fibre impregnation with sodium silicate, sodium sulphite or magnesium sulphate. Ghavami (1995) reported that the use of a water repellent in bamboo fibres allowed only 4% water absorption. The use of organic compounds like vegetable oils reduced the embrittlement process, but not completely (Filho et al., 2003). A recent finding shows that silane coating of fibres is a good way to improve the durability of natural fibre reinforced concrete. Other authors mentioned that using pulped fibres can improve durability performance, while some reported that the fibre extraction process can prevent durability reductions (Savastano et al., 2001; Juarez et al., 2007).

A feasibility study has been conducted on making coir fibre reinforced corrugated slabs for use in low cost housing. Tests for flexural strength and thermal and acoustic properties were performed. Producing slabs with a flexural strength of 22 MPa, a volume fraction of 3%, a fibre length of 2.5 cm and a casting pressure of 0.15 MPa were recommended. The thermal conductivity and sound absorption coefficient for low frequency were comparable with those of locally available asbestos boards.

8.6 Summary

This chapter provides a review on the inclusion of natural fibre as reinforcement in cement composites and application in construction. The application of natural fibres as construction materials and the benefits of adding fibres to concrete were discussed. Information about improving the durability of the fibres in reinforced concrete as well as the structural composition were mentioned.

References

Abiola, O.S., Kupolati, W.K., Sadiku, E.R., Ndambuki, J.M., 2014. Utilisation of natural fibre as modifier in bituminous mixes: a review. Construction and Building Material 54, 305−312.

Agopyan, V., Savastano, H., John, V., Cincolto, M., 2005. Developments on vegetable fibre-cement based materials in Sao Paulo, Brazil: an overview. Cement Concrete Composites 27 (5), 527−536.

Bledzki, A.K., Gassan, J., 1999. Composites reinforced with cellulose based fibres. Progress in Polymer Science 24 (2), 221−274.

Fakirov, S., Bhattacharyya, D. (Eds.), 2007. Engineering Biopolymers: Homopolymers, Blends and Composites. Munich Hanser Publishers.

Filho, R., Scrivener, K., England, G., Ghavami, K., 2000. Durability of alkali-sensitive sisal and coconut fibres in cement and mortar composites. Cement Concrete Composites 22 (2), 127−143.

Filho, R., Ghavami, K., England, G., Scrivener, K., 2003. Development of vegetable-fibre mortar composite of improved durability. Cement and Concrete 25, 185−196.

Ghavami, K., 1995. Ultimate load behavior of bamboo-reinforced light weight concrete beams. Cement and Concrete Composites 17, 281−288.

Juarez, C., Duran, A., Valdez, P., Fajardo, G., 2007. Performance of "*Agave lecheguilla*" natural fibre in Portland cement composite exposed to severe environment conditions. Building and Environment 42 (3), 1151−1157.

Kabir, M.M., Wang, H., Lau, K.T., Cardonna, F., 2012. Chemical treatments on plant-based natural fibre reinforced polymer composites: an overview. Composites Part A 43, 2883−2892.

Mohanty, A.K., Misra, M., Himrichen, G., 2000. Biofibres, biodegradable polymers and biocomposites: an overview. Macromolecular Materials and Engineering 266−277.

Natural Fibres: Ancient Fabrics, High Tech Geotextiles, 2009. International Year of Natural Fibre. www.naturalfibres20009.org/en/fibres/hemp.html.

Ramakrishna, G., Sundararajan, T., 2005. Impact strength of a few natural fibre reinforced cement mortar slabs: a comparative study. Cement and Concrete Composites 27 (5), 547−553.

Savastano, H., Warden, P., Coutts, R., 2001. Ground iron blast furnace slag as a matrix for cellulose-cement material. Cement and Concrete Composites 23, 389−397.

Sedan, D., Pagnoux, C., Smith, A., Chotard, T., 2008. Mechanical properties of hemp fibre reinforced cement: influence of the fibre/matrix interaction. Journal of European Ceramics Society 28, 183−192.

Natural fibre rebar cementitious composites

9

T. Rousakis
Democritus University of Thrace, Xanthi, Greece

9.1 Short introduction

The continuous and prosperous growth of mankind within a healthier environment urges for the adoption of the principle for 'green', sustainable development. In the construction sector, limited raw material resources, technologies and production processes with high embodied energy, as well as the deterioration of existing structures because of steel corrosion, ageing, etc. have to be faced. They all constitute significant issues under consideration that jeopardize sustainability. Therefore the additional terms of recyclability, low CO_2 footprint and nonmetallic reinforcements have already become part of the desirable future development prerequisites. Among the numerous materials and retrofit systems, cementitious composites reinforced with natural fibres seem to be the most promising of all, to fulfil the aforementioned aspects. Despite the highly demanding interdisciplinary material and structure research, they combine the great potential for recyclability, biodegradability and the endless cultivation process, with lower overall embodied energy than common minerals for the final structural fibres. They also rely on abundant local resources and common technology for the production of the cementitious matrices. Growing interlinks among industry, researchers and practitioners favour the introduction of advanced natural-based materials per a different kind of structure, application and retrofit technique (Rousakis, 2014b). Application of natural fibre rebar cementitious composites in construction is already a reality in structural seismic retrofit. Yet certain unidentified gaps in knowledge have to be addressed to enable broader applications.

This chapter presents the variety of natural fibre reinforcements and suitable cementitious matrices used in construction, especially in the field of strengthening existing masonry and concrete structures. Several applications are discussed. The study also refers to internal natural reinforcements suitable for use in new concrete structures.

9.2 Natural fibre rebar materials

9.2.1 Organic fibres

Natural fibres may be divided into two major categories: organic and inorganic natural fibres (Mallick, 2008; Müssig, 2010; Torgal and Jalali, 2011). Organic natural fibres may be further classified into plant or animal ones. Plant fibres include (1) seed fibres,

Advanced High Strength Natural Fibre Composites in Construction. http://dx.doi.org/10.1016/B978-0-08-100411-1.00009-1

such as cotton and akon; (2) fibres of stems, such as flax, hemp, jute and kenaf; (3) fruit hair, such as kapok and paina; (4) fibres of leaves, such as sisal and banana fibre; (5) fruit fibre, such as coir; and (6) fibres of spears, such as bamboo. Animal fibres include hairs and threads, such as cocoons or spider threads. There is a variety of uses of biocomposites in different aspects of life, from ancient years up to now (Staiger and Tucker, 2008).

In construction, natural fibres have been traditionally used for thousands of years and still are in order to produce adobe bricks (Rowell, 2008) or clay walls with wooden reinforcements in rural housing (Balázs, 2012). Fig. 9.1 shows the representation of a Neolithic lakeshore structure.

Plant or vegetable or cellulosic natural fibres (Brandt, 2009) are used to replace expensive and dangerous-to-health asbestos fibres since 1983 (for example, flax fibres in Coutts, 1983). The use of vegetable fibres as reinforcement for low-cost concrete elements has been proposed by Nilsson since 1975. Natural fibres such as hemp, sisal and flax, as well as bamboo fibres, have been also investigated experimentally in Fibre Reinforced Polymers (FRPs).

Hemp fibres have a tensile modulus of elasticity around 30−70 GPa, a tensile strength between 310 and 900 MPa and ultimate strain around 1.6−6%. The mechanical properties of flax fibres range between 24 and 80 GPa for the modulus of elasticity, between 300 and 1500 MPa for the tensile strength and between 1.3% and 10.0% for the ultimate strain. Sisal fibres present a lower modulus of elasticity around 9−38 GPa, tensile strength between 80 and 840 MPa and ultimate strain between 2.0% and 25.0% (Mallick, 2008; Cheung et al., 2009; Ansell and Mwaikambo, 2009; Faruk et al., 2012). It is evident that they reveal different properties because of the nonuniformity of their structure (moisture content, defects, cell dimensions, morphology of the plant). In Staiger and Tucker (2008) the large spread of properties is attributed to the variation in cellulose content of different fibre types and to the natural heterogeneity of the fibres themselves. The compressive mechanical properties of natural fibres have received

Figure 9.1 Representation of traditional application of natural fibre rebars: clay wall with reed reinforcement in Dispilio, Kastoria Lake, Greece (settlement older than 5000 BC).

less attention. In Wecławski et al. (2014), advanced composite tubes reinforced with hemp yarns provided enhanced mechanical properties under compression.

The mechanical properties of different natural fibres are gathered in Table 9.1 together with common reinforcing fibres used in construction, made of carbon, glass, aramide etc. (the mechanical properties of these fibres have been cited in Rousakis, 2014b). It seems that some of the natural organic fibres have mechanical properties that are similar to glass. Thus numerous applications that currently use glass reinforcing fibres may be reviewed in order to investigate the potential of alternative natural organic reinforcement.

Sustainability and recyclability issues are expected to become important drivers in the construction industry for the broader use of natural fibres in commercial FRP

Table 9.1 Range of mechanical properties of natural and man-made reinforcing fibres

	Fibres	Modulus of elasticity (GPa)	Tensile strength (MPa)	Ultimate strain
Natural organic	Hemp	30–70	310–900	0.016–0.06
	Flax	24–80	300–1500	0.013–0.1
	Sisal	9–38	80–840	0.02–0.25
Natural inorganic	Asbestos	110	1000	0.01–0.02
	Basalt	89–95	3000–4900	0.03–0.05
Man-made	Carbon fiber	215–300	3500–6000	0.015–0.023
	High modulus carbon	370	3500–4410	0.0095–0.012
	Ultra high modulus carbon	570–800	1800–2300	0.002–0.0166
	Glass	70–90	1900–4800	0.03–0.057
	Aramide	70–130	2750–4100	0.024–0.05
	PBO	270	5200–5400	0.01–0.02
	PEN	22–27	790–1030	0.045–0.05
	PET	6.7–18	740–920	0.07–0.138
	Vinylon	16	735	0.046
	Polypropylene	2	400	0.20
	UHMW polyethylene	175	2400	0.019

products (Bank, 2006). In conclusion, natural organic fibres may offer a 'sustainable' alternative material to common, carbon, glass or plastic fibres. Indeed, local cultivation may ensure a sustainable production chain besides their low environmental impact both in production and in the disposal phase (Asprone et al., 2011).

9.2.2 Inorganic fibres

Inorganic natural fibres correspond to mineral fibres such as asbestos (Vickers et al., 2015) and basalt fibres, as well as Silexil (siliceous needles coming from Spongolite, Saliba et al., 2005), which is close to 100% SiO_2. Inorganic basalt fibres reveal superior corrosion resistance and similar mechanical properties to glass fibres (Bank, 2006; Dhand et al., 2015). The mechanical properties of basalt fibres range between 89 and 95 GPa for the modulus of elasticity, between 2800 and 4900 MPa for the tensile strength and between 3.00% and 5.00% for the ultimate strain. Generally, the mechanical properties of the FRP (fibres and polymers) depend on the fibre volume fraction, the orientation of the fibre, the method of manufacture, the temperature and duration of the cure cycle and the age of the polymer composite (Hollaway and Teng, 2008; Fiore et al., 2015). The fibre volume fraction in most FRP bars is estimated between 50% and 60% and between 60% and 70% (Bank, 2006) for FRP strips.

Natural inorganic basalt fibres are derived from volcanic deposits in a single melt process and offer better thermal stability, heat and sound insulation properties, vibration resistance and durability than glass fibres (Balaguru et al., 2009). Basalt differs from granite in being a fine-grained extrusive rock with a higher content of iron and magnesium with a density between 2.7 gr/cm^3 and 2.8 gr/cm^3. It is extremely hard (between five and nine on Moh's scale) and thus has superior abrasion resistance (Di Ludovico et al., 2010). Continuous basalt fibres can be produced, utilizing the same technology used for glass fibres. The extrusion process of basalt fibres is energy efficient and simpler than that of any competing fibres (Dhand et al., 2015). In addition, the raw materials are distributed worldwide (Di Ludovico et al., 2010). Basalt fibres are stable, inert, ecofriendly, nontoxic and nonreactive reinforcement materials (Dhand et al., 2015). Basalt fibres may reveal a wide range of mechanical properties by modifying the chemical composition. Thus the quality control of the production process is very important in obtaining basalt fibres with low dispersion. Basalt fibres with a higher modulus of elasticity than glass fibres are available (see Table 9.1).

Another important aspect of the basalt fibres is the potential for high biosolubility (biodegradability) with respect to many advanced man-made fibres (Di Ludovico et al., 2010; Dhand et al., 2015). Biosolubility (biodegradability) is a key property for basalt fibres, as inorganic fibres with advanced mechanical properties (similar to glass or carbon) possess features attributed to their natural origin such as recyclability and nontoxicity that favor 'green retrofitting'. Advanced basalt fibre reinforcements present a better ecofootprint than alternative materials of equivalent structural performance. The substitution of steel fibre or steel rebar as concrete reinforcement in future applications in construction by basalt ones may lead to reduced energy consumption and CO_2 quantity emitted to air.

9.3 Cementitious matrices

Natural fibre composites include not only polymers but alternative cementitious matrices as well. Organic natural fibre cementitious composites or cementitious biocomposites are investigated in Toledo et al. (2003). They belong to the category of natural fibre reinforced cementitious composites or NFRCM. They are renewable materials with low environmental impact with respect to advanced FRPs and favour sustainable development of the building industry.

Cementitious matrices may also overcome the following certain drawbacks that are related to organic epoxy resins, used for bonding fibres, such as (Di Ludovico et al., 2010): (1) the low performance under elevated temperature (above Tg) and under direct fire, (2) the potential for emission of poisonous fumes under elevated temperature, (3) relatively high costs, (4) potential hazards for workers due to solvent contents, (5) nonapplicability in the case of wet surfaces or low temperatures, (6) lack of vapour permeability, (7) incompatibility of resins and substrate materials and (8) quality control of chemical reactions. In any case, the epoxy resin surplus has to be treated as special waste.

In historical structures, the issues of retrofit reversibility, compatibility and sustainability are very critical. Therefore NFRCMs seem to be ideal for strengthening historical masonry buildings that possess moderate compressive and shear strength, very low tensile strength and low to moderate stiffness. They have similar stiffness and adequate tensile capacity. Consequently, they achieve better mechanical compatibility with the substrate at lower cost than high-performance carbon fibres, which have high stiffness, are hardly compatible with the substrate andhave nonexploitable tensile strength and high embodied energy and CO_2 production (De Felice, 2014; Codispoti et al., 2015). Issues related to the nonimpregnation of reinforcing fibres by cementitious matrices resulted in the development of fabrics or textiles in the form of open single or multiple meshes (Babaeidarabad et al., 2013; De Felice, 2014; Codispoti et al., 2015). Most cementitious matrices are based on materials available in most of the world. Therefore similar to sustainable natural fibres, suitable cementitious matrices may extend the local supply chain for the whole composite system.

9.4 Natural fibre reinforcements

9.4.1 Resin impregnated rebars

Basalt resin impregnated bars (Fig. 9.2) are already available in the market for use as structural reinforcement in new concrete structures or for the strengthening of existing ones (Kamenny Vek Basfiber Rebar, MagmaTech Rockbar, Sudaglass Rod, Incotelogy Basalt Fiber Rebars, Technobasalt, GBF Basalt Rebars among others). The main advantages of basalt rebars are (Fiore et al., 2015):

- tougher and lighter than steel;
- naturally resistant to alkali, rust and acids;
- moisture penetration from concrete does not spall;

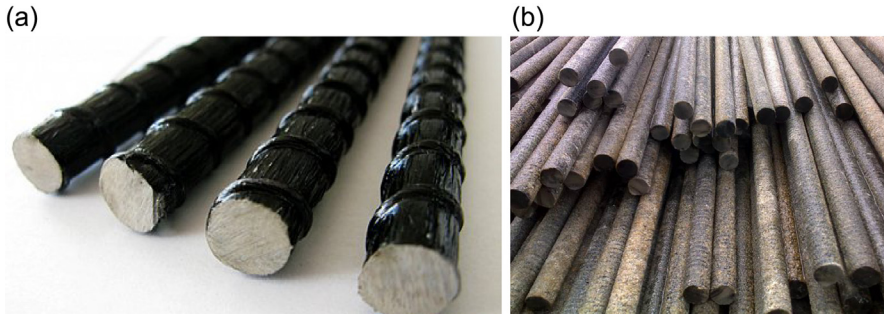

Figure 9.2 Basalt bars by (a) Technobasalt (http://www.technobasalt.com/products/item/basalt-rebar-1/.) and by (b) MagmaTech Rockbar (http://magmatech.co.uk/downloads/RockBar.pdf.).

- no need for special coating like fibreglass rods;
- same thermal expansion coefficient as concrete;
- easily cut to length with regular tools;
- does not conduct electricity; and
- optimal for use in harsh environments.

The use of basalt rebars as internal reinforcement in new concrete structures is already covered by design recommendations (*fib* bulletin 40, 2007), while there is comprehensive ongoing research addressing the time-dependent, long-term performance of rebars and tendons (Wang et al., 2014; Wu et al., 2014; Zhao et al., 2016 among others). Basalt fibres are also used as cheap mass reinforcement in cement paste and concrete as a competitive alternative product to polypropylene and polyacrylonitrile fibres (Fiore et al., 2015). As far as natural rebars are concerned, Ghavami (2005) presents early investigations (since 1981) on concrete beams, slabs or columns reinforced with alternative bamboo bars.

Furthermore, resin impregnated (coated) natural reinforcements are met in the form of textile grids. As already mentioned above, they are extensively used combined with cementitious matrices to strengthen masonry structures as well as concrete ones. The design of Externally Bonded Fabric Reinforced Cementitious Matrix (FRCM) Systems for Repair and Strengthening Concrete and Masonry Structures is already covered by advanced recommendation (ACI 549.4R-13, 2013). It covers common advanced fibres and natural inorganic basalt ones. Natural organic fibres are not included even for the strengthening of masonry structures, as further research is required. Yet ACI 549.4R-13 constitutes a solid basis for the further development of fabric reinforced cementitious composites for structural retrofit, while it cites several masonry repair applications since 2007 (Triantafillou, 2007).

9.4.2 Organic natural fibre grid

In Asprone et al. (2011), hemp fibres and pozzolanic mortars are used to propose a seismic retrofit system for existing masonry while significant durability aspects are

addressed. The immersion of hemp fibres into alkaline water resulted in a very significant reduction of mechanical properties of the fibres because of the alkali attack on the fibres and the volume variation due to water absorption. Therefore the latex coating of fibres was used to enhance durability performance. The mechanical performance of the cementitious matrix, in terms of stress-flexural strain, was remarkably enhanced when reinforced with a natural organic hemp fibre grid coated with latex or resin. Similarly, Olivito et al. (2014) investigated sisal and flax fabrics in cementitious seismic strengthening systems for masonry structures. They used natural hydraulic lime-based mortar and lime-based grouting with carbonate filler and pure pozzolan. The lime-based grouting did not reduce the mechanical performance of the sisal or flax fabrics with time. Higher fibre volume fractions are proposed to enhance the tensile performance of the cementitious composite. Cevallos and Olivito (2015) perform direct tensile tests in cementitious composites with the lime-based grouting matrix and flax or sisal fabrics in higher volume fraction. Grouts were reinforced with bidirectional woven fabrics made from single yarns of natural fibres. Flax and sisal fabrics were symmetrically woven. Both seismic strengthening systems revealed a three-stage stress-strain behavior typical for cementitious composites. They presented enhanced axial strain ductility and tensile strength with the number of fabric layers. In Cevallos et al., 2015, the flax cementitious composite with the grout matrix is applied on masonry specimens of different sizes (square or rectangular section and different slenderness ratio) to enhance their capacity under eccentric axial load (Figs 9.3 and 9.4). In all cases the NFRCM improved the strength and deformability of masonry elements under eccentric axial load. Flax FRCM with lime-based grouting maintained the bond with the brick walls, releasing the stored stress through the formation of cracks in the matrix.

9.4.3 Inorganic natural fibre grid: basalt fiber reinforced polymer grid

Basalt fibre grids embedded in cement-based mortar have been used as external confinement of concrete cylinders (Di Ludovico et al., 2010). The application required

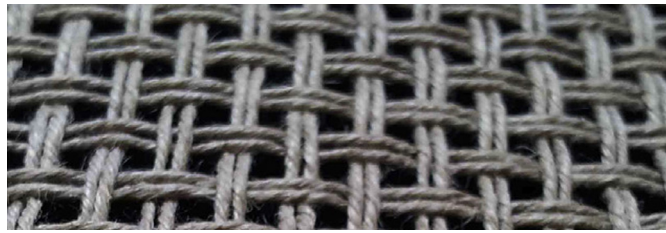

Figure 9.3 Bidirectional reinforcing flax fabric.
Adapted from Cevallos, O., Olivito, R.S., Codispoti, R., Ombres, L., 2015. Flax and polyparaphenylene benzobisoxazole cementitious composites for the strengthening of masonry elements subjected to eccentric loading. Composites Part B: Engineering, 71, 82–95. http://dx.doi.org/10.1016/j.compositesb.2014.10.055.

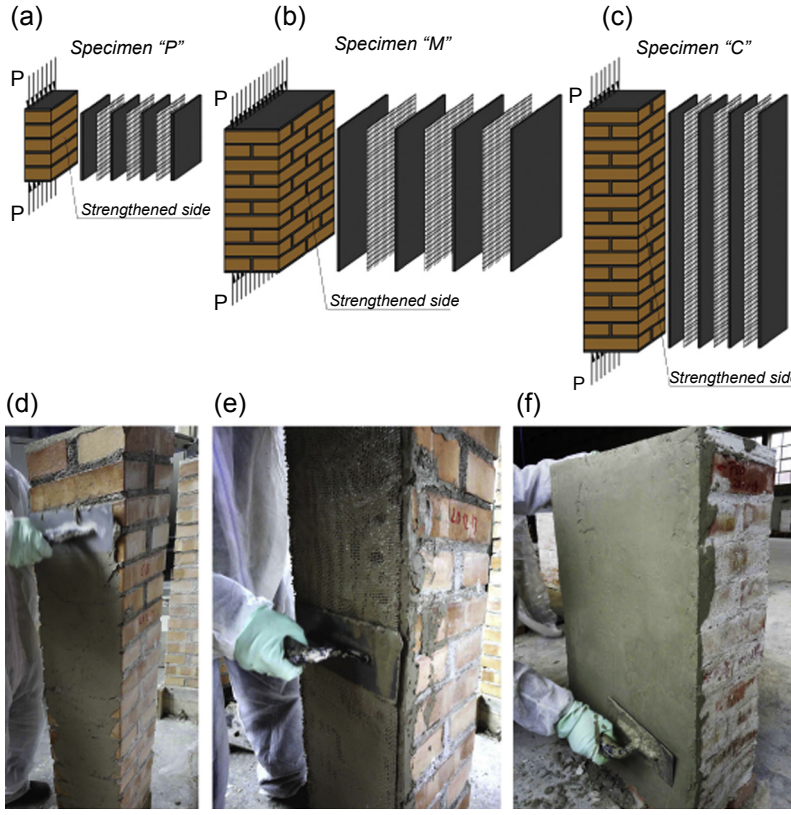

Figure 9.4 Application of the mortar composite containing flax fabrics: (a)–(c) strengthening of different specimens with three layers of natural fabrics; (d) application of the first layer of mortar; (e) embedment of the fabric into the mortar layer; and (f) application of the final mortar layer.
Adapted from Cevallos, O., Olivito, R.S., Codispoti, R., Ombres, L., 2015. Flax and polyparaphenylene benzobisoxazole cementitious composites for the strengthening of masonry elements subjected to eccentric loading. Composites Part B: Engineering, 71, 82–95. http://dx.doi.org/10.1016/j.compositesb.2014.10.055.

the patching of a layer of cement-based mortar with a thickness higher than 4 mm. Then the bidirectional basalt fibre grid was preimpregnated with epoxy resin or latex. Finally, a second layer of cement-based mortar was applied with a thickness higher than 4 mm. The experimental results showed a substantial gain in strength and ductility of columns and a gradual failure of the specimens. The results also revealed the need for higher mechanical interaction between the cementitious matrix and the grid.

In a later investigation, Al-Salloum et al. (2012) applied two different cementitious mortars reinforced with basalt textiles to increase the shear strength of reinforced concrete beams. The first mortar was a common cementitious one and the second polymer modified cementitious mortar. External shear strengthening of concrete members is

extremely demanding, as it is a bond critical application, while the developed inclined tensile strains are very low prior to shear cracking formation. Therefore successful external strengthening requires a high bond between the mortar and concrete substrate, as well as a high interaction between the mortar matrix and basalt textile grid. The experimental results of the study were very promising, as the shear capacity of the beams was substantially raised. Retrofits with polymer-modified cementitious mortar matrix presented a higher shear strength increase.

Larrinaga et al. (2013) investigated, both experimentally and analytically, the behavior of mortar reinforced with basalt textiles under direct tension. Basalt textile was covered with a bitumen coat to improve the bond with the mortar. The mortar matrix presented multiple cracking, denoting a good bond of the system in multiple layers of basalt textiles (Fig. 9.5). Also the model provided a satisfactory prediction of the whole stress-strain behavior of the cementitious composite.

Basalt fibre grids are widely applied in masonry structures. In Balsamo et al. (2014), basalt textile grids were embedded in lime-based mortar of very low strength and bonded externally on both sides of masonry panels. Masonry panels consisting of uncoursed masonry were representative of existing buildings in L'Aquila, Italy. Also, a yellow tuff masonry panel was included. The shear performance of the panels was remarkably enhanced. The failure mode of strengthened masonry panels was far more ductile. External seismic strengthening of masonry buildings with cementitious basalt grids may provide a reliable, efficient and sustainable alternative. Further analytical research is required to accurately quantify the enhancement of this technique with respect to the retrofit system, the reinforcement layout and the masonry type. Efficient analytical tools will allow for the retrofit of a large number of existing masonry structures with damages (environmental deterioration, inadequate construction techniques and materials, design for gravity loads only) or high seismic vulnerability. A basalt grid with an inorganic matrix provides high strength-to-weight ratio, low influence on global structural mass, corrosion and fatigue resistance, easy handling and installation and negligible architectural impact (Balsamo et al., 2014).

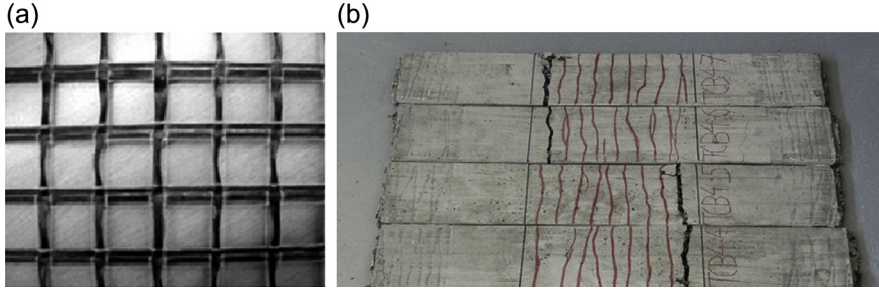

Figure 9.5 Reinforcing basalt textile (a) and different textile reinforced mortar specimens (b) after failure.
Adapted from Larrinaga, P., Chastre, C., San-José, J.T., Garmendia, L., 2013. Non-linear analytical model of composites based on basalt textile reinforced mortar under uniaxial tension. Composites Part B: Engineering 55, 518−527. http://dx.doi.org/10.1016/j.compositesb.2013.06.043.

Basalt textile reinforcements are also included (together with carbon, glass and steel ones) in the study by Ascione et al. (2015). The authors proposed a method for the qualification of externally bonded FRCM systems, based on combined direct tension and shear bond tests. The maximum stress and mode of failure of the FRCM system are estimated with shear bond tests. Then the qualification strain is estimated more reliably with direct tension tests, given the failure stress (from shear bond tests). The study presents the characteristic three-stage behavior of FRCMs under tension, as well as their typical force-slip behavior for different modes of failures. The study considers cement or lime mortars as matrices and modern bricks or historic bricks or tuff units as substrates.

9.4.4 Natural fibre sheets

Basalt fibre sheets combined with glass and PVA fibres have been used in De Caso Y Basalo et al. (2012) as reinforcement in two different cement-based matrices. The different systems were used to confine concrete cylinders. Bonded and unbonded systems to the concrete surface were investigated. They both reached similar strength levels of confined concrete. Unbonded external confinement provided a high potential for reversibility. However, the bonded jacket ensured adequate contact with concrete substrate, resulting in a superior and more reliable increase in deformability. For both bonded and unbonded confinement the predominant mode of failure was fibre-matrix separation and subsequent loss of compatibility in the external reinforcement.

The review by Ardanuy et al. (2015) gathers different kinds of cellulosic fibres used as reinforcement in cementitious composites. They discuss the different compositions, preparation methods, mechanical properties and strategies to improve fibre-matrix bonding and composite durability. They identify that the main challenges, towards more ecofriendly solutions, are the improvement of the durability and of the mechanical performance of the composites without increasing the production cost. Ardanuy et al. (2015) focus on recent manufacturing processes of aligned cellulosic fibres inside the matrix, in order to allow for a higher load capacity of the composite. In that respect, Silva et al. (2009), Toledo Filho et al. (2009) have used aligned sisal strands to produce high-performance cementitious composites. They replaced Portland cement with calcined clay in order to exclude calcium hydroxide. The aligned sisal fibres were placed into the aforementioned matrix layer by layer, up to a total of five layers (with matrix in between) and fibre volume fraction of 10%. The composite was vibrated and then it was subjected to compression. Finally, the specimens followed the standard curing treatment. The final composite laminate presented enhanced durability performance with ageing.

9.4.5 Natural fibre ropes

Different studies have addressed the promising confining effects of continuous fibre tapes (or strips) or fibre ropes, when wrapped around plain concrete columns (by hand), without resin impregnation or resin bonding on the concrete surface (Karantzikis et al., 2005; Triantafillou and Papanicolaou, 2005; Triantafillou et al., 2006; Shimomura and Phong, 2007). In Shimomura and Phong (2007), three different

kinds of continuous fibre ropes were used as external seismic strengthening of columns, alone or embedded in a concrete jacket. Furthermore, continuous fibre rope has been used as internal shear reinforcement in reinforced concrete beams.

Rousakis (2013a,b, 2014a) investigated further the confining effects of structural fibre ropes without resin impregnation or bonding to the surface of cylindrical plain concrete columns. Different fibre ropes (FR) of high extension, with adequate detailing and lateral rigidity, enabled the ever-increasing stress-strain behavior of concrete under monotonic or cyclic compression. FR confined concrete cylinders revealed a concrete strength increase more than six times the respective unconfined one and a concrete axial strain ductility of 40 (Rousakis, 2014a). The enhancement corresponds to enormous amounts of dissipated energy. This issue is very crucial in cases of seismic overloads or overdisplacements and provides a significant structural capacity reserve. Such high concrete axial strain ductility levels may eliminate failures in RC members related to the fracture of the external confining reinforcement (or of concrete under compression or degradation of compressive strength observed in steel confinement) for practical applications. Therefore it may easily lead exclusively to failures related to second-order effects or to the longitudinal bar's fracture. In cases of external FR wrapping of concrete columns already confined by FRP jackets, FR could sustain the abrupt fracture of FRP and balance the temporary load loss within desirable levels (Rousakis, 2013b; Rousakis et al., 2014).

Further testing concerned reinforced concrete columns of square sections with slender bars and very low corner radius (prohibitive for the use of FRPs), wrapped externally with common FR or pretensioned FR (Rousakis and Tourtouras, 2014). The experiments revealed the high potential of FR in confining noncircular columns. Nonimpregnated FR wrapping possesses a very high stress redistribution capacity around the section and along the column axis. It preserves full contact with the dilating and variably damaged the concrete core throughout loading. All columns could succeed axial strains higher than 5% without fracture of the fibre rope. The novel pretensioning technique increased the efficiency of the FR and prolonged the elastic stress-strain behavior of the columns. Except for the design relations provided in the aforementioned papers, in the study by Rousakis and Tourtouras (2015), a stress-strain model is presented for the prediction of common FR and pretensioned FR wrapping of RC columns. The review of the FR wrapping technique is very significant for the development of suitable natural reinforcements. In the aforementioned published investigations, the FR wrappings were not of natural fibre origin. However, they possess a relatively low modulus of elasticity (around only 2 GPa for polypropylene fibre rope) and tensile strength. The most important structural feature of suitable FR is the relatively high extension capacity. Therefore the use of alternative, durable and natural fibre ropes, organic or inorganic ones, is highly favored. The study by Shimomura and Phong (2007) has already proven the compatibility of FR with concrete or other cementitious jackets (matrices) to form cementitious composites.

Recently, Rousakis et al. (2015) used alternative natural inorganic basalt fibre rope (unbonded and nonimpregnated with resin) to wrap reinforced concrete columns (Fig. 9.6) and utilize the high temperature resistance potential of the material. Despite the lower extension capacity of the basalt fibre rope, its stress redistribution capacity

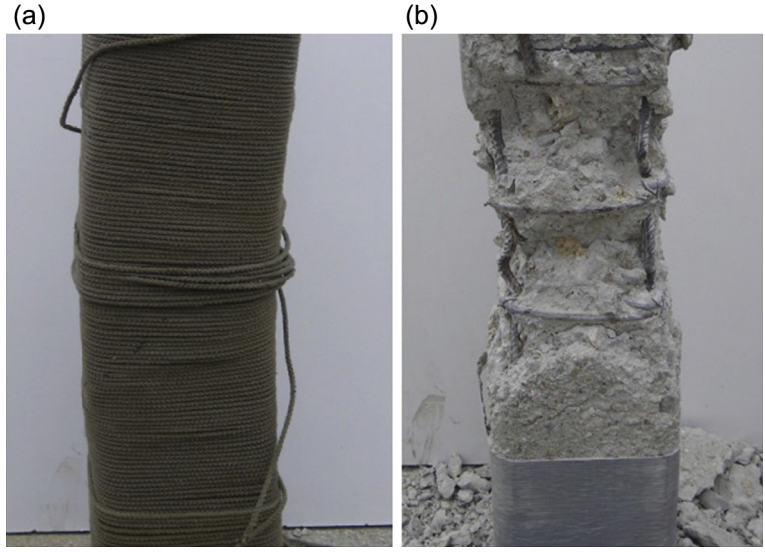

Figure 9.6 Reinforced concrete column wrapped by one layer of glass FRP sheet and two layers of BFR after the end of the experiment (Rousakis et al., 2015). Extensively deformed concrete core with no fracture of BFR (a). Specimen after the removal of BFR and fractured GFRP. Multiple buckling of bars and severely cracked concrete core (b).

was remarkable. While column RCGL1 presented fracture of the GFRP followed by full load drop, columns with Basalt Fibre Rope (BFR) wraps presented remarkable axial shortening while maintaining their axial compressive load. No column failed with fracture of the BFRs despite their multiple use. Tests were stopped early (at strain levels higher than 5%) for safety reasons imposed by extensive global buckling of the columns. After removal of the wraps, extensive disintegration of the concrete core was evidenced as well as steel bars' buckling. RC columns with hybrid GFRP and BFR

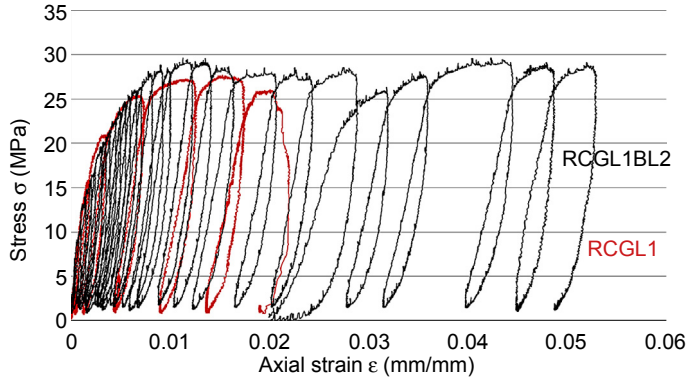

Figure 9.7 Stress-axial strain behavior of RC column wrapped by one layer of glass FRP sheet compared with RC column with hybrid GFRP and two layers of BFR.

confinement managed to maintain the integrity of concrete core after the fracture of the GFRP. A temporary, controlled load drop occurred, followed by the increase of the bearing load (see Fig. 9.7). Thus recent findings further support the need for the investigation of 'green', more sustainable natural fibre ropes, such as sisal, etc., in external strengthening, forming suitable cementitious composites.

9.5 Current applications

The potential of natural fibre reinforcements to strengthen masonry or concrete members is very high. Numerous construction-related applications have been already discussed in previous sections, related to the seismic retrofit of such structures. This crucial field of applications requires highly efficient, safe and reliable solutions, as the main target of the redesign is to fully utilize the potential of the structure as a whole and avoid structure collapse and human loss.

In general, natural fibre-based applications range from the automotive industry and the construction of nonstructural elements to casings, and structural and infrastructure applications (Pickering, 2008) such as beams, roofs, multipurpose panels, water tanks and pedestrian bridges (Ticoalu et al., 2010). In Satyanarayana et al. (1986), a detailed presentation of the fabrication process is given for the construction of polyester composite laminates, helmets, roofing, mirror casings, chair seats and boxes. Recent reviews include extensive applications of natural fibre reinforced cementitious composites or even concrete beams exclusively reinforced with bamboo rebars (Pacheco-Torgal and Jalali, 2011). Furthermore, natural reinforcements (sisal fibre, etc.) have been used to produce composite pipes, silos, tanks or low-budget housing projects (Vickers et al., 2015). Basalt FRP reinforcement (rebars, tendons, etc.) has already been utilized as internal reinforcement for the construction of concrete slabs (in bridge decks or roads, Fig. 9.8) and other concrete structures such as seismostations with nonmagnetic requirements (Fig. 9.9, Wu et al., 2010), in which basalt FRP barbending technology had to be developed to manufacture suitable stirrups, etc. (Fig. 9.10, Wu et al., 2010).

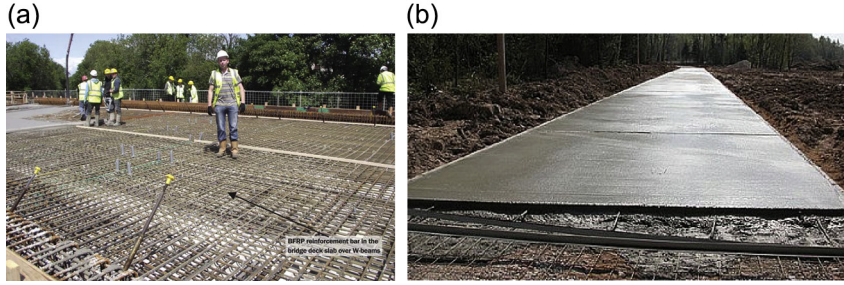

Figure 9.8 Bridge deck slab (http://magmatech.co.uk/downloads/Thompson_Bridge_Concrete_ Magazine.pdf.) or road construction with basalt bars (http://www.technobasalt.com/applications/ item/road-construction-1/.)

Figure 9.9 Use of basalt composite bars in seismostation in Lanzhou, China.
Adapted from Wu, Z., Wu, G., Wang, X., Hu, X., Jiang, J., 2010. New Progress in R & D of basalt fibres and BFRP in infrastructure engineering. Chinagbf.Com. Retrieved from: http://www.chinagbf.com/manage/webedit/uploadfile/2011221163046809.pdf.

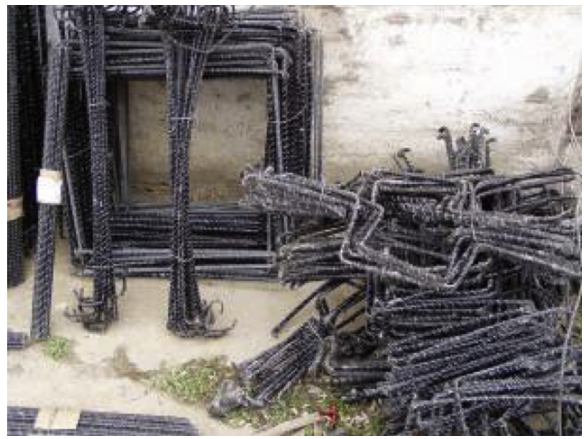

Figure 9.10 Bent bars and stirrups for use in reinforced concrete structure
Adapted from Wu, Z., Wu, G., Wang, X., Hu, X., Jiang, J., 2010. New Progress in R & D of basalt fibres and BFRP in infrastructure engineering. Chinagbf.Com. Retrieved from: http://www.chinagbf.com/manage/webedit/uploadfile/2011221163046809.pdf.

9.6 Concluding remarks and future trends

Natural fibre reinforced cementitious composites may provide a cheap and sustainable alternative to metallic or synthetic fibre-based reinforcements and jackets. They are light weight, with low environmental impact and biodegradability. As already mentioned, sustainability and recyclability issues are expected to become important drivers in the construction industry for the broader use of natural fibre reinforced cementitious

composites in commercial FRP products (Bank, 2006). Inorganic natural basalt fibres are in many cases a more advantageous alternative than common glass fibres and in some cases more than carbon ones. Several commercial products are already available in the construction industry, and there is a high potential for broader use, by ensuring optimized compatibility with cementitious matrices and enhanced durability.

As far as organic natural fibres are concerned, local cultivation may ensure a sustainable production chain besides their low environmental impact both in production and in the disposal phase (Asprone et al., 2011). On the other hand, the following barriers have been already acknowledged, restricting the broader development of organic natural fibres as building materials: variability in properties, less durability than common inorganic fibres because of high moisture and chemical absorption, cracking of cementitious matrices because of swelling and volume changes, weakening in alkaline environment and fibre-matrix bond-related issues (Parveen et al., 2012). In conclusion, more efforts should consider durability-related issues.

External seismic strengthening of masonry (and concrete) structures with cementitious natural fibre grid composites may provide a reliable, efficient and sustainable alternative. Further analytical research is required to quantify with accuracy the enhancement of this technique with respect to the retrofit system, the reinforcement layout and the masonry type (or concrete member). Efficient analytical tools will allow for the retrofit of a large number of existing masonry (or concrete) structures with damages (environmental deterioration, inadequate construction techniques and materials, design for gravity loads only) or high seismic vulnerability.

Basalt fibre ropes have revealed a remarkable potential in the efficient external wrapping of reinforced concrete columns that is superior to the already proven potential of FRs of high extension capacity. Therefore BFRs may combine the unique properties of their natural origin and high temperature resistance and easily be used with cementitious matrices (to serve mainly as a protective measure), as common or pretensioned wrapping. Seismic BFR wrapping (especially pretensioned), with suitable detailing, may restrict efficiently premature bar buckling (even of intermediate ones) in reinforced concrete columns, prevent relative slip of insufficiently lap-spliced bars and remarkably increase the shear strength capacity and axial strain ductility of concrete. Furthermore, it could prolong the elastic stress-strain behaviour of the column to increase its global antibuckling resistance and increase the axial load capacity (in cases that other more favourable strengthening measures could not be used). Already available design and predictive models may be utilized. Similarly, the use of BFRs as internal reinforcement in the partial replacement of steel stirrups in concrete beams seems to be a viable solution. Other natural organic fibre ropes may also be investigated in suitable applications.

References

Al-Salloum, Y., Elsanadedy, H.M., Alsayed, S.H., Iqbal, R.A., February 2012. Experimental and numerical study for the shear strengthening of reinforced concrete beams using textile-reinforced mortar. Journal of Composites for Construction 74−90. http://dx.doi.org/10.1061/(ASCE)CC.1943-5614.0000239.

ACI Committee 549.4R-13, 2013. Guide to Design and Construction of Externally Bonded Fabric - Reinforced Cementitious Matrix (FRCM) Systems for Repair and Strengthening Concrete and Masonry Structures. American Concrete Institute, Michigan, 2013.

Ansell, M.P., Mwaikambo, I.Y., 2009. The structure of cotton and other plant fibres. In: Eichhorn, S.J., Hearle, J.W.S., Jaffe, M., Kikutani, T. (Eds.), Handbook of Textile Fibre Structure, Natural, Regenerated, Inorganic and Specialist Fibres, vol. 2. Woodhead Publishing in Textiles. Number 88.

Ardanuy, M., Claramunt, J., Toledo Filho, R.D., 2015. Cellulosic fiber reinforced cement-based composites: a review of recent research. Construction and Building Materials 79, 115–128. http://dx.doi.org/10.1016/j.conbuildmat.2015.01.035.

Ascione, L., de Felice, G., De Santis, S., 2015. A qualification method for externally bonded Fibre Reinforced Cementitious Matrix (FRCM) strengthening systems. Composites Part B: Engineering 78, 497–506. http://dx.doi.org/10.1016/j.compositesb.2015.03.079.

Asprone, D., Durante, M., Prota, A., Manfredi, G., 2011. Potential of structural pozzolanic matrix-hemp fiber grid composites. Construction and Building Materials 25 (6), 2867–2874. http://dx.doi.org/10.1016/j.conbuildmat.2010.12.046.

Bank, L.C., 2006. Composites for Construction: Structural Design With FRP Materials. John Wiley & Sons, ISBN 0-471-68126-1, 551 pages.

Balaguru, P., Nanni, A., Giancaspro, J., 2009. FRP Composites for Reinforced and Prestressed Concrete Structures. In: A Guide to Fundamentals and Design for Repair and Retrofit. Taylor & Francis.

Balázs, G., 2012. Fibres in concrete structures [Chapter 9]. In: Fardis, M.N. (Ed.), Innovative Materials and Techniques in Concrete Construction. ACES Workshop.

Babaeidarabad, S., De Caso, F., Nanni, A., 2013. Out-of-plane behavior of URM walls strengthened with fabric-reinforced cementitious matrix composite. Journal of Composites for Construction. http://dx.doi.org/10.1061/(ASCE)CC.1943-5614.0000457.

Balsamo, A., Iovinella, I., di Ludovico, M., Prota, A., 2014. Masonry reinforcement with IMG composites: experimental investigation. Key Engineering Materials 624, 275–282. http://dx.doi.org/10.4028/www.scientific.net/KEM.624.275.

Brandt, A.M., 2009. Cement-based Composites Second Edition. Materials, Mechanical Properties and Performance. Taylor & Francis.

Cevallos, O., Olivito, R.S., Codispoti, R., Ombres, L., 2015. Flax and polyparaphenylene benzobisoxazole cementitious composites for the strengthening of masonry elements subjected to eccentric loading. Composites Part B: Engineering 71, 82–95. http://dx.doi.org/10.1016/j.compositesb.2014.10.055.

Cevallos, O., Olivito, R.S., 2015. Effects of fabric parameters on the tensile behaviour of sustainable cementitious composites. Composites Part B: Engineering 69, 256–266. http://dx.doi.org/10.1016/j.compositesb.2014.10.004.

Cheung, H.Y., Ho, M.P., Lau, K.T., Cardona, F., Hui, D., 2009. Natural fibre-reinforced composites for bioengineering and environmental engineering applications. Composites Part B: Engineering 40 (7), 655–663. http://dx.doi.org/10.1016/j.compositesb.2009.04.014.

Codispoti, R., Oliveira, D.V., Olivito, R.S., Lourenço, P.B., Fangueiro, R., August 2015. Mechanical performance of natural fiber-reinforced composites for the strengthening of masonry. Composites Part B: Engineering 77, 74–83. http://dx.doi.org/10.1016/j.compositesb.2015.03.021. ISSN 1359-8368. http://www.sciencedirect.com/science/article/pii/S1359836815001407.

Coutts, R.S.P., 1983. Flax fibres as a reinforcement in cement mortars. International Journal of Cement Composites and Lightweight Concrete 5 (4), 257–262.

De Caso Y Basalo, F.J., Matta, F., Nanni, A., 2012. Fiber reinforced cement-based composite system for concrete confinement. Construction and Building Materials 32, 55–65. http://dx.doi.org/10.1016/j.conbuildmat.2010.12.063.

Dhand, V., Mittal, G., Rhee, K.Y., Park, S.-J., Hui, D., 2015. A short review on basalt fiber reinforced polymer composites. Composites Part B: Engineering 73, 166–180. http://dx.doi.org/10.1016/j.compositesb.2014.12.011.

De Felice, G., De Santis, S., Garmendia, L., Ghiassi, B., Larrinaga, P., Lourenço, P.B., Papanicolaou, C.G., 2014. Mortar-based systems for externally bonded strengthening of masonry. Materials and Structures 2021–2037. http://dx.doi.org/10.1617/s11527-014-0360-1.

Faruk, O., Bledzki, A.K., Fink, H.P., Sain, M., 2012. Biocomposites reinforced with natural fibers: 2000-2010. Progress in Polymer Science 37 (11), 1552–1596. http://dx.doi.org/10.1016/j.progpolymsci.2012.04.003.

Fiore, V., Scalici, T., Di Bella, G., Valenza, a, 2015. A review on basalt fibre and its composites. Composites Part B: Engineering 74, 74–94. http://dx.doi.org/10.1016/j.compositesb.2014.12.034.

fib Bulletin 40, 2007. FRP Reinforcement in RC Structures, Fib Lausanne, 2007 (Convener of TG 9.3 Luc Taerwe).

Ghavami, K., 2005. Bamboo as reinforcement in structural concrete elements. Cement and Concrete Composites 27 (6), 637–649. http://dx.doi.org/10.1016/j.cemconcomp.2004.06.002.

Hollaway, L.C., Teng, J.G., 2008. Strengthening and Rehabilitation of Civil Infrastructures Using Fibre-reinforced Polymer (FRP) Composites. Woodhead Publishing Series in Civil and Structural Engineering No. 25.

Karantzikis, M., Papanicolaou, C.G., Antonopoulos, C., Triantafillou, T.C., 2005. Experimental investigation of non-conventional confinement for concrete using FRP. Journal of Composites for Construction, ASCE 9 (6), 480–487.

Di Ludovico, M., Prota, A., Manfredi, G., 2010. Structural upgrade using basalt fibers for concrete confinement. ASCE – Journal of Composites for Construction 14 (5), 541–552. Sept- Oct. 2010 (ISSN: 1090-0268).

Larrinaga, P., Chastre, C., San-José, J.T., Garmendia, L., 2013. Non-linear analytical model of composites based on basalt textile reinforced mortar under uniaxial tension. Composites Part B: Engineering 55, 518–527. http://dx.doi.org/10.1016/j.compositesb.2013.06.043.

Mallick, P.K., 2008. Fiber-reinforced Composites: Materials, Manufacturing and Design, third ed. CRC Press, Taylor & Francis, Boca Raton, FL.

Müssig, J., 2010. In: Mussig, J. (Ed.), Industrial Applications of Natural Fibres Structure, Properties and Technical Applications. John Wiley & Sons Ltd.

Nilsson, L., 1975. Reinforcement of Concrete With Sisal and Other Vegetal Fibres. Swedish Council for Building Research. Doc. D14.

Olivito, R.S., Cevallos, O., Carrozzini, A., 2014. Development of durable cementitious composites using sisal and flax fabrics for reinforcement of masonry structures. Materials and Design 57, 258–268. http://dx.doi.org/10.1016/j.matdes.2013.11.023.

Pacheco-Torgal, F., Jalali, S., 2011. Cementitious building materials reinforced with vegetable fibres: a review. Construction and Building Materials 25 (2), 575–581. http://dx.doi.org/10.1016/j.conbuildmat.2010.07.024.

Parveen, S., Rana, S., Fangueiro, R., 2012. Natural fiber composites for structural applications. In: Ferreira, A.J.M., Carrera, E. (Eds.), Mechanics of Nano, Micro and Macro Composite Structures. Politecnico di Torino, 18–20 June 2012. http://paginas.fe.up.pt/~icnmmcs/.

Pickering, K., 2008. In: Pickering, K.L. (Ed.), Properties and Performance of Natural-fibre Composites. Woodhead Publishing Limited, Cambridge, England.

Rousakis, T.C., 2013a. Hybrid FRP sheet – PP fiber rope strengthening of concrete members [Chapter 5]. In: Masuelli, M. (Ed.), Fiber Reinforced Polymers - the Technology Applied for Concrete Repair, ISBN 978-953-51-0938-9. http://dx.doi.org/10.5772/51425. Available from. http://www.intechopen.com/books/fiber-reinforced-polymers-the-technology-applied-for-concrete-repair/hybrid-frp-sheet-pp-fiber-rope-strengthening-of-concrete-members.

Rousakis, T., 2014a. Elastic fiber ropes of ultrahigh-extension capacity in strengthening of concrete through confinement. ASCE Journal of Materials in Civil Engineering 26 (1), 34–44.

Rousakis, T., 2013b. Hybrid confinement of concrete by FRP sheets and fiber ropes under cyclic axial compressive loading. ASCE Journal of Composites for Construction 17 (5), 732–743.

Rousakis, T.C., Kouravelou, K.B., Karachalios, T.K., 2014. Effects of carbon nanotube enrichment of epoxy resins on hybrid FRP – FR confinement of concrete. Elsevier, Journal of Composites Part B: Engineering 57, 210–218.

Rousakis, T.C., Tourtouras, I.S., 2014. RC columns of square section – passive and active confinement with composite ropes. Elsevier, Journal of Composites Part B: Engineering 58, 573–581.

Rousakis, T., 2014b. Retrofitting and strengthening of contemporary structures: materials used. In: Beer, M. (Ed.), Encyclopedia of Earthquake Engineering: Springer Reference. Springer-Verlag Berlin Heidelberg, 2013. 2014-03-23 12:12:26 UTC. www.springerreference.com.

Rousakis, T.C., Tourtouras, I.S., 2015. Modeling of passive and active external confinement of RC columns with elastic material. ZAMM Journal 95 (10), 1046–1057. http://dx.doi.org/10.1002/zamm.201500014. By Wiley-VCH Verlag GmbH & Co. KGaA, Article first published online: 6 AUG 2015.

Rousakis, T.C., Panagiotakis, G., Kostopoulos, A., Archontaki, E., 2015. Experimental testing of prismatic concrete columns confined by FRP and composite fiber ropes. In: Hui, D. (Ed.), Proceedings of the Twenty-third Annual International Conference on COMPOSITES/NANO ENGINEERING (ICCE-23). Chengdu, China 12–18/7/2015.

Rowell, R.M., 2008. Natural fibres: types and properties [Chapter 1]. In: Pickering, K.L. (Ed.), Properties and Performance of Natural-fibre Composites. Woodhead Publishing Ltd.

Saliba, C.C., Oréfice, R.L., Carneiro, J.R.G., Duarte, A.K., Schneider, W.T., Fernandes, M.R.F., 2005. Effect of the incorporation of a novel natural inorganic short fiber on the properties of polyurethane composites. Polymer Testing 24, 819–824. http://dx.doi.org/10.1016/j.polymertesting.2005.07.008.

Satyanarayana, K.G., Sukumaran, K., Kulkarni, a. G., Pillai, S.G.K., Rohatgi, P.K., 1986. Fabrication and properties of natural fibre-reinforced polyester composites. Composites 17 (4), 329–333. http://dx.doi.org/10.1016/0010-4361(86)90750-0.

Shimomura, T., Phong, N.H., 2007. Structural Performance of Concrete Members Reinforced with Continuous Fiber Rope. FRPRCS-8 Conference University of Patras, Patras, Greece, July 16–18.

Silva, F.D.A., Mobasher, B., Filho, R.D.T., 2009. Cracking mechanisms in durable sisal fiber reinforced cement composites. Cement and Concrete Composites 31 (10), 721−730. http://dx.doi.org/10.1016/j.cemconcomp.2009.07.004.

Staiger, M.P., Tucker, N., 2008. Natural-fibre Composites in Structural Applications [Chapter 8]. In: Pickering, K.L. (Ed.), Properties and Performance of Natural-fibre Composites. Woodhead Publishing Ltd.

Ticoalu, A., Aravinthan, T., Cardona, F., 2010. A review of current development in natural fiber composites for structural and infrastructure applications. Southern Region Engineering Conference. November, pp. 1−5.

Toledo Filho, R.D., Silva, F.D.a, Fairbairn, E.M.R., Filho, J.D.a M., 2009. Durability of compression molded sisal fiber reinforced mortar laminates. Construction and Building Materials 23 (6), 2409−2420. http://dx.doi.org/10.1016/j.conbuildmat.2008.10.012.

Toledo, R., Ghavami, K., England, G., Scrivener, K., 2003. Development of vegetable fibre mortar composites of improved durability. Cement and Concrete Composites 25, 185−196.

Torgal, F.P., Jalali, S., 2011. Eco-efficient Construction and Building Materials, ISBN 9780857298911.

Triantafillou, T.C., Papanicolaou, C.G., 2005. Textile reinforced mortars (TRM) versus fiber reinforced polymers (FRP) as strengthening materials of concrete structures. In: 7th International Conference on Fiber-reinforced Polymers in Reinforced Concrete Structures −FRPRCS7, Kansas City, USA, November 7−10.

Triantafillou, T.C., Papanicolaou, C.G., Zisimopoulos, P., Laourdekis, T., 2006. Concrete confinement with textile reinforced mortar (TRM) jackets. ACI Structural Journal 103 (1), 28−37.

Triantafillou, T.C., 2007. Textile-reinforced mortars (TRM) versus fibre-reinforced polymers (FRP) as strengthening and seismic retrofitting materials for reinforced concrete and masonry structures. In: International Conference on Advanced Composites in Construction (ACIC07). University of Bath.

Vickers, L., van Riessen, A., Rickard, W.D., 2015. Fire-resistant Geopolymers. SpringerBriefs in Materials. http://dx.doi.org/10.1007/978-981-287-311-8.

Wecławski, B.T., Fan, M., Hui, D., 2014. Compressive behaviour of natural fibre composite. Composites Part B: Engineering 67, 183−191. http://dx.doi.org/10.1016/j.compositesb.2014.07.014.

Wang, X., Shi, J., Liu, J., Yang, L., Wu, Z., April 2014. Creep behavior of basalt fiber reinforced polymer tendons for prestressing application. Materials and Design 59, 558−564. http://dx.doi.org/10.1016/j.matdes.2014.03.009.

Wu, G., Dong, Z.-Q., Wang, X., Zhu, Y., Wu, Z.-S., 2014. Prediction of long-term performance and durability of BFRP bars under the combined effect of sustained load and corrosive solutions. Journal of Composites for Construction 1−9. http://dx.doi.org/10.1061/(ASCE)CC.1943-5614.0000517.

Wu, Z., Wu, G., Wang, X., Hu, X., Jiang, J., 2010. New Progress in R & D of basalt fibres and BFRP in infrastructure engineering. Chinagbf.Com. Retrieved from: http://www.chinagbf.com/manage/webedit/uploadfile/2011221163046809.pdf.

Zhao, X., Wang, X., Wu, Z., Zhu, Z., April 2016. Fatigue behavior and failure mechanism of basalt FRP composites under long-term cyclic loads. International Journal of Fatigue 88, 58−67. http://dx.doi.org/10.1016/j.ijfatigue.2016.03.004.

Manufacturers of basalt products:

Kamenny Vek Basfiber Rebar, http://www.basfiber.com/Sites/basfiber/Uploads/Basfiber%20for%20construction%20%28SI%29.8A53BF0AC6BB4E2C801A5CF5485F4E15.pdf, http://www.basfiber.com/src/bridges.pdf.

MagmaTech Rockbar, http://magmatech.co.uk/downloads/RockBar.pdf.

Sudaglass Rod, http://www.sudaglass.com/rods.html, http://www.sudaglass.com/chars.html.

Incotelogy Basalt Fiber Rebars, http://incotelogy.de/produkte/kunststoffe/?lang=en.

GBF Basalt Rebar, http://www.basaltfiber-gbf.com/basalt-rebar-manufacturer.html.

Technobasalt, http://www.technobasalt.com/products/item/basalt-rebar-1/.

Development of bamboo fiber-based composites

10

G. Wang, F. Chen
International Centre for Bamboo and Rattan, Beijing, People's Republic of China

10.1 Introduction

Bamboo is one of the strongest and fastest growing plants in the world. About 22 million hectares of world's surface is covered in bamboo forest. One-third of the land mass of bamboo forest resides within China, which makes it the richest nation in the world (Peng et al., 2013). There are a multitude of advantages for using bamboo as a product, which include fast growth (needs only three to five years to grow into useful timber), sustainable utilization (a bamboo timber can be harvested multiple times from a single planting), high strength and stiffness (about two to three times when compared to wood), easy to process, and eco-friendly (list how much carbon it pulls out of air) (Zakikhani et al., 2014; Xiao et al., 2013; Yu et al., 2014b). In the past seven thousand years, people have continued utilizing and researching bamboo. Bamboo has provided abundant and high-quality cellulose fibers for centuries, becoming a primary feedstock for weaving, pulp, paper, and fiber-based composite industries in China. Bamboo products include traditional daily necessities and handcrafted articles, such as bamboo plywood, bamboo pulp-based products, bamboo fiber products, bamboo charcoal, bamboo vinegar, bamboo shoot-processed products, bamboo leaf extracts, etc. (Chen et al., 2011; Lugt et al., 2005). There is a total of 10 categories of bamboo products that include more than 100 series and thousands of varieties. The total volume of bamboo products exported annually reached over 28 billion dollars in China and were sold in more than 30 countries. Since 1995, the field research concerning bamboo fiber reinforced composites (BFRCs), dedicated to developing economical and lightweight green composites, has become more prominent with each passing year (Rassiah et al., 2014; Nugroho and Ando, 2001; Deng et al., 2014a,b).

Even though the bamboo industry uses bamboo to make crafts, furniture, plywood, bamboo wood composites, and more while taking advantage of bamboo's strong material properties, it fails to maximize on the economic and ecological strengths. The problem of the current bamboo industry is that it has a low comprehensive utilization rate of bamboo resources and very little automation, it produces little to no high value products, and there is not a degree of scale to it (Wang et al., 2013). BFRCs encountered many challenges during their development and manufacturing, summarized as follows:

1. It is difficult to obtained long, fine, and straight fibers directly from bamboo culm, while keeping the original bamboo characteristics. There are mainly three methods used to

Advanced High Strength Natural Fibre Composites in Construction. http://dx.doi.org/10.1016/B978-0-08-100411-1.00010-8

ret bamboo fiber. Mechanical extraction (steam explosion method, retting, crushing, grinding, rolling mill), chemical extraction (degumming, alkali or acid retting, chemical retting) and combined mechanical and chemical extraction (Zakikhani et al., 2014). However, the treatment of steam explosion or chemical separation likely damages the orientation of the natural bamboo fibers and usually produces only short fibers (Shao et al., 2008).

2. Compared to wood, it is relatively difficult for bamboo to obtain the fibrillation veneer with an even thickness and uniform size due to the change in diameter of the bamboo from the bottom of the stalk to the top (Chen et al., 2014b). Furthermore, the mechanical and physical properties of the main body in the middle part of bamboo culm are significantly different from that of the outer layer and inner layer, which have wax and silicium compounds on the surface, which make it difficult to glue (Grosser and Liese, 1971).
3. It is difficult to obtain a dedicated design for BFRC as a structural material. It is important for a biomaterial to have superior stability and uniformity when used for architectural purposes. The improvement of uneven stress distribution and a decrease in the coefficient of variation for the BFRC is a major concern (Chen et al., 2014a).

The main objective of this chapter is to provide the basic knowledge required to make BFRC an efficient, sustainable, and competitive structural material. Major areas of focus include understanding the characteristic and behavior of bamboo fiber and their functional contributions to advanced BFRC as a high-strength composite (Part I); discussing three advanced bamboo-based composite materials, along with their processing techniques, performance, and application (Part II); and discussing the prospects of scientific R&D of bamboo fiber-based composites with unconventional structures (Part III). The R&D for advanced bamboo fiber-based composites will propel the bamboo industry past traditional fields of bamboo manufacturing to newer forms of production and automation.

10.2 The characteristics of bamboo and its fiber

10.2.1 The characteristics of bamboo

From the macrolevel, bamboo has a structure of a hollow section and a thin wall with a certain tapering shape (Liu et al., 2012). From the tissue level, bamboo consists of unidirectional fibers that are reinforced by parenchymatous ground tissue that functions as a matrix (Fig. 10.1). The nonuniform distribution of vascular tissue along the radius direction indicates the feature of functionally graded materials for bamboo. Bamboo has more than 10 cellular layers in its cell structure, with each dissimilar microfibril orientation with thick layers and thin layers in alternate arrangement on the cell wall of bamboo fibers.

The main chemical compositions of bamboo include cellulose, hemicellulose, and lignin, all kinds of extractions, a little ash, and silicon dioxide. All of these structures and characteristics contribute to bamboo's superior strength, toughness, bending ductility, and low density.

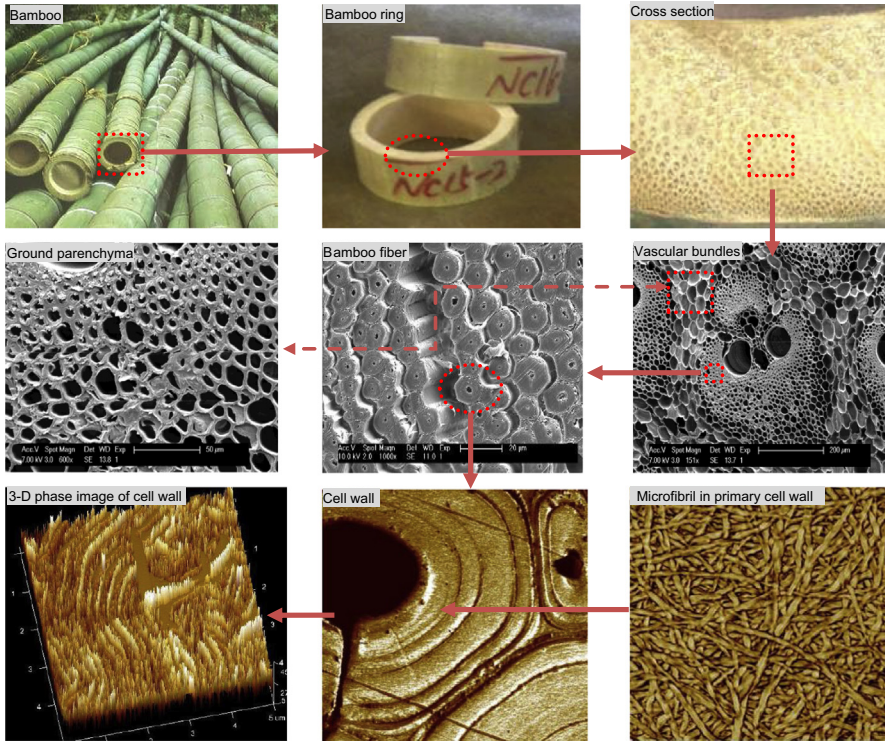

Figure 10.1 The morphology and composition of bamboo on different levels.

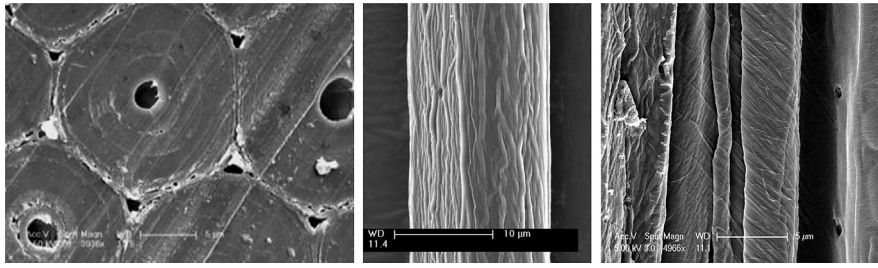

Figure 10.2 The typical Emission Scanning Electron Microscope (ESEM) images of a longitudinal section of a single fiber.

10.2.2 The characteristic of a single bamboo fiber

10.2.2.1 Morphology

The microstructure of a single bamboo fiber, as shown in Fig. 10.2, has a multilayered wall structure that is in concentric circles. The layers consist of a thick cell wall, small lumen, a few pits, and a small microfibril angle. The size of single bamboo fibers are 10−30 µm in diameter and 1−4 mm in length (Wang et al., 2011; Yu et al., 2014a).

10.2.2.2 Surface wettability

The research of surface wettability for different materials characterized by contact angle (CA) testing has contributed to the investigation of interfacial bonding behaviors and improved the permeability of BFRC. The CA of single bamboo viscose fiber and terylene fiber measured at different temperatures and relative humidity were compared. In Fig. 10.3, the temperature and humidity have a significant effect on the CA of natural plant fiber, such as bamboo, due to its unique structure and chemical composition. While the CA of terylene as a chemical synthetic fiber varied little with changing temperature and almost remained the same when the humidity changed (Chen et al., 2013a).

10.2.2.3 Tensile properties

The mechanical properties of a single fiber are essential for predicting the performance of bamboo fiber-based composites. The length and diameter of single bamboo fibers are very small and require a custom designed microtester (SF-I). The microtester was developed by the International Center for Bamboo and Rattan (ICBR) and consisted of a ball and socket system, which was observed using a confocal laser scanning microscope (Wang et al., 2011) (Fig. 10.4).

The tensile properties of different forms of bamboo in Table 10.1 show that the highest value of tensile strength and modulus (MOE) are observed in single bamboo fiber chemical isolation, and then in mechanical separation, followed by vascular bundle mechanical separation, bundle fiber, and finally with bamboo strip as the weakest. It can be seen that bamboo treated with chemical isolation perform much better than those prepped using mechanical separation. As the unit size of bamboo increases, the mechanical properties of the bamboo decline. The decline is probably due to the effect of weak interfaces that exist in the bamboos fiber middle lamella and fiber damage caused by sample preparation and treatment. In order to maintain fiber strength, it is critical to damage fiber during preparation processing.

10.2.3 The characteristics of bamboo bundle fiber and veneer

10.2.3.1 Preparation of bamboo bundle fiber veneer

Bamboo bundle veneer is processed by extracting long fibers with a mechanical treatment, and then the veneers are linked together via one-piece veneer formation technology (Chen et al., 2013b). The bamboo has been split, and the nodes along the sides are removed using a hatchet. The bamboo stalk is then fed into an untwisting machine, which will broom and roll the bamboo strips into a bamboo bundle, which is a loosely laminated reticulate sheet. Stalks are fed through the untwisting machine between five and seven times, until the outer green bark is removed and the fibers are fully separated (the number of times is dependent on species). A laminated bamboo bundle veneer is made by sewing the untwisted bamboo bundles in the width direction with cotton thread (Fig. 10.5).

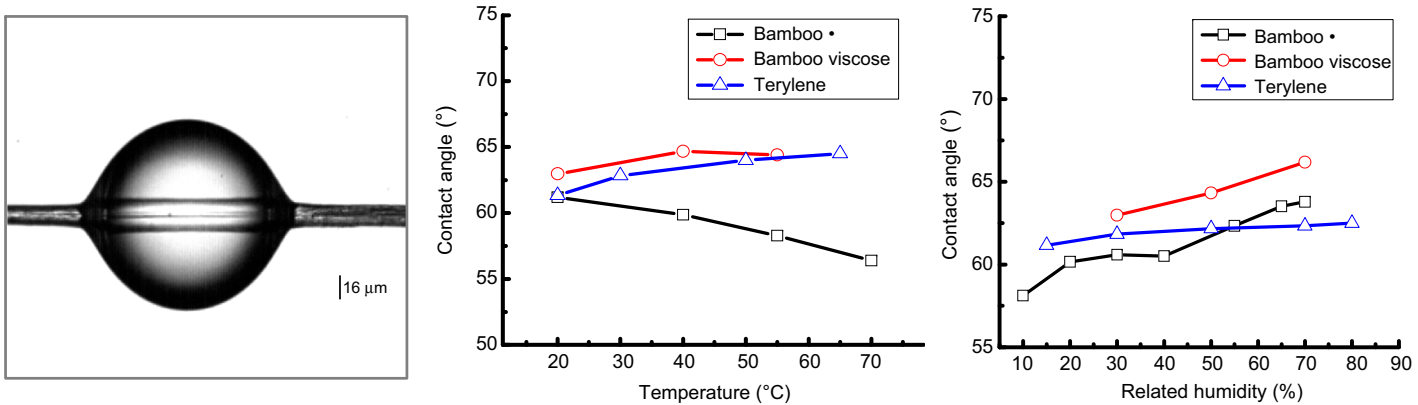

Figure 10.3 Contact angle of bamboo and terylene in different humidity and temperature.

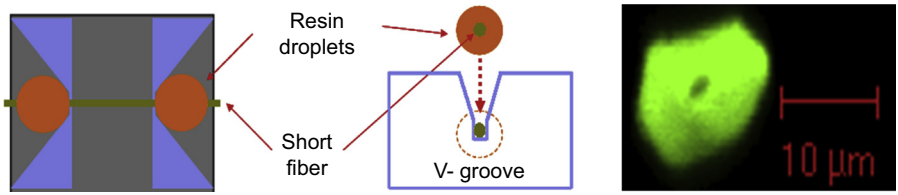

Figure 10.4 Ball and socket system and typical confocal laser scanning microscope (CLSM) images of the cross section of single bamboo fibers.

Table 10.1 Comparison of tensile properties of different form units of bamboo

Bamboo unit	Preparation method	Tensile strength (MPa)	Tensile modulus (GPa)	Elongation (%)
Single fiber	Chemical isolation	1770.00 (0.15)	26.85 (0.06)	2.89 (0.16)
	Mechanical separation	930.00 (0.19)	34.62 (0.17)	4.30 (0.17)
Vascular bundle	Mechanical separation	470.87 (0.21)	28.59 (0.16)	–
Bundle fiber	Chemical isolation	610.00 (0.37)	23.56 (0.35)	2.61 (0.32)
	Mechanical separation	290.00 (0.71)	16.50 (0.42)	1.68 (0.31)
Bamboo strip	Mechanical separation	192.84 (0.80)	14.72 (0.74)	4.28 (0.46)

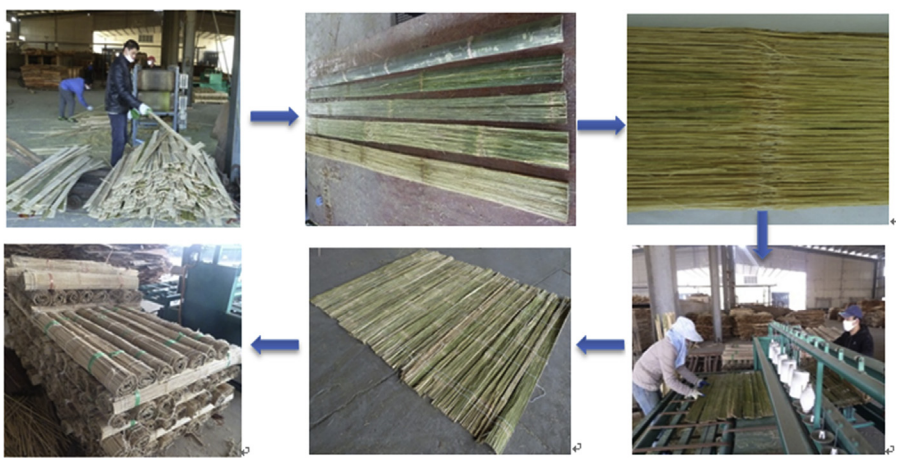

Figure 10.5 Production of bamboo bundle veneer.

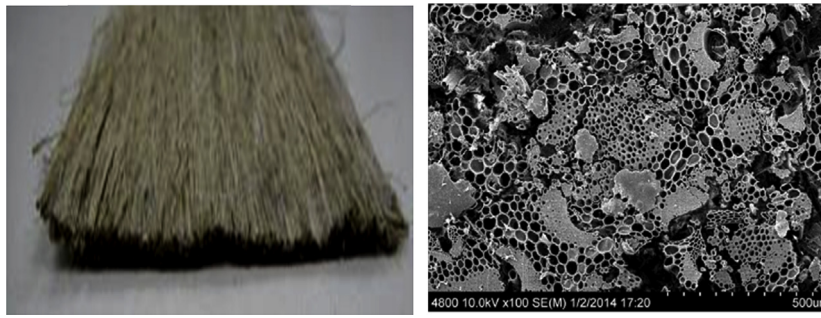

Figure 10.6 The brooming bundle fiber and its Emission Scanning Electron Microscope (ESEM) images of the cross section of a bamboo bundle.

Besides the use of an untwisting machine to physically broom the bamboo strips into bamboo bundle fibers, chemical isolation was also used. The benefit of chemical isolation is that it can remove the lignin and part of hemicellulose. A sodium sulfite pulping method is a chemical isolation process that is traditionally used in the textile industry in order to obtain the recombination of cellulose molecules. While chemical isolation does give a larger tensile strength and MOE, the fibers that are created using this method are too short for making bamboo bundle veneer, whereas the fibers from physical booming are large enough to be used in bamboo bundle veneers. The physical brooming method is broadly applied in the process of bamboo scrimber and laminated veneer lumber (LVL) (Zhang et al., 2014).

10.2.3.2 The effect of brooming times on bamboo fiber

Bamboo bundle fiber cross sections observed by Field Emission Scanning Electron Microscope (FESEM) Fig. 10.6 show that under the effect of mechanical rolling and untwining, the basic cellar structure of bamboo was totally smashed. The vascular bundle and parenchymatous ground tissue of bamboo was separated (Yu et al., 2014b). A large amount of microfractures occurred between each fiber. These microfractures are beneficial due to the fact they allow resins to be immersed into them, which creates a stronger interface between the fiber and resin (Qin et al., 2013). By creating stronger interfaces the material characteristics of BFRC are greatly increased.

In addition to the strengthened interface caused by brooming, the number of times the bamboo bundle goes through brooming will greatly affect the size of the bamboo bundle breadth and its mechanical properties. The breadth of a bamboo bundle increases with each time it goes through the brooming process, and by the sixth time it is broomed the process has very little effect on the characteristics and dimensions of the bundle. The tensile strength of a bamboo bundle fiber decreases with each time it goes through brooming. For the *Ci* zhu species of bamboo the internode bundle could maintain a tensile strength of 100 MPa before its sixth brooming, indicating that the sixth brooming is the optimized number of times for this species of bamboo in order for it to be a suitable bundle fiber (Fig. 10.7).

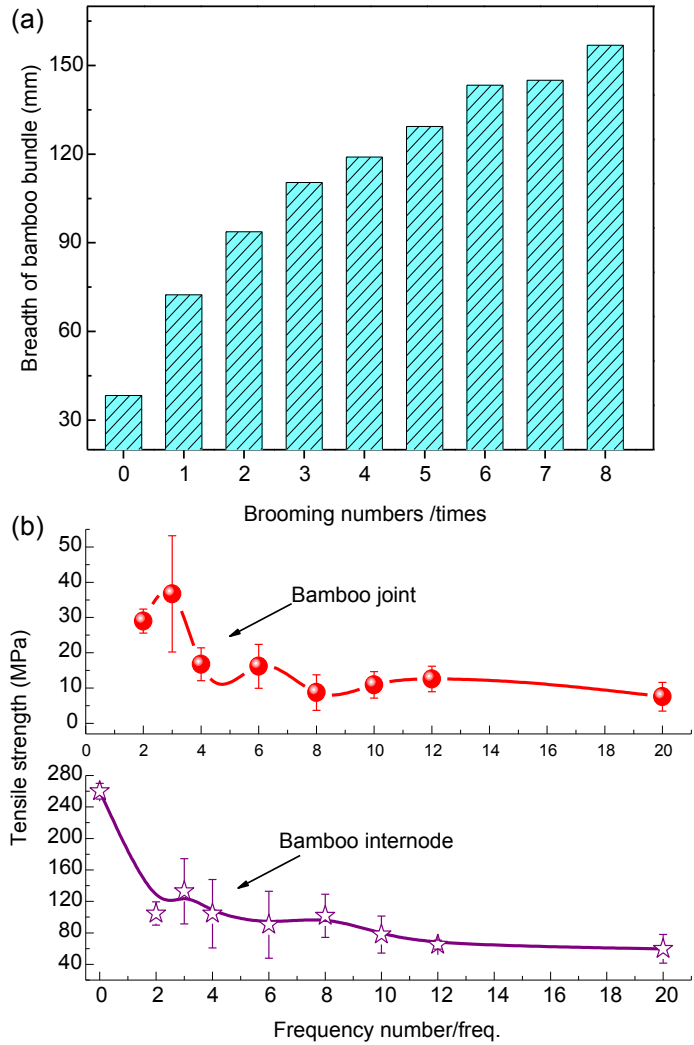

Figure 10.7 The effect of brooming on bamboo bundle fibers: (a) size of cross section and (b) tensile property.

10.3 Development of advanced bamboo fiber composites

10.3.1 Bamboo bundle veneer lumber

10.3.1.1 Manufacturing technique

Bamboo scrimber is a bamboo-based product widely used in the construction of furniture and architecture materials in China. Due to the high density, uneven ply

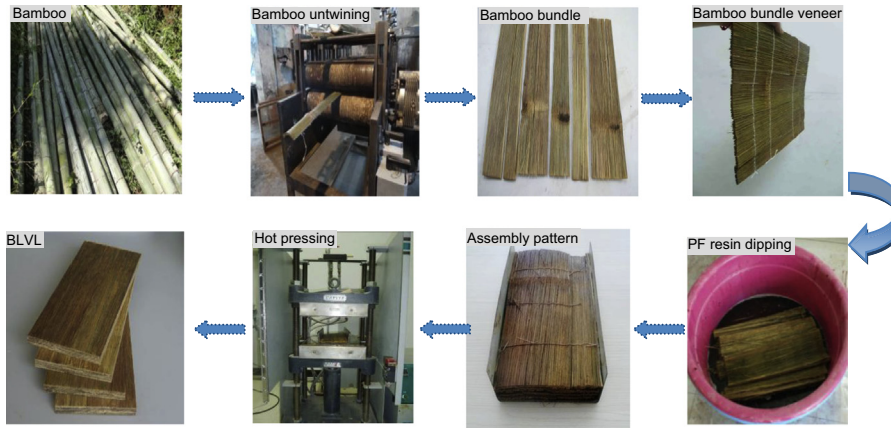

Figure 10.8 Production of bamboo bundle laminated veneer lumber.

organization, and large residual stress of scrimber, its use is limited in construction (Yu and Yu, 2013). In order to overcome the drawbacks of using scrimbers a process of brooming bamboo bundles was developed by the ICBR (Fig. 10.5). This process allows a bamboo bundle fiber to be made into a large uniform bamboo bundle veneer. The specific production of BLVL Fig. 10.8 begins with a veneer being immersed in the phenol formaldehyde resin for five to seven minutes and dried to an moisture content(MC) of 10−12% under an ambient environment. Then the resin-soaked veneers are layered symmetrically along the grain direction with the outer layer of bamboo bundle facing upward. The layered bamboo veneers are placed in a hot press, where they are pressed down to the desired thickness and the press is heating up to 150°C over a 10-min period. The veneers remain pressed at the desired thickness at 150°C for 10 min, after which the press maintains the same thickness while being cooled back to room temperature over a 10-min period. By using cooling cycle water, the upper and lower press plates of the hot press are maintained at room temperature before closing and opening. This "cold−cold" process is used to ensure a complete curing of the resin, which helps to prevent bubbling in the composites (Li et al., 2014; Cheng et al., 2009).

10.3.1.2 Mechanical and physical properties of bamboo bundle laminated veneer lumber

The untwining process coupled with the veneer laminating process made it possible to use bamboo scrimber to produce structural materials with uniform density and stable performance. A series of studies about the properties of BLVL were performed about its density uniformity, static mechanical performance (bending and shear), dynamic impact resistance, uniform load performance, termite resistance, hydrothermal property, dimension stability, connection behavior, and other aspects (Deng et al., 2014c; Yu et al., 2012a,b, 2014c).

Table 10.2 Physical and mechanical properties of bamboo wood laminated veneer lumber corresponding to different loading direction and ply organization types

Assembly types	Air-dry density (g/cm^3) $F_{sum} = 11$, $p < .01$	MOR (MPa)		MOE (GPa)		Shearing strength (MPa)	
		Perpendicular $F_{sum} = 30$, $p < .01$	Parallel $F_{sum} = 25$, $p < .01$	Perpendicular $F_{sum} = 60$, $p < .01$	Parallel $F_{sum} = 38$, $p < .01$	Perpendicular $F_{sum} = 82$, $p < .01$	Parallel $F_{sum} = 32$, $p < .01$
7B	1.028	253.06a	220.61a	25.39c	23.40c	22.43e	25.25f
	(0.04)	(40.71)	(27.71)	(1.69)	(1.89)	(2.02)	(2.57)
7P	0.500	81.22a	110.64b	11.67c	12.77c	5.27e	9.64f
	(0.02)	(27.38)	(7.86)	(1.15)	(0.87)	(1.36)	(1.43)
BPPPPPB	0.660	196.07a	130.25b	19.89c	14.29d	14.24f	15.68f
	(0.05)	(19.24)	(25.62)	(1.64)	(1.85)	(1.87)	(3.62)
BPBPBPB	0.810	219.44a	173.10b	21.84c	18.65d	14.86f	16.77f
	(0.04)	(23.03)	(21.32)	(1.46)	(1.57)	(2.51)	(2.45)
BBPPPBB	0.811	243.39a	177.72b	22.83c	18.60d	16.66e	20.33f
	(0.04)	(36.57)	(12.42)	(2.20)	(1.15)	(1.22)	(2.14)
BBPBPBB	0.886	240.80a	193.09b	23.65c	20.39d	16.51f	19.58f
	(0.06)	(26.09)	(13.45)	(1.25)	(0.83)	(3.09)	(3.73)
BPPBPPB	0.756	193.60a	189.44a	20.14c	19.74c	14.97f	14.44f
	(0.04)	(23.92)	(19.27)	(1.76)	(1.97)	(2.34)	(1.18)
PBPBPBP	0.717	153.06a	134.65a	17.17c	16.38c	11.85f	11.78f
	(0.03)	(30.30)	(23.32)	(1.21)	(1.27)	(1.32)	(1.53)

P represents poplar wood veneer and B represents bamboo bundle veneer; the values in parentheses are standard deviations, and a lowercase letter represents a significant difference of the effect of loading way on the mechanical properties on 0.05 level.

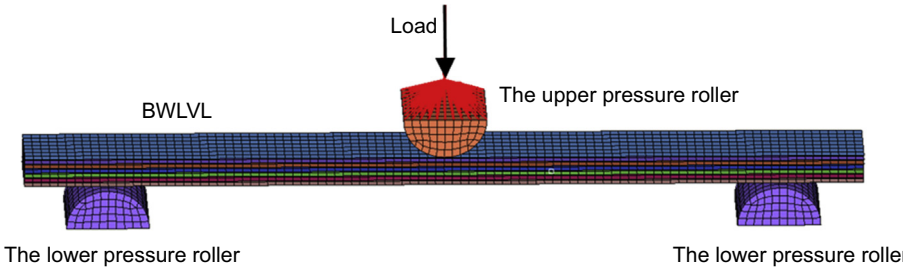

Figure 10.9 The finite element model for seven-layer bamboo and wood laminated lumber.

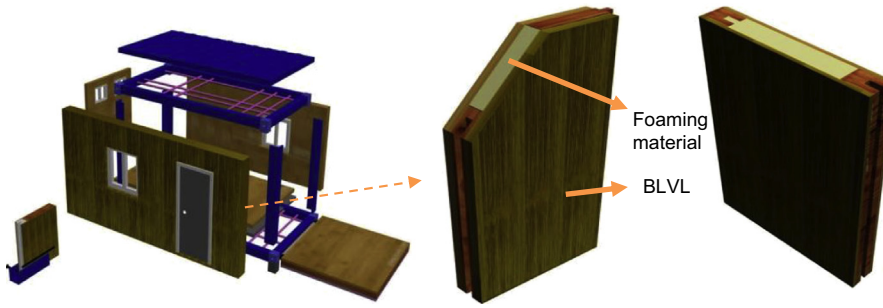

Figure 10.10 Application of lightweight bamboo-based wall in bamboo steel house.

The results indicated BLVL possessed excellent mechanical properties (Table 10.2), with a density of 1.0 g/cm^3, tensile strength and modulus of 203 MPa and 20.3 GPa, horizontal shear strength of 22.4 MPa, static bending strength (MOR) and modulus (MOE) of 253.1 and 25.4 MPa, and thickness swelling rate less than 8% in 24 h. The performance of BLVL is a combination of high strength, dimensional stability, durability, reliable structural properties, and flexible design. All of these characteristics represent why BLVL is an ideal green building material for all forms of structures.

10.3.1.3 Application of bamboo bundle laminated veneer lumber

BLVL has excellent longitudinal mechanical properties that make it an effective structural component for columns, beams, and girders. BLVL has been used to construct walls in bamboo/wood structure housing in Wuxi, Jiangsu Province, China. Due to its thermal properties, BLVL makes a far superior insulator when compared to the standard concrete that is used to construct walls. In addition, the hallow core of the BLVL walls can be filled with bamboo fiber foam, which further improves the insulation of the material and makes it fire-retardant (Fig. 10.10).

The use of BLVL for the construction in bamboo/wood structures has led to it being used in the development of lightweight walls in modular steel frame structures (Fig. 10.10).

Figure 10.11 Large-span double beam component made by bamboo bundle wood hybrid laminated composites.

With the market in China for large-scale green construction growing, there has been an urgent need for the development of a product to fill this ever-growing demand. Large-span BLVL was developed to fill the role of a large-scale green structural material (Fig. 10.11). Large-span BLVL is constructed by using two pieces of BLVL and bolting them together using a series of clamps to form a double beam (Fig. 10.11). The pieces of BLVL used to construct the large-span BLVL are a continuous length and are manufactured using an intermitted hot press process that allows for longer pieces of BLVL. In order to further improve the properties of large-span BLVL, the BLVL was replaced with bamboo bundle wood laminated veneer lumber (BWLVL), seen in Table 10.2 and Fig. 10.9. BWLVL was an improvement over BLVL, due to it effectively combining the advantages of bamboo and wood. In BWLVL the low density wood core helped to reduce weight and improve the stability, while the bamboo veneer surface layers provided the stiffness and strength needed for large-scale construction. The finite element model for seven-layer bamboo and wood laminated lumber was developed and successfully simulated the variation tendency of bending behaviors for the different laminated pattern of BWLVL under elastic and plastic limit loads (Chen, 2014).

In Qingdao, Shandong, China, the designs for a villa using large-span BWLVL is being planned, and one of the major concerns is how to properly protect large-span BWLVL from the weather and decay. A process has been developed where the bamboo bundles are treated with preservatives before being turned into veneer, and once the beam is constructed, epoxy paint and petroleum asphalt are applied for further protection. With this protection, large-span BLVL can be used as exterior support elements in outdoor structures, as shown in Fig. 10.11.

10.3.2 Core-shell structured bamboo plastic composites

10.3.2.1 Materials and preparation

Bamboo residue fiber (BR), bamboo pulp fiber (BPF), and white mud (WM) were supplied by Guizhou Chitianhua Co. Ltd. (Chishui, China). The lubricant PE-wax was obtained from Yi-li Chemical Reagent Company (Beijing, China) and was used to improve the processing of the BPC profile. Virgin high-density polyethylene (V-HDPE, DGDK-3364) with a density of 0.945 g/cm^3, a melt flow index of 0.075 g/min (190°C, 2.16 kg),

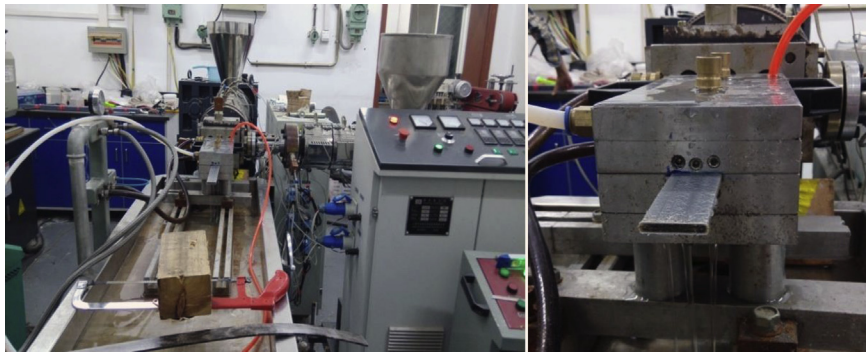

Figure 10.12 Production line of core-shell structured bamboo plastic composites

and a tensile strength of 22.1 MPa was provided by Zhangmutou Plastic Co. Ltd. (Guangzhou, China). The compatibility of fiber/plastic blends was improved with the addition of Maleic anhydride, in the form of maleated polyethylene (MAPE, CMG9801), also acquired from Zhang Mu Tou Co. Ltd. (Guangzhou, China). BR and BPF were dried at 80°C for 24h before blending with V-HDPE. WM was grinded to 800-mesh before blended with other materials. Before the coextrusion process, the core and shell systems were pelletized using a twin-screw extruder at 150°C,160°C,165°C,175°C, and 150°C die temperature. V-HDPE and BR were used as core systems. Materials used for the shell were V-HDPE, BPF/HDPE, and WM/HDPE, and the abbreviations of the corresponding core-shell structured BPC are CSHDPE, CSBPF, and CSWM, respectively (Xian et al., 2016).

10.3.2.2 Manufacture process of core-shell structured bamboo plastic composites

The core-shell structured BPC were directly prepared using a single-screw/single-screw coextruder system. Coextrusion is a process in which two or more polymer materials are extruded together to produce different multilayer structures, e.g., pipes, panels, and core-shell profiles (Kirchmajer 2015; Negendank et al., 2012; Koh et al., 2002). The final products have shown excellent properties for different types of material used. In addition, coextrusion is suitable for the use of certain waste materials, thereby significantly reducing the production costs. Because of its advantages, coextrusion technology has been recognized for potential applications in wood/bamboo plastic composites (Kim et al., 2013). Also, the work focused on the application of coextrusion in BPC is very limited.

The composites were formulated with three shell types per core system. The core system was V-HDPE:BR:MAPE = 65:30:4:1*wt%* PE-wax. The three shell types were V-HDPE:MAPE=95:4:1*wt%* PE-wax, V-HDPE:BPF:MAPE=90:5:4:1*wt%* PE-wax, and V-HDPE:WM:MAPE=90:5:4:1*wt%* PE-wax, respectively. The composites were manufactured with a coextrusion system. The system consists of a 30-mm single-screw extruder (Shanghai Sunlight Plastic Machinery Manufacturing

Co., Ltd.) for the core and a 20-mm single-screw extruder (Shanghai Sunlight Plastic Machinery Manufacturing Co., Ltd.) for the shell. A specially designed die, with a cross-sectional area of 4×30 mm^2 was used in combination with the core; the shell thickness was controlled by adjusting the ratio core/shell extruder rotational speed to 1:2. Manufacturing temperatures at the die for the core systems were 160°C,165°C,170°C,170°C, and 165°C; the same for shell formulations were from 160−180°C. The coextruded BPC are cooled using a 2-m water tank with controlled water spray. The extrusion speed is maintained by a speed-controlled puller. The details can also be found in the literature.

10.3.2.3 The characteristic of core-shell structured bamboo plastic composites

As can be observed from the cross section of BPC, the mechanical performance of the core-shell structured BPC is dependent upon the quality of the core-shell adhesion. There are almost no gaps existing in the core and the shell layer. This morphology suggests that a better surface contact area between the core and the shell has been realized (Fig. 10.13A(a)). The cross section of core-shell structured BPC with BPF/HDPE shell materials can be seen in Fig. 10.13A(b). One may observe that the section of the core-shell structured BPC became rougher with the presence of BPF. In general, the section with fibers that are surrounded by a large quantity of matrix material can be commonly associated with good fiber-matrix interfacial adhesion.[25] But Fig. 10.13 A(b) shows that exposed fibers are more frequent for this sample. This may indicate that the fibers are unevenly dispersed in the HDPE. The SEM micrographs taken from the section of the composites with the WM/HDPE shell layer are shown in Fig. 10.13A(c). It can be concluded that there are noticeable gaps (insufficient contact) between the core and the shell layer. Small gaps that can be observed at the interface revealed weak interfacial

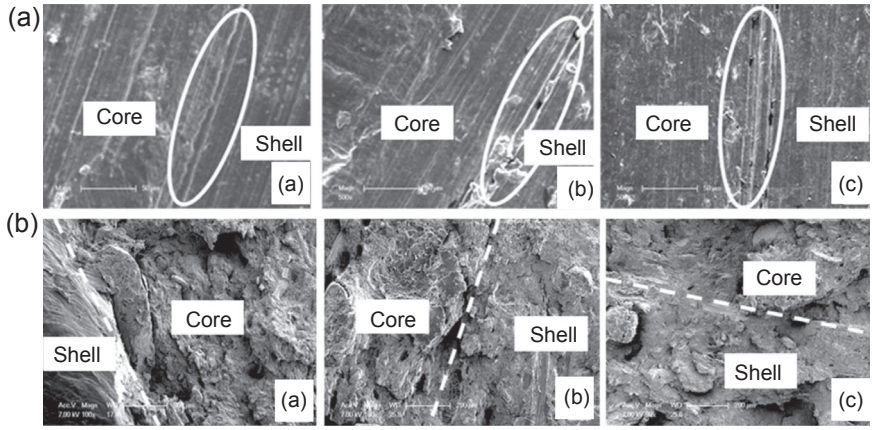

Figure 10.13 SEM micrographs of the core-shell structured bamboo plastic composite: the cross section (A), the fractured surface (B), (a) core-shell high-density polyethylene, (b) core-shell bamboo pulp fiber, and (c) core-shell white mud.

bonding. In other words, the poor mechanical properties can be due to the lack of good interfacial bonding between the core and the shell layer. This can be correlated with the degradation of flexural properties, as discussed in the previous section. The degradation of the flexural properties of the core-shell BPC can be caused by the weak interfacial adhesion in the presence of BPF or WM. In other words, the BPF or WM has negative effects on the interface properties of the ITZ. Fig. 10.13B shows the impact fractured surfaces of the core-shell structured BPC. Fig. 10.13B(a) is evidence that the fractured section of the V-HDPE is smooth. From Fig. 10.13B(b), it can be seen that the BPF pull out with the addition of BPF in the shell. As shown in Fig. 10.13B(c), when loading WM in the shell, the fractured section shows many defects, like holes. Even the agglomerates begin to appear; this is because WM partly forms the clusters or agglomerated structures in the HDPE matrix. The pullout and the presence of voids in the fractured section are probably responsible for the poor mechanical and interface properties.

Dynamic mechanical analysis was used to investigate the storage modulus, the loss modulus, and the mechanical loss factor (tanδ) of composites under dynamic temperature or frequency conditions. The dynamic behavior of polymer composites can essentially reflect the structure of composites, relations between the molecular movement and performance, and the compatibility of each component in the composites. The total energy dissipation under cyclic load can be divided into the core, the shell layer, and the interface between them. If the interfacial adhesion is poor, continuous cyclic loading of composites results into higher energy dissipation at the interface (Kennedy et al., 1992).

Fig. 10.14 shows the frequency dependence of storage modulus (E'), loss modulus (E''), and mechanical loss factor (tanδ) for the core-shell structured BPC. As shown, the E' for the three composites increases with the frequency, with the same consistently at a high frequency as compared to a low frequency. In other words, the dynamic stiffness of composites was higher than the static stiffness; it states that the structure stability of the material is good under high frequency. This is because under a constant force, the viscoelasticity of polymers is a function of temperature, time, and frequency. As the external force is maintained constant, the molecules of composites reduce the effect of external stress through recombination. The molecule of composites recombines fast within a short period of time. So the modulus of composites at high-frequency loading was higher than that for low-frequency loading. The increase of storage modulus of the core-shell structured BPC indicates that the composites exhibited better interactions between the core and the shell. This performance achieves a higher modulus for CSHDPE. The highest value of the dynamic modulus can be achieved for CSHDPE, rather than for CSBPF or CSWM. This tendency statistically correlates to the bending test as well. In that way, the imperfect interfaces between the core and shell layer in the CSBPF and CSWM. Fig. 10.14 b shows the loss modulus of the three composites being decreased with the increase of frequency. It is noteworthy that the E'' of the core-shell structured BPC with the V-HDPE shell is higher than that of the other BPC. The results indicate that the heat generated by molecular movement was less, and as a result the energy loss in the composites was lower. A similar trend was observed in mechanical loss factor (tanδ) of the

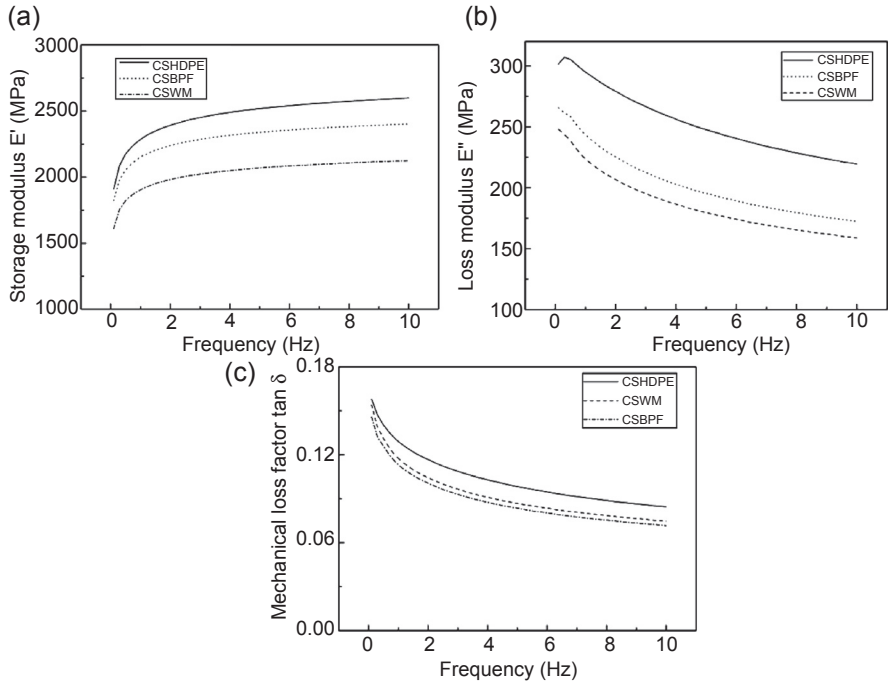

Figure 10.14 Effects of shell materials on the E', E'', and tanδ of the core-shell structured bamboo plastic composite: (a) E', (b) E'', and (c) tanδ.

composites, as shown in Fig. 10.14 c. This is mainly related to the fact that the mechanical loss of composites at a high frequency was lower than that at a low frequency. The tanδ of the composites decreased with the increase of frequency. Generally the energy dissipation of the core-shell structured BPC involves the core, the shell layer, and the interface damping. The results showed that the movement of the matrix chain segment was restricted due to the addition of the bamboo powder, which makes its damping performance degrade. At the same time, interface damping has significant effects on damping properties of wood plastic composites. The tanδ of CSHDPE composites was greater than that of CSBPR and CSWM at the same frequency. The influence of BPF as well as WM on the damping behavior of the core-shell structured BPC can be explained by two possible factors. One factor is the energy of thermally activated molecular movement is different for core-shell structured BPC with different shell layers. The other factor is that the incorporated BPF or WM has restricted the mobility of the HDPE chains and has the tendency to render higher elastic stiffness.

A line of indents, spanning from the shell to the core layer, was made. The response nuances of nanoindentation were investigated in context of the ITZ property variation. Seven test points were designed with 350-nm indentation depth. In order to avoid overlapping of the impact zones of neighboring indents, the spacing of indentation was

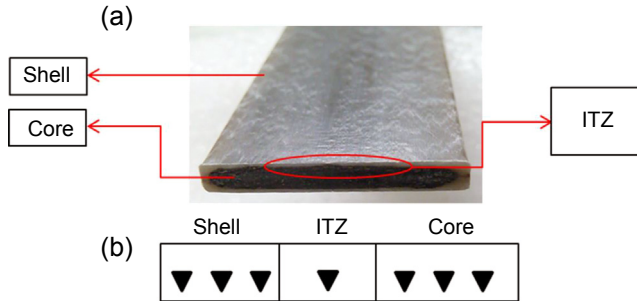

Figure 10.15 The relative position of ITZ: (a) the diagram of ITZ and (b) the position distribution of all depenetration in quasistatic nanoindentation.

chosen to be, at minimum, seven times the indentation depth.[35] The hardness and elastic modulus of the samples were obtained from the seven indentations at different locations, as shown in Fig. 10.16. It also illustrates the profiles of elastic modulus and hardness across the interphase regions, which were obtained after unloading at the final indentation. The mean elastic modulus and hardness of the V-HDPE shell layer were 1.8−2.2 GPa and 0.12−0.14 GPa respectively, in the shell layer made with BPF/HDPE they were 3.2−16 GPa and 0.18−0.8 GPa respectively, whereas in the WM/HDPE shell system they were 5−6 GPa and 0.11−0.28 GPa respectively. The mean hardness and elastic modulus of the core layer were 0.19−0.25 GPa and 3−4.5 GPa respectively. One out of the seven indentations showed distinct hardness and elastic modulus in ITZ, with intermediate properties between those for the core and the shell (Fig. 10.16). The corresponding values of hardness and elastic modulus in ITZ are lower than the same for the individual core and shell layer. It further illustrates that the elastic modulus and hardness of ITZ were different from zones on either side. It is notable from the indentation made in ITZ that the properties of the indentation close to the core should be affected less than those close to the shell. In other words, the results provided by these indents could be more influenced by the different shell layer materials. The effect of incorporation of BPF as well as WM on the ITZ properties of core-shell structured BPC can be partially explained as follows: if BPF and WM of high elastic modulus are well dispersed through a low elastic modulus matrix, it is obvious that the modulus of the composites will be higher than that of the matrix. However, for the fillers in the shell to be really weakened in nature, many other factors come into the picture: the most important being the force of adhesion of the core and shell layer, which plays a crucial role. Based on these results, it can be said that the ITZ properties are poorly contrasting them with respect to the shell layer and the core.

10.4 Prospects

Bamboo has a more significant effect on preserving the environment than any other plant. A series of innovative products and techniques related to bamboo-based composites in future scientific research and engineering applications were proposed:

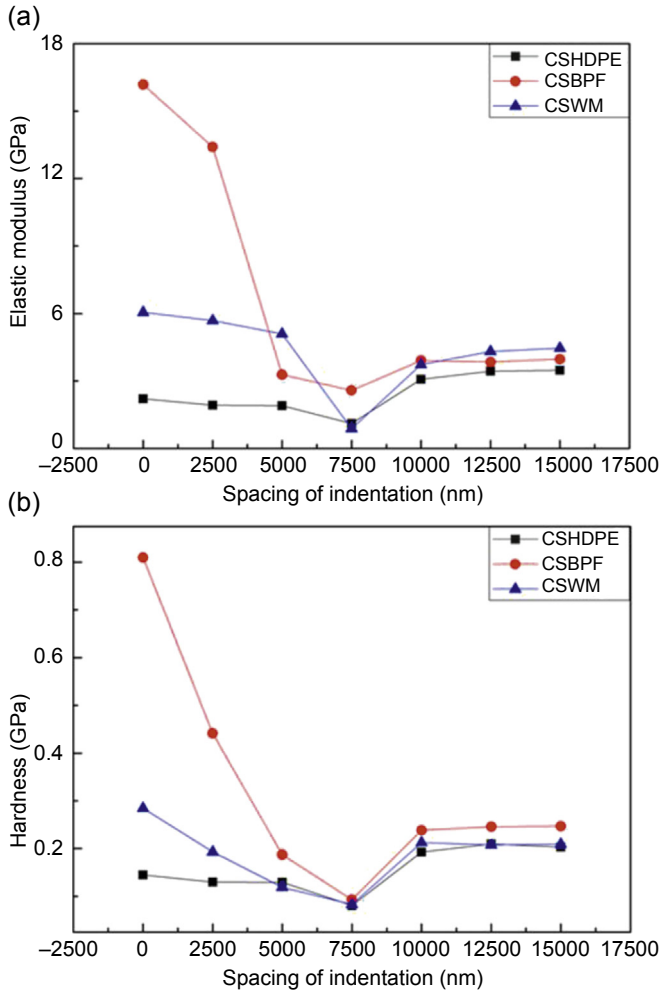

Figure 10.16 Effects of shell materials on the elastic modulus and hardness of core-shell structured bamboo plastic composites: (a) elastic modulus and (b) hardness.

1. The relationship between the mechanical and physical properties of bamboo fiber and its characteristic in its growth processes

   To optimize the application of bamboo and obtain reasonably useful fiber, the relationship between the mechanical and physical properties of bamboo fiber and its growth, lignifying, and maturing processes from the initial stage of bamboo shoots to mature bamboo and recession.
2. Manufacture technology of bamboo bundle veneer cross-laminated composites (BCLC) and its assembly technique for the container house

   The container house is a prefabricated structure in development that is intended for use as a temporary scenic house, an open-air dwelling, and a military structure. The standard wall components are made of BCLC, but an effect system for connecting and assembling the BCLC wall units still needs to be designed.

3. Development of bamboo-based engineering materials with continuous length and large-span components

   To produce large-scale green structures, eg, a bamboo wood exhibition room, conference hall, library, and bridge, the development of large-span bamboo-based engineering materials and components is necessary. In order to produce these products the development of automation control and large-scale production is imperative.
4. Scientific R&D of value-added BFRC with heterotypic structure

   To improve the scope of applications for a bamboo fiber-based composite, a series of innovative products with a heterotypic structure that could meet the nonplanar requirement by the weave forming, filament-wound processing, and vacuum molding, among others. Examples include bamboo-based shell materials for mobile phone cases,other electronic housing, interior paneling for various forms of transportation, and storage containers.

Acknowledgments

The authors are grateful for the financial support of the Fundamental Research Funds of the International Center for Bamboo and Rattan (1632015003).

References

Chen, H., Wang, G., Cheng, H.T., 2011. Properties of single bamboo fibers isolated by different chemical methods. Wood and Fiber Science 43 (2), 1−10.

Chen, H., Cheng, H.T., Jiang, Z.H., Wang, G., Fei, B.H., et al., 2013a. Contact angles of single bamboo fibers measured in different environments and compared with other plant fibers and bamboo strips. BioResources 8 (2), 2827−2838.

Chen, F.M., Jiang, Z.H., Wang, G., et al., 2013b. Bamboo bundle corrugated laminated composites. Part I. Three-dimensional stability in response to corrugating effect. Journal of Adhesive 89 (3), 225−238.

Chen, F.M., Deng, J.C., Cheng, H.T., Li, H.D., Jiang, Z.H., Wang, G., Zhao, Q.C., Shi, S.Q., 2014a. Impact properties of bamboo bundle laminated veneer lumber by preprocessing densification technology. Journal of Wood Science. http://dx.doi.org/10.1007/s10086-014-1424-0.

Chen, F.M., Deng, J.C., Jiang, Z.H., Wang, G., Zhang, D., Zhao, Q.C., Cai, L.P., Shi, Q.S., 2014b. Evaluation of the uniformity of density and mechanical properties of bamboo-bundle laminated veneer lumber (BWLVL). BioResources 9 (1), 554−565.

Chen, F.M., 2014. Technology and Theory of Bamboo Bundle Laminated Veneer Lumber With Continuous Plate Process (Dissertation for the Degree). Chinese Academy of Forestry, Beijing, China.

Cheng, L., Wang, X.M., Yu, Y.L., 2009. Effect of glue immersion parameters on performance of reconstituted *Dendrocalamopsis oldhami* lumber. China Wood Industry 23 (3), 16−19.

Deng, J.C., Chen, F.M., Li, H.D., Wang, G., Shi, S.Q., 2014a. The effect of PF/PVAC weight ratio and ambient temperature on moisture absorption performance of bamboo-bundle laminated veneer lumber. Polymer Composites. http://dx.doi.org/10.1002/pc.23255.

Deng, J.C., Chen, F.M., Wang, G., et al., 2014b. Hygrothermal aging properties, molding and abrasion resistance of bamboo keyboard. European Journal of Wood and Wood Products 72 (5), 659−667.

Deng, J.C., Li, H.D., Zhang, D., et al., 2014c. The effect of joint form and parameter values on mechanical properties of bamboo-bundle laminated veneer lumber (BLVL). BioResources 9 (4), 6765−6777.

Grosser, D., Liese, W., 1971. On the anatomy of Asian bamboos, with special reference to their vascular bundles. Wood Science and Technology 5, 290−312.

Kennedy, J.M., Edie, D.D., Banerjee, A., Cano, R.J., 1992. Characterization of interfacial bond strength by dynamic analysis. Journal of Composite Materials 26 (6), 869−882.

Kirchmajer, D.M., Gorkin III, R., 2015. An overview of the suitability of hydrogel-forming polymers for extrusion-based 3D-printing. Journal of Materials Chemistry B 3 (20), 4105−4117.

Koh, Y.H., Kim, H.W., Kim, H.E., Halloran, J.W., 2002. Fabrication of macrochannelled-hydroxyapatite bioceramic by a coextrusion process. Journal of the American Ceramic Society 85 (10), 2578−2580.

Kim, B.J., Yao, F., Han, G., Wang, Q., Wu, Q., 2013. Mechanical and physical properties of core−shell structured wood plastic composites: effect of shells with hybrid mineral and wood fillers. Composites Part B Engineering 45 (1), 1040−1048.

Li, H.D., Chen, F.M., Cheng, H.T., et al., 2014. Large-span bamboo fiber-based composites, part I: a prediction model based on the Lucas-Washburn equation describing the resin content of bamboo fiber impregnated with different PVAC/PF concentrations. BioResources 9 (4), 6408−6419.

Liu, D.G., Song, J.W., Anderson, D.P., Chang, P.R., Hua, Y., 2012. Bamboo fiber and its reinforced composites: structure and properties. Cellulose 19 (5), 1449−1480.

Lugt, P., Dobbelsteen, A.A.J.F., Janssen, J.J.A., 2005. An environmental, economic and practical assessment of bamboo as a building material for supporting structures. Construction and Building Materials 20, 648−656.

Negendank, M., Mueller, S., Reimers, W., 2012. Coextrusion of Mg−Al macro composites. Journal of Materials Processing Technology 212 (9), 1954−1962.

Nugroho, N., Ando, N., 2001. Development of structural composite products made from bamboo II: fundamental properties of laminated bamboo lumber. Journal of Wood Science 47 (3), 237−242.

Peng, Z., Lu, Y., Li, L., Zhao, Q., Feng, Q., Gao, Z., Jiang, Z., 2013. The draft genome of the fast-growing non-timber forest species moso bamboo (*Phyllostachys heterocycla*). Nature Genetics 45 (4), 456−461.

Qin, L., Yu, W.J., Yu, Y.L., 2013. Research on properties of reconstituted bamboo lumber made by thermo treated bamboo bundle curtains. Forest Products Journal 62, 545−550.

Rassiah, K., Megat, A.M.M.H., Ali, A., 2014. Mechanical properties of laminated bamboo strips from Gigantochloa Scortechinii/polyester composites. Materials and Design 57, 551−559.

Shao, S.L., Wen, G., Jin, Z.F., 2008. Changes in chemical characteristics of bamboo (Phyllostachyspubescens)components during steam explosion. Wood Science and Technology 42, 439−451.

Wang, G., Yu, Y., Shi, S.Q., Wang, J.W., Cao, S.P., Cheng, H.T., 2011. Microtension test method for measuring tensile properties of individual cellulosic fibers. Wood and Fiber Science 43 (3), 251−256.

Wang, G., Jiang, Z.H., Chen, F.M., Cheng, H.T., Sun, F.B., 2013. Manufacture situation and problem analysis for large span bamboo engineering material in China. China Forest Products Industry 40 (6), 49−53.

Xian, Y., Wang, C., Wang, G., Ren, W., Cheng, H., 2016. Understanding the mechanical and interfacial properties of core−shell structured bamboo−plastic composites. Journal of Applied Polymer Science 133 (10).

Xiao, Y., Yang, R.Z., Shan, B., 2013. Production, environmental impact and mechanical properties of glubam. Construction and Building Materials 44, 765−773.

Yu, W.J., Yu, Y.L., 2013. Development and prospect of wood and bamboo scrimber industry in China. China Wood Industry 27 (1), 5−8.

Yu, Z.X., Jiang, Z.H., Wang, G., Cheng, H.T., Zhang, W.F., Qiu, Y.X., 2012a. Impact resistance properties of bamboo scrimber. Journal of Northeast Forestry University 40 (4), 46−48.

Yu, Z.X., Jiang, Z.H., Wang, G., Zhang, W.F., Chen, F.M., 2012b. Mechanical properties of laminated bamboo scrimber in hygrothermal environment. Journal of Central South University of Forestry and Technology 32 (8), 127−130.

Yu, Y., Wang, H.K., Lu, F., 2014a. Bamboo fibers for composite applications: a mechanical and morphological investigation. Journal of Materials Science 49, 2559−2566.

Yu, Y.L., Huang, X., Yu, W.J., 2014b. A novel process to improve yield and mechanical performance of bamboo fiber reinforced composite via mechanical treatments. Composites: Part B 56, 48−53.

Yu, Y.L., Zhu, R.X., Wu, B.L., Hu, Y.-A., Yu, W.J., 2014c. Fabrication, material properties, and application of bamboo scrimber. Wood Science and Technology. http://dx.doi.org/10.1007/s00226-014-0683-7.

Zakikhani, P., Zahari, R., Sultan, M.T.H., Majid, D.L., 2014. Extraction and preparation of bamboo fibre-reinforced composites. Materials and Design 63, 820−828.

Zhang, D., Wang, G., Ren, W.H., 2014. Effect of different veneer-joint forms and allocations on mechanical properties of bamboo-bundle laminated veneer lumber. BioResources 9 (2), 2689−2695.

Straw fibre-based construction materials

11

S.H. Ghaffar
Brunel University London, London, United Kingdom

11.1 Introduction

Straw is a promising biomass for the production of bioproducts, which could present a novel source for the eco-building materials and systems. The European countries (27 countries) produce 137.49 million tonnes of wheat collectively, which is 16.59% higher than that produced in China (Zhang et al., 2012). It is evident that straw biomass is an abundant and inexpensive lignocellulosic resource for manufacturing eco-building materials. For instance, straw can be utilised as alternatives to wood flour or other bast fibre composites with comparable density and could reduce the cost of building products. On the other hand, utilisation of these inexpensive raw materials in composites leads to socioeconomic and environmental benefits by making additional income for the farmers, generating cost-effective high performing products and minimising the burning of the straw in the field. Compared to wood, straw is much lighter in weight and has more water resistance. The main chemical constituents of straw are similar to those of wood: cellulose, hemicellulose, lignin and extractives; however, straw has a higher content of hydrophobic waxy cuticle layers and a high amount of inorganic silica and extractives.

The development of commercially viable 'green products' based on natural resources for both matrices and reinforcements in construction applications is rising. This emergence includes novel pathways to manufacture natural polymers with enhanced mechanical properties and thermal stability using new technologies such as nano and/or biotechnology for natural polymers to make biodegradable plastics and their biocomposites with lignocellulosic fibres. The research concerning straw optimisation for bioproducts have developed extensively over the past few years (Ghaffar and Fan, 2013, 2014, 2015a,b; del Rio et al., 2013; Stelte et al., 2013; Zhu et al., 2012; Hansen et al., 2011, 2013; Halvarsson et al., 2009; Han et al., 2009; Jiang et al., 2009; Zhang et al., 2003; Alemdar and Sain, 2008a; Borrion et al., 2012; Lindedam et al., 2012; Larsen et al., 2012). Straw-based natural fibres have gained much attention because they have the advantages of low cost, low density, full biodegradability and nonabrasive behaviour during processing, as well as high toughness with acceptable mechanical properties (Mohanty et al., 2000; Liu et al., 2005a; Satyanarayana et al., 2009). The big challenge in working with natural fibre reinforced composites is their variation in properties and characteristics. The general characteristics of reinforcing fibres used in biocomposites for construction, including source, type, structure, composition, mechanical, physical and chemical properties, must be

Advanced High Strength Natural Fibre Composites in Construction. http://dx.doi.org/10.1016/B978-0-08-100411-1.00011-X

studied in detail in order to enable the success in the development of novel products that can be useful for construction.

This chapter will provide an extensive review of the existing and emerging technologies and pretreatments for the straw biomass and its optimisation as a construction material. Renewable materials for construction and the use of straw in construction are discussed in detail, as well as the evidence for the success in bioconversion, along with the associated limitations for the application of biocomposites. The information in this chapter will serve as great scientific insights and directive fundamentals for researchers and industries for further developments and investments in straw biomass and its optimised utilisation in construction.

11.2 Renewable bio-based construction materials

Worldwide, buildings are responsible for more than 40% of global energy consumption and as much as 33% of carbon dioxide equivalent emissions (CO_2e), which sums to about 8.1 Gt annually (Lawrence, 2015). Therefore, strategies to reduce the environmental impact of construction by using bio-based renewable materials should be the main goal of the construction sector. Various strategies have been developed to reduce carbon emissions, including: 1) improved thermal insulation for both new build and retrofit; 2) better building design (eg, PassivHaus); 3) enhanced efficiency of heating; 4) reduction in the carbon emissions of energy production through the use of nuclear energy ventilation and air conditioning systems; and 5) renewable energy sources (hydro, wind, tidal, photovoltaic, biomass, etc.). However, not much emphasis is placed on reducing the embodied energy within buildings. Building materials traditionally were sourced locally, and it is the variety of local materials that created the character of the historic built environment. Vernacular buildings depend on small-scale construction technologies, which are not appropriate for the high volume, mass-produced built environment needed to service the large and always-growing global population.

The transition from an oil-based economy towards a bio-based economy is very vital, and specific focus should be put on the integration of local sustainable cultivation of resources. The challenges with bio-based building materials must be tackled through the whole product chain (production and supply) of straw-based building materials, as well as in the marketing of these products so that this bioeconomical business could develop in a sustainable and profitable method. This business should be profitable for every stakeholder in the product chain. The challenges are within different fronts, including the need for technical development and product innovation, and a huge effort must be focused on partner matching to develop new businesses. Of course, significant work must be carried out to increase the bio-based construction market demand. Gathering adequate and robust information about specific variations in material properties is not straightforward, specifically when it comes to natural materials such as sheep wool, cork, hemp-crete and straw biomass. Information about the physical properties of such materials is either very limited or differs significantly according to different sources and measurement techniques (McLeod and Hopfe, 2013). This will then require a comprehensive and harmonised set of product standards, which

could only be significant if there is more investment in the research of renewable material science and collaboration between different sectors within the construction industry, from farmers to policy makers.

11.2.1 Straw in construction

An innovative straw−bale construction method is being used in northern China to build houses and other public buildings using waste rice straw. In Europe there are plans for large buildings from straw; thousands of tightly packed cubes of compressed straw will form the core walls of a big complex. The straw construction helps to bring in sustainability funding sourced from the European Union. The straw walls should be dense enough with brick pillars as additional loadbearing support. Nonload-bearing straw bale walls are mostly used for external infill above the damp-proof course level in moderate environments. Straw bale walls can be constructed either on site or as prefabricated panels brought to the site and enclosed in a protective outer finish (ie, lime render). In addition to the other general benefits of off-site construction (such as speed of construction and reduced waste), straw bale walls are particularly very suitable for the prefabricated construction methodology. In this way the risk of water damage and the risk of fire associated with loose cut straw during construction is minimised. Various prefabricated straw bale systems are developed in the United Kingdom and elsewhere (Sutton et al., 2011). Prefabricated straw bale panels could be designed and manufactured throughout the year and require minimal specialist machinery (ie, primarily lifting equipment). On the other hand, rendering and initial hardening could be carried out off site, with final finishes applied on site as necessary. Straw bales could also be used for lightly loaded structural walls (up to two stories high). The compressive strength of the straw bale wall is low due to displacement rather than material failure; however, a 450 mm-thick bale wall is able to support 0.8−1.0 tonnes/m length, which is adequate for domestic scale buildings and loadings (Sutton et al., 2011). The render's role is significant for structural capability, in terms of increasing resistance and improving stiffness by minimising movement, as well as protecting the straw from decay and improving fire resistance. Although weather protection to load-bearing walls during construction could be more challenging than when a straw bale is used as infill. Straw bale walls are thick, which give good insulation and thermal inertia that is a product of phase changes of residual moisture. Straw bale walls must be protected against driving rain by the coating and by deep, overhanging eaves. There are some challenges with straw bales that, if solved, could further increase their application in construction:

1. The straw directions are random, which means condensation droplets near the outside could drip inwards and downwards and the base of the wall could become permanently moist over time.
2. The bale size is determined by the manufacturer of the combine harvester, not by the structural engineer or architect.
3. The straw is not fully compacted. When placed under load from floors and roofs, the straw bales in the wall will compress. Height reduction in the wall could be as great as 60 mm in a two story home. Adjustments must be made at all openings to rectify this dimensional problem.

A straw bale is very suitable as infill (nonload-bearing) insulation for timber frame buildings with either an external render or timber rain screen finish. Straw enables vapour permeable walls, which are locally sourced and have low-impact for construction. Nonetheless, it needs careful and accurate detailing in the construction stage to fully avoid the ingress and retention of moisture.

Another solution, which would eliminate the issues associated with straw bale construction, is strawboards. The commercial strawboard industry is relatively new and growing in the United States, the United Kingdom and China. Strawboards compete with reconstituted wood products, such as particle and fibreboards in markets for wall panels, ceiling panels, floor underlays, furniture and cabinet construction. The variety of hybrid strawboards are suitable for use in many different applications, for instance, low density strawboards provide excellent thermal and acoustic insulation, whilst higher densities allow for structural applications. Waste agricultural raw materials for the production of panels, such as wheat strawboard and rice strawboard, have the potential of being utilised as construction materials. To achieve the full commercialisation of strawboards, several fundamental issues such as the strength and durability, the compatibility and interface of matrix and straw particles must be overcome. The issues associated with straw biomass for strawboard biocomposite application through a detailed material science (ie, morphology, surface and interface science, chemical and mechanical properties, etc.) is assessed later on in this chapter.

11.3 Straw material science

11.3.1 Main constituents of straw biomass

Lignocellulosic material from cereal straws essentially consists of three different polymeric entities: linear and crystalline (cellulose), branched noncellulosic and noncrystalline heteropolysaccharides (hemicelluloses), and branched (noncrystalline) lignin (Glasser et al., 2000). Cellulose is a long chain of glucose molecules, connected to each other primarily by β $(1 \rightarrow 4)$ glycosidic bonds; the noncomplicated structure of cellulose indicates that it could be biodegraded. The main difficulty in the bioconversion procedure is the crystalline nature of cellulose, therefore it must be pretreated to expose the cellulose structure and change it to be more vulnerable to cellulase action (van Wyk, 2001). Hemicellulose, just like cellulose, is a macromolecule from different sugars but alters from cellulose in that it is not chemically homogeneous and is a polysaccharide, which has lower molecular weight compared to cellulose. A key alteration among cellulose and hemicellulose is that the latter possesses branches with short lateral chains containing various sugars, and cellulose contains easily hydrolysable oligomers. Hemicelluloses in straw biomass are made mainly of xylan, whereas softwood hemicelluloses have glucomannan. Lignin is connected to both hemicellulose and cellulose, founding a physical cover that is an impermeable wall in the plant cell wall. The existence of lignin in the cellular wall offers rigidity, impermeability and a confrontation to microbial attack. Lignin is a complex three-dimensional polymer formed by radical coupling polymerisation of *p*-hydroxycinnamyl, coniferyl and

Table 11.1 Compositions of straw biomass (% dry matter)

Category	Lignin	Cellulose	Hemicellulose	Water-soluble	Wax	Ash	Others
Wheat straw	14.1	38.6	32.6	4.7	1.7	5.9	2.4
Rice straw	12.3	36.5	27.7	6.1	3.8	13.3	0.3
Rape straw	21.3	37.6	31.4	–	3.8	6.0	0
Oat straw	16.8	38.5	31.7	4.6	2.2	3.1	3.1
Rye straw	17.6	37.9	32.8	4.1	2.0	3.0	2.6
Barley straw	14.6	34.8	27.9	6.8	1.9	5.7	8.3

sinapyl alcohols; these three lignin precursors' monolignols induce the *p*-hydroxyphenyl (H), guaiacyl (G) and syringyl (S) phenylpropanoid units (Ghaffar and Fan, 2013). Lignin extraction from lignocellulosic biomass such as wood and straw represents the key point to its utilisation for industrial applications. The major problem is its vaguely defined structure and its versatility according to the origin, separation and fragmentation processes. Lignin could be exploited as a raw material for chemical production. It may also be a good candidate for chemical modifications and reactions due to its highly functional character (ie, rich in phenolic and aliphatic hydroxyl groups) for the development of new bio-based products (Laurichesse and Avérous, 2014). Extractives are also amongst the main constituents of straw biomass. They are a heterogeneous group of substances, and the main extractives are resin acids, steryl esters, triglycerides, fatty acids, sterols, fatty alcohols, and a selection of phenolic compounds (Sun, 2010). Generally the extractives are low molecular weight compounds, and their chemical behaviour varies for different classes of extractives.

The composition and quantities of these complex constituents differ between straw biomass, which can however be summarised in Table 11.1.

11.3.2 Surface chemical distribution

The chemical distribution of straw is not consistent throughout the anatomical parts, although it might have similarities in general terms, but the differences may not be negligible. Understanding these differences could be useful for the pretreatment and processing design; for example, the chemical properties of straw surfaces are vital for establishing the interfacial bonding properties in composites, hence effective modification to improve fibre matrix adhesion requires relevant quantitative analyses of the surface. ATR-FTIR is a useful analytical tool to investigate the surface of straw in

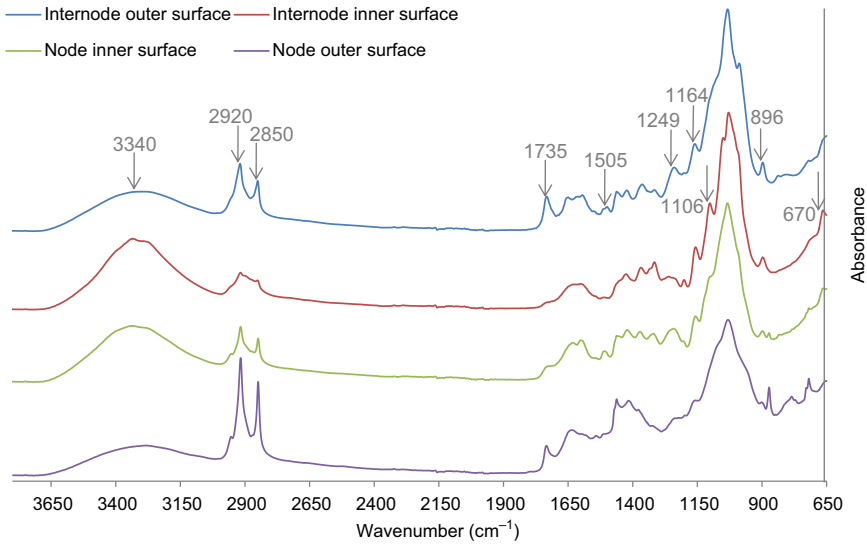

Figure 11.1 ATR-FTIR spectra of wheat straw internode and node outer and inner surface.

terms of functional groups (Fig. 11.1). For instance, the surface chemical distributions of wheat straw node and internode and inner and outer surface are shown in Fig. 11.1. The band of 985 cm^{-1}, which is most likely attributed to the Si−O stretching vibration (Frost and Mendelovici, 2006), was observed in the spectrum of the outer surface, but absent in the inner surface of the internode. It is interesting that for the outer surface node, this is represented as the band of 790 cm^{-1} attributed to the Si−C stretching vibration (Frost and Mendelovici, 2006), and again it is absent in the inner surface of the node. This means that the components containing silicon are primarily on the outer surface and the finding is the most important for the pretreatment of the biomass either for composite development due to the inhibiting of interfacial bonding. The peak at 1164 cm^{-1} is assigned to a C-O-C antisymmetric bridge in hemicelluloses and cellulose and to aromatic C-H deformation of the syringyl and guaiacyl units in lignin (Fang et al., 2002). This band had a prominent intensity in the internode inner and outer surface. The peak at 1385 cm^{-1} reflects C-H asymmetric deformations (Sun et al., 2005) with polysaccharide sources (Le Troëdec et al., 2009). The C=C stretch of aromatic rings of lignin are presented at peaks 1425 and 1510 cm^{-1} (Sain and Panthapulakkal, 2006; Xiao et al., 2001). The intensity of these peaks was highest in the node outer surface, followed by internode outer surface, hence the outer surface has a higher concentration of aromatic rings of lignin. The aromatic skeletal vibration coupled with C-H in plane deformations is at 1600 cm^{-1} peak (Jiang et al., 2009).

Peak at 1738 cm^{-1} is assigned to the acetyl and uronic ester groups of the hemicelluloses or the ester linkage of carboxylic group of the ferulic and *p*-coumeric acids of lignin and/or hemicelluloses (Alemdar and Sain, 2008b; Kristensen et al., 2008). Two strong and sharp peaks at 2850 and 2920 cm^{-1} are assigned to the asymmetric and symmetric stretching of the CH_2-group comprising the majority of the aliphatic

fractions of waxes, respectively (Inglesby et al., 2005; Merk et al., 1997). The outer part of the straw surface (epidermis) contains wax and inorganic substances on the surfaces, and hence the intensity of the bands associated with aliphatic fractions of waxes is much higher in the outer surface of the node and internode. Additionally the intensity of these bands in the node outer surface is higher than the internode outer surface, as the epidermis size in node is larger than internode.

11.3.3 Surface elemental composition

The elemental composition of node and internode inner and outer surface of wheat straw was gathered using the EDX-SEM technique in order to get the chemical information of the localised surface. The EDX spectra were obtained using an INCA Energy 350 microanalysis system (Oxford instruments, England). The elements detected were quantitatively analysed using the database of standard samples programmed in the software. The elemental ratio of all elements detected was automatically calculated from their normalised peak areas. The results are an average of the 10 measurements taken at different areas for each section (Table 11.2). It is apparent that the bulk structure of the wheat straw consisted of carbohydrates and lignin with a considerable amount of C and O and trace amounts of Si (wt%). The outer surface of the internodes had considerably higher Si weight percentage than the inner surface: the former is 3.63% and the latter is 0.83%. By contrast, the Si weight percentage for the outer surface of nodes is about two times that of the inner surface. It is most surprising that the Si weight percentage of the nodes is much lower than that of internodes, only about one-fourth. It could be concluded that more silicon (in the form

Table 11.2 Wheat straw node and internode elemental composition

	Elemental content (wt%)			
	C	**O**	**Si**	**O/C**
Node inner surface	50.99 (1.51)	48.70 (1.0)	0.31 (7.02)	0.95
Node outer surface	52.23 (6.24)	47.10 (3.75)	0.67 (4.56)	0.90
Internode inner surface	54.52 (1.54)	44.65 (2.04)	0.83 (7.87)	0.82
Internode outer surface	51.22 (8.7)	45.14 (5.98)	3.64 (9.5)	0.88
Average node (inner and outer)	51.61	47.90	0.49	0.92
Average internode (inner and outer)	52.87	44.89	2.23	0.85
Average inner surface (node and internode)	52.75	46.67	0.57	0.88
Average outer surface (node and internode)	51.72	46.12	2.15	0.89

Values in () are coefficient of variance percentage.

of silica) is located mainly in the epidermis of wheat straw. The theoretical O/C ratio of cellulose was reported as 0.83 and that of lignin as 0.33 (Linxin et al., 2010; Zhao and Boluk, 2010). The O/C ratio for wheat straw in all areas is similar to cellulose, indicating the presence of a carbohydrate-rich surface (Table 11.2). The lowest O/C ratio of wheat straw internode inner surface is because of the associated lignin and hydrocarbons. A comparatively higher proportion of carbon atoms in the internode inner surface may be attributed to the predominance of lignin (Sutton et al., 2011). It is worth mentioning that a higher content of C on the node outer surface is an indication of a high quantity of wax (Zhao and Boluk, 2010).

11.3.4 Crystallinity

Wheat straw was subjected to a powder X-ray diffraction method analysis, which was carried out using a D8 advanced Bruker AXS diffractometer, Cu point focus source, graphite monochromator and 2-D area detector GADDS system. The diffracted intensity of CuKa radiation (wavelength of 0.1542 nm) was recorded between 5 and 40 degree (2θ angle range) at 40 kV and 40 mA. Samples were analysed in transmission mode. The crystallinity index was evaluated by using the Segal et al. (1959) empirical method as follows:

$$\mathrm{CI}\% = \frac{I_{002} - I_{\mathrm{amorph}}}{I_{002}} \times 100 \tag{11.1}$$

I_{002} is the maximum intensity of diffraction of the (002) lattice peak at a 2θ angle of between 21 and 23 degree, which represents both crystalline and amorphous materials. I_{amorph} is the intensity of diffraction of the amorphous material, which is taken at a 2θ angle between 18 and 20 degree, where the intensity is at a minimum. It should be mentioned that the crystallinity index is valuable only on a comparative basis, as it is used to specify the order of crystallinity rather than the crystallinity of crystalline regions. Crystalline microfibrils of cellulose are surrounded by amorphous hemicellulose, and the whole is embedded in the matrix of lignin. The crystalline structure of cellulose and hemicellulose exhibits variability in both structure and constitution. Lignin and hemicelluloses are fundamentally amorphous polymers, while cellulose has both amorphous and crystalline regions. An example of X-ray powder diffraction spectra from the wheat straw node and internode is given in Fig. 11.2.

The X-ray diffraction patterns of wheat straw nodes and internodes showed spectra typical of cellulosic materials with the major peak at a diffraction angle (2θ) of 21−22 degree and a broader, secondary peak at 18 degree, which indicates that the cellulose is in its cellulose I crystal form. The crystallinity index for wheat straw node and internode was calculated to be 34.73% and 45.00%, respectively, which indicated that the node has much more amorphous regions than the internode. The result thus could also reflect that there is more concentration of lignin and hemicellulose in the node area or that the cellulose in the node has more amorphous regions when compared to the internode. Also, the increasing of crystalline regions

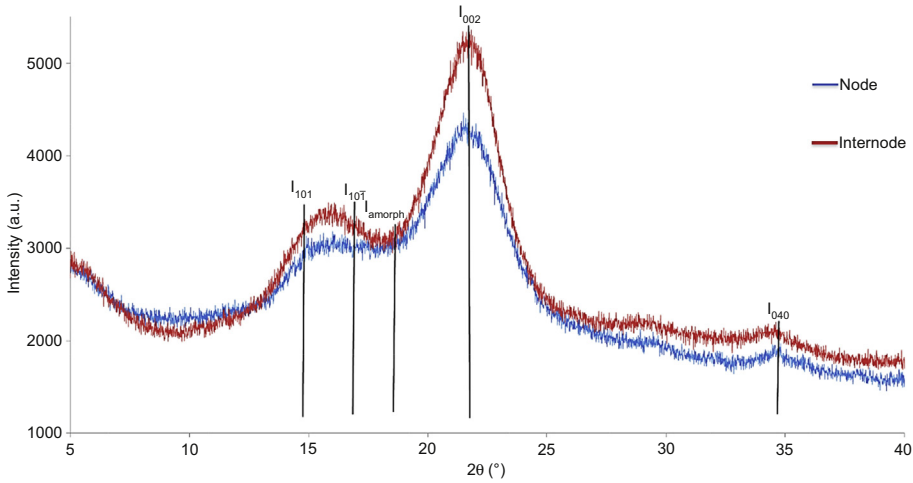

Figure 11.2 X-ray diffractogram of wheat straw node and internode.

Table 11.3 Crystallinity index calculation of wheat straw node and internode

	2θ (degree)		Intensity (a.u.)		Crystallinity index (%)
	I_{amorph}	I_{002}	I_{amorph}	I_{002}	
Node	18.32	21.49	2913	4463	34.73
Internode	18.51	21.71	2950	5364	45.00

increases the rigidity of cellulose but decreases the elasticity of polymeric substances. In addition, the ratio of the crystalline region to the amorphous region in a cellulose structure affects the accessibility of cellulose molecules. When it comes to the crystallinity of straw biomass, most of the pretreatments are designed in a way to increase the crystallinity, which is achieved by the removal of lignin and hemicellulose. It is important to know the untreated crystallinity of anatomical parts (ie, node, internode) of straw biomass before any type of pretreatment that focuses on the changes in crystallinity. The crystallinities of wheat straw in different anatomical parts are different and fairly low, about 40% on average of node and internode (Table 11.3). This means that the cellulose from wheat straw is a suitable parent polymer for the preparation of cellulose derivatives (Helbert et al., 1997).

11.3.5 Straw biomass morphology

In this section the morphology of wheat straw is specifically analysed amongst all the straw biomasses. However, in general, the straw stem comprises internodes separated by nodes, at which leaves are attached to the stem (Fig. 11.3). The internodes are formed

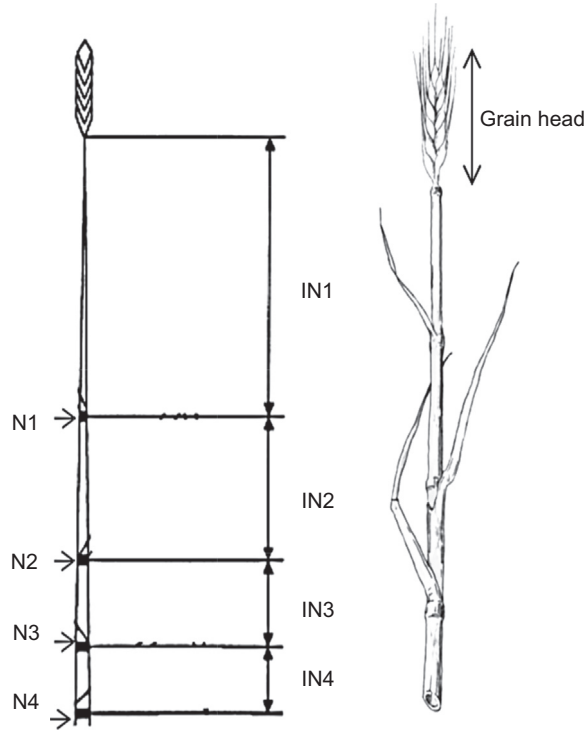

Figure 11.3 Schematic diagram of wheat straw with nodes (N) and internodes (IN).

as concentric rings leaving a void or lumen in the centre. The outermost ring is a cellulose-rich dense layer (termed the epidermis), which has a concentration of silica on the surface. Beneath the epidermis is a loose layer containing parenchyma and vascular bundles. The internodes are the parts containing the fibres of sufficient amount and quality that are of interest for the refining and manufacture of biocomposites. Nodes contain smaller amounts of fibre cell elements. The length of the internodes increases from the ground to the top. Wheat straw is less homogenous than the perennial softwoods or hardwoods in the morphological structure and consists of solid nodes and hollow internodes. The stem of wheat straw is inherently formulated in a multilayered structure. The top layer is a cuticle, which is defined as the continuous noncellular membrane lying on the epidermal walls. The estimated cuticle thickness is generally 1 mm and contains a wax layer in the form of an unspecified thin film or characteristic wax crystals. The cuticular waxes are formidable barriers of the straw plants to control the exchange of water, solutes and even gases and vapours (Wiśniewska et al., 2003).

11.3.5.1 Node

The node structure along the longitudinal direction was investigated by taking cross-sectional images after carefully grinding layer by layer with smooth abrasive paper (grit size: SiC Abrasive paper, P180, Buehler) moving towards the wheat grain (Fig. 11.4). The investigation starts from the internode immediately before the node

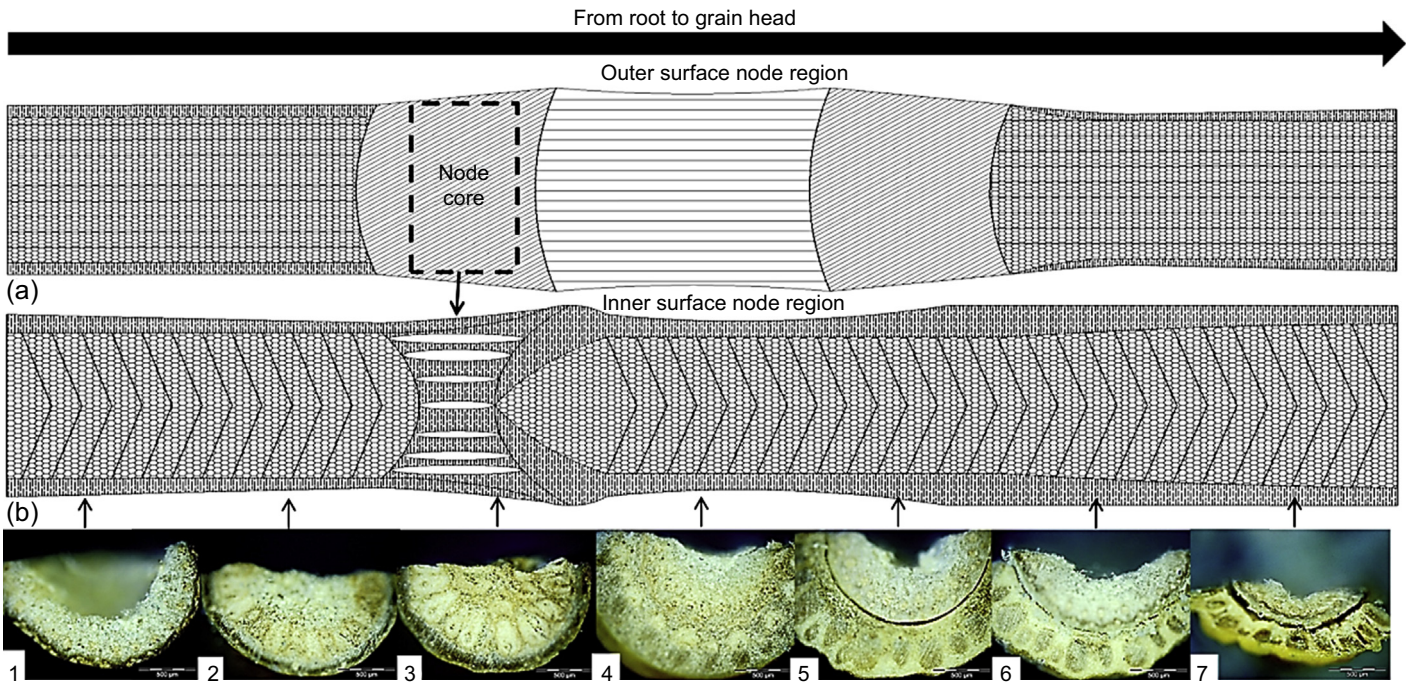

Figure 11.4 The schematic image of the node outer (a) and inner (b) surface longitudinal view and the optical microscopy images corresponding to the position in the node shown by the *arrows*.

and then enters the node core zone and continues forward to where the brown elliptical rings get smaller and the beginning of the upper internode reveals. Those brown elliptical rings that start to get smaller and smaller until they disappear, ie, the start of the hollow upper internode. Fig. 11.4 shows the outer and inner surfaces of the node region, and their corresponding optical microscopy (OM) images are shown by the *arrows*, indicating their positions in the node region. It is apparent that the structure of the node is not symmetrical along the length direction and the morphology changes clearly from left to right (moving upwards to the grain head) in the node region. The outer ring of the node is revealed after the dense area of node core in the fourth image from the left. There are some significant characteristics between the first OM image, which is the end of the lower internode and just the beginning of the node core, with the seventh OM image, which is the end of node region and the start of the upper internode. In the first image the elliptical rings associated to the node region are absent, whereas in the seventh image the elliptical rings are apparent and the cut between the upper (new) internode is quite clear. It is also observed that after the seventh image the outside elliptical ring of the node region disappears (image not shown). The second and third OM images are quite similar in morphology, but the detailed differences are in the size and the occurrence of the elliptical rings, which become more prominent in the third image, hence it is labelled as the node core. In the fourth image the cut between the outer elliptical rings and the internode is not visible, whereas in the fifth image the internode becomes distinguishable from the outer elliptical rings. Therefore it is gathered that in the initial stage of the internode, the morphology is not hollow and is filled with small, white and soft circular or bubbled-shaped cells. The sixth image is morphologically quite similar to the fifth, except that the internode is slowly becoming hollow. It can be concluded that after the node core zone the internode starts to appear from the centre, and the elliptical rings become smaller and smaller until the upper internode becomes hollow and hence the outer elliptical rings disappear. This detailed morphological investigation of node region reveals why the node is the hardest anatomical part of the wheat straw stem. The investigation of the node region profile across the diameter of the node was performed along a 1.8 mm distance, as shown in Fig. 11.5. The cross section of the node core, as the whole straw was cut in transverse direction in the node region, shows that the node core is very dense with tightly packed bubbled-shaped cells in the centre (Fig. 11.5(a)), and there are brownish-coloured elliptical-shaped rings, which are ordered in a circle occupying the overall node core. The centre of these elliptical-shaped rings is white and is constituted with small circular cells that are very soft, and some cuts are visible within the brown elliptical-shaped rings (Fig. 11.5(a)). Fig. 11.5(b) shows the morphology of the brown elliptical rings in longitudinal direction with the white cells occupying the centre of these rings. The longitudinal length of elliptical-shaped rings in the node core is about 150−160 μm.

11.3.5.2 Internode

Unlike the node, the morphological longitudinal profile of the internode was found to be consistent. The only morphological difference exists in the beginning stages and termination of the same internode from the lower node to the upper node. This

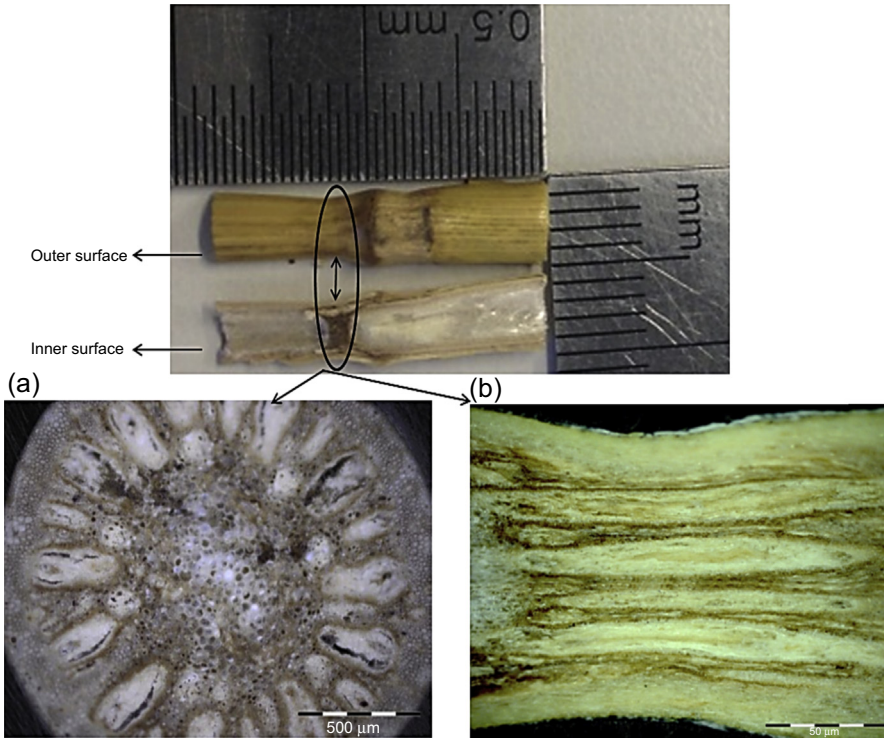

Figure 11.5 (a) Node cross section and (b) node transverse inner surface view.

difference is simply in the partial occupation of small cellular cells that exist in the termination of the internode, which is not present in the beginning stages, which are immediately hollow. The outer part of the straw (epidermis) internode contains wax and inorganic substances on the surfaces and then follows a region with fibre bundles (vascular bundles) integrated in a region of parenchyma and vessel elements. The lignin material forms a thin layer around the parenchyma, and although it contains vascular bundles, its main function is considered to stiffen the stem structure. The epidermis is a complex tissue with bubble-shaped polygonal short and long cell types (Fig. 11.6). The wheat straw epidermis is thin but has dense and thick-walled cells with an outer wall coated with a waxy film of cutin cuticle. The function of the epidermis is to control gas exchange and water balance; it also protects and supports the plant body. The vascular system has xylem tissue with dense lignified structures in the secondary wall, surrounded by a strong sheath of sclerenchyma cells, which have elongated thick lignified cell walls resistant to microbial degradation; the observations are in agreement with the earlier report (Hansen et al., 2011). In wheat straw the protoxylem vessels are developed with a very strong lignified cell wall. These cells have an extreme length and honeycomb shape (Fig. 11.6). The dense layers of epidermal cells may give additional mechanical strength to the stem. In addition to two rings of vascular bundles, there is a considerable amount of extra vascular fibres (Fig. 11.6). Fibres on

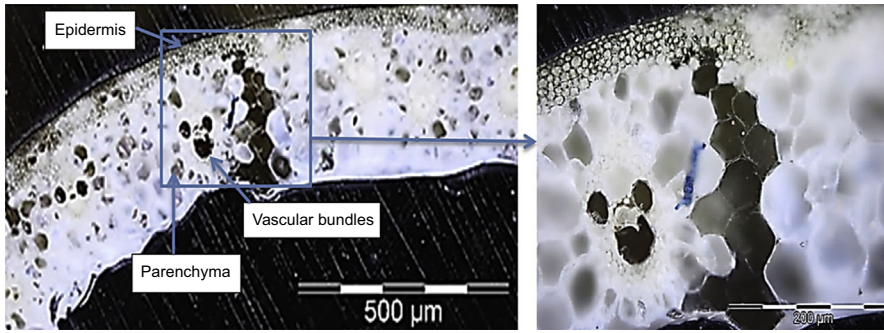

Figure 11.6 Optical microscopy image of internode cross section.

the phloem side of the vascular bundles represent the most valuable fibrous material in the stem strongly bounded to the epidermis. The longitudinal section of vascular bundles has some parts of densely lignified thickenings in the secondary wall, arranging as annular rings or spiral structures to form vessels, which are capable of stretching. It has been reported that the protoxylem vessels are formed early in the season, then during growth they are partially broken down and form an internodal cavity called lacuna (Liu et al., 2005b). The strengthening tissue of sclerenchyma fibres surrounds the vascular cells. The spiral structure is in the lignified thickening secondary wall, which mainly consists of cellulose surrounded by the primary wall. The annular and spiral vessels arise at the earlier growth stage, during which the plant growth is very fast, and a higher stress exists during the formation process of the two types of structures, which leads to a higher orientation order of cellulose chains in the biosynthesis process of cellulose (Yu et al., 2005). Scanning electron microscopy was used to further examine the microstructure and the surface morphology of the wheat straw. Fig. 11.7 shows that the internode cross section of wheat straw and the observations are similar to those of the OM images. The morphology of cellulose in vascular protoxylem consists of annular rings or spiral form backbones with thin cellulose films around them. The parenchyma consists of vascular bundles embedded in a soft cellular material composed mainly of cellulose. The cellulose-rich epidermis forms a hard, rigid outer layer, which protects the living cells within and stiffens the stem in conjunction with the lignin material. Cellulose microfibrils are very important in wheat straw tissues and make the major contribution to the mechanical strength; they also act as the framework of cell walls in the vascular bundles. The distance between the spiral vessels in the vascular bundle is measured to be roughly 200 µm (see Fig. 11.7).

11.4 Pretreatment and processing of straw biomass

Major research efforts have been spent to find efficient and fast pretreatment methods. The pretreatment has a large impact on all the other steps in the process. Due to environmental and sustainability issues, this century has witnessed remarkable

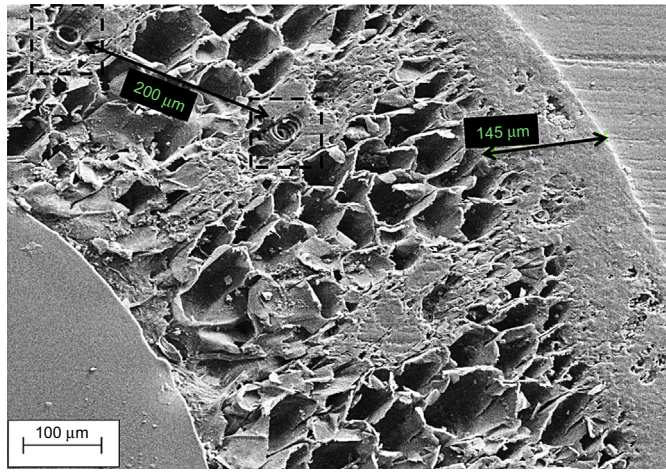

Figure 11.7 An example of internode cross section showing the epidermis and distance between spiral vessels in vascular bundles.

achievements in green technology in the field of material science through the development of biocomposites. The waxy layer on the outer surface of straw biomass is one of the main inhibiting factors for the reduction of bonding quality in biocomposites, and on the other hand, it makes the straw less accessible to the main components, such as cellulose and hemicellulose, which could be utilised as a bioenergy source. The wax is normally made up of a mixture of primarily long-chain fatty acids and fatty alcohols, sterols and alkanes (Deswarte et al., 2006). The biocomposites from straw biomass will experience low quality without any pretreatments to address the issues raised from the waxy layer on the surface (Shen et al., 2011). The pretreatments should not only be environmentally sustainable but also should not deteriorate the mechanical integrity and rigidity of each individual straw. Traditionally the wax layer was extracted by the organic solvents like ethanol/benzene. Han et al. (1999) reported that the wettability of the wheat straw surface was enhanced through ethanol/benzene extraction, and the bondability of particleboards made from extracted wheat straw was improved due to the removal of wax-like substances and other nonpolar extractives from the straw surface. Other approaches have been used to increase interfacial adhesion between the straw surface and resin system, such as steam explosion (Han et al., 2010; Li et al., 2011), acid or alkali treatment (Mo et al., 2001; Zheng et al., 2007), coupling agents modification (Han et al., 2001a) and enzyme treatment (Zhang et al., 2003; Schmidt et al., 2002).

In our previous research on the differential behaviour of wheat straw with various pretreatments (Ghaffar and Fan, 2015b), we focused on understanding wheat straw (node and internode) by investigating important properties for the processing and further production of biocomposites. A combination of mild physical treatments and the synergetic effect of each physical treatment were investigated in terms of chemical, surface and mechanical properties. Functional group changes were monitored in two

anatomical sections of the inner and outer surface of the wheat straw stem, and the results showed a reduction in the intensities assigned to aliphatic fractions of waxes and silica after each stage of pretreatment when compared to the untreated samples. The penetration rate (wettability) and hydrophobicity of wheat straw internode outer surface was analysed through contact angle measurements, which indicated a 35% decrease in the hydrophobicity of straw surface, therefore increasing the wettability after the combinational pretreatment. This is advantageous for water-based adhesives used in biocomposite production. The relationship of surface characteristics to the mechanical properties of wheat straw was also investigated by testing the single strand tensile strength of nodes and internodes. The results revealed a 35% increase in tensile strength of wheat straw after the pretreatment in comparison to untreated wheat straw. The thermogravimetric analysis also indicated that the thermal stability of the wheat straw increased after the pretreatment, which is encouraging for the biocomposite application.

Alemdar and Sain (2008b) researched cellulose nanofibers that were extracted from wheat straw by a combination of chemical and mechanical treatment. Chemical composition, morphology and physical and thermal properties of the nanofibers were characterised to investigate their capability in biocomposite applications. Results showed that the produced wheat straw nanofibers' diameters are within the range of 10−80 nm with lengths of a few thousand nanometers. The crystallinity of the nanofibers was increased by 35% for the wheat straw nanofibers following the treatment. The nanofibers also exhibited enhanced thermal properties, where thermal degradation temperatures increased by 45%, making them promising candidates for use in thermoplastic composites. It can be concluded from these results that the cellulose nanofibers obtained from wheat straw can find potential application in biocomposites such as consumer goods and building products.

Biocomposites from wheat gluten and wheat straw fibres were prepared using a thermomechanical process (Montaño-Leyva et al., 2013). Three types of wheat straw fibres were prepared by successive grinding processes: cut milling, impact milling and ball milling with sizes of 1.1 mm, 62 μm and 8 μm, respectively. It was shown that the adhesion at the interface wheat straw fibre/wheat gluten was improved by a higher specific area of fibres, which was favoured in the case of small fibres. It was shown that the interfacial adhesion was improved in the ball milling > impact milling > cut milling order (Montaño-Leyva et al., 2013). Mechanical properties of a short fibre reinforced composite depend on several factors such as fibre volume content, fibre aspect ratio, fibre orientation and fibre/matrix adhesion. The tensile strength is mainly dependent on the compatibility between the filler and the matrix, while the Young's modulus is more influenced by the fibre impregnation and aspect ratio.

11.4.1 Biocomposites

Industrial applications of straw biomass are still under investigation. One of such applications is using straw biomass in composites that would fit in the construction sector well. A major approach is to chop and mill straw biomass directly into particles and then use the particles to make composites (Panthapulakkal et al., 2006;

Han et al., 2001a; Schirp et al., 2006; Hornsby et al., 1997a). Other approaches include acid hydrolysis before milling (Le Digabel et al., 2004), steam explosion and thermomechanical processes (Halvarsson et al., 2009; Avella et al., 1995), chemical pulping before shearing (Panthapulakkal et al., 2006) and a chemimechanical technique to produce straw biomass fibres (Alemdar and Sain, 2008a; Ye et al., 2007). Finding the limitations with the straw biomass for the targeted product is the key to outstanding research and development; hence the detailed study of straw is required to finding the limitations associated with it in biocomposite applications. Interestingly, research on the biocomposites from straw has been on utilising straws in particle form with very short length (ie, Halvarsson et al., 2008, 2009; Alemdar and Sain, 2008a; Panthapulakkal et al., 2006; Le Digabel et al., 2004; Avella et al., 1995), whereas the mechanical properties could potentially be increased by using longer straws and the energy consumption of the processing of raw materials could be lowered.

Several strategies have been developed to utilise the binding material that binds natural wood together for the binding of wood composites. Water-resistant bonds can be obtained by pressing at high forces (100 g cm^{-3}) and temperatures (200°C) for rather long periods of time. Under these conditions, binding is obtained by the pyrolytic degradation of the cell wall constituents (Zavarin, 1984). Using the procedures described, wood composites with reasonable mechanical properties can be achieved. The main principle is to activate the outer surface layer of the fibre before pressing and create chemical bonding between adjacent fibres during hot pressing. In straw biomass, the constituents such as lignin, protein, starch, fat and water soluble carbohydrates are 'natural binders' (Kaliyan and Morey, 2010). These natural binders can be softened or melted locally either by high moisture or elevated temperature and steam to utilise their binding functionality.

Biocomposites, in general, might not possess high strength as in the case of advanced composites made from synthetic fibres. Nevertheless, there are many mass volumes, both noncritical and/or nonstructural applications, at present where composites with moderate strength are needed.

11.4.1.1 Bioengineering of straw biomass to biocomposites

Innovative approaches to minimise the amount of binder while ensuring product quality is vital for the industry. In this context the forest industry is increasingly approaching enzyme technology in the search of solutions. Biocomposite properties made from biological pretreatment of raw materials are discussed and compared in the following sections where the optimised parameters (ie, press time, press temperature, enzyme dosage, etc.) are identified in order to achieve an overall satisfactory composite for construction purposes. The lignin enzymatic activation for biomass biocomposites could contribute to the self-bonding characteristics of the biomass by oxidation of their surface lignin (Widsten and Kandelbauer, 2008). The in situ cross-reaction of lignin via laccases were used to produce biocomposites, and the inclusion of hot pressing to this process further increased the cross-linking (Felby et al., 2002, 2004; Lund et al., 2000). The bonding mechanism of fibreboards produced from laccase pretreated fibres could be related to phenoxy radicals on biomass surfaces that cross-link when

the biomass is pressed into boards (Felby et al., 1997, 2002, 2004; Kharazipour et al., 1997; Widsten et al., 2003). The condensation of hemicellulose degradation products, hydrogen bonding and molecular entanglement are also other contributions to the enhanced bonding quality effect (Felby et al., 2004; Widsten et al., 2003).

In small-scale trials by Felby et al. (1997) and Kharazipour et al. (1997, 1998), biomass fibres were incubated with laccase (Felby et al., 1997; Kharazipour et al., 1997) or peroxidase (Kharazipour et al., 1998) at a low consistency in H_2O medium at an appropriate pH, or laccase solution was sprayed on wood fibres (Kharazipour et al., 1997). According to the European standard (BS EN 622−5, 2009), none of the enzymatically bonded medium density fibreboard (MDF) obeys with the standards for mechanical strength and dimensional stability (Widsten and Kandelbauer, 2008). Nevertheless, higher density biocomposites of great mechanical strength and adequate dimensional stability were developed on laboratory/pilot-scale, which passed the European specifications (BS EN 622−2, 2004) (Kharazipour et al., 1993; Qvintus-Leino et al., 2003).

The physical and mechanical properties along with the processing parameters of biocomposites made through biological pretreatment from forest and agricultural biomass are presented in Table 11.4.

Halvarsson et al. (2009) used wheat straw for fibreboard production without synthetic resin. The bonding was triggered by the activation of fibre surface by oxidative pretreatment and Fenton's reagent (ferrous chloride and hydrogen peroxide), during the defibration process. Particleboards using flax and hemp, treated by laccase enzyme and its mediators (ABTS, 1-hydroxybenzotriazole (HBT), 3′-Hydroxyacetanilide (NHA)), were processed by Batog et al. (2008). The particleboards treated by laccase had better strength than in the absence of laccase; the laccase mediators improved the enzymatic oxidation of lignin. The improvement of laccase activity was realised by adding its mediators and the processing medium (by using a buffer and an organic solvent: dioxane solution).

The surface is important in the bonding mechanisms of enzymatically activated biomass for biocomposites. For example, the surface (fibre/particle) entanglement on a macroscale and the level of contact, which is induced by changes in surface morphology, is vital in the determination of bonding mechanism. The enzyme catalysis initiates stable lignin radicals, which face thermal decay by cross-linking across biomass fibres or particles during the hot press procedure. These robust covalent bonds increase interfacial adhesion and are resistant to moisture so biocomposites should have a relative strength improvement (Felby et al., 2004). The enzyme pretreatment could also produce radical decay products, leading to improved level of carbonyl groups that induce robust Lewis acid−base bonding (hydrogen bonding) links.

11.5 Interfacial bonding in biocomposites

One of the most important parameters dominating the overall behaviour in the mechanical and physical performance of biocomposites is the interfacial bonding. The

Table 11.4 Fibreboard produced from enzymatic activation of agricultural and forest biomass fibres

		Incubation parameters				Pressing parameters					Fibreboard properties					
Enzyme	**Fibre**	***T*, °C**	***t*, h**	**pH**	**Enzyme dosage U/g**	**Mat water content %**	***T*, °C**	***t*, min**	***P*, MPa**	**ρ, g/cm^3**	**Thick-ness, mm**	**IB, MPa**	**MOR, MPa**	**MOE, GPa**	**24 h TS %**	**References**
Laccase SP504 (*Tramates versicolor*)	80% spruce/pine mixture with 20% beech	35	12	5	26,900	Dry fibres	190	5	1	0.78	5.4	0.95	–	–	23	Kharazipour et al. (1997)
Laccase SP504 (*Tramates versicolor*)	Beech	20	1	4.5	–	12	200	5	n/a	0.90	3	1.57	44.6	3.36	19	Felby et al. (1997)
Peroxidase SP502	80% spruce/pine mixture with 20% beech	RT	4	7	4200	Dry fibres	190	5	1	0.8	5	0.63	41.7	4.02	28	Kharazipour et al. (1998)
Tramates versicolor medium	Rape straw	–	–	–	–	Dry fibres	–	–	–	0.8	–	0.35	20	–	50	Unbehaun et al. (2000)
Laccase (*Myceliophtora thermophila*)	Beech	50	0.5	7	24	11–13	200	5	n/a	0.85	8	0.93	46	3.95	46	Felby et al. (2002)
Laccase (*Trametes villosa*)	Beech	20	1	4.5	3	Dry fibres	200	5	n/a	0.85	3	–	40.3	4.08	–	Felby et al. (2004)
Laccase (*Myceliophtora thermophila*)	Beech (TMP)	RT	6	6.7	500	40	190	7	0.3	0.92	4–45	1.4	53	4.8	26	Petri et al. (2009)
Peroxide (4% H_2O_2 + 1% ferrous sulphate) based on dry wheat straw	Wheat straw	–	–	–	–	Wet fibres	200	1.3	0.5	1.0	6	0.67	23	3.5	85	Halvarsson et al. (2009)

mechanism of interfacial bonding will help the further development in designing an innovative matrix and substrate surface treatments. Good adhesion and bonding at the interface is dominant for achieving high interfacial shear and off-axis strength. Good adhesion is also necessary for efficient load transfer and long-term property retention. An important aspect with respect to optimal mechanical performance of straw biocomposites in general, and durability in particular, is the optimisation of the interfacial bond between the straw surface and resin. Comprehensive knowledge of the microstructure in relation to the interface is vital for the development of biocomposites. Several analytical techniques must be used in combination in order to have a reliable method for investigating and evaluating the interfacial bonding mechanism. Besides the properties of the reinforcing fibre and the polymer matrix, the fibre/matrix interaction has a critical impact on the properties of a biocomposite (Rao et al., 1991; Herrera-Franco and Drzal, 1992). The chemical composition of the fibre and the composition of the fibre surface have a crucial part (Adusumali et al., 2006; Narkis et al., 1988; Luo and Netravali, 1999). The optimal interface between a strong fibre and the matrix leads to a strong composite with high tensile strength, whereas a weak fibre/matrix interface, in which force transfer from the matrix to the fibre is impossible, leads to a reduction in the tensile properties. For the interpretation of the mechanical properties of a composite, the characterisation of fibre/matrix adhesion is important (Graupner et al., 2014).

The interfacial shear strength in biocomposites mainly depends on mechanical interlocking and chemical bonding. Hydrogen bonding is probable between the ester groups of the resin and -OH groups on the fibre. The surface irregularity and/or roughness mainly attributes to the mechanical entanglement. Bonding performance is presumed to be influenced by the degree of penetration of the adhesive into the porous network of interconnected cells of straw. Mechanical interlocking happens on a millimetre and micron length scale, and diffusion entanglement within the cell wall pores could occur on a nanoscale.

It is necessary to enhance the surface morphology at the interfaces to maximise the load-bearing capacity of bonded joints and to improve their deformational characteristics. The usage properties of the adhesive joints depend on the quality of the interface that is formed between the substrates.

11.5.1 Matrices for biocomposites

Composite products from agricultural and forest biomass are conventionally made with the expensive petroleum-derived adhesives; manufacturers of MDF, particleboard, plywood and oriented strand board are under pressure to reduce production costs and harmful formaldehyde emissions from the petroleum-derived adhesives and to improve product recyclability. Matrices are important part of composites, in particular for biocomposites it is necessary to find alternatives derived from biobased resources that can replace petroleum-based polymers. Thermosetting resins originating from renewable resources such as vegetable oils, starch, hemicellulose, etc. have been developed; several sources for natural-based binders are known, such as lignin, tannin, starch, pulp and protein (Ghaffar and Fan, 2014; Alemdar and Sain,

2008a; Kaliyan and Morey, 2010; Norström et al., 2015). This development is motivated by the climate change concerns (ie, renewable bio-based matrices are CO_2 neutral) and the necessity to lower dependency of fossil oil as raw material, since the increasing demand for products should not rely entirely on a limited resource. Bio-based polyester resin and polyfurfuryl alcohol resins have a great potential to be used for biocomposites. A fully bio-based polyester resin is hard to achieve due to the lack of cost-effective methods to synthesise styrene from a biological precursor; however, styrene replacements are being proven (Liu et al., 2015c,d). Polyfurfuryl alcohol resin is derived from agricultural wastes rich in hemicellulose. For these new resins to be accepted by the industries, their properties need to be well understood and a comparison with conventional resins, such as vinylesters and epoxies, must be investigated in detail. If such resins are compatible with straw fibres, in terms of establishing a good interfacial bonding, which dominates the overall performance of any composite, then completely bio-based composites can be commercialised.

The most commonly used matrix materials for the wheat straw composites are polypropylene and high-density polyethylene (Panthapulakkal et al., 2006; Schirp et al., 2006; Avella et al., 1995; Le Digabel et al., 2004; Frounchi et al., 2007; Hornsby et al., 1997b; Panthapulakkal and Sain, 2006; Shakeri and Hashemi, 2004). Other matrix materials used for the wheat straw composites include urea formaldehyde (UF) resin (Zhang et al., 2003; Han et al., 2001b) or melamine-UF resin and phenol–formaldehyde resin (Halvarsson et al., 2008; Hervillard et al., 2007). Various coupling agents were also used to increase the adhesion between wheat straw and resin for the improvement of the mechanical properties of the composites (Zou et al., 2010).

For manufacturing good quality straw-based biocomposites, polymeric methane diphenyl diisocyanate (PMDI) is currently a required adhesive to make particleboards, which could satisfy the commercial and/or industrial requirements. However, PMDI is more expensive than other water-based adhesives such as UF and phenol formaldehyde (PF). PMDI is also more environmentally harmful, because it is an isocyanate-based composition and should be of certain toxicity. It could cause mild eye irritation and slight skin irritation. Vapour hazard arises if the PMDI material is heated to temperatures above 40°C (ie, when hot pressing). These hazards have a serious effect on the health of workers. Under such conditions, it is essential to wear a gas mask and a respirator since repeated inhalation of the vapour at levels above the ceiling threshold limit value causes respiration sensitisation (Zhang and Hu, 2014).

A primary objective of lignin utilisation research has been to use industrial lignin as binders; most of the research for this specific property has focused on the incorporation of lignin with phenolic wood adhesives for panel products. A detailed report of the development of lignin-based wood adhesives has been produced by the previous researchers (Nimz, 1983). Lignin acts together with hemicellulose as a perfect natural adhesive for straw, and the isolated technical lignins generally are poor binders for wood composites when compared to conventional resin systems such as PF resins (Lewis et al., 1989), although industrial soda bagasse lignin was shown to have much higher reactivity toward formaldehyde, which was considered to be due to a lower degree of condensation and more phenylpropanoid units that maybe from *p*-coumarate (Ysbrandy et al., 1992).

11.6 Conclusions and future perspectives

Straw has been used as a building material worldwide for most of the last 9000 years; only since industrialisation has its use declined. Configuring straw to exploit its intrinsic strength and resistance to decay when kept dry, and good thermal properties could bring it back into favour as a building material. Straw is cheap, nontoxic, easy to handle and use, abundant and carbon capturing. It provides good comfort to building occupants and it is safe to dispose of at the end of life as it is biodegradable. Sustainability, industrial ecology and eco-efficiency establish the principles that are guiding the developments of new generations of green materials for construction. Renewable-based building products must be produced as full-scale components using biocomposite materials. This must be carried out to prove that such components could be made and would have properties that enable them to comply with the requirements of the application. Biocomposites are being applied to a wide range of materials derived wholly or in part from renewable biomass resources. Utilising biocomposites to reduce the embodied energy in building facades, supporting structures and internal partition systems must be explored; this will result in a step change in the use of sustainable, low-carbon construction materials. With the developments in technology, it is compulsory to stop developing materials that are environmentally hazardous. Biofibres from straw, sisal, coir, hemp, etc. are being explored to find applications in a wide range of industries other than the construction sector.

Developing biocomposite materials for construction products with a long life span is possible by protecting the straw-based fibres with novel pretreatments and coatings to enhance the overall biocomposite properties. Therefore a system should be designed, taking into consideration all the aspects related to construction, which could replace the high embodied energy construction materials currently in use. The aim should be to integrate a cohesive and efficient construction system and prove the technology by means of full-size demonstration installations. Facilitating the interregional and transnational product chain development concerning straw-based construction materials through the informing of, and collaboration with, all relevant stakeholders must be the main topic to be focused on for the emerging sustainable developments. It is also important to keep improving the performance of straw-based building products through innovation in pretreatment strategies and technologies.

References

Alemdar, A., Sain, M., 2008a. Biocomposites from wheat straw nanofibers: morphology, thermal and mechanical properties. Composites Science and Technology 68, 557−565.

Alemdar, A., Sain, M., 2008b. Isolation and characterization of nanofibers from agricultural residues − wheat straw and soy hulls. Bioresource Technology 99, 1664−1671.

Avella, M., Bozzi, C., dell'Erba, R., Focher, B., Marzetti, A., Martuscelli, E., 1995. Steam-exploded wheat straw fibers as reinforcing material for polypropylene-based composites. Characterization and properties. Die Angewandte Makromolekulare Chemie 233, 149−166.

Adusumali, R., Reifferscheid, M., Weber, H., Roeder, T., Sixta, H., Gindl, W., 2006. Mechanical properties of regenerated cellulose fibres for composites. Macromolecular Symposia 244, 119−125.

Borrion, A.L., McManus, M.C., Hammond, G.P., 2012. Environmental life cycle assessment of bioethanol production from wheat straw. Biomass Bioenergy 47, 9−19.

BS EN 622−5, 2009. Fibreboards. Specifications. Requirements for Dry Process Boards (MDF).

BS EN 622−2, 2004. Fibreboards. Specifications. Requirements for Hardboards.

Batog, J., Kozlowski, R., Przepiera, A., 2008. Lignocellulosic composites bonded by enzymatic oxidation of lignin. Molecular Crystals and Liquid Crystals 484, 35/42/408.

Deswarte, F.E.I., Clark, J.H., Hardy, J.J.E., Rose, P.M., 2006. The fractionation of valuable wax products from wheat straw using CO_2. Green Chemistry 8, 39−42.

Le Digabel, F., Boquillon, N., Dole, P., Monties, B., Averous, L., 2004. Properties of thermoplastic composites based on wheat-straw lignocellulosic fillers. Journal of Applied Polymer Science 93, 428−436.

Frost, R.L., Mendelovici, E., 2006. Modification of fibrous silicates surfaces with organic derivatives: an infrared spectroscopic study. Journal of Colloid and Interface Science 294, 47−52.

Fang, J.M., Fowler, P., Tomkinson, J., Hill, C.A.S., 2002. Preparation and characterisation of methylated hemicelluloses from wheat straw. Carbohydrate Polymers 47, 285−293.

Felby, C., Hassingboe, J., Lund, M., 2002. Pilot-scale production of fiberboards made by laccase oxidized wood fibers: board properties and evidence for cross-linking of lignin. Enzyme and Microbial Technology 31, 736−741.

Felby, C., Thygesen, L.G., Sanadi, A., Barsberg, S., 2004. Native lignin for bonding of fiber boards—evaluation of bonding mechanisms in boards made from laccase-treated fibers of beech (Fagus sylvatica). Industrial Crops and Products 20, 181−189.

Felby, C., Pedersen, L., Nielsen, B., 1997. Enhanced auto-adhesion of wood fibres using phenol oxidases. Holzforschung 51, 281−286.

Frounchi, M., Dadbin, S., Jahanbakhsh, J., Janat-Alipour, M., 2007. Composites of rice husk/wheat straw with pMDI resin and polypropylene. Polymers & Polymer Composites 15, 619.

Ghaffar, S.H., Fan, M., 2015a. Revealing the morphology and chemical distribution of nodes in wheat straw. Biomass Bioenergy 77, 123−134.

Ghaffar, S.H., Fan, M., 2014. Lignin in straw and its applications as an adhesive. International Journal of Adhesion and Adhesives 48, 92−101.

Ghaffar, S.H., Fan, M., 2013. Structural analysis for lignin characteristics in biomass straw. Biomass Bioenergy 57, 264−279.

Ghaffar, S.H., Fan, M., 2015b. Differential behaviour of nodes and internodes of wheat straw with various pre-treatments. Biomass Bioenergy 83, 373−382.

Glasser, W., Kaar, W., Jain, R., Sealey, J., 2000. Isolation options for non-cellulosic heteropolysaccharides (HetPS). Cellulose 7, 299−317.

Graupner, N., Rößler, J., Ziegmann, G., Müssig, J., 2014. Fibre/matrix adhesion of cellulose fibres in PLA, PP and MAPP: a critical review of pull-out test, microbond test and single fibre fragmentation test results. Composites Part A: Applied Science and Manufacturing 63, 133−148.

Hansen, M.A.T., Kristensen, J.B., Felby, C., Jørgensen, H., 2011. Pretreatment and enzymatic hydrolysis of wheat straw (*Triticum aestivum* L.) − the impact of lignin relocation and plant tissues on enzymatic accessibility. Bioresource Technology 102, 2804−2811.

Halvarsson, S., Edlund, H., Norgren, M., 2009. Manufacture of non-resin wheat straw fibreboards. Industrial Crops and Products 29, 437−445.

Han, G., Cheng, W., Deng, J., Dai, C., Zhang, S., Wu, Q., 2009. Effect of pressurized steam treatment on selected properties of wheat straws. Industrial Crops and Products 30, 48–53.

Hansen, M.A.T., Jørgensen, H., Laursen, K.H., Schjoerring, J.K., Felby, C., 2013. Structural and chemical analysis of process residue from biochemical conversion of wheat straw (*Triticum aestivum* L.) to ethanol. Biomass Bioenergy 56, 572–581.

Helbert, W., Sugiyama, J., Ishihara, M., Yamanaka, S., 1997. Characterization of native crystalline cellulose in the cell walls of Oomycota. Journal of Biotechnology 57, 29–37.

Han, G., Umemura, K., Kawai, S., Kajita, H., 1999. Improvement mechanism of bondability in UF-bonded reed and wheat straw boards by silane coupling agent and extraction treatments. Journal of Wood Science 45, 299–305.

Han, G., Deng, J., Zhang, S., Bicho, P., Wu, Q., 2010. Effect of steam explosion treatment on characteristics of wheat straw. Industrial Crops and Products 31, 28–33.

Han, G., Umemura, K., Wong, E., Zhang, M., Kawai, S., 2001a. Effects of silane coupling agent level and extraction treatment on the properties of UF-bonded reed and wheat straw particleboards. Journal of Wood Science 47, 18–23.

Hornsby, P.R., Hinrichsen, E., Tarverdi, K., 1997a. Preparation and properties of polypropylene composites reinforced with wheat and flux straw fibres: Part I Fibre characterization. Journal of Materials Science 32, 443–449.

Halvarsson, S., Edlund, H., Norgren, M., 2008. Properties of medium-density fibreboard (MDF) based on wheat straw and melamine modified urea formaldehyde (UMF) resin. Industrial Crops and Products 28, 37–46.

Herrera-Franco, P.J., Drzal, L.T., 1992. Comparison of methods for the measurement of fibre/matrix adhesion in composites. Composites 23, 2–27.

Hornsby, P., Hinrichsen, E., Tarverdi, K., 1997b. Preparation and properties of polypropylene composites reinforced with wheat and flax straw fibres: Part II Analysis of composite microstructure and mechanical properties. Journal of Materials Science 32, 1009–1015.

Han, G., Kawai, S., Umemura, K., Zhang, M., Honda, T., 2001b. Development of high-performance UF-bonded reed and wheat straw medium-density fiberboard. Journal of Wood Science 47, 350–355.

Hervillard, T., Cao, Q., Laborie, M.G., 2007. Improving water resistance of wheat straw-based medium density fiberboards bonded with aminoplastic and phenolic resins. BioResources 2, 148–156.

Inglesby, M.K., Gray, G.M., Wood, D.F., Gregorski, K.S., Robertson, R.G., Sabellano, G.P., 2005. Surface characterization of untreated and solvent-extracted rice straw. Colloids and Surfaces B: Biointerfaces 43, 83–94.

Jiang, H., Zhang, Y., Wang, X., 2009. Effect of lipases on the surface properties of wheat straw. Industrial Crops and Products 30, 304–310.

Kristensen, J., Thygesen, L., Felby, C., Jorgensen, H., Elder, T., 2008. Cell-wall structural changes in wheat straw pretreated for bioethanol production. Biotechnology for Biofuels 1, 5.

Kaliyan, N., Morey, R.V., 2010. Natural binders and solid bridge type binding mechanisms in briquettes and pellets made from corn stover and switchgrass. Bioresource Technology 101, 1082–1090.

Kharazipour, A., Huettermann, A., Luedemann, H.D., 1997. Enzymatic activation of wood fibres as a means for the production of wood composites. Journal of Adhesion Science and Technology 11, 419–427.

Kharazipour, A., Bergmann, K., Nonninger, K., Hüttermann, A., 1998. Properties of fibre boards obtained by activation of the middle lamella lignin of wood fibres with peroxidase and H_2O_2 before conventional pressing. Journal of Adhesion Science and Technology 12, 1045–1053.

Kharazipour, A., Hüttermann, A., Kühne, G., Rong, M., 1993. Process for gluing wood chips and articles produced by this process. European Patent Application. EP0565109.

Lindedam, J., Andersen, S.B., DeMartini, J., Bruun, S., Jørgensen, H., Felby, C., et al., 2012. Cultivar variation and selection potential relevant to the production of cellulosic ethanol from wheat straw. Biomass Bioenergy 37, 221−228.

Larsen, S.U., Bruun, S., Lindedam, J., 2012. Straw yield and saccharification potential for ethanol in cereal species and wheat cultivars. Biomass Bioenergy 45, 239−250.

Liu, W., Misra, M., Askeland, P., Drzal, L.T., Mohanty, A.K., 2005a. 'Green' composites from soy based plastic and pineapple leaf fiber: fabrication and properties evaluation. Polymer 46, 2710−2721.

Lawrence, M., 2015. Reducing the environmental impact of construction by using renewable materials. Journal of Renewable Materials 3, 163−174.

Laurichesse, S., Avérous, L., 2014. Chemical modification of lignins: towards biobased polymers. Progress in Polymer Science 39, 1266−1290.

Linxin, Z., Shiyu, F., Feng, L., Huaiyu, Z., 2010. Chlorine dioxide treatment of sisal fibre: surface lignin and its influences on fibre surface characteristics and interfacial behaviour of sisal fibre/phenolic resin composites. BioResources 5, 2431−2446.

Liu, R., Yu, H., Huang, Y., 2005b. Structure and morphology of cellulose in wheat straw. Cellulose 12, 25−34.

Li, X., Cai, Z., Winandy, J.E., Basta, A.H., 2011. Effect of oxalic acid and steam pretreatment on the primary properties of UF-bonded rice straw particleboards. Industrial Crops and Products 33, 665−669.

Lund, M., Hassingboe, J., Felby, C., 2000. Oxidoreductase catalyzed bonding of wood fibres. Bordeaux, France. In: Proceedings of the 6th European Workshop on Lignocellulosics and Pulp, pp. 113−116.

Luo, S., Netravali, A., 1999. Interfacial and mechanical properties of environment-friendly "green" composites made from pineapple fibers and poly (hydroxybutyrate-co-valerate) resin. Journal of Materials Science 34, 3709−3719.

Liu, W., Xie, T., Qiu, R., 2015c. Styrene-free unsaturated polyesters for hemp fibre composites. Composites Science and Technology 120, 66−72.

Liu, W., Xie, T., Qiu, R., Fan, M., 2015d. N-methylol acrylamide grafting bamboo fibers and their composites. Composites Science and Technology 117, 100−106.

Lewis, N., Lantzy, T., Branhm, S., 1989. Lignin in adhesives: introduction and historical perspective. In: Hemingway, R., Conner, A. (Eds.), Adhesives from Renewable Resources. Oxford University Press, Oxford, pp. 13−26.

Mohanty, A.K., Misra, M., Hinrichsen, G., 2000. Biofibres, biodegradable polymers and biocomposites: an overview. Macromolecular Materials and Engineering 276-277, 1−24.

McLeod, R.S., Hopfe, C.J., 2013. Hygrothermal implications of low and zero energy standards for building envelope performance in the UK. Journal of Building Performance Simulation 6, 367−384.

Merk, S., Blume, A., Riederer, M., 1997. Phase behaviour and crystallinity of plant cuticular waxes studied by Fourier transform infrared spectroscopy. Planta 204, 44−53.

Mo, X., Hu, J., Sun, X.S., Ratto, J.A., 2001. Compression and tensile strength of low-density straw-protein particleboard. Industrial Crops and Products 14, 1−9.

Montaño-Leyva, B., Ghizzi, D., da Silva, G., Gastaldi, E., Torres-Chávez, P., Gontard, N., Angellier-Coussy, H., 2013. Biocomposites from wheat proteins and fibers: structure/mechanical properties relationships. Industrial Crops and Products 43, 545−555.

Narkis, M., Chen, E., Pipes, R., 1988. Review of methods for characterization of interfacial fiber-matrix interactions. Polymer Composites 9, 245−251.

Norström, E., Fogelström, L., Nordqvist, P., Khabbaz, F., Malmström, E., 2015. Xylan − a green binder for wood adhesives. European Polymer Journal 67, 483−493.

Nimz, H., 1983. Lignin-based wood adhesives. In: Pizzi, A. (Ed.), Wood Adhesive: Chemistry and Technology. Marcel Dekker, New York, pp. 247−288.

Panthapulakkal, S., Zereshkian, A., Sain, M., 2006. Preparation and characterization of wheat straw fibers for reinforcing application in injection molded thermoplastic composites. Bioresource Technology 97, 265−272.

Petri, W., Alfred, H., Carol, H., Andreas, K., 2009. A preliminary study of green production of fiberboard bonded with tannin and laccase in a wet process. Holzforschung 63, 545.

Panthapulakkal, S., Sain, M., 2006. Injection molded wheat straw and corn stem filled polypropylene composites. Journal of Polymers and the Environment 14, 265−272.

Qvintus-Leino, P., Widsten, P., Tuominen, S., Laine, J., Kunnas, J., 2003. Method of producing compressed layered structures such as fiberboard or similar wood-based products. International Patent Application. WO03047826.

del Rio, J.C., Prinsen, P., Gutierrez, A., 2013. A comprehensive characterization of lipids in wheat straw. Journal of Agricultural and Food Chemistry 61, 1904−1913.

Rao, V., Herrera-Franco, P., Ozzello, A., Drzal, L., 1991. A direct comparison of the fragmentation test and the microbond pull-out test for determining the interfacial shear strength. The Journal of Adhesion 34, 65−77.

Stelte, W., Nielsen, N.P.K., Hansen, H.O., Dahl, J., Shang, L., Sanadi, A.R., 2013. Pelletizing properties of torrefied wheat straw. Biomass Bioenergy 49, 214−221.

Satyanarayana, K.G., Arizaga, G.G.C., Wypych, F., 2009. Biodegradable composites based on lignocellulosic fibers—an overview. Progress in Polymer Science 34, 982−1021.

Sutton, A., Black, D., Walker, P., 2011. Straw Bale: An Introduction to Low-impact Building Materials. IHS BRE Press.

Sun, R., 2010. Extractives. In: peng, P., Bian, J., Sun, R. (Eds.), Cereal Straw as a Resource for Sustainable Biomaterials and Biofuels. Elsevier, United Kingdom, pp. 49−72.

Sun, X.F., Xu, F., Sun, R.C., Fowler, P., Baird, M.S., 2005. Characteristics of degraded cellulose obtained from steam-exploded wheat straw. Carbohydrate Research 340, 97−106.

Sain, M., Panthapulakkal, S., 2006. Bioprocess preparation of wheat straw fibers and their characterization. Industrial Crops and Products 23, 1−8.

Segal, L., Creely, J.J., Martin, A.E., Conrad, C.M., 1959. An empirical method for estimating the degree of crystallinity of native cellulose using the X-ray diffractometer. Textile Research Journal 29, 786−794.

Shen, J., Liu, Z., Li, J., Niu, J., 2011. Wettability changes of wheat straw treated with chemicals and enzymes. Journal of Forestry Research 22, 107−110.

Schmidt, A.S., Mallon, S., Thomsen, A.B., Hvilsted, S., Lawther, J.M., 2002. Comparison of the chemical properties of wheat straw and beech fibers following alkaline wet oxidation and laccase treatments. Journal of Wood Chemistry and Technology 22, 39−53.

Schirp, A., Loge, F., Aust, S., Swaner, P., Turner, G., Wolcott, M., 2006. Production and characterization of natural fiber-reinforced thermoplastic composites using wheat straw modified with the fungus *Pleurotus ostreatus*. Journal of Applied Polymer Science 102, 5191−5201.

Shakeri, A., Hashemi, S., 2004. Effect of coupling agents on mechanical properties HDPE/wheat straw composites. Polymers & Polymer Composites 12, 449−452.

Le Troëdec, M., Peyratout, C.S., Smith, A., Chotard, T., 2009. Influence of various chemical treatments on the interactions between hemp fibres and a lime matrix. Journal of the European Ceramic Society 29, 1861−1868.

Unbehaun, H., Dittler, B., Kühne, G., Wagenführ, A., 2000. Investigation into the biotechnological modification of wood and its application in the wood-based material industry. Acta Biotechnologica 20, 305−312.

van Wyk, J.P.H., 2001. Biotechnology and the utilization of biowaste as a resource for bioproduct development. Trends in Biotechnology 19, 172−177.

Wiśniewska, S.K., Nalaskowski, J., Witka-Jeżewska, E., Hupka, J., Miller, J.D., 2003. Surface properties of barley straw. Colloids and Surfaces B: Biointerfaces 29, 131−142.

Widsten, P., Kandelbauer, A., 2008. Adhesion improvement of lignocellulosic products by enzymatic pre-treatment. Biotechnology Advances 26, 379−386.

Widsten, P., Laine, J.E., Tuominen, S., Qvintus-Leino, P., 2003. Effect of high defibration temperature on the properties of medium-density fiberboard (MDF) made from laccase-treated hardwood fibers. Journal of Adhesion Science and Technology 17, 67−78.

Xiao, B., Sun, X.F., Sun, R., 2001. Chemical, structural, and thermal characterizations of alkali-soluble lignins and hemicelluloses, and cellulose from maize stems, rye straw, and rice straw. Polymer Degradation and Stability 74, 307−319.

Yu, H., Liu, R., Shen, D., Jiang, Y., Huang, Y., 2005. Study on morphology and orientation of cellulose in the vascular bundle of wheat straw. Polymer 46, 5689−5694.

Ye, X.P., Julson, J., Kuo, M., Womac, A., Myers, D., 2007. Properties of medium density fiberboards made from renewable biomass. Bioresource Technology 98, 1077−1084.

Ysbrandy, R., Sanderson, R., Gerischer, G., 1992. Adhesives from autohydrolysis bagasse lignin, a renewable resource − Part II. DSC thermal analysis of novolac resins. Holzforschung 46, 253−256.

Zhang, Y., Ghaly, A., Li, B., 2012. Physical properties of wheat straw varieties cultivated under different climatic and soil conditions in three continents. American Journal of Engineering and Applied Sciences 5, 98−106.

Zhu, X., Wang, F., Liu, Y., 2012. Properties of wheat-straw boards with FRW based on interface treatment. Physics Procedia 32, 430−443.

Zhang, Y., Lu, X., Pizzi, A., Delmotte, L., 2003. Wheat straw particleboard bonding improvements by enzyme pretreatment. Holz als Roh- und Werkstoff 61, 49−54.

Zhao, L., Boluk, Y., 2010. XPS and IGC characterization of steam treated triticale straw. Applied Surface Science 257, 180−185.

Zheng, Y., Pan, Z., Zhang, R., Jenkins, B.M., Blunk, S., 2007. Particleboard quality characteristics of saline jose tall wheatgrass and chemical treatment effect. Bioresource Technology 98, 1304−1310.

Zavarin, E., 1984. Activation of wood surface and nonconventional bonding. In: Rowell, R. (Ed.), The Chemistry of Solid Wood. Advances in Chemistry Series 207. American Chemical Society, Washington DC, pp. 349−400.

Zou, Y., Huda, S., Yang, Y., 2010. Lightweight composites from long wheat straw and polypropylene web. Bioresource Technology 101, 2026−2033.

Zhang, L., Hu, Y., 2014. Novel lignocellulosic hybrid particleboard composites made from rice straws and coir fibers. Materials & Design 55, 19−26.

Electricity functional composite for building construction

12

F. Fu, Q. Yuan
Research Institute of Wood Industry, Chinese Academy of Forestry, Beijing, China

12.1 Introduction

Natural wood fiber-based electricity functional composite refers to these wood-based composites with certain electric conductivity obtained through directly carbonizing the composites or combining them with excellent electrical and magnetic functional units by the surface coating, built-in composite, confounding, and so on.

According to the structure, it can be classified as follows: (1) surface conduction type, (2) built-in conduction type, and (3) whole conduction type.

According to the functionalities, it can be classified as follows: (1) electromagnetic shield (reflection, absorption, and multiple reflections), (2) antistatic function, (3) electric heating, (4) piezoelectricity, and (5) electrochromism.

Natural fiber-based material, such as wood, under an air-dried state belongs to a poor conductor of electricity with the resistivity of more than 10^{12} Ω m. Wood therefore is seen as one of the most important insulating materials in construction, transportation, and other industries. The electrical properties of natural wood fiber-based composites have been investigated a great deal, especially for providing good reference information for continuous nondestructive testing of moisture content, high frequency heating, and microwave drying technology. Natural aesthetics and some other inherent functionalities have prompted its applications in construction industries. The natural wood fiber-based electricity functional composite introduced in this chapter, produced by the laminating, confounding, or surface decorating technology, aims to be used for antistatic, electromagnetic shielding, and/or electric heating. The advanced composites and their technologies shall allow the effective and efficient expansion of the applications of wooden composites in construction.

12.2 Natural wood fiber-based antistatic composites

12.2.1 Antistatic mechanisms

Advantages of the natural fibers, eg, wood, in the electric insulation turn it into disadvantages in the uses, such as advanced office furniture and flooring with higher demand. The electrostatic charge is observed to generate on the surface of furniture due to the piezoelectric effect caused by friction or mechanical effect. Electrostatic charges are prevented from escaping and form electrostatic accumulation on the surface because of the

Advanced High Strength Natural Fibre Composites in Construction. http://dx.doi.org/10.1016/B978-0-08-100411-1.00012-1

high electrical resistivity. This can exhibit high voltage and a low current, resulting in the phenomena of discharge once it reaches to a certain degree. It also leads to a numbing in the arms of operators. The accumulation of electrostatic on the surface of furniture could result in potential hazards to human beings and electrical equipment due to the leakage of the generated electrostatic charge. Antistatic treatment on furniture (by improving the electrical conductivity) has been regarded as an effective method to eliminate the hazards caused by the efficient electrostatic. The electrostatic hazards could be prevented by reducing friction, and the leakage of the electrostatic charge could be redirected by conductive charge through the circuit. Reducing the relative humidity in the surrounding environment and the addition of antistatic elements can also be helpful.

12.2.2 Antistatic modification and performance

12.2.2.1 Production of antistatic elements

External coating

The antistatic agents, appropriate dispersant, and additives are generally blended uniformly and then coated on the surface of component, eg, furniture. The antistatic agent can also be mixed with the other paints for the applications. Two approaches generally have the same chemical compositions for the antistatic effectiveness. Nevertheless, the finishing technology is a simpler process and costs less in comparison with the former approach. Therefore it is recommended to mix the antistatic agent with coating to generate an antistatic coating surface. Antistatic coating results in an effective reduction of surface resistance of the coated component, eg, furniture, and hence its antistatic performance can be improved after the application of external coating. In addition the external environmental conditions (ie, surface dust and environment humidity) can also affect the surface resistance of the furniture significantly and result in the instability of the antistatic performance.

Volume impregnation

The antistatic agent has been introduced to the inside of wood by impregnation at the atmospheric pressure and room temperature, or by steaming and pressure cooking to prepare antistatic wood fiber-based composites. The later approach requires a more complex process and equipment. The antistatic composites developed through the internal impregnation need to be further dried to remove the solvent and moisture. Compared to the coating method, the volume impregnation gives rise to a greater declination in the volume resistivity of the composites. The electrostatic charges pass through the composite materials and escape to a low potential along the shorter path. The furniture of such antistatic composites exhibits a more stable antistatic performance.

12.2.2.2 Performance of antistatic agents in the composites

Antistatic agent

The antistatic agent has been widely used in the plastic industry and exhibits a broad application prospect in the furniture industry. The antistatic agent is a kind of

amphiphilic molecule belonging to the organic polymer surfactant. The structural formula of the antistatic agent can be abbreviated to *R-Y-X*. The *R* terminal is nonpolar lipophilic hydrocarbon chain, such as −CH, C_6H_5, and so on. The *X* terminal is hydrophilic polar end groups, such as −OH, −COOH, and NH_2. The *Y* terminal in the middle is a linking group. Most of the *R* terminals are adsorbed on the surface of wood fiber due to its hydrophobic effect after the addition of antistatic agent in the fibers or on the surface of furniture. Such adsorbent comprises ion exchange, ion pair, π electron polarized absorption, and hydrogen bonding and dispersion forces. The *X* terminal departs from the wood fiber and forms a layer of continuous hydrophilic group on the surface of fiber. As illustrated in Fig. 12.1, a trace of water molecules is absorbed by the hydrophilic group from the surrounding environment. A continuous phase of conductive monomolecular layer is formed and results in the reduction of resistivity and the escaping of static electricity. The antistatic agents can be divided into ionic, amphoteric, and nonionic points. The ionic can be divided into anionic and cationic. Comprised of other antistatic agents, it is easier to form water molecule film through absorbing water molecules from the surrounding environment for the ionic surfactant. The ionic antistatic agent exhibits stronger adsorption capacity, longer duration, and better antistatic effect. Additionally, the arrangement of antistatic agents provides an ionized occasion to trace the electrolyte in the timber/fiber. A small quantity of solid solution is formed and results in the enhancement in its own antistatic performance of the composites.

The commonly used antistatic agents can be divided into higher alcohol sulfuric acid ester salt anionic, quaternary ammonium salt type cationic surfactant, betaine amphoteric surfactant, and polyethylene glycol fatty acid ester nonionic. The anionic antistatic treatment, for a negative charge in the water, exhibits good compatibility with the negatively charged fiber. In the adsorption process between antistatic agents and natural wood fibers, the fibers and the hydrophilic end are mutually exclusive due to the properties of negatively charge, so that the lipophilic end and fiber adsorption hydrophilic end link back to the natural wood fiber and make it easier to form a continuous conductive film on the surface of the fiber and the furniture once wood or composites are made into the furniture.

Hygroscopic inorganic salt (ie, NaCl)

The inorganic substance plays an antistatic effect once impregnated in composites due to its strong polarity and hygroscopicity. They still belong to the category of the ionic conductivity in principle, and the salt after hygroscopicity turns to be a conductor due

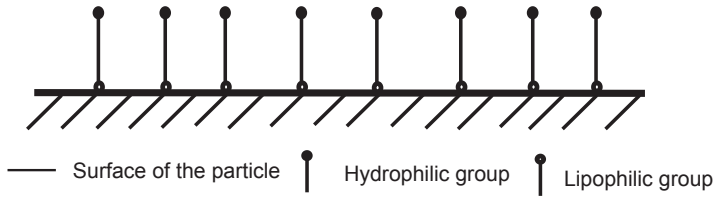

Figure 12.1 Absorption of the octadecyl dimethyl hydroxyethyl quaternary ammonium nitrate (SN) antistatic agent.

to its ionization. However, a significant increase in the moisture content of the components or furniture is observed due to the strong moisture absorption of inorganic salts with the prolonged use of furniture. The increased moisture absorption of the inorganic salts would result in a decrease in the dimensional stability of the furniture products, such as a phenomenon of frosting on its surface.

Metal powder and graphite powder

The metal or graphite powder exhibits an excellent electrical conductivity. The undoped π electronic can move freely between the layers of graphite in its special layered molecular structure. Their role in conducting free electrons is considered, and the use of drift drag free electrons results in the escape of accumulated electrostatic charge. For the efficient escapes of the electrostatic charge, a certain degree of continuous phase must be formed in the surface or inside the furniture. It will seriously affect the decorative effect of furniture after the antistatic treatment due to the black color of powder.

Different antistatic function bodies (ie, single aluminum powder, copper powder, graphite, or glycerin) have been applied to the particleboard composites through various methods (Table 12.1) to prepare the antistatic particleboard composites (Fu and Hua, 1994), which result in different enhancements in antistatic performance (Table 12.2). The ranking order was found as follows: aluminum powder < copper powder < graphite < glycerin. The graphite or glycerin is most effective.

Application of the SN significantly improved the antistatic performance of particleboard. As showed in Fig. 12.1, one end of lipophilic groups with a hydrophobic characteristic will facilitate its adsorption on the surface of wood particles, while the other

Table 12.1 Technologies of doping antistatic additives

Sample number	Antistatic additive	Applied amount (%)	Addition method
1	—	—	—
2	Aluminum powder	7.5	Spraying after dilution of adhesive
3	Copper powder	7.5	Spraying mixed with adhesive solution
4	Graphite	7.5	Spraying mixed with adhesive solution
5	Glycerin	7.5	Spraying directly after gluing
6	—	—	—
7	SN	7.5	Spraying directly after gluing
8	SN + graphite	5.6 + 1.9	Mixed spraying after gluing
9	SN + glycerin	3.9 + 3.6	Spraying respectively after gluing

Table 12.2 **Volume resistivity of particleboard composites**

Sample number	Oven-dry density (g/cm^3)	MC (%)	Resistivity (Ω cm)	MC (%)	Resistivity (Ω cm)	MC (%)	Resistivity (Ω cm)
1	0.73	4.95	1.36×10^{10}	7.97	5.93×10^{8}	11.13	1.23×10^{7}
2	0.75	4.79	2.42×10^{9}	7.34	2.00×10^{8}	10.44	5.50×10^{6}
3	0.74	4.99	1.04×10^{9}	7.78	1.35×10^{8}	10.90	$<2 \times 10^{6}$
4	0.76	4.88	8.38×10^{8}	7.44	1.35×10^{8}	10.80	$<2 \times 10^{6}$
5	0.76	4.65	2.83×10^{8}	7.51	3.42×10^{7}	10.72	$<2 \times 10^{6}$
6	0.63	5.39	7.05×10^{10}	8.35	2.14×10^{9}	11.25	6.19×10^{7}
7	0.62	5.23	1.04×10^{10}	8.00	5.50×10^{8}	11.16	2.98×10^{7}
8	0.62	5.11	3.53×10^{9}	9.00	6.28×10^{7}	11.26	$<2 \times 10^{6}$
9	0.65	4.97	5.83×10^{8}	7.50	7.80×10^{7}	10.68	$<2 \times 10^{6}$

end of the hydrophilic group is back to the surface of wood particles, and a layer of hydrophilic group is formed. The antistatic performance can be significantly enhanced when the SN is mixed with graphite or glycerin. Volume resistivity of the antistatic particleboards decreases by about two orders. Water can also be seen as a kind of antistatic agent. It can be seen from Table 12.2 that the moisture content has a significant effect on the antistatic performance of particleboard composites, and a positive correlation has been found between the two.

12.2.3 Application of natural wood fiber-based antistatic composites

The system resistance of the antistatic wood-based moveable floor shall be $1.0 \times 10^5 \sim 1.0 \times 10^9\ \Omega$ at the condition of $50\% \pm 5\%$ relative humidity and $20 \pm 2°C$ in accordance with the Chinese Forest Industry Standard of LY/T 1330−2011 "Antistatic Wood-Based Moveable Floor." It is apparent that the wood fiber-based antistatic composite as discussed has great potential as an antielectrostatic floor, wallboard, and top panel of the furniture. Application of antistatic furniture will possess a considerable market prospect with the popularization of electronic equipment.

12.3 Wood-based electromagnetic shielding composites

12.3.1 Electromagnetic shielding mechanisms

Electromagnetic (EM) shielding is an electromagnetic shell (entity or nonentity) made of the shielding materials (conductive or magnetic material), which forms a close electromagnetic shielding region and shields the electromagnetic wave. The electromagnetic filed is enclosed in the inner region, and the external electromagnetic radiation cannot enter the inner area either (or out of electromagnetic energy in the region will be greatly attenuated). Refection, absorption, and attenuation of the shielding materials are applied to reduce the effects of the electromagnetic field of the radiation sources. When the EM signal reaches the surface of shield materials, it will be reflected, absorbed, and refracted (Fig. 12.2).

Shielding effectiveness (SE), a measurement of the attenuation of an EM signal through a shielding material, is commonly used to examine the electrical shielding performance. A significant amount of energy of the EM signal will be lost due to the reflection, absorption, and refraction in accordance with the electromagnetic shielding theory of Schelkunoff (1943). The SE of a material under the interference of an ambient electromagnetic signal is expressed as:

$$\mathrm{SE} = R + A + B \tag{12.1}$$

where, SE is the shielding effectiveness in dB, R is the reflection loss in dB, A is the absorption loss in dB, and B is the correction factor due to multiple reflections within the material.

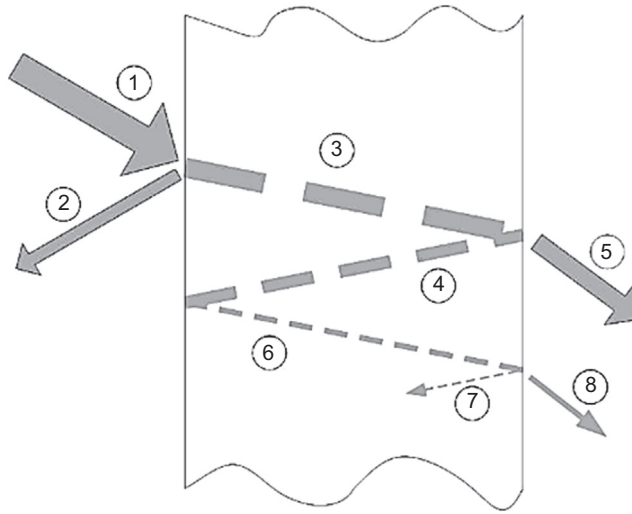

Figure 12.2 Absorption and reflection of electromagnetic wave: (1) is the incident electromagnetic wave; (2) is the reflected part of electromagnetic wave from the first interface; (3), (4), (6), and (7) are the multiple refraction and absorption of electromagnetic wave in the materials; (5) and (8) are the transmitted electromagnetic wave.

Neglecting the effect of the multiple reflections (B) within the material, Eq. (12.1) can be rewritten as Eq. (12.2).

$$\mathrm{SE} = R + A \tag{12.2}$$

For a plane electromagnetic field, the reflection loss R and the absorption loss A can be calculated by Eqs. (12.3) and (12.4), respectively.

$$R = 168 + 10\log_{10}(\sigma_r/\mu_r f) \tag{12.3}$$

$$A = 0.131t(f\mu_r\sigma_r)^{1/2} \tag{12.4}$$

where, σ_r is the electrical conductivity relative to copper, μ_r is the permeability relative to free space, f is the frequency of the signal in Hz, and t is the thickness of the material in millimeters.

From the previous research, most of the SE test is conducted by using the coaxial cable method. The setup consists of a vertical flanged test device with the input and output connected to a Hewlett–Packard 7401A EMC Analyzer (Fig. 12.3).

12.3.2 Methodology and performance of shielding composites

Wood-based electromagnetic shielding composites can be divided into compound electromagnetic shielding composites, including surface conduction type, laminating

Figure 12.3 Setup for the electromagnetic shielding effectiveness test.

type and hybrid type, and carbonized electromagnetic shielding composite. From the previous research, a wooden element is composited with conductive materials by coating, laminating, and filling to prepare wood-based electromagnetic shielding composites. In addition, the carbonized electromagnetic shielding composite with electrical conductivity is prepared through heat treatment to make the overall substrate or surface charring under vacuum or atmosphere conditions.

12.3.2.1 Surface coating

Chemical metallized

Earlier research on the electroless plating is conducted on wood particles to prepare composite particleboard with shielding performance (Nagasawa and Kumagai, 1989; Nagasawa et al., 1990; Nagasawa et al., 1992). The particleboard was prepared by using 10 g of nickel plating particles and pressed at the pressure of 2.5 MPa (Nagasawa et al., 1999). SE of the particleboard reached to more than 40 dB in the frequency of 10 MHz−1 GHz. Electroless plating was also applied to nickel plating on the surface of wood veneers afterward. The veneer after nickel plating exhibits SE of 55−60 dB in the frequency ranged from 9 KHz to 1.5 GHz (Wang et al., 2005, 2006). The metal layer was separated out to form a uniform layer of electromagnetic shield coating on the surface of matrix materials by a reduction reaction under the function of metal ions as the reducing agent during the electroless plating process. The layer of electromagnetic shield coating bonded with the matrix material tightly and exhibited stable electromagnetic shielding performance. It also has a low production cost and advantages in the size and shape. However, the electroless plating metal layer is easy to peel off and has poor secondary processing performance. Therefore it is a key point for the electroless plating technology to improve the bonding strength between the coating layer and the substrate.

Surface pretreatment, such as edulcoration, roughening, or coupling agents, has been conducted to improve the bonding strength between the metal coating layer and matrix material. The surface of the substrate was firstly pretreated by the γ-aminopropyl trihydroxysilane and then the electroless plating was operated (Liu et al., 2010). The experimental results revealed that SE of the substrate was greater than 60 dB at the frequency range of 10 MHz−1.5 GHz and the coating bond strength was greater than 2.5 MPa.

It is difficult for the wood-based electromagnetic shielding composite prepared by a single electroless copper plating or a nickel plating process to meet a certain SE requirements for the special applications. In order to obtain a thicker, more uniform composite metal coating or plating layer, the Ni-Cu-P alloy was applied to the *Fraxinus mandshurica* veneer to prepare a wood-based electromagnetic shielding composite (Hui et al., 2014). A continuous and dense layer of Ni-Cu-P alloy plating was observed to form on the surface of wood veneer, and the SE of the veneer was 55−60 dB.

Metal diaphragm or metal mesh on the surface

The easiest method to prepare surface conductive composites is to apply a conductive foil to the surface of a substrate directly. The iron foil (50 μm in thick), copper foil (10, 18, 35, 50 μm), and aluminum foil (20 μm) have been attempted to cover the surface of a 5 cm-thick plywood (Shiro et al., 1991), and then pasted the PCM (polymer cement mortar) film on the metal foil or decorative plate on the surface of the metal powder layer to prepare three-layered composites (plywood/metal foil/PCM). SE of the three-layered composite covered with iron foil is greater than 30 dB within the frequency of 30−500 MHz and that of the composite covered with copper foil and aluminum foil is 50−80 dB and 30 −60 dB, respectively. The nickel-plated fabric and roughened copper foil also have been stacked to the surface of wood-based composites with the mixture of polyvinyl acetate emulsion and epoxy resin as resin (Wang et al., 2009). It was found that the composited wood-based panel exhibits greater mechanical performance than the wood-based panel. It was also found that the SE of the panel covered with nickel-plated fabric was about 60 dB and that of the panel covered with copper foil was greater than 70 dB; both met the SE requirements of construction timber applied to the shielded room.

Magnetron sputtering

The principle of magnetron sputtering is that the plasma generated at the condition of abnormal glow discharge bombards the surface of cathode target due to the action of an electric field and results in the sputtering of molecules, atoms, ions, and electrons on the surface of the target in the rarefied gas environment (Yu et al., 2009). The sputtered particles with a certain kinetic energy toward the surface of substrate in a certain direction form a uniform and dense coating on the surface of substrate. The copper-plated substrate exhibits twice the value of SE than that of the nickel-plated substrate in the same circumstance. However, the nickel-plated substrate has good resistance to rust wear (Li et al., 1996).

The fiberboard substrate with a precoating thickness of 30 μm was plated with copper and aluminum from the double side by magnetron sputtering for 90 s. Results revealed that SE of the plated fiberboard is above 30 dB in the frequency ranging from 30 MHz to 1.5 GHz. Some fiberboards plated with aluminum from the single side can achieve the SE values of the shielding requirements, high bonding strength between the coating layer and fiber surface, and the improved coating abrasion resistance (Qiu, 2008).

12.3.2.2 Laminated composites

The single layer of electromagnetic shielding material has some limitations in the SE, and it is difficult to meet the requirements of high electromagnetic shielding effectiveness. A single layer of an electromagnetic shielding material only has a good SE in certain frequency bands, and it is difficult to achieve broadband shielding performance. The multiple composite ideas have been introduced to prepare a multilayer electromagnetic shielding composite with excellent performance according to the electromagnetic theory. The electromagnetic shielding materials with high absorption and low reflection were also designed. The more mature multiple shielding theory is the multlayer electromagnetic shielding theory of Schelkunoff and Tao Линь BT. The former is a departure from the perspective road and derived Schelkunoff shielding theory by using the principle of equivalent transmission line. The latter is from the perspective field of view and derived the electromagnetic theory by solving Maxwell equations.

Electromagnetic shielding plywood laminated with conductive sheets

The process of "spreading-scattering-molding-pressing" has been adopted to prepare copper fiber/urea-formaldehyde conductive film, and then its structural features, conductivity, piezo resistivity, and electromagnetic shielding effectiveness were studied (Lu et al., 2011a). Meanwhile, the self-made copper fiber-filled conductive sheets are laminated with wood veneers to manufacture electromagnetic shielding plywood which their structure (Fig. 12.4) and are designed based on the multilayer electromagnetic shielding theory of Schelkunoff and the model of sandwich shielding.

SE of the electromagnetic shielding plywood laminated with double layers of conductive films increases with the rising of the filling ratio of the copper fiber (Fig. 12.5). SE of the plywood laminated with two pieces of conductive sheets

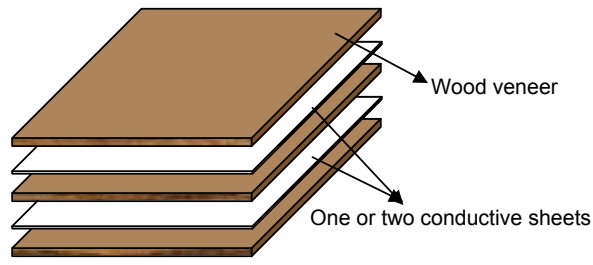

Figure 12.4 Structural model of laminated electromagnetic plywood.

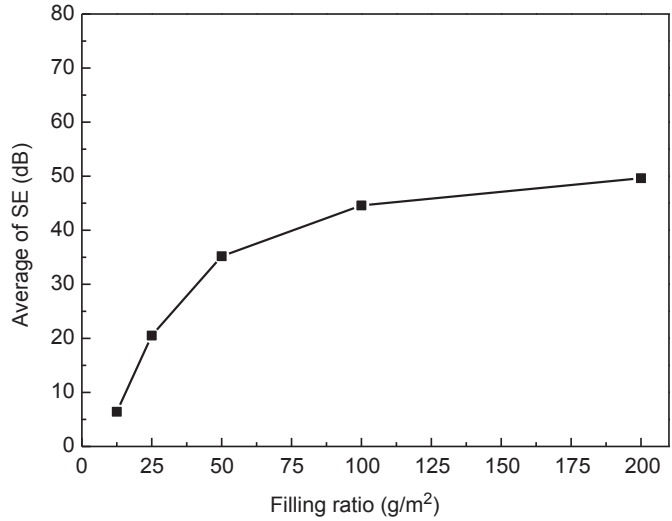

Figure 12.5 Average shielding effectiveness change of plywood with double-layered conductive sheets in different filling ratio.

(200 g/m^2) ranged from 39.3 to 61.75 dB and had good bonding properties, indicating the plywood had medium shielding effect and could be used commercially as an effective shielding material for electromagnetic radiation (Fig. 12.6). It was found that under the precondition of equal total filling volume, with the increase of filling volume, the SE of double-layered conductive sheet-laminated plywood started to become stronger than that of single-layered conductive sheet-laminated plywood. The more the

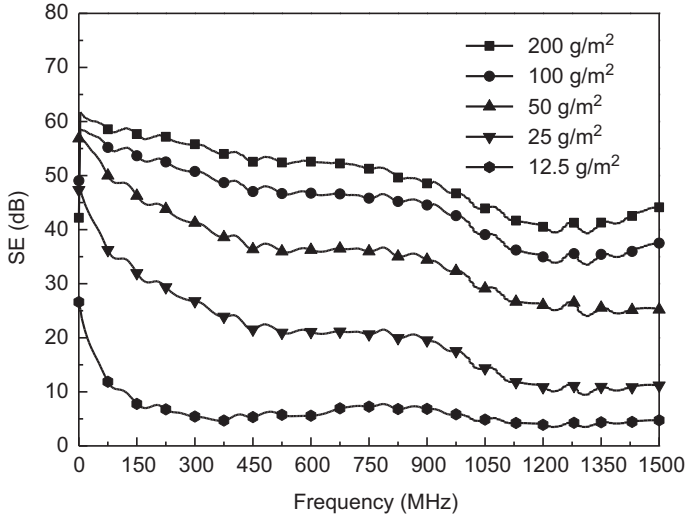

Figure 12.6 Shielding effectiveness of plywood with double-layered conductive sheets.

filling volume was, the greater the difference between the effectiveness of the foregoing two types of plywood. It was the first time this filling volume was called "double-layered shielding reversion point." In this experiment, the reversion point of the copper fiber filling volume is 50 g/m^2, which may have strong directive significance on real production and proved the advantage of laminated structure (Fig. 12.7). It was also found that total SE of the plywood laminated with double layers of conductive sheets is less than double of the SE for the plywood laminated with a single layer of conductive film (Fig. 12.8).

Metal mesh and plate

In addition to the application of metal fiber-filled conductive sheets, the metal plate and network, such as barbed wire, stainless steel wire mesh, copper wire mesh, and other mesh shielding materials, have also been applied to the preparation of wood-based electromagnetic shielding composites. The stainless steel and copper mesh were composited with wood veneers using urea-formaldehyde or phenol-formaldehyde adhesive as resin. The experimental results revealed that the SE of the composited plywood reaches to 40 dB in the frequency ranged from 1 to 1000 MHz. The metal mesh layer affected the SE of composited plywood significantly (Luo and Zhu, 2000).

The roughened aluminum alloy sheets were also laminated with Oriented Strand Boards (OSB) to prepare wood−aluminum composites according to the laminated electromagnetic shielding model (Lu et al., 2011b). It was found that the lamination of aluminum alloy sheets remarkably improved SE the of wood−aluminum composites (Fig. 12.9). The impregnation stripping performance also met the requirements of physical and mechanical performance. The SE of the wood−aluminum composites with double layers of 1 mm-thick aluminum alloy sheets on the surface 60−109 dB in the frequency ranged from 1 to 10 GHz.

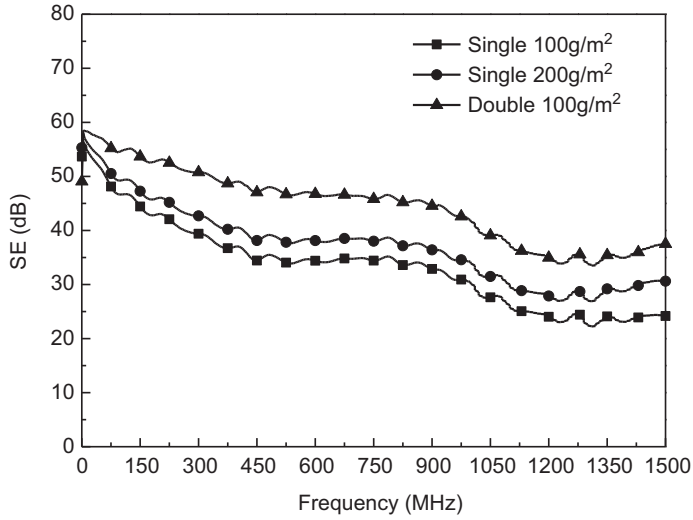

Figure 12.7 Shielding effectiveness of plywood laminated conductive films.

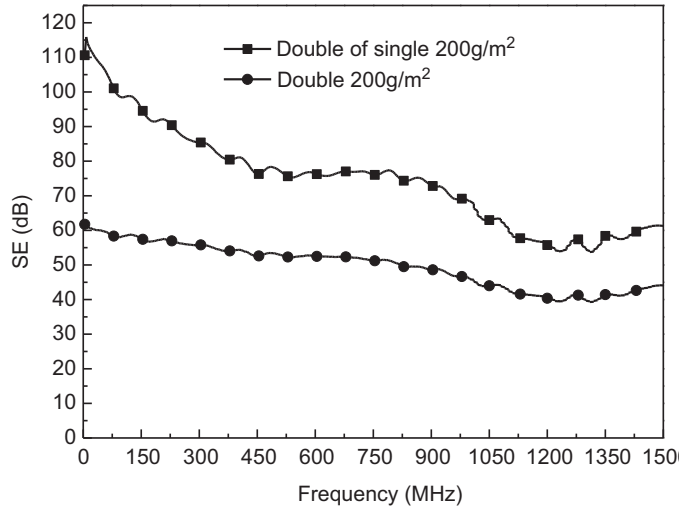

Figure 12.8 Shielding effectiveness of plywood laminated conductive films.

Carbon fiber felt and carbon fiber paper

Except for the metal lamellar material, a carbon material with excellent electromagnetic property, such as carbon fiber paper, sheet, panel, and net, has been laminated in the wooden composite for the application of electromagnetic shielding.

Based on the structural model of laminated electromagnetic shielding, the conductive carbon felts with excellent electrical conductivity were laminated with poplar veneers to manufacture electromagnetic shielding plywood. The SE of the plywood,

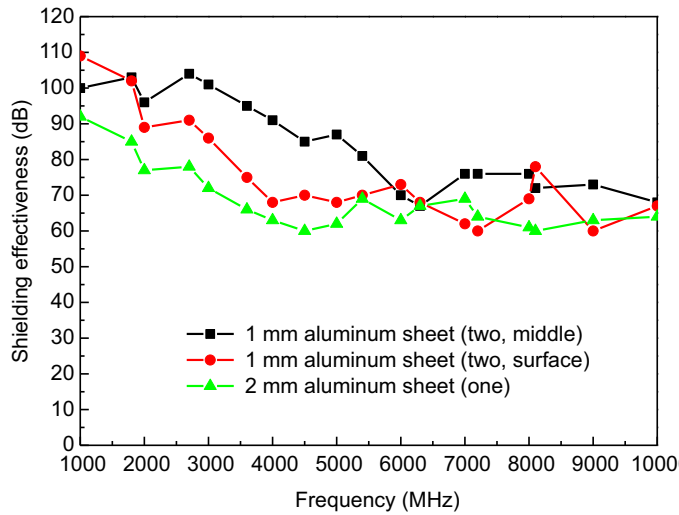

Figure 12.9 Shielding effectiveness of the wood−aluminum composites with different structures.

which was laminated with the double-layered conductive carbon felts with carbon fiber filler amount of 60 and 120 g/m^2, was 45.62−65.45 dB and 52.61−68.37 dB within the test frequency of 100 KHz−1.5 GHz, respectively. It had medium shielding performance and could be used under the high requirements of electromagnetic compatibility. It was also found that the double-layered conductive carbon felt-laminated plywood exhibited greater SE than that of the plywood laminated with single-layer conductive carbon felt at the same total carbon fiber filler content. The laminated structure model (Fig. 12.4) was proven to be feasible.

Carbon fiber paper (CFP), a type of flexible planer electromagnetic shielding material with thin thickness, low density, and good adhesion property and permeability, was laminated with wood veneer to produce a plywood composite with good shielding effectiveness (Yuan et al., 2014). A hot-pressed pressure of 1.2 MPa and a double-sized adhesive concentration of 380 g/m^2 were found most appropriate for the production of CFP plywood composites. SE of plywood composite laminated with single-layer CFP was better than before hot pressing, which results from the formation of three-dimensional and smaller conductive carbon fiber circuitries (Fig. 12.10). The space between two-layered CFPs and the thickness of the surface-layer veneer had significant influence on SE. The SE of the composites laminated with two-layered CFPs was significantly higher than those with one layer of CFP (Fig. 12.11). The SE in the

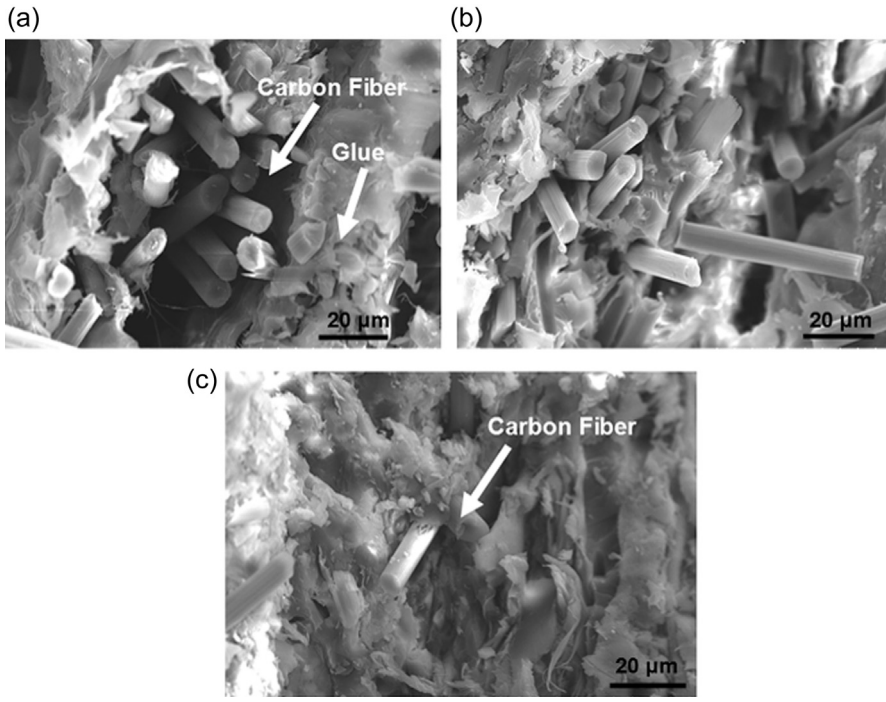

Figure 12.10 SEM for cross section of the glued carbon fiber paper with different adhesive concentration: (a) 180 g/m^2; (b) 330 g/m^2; (c) 430 g/m^2.

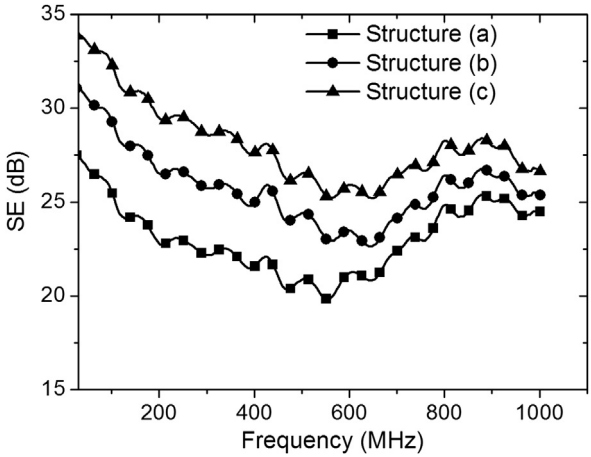

Figure 12.11 Shielding effectiveness of three different structures of plywood composite with two-layered carbon fiber papers: (a) three layers with two-layered carbon fiber papers; (b) five layers with two-layered carbon fiber papers; (c) seven layers with two-layered carbon fiber papers.

frequency range of 30 MHz to 1 GHz reached above 30 dB depending on the space between two-layered CFPs and the thickness of the surface veneer, which was sufficient SE for commercialization and the use of plywood composites.

On the basis of the multilayer electromagnetic shielding structure model, results revealed that the reflection losses between the two layers of shielding composites were determined by the distance. Increasing the distance resulted in the increase of multiple reflection loss. It also found that thickness of the surface layer of wood-based materials influenced the incident angle of electromagnetic waves, which affects the multiple electromagnetic emission losses between the two layers of shielding composites.

Carbon fiber mesh

A mesh of conductive material helps improve the bonding properties of the substrate, and the conductive paths in the micronetwork structure can effectively reflect the loss of the incident electromagnetic field. The mesh prepared by carbon fiber materials was regarded as an efficient way to shield the electromagnetic wave effectively due to the poor bonding performance between metal mesh and wooden materials caused by the existing stress in the metal mesh.

In order to further improve the overall shielding performance of carbon fibers, the carbon fibers after electroless nickel plating were arranged on the shielding specimen with a diameter of 115 mm by a grid (19 × 19) (Yuan et al., 2013) and then were composited with fiberboard using the modified white latex as resin to prepare the composited fiberboard. The composited fiberboard exhibits the SE of 41.54−63.73 dB within the test frequency of 200−1000 MHz. Therefore the carbon fiber sheet-like materials have good prospects in the preparation of electromagnetic shielding materials.

12.3.2.3 Hybrid composites

The conductive powder (ie, metal powder, carbon black, and carbon fiber powder) or fiber (ie, metal fiber and carbon fiber) is blended with the wooden units (ie, wood fiber,

wood particles, wood veneer) directly to prepare a wood-based electromagnetic shielding composite filled with conductive materials. The conductive or magnetic treatment also has been applied to the preparation of wood-based electromagnetic shielding composites. Additionally, the shield powder material is uniformly mixed with the adhesive and then applied to the preparation of wood-based electromagnetic shielding composites.

Conductive powder

Two conductive powders with different sizes and an electrically conductive liquid are mixed with the urea-formaldehyde resin to prepare conductive adhesives and then are composited with the poplar veneers to prepare conductive plywood (Hua and Fu, 1995). Application of three conductive media improves the conductivity of plywood, and the area-specific resistance of the glue layer decreased to 100 Ω or less: using conductive metal powder with a greater size affects the conductive performance of conductive plywood significantly. However, the conductive plywood containing conductive powder with a smaller size exhibits a better uniformity of resistance. The graphite powder, copper powder, and nickel powder are also mixed with adhesive to prepare conductive plywood, respectively, and the SE of the conductive plywood were investigated (Liu, 2005). Effects of the nickel powder on the SE are more significant than that of the graphite powder under the same volume-filling condition. When the adhesive capacity increases to 250 g/m^2, the average and the maximum SE of electromagnetic shielding composites is 2.73−7.86 dB and 5.28−13.13 dB, respectively. The corresponding percolation threshold is 34.3%−38.5%.

Metal fiber

The application of fibrous conductive materials in the preparation of shielding materials results in a decrease in the required amount of conductive materials. Most of the previous research has focused on the application of metal fiber and carbon fiber. For example, the stainless steel fibers and wood fibers are mixed by a certain percentage (steel/wood fiber mixing ratio of 3:1) and composited with the medium-density fiberboards (MDF) on the surface of both sides. Results revealed that the SE of the composited MDF is greater than 55 dB. The loading of the stainless steel fiber affects mechanical properties of the composited MDF significantly. Furthermore, application of a certain amount of isocyanate adhesive in the mixture of stainless steel and wood fibers can improve the bonding performance of MDF significantly and makes it meet the requirements determined by the national standard (Zhang and Liu, 2005).

Carbon fiber

Carbon fibers (CF) are characterized by their superior electrical properties, light weight, and high strength, and they have been widely used in the preparation of electromagnetic shielding composites made with wood and carbon fibers. The carbon fiber was treated by the pretreatment process of oven-drying in a circulation oven at 103°C and soaking in the alcohol oven-dried in a circulation oven at 103°C (Hou, 2015). The number of grooves increased on the surface of the carbon fiber after the pretreatment

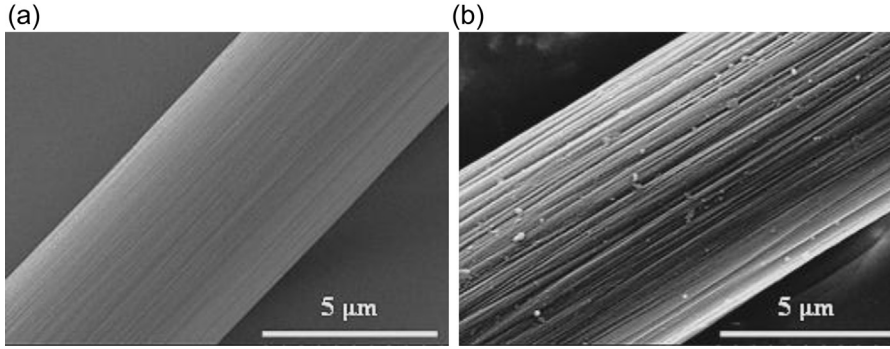

Figure 12.12 Carbon fiber surface morphology (a) before and (b) after surface pretreatment.

process (Fig. 12.12) resulted in the generation of a stronger interfacial bonding surface between the carbon and wood fibers. The pretreated carbon fiber was mixed with wood fiber by the solution blend method and was then composited with the diphenylmethane diisocyanate (MDI) resin to prepare carbon-based electromagnetic shielding fiberboard with a high conductivity, stable shielding performance, and physical and mechanical properties. As illustrated in Figs. 12.13 and 12.14, a cross-linked conductive network was observed to form in the carbon-based electromagnetic shielding fiberboard as the CF content increased to 20%. It was found that SE of the carbon-based fiber was increased with the increase in filling amount (Figs. 12.15−12.17). At the CF content of 20%, the SE of the fiberboards with increasing length was between 31.96 and 44.43 dB, 36.67 and 46.65 dB, and 34.07 and 44.90 dB, respectively. These values met the requirements for commercial application (30−60 dB). The mechanical properties of carbon-based fiberboards were improved because of the addition of carbon fibers. When the carbon fiber filling amount increases to 20%, the increment of MOR was 65.21% (2 mm), 80.69% (5 mm), and 56.36% (10 mm); its modulus of elasticity (MOE) was increased by 139.96% (2 mm), 181.78% (5 mm), and 155.86% (10 mm).

In addition, the carbon and wood fires were blended with adhesive, respectively, and then compounded to prepare carbon fiber filled electromagnetic shielding MDF by a hot-pressing process (Zhang et al., 2013). Surface resistivity of the MDF decreases to 1.48 Ω cm, and the corresponding average SE is 28.62 dB as the doping rate of carbon fiber increases to 50%.

When the mixture of carbon and wood fiber (mass ratio of carbon and wood fiber is 3:1) was placed on both sides of the MDF, average SE of the MDF reached to 47.89 dB (Zhang et al., 2013). The chopped carbon fibers were blended with wood fibers directly to prepare composited fiberboard (Piao and Xu, 1993). The composited MDF exhibits the SE of above 30 dB as the carbon fiber content increases to 25%.

12.3.2.4 Carbonized electromagnetic shielding composite

The carbonized electromagnetic shielding composite has illustrated good overall conductivity due to the natural mixed carbonized fiber and simple production process.

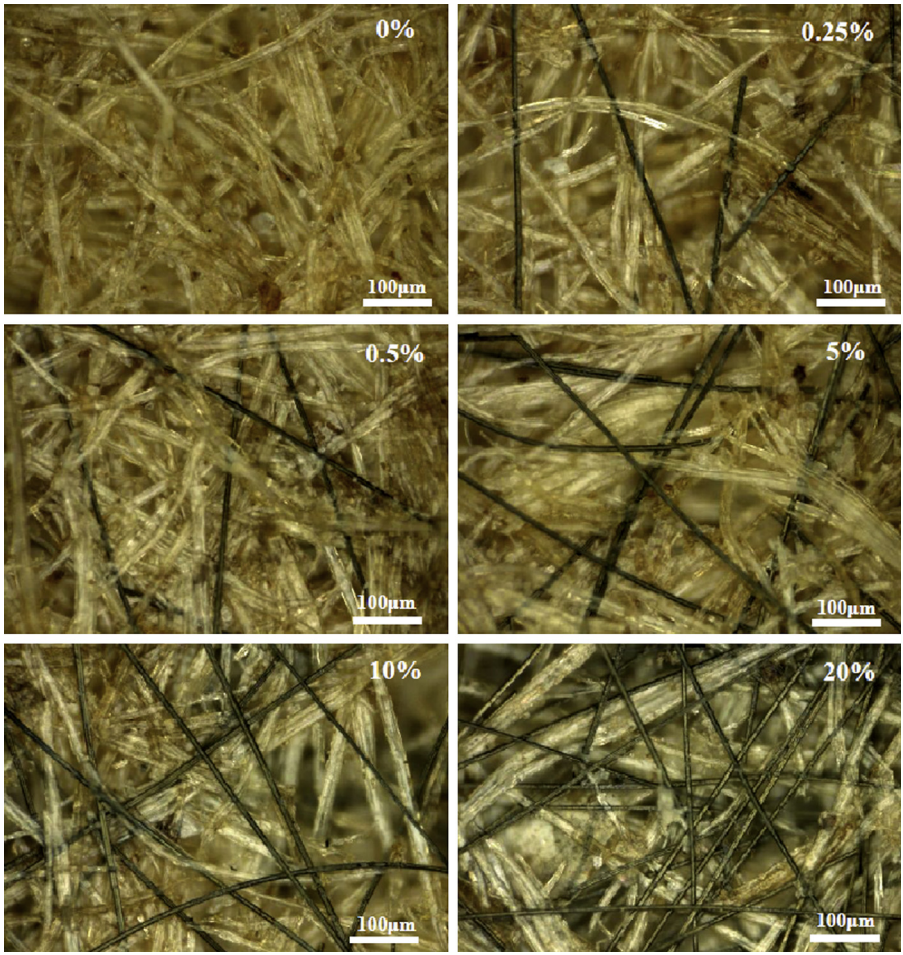

Figure 12.13 Carbon fiber distributions in the plane of the electromagnetic shielding fiberboard (the *black fibers* are carbon fibers, and the *brown fibers* are wood fibers).

However, a good mature technology and carbonization equipment with excellent performance are needed. The size of the carbonized material can be limited by the carbonization equipment. Furthermore, high energy consumption is also needed during the preparation of carbonized electromagnetic shielding composite. The carbonized MDF was prepared under the carbonization temperature range from 900 to 1500°C (Jin et al., 2012). Average SE of the carbonized MDF ranges from 66.8 to 84.6 dB in the frequency ranging from10 MHz to 1 GHz. The influence of species, thickness, and density of the wood panel materials on the SE of carbonized wood panels are significant. The carbonized materials with thicknesses of 2, 5, and 7 mm were prepared from the acacia panels (Cai and Wang, 2002). The maximum SE of carbonized acacia panels increase remarkably with the increasing thickness and is up to 28.4, 54.2, and 69.5 dB in the frequency range of 1.5−2.7 GHz.

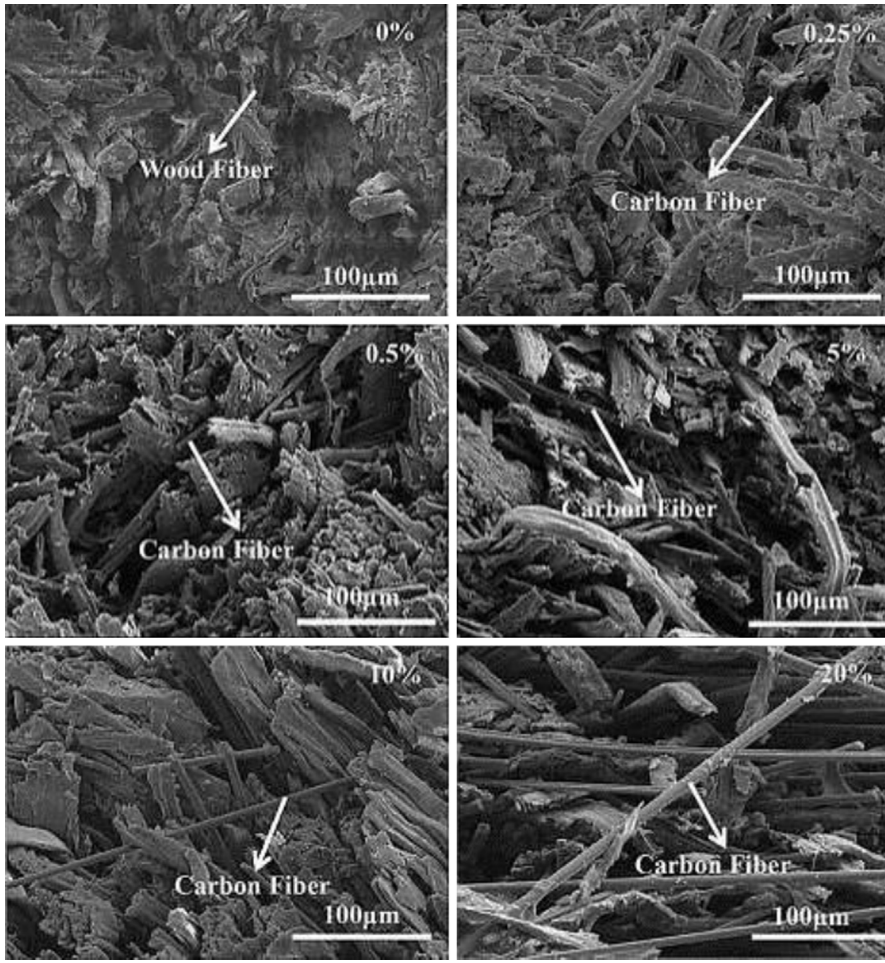

Figure 12.14 Carbon fiber distributions in the cross section of the electromagnetic shielding fiberboard.

Six species of wood were carbonized in the carbonization temperature range from 500 to 1000°C to prepare carbide plates (Wang and Hung, 2003). The increment of SE is as much as 24.4−49.5 dB in the 1.5−2.7 GHz frequency range for the increasing of carbonization temperature. The maximum SE of carbonized American western hemlock and paulownia carbide plate increases to 36 and 61 dB, respectively.

The powder of White poplar, Chinese fir, and Mason pine was carbonized to study the electrical performance of different species of the wood carbonized material (Hu, 2011). The wood powder was carbonized at the temperature of 1500°C for 1.5 h with Fe_2O_3 as a catalyst. The applied amount of Fe_2O_3 in this study is 6%. The carbonized Mason pine powder achieves the lower resistivity due to the grater content in lignin and extract, and a higher content of fixed charcoal powder is obtained during

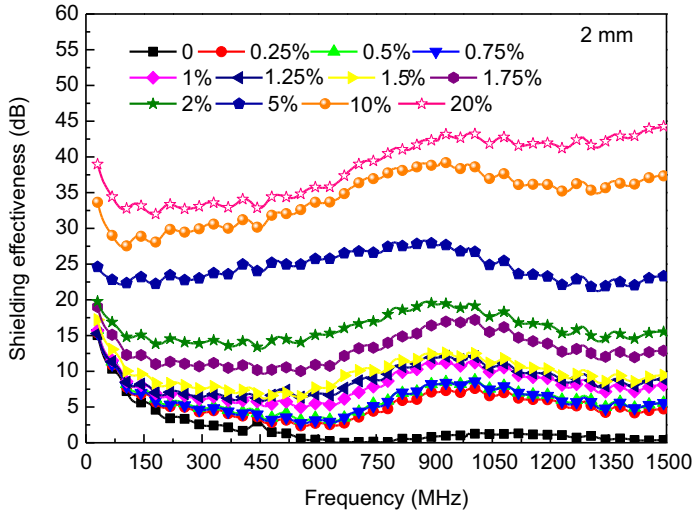

Figure 12.15 Shielding effectiveness of electromagnetic shielding fiberboard (2 mm).

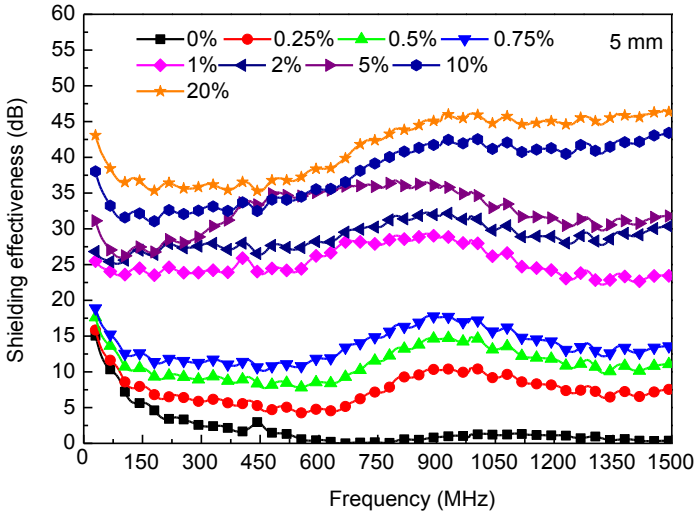

Figure 12.16 Shielding effectiveness of electromagnetic shielding fiberboard (5 mm).

the carbonization process. Increasing the content of fixed charcoal powder resulted in the formation of a layered crystal structure of the graphite. The charcoal powder made from Mason pine powder exhibits the lower resistivity, as low as 0.046 Ω cm. Furthermore, the charcoal powder was composted with PF resin (mass ratio of the charcoal powder and phenol formaldehyde (PF) resin was 0.5) to prepare charcoal-based functional thin panels, and the SE of the charcoal-based functional thin panel was increased with the increase of thickness and density of the thin sheet. Experimental results

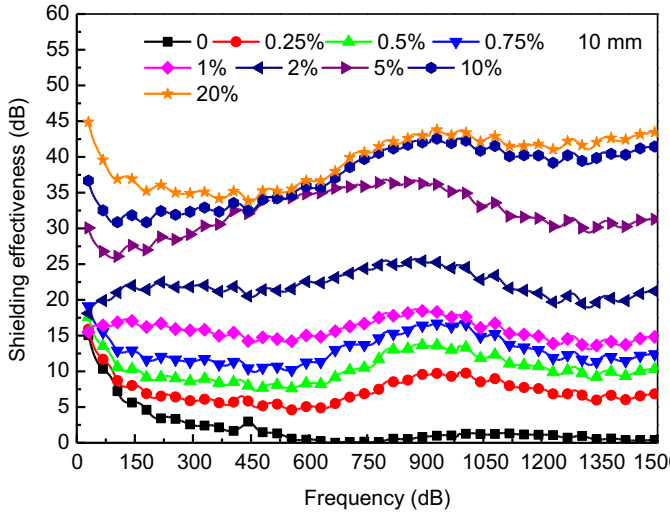

Figure 12.17 Shielding effectiveness of electromagnetic shielding fiberboard (10 mm).

revealed that the SE of the thin panel was above 30 dB in the frequency of 0.1−1500 MHz and reached the medium shielding effect.

12.3.3 Joints and engineering applications

The electromagnetic shielding materials have been applied to prepare electromagnetic shield products by the bonding technology of welding, riveting, screw, or adhesive bonding. However, the bonding quality of the electromagnetic shielding materials affects the SE of the entire system directly. Increasing in the bonding seam generated in the bonding process always results in the increase of electromagnetic leakage and weakens the SE of electromagnetic shielding.

Most previous research focuses on the development of electromagnetic shielding materials. Few studies have been carried out on the engineering applications of electromagnetic shielding materials. Bonding technology of the self-made electromagnetic shielding plywood was investigated (Lu et al., 2013). An attempt on the integration research and development from the electromagnetic shielding material to final products have also been taken (Lu, 2007).

12.3.3.1 Bonding definitions and methods

Bonding is often defined as the generation of a low impedance path applied to the supply current flow between two objects and electrically on the whole. A potential difference in the framework or equipment is avoided because the presence of potential difference can lead to electromagnetic interference. The objectives were generally fixed by using mechanical or chemical methods in structure. Realization of bonding can be summarized as direct and indirect bonding. Among which, the direct bonding

can be divided into welding, brazing, soldering, bolting, riveting, and conductive adhesive connection, etc.

However, the indirect bonding is hard to realize due to the operating requirements of equipment or the positional relationship. It is necessary to import the auxiliary conductor as a bonding bar in the bonding process. Resistance of the electromagnetic shield bonded by indirect bonding is equal to the sum of intrinsic resistance of each lap and that of the contact resistance between the metals on the head of the bonding joint. The bonding resistance should be less than 0.1 mΩ for the aluminum, copper, or brass as bonding bars. The fastening in the indirect bonding methods can be realized through bolting, riveting, welding, or brazing.

12.3.3.2 Bonding technology in the laminated electromagnetic shielding plywood

Design of the ride interface should be selected according to their different structural characteristics in the bonding structures. Characteristics of the laminated electromagnetic shielding plywood are the following:

1. Upper and lower surfaces of the plywood are wood materials (insulating material).
2. Two layers of conductive material are located in the middle layer and spaced by a layer of wood veneer in the middle.
3. A discontinuous metal point is observed to generate in the cross section of the conductive layer in the plywood after sawing.

It is necessary to form a good electrical connection between the two layers of conductive materials in the glue line of the electromagnetic shielding plywood. The ride interface was designed as an inclined joint, opposite joint, and step joint in accordance with the processing characteristic in the engineering application (Lu et al., 2013).

In accordance with the processing characteristic in the engineering application, there were two fixed methods applied to the bonding of the electromagnetic shielding plywood, namely:

1. Inclined joints and opposite joints are chosen to fix conductive adhesives and ordinary adhesive directly (Lu, 2007).
2. The step joint was chosen to fix ordinary adhesive directly. Among which, the conductive layer is formed by the copper foil, and the stepped surface is copper foil (Lu, 2007).

Effects of interfaces and fixed ways on the resistance of bonding seams and SE of the electromagnetic shield are different. The electromagnetic shielding plywood with different bonding structures has been prepared using different bonding methods according to the production process of flow diagram shown in Fig. 12.18. The SE of the electromagnetic shielding plywood with different bonding structures was investigated through a coaxial method and a window method, as shown in Figs. 12.19 and 12.20.

The SE of the electromagnetic shielding plywood with different bonding structures is illustrated in Table 12.3 and Fig. 12.21. Bonding methods, namely copper connections,

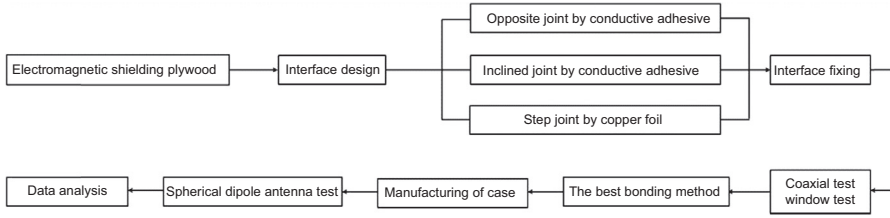

Figure 12.18 Bonding experiment process diagram.

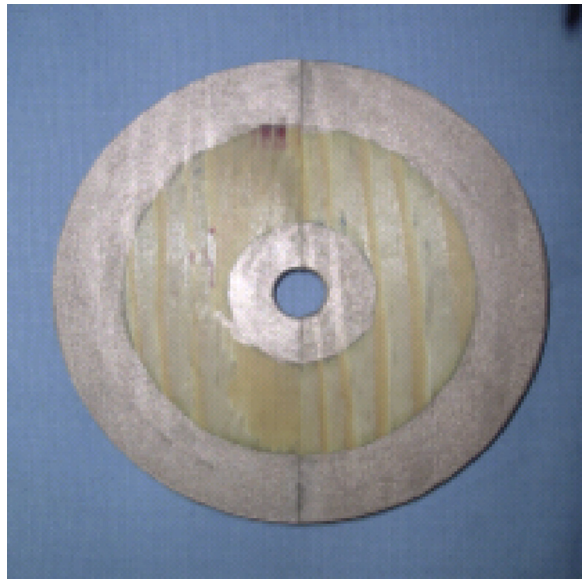

Figure 12.19 Sample of coaxial test.

Figure 12.20 Sample of window test.

Table 12.3 Shielding effectiveness of electromagnetic shielding plywood after bonding (window test)

Frequency (MHz)	Common plywood (dB)	Nonbonding seam (dB)	Connecting by copper foil (dB)	Inclined joint by conductive resin (dB)	Butting by conductive resin (dB)	Butting by nonconductive resin (dB)
30	0.42	65.71	62.98	42.12	42.93	49.68
65	0.00	68.46	62.75	42.29	50.28	51.38
110	0.00	79.26	67.06	40.09	44.56	48.59
190	0.00	79.45	74.22	49.92	55.70	59.12
300	0.00	68.90	75.15	44.97	39.16	50.89
400	0.00	63.21	69.69	40.70	35.46	37.05
500	0.00	62.15	68.03	35.13	34.19	34.58
600	1.24	71.96	66.92	44.55	44.45	30.32
700	2.11	75.78	66.88	49.03	49.31	40.12
800	2.54	66.18	58.50	47.56	47.92	42.13
900	0.34	63.09	56.39	40.07	36.83	38.21
1000	2.61	67.62	61.73	48.15	32.50	36.05
Average	0.77	69.31	65.86	43.71	42.77	43.17

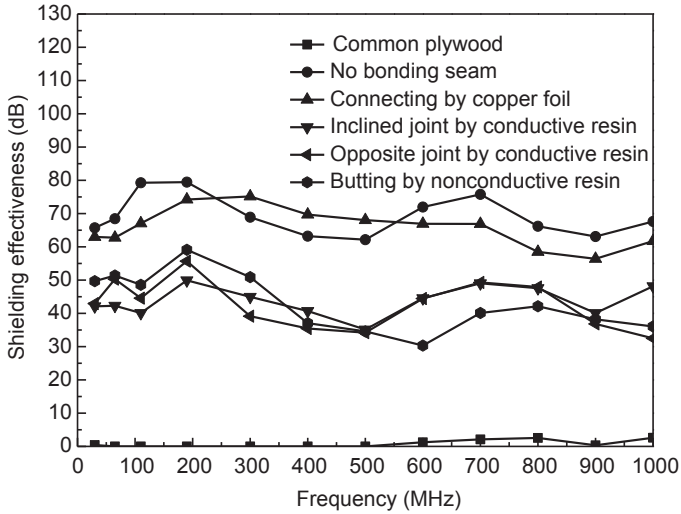

Figure 12.21 Comparison of shielding effectiveness after bonding.

opposite joints by conductive adhesive, inclined joints by conductive adhesive, joints by nonconductive adhesive, and nonbonding seams, are applied to the electromagnetic shielding plywood.

The ordinary plywood (nonconductive film lamination) has almost no shielding effect and the corresponding SE ranges from 0 to 2.61 dB. SE decrement of the electromagnetic shielding plywood bonded by copper foil ranges from 0 to 12.20 dB. The average decrement of SE is 5.17 dB (5%) and illustrates the smallest decline. SE decrement of the electromagnetic shielding plywood bonded by using an inclined joint by conductive adhesive, opposite joint by conductive adhesive, and joint by nonconductive adhesive is 18.63−39.18 dB, 18.19−35.13 dB, and 16.04−41.64 dB, respectively. The corresponding average decrement is 25.60 dB (36.9%), 26.54 dB (38.3%), and 26.14 dB (37.7%), respectively, which exhibits greater SE decrement than that of the electromagnetic shielding plywood bonded by copper foil.

Therefore the copper foil connection has been regarded as the best bonding method in the engineering application of electromagnetic shielding plywood. For the copper foil connections, the copper is a good conductor and can form a good electrical connection between the copper foil and copper fiber in the conductive film during the hot-pressing process. Therefore a low impedance path applied to the supply current flow is observed to generate among the conductive layers and forms the overall electrical connection on the whole. Electromagnetic leakage from the bonding seams is avoided, which prevents the sharp reduction of SE.

For the opposite joint by conductive adhesive and inclined joint by conductive adhesive, the electrical connection among the conductive layers is realized by the conductive adhesive. It is hard to form an effective conductive path in the adhesive system due to the greater resistance ($2 \times 10^6\ \Omega$) of the cured conductive adhesive. Therefore the expected electrical connection between the conductive layers is not

achieved. A larger decline in the value of SE is generated due to electromagnetic leakage formed in the glue layer.

For the nonconductive adhesive connection, it is unable to form an electrical connection between the conductive layers due to the poor conductivity of nonconductive adhesive. A larger decline in the value of SE is generated due to electromagnetic leakage formed in the glue layer. It is also noted that SE decrement of the electromagnetic shielding plywood bonded by the inclined joint by conductive adhesive, opposite joint by conductive adhesive, and joint by nonconductive adhesive is almost the same.

12.3.3.3 Electromagnetic shielding case and its performance

The electromagnetic shielding case (460 mm × 460 mm × 230 mm, Fig. 12.22) was made with electromagnetic shielding plywood (500 mm × 500 mm × 2 mm) using the copper foil connection in accordance with the process illustrated in Fig. 12.18 (Lu et al., 2014). Fig. 12.23 shows the SE of the case (spherical dipole antenna test) and electromagnetic shielding plywood (window test). It was found that the SE of plywood declined sharply after bonding, especially at high frequencies due to electromagnetic leakage from the bonding seams. Therefore it is critical to study seam leakage problems in developing the wood-based electromagnetic shielding materials into final products.

Figure 12.22 Electromagnetic shielding case.

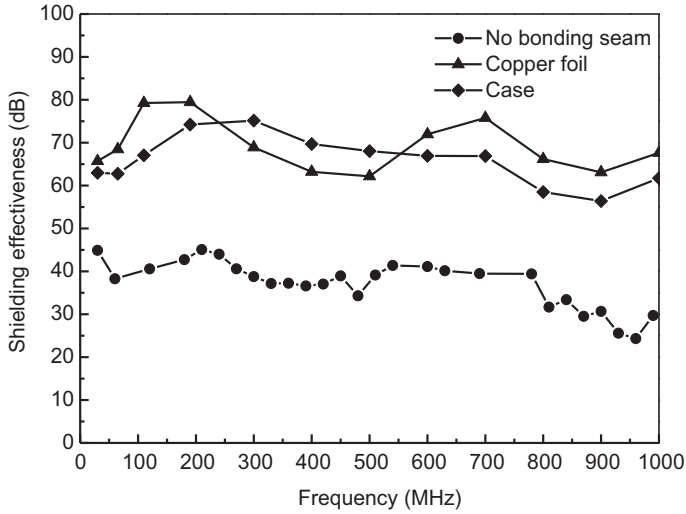

Figure 12.23 Shielding effectiveness of case and electromagnetic shielding materials.

12.3.3.4 Electromagnetic shielding wooden door

It is critical to suppress the electromagnetic leakage occurring between the door seams in the preparation of electromagnetic shielding wooden doors. The bonding technology of electromagnetic shielding materials has been improved by the Research Institute of Wood Industry, Chinese Academy of Forestry (Lv and Fu, 2013), to solve the problem of electromagnetic leakage formed in the application of wood-based electromagnetic shielding composites. The conductive layer in the electromagnetic shielding material was exported out by the copper foil or conductive materials to form an individual electrical connection with the doorframe (including slots and copper plate), and an effective electrical connection among the electromagnetic shielding door, doorframe, and wood-based electromagnetic shielding materials can be generated and prevents the electromagnetic leakage efficiently.

12.3.3.5 Design and construction of electromagnetic shielding room

The copper foils were laminated on the surface of MDF by a hot-pressing process to prepare electromagnetic shielding MDF by the researchers from the Research Institute of Wood Industry (Chinese Academy of Forestry) and Beijing University of Technology. The electromagnetic shielding MDF was then applied to construct a wood-based electromagnetic shielding room (Fig. 12.24). The electromagnetic shielding MDF was firstly laid on the roof surface, then the surrounding walls, and finally the ground in accordance with the construction program. The basic steps of the construction process are as follows:

1. construction of steel frames;
2. construction of wood-based materials on the wall;

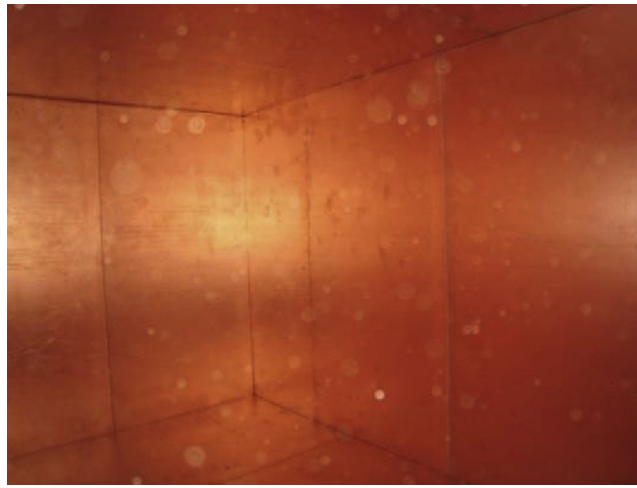

Figure 12.24 Wood-based electromagnetic shielding room.

3. installation of the electromagnetic shielding wood-based panels;
4. installation of electromagnetic shielding door and doorframe; and
5. installation of aluminum-plastic panels and lying of the power.

Overall, SE of the wood-based electromagnetic shielding room reached to 80 dB.

12.4 Electric heating composites

12.4.1 Mechanisms for electric heating and heat transfer

12.4.1.1 Mechanisms for electric heating

Natural wood fiber-based electric heating composites, normally metal and carbon material as its electric heating layer, and metal foil or conductive adhesive as the electrodes pasted on two ends of the electric heating layer, can be manufactured with solid panel, fiberboard, or multilayered wood composite panel. The electric heating material can be placed in the groove prefabricated on the substrate panels or can be coated and printed on the surface. In addition the functional elements, such as decorative layer, heat dissipating layer, far infrared emitting layer, heat reflecting layer, and heat insulating layer, can also be laminated with the composites. The electric heating composite can mainly be divided into electric heating multiply wood composite, electric heating fiberboard composite, and wood−bamboo electric heating composite (Fig. 12.25). The temperature distribution of common materials for electric heating, such as cable, carbon fiber paper, and carbon ink printing paper, can be seen in Fig. 12.26. Carbon fiber paper has the most uniform temperature distribution, exhibiting the unevenness of less than 5°C in the intermediate region.

Before loaded with electricity, electrodes on both ends of the electric heating layer are connected with the power source to form a conductive loop. Then current carriers

Figure 12.25 Wood−bamboo electric heating composite.

in the conductive elements and the lapping interface of the conductive structure collide and rub intensely with each other under the function of electric field, by which electric energy will be changed into heat.

Carbon electric heating material has a six-sided graphite crystal structure. On one surface, a regular hexagon consisting of six carbon atoms extends to form the lamellar structure. In this structure, each atom bonds with the other three atoms with sp2 hybrid covalent bond. There is also a free electron on the overlapping *P* orbit similar to a free electron and carrier of metal, making it conductive (He, 2005).

With respect to the carbon fiber loaded with electricity, a free electron (π electron) in *P* orbit of a carbon atom of graphite crystallite migrates directionally to a certain free path. Among which, it absorbs electric energy when moving apart from the atomic nucleus continuously and releases energy when getting closer to the atomic nucleus. In terms of molecular kinetics, current carriers in the conductive elements, and lapping interface of the conductive structure collide and rub intensely with each other under the function of electric field, by which electric energy will be changed into heat. However, carbon fiber is made up of turbostraticgraphitic structure, and its structure regularity decides the number of π electrons per unit volume and the average free path. It has been indicated that the higher the regularity is and the larger the dimension of graphite crystal (L_a and L_c) is, the smaller the interlayer spacing of crystallite is and the larger the number of π electrons per unit volume and the average free path is (He, 2005). Consequently, more heat generates under the same field function if its structure of graphite crystallite is more regular.

12.4.1.2 Mechanisms of heat transfer

The electric heating membrane made with carbon fiber paper can reach to a steady state after working for five minutes (Yuan and Fu, 2014). In the wood-based electric heating composite, the heat generated by the fast Joule effect of the electric heating layer transfers to the composite substrate simultaneously in the form of heat conduction and heat radiation to make the temperature on the surface of the composite rise. Then the heat releases outward in the form of convection and radiation from the surface (Yao and Zhang, 2007).

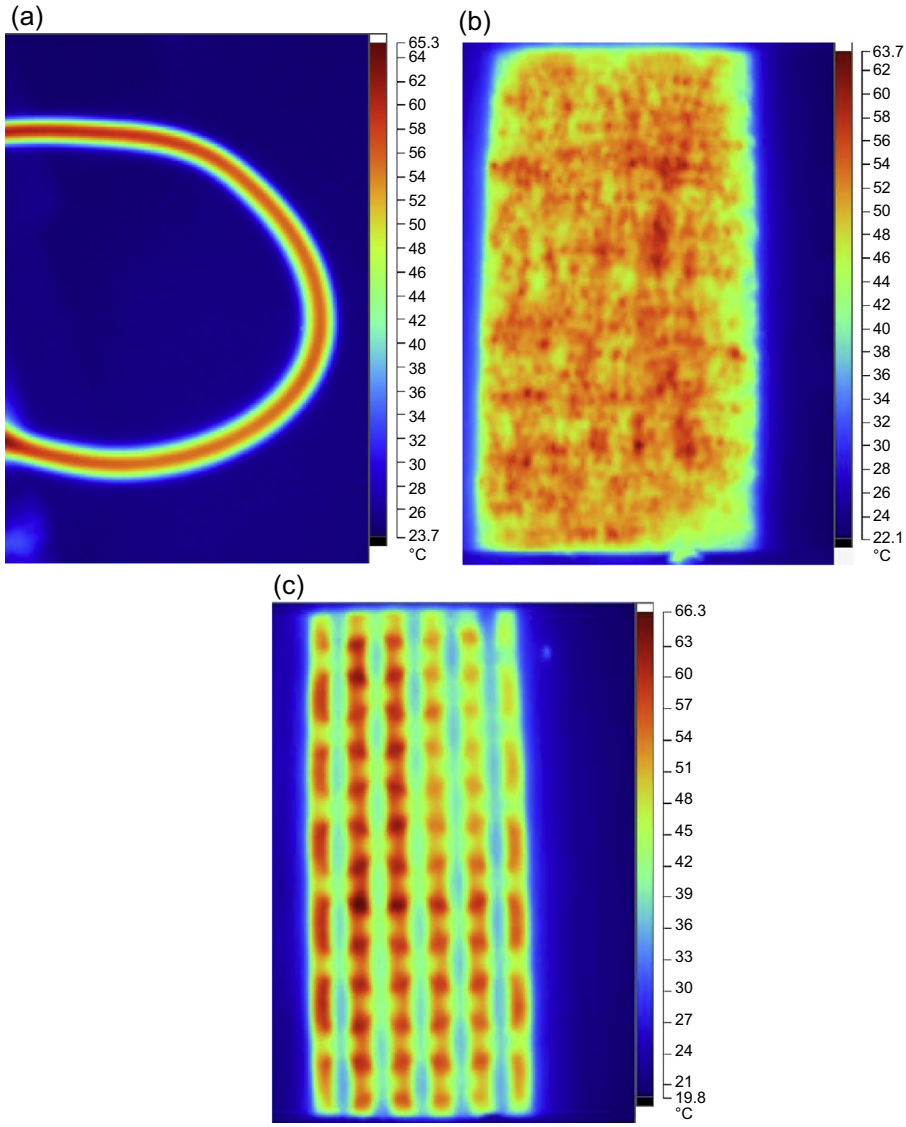

Figure 12.26 Temperature distributions for different electric heating materials: (a) electric heating cable (500 W/m^2); (b) carbon fiber paper (500 W/m^2); (c) carbon ink printing paper (500 W/m^2).

On the basis of conservation of energy, the quantity of heat changed from the electric energy by Joule effect (calorific value) is equal to the sum of total heat storage of the composite and heat transferring with the external environment. It can be shown as Eq. (12.5) (Yao and Zhang, 2007).

$$dQ = dQ_h + dQ_x, \tag{12.5}$$

Where, dQ is the differential increment of the calorific value, dQ_h is the differential increment of heat transfer, and dQ_x is the differential increment of heat storage.

$$dQ = Pdt \tag{12.6}$$

$$dQ_h = Fa_t \Delta T dt \tag{12.7}$$

$$dQ_x = cmd(\Delta T) \tag{12.8}$$

Where, d_t, c, and m are the heat transfer coefficients between surface and environment, specific heat, and quality of the composite, respectively. The involved composite includes glue layer, electric heating element, and wood−bamboo material with remarkable anisotropy, which leads to the difficulty and complexity in the calculation of equivalent specific heat.

The d_t is proportional to the difference between surface temperature (T_s) and environment temperature (T_0) (Dai, 1991). It can be described as Eq. (12.9), generally.

$$a_t = a + b(T_s - T_0) = a + b\Delta T \tag{12.9}$$

For that,

$$\Delta T = T_s - T_0 \tag{12.10}$$

The relationship between surface temperature and loading time could be approximately seen as Eq. (12.11):

$$T_s = \frac{\left[A - \frac{a}{2b}\right]\left[1 - e^{-\frac{2FbA}{cm}t}\right]}{1 - \frac{a-2bA}{a+2bA}e^{-\frac{2FbA}{cm}t}} + T_0 \tag{12.11}$$

$$A = \sqrt{\frac{P}{Fb} + \frac{a^2}{4b^2}}$$

Therefore it is a relationship of exponential function that surface temperature increases monotonically along with time in the loading process. Surface temperature is decided by the loading time, power, interface temperature difference, and temperature-specific quality of the composite. It can be seen from Fig. 12.27 and Eqs. (12.12)−(12.14) that the correlation between time and temperature is exponential under a power density of 500 W/m^2. All correlation coefficients (R^2) are higher than 0.99.

$$T_s = 17.9163 + 22.2751\left(1 - e^{-0.0012t}\right) + 7.0552\left(1 - e^{-0.0095t}\right) \tag{12.12}$$

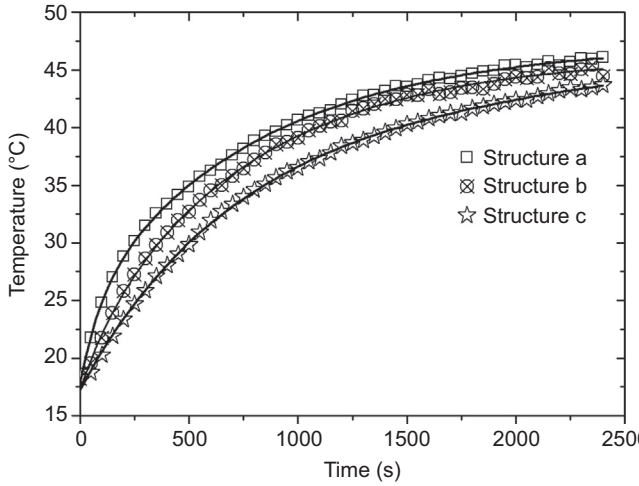

Figure 12.27 Correlation of time and temperature.

$$T_s = 17.3066 + 25.0349\left(1 - e^{-0.0013t}\right) + 3.9647\left(1 - e^{-0.0057t}\right) \tag{12.13}$$

$$T_s = 17.23 + 22.9899\left(1 - e^{-0.0015t}\right) + 1.2888 \times 10^9\left(1 - e^{-1.333\times10^{-12}t}\right) \tag{12.14}$$

12.4.1.3 Heat transfer of radiation

Heat radiation is the most effective way for heat transfer among three mechanisms of conduction, convection, and radiation. The radiation is the main transferring mechanism of carbon material after it is loaded with electricity. It is also an electromagnetic wave in infrared frequency. Fig. 12.28 shows that an infrared wave emitted from the three kinds of composites is in the wavelength from 4 to 25 μm, and its electric-to-radiant power transfer efficiency reaches more than 80% (Table 12.4).

Normal total emissivity is another key index for evaluating the heat radiation performance of a heating material. It is confirmed that the carbon material has a good heat radiation performance, but the performance will weaken after the carbon heating material is laminated in the middle layer of the composite substrate. As seen from Table 12.4, the normal total emissivity of the composite loaded with power density of 500 W/m^2 reduces slightly from 0.883 (structure a) to 0.881 (structure c) as the electric heating layer toward the middle layer.

Earlier researches on the wood infrared drying technology have indicated that cellulose, hemicellulose, lignin, and water in wood are the strongest absorbers for infrared waves. Of which, cellulose has an absorptivity of 60%−80%, mainly in the wavelength range from 2.5 to 20 μm (Wang, 1983c; Liang, 1991). The fact that pine wood veneer in the thickness of 0.1 mm exhibited only 5% transmissivity shows that wood has a very strong absorption power for infrared waves (Wang, 1983b).

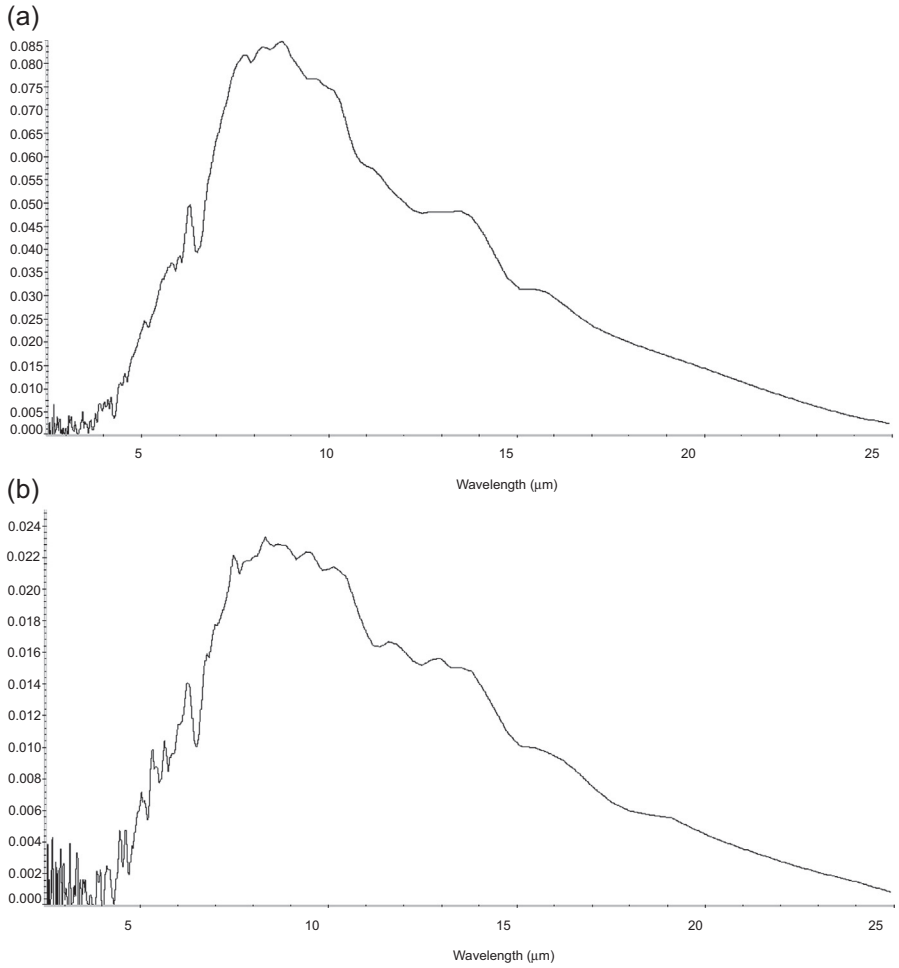

Figure 12.28 Radiant spectrogram of composites with different structures (500 W/m^2): (a) structure a; (b) structure c.

Table 12.4 Emissivity of wood−bamboo electric heating composite

Specimens	Normal total emissivity	Electric-to-radiant power transfer efficiency (double surface) (%)
Structure a	0.883	82.27
Structure b	0.881	78.55
Structure c	0.881	71.61

Once the composite is working, the absorber (eg, cellulose) of wood material next to the electric heating material firstly absorbs the infrared wave and emits the wave with the same length. That is to say the heat transfer can be seen as a dynamic process of "radiation-absorption- radiation-reuptake" (Wang, 1983a). However, there is a certain amount of loss in this process. For the electric heating layer close to the middle position, the transfer efficiency of electric-to-radiant power for all three structures reduces from 82.27% to 71.61%, a decrement of 10.66%.

12.4.2 Methodology and performance of electric heating composites

12.4.2.1 Preparation process and drop rate of resistance

Preparation methods for wood-based electric heating materials include laminated cold press or hot press and embedding inside. Matsushita Electric Works Ltd. in Japan has prepared an electric heating product by embedding the inside method since 1993. Many enterprises in China have been concentrating on the laminating press technology for many years. Recently, an electric heating cable embedded process has been developed as another popular technology for its simple and feasible electric connection, insulation, and waterproofness. Melamine modified urea-formaldehyde resin (MUF) has been seen as a common adhesive for the laminating hot-press process. With this process, there is a drop rate of resistance (DRR) of about 30% of the electric heating layer when carbon fiber paper was used (Yuan and Fu, 2014). The resistance deviation of the composite can be influenced by the process factors, such as glue spread, pressure, pressing time, and temperature of pressing plate. It can be seen in Fig. 12.29. DRR declines linearly with the increase of glue spread. This result is different from that of the composite made with epoxy resin prepreg, which exhibits fluctuant increasing firstly and then decreasing (Yang et al., 2000).

12.4.2.2 Structure design and performance

The structure design should take into account humidity and heat resistance, dimensional stability, efficiency of heat transfer, and security in long-term use. The electric heating layer should be close to the surface to improve the transfer efficiency by taking dimensional stability and security into account. For instance, plywood-based composites could follow structure a (electric heating layer between veneer layer one and two), structure b (electric heating layer between veneer layer two and three) or structure c (electric heating layer between veneer layer three and four) (Fig. 12.30).

Time—temperature effect

Heating up surface temperature along with loading time, as a direct index to evaluate the efficiency of heat transfer, mainly depends on the input power, structure, and thermal conductivity of the substrate, as well as the increase in and maximum temperature increase with the addition of power (Fig. 12.31). Moreover, the position of the electric heating layer also has an effect on its temperature rising. Temperature and rising speed

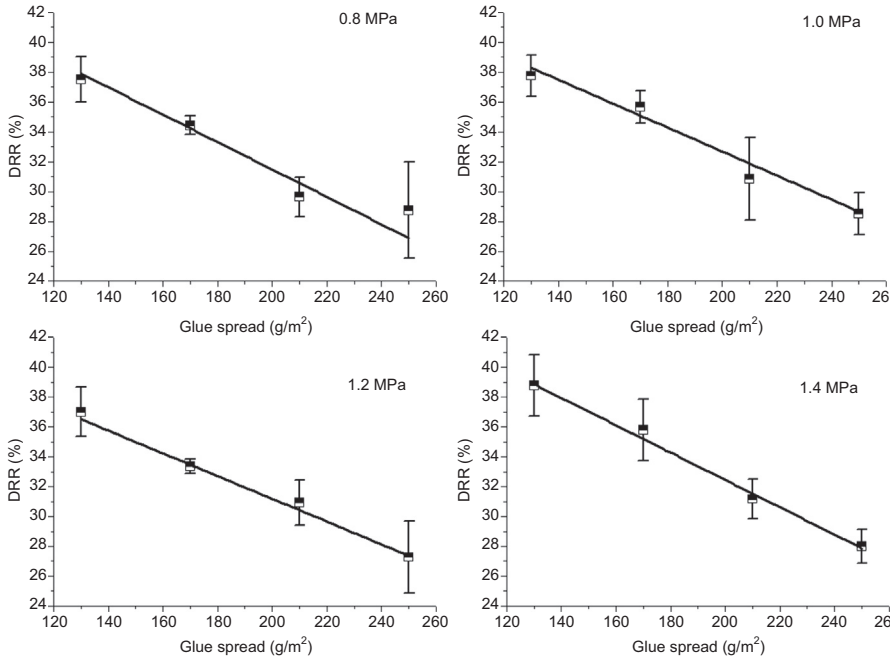

Figure 12.29 Relation between glue process and drop rate of resistance after hot pressing (two-layered fiberboard composite).

Figure 12.30 Structure of the multiply composite.

decline slightly when the electric heating layer moves towards the middle layer (Fig. 12.32). The surface temperature ascends quickly at beginning for the large temperature difference existing among the electric heating layer, wood substrate, and ambient air. Heat dissipation speed is then close to the heating speed (input power) as the temperature gradient decreases, when the surface temperature tends to be stable.

Improving the efficiency of heat transfer can be achieved by reducing the heat transferring to the bottom of the composite. The top surface temperature is normally higher than that of the bottom surface and the rising speed of the bottom temperature delays compared to the top surface (Fig. 12.33). By contrast, as the electric heating layer moves to the middle position, the top surface temperature, such as structure c, can be lower than its bottom surface, and temperature rising speed was similar. What is more, in terms of structure c, an increase in the volume of material, such as the

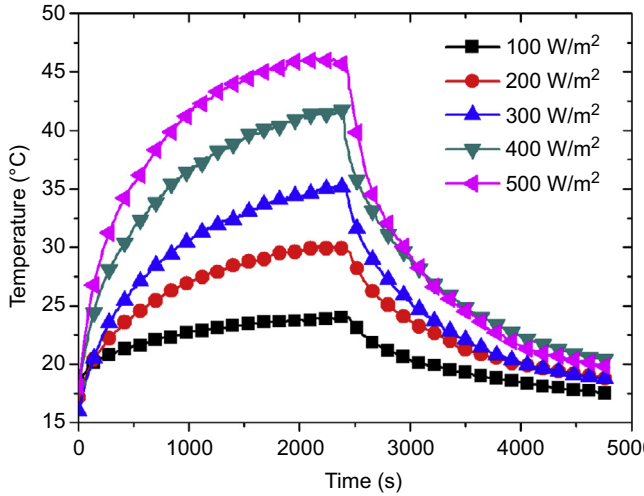

Figure 12.31 Time−temperature effect of structure a.

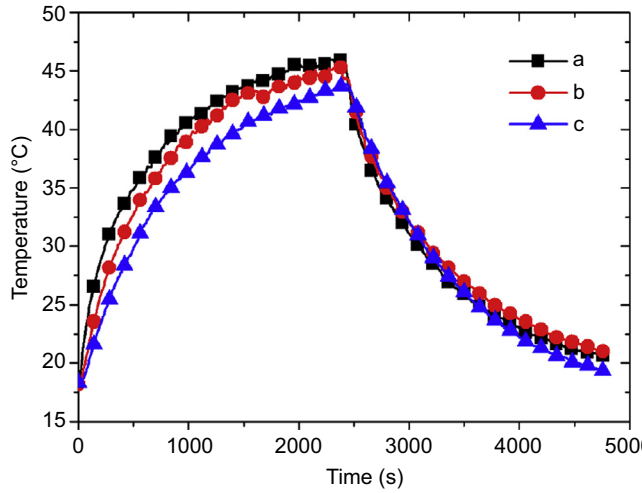

Figure 12.32 Comparison among the effect of structure a, b, and c (500 W/m^2).

structure c above the electric heating layer, leads to an increase of the heat storage and reduction of the heat dissipation, and the temperature on the surface decreases. Therefore the closer the heating region is, the higher the heating efficiency is.

As a poor conductor for heat, natural wood material has a certain thermal diffusivity (Yu et al., 2011; Kawasaki and Kawai, 2006). This could be magnified when the thickness of the wooden material above the electric heating layer increases, which makes temperature unevenness on surfaces decline slightly (Fig. 12.34), eg, the temperature unevenness of structure a, b, and c is 5.28, 4.33, and 4.26°C, respectively.

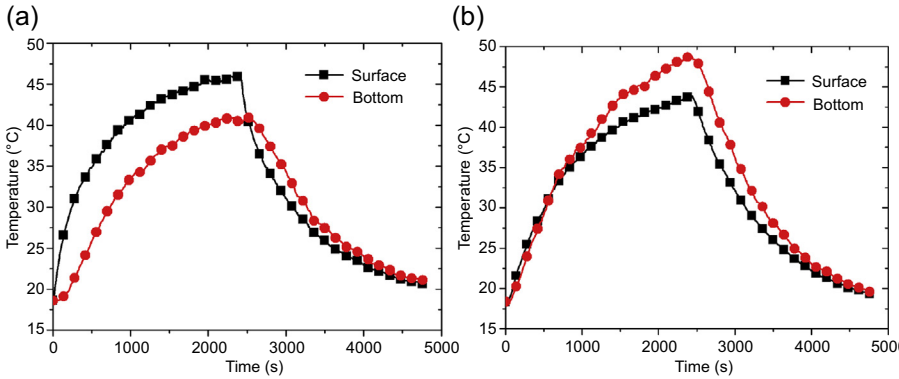

Figure 12.33 Time−temperature effect on the surface and bottom (500 W/m^2): (a) structure a; (b) structure c.

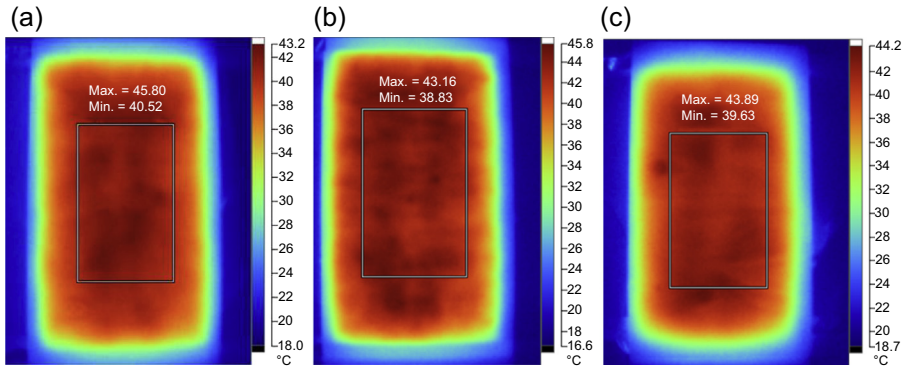

Figure 12.34 Surface temperature distribution of the composite with heating layer in different positions (500 W/m^2): (a) structure a; (b) structure b; (c) structure c.

Physical property of electric heating composites

Dimensional stability as a basic index for the application of composites largely depends on its structure. With respect to the multiply solid wood composite electric heating material, the embedded electric heating layer has almost no influence on its dimensional stability (Table 12.5). The dimensional change due to heat and humidity was less than 0.16% and 0.11%, respectively, which conforms to the China criteria LY/T 1700−2007 "wood-based flooring with underfloor heating." Furthermore, Fig. 12.35 shows that there is no craze in glue line after a peeling test.

12.4.3 Electrical safety of electric heating composites

The application of wood-based electric heating composite mainly focuses on the electric heating wood-based floor. The electrical safety, control for the volatile organic compounds, and harmful electromagnetic radiation are strictly required to ensure

Table 12.5 Dimensional stability of multiply electric heating composites

Specimens	Heat resistance		Humidity resistance	
	Length variation (%)	Width variation (%)	Length variation (%)	Width variation (%)
Structure a	0.12	0.11	0.08	0.09
Structure b	0.16	0.16	0.11	0.05
Structure c	0.16	0.06	0.09	0.07

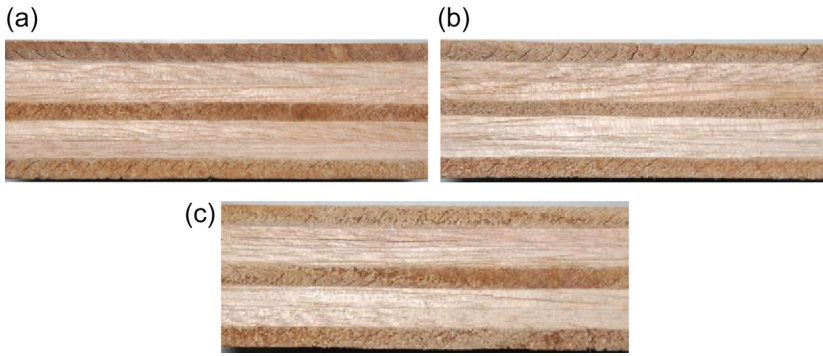

Figure 12.35 End surfaces of specimens after dip peel test: (a) structure a; (b) structure b; (c) structure c.

safety and environment protection during use, improved by designing electric connection and other protection treatment.

12.4.3.1 Electrical safety protection

Electrical safety is of prime importance for the electric heating floor. Currently the insulations for electric heating layers are carried out as follows: insulating resin plates or films are composited on the two faces of the electric heating composites, which have good performance for waterproofness, insulation, and electrical safety; on the other hand, common modified formaldehyde adhesive with good insulation performance can form two-layered insulating films on the electric heating layer after a proper hot-press process. After waxing mortise in the end, the electric heating floor will have a good electrical safety property. Table 12.6 shows the electrical safety performance of the three kinds of composites with different structures. All meet the requirements of China criteria JG/T 286−2010 "Electric radiant heating film for low temperature" and GB/T 7287-2008 "Test method of infrared heater."

Table 12.6 Electrical safety performance of a multilayered electric heating composite with built-in carbon fiber paper in different structures

Specimens	Leakage current under working temperature (mA)	Electric strength under working temperature (3750 V)	Leakage current under wet condition (mA)	Electric strength under wet condition (3750 V)
Structure a	0.008	Passed	0.010	Passed
Structure b	0.007	Passed	0.010	Passed
Structure c	0.009	Passed	0.012	Passed

In the structure a, b, and c, the electric heating layer moved toward the middle position. Performance was tested based on JG/T 286−2010 "Electric Radiant Heating Film for Low Temperature," but the humidity resistance testing was based on the GB/T 7287-2008 "Test Method of Infrared Heater."

12.4.3.2 Electric connection

The electric connection, as another key technology for the electric heating wood-based floor, includes two connecting points. (1) The connection between electric heating material and electrodes: electrodes contact the electric heating material in the composite. In order to minimize the contact resistance and prevent overheating effectively, a conductive coating is sometime applied on the surface of the electric heating material, which is placed in contact with the electrodes. (2) The connection between electrodes and external power supply, which can be achieved in two ways: (1) after power, an input wire with a connector is welded on the electrodes through the preset hole in a wooden substrate, and insulating sealant is padded in the hole; (2) a conductive connector is firstly set inside the substrate and tightly connected with electrodes under the bonding pressure, then a snap-in, inflatable, or retractable type male plug with a power connection wire is put in the preset connector. The final connection, electric connection, and installation among the floors can be simultaneously realized, as the electrical connector is preset in the mortise of the floor.

12.4.3.3 Supply voltage

Except for commonly used 220 V AC power supply, safety 36 V converted from 220 V by a transformer has also been used for the improvement of electrical safety. However, a higher current will be brought in for the same total power and heating effects. In addition, lower and safety voltage can also be applied to the floors because a certain number of floors are connected in a series to a group, and then some groups can be connected in parallel to the power source. The final voltage of one floor will be lower or even much lower than 36 V.

In addition to the aforementioned technology for the electrical safety, the scheme, such as short circuit, overload, and leakage protection, included in the supply system of the whole heating element can also play improved protection performance, although

it needs the relative product technology and acceptance specification for guaranteeing the safety quality.

12.4.3.4 Reducing volatile organic compounds

Heat generated from the Joule effect can accelerate the volatilization of organic compounds in the floor. As the temperature gradient in the working floor is from the middle layer to the surface, the volatilization has an advantage of shorter volatilizing distance compared to the general heating floor. The modified MUF adhesive with low aldehyde has been another contributor.

12.4.3.5 Shielding harmful electromagnetic radiation

Electromagnetic radiation always generates from a conductive material after it is loaded with electricity. A shielding material, such as conductive ink and aluminum foil, had been used for shielding harmful radiation and improving heat transfer at same time. If two electric heating layers are laminated in different positions of the floor, respectively, the harmful radiation can counteract each other. However, the infrared wave generating from the carbon heating material is also a kind of electromagnetic radiation, and the shielding treatment could attenuate the infrared effect. In practice, the electromagnetic radiation of an electric heating membrane made of carbon fiber paper is much lower than the limiting value of GB8702-2014 "Protection regulation of electromagnetic radiation" (Tables 12.7 and 12.8).

12.5 Application and future trends

Natural wood fiber-based electricity functional composites have been developed for their antistatic, shielding, and electric heating effects. Of these, natural wood fiber-based antistatic composites can be used for antistatic floors, desks, and doors (Fig. 12.36) to avoid electrostatic hazards to human beings. In order to reduce the harm or interference of electromagnetic radiation, electromagnetic shielding composites

Table 12.7 Electromagnetic radiation of carbon fiber paper loading with different power

Input power density (W/m^2)	Electric field intensity (V/m)		Magnetic field intensity (I/m)		Radiation power density (W/m^2)	
300	1.7543	±0.2509	0.00643	±0.00157	0.0079	±0.0021
500	1.2571	±0.1960	0.00340	±0.00061	0.0044	±0.0011
700	1.1550	±0.2081	0.00323	±0.00062	0.0042	±0.0011

The test probe of NBM550 electromagnetic radiation analyzer was contacted closely on the electric heating membrane to test in the testing frequency range 100 KHz ~ 3 GHz, and seven points had been tested.

Table 12.8 Electromagnetic radiation of three multilayer electric heating composites

Structure type	Electric field intensity (V/m)		Magnetic field intensity (I/m)		Radiation power density (W/m^2)	
a (1/2 layer)	1.97	±0.20	0.0086	±0.0020	0.0083	±0.0017
b (2/3 layer)	1.77	±0.18	0.0046	±0.0003	0.0069	±0.0014
c (3/4 layer)	1.83	±0.24	0.0051	±0.0005	0.0077	±0.0017

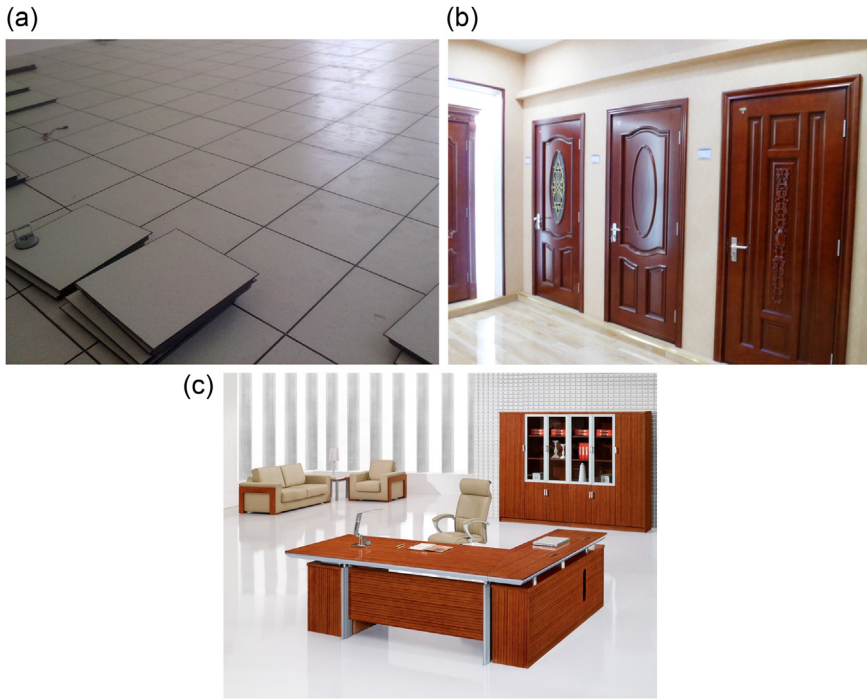

Figure 12.36 Natural wood fiber-based antistatic products: (a) antistatic floor; (b) antistatic door; (c) antistatic desk.

have been manufactured as shielding floors, wall panels, and high-precision test rooms (Fig. 12.37). As the high-efficiency electric heating effect, electric heating composites have been developed as indoor electric heating floors, wall panels, Kang, and arm chairs (Fig. 12.38). Because of the dehumidification and far infrared effect for electric heating, moisture−mildew proof floors, electric heating bureaus, and steam rooms (Fig. 12.39) have also been developed to extend the lifetime of furniture. It can be seen that the composites are widely applicable and upscale.

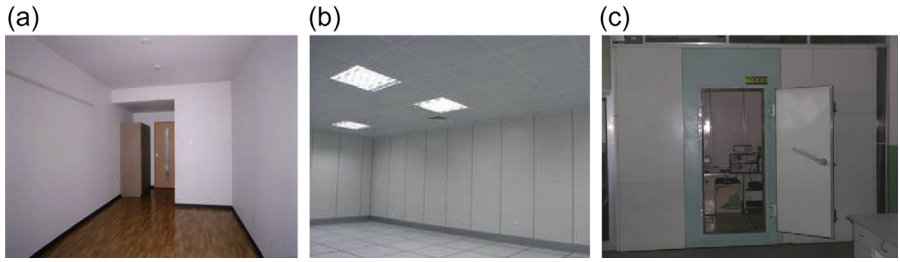

Figure 12.37 Wood-based electromagnetic shielding products: (a) shielding floor; (b) shielding wall panel; (c) high-precision test room.

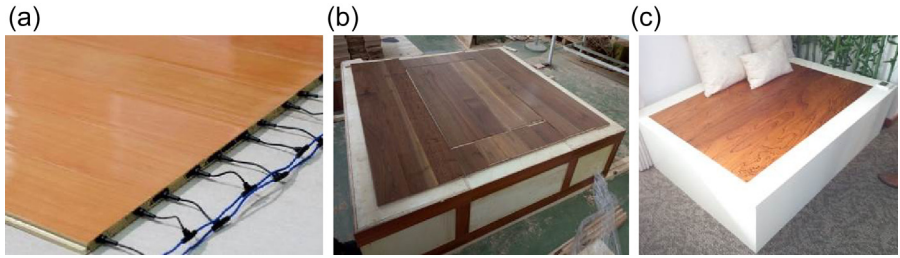

Figure 12.38 Natural wood fiber-based electric heating products for indoor heating: (a) electric heating floor; (b) electric heating Kang; (c) electric heating armchair.

Figure 12.39 Natural wood fiber-based electric heating products for mildew proofing and health care: (a) moisture−mildew proof floor; (b) electric heating bureau; (c) steam room.

The key of electromagnetic shielding composites is to develop simple and efficient jointing technology. Electrostatic charge always generates and gathers on the surface of the furniture or composite components, so antistatic composites and durable antistatic agents for surfaces have a promising future.

The increasing indoor heating demand is leading to the development of electric heating composites. Many floor enterprises in China have rich experiences in research and production, and the key technologies are improving all the time. However, in order

to further address the bottlenecks and promote markets healthily and continuously, more efforts could be centered in the following directions: (1) developing more homogeneous electric heating materials and improving heating performance of uniformity, stability, and age resistance; (2) developing a new type of electric heating material with positive temperature coefficient property to realize the self-limiting temperature function of an electric heating floor and fully enhance the security of products; (3) developing high-efficiency insulation technology and cracking the contradiction between electrical safety and processing efficiency; (4) designing simpler electric connectors and connecting structures to achieve efficient installation and resolve the insecure splice; (5) developing automatic and efficient manufacturing devices to enhance manufacturing accuracy and efficiency and improve product power deviation; (6) strengthening the basic research on the electric heating effect and its response rules, mechanisms, and the evolution law of aging and antiaging. Finally, the composites endowed with piezoelectricity and electrochromic functions will be emphasized with its practicability.

Acknowledgments

This work was financially funded by the National Science and Technology Pillar Program during the Twelfth Five-year Plan Period of China (No. 2015BAD14B04) and the Nonprofit Project of Science and Technology Agency of Zhejiang Province of China (No. 2014NM009).

References

Cai, X.F., Wang, Y.S., 2002. Electromagnetic wave shielding effect of wood composite panels coated with charcoal and charcoal powder. Forestry Industry (Taiwan) 21 (3), 207−216.

Dai, G.S., 1991. Heat Transfer, first ed. Higher Education Press, Beijing.

Fu, F., Hua, Y.K., 1994. A study on antistatic properties of particleboard. China Wood Industry 8 (3), 7−10.

He, F., 2005. The electrothermal property and application of carbon fiber. New Chemical Materials 33 (3), 7−8, 38.

Hou, J.F., 2015. Study on Properties of Carbon-Based Electromagnetic Shielding Fiberboard. Zhejiang Agriculture & Forestry University, Lin'an, pp. 15−39.

Hu, N.N., 2011. Study on Preparation and Application of Conductive Wood Charcoal. Chinese Academy of Forestry, Beijing, pp. 100−101.

Hua, Y.K., Fu, F., 1995. Research on electrically conductive plywood. Scientia Silvae Sinicae 31 (3), 254−259.

Hui, B., Li, G.L., Li, J., Wang, L.J., 2014. Preparation of electromagnetic shielding wood-based composite by electroless Ni-Cu-P plating on fraxinus mandshurica veneer. Journal of Functional Materials 10 (45), 10123−10127.

Jin, H.K., Sang, B.P., Nadir, A., Nam, H.K., Sung, M.K., 2012. Electromagnetic interference shielding effectiveness, electrical resistivity and mechanical performance of carbonized medium density fiberboard. Journal of Composite Materials 47 (16), 1951−1958.

Kawasaki, T., Kawai, S., 2006. Thermal insulation properties of wood-based sandwich panel for use as structural insulated walls and floors. Journal of Wood Science 52 (1), 75−83.

Li, W.M., Zhang, L.F., Liu, J.L., Ren, B.L., Shi, D.P., 1996. Composite material for shielding electromagnetic wave prepared by means of magnetron controlling sputter. Journal of Jilin University 3, 65−66.

Liang, J.H., 1991. Experimental research on internal temperature of lumber dried by electric heat far infrared radiation. Scientia Silvae Sinicae 27 (2), 154−159.

Liu, H.B., Li, J., Wang, L.J., 2010. Electroless nickel plating on APTHS modified wood veneer for EMI shielding. Applied Surface Science 257 (4), 1325−1330.

Liu, X.M., 2005. Processing and Performances of Electromagnetic-Shield Effectiveness Functionally Wood-Based Laminated Composites. Chinese Academy of Forestry, Beijing, pp. 119−121.

Lu, K.Y., Fu, F., Cai, Z.Y., Fu, Y.J., Zhang, Y.M., 2011a. Study of properties of electromagnetic conductive shielding plywood laminated with sheets. Journal of Building Materials 14 (2), 207−211, 235.

Lu, K.Y., Fu, F., Fu, Y.J., Cai, Z.Y., 2011b. Study to wood electromagnetic shielding composites laminated with aluminum plates. Advanced Materials Research 280, 159−164.

Lu, K.Y., Fu, F., Sun, H.L., Fu, Y.J., 2013. Bonding technology of electromagnetic shielding plywood laminated with conductive sheets. Wood Research 58 (3), 465−474.

Lu, K.Y., Hou, J.F., Yuan, Q.P., Fu, F., Zhang, Y.M., 2014. Properties of electromagnetic shielding case made of plywood laminated with conductive sheets. Wood Research 59 (4), 547−556.

Lu, K.Y., 2007. A Study on Preparation and Bonding of Electromagnetic Shielding Plywood Laminated with Conductive Films. Chinese Academy of Forestry, Beijing, pp. 79−107.

Luo, Z.H., Zhu, J.Q., 2000. Review of wood/metal composite materials. China Wood Industry 14 (6), 25−27.

Lv, B., Fu, F., 2013. Wood Door. China Building Materials Industry Press, Beijing.

Nagasawa, C., Kumagai, Y., 1989. Electromagnetic shielding particleboards with nickel-plated wood particle. Journal of Wood Science 35 (12), 1092−1099.

Nagasawa, C., Kumagai, Y., Urabe, K., 1990. Electromagnetic shielding effectiveness particles board containing nickel-metalized wood particles in the core layer. Journal of Wood Science 36 (7), 531−537.

Nagasawa, C., Kumaga, Y., Koshizaki, N., 1992. Changes in electromagnetic shielding properties of particleboards made of nickel-plated wood particles formed by various pretreatment processes. Journal of Wood Science 38 (3), 256−263.

Nagasawa, C., Kumagai, Y., Urabe, K., Shinagawa, S., 1999. Electromagnetic shielding particleboard with nickel-plated wood particles. Journal of Porous Materials 6, 247−254.

Piao, Z.Y., Xu, S.A., 1993. Performance improvement of medium fiberboard by combining with various non-wood materials. Research Report of South Korea Academy of Forestry 47, 35−48.

Qiu, Y.T., 2008. The Research of Electromagnetic Shielding Materials Made of Wood. Chinese Academy of Forestry, Beijing, pp. 29−39.

Schelkunoff, S.A., 1943. Electromagnetic Waves. D.Van Nostrand Company, Inc., New York.

Shiro, A.K., Hiroshi, B.B., Toshihiro, M., 1991. Manufacturing and electromagnetic shielding characteristics of multilayer laminated wood-based composites. Report of Research Institute of Forestry 360, 171−184.

Wang, S.Y., Hung, C.P., 2003. Electromagnetic shielding efficiency of the electric field of charcoal from six wood species. Journal of Wood Science 49 (5), 450−454.

Wang, L.J., Li, J., Liu, Y.X., 2005. Surface characteristics of electroless nickel plated electromagnetic shielding wood veneer. Journal of Forestry Research 16 (3), 233−236.

Wang, L.J., Li, J., Liu, Y.X., 2006. Preparation of electromagnetic shielding wood-metal composite by electroless nickel plating. Journal of Forestry Research 17 (1), 53−56.

Wang, J.L., Guo, H.X., Li, R.Q., Wang, Q., 2009. Preparation and characteristics of surface-type electromagnetic shielding wood-based composites. China Wood Industry 23 (1), 21−23.

Wang, D.A., 1983a. Study on mechanism for wood infra-red drying (Ⅰ). Infrared Technology 5 (1), 1−3.

Wang, D.A., 1983b. Study on mechanism for wood infra-red drying (Ⅱ): penetration depth of infrared ray on wood. Infrared Technology 5 (2), 22−24.

Wang, D.A., 1983c. Study on mechanism for wood infra-red drying (Ⅲ): absorption theory of dry wood. Infrared Technology 5 (4), 35−38.

Yang, X.P., Rong, H.M., Dai, X.J., 2000. Electrical properties of laminated rubber/carbon fibre facial conductive and heat generating sheet. China Rubber Industry 47 (1), 9−13.

Yao, W., Zhang, C., 2007. Electro-thermal effect of carbon fiber reinforced cement composites. Development and Application of Materials (China) 22 (1), 17−20.

Yu, D.H., Wang, C.Y., Cheng, X.L., Song, Y.X., 2009. Recent development of magnetron sputtering processes. Vacuum 46 (2), 19−25.

Yu, Z.T., Xu, X., Fan, L.W., Hu, Y.C., Cen, K.F., 2011. Experimental measurements of thermal conductivity of wood species in China: effects of density, temperature, and moisture content. Forest Products Journal 61 (2), 130−135.

Yuan, Q.P., Fu, F., 2014. Application of carbon fiber paper in integrated wooden electric heating composite. BioResources 9 (3), 5662−5675.

Yuan, Q.P., Su, C.W., Huang, J.D., Gan, W.X., Huang, Y.Y., 2013. Process and analysis of electromagnetic shielding in composite fiberboard laminated with electroless nickel-plated carbon fiber. BioResources 8 (3), 4633−4646.

Yuan, Q.P., Lu, K.Y., Fu, F., 2014. Process and structure pf electromagnetic shielding plywood laminated with carbon fiber paper. The Open Material Science Journal 8, 99−107.

Zhang, X.Q., Liu, Y.X., 2005. Research on stainless steel fiber/wood fiber composited MDF. China Wood Industry 19 (2), 12−16.

Zhang, Y.L., Qi, W.Z., Sun, L.P., 2013. Charcoal composite electromagnetic shielding characteristics analysis. Forest Engineering 29 (1), 54−56, 60.

Sound absorption and insulation functional composites

13

L. Peng
Research Institute of Wood Industry, Chinese Academy of Forestry, Beijing, China

13.1 Introduction

Noise pollution, together with air pollution and water pollution, have become the three most serious environment pollution that affect human health. According to the investigation report of the World Health Organization, noise can harm human health physically and psychologically, like auditory fatigue, hearing loss, disturbing people's lives, and affecting work. Nowadays it has been widely realized that industry noise pollution has a critical negative effect and indoor noise pollution is still concerned (Wu, 2006).

Wood and wood-based composite materials are widely used as construction and decoration products, which have significant influence and regulation on indoor acoustical environments. Therefore research on sound insulation properties of wood and wood-based materials have a broad and general significance. This chapter attempts to introduce the following research on the acoustic properties of wood and wood-based composites and some wooden sound attenuation functional materials for absorption and insulation. It is of vital significance to improve the indoor acoustical environment and expand the functional areas of wood-based materials.

13.1.1 Sound transmission through barriers

Indoor noise can be caused by many aspects, such as outdoor traffic, public activities, and household appliances. The construction site noise, vehicle noise, or entertainment-gathering noise from outside, as well as noise from neighbors, are propagated through walls, doors, or windows, which are defined as airborne sound. Based on the propagation path of sound, the control of noise involves the following three ways: alterations at noise and vibration sources, modifications along the sound propagation path, and dealing with sound receivers. To control the noise in the interior space, noise barriers and absorption materials are often utilized to attenuate the acoustic energy.

When the acoustic wave is incidentally on the object, some of the acoustic energy is reflected, and some is converted into heat and attenuated due to friction and viscous resistance, which is defined as sound absorption. And some are transmitted through the object and vibrate the air on the other side. As shown in Fig. 13.1, E_i, E_r, E_a, and E_τ are incident acoustic energy, reflected energy, and absorbed energy, respectively. According to the conservation laws of energy, they have the following relationship:

$$E_i = E_r + E_a + E_\tau \tag{13.1}$$

Advanced High Strength Natural Fibre Composites in Construction. http://dx.doi.org/10.1016/B978-0-08-100411-1.00013-3

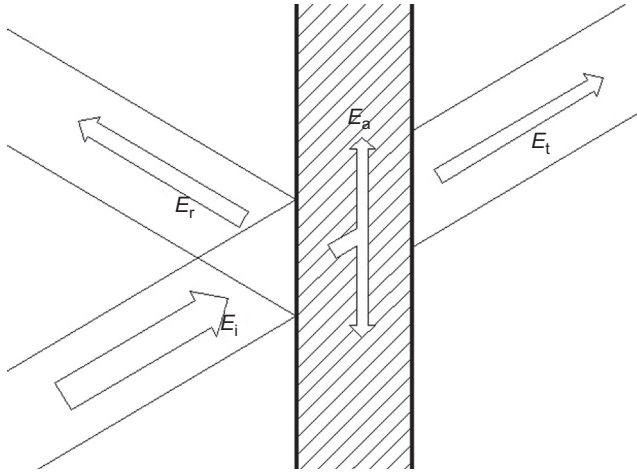

Figure 13.1 Diagram of sound transmission through material.

13.1.2 Definitions

Sound absorption coefficient is used to evaluate the sound absorption efficiency of materials. It is the ratio of absorbed energy to incident energy and is represented by α. If the acoustic energy can be absorbed entirely, then $\alpha = 1$.

$$\alpha = \frac{E_a}{E_i} = 1 - \frac{E_\tau}{E_i} \tag{13.2}$$

The sound absorption coefficient of materials is correlated with frequency, and it varies with different frequencies. The sound absorption coefficient frequency characteristic curves can be used to illustrate the sound absorption properties of different frequencies exactly. It is not convenient to compare and state, so the average sound absorption coefficient, which is the average of an acoustic material's absorption coefficients at a specified set of frequencies, is used for simplification. The average sound absorption coefficient is represented by $\overline{\alpha}$.

The sound absorbed capacity of a certain building element is characterized by sound absorption A, which equals the sound absorber surface area multiplied by the sound absorption coefficient.

$$A = \sum_{1}^{n} s_i \alpha_i \tag{13.3}$$

where, s_i and α_i are the surface area and sound absorption coefficient of the ith wall.

Transmission coefficient is the ratio of transmitted energy to incident energy and is presented by τ. In engineering, the sound insulation capacity of material or building

elements is represented by sound reduction index, which is also called sound transmission loss (STL) and is expressed in decibels.

$$R = 10\lg\frac{1}{\tau} = 10\lg\frac{E_{\mathrm{i}}}{E_{\tau}} \tag{13.4}$$

The STL of a certain object varies with frequencies. Usually the STL in high frequencies is greater than that in low frequencies. The sound insulation properties of different materials are also different (Ma, 2002). According to ISO 140-4, sound insulation measurements are conducted at least in third-octave bands of 100−3150 Hz, while additional information can be obtained by extending the frequency range of 50−5000 Hz. The sound insulation properties of materials can be rated with three factors: sound insulation frequency spectra, average sound reduction index, and weighted sound reduction index R_{w}. Sound insulation frequency spectrum is a sound reduction curve based on the STL values on different frequencies. Average sound reduction index is the arithmetic average value of sound reduction indexes of center frequencies of one-third octave bands.

Weighted sound reduction index R_{w} is a single-number quantity that is intended for rating the airborne sound insulation and for simplifying the formulation of acoustical requirements in building codes. According to the method described in ISO 717-1:1996 and GB/T 50121-2005, R_{w} is determined by comparing the measurement results to the values of the reference curve. The reference curve is shifted in 1 dB steps to the highest possible position, at which the sum of unfavorable deviations between reference and measured values is as large as possible but does not exceed 32 dB. Unfavorable deviation means that the measured value of the sound reduction index at a certain frequency band is lower than the corresponding reference value. When the ISO 717-1 reference curve has been shifted to the correct position, the weighted sound reduction index R_{w} can be read from the reference curve at 500 Hz.

In America, Sound Transmission Class (STC) rating is generally used instead. The determination of STC is similar to the weighted sound insulation index. However, they diverge to a significant degree in the details, and in the numerical results produced.

Footsteps or heavy movements on upstairs floors stimulate floor vibration. The vibration spreads along the structure and radiates downstairs, turning out to be noise, which is called impact sound. Other than airborne sound insulation, the impact sound insulation property is rated by the normalized impact sound pressure level in the receiving room that is stimulated by the impact on the upstairs floors. The higher impact sound pressure level downstairs means poorer impact sound insulation property of floors, whereas the floors get better impact sound insulation characteristics.

The impact sound downstairs is related to the room sound absorption areas. In order to eliminate the influence of sound absorption, normalized impact sound pressure level L_{P_n} is expressed by:

$$L_{P_{\mathrm{n}}} = \overline{L_{P_{\mathrm{i}}}} + 10\lg\frac{A}{A_0} \tag{13.5}$$

where, $\overline{L_{P_i}}$ is the average impact sound pressure level in the receiving room in decibels. A is sound absorption area in the receiving room and A_0 is the reference sound absorption area, which usually is 10 m^2.

Impact sound pressure level differs with frequencies. A single-number value that normalized weighted sound pressure level $L_{P_n,W}$ in decibels is used to rate impact sound insulation properties of different floors. A rating curve with octave-band sound pressure levels from 125 to 2000 Hz is used for determining $L_{P_n,W}$ (Zhong, 2012). The floor impact sound insulation rating method is stated in standard ISO 717-2:1996. In North America, impact insulation class is used to rate the impact sound attenuation of the floors.

13.2 Sound absorption functional composites

13.2.1 Sound absorption mechanism

According to the different structures, the sound absorption materials can be classified into porous absorption material, resonance absorption material, and special sound absorption structure. The porous sound absorbing material holds the maximum category and is widely used. The resonance absorption material includes sheet resonance, perforated plates, and microperforated panels. In this section, the sound absorbing mechanisms of porous absorption material and resonance absorption material are introduced.

13.2.1.1 Mechanism of porous absorption materials

Porous sound absorption material is most widely used as sound absorption functional material, which is made of glass fiber, wool fiber, wood fiber, or polyester fiber and adhesive as board or sound proof felt. There are many macropores and micropores that are interconnected and opened to the surface inside the material. It can be seen as a complicated channel system with many solid frames and capillaries. The mechanism of sound absorption mainly involves three physical processes (Zhu et al., 2014). First, when the sound wave is in the porous material, the viscous effect between the solid frame and numerous air cavities will attenuate part of the sound energy and convert it into heat. Second, heat transfer will happen due to temperature distinction between different parts caused by friction, which is an isothermal process. And this process will further dissipate sound energy. Third, the vibration of air in the bulk materials will also lead to the vibration of fibers. Usually the sound absorption property in high frequencies is better than that in low frequencies.

13.2.1.2 Mechanism of resonate absorption materials

It presents a sound absorption effect when there is a cavity between sheet and rigid back, for instance, wooden or metal sheets as ceilings and wall slabs. The absorption mechanism of the structure is sheet resonance sound absorption. The sheet is

stimulated to vibrate and yield in the acoustic field. The vibration energy is attenuated, due to internal friction or viscosity of the board and constraint of the fixed boundary, and is converted into heat and dissipated. Since low frequency sound waves are more likely to arouse the vibration than high frequency waves, the sheet resonance structure yields good sound absorption performance at low frequencies. When the frequency of the incident sound wave is equal to the sheet inherent frequency or natural frequency, the vibration amplitude reaches its maximum and the structural resonance occurs. The resonance frequencies of common sheet sound absorption structures are 80−300 Hz. The resonance frequency of sheet sound absorbing structure f_r can be estimated by Eq. (13.6):

$$f_r = \frac{60}{Md} \tag{13.6}$$

where M is surface density of the sheet and d is the thickness of the air cavity. The sound absorption peak value can be improved by filling the cavity with porous sound absorption material.

A perforated panel can be seen as many parallel Helmholtz resonators. As shown in Fig. 13.2, a single Helmholtz resonator is made up from a large chamber and a narrow neck. The internal cavity is connected to the outside by a narrow neck. In the acoustic field, the air column in the neck keeps doing circular motions like pistons. Vibrated air in the openings is damped for friction. And part of the acoustic energy is converted into thermal energy. The structure resonates when the frequency of the incident sound wave is equal to the inherent frequency, and the damping effect at neck reaches maximum. Sound energy is absorbed to the largest extent and the sound absorption coefficient reaches the peak value. The sound absorption feature of resonate structure is strong selectivity on frequencies, which only shows good sound absorption performance near resonate frequency. Neither higher nor lower frequencies get high sound absorption coefficients. The width of the sound absorption frequency band is small and

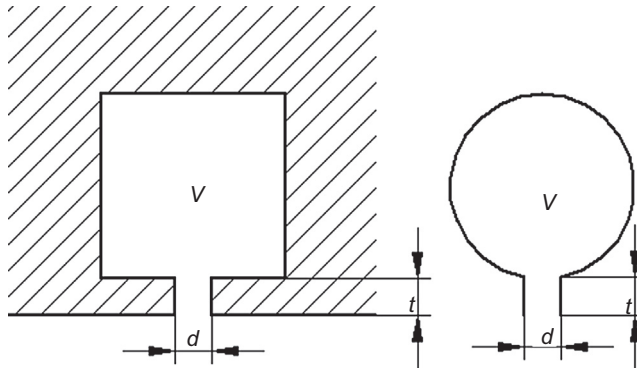

Figure 13.2 Helmholtz resonator.

from dozens to 200 Hz. Fabric or porous sound absorption material is often struck to the back of a perforated panel to widen its frequency band.

The resonance frequency f_r of a Helmholtz sound absorption structure can be calculated by the Eq. (13.7) (Liu, 2000):

$$f_r = \frac{c}{2\pi}\sqrt{\frac{p}{d(l+0.8D)}} \tag{13.7}$$

where c is sound velocity, p is perforated rate, namely the ratio of perforated area to total area, d is the thickness of air cavity, l is the thickness of panel, and D is the diameter of pore.

The sound absorption coefficient of a perforated panel near resonance frequency is large, while it decreases sharply when incident wave frequency gets larger or smaller. The width of absorption frequency bend is small and the resonant frequency is low. It is not often used alone in civil engineering (Hou, 2012).

13.2.2 Sound absorption measurement

The sound absorption properties of wooden materials can be characterized by a sound absorption coefficient, which can be measured in the standing wave tube method, the transfer function method, and the reverberation room method. Both standing wave tube methods and transfer function methods are carried out in sonic tubes and sound absorption coefficients of normal incident are obtained. The sample size required in the tube method is small and the experiments are low cost and easy to carry out. The reverberation room method is conducted in a room and absorption coefficients of a random incident are obtained. The sample size of the reverberation room method is large and the measurement is less convenient to carry out while the results are close to actual situation. For the research, the standing wave tube method or the transfer function method can be used in preliminary research to study sound absorption regularity of the material. Then the absorption properties in space can be measured in the reverberation room (Chen et al., 2005).

13.2.2.1 Standing wave tube method

A standing wave tube is a metal or plastic straight pipe, of which the sample is fixed on one side and a loudspeaker is fixed on the other side. A single frequency wave is generated by a loudspeaker and is magnified by an amplifier. Sound waves propagate rectilinearly in the tubes, and it can be regarded as plant waves. A standing wave field is contributed by incident waves and reflected waves. And the maximum and minimum sound pressure values are distributed alternately from material surface. The difference between the maximum value and the minimum value can be measured by a moving microphone, and the absorption coefficients are calculated. This method is described in standard GB/T 19696.1-2004. Fig. 13.3 illustrates the diagram of standing wave tubes for sound absorption measurement.

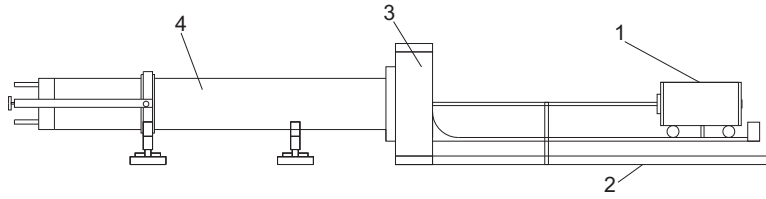

Figure 13.3 Standing wave tubes for sound absorption measurement. (1) Testing vehicle; (2) rails; (3) sound source; and (4) standing wave tubes (for low frequency and high frequency test).

The ratio of sound pressure minimum value to the maximum value is marked as standing wave ratio G. The absorption coefficient can by expressed by:

$$\alpha = \frac{4G}{(1+G)^2} \tag{13.8}$$

Eq. (13.8) illustrates that the normal incidence absorption coefficient can be calculated once the standing wave ratio is determined. Actually, the measured result in standing wave tubes is the sound pressure level difference L between the maximum value and minimum value, $L = 20\lg G$. And the absorption coefficient can be calculated by the Eq. (13.9):

$$\alpha = \frac{4 \times 10^{\frac{L}{20}}}{\left(1+10^{\frac{L}{20}}\right)^2} \tag{13.9}$$

13.2.2.2 Transfer function method

In 1980, Chung and Blaser proposed an absorption coefficient measuring approach in the transfer function method using impedance tubes with two microphones. The transfer function method is also conducted in sonic tubes like the standing wave method, while the sliding microphone is replaced by two microphones fixed on the tube wall. The sound source generates plane waves in the tubes. Sound pressure is tested by two microphones closed to the test sample, and the sound propagation function of two microphone signals can be obtained. Normal incident absorption coefficient and surface impedance are derived from complex calculation. The transfer function method is more convenient and advanced compared with the standing wave method. The measurement method is stated in standard ISO10534-2 and GB/T18696.2-2002.

13.2.2.3 Reverberation room method

The reverberation time, which characterizes the rate of sound decay, is considered to be the most important acoustic parameter for various kinds of rooms. The absorption coefficient measurement in a reverberation room is estimated from the decay of sound under measurement conditions (Kanev, 2012). The measurement is conducted in a reverberation room where volume is no less than 150 m^3 and the area of the tested

sample is about 10−12 m^2. The reverberation time t_1 of the vacant room is measured before the sample is mounted. Sound absorption coefficient of the surface of reverberation room α_1 can be calculated according to the Sabine reverberation formula.

$$t_1 = \frac{0.161\ V}{A} = \frac{0.161\ V}{S_1\alpha_1} \tag{13.10}$$

where, V is the volume of reverberation room, A is sound absorbed capacity, and S_1 is total surface area of the reverberation room.

Then the test sound absorption material is mounted in the reverberation room. The reverberation time t_2 is measured and can be expressed by:

$$t_2 = \frac{0.161\ V}{A + \Delta A} = \frac{0.161\ V}{S_1\alpha_1 + S_2\alpha_2} \tag{13.11}$$

where, ΔA is the additional sound absorbed capacity of sound absorption material, S_2 is the surface area of the tested sample, and α_2 is the sound absorption coefficient of the tested sample, which can be calculated by Eq. (13.12):

$$\alpha_2 = \frac{0.161\ V}{S_2}\left(\frac{1}{t_2} - \frac{1}{t_1}\right) \tag{13.12}$$

The reference standards of the measurements are ISO 354-2003 or GB/T 20247-2006.

13.2.3 Sound absorbing of wooden materials

13.2.3.1 Porous sound absorption materials

As is widely known, wood is a kind of porous material. The sound absorption properties of solid wood are related to wood species, moisture content, grain direction, and other factors.

Wood species

The absorption properties of individual wood species can be very different. Fig. 13.4 shows the experimental results of absorption properties of 10 wood species at tangential sections (LT) (Smardzewski et al., 2014), namely, alder (*Alnus glutinosa* L. Fearthn.), ash (*Fraxinus* excelsior L.), balsa (*Ochroma lagopus* Sw.), birch (*Betula pendula* Roth.), elm (*Ulmus minor* Mill.), meranti (Shorea spp.), oak (*Quercus robur* L.), pine (*Pinus sylvestris* L.), poplar (*Populus nigra* L.), and sapeli (*Entanrdophragma cylinfricum* (Sprague)). As shown in the figure, the tendencies of sound absorption curves of different wood species are alike. And average absorption coefficients of them all are below 0.2. Since the densities and microstructure vary with species, the absorption properties also differ in terms of species. In general, wood with a lower density gets better absorption performance. The absorption property of hardwood is better than softwood of the same density.

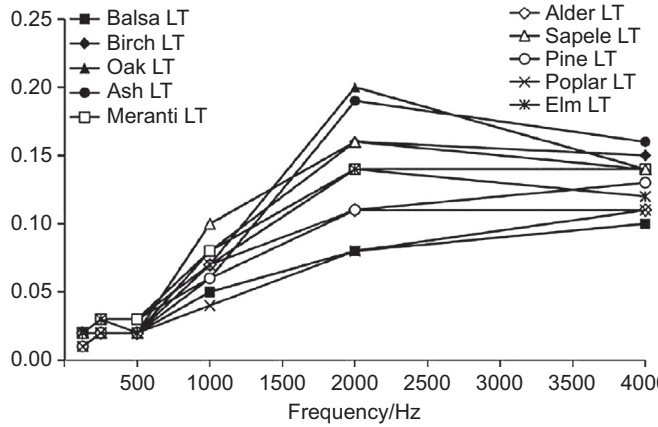

Figure 13.4 Experimental results of sound absorption coefficients of 10 species (Smardzewski et al., 2014).

Moisture content

Fig. 13.5 shows the sound absorption coefficient spectrums of Japan cedar (*Cryptomeria fortune* Hooibrenk ex Otto et Dietr) in different moisture contents (6%, 19%, 24%, and 64%). The sound absorption properties are decreased with the increase of moisture content, and the impact of moisture content is significant in high frequencies.

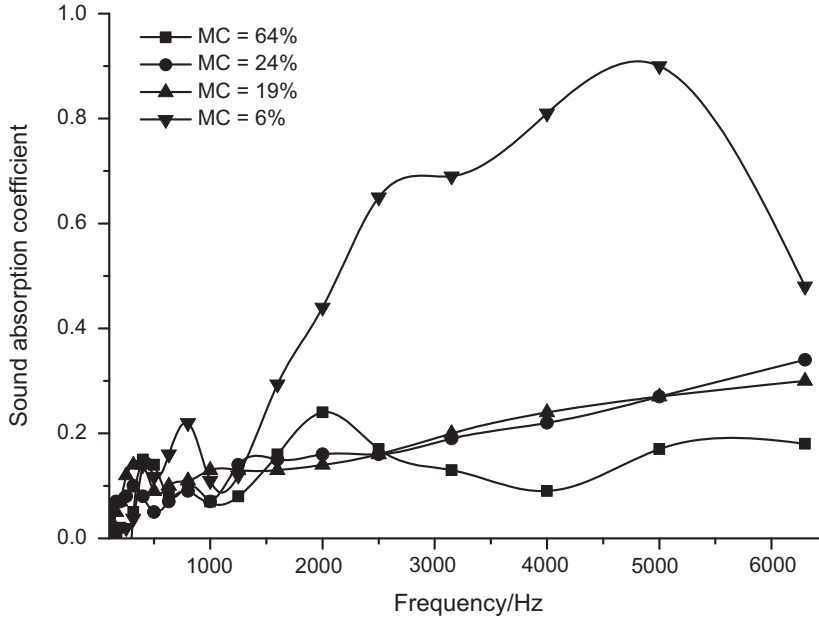

Figure 13.5 The sound absorption coefficient spectrums of Japan cedar in different moisture contents.

Pores of porous materials like wood are narrowed when absorbed or during water uptake. Air in voids and micropores are replaced by water, and the porosity is decreased so that sound absorption property is also diminished (Wang et al., 2014).

Wood grain direction

The properties of solid wood vary with anatomical structure and sound wave incident plate. Fig. 13.6 illustrates the comparison of sound absorption properties of Mongolian Scotch pine (*P. sylvestris* var. *mongolica*) in three dimensions. It concluded that the sound absorption property of a cross section is better than those of longitudinal section and tangential section. Wood is made up of many axial cells, and it presents a honeycomb structure in cross sections, which is easy for acoustic waves to transmit into. While longitudinal sections and tangential sections are made up of many axial sections of cells, there are less pores and voids, so that absorption properties of longitudinal sections and tangential sections are weaker than that of cross sections. There is a small amount of xylem ray cross sections in a tangential section that makes the tangential section sound absorption performance better than a longitudinal section.

Wooden panels are made from wooden elements and adhesive, which is also a porous structure. Researchers of Northeast Forestry University have measured and compared sound absorption characteristics of solid wood (pine), plywood, particleboard, and medium density fiberboard in a standing wave tube method (Liu et al., 2007). The comparison of sound absorption coefficient curves of timber and common wooden

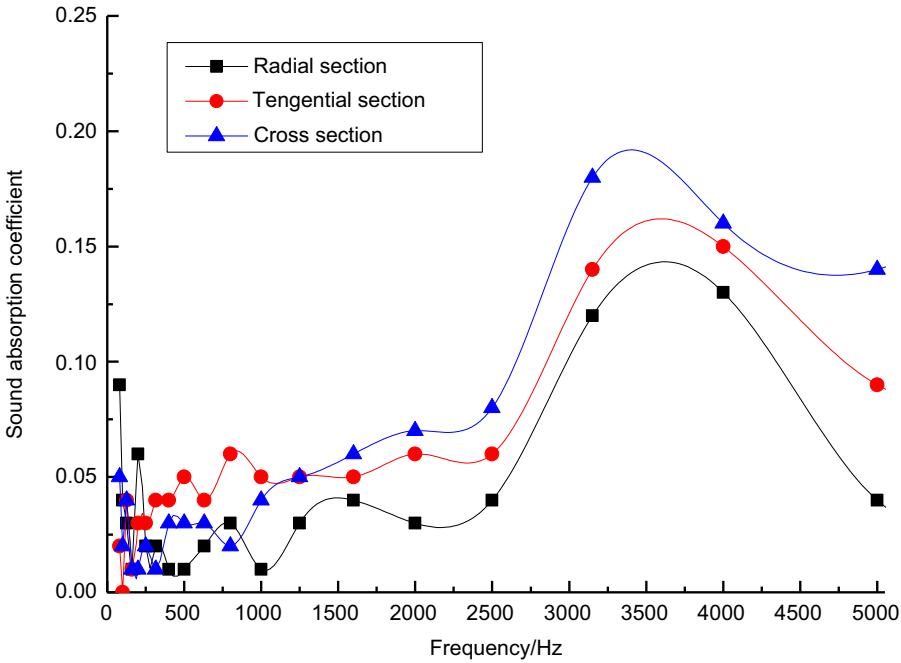

Figure 13.6 Sound absorption coefficients of three dimensions of Mongolian Scotch pine.

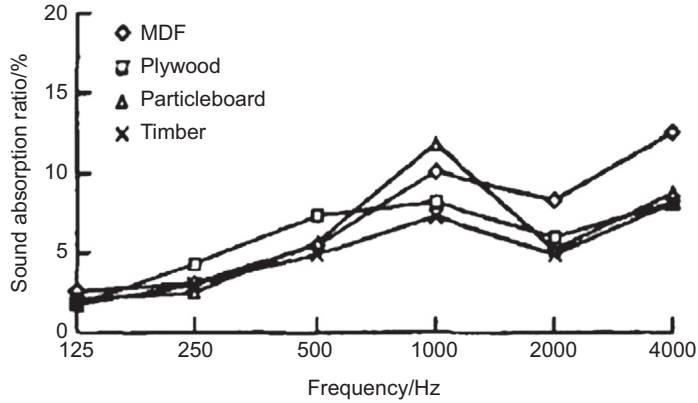

Figure 13.7 Comparison of sound absorption properties of four different wooden materials of the same thickness (in 8 mm) (Liu et al., 2007).

panels of the same thickness are shown in Fig. 13.7. It can be concluded that the sound absorption spectrum patterns of different wooden materials are alike. Sound absorption coefficients are increased with the increase of frequency, and the peak values are close to 1000 Hz. The absorption properties of wood and wooden panels are presented in turn: fiberboard > plywood > particleboard > solid wood.

It can be concluded from Fig. 13.7 that the sound absorbing rate of four kinds of materials are no larger than 20%, and the average absorption coefficients are less than 0.1. A sound absorption material is defined as one with an average absorption coefficient larger than 0.2. Thus the properties of all the earlier four materials are poor. Although there are plenty of cell lumina in the solid wood, the porosity is about 50%. The connectivity between lumina is poor, and it is difficult for an acoustic wave to motivate unconnected air particle vibration. Thus solid wood and wooden panels are not good absorption materials.

Natural fiber material is the earliest sound absorption material. The composites of natural fibers like hemp fibers, coconut shell fibers, and others have wide sound absorption frequency bands. While the use of those natural fiber composites is restricted due to their poor fireproof, damp-proof, and decay properties. Then, when inorganic fibers like mineral wool fibers and glass fibers were developed, the shortcomings of the natural fibers mentioned before were overcame. However, it is reported that inorganic fibers polluted the environment and harmed people's health. With the development of the chemical industry, polyester fibers and other synthetic fibers are widely used as new fibrous sound absorption materials, which have advantages of both natural fibers and inorganic fibers. In order to enhance the sound absorption of polymer fiber composite materials, different kinds of natural fibers and polymer fibers are blended and made into a new composite material, which also shows good physical and mechanical properties.

Researchers of the Wood Functional Material Lab in the Chinese Academy of Forestry developed a high sound absorption property composite material made of

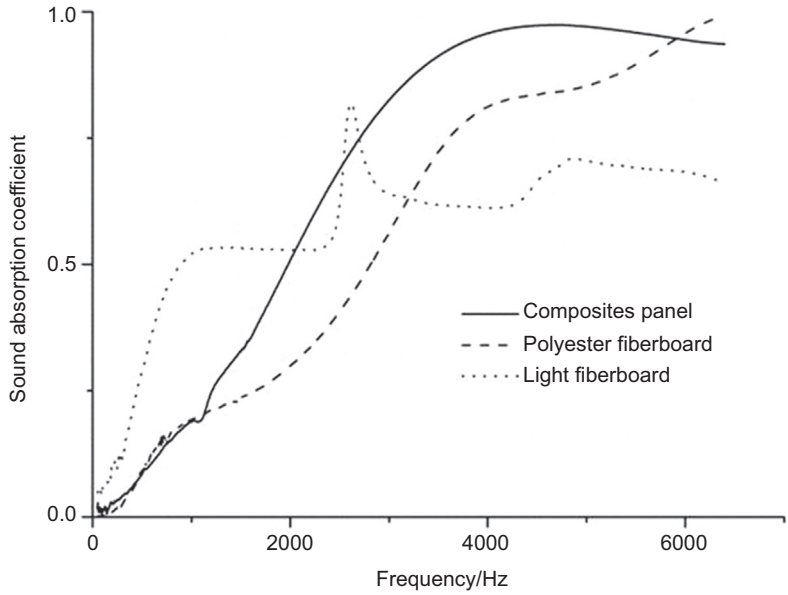

Figure 13.8 Comparison of absorption coefficient of composite material with polyester fiberboard and light fiberboard.

wood fiber and polyester fiber with the adhesive PMDI. The density of the composites is in the range of 0.1−0.3 g/cm^3. The transfer function method was used to measure the sound absorption properties of the composites, as well as polyester fiberboard and light fiberboard. The comparison of absorption properties of the three is shown in Fig. 13.8 (Wang, 2013).

It can be concluded from Fig. 13.8 that the sound absorption property of light fiberboard is better than that of polyester fiberboard and wood/polyester fiber composites at the range of 50−1800 Hz. And there is an absorption peak value at 2600 Hz, which is caused by resonance. The absorption coefficients of the composites are higher than those of polyester fiberboard and light fiberboard at the frequency of 2700−6400 Hz. Both wood/polyester composite material and polyester fiberboard are porous fibrous sound absorbing materials. They share the same absorption mechanism and similar sound absorption regularity.

There are many aspects that affect the sound absorption properties of porous fibrous materials, namely acoustic impedance, flow resistance, porosity, and structural factors (tortuosity) on account of the structure, and thickness, bulk density, and cavity behind the board in engineering.

Airflow resistance and resistivity

Airflow resistance is the resistance of an air particle going through a material, which can be expressed by the ratio of pressure gradient in a material to airflow linear velocity in steady airflow conditions. Resistivity is defined as the ratio that pressure gradient of

unit thickness to airflow linear velocity in the plate that is vertical to the airflow in steady conditions. The airflow resistance is related to impedance and can adjust sound absorption characteristics in this way. The sound absorption property is improved with the increasing resistivity of fibrous material, while it decreases when the resistivity gets over a certain value. If the airflow resistance is too small, the acoustic energy attenuation caused by internal friction is minor and the absorption effect is poor. If the resistance is too large, most of the acoustic waves are reflected and the absorption becomes weaker. The sound absorption curves move toward low frequency with increasing resistivity. As for low airflow resistance materials, absorption coefficient at low frequency is low, and it increases sharply at medium and high frequencies. Compared with low airflow resistance materials, the absorption coefficient of high-resistance materials in high frequencies is decreased, and the absorption coefficients at low and medium frequencies are increased. Airflow resistivity of a fibrous porous material is related to the fiber morphology, size, density, porosity, tortuosity, and arrangements.

Thickness

The length of a wave transmitting path is determined by the thickness of fibrous material. The thicker the material, the longer the transmission path, and more acoustic energy is attenuated. The absorption peak value often occurs at the fourth wavelength. With an increase of thickness, the average absorption coefficient is improved and the peak value moves toward low frequency. However, it is impractical to improve the absorption performance by increasing thickness.

Bulk density

At a certain thickness, the increase of density can improve the absorption performance at low frequencies. However, the improvement is less than that by increasing thickness. Nor too high nor too low, the density will get a good sound absorption property. The influence of density is complex, which is also affected by the morphology of fibers, porosity, and airflow resistance.

Opened porosity

The opened porosity of fibrous material is the volume percentage of the interconnected channels and pores opened to out space to the porous material. Larger porosity means more interconnected pores inside the material and larger specific surface area. There is more internal friction between air and fibers, resulting in higher sound absorption coefficients.

Thickness of air cavity behind

There usually is an air cavity of certain thickness between a porous absorption material and rigid back in applications. The reflected waves by rigid back and the incident wave form a phase difference of 180 degree. The absorption material yields the optimized performance when the thickness of the air cavity is integral in multiples of one-fourth incident wavelength. On the contrary, when the air cavity thickness is integral

in multiples of one-half incident wavelength, the incident waves are overlaid with reflected waves and the absorption performance is the worst.

13.2.3.2 Wooden perforated panels

As shown in Fig. 13.9, a wooden perforated panel is a kind of product that small holes are cut regularly or grooves are on a visible side and the holes are on the rear. And their core materials are medium density fiberboard (MDF) as substrate with high strength and rigidity for standing up to an impact to some extent. The panel veneer sheets are often solid wood bark or melamine decorative facing (Yu et al., 2010).

The sound absorption properties of perforated panels depend on panel thickness, pore diameter, perforated rate, depth of cavity from rigid back, and so on. To adequately make full understanding of the sound absorption properties of perforated panels, this section presents some research conducted by scholars of the Wood Functional Material Lab of the Chinese Academy of Forestry (Zhu et al., 2015).

Materials: medium density fiberboard (MDF), moisture content is 8.5%, density is 0.72 g/cm^3. The thickness of panels are 10, 15, and 20 mm. The computer-controlled manufacture system Ncstudio and a carved machine are used to perforate the panels. The pore diameters are 3, 6, and 9 mm, separately. And the depths of cavity behind to the rigid back are 25, 50, and 100 mm.

Measurements and instruments: The sound absorption coefficients were tested with impedance tubes (model number: SW 422 and SW 477, BSWA Technology Co., Ltd., China) in the transfer function method. The measurements were carried out according to the related standard.

Panel thickness

Fig. 13.10 shows the sound absorption coefficient spectrums of three perforated panels in the thickness of 10, 15, and 20 mm. The pore diameters are 3 mm, pore center distances are 12 mm, and perforated rate is 4.91%. The depth of cavities behind the panels is 100 mm.

For the effect of different panel thickness, it can be concluded from Fig. 13.9 that thickness has a significant influence on the absorption properties of perforated panels

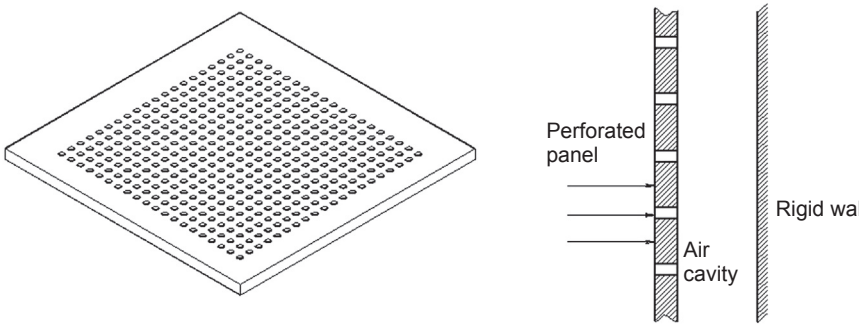

Figure 13.9 Perforated panel and perforated panel sound absorbing structure.

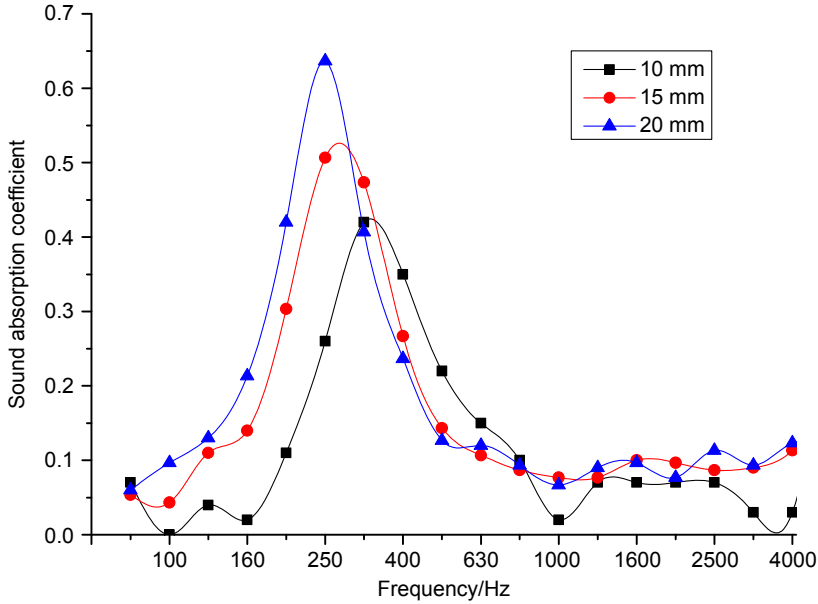

Figure 13.10 Sound absorption coefficient spectrums of different thickness-perforated panels.

below 1000 Hz. With the increase of panel thickness, the widths of absorption frequency bands are narrowed slightly and the absorption coefficient peak values are improved. In the frequency range of 50−1000 Hz the absorption coefficients of a perforated panel are first increased with frequencies, and the resonant frequency is shifted to low frequency. The thicker panel is larger than the absorption coefficient before the coefficient reaches the peak value. As the frequency goes up beyond the resonant frequency, the sound absorption coefficient is decreased. The absorption coefficients of the thinner perforated panel are greater than those of the thicker panels in 315−1000 Hz. The sound absorption coefficients of the perforated panels are no larger than 0.1 beyond 1000 Hz, which illustrate that the thickness of the panels has no influence on the absorption properties of high frequencies.

The improvement of perforated panel thickness has little influence on the sound absorption of high frequencies. So it is useless to increase the thickness for the purpose of high frequency sound absorption properties, which may also result in waste. However, it cannot satisfy the strength and rigidity requirements if the panels are too thin. Practical situations and conditions should be involved in comprehensive consideration to choose the proper thickness. The most common perforated panel thickness is 15 mm.

Pore diameter

Fig. 13.11 shows the sound absorption coefficient spectrums of perforated panels of three different pore diameters at 3, 6, and 9 mm. The thickness of perforated panels is 20 mm, the perforated rate is 3.14%, and the depth of cavity behind is 50 mm.

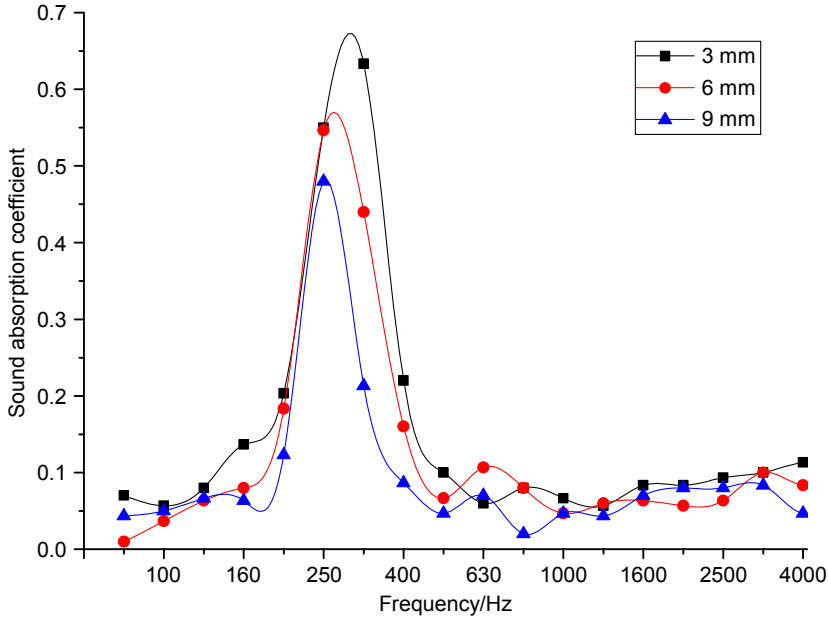

Figure 13.11 Sound absorption coefficient spectrums of perforated panels of different pore diameters.

As shown in Fig. 13.11, with the increase of pore diameters, the sound absorption frequency band is narrowed and the peak values are decreased. The resonant frequency of a perforated panel with a pore diameter of 3 mm is larger than those of 6 and 9 mm. The variability of absorption coefficients of panels of different pore diameters is small below the resonant frequency and at medium and high frequencies. The absorption coefficients near resonant frequencies vary: the smaller the pore diameters, the larger the coefficients.

Perforated rate

Fig. 13.12 shows the sound absorption coefficient spectrums of perforated panels of three different perforated rates at 7.07%, 4.91%, and 3.14%. The thickness of perforated panels is 15 mm, the pore diameter is 3 mm, and the depth of cavity behind is 50 mm.

As shown in Fig. 13.12, with the increase of perforated rate, the widths of sound absorption frequency bend are increased, the peak values are diminished, and the resonant frequencies are moved to high frequencies.

Depth of cavity behind

Fig. 13.13 shows the absorption properties of perforated panels in different installing conditions. The depths of the cavities behind panels to the rigid back are 25, 50, and 100 mm, with 15 mm thickness, 3 mm pore diameter, and 7.07% perforated rate. It can

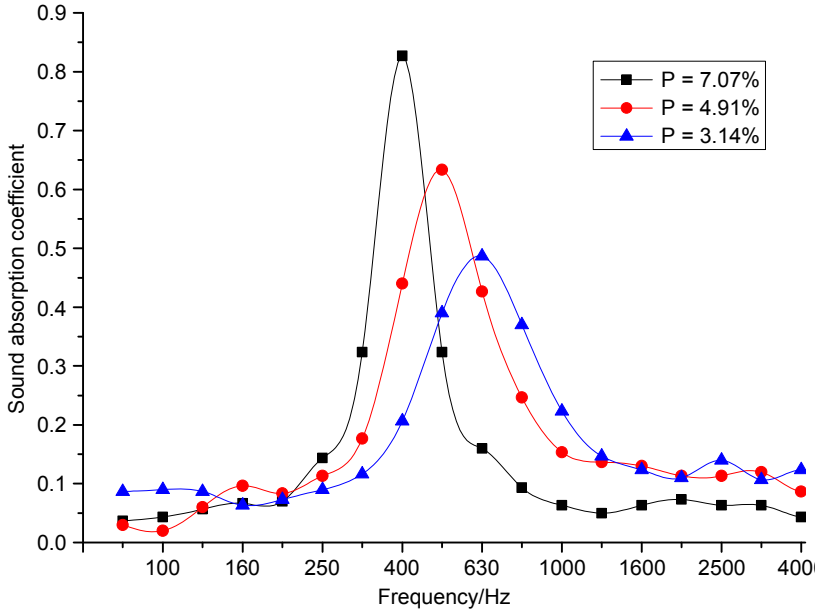

Figure 13.12 Perforated panels absorption coefficient spectrums of different perforated rates.

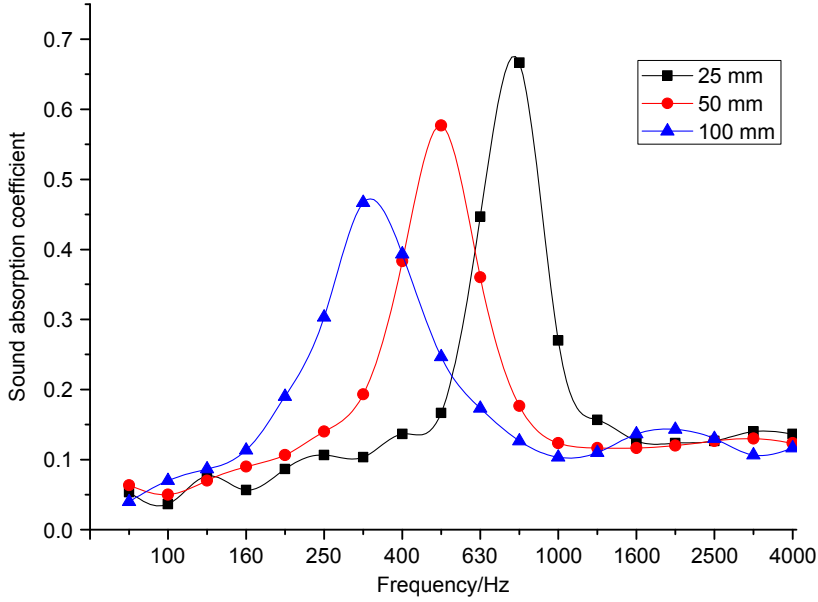

Figure 13.13 Absorption coefficient spectrums of perforated panels of different cavity depths behind.

be concluded that with the increase of the depth of cavities, the absorption coefficient peak value is decreased and the resonant frequency moves to low frequencies. The widths of the absorption frequency band remain about the same.

13.2.4 Theoretical models of porous fibrous absorption materials

Nowadays the research of porous fibrous absorption materials is mainly a combination of experimental study and theoretical analysis. The sound absorption theories of porous material are used to analyze the properties of materials and contribute to the material innovations. An accurate prediction of sound absorption characters by its structural parameters is one of the main research interests. The prediction research of porous fibrous materials is mainly based on the following three theories (Garai and Pompoli, 2005).

13.2.4.1 Empirical model theory

The empirical model theory is mainly based on Delany-Bazley's theoretical research (Delany and Bazley, 1970). Delany and Bazley developed a simple Power-law Function model to illustrate the complicated relationships between airflow resistance, frequencies, surface characteristic impedance, and propagation wave numbers. The empirical model has only one impendent variable, resistivity, and it is easy to measure. The impedance Z of a rigidly backed layer of thickness l can be calculated from the Eq. (13.13).

$$Z = Z_0 \coth \gamma l \tag{13.13}$$

where Z_0 is the surface impedance of the configuration and γ is the propagation coefficient that $\gamma = \alpha + j\beta$. The normal incidence absorption coefficient α_n is derived from the impedance and is defined by the Eq. (13.14), where ρ_0 is the density, c_0 is the velocity of sound, and $\rho_0 c_0$ is the characteristic impedance of air.

$$\alpha_n = 1 - \left|\frac{Z - \rho_0 c_0}{Z + \rho_0 c_0}\right|^2 \tag{13.14}$$

The empirical model has been widely used in porous fibrous absorption material research since the 1970s. Later the model was expanded to the research on foam porous materials (Dunn and Davern, 1986). However, the fitting correlations of the Delany-Bazley empirical model in low frequencies is poor and is largely affected by fiber alignment and processing parameters.

Miki (1990) took nonacoustic parameters like porosity and tortuosity structure factors into account and made revisions on the Delany-Bazley empirical model. The empirical models only involve airflow resistance. And it is a more numerical model that states the quantitative relations between impedance and propagation coefficients with no physical meanings.

13.2.4.2 Microstructural model theory

The microstructural theory consists in deriving the wave propagation inside individual pores from the first principles and then generalizing the results to the macroscopic scale. Attenborough, Champoux, and Stinson proposed an absorption theoretical model for complex microstructural porous materials based on five parameters including porosity, dynamic/static shape factors, tortuosity, and airflow resistance (Attenborough, 1983; Champoux and Stinson, 1992). In general, the microstructural models provide a deep physical insight of sound energy dissipation mechanisms but are inherently more complex and contain some parameters to be determined from a detailed knowledge of the material microstructure.

13.2.4.3 Phenomenological model theory

The phenomenological approach consists in replacing a fluid-saturated porous solid with an equivalent dissipative fluid, taking into account both viscous and thermal dissipation. As shown in Fig. 13.14, the bulk Young's modulus of equivalent fluid is marked as K, and the equivalent density is ρ. Two major parameters that characterize the propagation of acoustic waves in fluid are characteristic impedance $Z_c = (\rho K)^{1/2}$ and propagation constant $k = \omega(\rho/K)^{1/2}$. In other words, the phenomenological model theory is mainly focused on the Young's modulus and the density of equivalent fluid. Morse's research has demonstrated fine theoretical applicability of a phenomenological model on sound wave propagation in a porous structure with a rigid frame (Morse and Ingard, 1986). A fundamental advancement was obtained by Biot (1956), who developed a general theory of propagation of elastic waves in a fluid-saturated porous solid with an elastic frame. Allard studied the absorption charateristics of glass fiber materials with Biot's theory and found that the correlations of Biot's model were more significant than those of rigid frame equivlent model. (Allard et al., 1991).

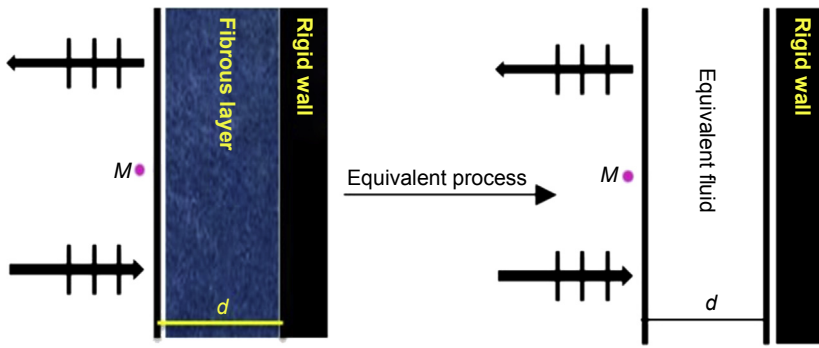

Figure 13.14 Equivalent fluid diagram of phenomenological theoretical model.

13.2.5 Developments and future trends

In general, the porosities of solid wood are about 50%. However, due to the weak interior connectivity, the sound absorption properties of untreated wood are relatively poor. Many studies show that the absorption performance of solid wood is related to the pore size and connectivity. So proper techniques like microwave explosion or hydrothermal treatment, which can enhance wood air permeability and pore sizes, can be used to improve the solid wood absorption properties.

Porous fibrous sound absorption materials are widely used to improve the indoor acoustic environment. With the improvement of the environment and health consciousness, it has become a new tendency to replace part of the synthetic fibers with natural fibers. So it is of practical significance to study the properties of natural and synthetic fiber composite materials and develop innovative acoustic products to satisfy different engineering demands.

Due to the shortage of timber resources, wooden perforated panels can make full use of branches, sawdust, and submarginal logs, which are widely used as wallboard and ceilings for their strength, decorativeness, and acoustic properties. On the basis of the wooden panel industry, it is a general trend to optimize the perforated panel structure for different applications.

With the advance of manufacturing technologies, it is convenient and feasible to process micropores, which can alter the characteristic acoustic impedance of perforated panels and improve the sound absorption properties. It is of great importance to utilize the microperforated technology on wooden panels.

In general, the valid absorption frequency band of perforated panels is too narrow to meet the demand of controlling and optimizing the acoustic conditions when the frequency range is wide. A porous absorption material with superior high frequency absorption properties can be used to combine with the perforated panel to enhance its absorption property and widen the frequency band.

13.3 Sound insulation functional composites

13.3.1 Sound insulation mechanism

13.3.1.1 Airborne sound insulation mechanism

When incident sound waves hit the material surface, the material is forced to flexural vibration due to the changes of ambient sound pressures. The bending waves propagate along the material, and due to the internal friction and viscoelastic effects, acoustic energy is converted into heat energy and dissipated. Then the acoustic waves are attenuated in transmission and air vibration of the other side is reduced. The airborne sound insulation of the material depends on three physical parameters: surface density or surface mass, stiffness, and damping. The sound reduction index is correlated with frequency, and it corresponds to the Mass Law. Moreover, there are other factors affecting the airborne sound insulation performance of a material than resonance phenomenon, coincidence effect, sound bridge, sound leak, and flanking transmission, etc.

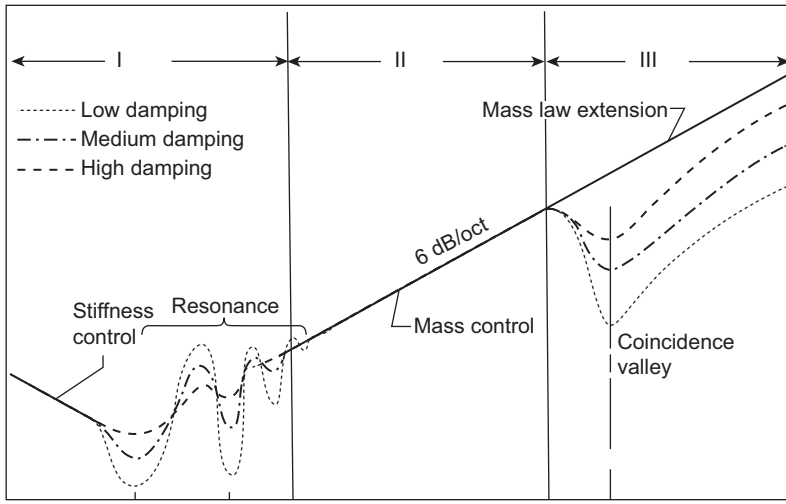

Figure 13.15 Sound insulation frequency characteristic curve of homogeneous single panel.

Fig. 13.15 shows the sound reduction index or transmission loss changes with frequencies. With the frequency increasing, the curve is divided into a stiffness-controlled region, mass-controlled region, and coincidence-controlled region.

The insulation properties of boards are mainly governed by stiffness in low frequencies, which is defined as a stiffness-controlled region. The stiffer the board is, the better the soundproof property. According to the definition, stiffness can be expressed by:

$$S = \frac{1}{12} \times \left(\frac{Eh^3}{1 - \upsilon^2} \right) \tag{13.15}$$

where, E, h, υ are Young's modulus, thickness, and Poisson's ratio, respectively. It proves that the thickness and Young's modulus have a positive relationship with stiffness.

The resonant frequency of single thin board is within the scope of hearing. Resonance occurs when the frequency of incident wave and the board inherent frequency are equal. Resonance phenomenon will reduce the sound insulation properties of boards in low frequency. The resonance amplitude is affected by damping factor: the larger the damping factor is, the less resonance amplitude. The resonant frequency of a thin board is related to size, thickness, Young's modulus, and surface density, which can be calculated by the following equation:

$$f_{\mathrm{r}} = \frac{\pi}{2} \sqrt{\frac{B}{M} \left(\frac{n^2}{l_{\mathrm{x}}^2} + \frac{m^2}{l_{\mathrm{y}}^2} \right)} \tag{13.16}$$

where, B is the stiffness of the board (N·m), $B = \frac{1}{12}Eh^3$, E is Young's modulus (Pa), h is thickness (m), and M is surface density (kg/m^2). It should be noted that the mounting method has a significant influence on the impact of resonance on transmission loss values (Satoh et al., 2014).

With the frequency increase, the sound reduction loss of the board is increased linearly. This frequency range is called the mass controlled region. Assuming that the board is infinite and homogenous, the sound reduction index of a random incident can be expressed by:

$$R = 20\lg Mf - 48 \tag{13.17}$$

where, M is surface density (kg/m^2) and f is incident wave frequency. It can be concluded from the Eq. (13.15) that in the mass controlled region the sound reduction index of the board is related to surface density and frequency. There is an increase in sound reduction index of about 6 dB for each doubling of surface mass or frequency in this region. This is often known as Mass Law.

The materials are induced to vibrate as sound waves are incidenting on the surface. A coincidence phenomenon occurs when the wavelengths of longitudinal sound waves in air and bending waves in a plate are equal. The frequency range is called the coincidence effect-controlled region, and the frequency is called critical frequency, which is determined by the following equation.

$$f_c = \frac{C^2}{2\pi}\sqrt{\frac{12m(1-\sigma)}{Eh^3}} \tag{13.18}$$

where, m is surface density, σ is Poisson's ratio, E is Young's modulus, and h is panel thickness. At the lowest coincidence frequency, or critical frequency, a plate constitutes virtually no obstacle for airborne sound hitting its surface and sound reduction is minimal. Although coincidence is a narrow-band phenomenon, it is detrimental to the sound reduction index if critical frequency occurs within the building acoustical frequency range.

13.3.1.2 Impact sound insulation mechanism

Vibration occurs when the floors upstairs are impacted. The vibration propagates along the structure and radiates downstairs, causing noise. As the impact energy is large and seldom is attenuated in transmission, the vibration is widely spread in a continuous structure. Wood is widely known as a viscoelastic material. Wooden floors used on upstairs bases can decrease the impact energy and weaken the vibration of floors. Theoretically the impact sound insulation improvement ΔL_n, after covering wooden floors, can be expressed by:

$$\Delta L_n = 40\lg\frac{f}{f_R} \tag{13.19}$$

where, f is frequency, f_R is the inherent frequency of wooden floors, $f_R = \frac{1}{2\pi}\sqrt{\frac{D}{M}}$, D is stiffness of floors, and M is the mass of tapping hummer and is 500 g in ISO standard. It is concluded from Eq. (13.17) that attenuation of floors impacting sound can be improved by increasing the inherent frequency. For this purpose, it can be derived from decreasing the stiffness or improving the elasticity.

Pritz T and Kyoung-Woo Kim have studied the influence factors of floor impact sound attenuation by testing different covering materials (felt, cork, solid PVC, and PVC foams). It is concluded that cover materials with larger elastic coefficients have better impact sound insulation properties (Pritz, 1996; Kim et al., 2009).

13.3.2 Sound insulation measurement

13.3.2.1 Airborne sound insulation measurement

Reverberation room measurement

The reverberation room method can be used to study the practical characteristics of acoustic materials in the later lab research of the application subject. As shown in Fig. 13.16, a source room and a receiving room are separated by a test element. According to the measured parameters the measurement approach can be divided into the sound pressure method and the sound intensity method. The sound pressure method is established under the assumption that two rooms are perfect diffuse sound fields and any indirect transmission can be ignored. The sound pressure levels in the source and receiving rooms and the absorption area in the receiving room will be measured. Sound reduction index is given by:

$$R = 10\lg\frac{1}{\tau} = 10\lg\frac{W_1}{W_2} = L_{P_1} - L_{P_2} + 10\lg\frac{S}{A} \tag{13.20}$$

where, W_1 and W_2 are sound power of source room and receiving room and L_{P_1} and L_{P_2} are the temporal and spatial average sound pressure levels in the source and receiving rooms, respectively. S is the area of the test element and A is the absorption area in the receiving room, which can be determined by the volume and reverberation

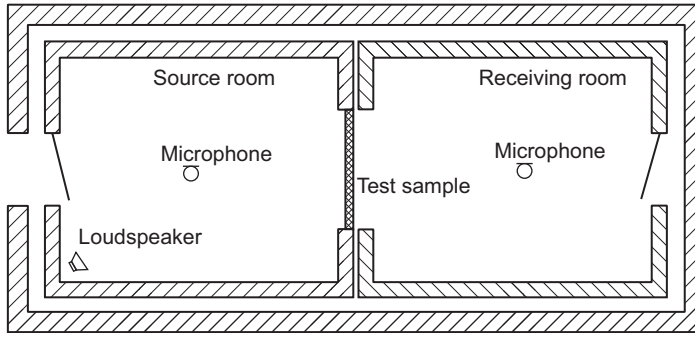

Figure 13.16 The diagram of airborne sound insulation measurement.

time of a room. Eq. (13.18) is the theoretical foundation of the reverberation room method. The method is stated in the standard ISO 140-3 and national standard GB/T 19889.3 and the relevant standards GB/T 19889 part 4, 5, and 10. This method is called the traditional sound pressure method.

With the development of computer and digital signal techniques, the acoustic measurement system based on computers is applied more and more widely. The impulse response measurements have been applied to measuring sound insulation. Acoustic fields are emitted by MLS or e-sweep signals, and the impulse responses in the source room and receiving room are measured to calculate sound pressure levels. This method is called the impulse sound pressure method. The impulse sound pressure method is described in ISO 18233-2006.

Compared with the traditional sound pressure method, the impulse sound pressure method has a higher signal-noise ratio. This method can determine presumably the flanking transmission path with the impulse sequence. The impulse method has the same shortcoming of low frequency errors like the traditional method.

Sound insulation properties of building elements can also be measured in the sound intensity method. Sound intensity is a vector describing the energy flux in the sound field and can be measured in P−U method and P−P method. Compared with the sound pressure method, the sound intensity method has higher signal-noise ratio, and the error in low frequencies is less. It can also suppress flanking transmission and determine the sound leakage path (Cai et al., 2011). This method is illustrated in standard ISO 15186 part 1, 2, and 3 and Chinese standard GB/T 31004.1-2014.

Sonic tubes measurement

In general, the sound source radiates diverging spherical wave in infinite space. When the acoustic waves are limited in a sonic tube, the transmission is affected by many factors such as tube diameter, shape, tube wall materials, and sound source conditions.

Fig. 13.17 shows the schematic diagram of a 4-channel impedance tube for sound insulation measurement. The equipment consists of sound source, front standing wave tube, back standing wave tube, and bottom absorption layer. The loudspeaker generates normal incident plant waves of different frequencies. The test sample is placed in the middle of standing wave tubes. Due to the wave reflection on the surface of a sample and the bottom absorption layer, it forms a standing wave field in the front

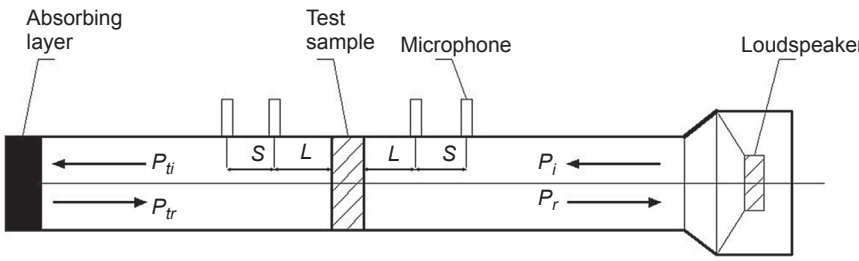

Figure 13.17 Schematic diagram of 4-channel impedance tube.

tube (incident field) and back tube (transmission field). The method of standing wave separation is used to separate the incident wave, transmitted wave, and reflected wave with two microphones. In order to simplify the analysis, the second reflection and transmission by sample and bottom layer are out of consideration. The incident and reflected sound pressure in the incident field, as well as transmitted pressure and bottom layer, reflected pressure in the transmission field can be calculated with the measured results by four microphones. The sound pressure transmitted coefficient t_p is obtained. The transmission loss is the logarithm of t_p (Zhang et al., 2010).

$$\mathrm{TL} = -20 \times \lg|t_p| \tag{13.21}$$

Compared with the reverberation room method, the measurement in sonic tubes is more convenient and low cost, which is suitable for the production line. The test results derived from the reverberation room, the transmission loss of random incidence, and the influence of edging conditions can be overlooked. At the same time, the results of sonic tubes are the transmission loss of normal incidence. And the edging conditions cannot be ignored. So there are differences between the measurement results of the two methods. In terms of wooden materials, the modal frequencies vary considerably under the influence of edging conditions of different sizes. Since the transmitting attenuation is decreased at resonant frequencies, the sound reduction index in low frequency differs greatly. And the sound reduction index in high frequency has little relationship with edging conditions, so that the difference of measured results is little.

13.3.2.2 Impact sound insulation measurement

The measurement methods of impact sound insulation properties are based on the standard ISO 717-2 and GB/T 19889.6-2005. The laboratory consists of two adjacent rooms, and there is structural isolation of certain thickness between the emitting room upstairs and the receiving room downstairs to avoid the measurement deviation caused by flanking transmission. There is a reserved hole for assembling a test sample. The standard area of the hole is 10 m^2, and the length of the short side is no less than 2.3 m. A standard tapping machine is used to impact the test floors. The sound pressure levels in 16 center frequencies of one-third octave frequency bands and the reverberation time are measured in the receiving room. According to the standard, normalized impact sound pressure level spectrum is obtained, and the normalized weighted levels can also be derived.

13.3.3 Sound insulation of wooden materials

13.3.3.1 Airborne sound insulation properties of wood and wood-based composites

Airborne sound insulation properties of wood and wooden panels

The timber or wooden panels of certain thicknesses have sound insulation properties. The sound insulation properties are poor due to the small surface density and porous

structure. For instance the weighted sound insulation loss of 2 mm steel panel equals that of 35 mm particleboard and is larger than that of 40 mm plywood. Table 13.1 shows the frequency characterized STLs of common wooden panels. It is concluded that for a certain material the surface density is increased with the thickness improved. And the average STL is improved, which confirms to Mass Law. The comparison of different material STLs shows that the average STL is not entirely increased with surface density. This is because there are some other factors that influence the STLs despite Mass Law.

Fig. 13.18 shows sound insulation properties of wooden panels (Liu et al., 2007). It shows that the insulation frequency spectrums of different wooden panels are similar in that STL is increased linearly with frequencies, and it accords with Mass Law. Moreover, there is a curve valley at high frequencies, which is called coincidence valley.

At low frequencies, the STL values depend on stiffness and resonance of the boards. The boards tend to bend as the sound waves incident on the surface. And the stiffer the board, the more resistant it is for bending. The stiffness of the boards is related to thickness, Young's modulus, and Poisson's ratio. The stiffness can be improved by increasing the thickness or Young's modulus.

Resonance has a significant influence on the sound insulation properties. In terms of building elements like reinforced concrete walls and solid brick walls, the thickness of walls is large enough that resonant frequencies are below 100 Hz and can be ignored. The resonant frequencies of timber or wooden panels are in the range of human hearing. Resonance phenomenon occurs when the frequency of incidence sound waves equals the inherent frequency and the sound insulation property is weakened. The negative effect of resonance can be improved by enhancing the damping or laminating with other materials.

Coincidence effect has a remarkable influence on the sound insulation properties of thin panels. Table 13.2 shows the critical frequencies of some solid wood and wooden panels. Note that for wood panels of 20−30 mm thickness, the critical frequency is in the low frequency range (<1000 Hz). It can be used to reduce the influence of coincidence effect by improving damping properties, improving the thickness, altering the stiffness, or adding rib-stiffeners (Bucur, 2006).

Nowadays the research of wooden material insulation properties is mainly concentrated on the rating and application of building elements. The Finnish Institute of Occupational Health has studied insulation properties of 27 kinds of common construction boards, including wooden panels in the reverberation room method. Physical parameters like damping factor, mass density, and Young's modulus are also tested to supply data support for architectural acoustic design and research (Larm et al., 2006).

Airborne sound insulation properties of wood polymer composites

Timber and wooden panels are porous materials due to their low surface densities. So they are seldom used alone as sound insulation functional materials. Viscoelastic polymer materials own chemical structures of macromolecular chains and yield excellent vibration damping effects. The mechanical properties of most of the polymers are

Table 13.1 Sound transmission loss of common wooden panels varied with frequencies (Liu et al., 2000)

Materials	Thickness/mm	Surface density/(kg/m^2)	STL/dB						
			125 Hz	250 Hz	500 Hz	1000 Hz	2000 Hz	4000 Hz	Average STL
Plywood	6	3	11	13	16	21	25	23	18.2
	12	8	18	20	24	24	25	30	23.5
	40	24	24	25	27	30	38	43	31.2
Particleboard	6	4.5	18	18	22	27	32	31	24.7
	20	13	24	27	26	27	24	33	26.8
	35	17	21	23	27	28	24	29	25.3
Light fiberboard	12	3.8	13	12	17	23	29	32	21
Hardboard	5	5.1	21	21	23	27	33	36	26.8

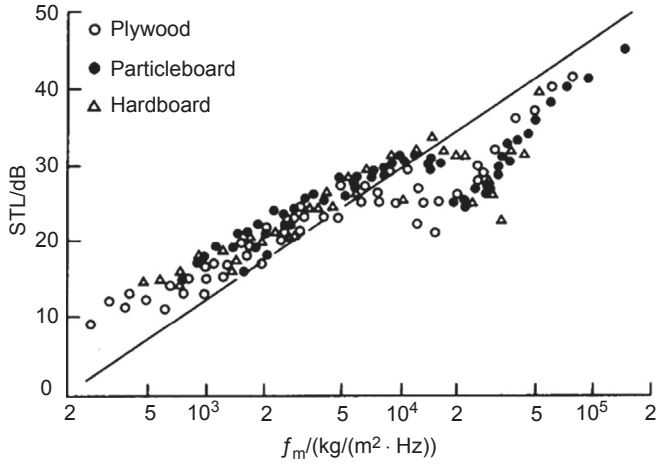

Figure 13.18 Sound insulation frequency characteristic curves of a wood panel (Liu et al., 2007).

Table 13.2 Critical frequency of wood and wooden panels (Bucur, 2006)

Materials	Density (g/cm^3)	Critical frequency (Hz)			
Thickness		2 mm	5 mm	20 mm	30 mm
Fir	0.50	–	–	500	330
Beech	0.75	–	2400	600	400
Plywood	0.55	7000	2800	700	470
Particleboard	0.66	–	4300	1090	725

poor, and they cannot be used as construction and decoration materials (Wang et al., 2011). The composite of wooden materials and polymers has better physical and mechanical properties, and the surface density and insulation properties are also improved.

A wood rubber composite panel is an innovative material that mixes wood elements, such as chips and fibers, with waste tire rubber particles and hot presses them into the board. The composite material has excellent vibration damping property, and it is a complex vibration system consisting of many single free oscillating systems when impacted by sound waves. Both wood and rubber particles are viscoelastic and polymeric materials. When they are subjected to the alternating stresses from vibration and sound waves, their forms would become highly and elastically deformed due to the movement of rubber molecule chains, which is characterized by the remarkable lag of deformation behind the stress change. The movement of lagged deformation works by overcoming great resistance, converting into thermal energy, and dissipating into the

environment. Based on this theory, the composites of wood and rubber particles have a good soundproof property.

The researches of scholars from Beijing Forestry University are presented in this section to illustrate the insulation properties of wood rubber composite materials. The sound insulation properties of wood rubber composite materials are related to factors of wood/rubber ratio, rubber size, and the resin ingredients (the ratio of UF to PMDI) (Zhao et al., 2010).

Fig. 13.19 illustrates a sound transmission loss comparison of four different wood-based materials. The transmission loss value increases with increasing sound frequency and reaches the maximum for each type at 1250 Hz. The particleboard performs the worst in sound insulation. It is expected that the wooden chips are randomly distributed in the board, and there are many microvoids between chips. Sound can transmit through air particle vibrations to the other side, thus the transmission loss of the particleboard is poor. The core layer of the wooden engineering floor is high density fiberboard. And there is a wear resistant layer of Al_2O_3 in the surface coating. The density of engineering floors is about 800 g/cm^3, which is higher that about 650 g/cm^3 of particleboard. Based on the Mass Law, the sound insulation property of wooden engineering floors is better than particleboards. It also can be concluded from the figure that the sound transmission loss of wood rubber composites is higher than particleboard and engineering floors. And the larger the rubber ratio, the higher the transmission loss values.

Fig. 13.20 illustrates that rubber crumb diameter has a great influence on the sound insulation of the composite. The insulation property is improved with increasing rubber crumb diameter. This phenomenon is probably attributed to having a great impediment to sound transmission of the larger rubber crumbs in the composite, as compared to the smaller rubber crumbs. It is expected that the impact of rubber crumb diameter on insulation property depends on the rubber content in the composites.

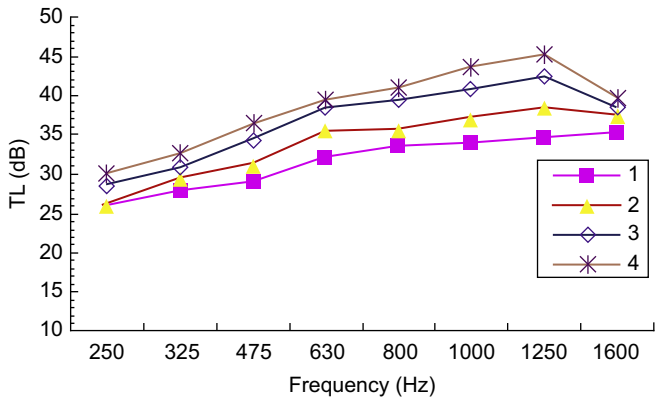

Figure 13.19 Sound transmission loss coefficients of test panels as a function of sound wave frequency: (1) wooden particleboard, (2) wooden engineering floorings, (3) wood rubber composite panel (wood/rubber ratio 60:40), and (4) wood rubber composite panel (wood/rubber ratio 50:50) (Zhao et al., 2010).

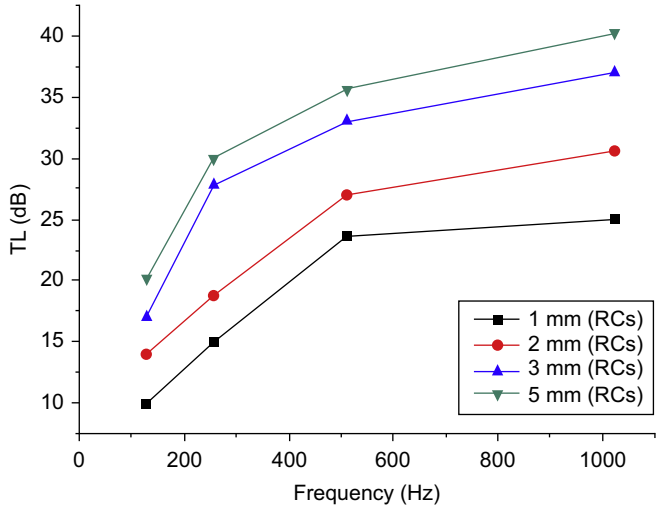

Figure 13.20 Influence of waste tire recycled rubber crumbs (RCs)size on sound transmission loss coefficients of a wood/rubber (60:40) composite as a function of sound wave frequency (Zhao et al., 2010).

As shown in Fig. 13.21, transmission loss values increase with an increase of PMDI (polymethylene polyphenyl polyisocyanate) dosage in the composites. This is because increasing the amount of PMDI will result in the extent of the surface of rubber crumbs coated by PMDI and improve the bond quality between wood particles and rubber crumbs, which in turn will be attributed to the improved viscoelastic property of the composites. PMDI resin may also improve the dynamic and mechanic properties of

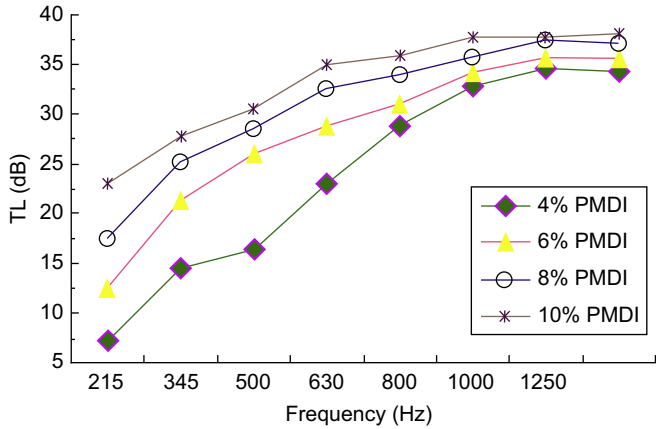

Figure 13.21 Influence of PMDI content on the sound transmission loss coefficients of wood/rubber (60:40) composites as a function of sound wave frequency (the rubber crumb average diameter is 5 mm) (Zhao et al., 2010).

rubber crumbs, so the composite panel will attenuate more acoustic energy due to the increased inner friction coefficient. However, the influence of PMDI dosage becomes less significant with frequency increasing, especially beyond 1000 Hz.

Wood plastic composites (WPCs) are composite materials made of wood fiber/wood flour and thermoplastics including PE, PP, PVC, etc. In addition to wood fiber and plastic, WPCs can also contain other lingo-cellulosic and/or inorganic fillers. WPCs do not corrode and are highly resistant to rot and decay. They are often considered a sustainable material because they can be made using recycled plastics and the waste products of the wood industry. The composites of wood and plastic have better sound insulation properties since the surface density and stiffness are improved. Joan Pere López developed composites that are prepared from polypropylene (PP) reinforced with mechanical pulp fibers from softwood (López et al., 2012). Acoustic properties of the composites from mechanical pulp and PP have been investigated and compared to fiberglass composites and gypsum plasterboards. The results showed that the composites reinforced by mechanical pulp or glass fiber have better soundproof property than gypsum plasterboards. And with the increase of fibers, the critical frequency of the composites is decreased and transmission loss values show little change.

The transmission loss of WPCs can be improved by adding inorganic fillers. Some scholars filled wood flour high-density polyethylene (HDPE) composites with precipitated $CaCO_3$ (Li et al., 2013) or nanoclay (Kim et al., 2015) and investigated the properties of the composites. It concluded that inorganic fillers can increase the composite surface density and stiffness, thus sound insulation property is improved. Fig. 13.22 shows a simplified internal structural model of acoustic wave propagation in the composites with inorganic fillers. The matrix represents the plastic component of WPC. The fillers include wood and inorganic particles, which are dispersed in the

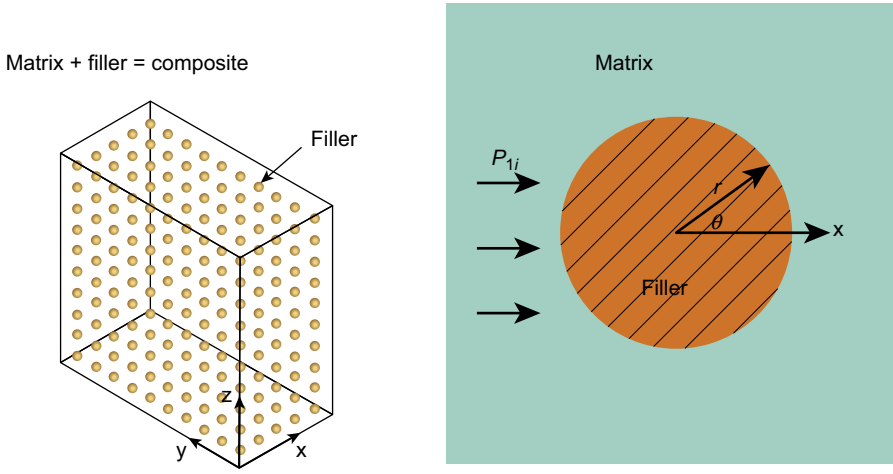

Figure 13.22 A simplified interior structure for the inorganic particle-filled wood plastic composites and sound scattering field around a filler element (Li et al., 2013).

matrix. It is assumed that the composite is homogeneous, and inorganic fillers are distributed uniformly in the matrix. A single filler particle and matrix is selected for propagation analysis. When a normal incident plane wave reaches the surface of particles, partial sound waves are penetrated through the particles and partial waves are scattered, which increase the propagation path of waves and more internal friction and energy attenuation (Liang et al., 1999). The sound transmission loss of inorganic particle-filled WPCs is affected by filler ratio and particle size. The more fillers, the larger energy attenuated. WPCs with larger filler particle size yield better soundproof property in high frequency.

13.3.3.2 *Impact sound insulation properties of wood and wood-based composites*

Cork floor is the earliest wooden material used for the sound insulation function. Cork is the bark of cork oak. The cork cells are similar to closed hexagonal prisms, which are filled with compressible air. Besides, there is suberin in cell walls and intercellular space, which makes the cell a sealed element (Gibson et al., 1981). The closed microstructure gives cork excellent elasticity and thermal and acoustic insulation properties. Panels made from cork have a good impact sound insulation property. However, the development of cork insulation material is limited by a finite source.

The impact sound pressure levels of particleboard and concrete floors are shown in Fig. 13.23. The peak value of impact sound pressure level varies little when the thickness of particleboard is altered. The peak value moves toward high frequencies with the thickness increasing. The variation of concrete floors impacting sound performance is similar to that of particleboard, in that it has little effect on insulation property improvements when the thickness is increased to a certain extent (Liu et al., 2007).

The impact sound insulation properties vary with wooden material species. The properties of wooden panels are ranked in descending order: light particleboard > light fiberboard > common particleboard > MDF > plywood. However, on

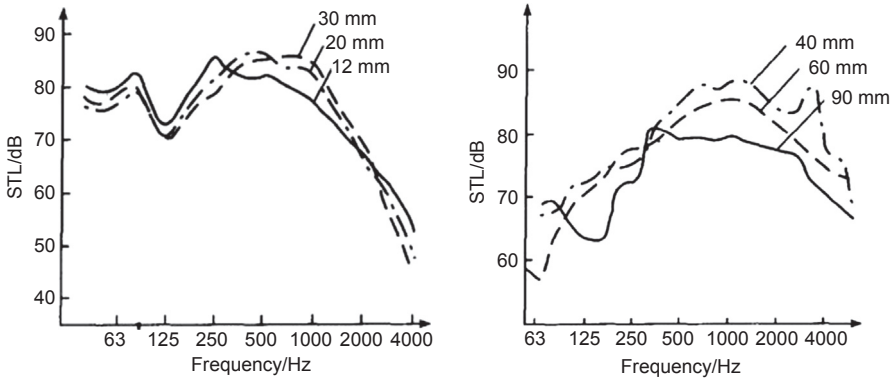

Figure 13.23 Impact sound insulation frequency spectra of particleboard floors and concrete floors (Liu et al., 2007).

the whole, wooden materials perform badly in impact sound insulation without any treatment. It can be improved by some modification and treatments.

Researchers in the wood functional materials lab of the Chinese Academy of Forestry proposed a wood rubber composite material (WRC) made from wood particles and rubber crumbs with adhesive PMDI. The influences of different manufacturing factors on impact sound insulation properties were also investigated (Sun, 2009). It is concluded that wood/rubber ratio in weight has the most significant influence on the impact sound, followed by the wood morphology, and the effect of size of rubber crumbs is least of them all. Fig. 13.24 presents the comparison of impact sound and impact sound insulation of MDF, plywood, and WRC. It shows the impact sound and insulations of MDF and plywood are similar. The insulation property of MDF is slightly better than plywood. And the impact sound insulation property of WRC is much better than both of them.

Eq. (13.17) shows that the impact sound insulation improvement of floors is corresponding to the inherent frequency of materials. The inherent frequency and damping ratio can be measured in a wooden thin panel elastic modulus method by cantilever deflection. Compared with plywood and MDF, WRC has lower inherent frequencies and weaker abilities to resist deformation under impact loadings, which means smaller bending rigidity and better elasticity. Meanwhile, WRC is more likely to resonate practically because of low modal inherent frequencies of each order in the low frequency range. The damping effects of rubber crumbs are fully exerted.

The damping factor of WRC is larger than those of MDF and plywood, which can fasten vibration attenuation. Acoustic energy is greatly dissipated during transmission so that acoustic radiation of the structure is suppressed. In the perspective of energy conversion, the structure with the larger damping factor can convert the vibration

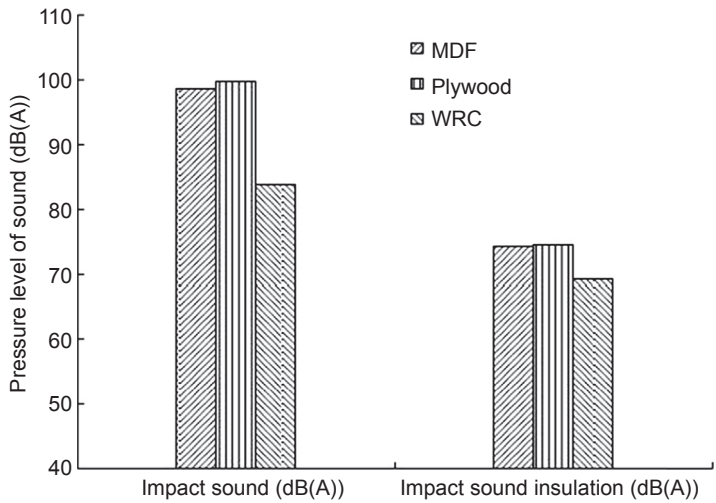

Figure 13.24 Impact sound and impact sound insulation pressure levels of MDF, plywood, and WRC.

energy into thermal energy and dissipate it more efficiently. In this way, structural acoustic radiated energy is also reduced. In a word, compared with MDF and plywood, the WRC gets better vibration reduction effect so that sound stimulated by impulse load is reduced efficiently.

13.3.4 Sound insulation applications of wooden materials

Nowadays, wooden material is widely used in human settlements. It is of vital significance for improving the resistant acoustic environment to improve the sound insulation properties of wooden materials. The acoustic insulation functional wooden elements in construction are wooden partitions, timber doors, and wooden floors.

13.3.4.1 Airborne sound insulation properties of wooden partitions and timber doors

The insulation property of a single wallboard is mainly governed by Mass Law, and it can be enhanced by improving the weight and thickness. However, the self-weight of the building element will be largely improved and it will occupy more space. In order to yield better soundproof property, especially for lightweight wallboards, possible solutions are limited to double-leaf partitions, consisting of plates over studding and an intervening cavity. As there is an elastic air cavity between two plates, the double-leaf insulation structure can be seen as a vibration system made of "mass-spring-mass." The incident waves are reflected twice and absorbed twice. The acoustic energy transmitted through the second panel is largely attenuated, and the sound insulation property is greatly enhanced. The double-leaf structure is also used in wooden insulation doors.

The sound insulation property of a wooden partition is correlated with factors such as surface density, stud dimensions and space, volume weight and thickness of filled absorption material, and sealing. Studies have shown that selecting the optimal face plate has a great effect on the insulation property in double-leaf structure design. The face plate is expected to have high critical frequency to avoid coincidence effects. Nevertheless, in some cases, the compound of a high critical frequency thin panel and a large surface mass panel can attenuate more vibration energy. Studs in wooden partitions play a role of supporting the facing plates, supplying stiffness and lateral shear resistance effects. The dimensions of studs determine the air thickness in the structure. Sound reduction is improved by increasing air thickness. However, as the cross area of studs increase, the rigidity of walls is improved, and the stiffness is increased in the same way. Transmission loss in a stiffness-controlled region is largely affected and improved in 100−500 Hz (Remes, 2009). The space between wall studs determines amounts of studs, which play a role of sound bridges in sound wave transmission. The sound absorption property of the air cavity is weakened necessarily with the increasing amount of studs, and the sound reduction index is also decreased. When the space of wall studs is increased, the resonant frequency moves toward low frequency. Usually the resonant frequency is projected below 100 Hz to avoid the influence of resonance effect. Under the consideration of the safety of the structure,

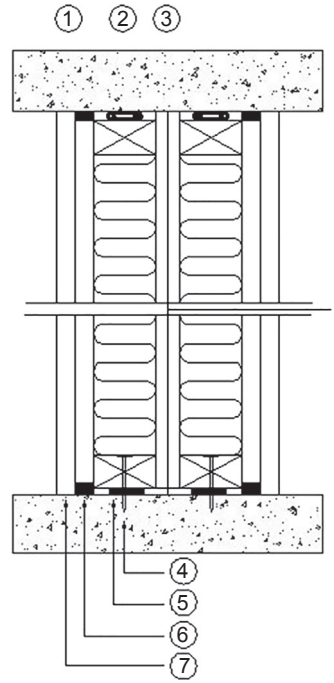

Figure 13.25 A typical structure of sound insulation partition (Remes, 2009): (1) two layers of chipboard or medium density fiberboard (screw fastening); (2) timber studding and mineral wool; (3) air space (empty, no connection between studs); (4) attachment with screws to floor slab; (5) sealing to floor slab with EPDM rubber band; (6) sealing of the inner plate to the floor slab with sealing mastic; and (7) outer plate layer extended to floor level.

it is suggested that the space between studs can be 400 or 600 mm, and the priority is given to 600 mm. Fig. 13.25 shows a typical sound insulation partition structure.

Fig. 13.26 shows a typical structure of sound insulation timber door. A porous, fibrous material filled between two wallboards or facing plates of doors cannot only block thermal conduction but also absorb acoustic energy, which has a positive effect on sound reduction. When sound waves propagate through facing plates and transmit to the air layer, the porous absorption material hung or put in the air cavity can attenuate partial acoustic energy and improve transmission loss of the structure.

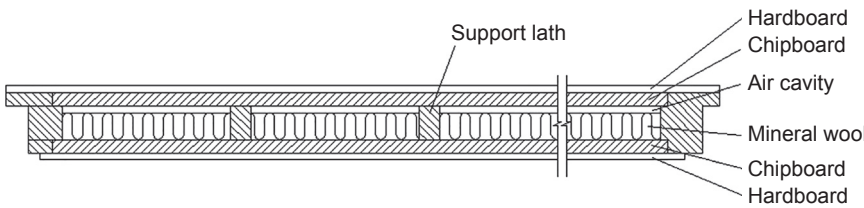

Figure 13.26 A typical structure of sound insulation timber door.

The additional sound reduction index of filled porous absorption material is commonly 5 dB. Taking the effects of volume weight of absorption material into account (it has occupied part of air layer thickness, which can also absorb sound energy), the practical sound reduction index is improved by 2−4 dB (Zhou, 2006).

Doors are usually the weakest sound insulating elements between rooms and therefore need careful acoustic design. Examination of the sound insulation of doors presupposes two separate transmission paths to be considered: the structural transmission through the door leaf and the leak transmission through the slits. Most doors are designed nowadays as double-panel structures with sound absorbing and fire-resistant materials in the air cavity to improve the mechanical and sound insulation properties of the door leaf. According to the research by Finnish scholars, the reduction of interpanel connections (glue and support laths) is the key point for structural improvements. The compromise between good stiffness and good insulation could be found by replacing laths with elastic contacts or honeycomb supports. Sound absorption materials filled in the core layer can enhance the soundproofing of the structure. But above all, sound leak has the most significant influence on the sound insulation property of doors. It can be improved by about 6 dB by slit-sealing improvements (Hongisto et al., 2000). The airborne sound insulation properties of doors are rated according to the standard GB/T 8485-2008.

13.3.4.2 Impact sound insulation properties of wooden floors

Wooden floors are often installed on the floor base to insulate impact sound. Usually there is a mat layer under wooden floors for waterproofing and damping effects. The impact sound insulation property of wooden floors depends on installing methods and mat layer. According to China engineering construction standard CECS 191-2005 "Technical specification for wood floor coverings," there are some common covering approaches: keel pavement, floating pavement, gluing direction pavement, etc. Scholars from the state key laboratory of subtropical building science, South China University of Technology, have researched the effects of different covering methods on the impact sound improvement of wooden engineering floors of 18 mm (Chen, 2013). As shown in Fig. 13.27, A-1 is wooden keen pavement, A-2 is direct pavement, and A-3 and A-4 are floating pavement. A-3 is paved with a moisture-proof isolation mat and A-4 is paved with damping mat. The measured results are illustrated in Figs. 13.28 and 13.29.

As shown in Fig. 13.29, four covering structures share a similar tendency in the spectrum that the impact sound insulation improvement performs well in medium and high frequencies, and the improvement is poor in low frequency. Wooden keen pavement has the highest improvement value in medium frequency (200−2000 Hz). In high frequency, the damping mat yields the best impact sound insulation property. From the installation perspective, wooden keen as mat layer is an option that both cost-saving and insulating impact sound efficiently.

Compared with paving directly on the floor base, an additional mat layer under wooden floors has a significant improvement on the attenuation of impact sound. There are many mat layer structures, for instance, mat panels, wooden keens, and damping

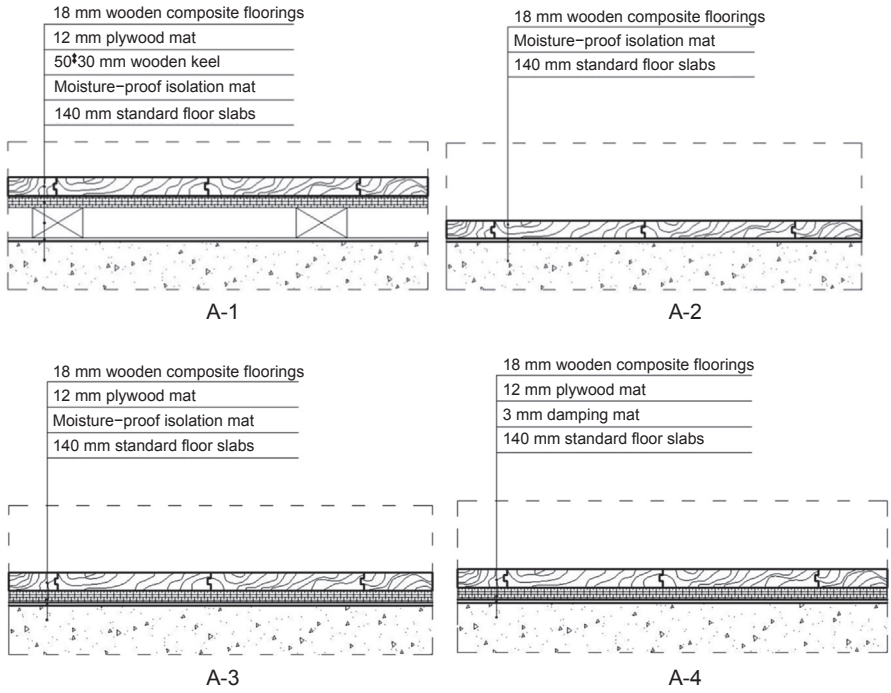

Figure 13.27 Wooden floors with different structural layers.

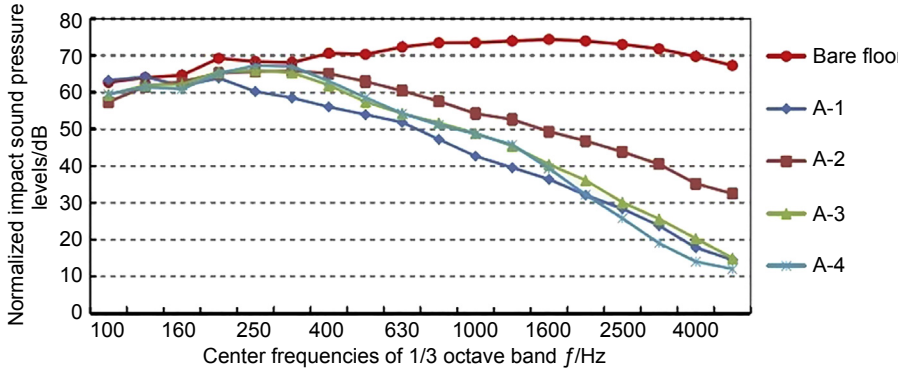

Figure 13.28 Normalized impact sound pressure levels of wooden engineering floors by different installing approaches (Chen, 2013).

mats. Research shows that altering keen space has little effect on insulation property. With the thickness of keens increasing, the floor's impact sound improvement is increased gradually. And the increasing tendency is descending: when the thickness of keens is doubled, the improvement value is increased by 2 dB, and it is increased by 3 dB when the thickness is tripled. Plywood as a mat layer has little effect on impact

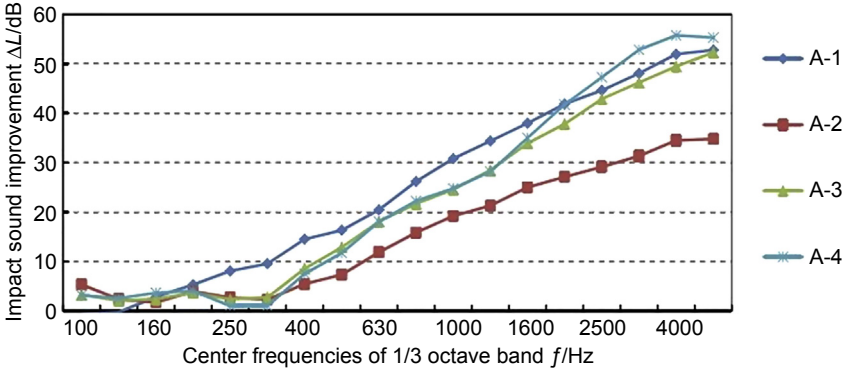

Figure 13.29 Impact sound improvements of wooden engineering floors by different installing approaches (Chen, 2013).

sound improvement, while a damping mat and glass fiber between keens can improve impact sound attenuation effectively.

The ratings of floors impacting sound insulation properties is based on the standard ISO 717-2:1996 and GB/T 50121:2005.

13.3.5 Developments and future trends

Wooden materials are widely used as construction and decoration materials. However, due to the porous structure and low surface density, the sound insulation properties of wood and wooden panels are poor. Nowadays the research of wooden material insulation properties is mainly involved in two aspects. The first is double-layer structures or laminated structures in building elements with good sound insulation properties, as well as mechanical properties and enhancing its insulation properties by structural optimization. The second includes improving the surface density and mechanical properties by compositing wooden elements with polymers and enduring its acoustic properties. Besides, many construction acoustic scholars have made some theoretical researches on the properties of wooden partitions and timber doors.

According to different transmission paths of vibration and sound, the approaches to control noise also differs. They all can be attenuated by absorption or insulation materials. In architectural acoustic design, a double-leaf structure is often used to block acoustic wave transmission. In vehicle and mechanic design, viscoelastic damping materials and compounded damping structures are used to avoid solid-borne noise. It has been researched that viscoelastic damping structures yield good insulation properties in an airborne acoustic field (Zheng and Chen, 1996). The attenuation of structural vibration is closely associated with airborne sound insulation properties. There have been many experimental and theoretical researches on the composites of metal and polymer damping materials utilizing the noise reduction of shipping and vehicles. It of great importance to develop a new airborne sound insulation functional construction material made from wood and viscoelastic damping material.

The impact sound can be attenuated effectively by covering wooden floors. Currently the research of wooden floors impacting sound insulation properties is mainly focused on the influence of different assemblies. Few works are involved with the effects of different physical and mechanical properties of wooden floors. Research on the relationships between different physical and mechanical characteristics of wooden floors and impact sound insulation properties has a great significance on the improvement of wooden material acoustic properties.

References

Allard, J.F., Depollier, C., Guignouard, P., Rebillard, P., 1991. Effect of a resonance of the frame on the surface impedance of glass wool of high density and stiffness. Journal of the Acoustical Society of America 89 (3), 999−1001.

Attenborough, K., 1983. Acoustical characteristics of rigid fibrous absorbents and granular materials. The Journal of the Acoustical Society of America 73 (3), 785−799.

Biot, M.A., 1956. Theory of propagation of elastic waves in a fluid-saturated porous solid. I. Low-frequency range. Journal of the Acoustical Society of America 28 (2), 168.

Bucur, V., 2006. Acoustics of Wood, second ed. Springer-Verlag Berlin Heidelberg, New York.

Cai, Y.S., Zhao, Y.Z., Wu, S.X., 2011. The summary of techniques on the airborne sound insulation measurement. In: Electric Technology and Civil Engineering (ICETCE), International Conference on. IEEE, pp. 1785−1788.

Champoux, Y., Stinson, M.R., 1992. On acoustical models for sound propagation in rigid frame porous materials and the influence of shape factors. The Journal of the Acoustical Society of America 92 (2), 1120−1131.

Chen, K.A., Zeng, X.Y., Li, H.Y., 2005. Acoustical Measurement. Science Press, Beijing (in Chinese).

Chen, X., 2013. Laboratory Measurements of the Reduction of Transmitted Impact Noise by Wooden Floors. Sound China University of Technology (in Chinese).

Chung, J.Y., Blaser, D.A., 1980. Transfer function method of measuring acoustic intensity in a duct system with flow. Journal of the Acoustical Society of America 68 (6), 1570−1577.

Delany, M.E., Bazley, E.N., 1970. Acoustical properties of fibrous absorbent materials. Applied Acoustics 3 (7), 105−116.

Dunn, I.P., Davern, W.A., 1986. Calculation of acoustic impedance of multi-layer absorbers. Applied Acoustics 19 (5), 321−334.

Garai, M., Pompoli, F., 2005. A simple empirical model of polyester fibre materials for acoustical applications. Applied Acoustics 66 (12), 1383−1398.

Gibson, L.J., Easterling, K.E., Ashby, M.F., 1981. The structure and mechanics of cork. Proceedings of the Royal Society A: Mathematical Physical & Engineering Sciences 377, 99−117.

Hongisto, V., Keranen, J., Lindgren, M., 2000. Sound insulation of doors-Part 2: comparison between measurement results and predictions. Journal of Sound and Vibration 230 (1), 149−170.

Hou, Q.Q., 2012. Study and Simulation of Wooden Perforated Panels Structure's Sound Absorption Performance. Northeast Forestry University (in Chinese).

Kanev, N.G., 2012. Sound decay in a rectangular room with impedance walls. Acoustical Physics 58 (5), 603−609.

Kim, B.J., Huang, R., Xu, X., Lee, S.Y., Kunio, J., Wu, Q., 2015. Sound transmission properties of mineral-filled high-density polyethylene (HDPE) and wood-HDPE composites. Bioresources 10 (1), 510−526.

Kim, K.W., Jeong, G.C., Yang, K.S., Sohn, J.Y., 2009. Correlation between dynamic stiffness of resilient materials and heavyweight impact sound reduction level. Building & Environment 44, 1589−1600.

Larm, P., Hakala, J., Hongisto, V., 2006. Sound Insulation of Finnish Building Boards. Work Environmental Research Report Series 22. Finnish Institute of Occupational Health.

Li, P., Kim, B.J., Wang, Q., Wu, Q., 2013. Experimental and numerical analysis of the sound insulation property of wood plastic composites (WPCs) filled with precipitated $CaCO_3$. Holzforschung 67 (3), 301−306.

Liang, J., Li, R., Tjong, S., 1999. Effects of glass bead content and surface treatment on viscoelasticity of filled polypropylene/elastomer hybrid composites. Polymer International 48 (11), 1068−1072.

Liu, X.T., 2000. Building Physics, second ed. China Architecture & Building Press, Beijing (in Chinese).

Liu, Y.X., Yu, H.P., Zhao, R.J., 2007. Wooden Environtology. Science Press, Beijing (in Chinese).

López, J.P., Mansouri, N.E.E., Alba, J., Rey, R.D., Mutjé, P., Vilaseca, F., 2012. Acoustic properties of polypropylene composites reinforced with stone groundwood. Bioresources 7 (4), 4586−4599.

Ma, D.Y., 2002. Noise and Vibration Control Engineering Handbook. China Machine Press, Beijing (in Chinese).

Miki, Y., 1990. Acoustical properties of porous materials-modifications of Delany-Bazley models. Journal of the Acoustical Society of Japan (E) 11 (1), 19−24.

Morse, P.M., Ingard, K.U., 1986. Theoretical Acoustics. McGraw-Hill, New York.

Pritz, T., 1996. Dynamic young's modulus and loss factor of floor covering materials. Applied Acoustics 49 (2), 179−190.

Remes, M., 2009. Sound Insulation of Wooden Double-leaf Partitions. Helsinki University of Technology.

Satoh, T., Kimura, M., Yamaguchi, M., Kunio, J., 2014. An impedance tube measurement technique for controlling elastic behavior of test samples. In: The 43rd International Congress on Noise Control Engineering, Melbourne, Australia.

Smardzewski, J., Batko, W., Kamisiński, T., Flach, A., 2014. Experimental study of wood acoustic absorption characteristics. Holzforschung 68 (4), 467−476.

Sun, W.S., 2009. Study on Wood-rubber Composite and Application in Soundproof Flooring. Chinese Academy of Forestry (in Chinese).

Wang, D., Peng, L.M., Fu, F., Wang, J.F., Zhu, G.Y., 2014. Study on sound absorption characteristics of *Cryptomeria fortunei* Hooibrenk ex Otto et Dietr. Journal of Central South University of Forestry & Technology 34 (10), 137−140 (in Chinese).

Wang, J.F., 2013. Study on the Sound-absorbing Materials with Wood Fiber and Polyester Fiber. Nanjing Forestry University.

Wang, X., You, F., Zhang, F.S., Li, J., Guo, S., 2011. Experimental and theoretic studies on sound transmission loss of laminated mica-filled poly(vinyl chloride) composites. Journal of Applied Polymer Science 122 (2), 1427−1433.

Wu, M.Q., 2006. Adverse effects of indoor noise on human health and noise control. Journal of Environment and Health 23 (2), 189−192 (in Chinese).

Yu, H.P., Guo, M.H., Hou, Q.Q., Wang, J.M., 2010. Research on influence factors of absorption performance for wooden perforated panels. Advanced Materials Research 113−116, 1959−1963.

Zhang, Z., Zhang, X., Zhang, N., Zhang, H., 2010. Study on acoustic transmission loss of materials with transfer matrix-impedance tube methods. Materials Review 24 (5), 118−121 (in Chinese).

Zhao, J., Wang, X.M., Chang, J.M., Yao, Y., Cui, Q., 2010. Sound insulation property of wood−waste tire rubber composite. Composites Science & Technology 70 (14), 2033−2038.

Zheng, H., Chen, D.S., 1996. Literature review of the study on the sound insulation properties of layered damping panels. Applied Acoustic 2, 1−6 (in Chinese).

Zhong, X.Z., 2012. Construction Sound Absorption and Insulation Materials, second ed. Chemical Industry Press, Beijing (in Chinese).

Zhou, H.B., 2006. Studies on Design Methods for Sound Insulation of Wood Structure Walls and Vibration Performance of Wood Structure Floors. Chinese Academy of Forestry (in Chinese).

Zhu, G.Y., Peng, L.M., Liu, Y., Fu, F., Wang, D., Song, B.Q., 2015. Sound absorption of perforated medium density fiberboard. China Wood Industry 29 (2), 5−8 (in Chinese).

Zhu, X., Kim, B.J., Wang, Q., Wu, Q., 2014. Recent advances in the sound insulation properties of bio-based materials. BioResources 9 (1), 1764−1786.

Fire performance of natural fibre composites in construction

14

M. Fan [1], *A. Naughton* [1], *J. Bregulla* [2]
[1]Brunel University London, London, United Kingdom; [2]Building Research Establishment, Watford, United Kingdom

14.1 Introduction

Most research into the fire performance of natural fibre composites (NFCs) is concerned with the reaction to fire parameters, not fire resistance (Naughton, 2013). Analysis techniques and current theories pertinent to the residual mechanical properties of fibre reinforced polymer (FRP) composites exposed to fire are not applicable to NFCs. Current models for residual mechanical properties did not account for the decomposition of fibres at relatively low temperatures. As of yet, there are no models that are specific to the residual mechanical properties of NFCs exposed to fire. The discrepancies between the current composite theory and NFCs have motivated some researchers (eg, Naughton et al., 2014) to re-evaluate the conceptual model for thermal decomposition of polymer composites and to develop a model for residual mechanical properties specific to NFCs, as well as to quantify some fire performance parameters, such as the char contribution of natural fibres.

Fire resistance in the construction industry is defined as the ability of a material or building element to maintain the structural integrity of the building and prevent catastrophic collapse for a prescribed period of time. A material or building element achieves a fire resistance rating by passing the performance criteria in a full-scale fire resistance test. A full-scale fire resistance test investigates the fire resistance of a building element in a configuration and size that is similar to that in practice. The full-scale fire resistance test is inhibitive for innovative materials such as NFCs due to the financial commitment and the prescriptive pass/fail information of the tests. It is not normally possible to develop a scientific understanding of the material parameters, which contribute to a successful or unsuccessful fire resistance test. However, a bench scale test method can be adopted to provide an indicative assessment of the likely performance in full-scale fire resistance tests, which are required for materials to meet building standards in the United Kingdom (Naughton, 2013).

The fire performance of FRPs is as important a design consideration as the modulus, yield stress and clarity. The main emphasis on fire performance is in adding fire retardants into the resin mixture. This approach is being extended to NFCs in terms of research and development with either fire retardant coatings on the fibres or fire retardant and intumescent fillers in the resin mixture. However, the additives used to improve fire resistance can have a detrimental effect on the processing techniques and on mechanical performance (Halliwell and Reynolds, 2003).

Advanced High Strength Natural Fibre Composites in Construction. http://dx.doi.org/10.1016/B978-0-08-100411-1.00014-5

Poor interfacial adhesion in NFCs can contribute to premature thermal degradation. Natural fibres start degrading at around 150°C. Low temperature degradation is associated with hemicellulose and lignin, whereas high temperature degradation is associated with the presence of cellulose. The thermal conductivity of NFCs has been shown to be dependent on fibre orientation. In-plane thermal conductivity is greater than transverse thermal conductivity (Behzad and Sain, 2007). Fibre type and fibre volume (V_f) also contribute to the failure characteristics and charring rates of NFCs. Composites with a high V_f display similar charring behaviour to wood-based composites. As with most other materials, substrate, thickness and moisture content all play an important role in the fire resistance characteristics of NFCs.

There are currently no standard tests specific to NFCs. However, current British standards acknowledge the use of natural fibres as reinforcement in polymer composites, and most experimental testing of NFCs is based on standards for traditional FRPs. A full-scale test would be required to verify whether an NFC meets building standards and fire safety requirements. Until the fire resistance and reaction characteristics of NFCs are fully understood, full-scale tests are the only indication of fire performance.

14.2 Synthetic polymers and biopolymers for natural fibre composites

Polymers can be classified as elastomers, plastics and fibres. Plastics can be further defined as either thermoplastic or thermoset. Thermoplastic and thermoset polymers form the matrix phase in an FRP composite. The matrix phase is required to transfer the loads to the fibres and must protect the fibres from impact, abrasion and chemical and moisture attack. It binds the fibres, providing rigidity to fibre bundles that would otherwise be relatively pliable. Most commercially available thermoplastics such as polypropylene and thermosets such as epoxy are derived from a petrochemical-based origin. Biopolymers, on the other hand, are polymers derived from natural resources such as polylactic acid from corn oil, cashew nut shell liquid oil and thermoplastic and thermoset products from soy (Mohanty, 2009). Biopolymers have some limitations in terms of cost versus performance. They are typically difficult to procure at the moment, but with increasing interest and continued research, they may become commercially viable in the near future. Alternatively, a copolymer of petrochemical origin can be used to create a hybrid matrix, which improves the performance of the biopolymer, inviting wider interest in various industries. The main advantage and attraction of a biopolymer is its ability to biodegrade at the end of its useful life.

14.2.1 Polyesters

Polymers can be further classified in terms of their chemical composition, which is an important indication of their reaction to heat and thermal decomposition (Beyler and Hirschler, 2002). Carbonaceous polymers and polyolefins are thermoplastic materials such as polyethylene and polypropylene. Oxygen-containing polymers are cellulosics,

polyacrylics and polyesters. Natural oxygen-containing polymers are cellulosics such as wood and paper products. Nitrogen-containing materials such as polyurethanes are principally used as foams for flexible and rigid thermal insulation. Nitrogen can also be contained in materials with carbon−carbon chains, such as polyacrylonitrile, which is mostly made into fibres and used as a constituent of engineering copolymers. The most common chlorine-containing polymer is polyvinylchloride (Rudnik, 2007). Fluorine-containing polymers are characterised by high thermal and chemical inertness and low coefficient of friction (Beyler and Hirschler, 2002).

Poly(ethylene terapthalate), which is a thermoplastic polymer, was purportedly discovered by Carleton Ellis (Fink, 2005). However, the first patents emerged in the 1930s and commercial production of glass fibre reinforced polyesters began in 1941 (Fink, 2005). Thermoplastic materials can be softened and deformed at temperatures below the minimum thermal decomposition temperature without causing permanent degradation of the material. Thermosets, on the other hand, cannot. This provides thermoplastic materials with the advantage of being easily formable and moulded into various products.

The formability of thermoplastic materials is dependent on the degree of order in molecular packing or 'crystallinity'. There are well-defined melting temperatures for crystalline materials (Beyler and Hirschler, 2002). The formability or deformability of a polymer can be defined as the ratio between the strain resulting from a constant applied stress. The Glass Transition Temperature (T_g) is a temperature at which a polymer material begins to transform into a rubbery state. T_g is then considered the upper limit for the use of a thermoplastic polymer that is required to be stiff and rigid. The melting temperature (T_m) is the point at which a material begins to melt and become viscous. As most materials are only partially crystalline, the melting temperature is less well-defined and falls within a range of 10°C or more (Beyler and Hirschler, 2002). Polyester has a glass transition temperature of 69°C (Rudin, 1999) and a melting temperature in the range of 250−300°C (Braun and Levin, 1986). The auto-ignition temperature in inert atmospheres has been shown to be approximately 450−500°C (Braun and Levin, 1986; Patten, 1961). Flash ignition has been found to be 400°C (Patten, 1961). Ignition temperature in an oxygen-rich environment has been found to be 364°C (Burchill et al., 2005).

14.2.2 Thermal decomposition of polymers

There are a number of important chemical mechanisms in the thermal decomposition process of polymers: namely the random chain scission, end chain scission, chain stripping and cross-linking. Thermal decomposition of a polymer generally incorporates more than one of these mechanisms (Beyler and Hirschler, 2002). They provide a useful conceptual framework in identifying and classifying thermal decomposition behaviour.

The ranking of fire resistance for thermoset polymers can be presented thus (Kozlowski and Wladyka-Przybylak, 2008):

Phenolic > Polyimide > Bisaleimide > Epoxy > Polyester > Vinylester

The formation of char can be a good criterion to measure the fire resistance of polymers. Fire-resistant polymers, such as phenolics, readily form a carbonatious char during the decomposition process by means of the cross-linking of polymer chains (Chapple and Anandjiwala, 2010). Char is formed at the expense of flammable volatiles and acts as an insulating barrier against heat, therefore retarding the process of thermal degradation.

14.3 Natural fibre reinforcements

The most commonly used reinforcing fibres in the construction industry are glass fibres. In many ways, natural fibres display similar mechanical properties and characteristics to glass fibres. Consequently, once extracted from the plant, natural fibres are used for reinforcement in much the same way as glass fibres such as yarns, woven or nonwoven mats and chopped fibres. However, natural fibres offer the advantage that they are not abrasive to machinery, they are not harmful to humans and they can be obtained from renewable sources.

Hemp and other natural fibres are often used as thermal insulations in the construction industry (Kymalainen and Sjoberg, 2008). Varieties of natural fibres used for reinforcement are normally defined as either 'wood' or 'nonwood' fibres. Nonwood fibres can be further defined as bast, leaf, fruit and seed fibres. Their properties are intrinsically dependent on their locality, yield, maturity, retting process and location of the fibre within the plant.

Bast fibre is found in the outer layer or skin of the plant's stem. Sisal is a form of leaf fibre, which is found in the large leaves of the cactus. An example of fruit fibre is the husk from coconut or 'coir'. Natural nanofibres can be extracted from a variety of plants and even vegetables such as carrots. Hemp, flax, jute, sisal and kenaf are all well-established sources of technical and industrial fibre and have been used for centuries to make a wide variety of products such as ropes, twine, clothes and canvas.

14.3.1 Hemp fibres

Hemp 'cannabis sativa' is known to be the oldest cultivated nonfood crop in the world, and evidence of materials made from hemp have been discovered in tombs dating back to 8000 BC (Cripps et al., 2004). It has been cultivated for thousands of years for food, recreation and industrial purposes (Stafford and Bigwood, 1992). Up until the middle of the 20th century, hemp was an integral material in a variety of mainstream industries from paper to rope and even oil. The US army even adopted the slogan 'Hemp for Victory' during World War II to promote the production of hemp for industrial purposes. The industrial use of hemp fell into decline with the advent of polyester in the 1930s and glass fibre technology in the 1940s (Fink, 2005). The development of technical hemp fibre was temporarily arrested due to the legislation leading to the prohibition of cannabinoids in the 1970s. Hemp contains only small traces of the

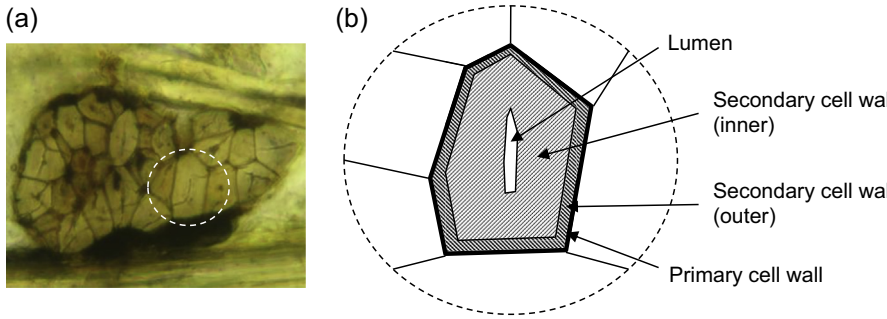

Figure 14.1 Composition of (a) technical fibre bundles and (b) elementary fibres.

psychoactive ingredient 'tetrahydrocannabinol', the substance to which the legislation pertains (Roulac, 1997). In recognising the distinction between industrial hemp crop and recreational 'marijuana', there has been a resurgence of hemp production in Europe.

Technical hemp fibre is classed as a bast fibre, which is extracted from the outer portion of the plant stem just below the outer layer of skin. Bast fibres are extracted from the plant by a microbial process known as 'retting', which breaks the chemical bonds that hold the stem together by the decomposition of lignin and hemicelluloses (Thygesen, 2006). After retting, hemp fibres are separated from the stalk by a mechanical decortication process. The properties of hemp fibres are dictated by the location, yield, type and processing methods (Roulac, 1997).

Hemp fibres are composed of cellulose (74%), hemicellulose (12%), lignin (5%), pectin (2%) and other extraneous material and are characterised by a cellular structure (Fig. 14.1). Each cell has one external wall and three side walls containing crystalline cellulose regions called microfibrils, which are interconnected via the lignin and hemicellulose fragments (Kozlowski and Wladyka-Przybylak, 2008). The individual cells are known as elementary hemp fibres (Dai and Fan, 2010). The cell walls are defined by the concentration of constituent materials and the microfibrilar angle. The cellulose microfibrils are almost parallel to the elementary fibre in the inner part of the secondary cell wall (0−2 degree), helical in the outer part of the secondary cell wall (25−30 degree) and helical in the primary cell wall (70−90 degree) (Thygesen, 2006). The lumen is hollow and allows the transport of moisture and nutrients within the plant by a capillary action, which can also lead to the ready absorption and retention of internal moisture, which is enhanced by the presence of lignin and hemicellulose (Pejic et al., 2008). The primary cell wall is rich in lignin and pectin with decreasing volumes of lignin towards the inner part of the fibre (Thygesen, 2006).

14.3.2 Mechanical properties of natural fibres

The mechanical properties of natural fibres vary greatly depending on yield, species, weather conditions, location and exposure, to name but a few (Table 14.1).

Table 14.1 Mechanical property of natural fibres

	σ_f (MPa)	E_f (GPa)	ε_f (%)	G_f (GPa)
Madsen et al. (2007)	755	62–68	–	8
Fan (2010)	529–1256	–	1.6	–
Pickering et al. (2007)	857	58		
Baley	788	44.5	1.8	–
Duval	394	19.3	2.6	–
Robson	900	25	–	–
Thygesen	1735	24.9		
Bodros	900	35	1.6	–
Symington	64	900	1.6	–
Charlet	1100	70	1.8	–

Additionally, natural fibres present a number of physical characteristics, such as flaws and a variable cross section, which makes an accurate analysis of the mechanical properties difficult. The primary and secondary cell walls of hemp fibres present different deformation and breaking behaviour, which is associated with the microfibril angle of each wall (Dai and Fan, 2010). Natural fibre mechanical properties are also dependent on temperature and moisture content (Placet, 2006). Given the high degree of variability, many researchers have adopted statistical analysis and probability distribution analysis to characterise hemp fibres (Fan, 2010; Virk, 2010; Pickering et al., 2007).

The stress-strain behaviour of many natural fibres is quasi-linear (Nechwatal et al., 2003). Every fibre shows a different initial curve shape. Therefore the calculation of modulus is uncertain. Nechwatal et al. (2003) found an interesting correlation between the initial curve range and the total curve range, resulting in a nonelongation corrected modulus E_n of:

$$E_n = \frac{L_{FV} F_{max}}{A \Delta L_{F_{MAX}}} \tag{14.1}$$

where, L_{FV} is the length at force F_v and $\Delta L_{F_{MAX}}$ is the elongation at maximum force (F_{max}).

Fan (2010) found that the tensile stress-strain curve of hemp fibres is linear, in agreement with Hooke's law. A relationship between tensile strength and fibre diameter was found, and tensile strength was reliably predicted from the power regression ($r^2 = 0.88$) (Fan, 2010):

$$\sigma_f = 44805 D^{-1.2093} \tag{14.2}$$

Placet et al. (2012) investigated the diameter dependence of Young's modulus in hemp fibres and found that the ultrastructural parameters such as cellulose crystallinity and microfibril angles are the main influencing factors (Placet et al., 2012). The strength of fibres is dictated by the arrangement of the microfibrils. The more parallel the microfibrils to the axis of the fibre, the stronger the fibre (Kozlowski and Wladyka-Przybylak, 2008).

A contribution to the failure of natural fibres is the presence of flaws (Silva et al., 2008; Fan, 2010). Natural fibres have naturally occurring flaws where stress concentrations can occur and lead to failure in tension. The defects have been observed as kink bands, dislocations, nodes and slip planes (Dai and Fan, 2010). It has been shown in tests that as the length of a sample fibre is increased, the volume of defects present in the sample also increases, leading to more mechanisms for failure in tension, as there is more potential for the linking of flaws and the propagation of cracks (Silva et al., 2008).

Another major problem in determining the mechanical properties of natural fibres is cross-sectional area. In order to calculate the stress, the cross-sectional area is required. The determination of the cross-sectional area in an individual strand of fibre is a notoriously difficult problem, as the cross section is rarely circular and invariably nonuniform along the length of the fibre (Dai and Fan, 2010). The cross-sectional area (A) can be calculated from the density (ρ) and the fineness of the fibre (T), and a good correlation between microscopic measurements has been found (Nechwatal et al., 2003). Virk (2010) developed a fibre area correction factor for the use of hemp fibres as reinforcement in polymer composites. The area correction factor is applied to models for composite strength and modulus where the cross-sectional area of fibres has been assumed to be circular.

Placet (2006) investigated the thermomechanical behaviour of hemp fibres. Under cyclic stress regimes, hemp fibres increase in stiffness. The mechanical properties stabilise after a number of cycles, suggesting that mechanical behaviour involves biochemical adaption and/or structural adaption such as microfibril reorientation (Placet, 2006). The rigidity and endurance of fibres are highly affected by temperatures above 150°C and up to 180°C (Placet, 2006).

14.3.3 Thermal decomposition of natural fibres

Since natural fibres are not thermoplastic, the pyrolysis temperature of natural fibres is lower than the glass transition temperature (Chapple and Anandjiwala, 2010). As such, they have poor fire resistance properties, but they do char quite readily due to the presence of cellulose and lignin. The thermal degradation of bast fibres such as hemp is a one-stage process that begins at around 150°C and is associated with the degradation of hemicellulose and lignin. The activation energy for this process is approximately 117 kJ/mol, which corresponds with the activation energy of hemicellulose (Kozlowski and Wladyka-Przybylak, 2008). Experimentally, hemp fibre has been shown to have a relatively low heat release rate, which could be associated with its relatively low lignin content (Kozlowski et al., 2002). Thermal decomposition of lignin involves cleavage of weak bonds at relatively low temperatures.

The flammability of natural fibres is dependent on crystallinity and orientation. The more crystalline the fibre, the more levoglucosan is produced during pyrolysis. Levoglucosan is a cellulose monomer and is evolved in the form of a highly flammable tar. Since the activation energy of cellulose pyrolysis increases with an increase in crystallinity, the flammability of fibres could theoretically be reduced by increasing their crystallinity (Kozlowski and Wladyka-Przybylak, 2008).

Although the decomposition process of hemicellulosic fibres such as hemp occurs at a relatively low temperature, hemicellulose produces more noncombustible gases and less tar than cellulose. Lignin contributes to more char formation than either cellulose or hemicellulose (Chapple and Anandjiwala, 2010). Fibres with low cellulose content, high lignin and high hemicellulose content should be less flammable than fibres such as cotton, which have a high cellulose content (Chapple and Anandjiwala, 2010).

The study on the thermal degradation mechanism of hemp fibre, including thermogravimetric analysis, indicated that there is evidence of dehydration in the form of desorption of chemically bound moisture between 150°C and 250°C (Ming and Qui-Ju, 2006). The onset of significant decomposition was found to occur at 300°C, coinciding with rapid mass loss between 300°C and 360°C and the formation of carbonaceous residues. Oxidisation of the char occurs between 360°C and 440°C, coinciding with a reduction in the rate of mass loss. Between 360°C and 440°C, flammable aliphatic groups, of which laevoglucose is the major constituent, are decomposed through homolytic cleavage of C−O and C−H bonds, resulting in the production of condensed and cross-linked aromatic components, which are more.

The rate of thermal degradation of hemp fibres was found to reduce with chemical treatment due to the lower contents of hemicellulose and lignin after treatment (Kaczmar et al., 2011). Feng et al. (2008) investigated the effect of high temperature alkali cooking on hemp fibre. It was found that the cooking process was effective at removing hemicellulose and lignin and can also improve the thermal stability of cellulose by increasing the crystallinity index. Pickering et al. (2007) also found that alkali cooking improved the mechanical properties. However, the maximum processing temperature was found to be 160°C before a reduction in tensile properties was observed. Fibres processed at 180°C had less than 50% of the tensile strength of fibres processed at 160°C.

The decomposition and degradation of fibres can be identified by discolouration of the fibre cell walls and the development of voids within the fibre cross section. The process can be illustrated chronologically in Fig. 14.2. The cross section of undamaged virgin fibres within a polyester matrix are characterised as a light grey colour. The cell walls are well defined and there are minimal voids at the interface between fibre and matrix (Fig. 14.2(a)). Fibres that have experienced the initial onset of thermal damage are characterised as a light red/orange, the cell walls are a light red colour and the interface is still intact at this stage (Fig. 14.2(b)). Further exposure and an increase in temperature leads to a deeper discolouration of the fibre, the primary cell walls begin to turn black and there is evidence of interfacial separation due to fibre shrinkage (Fig. 14.2(c)). The decomposition of the secondary cell walls, which are lignin poor, occurs within the char region (Fig. 14.2(d)). The lignin-rich primary cell walls

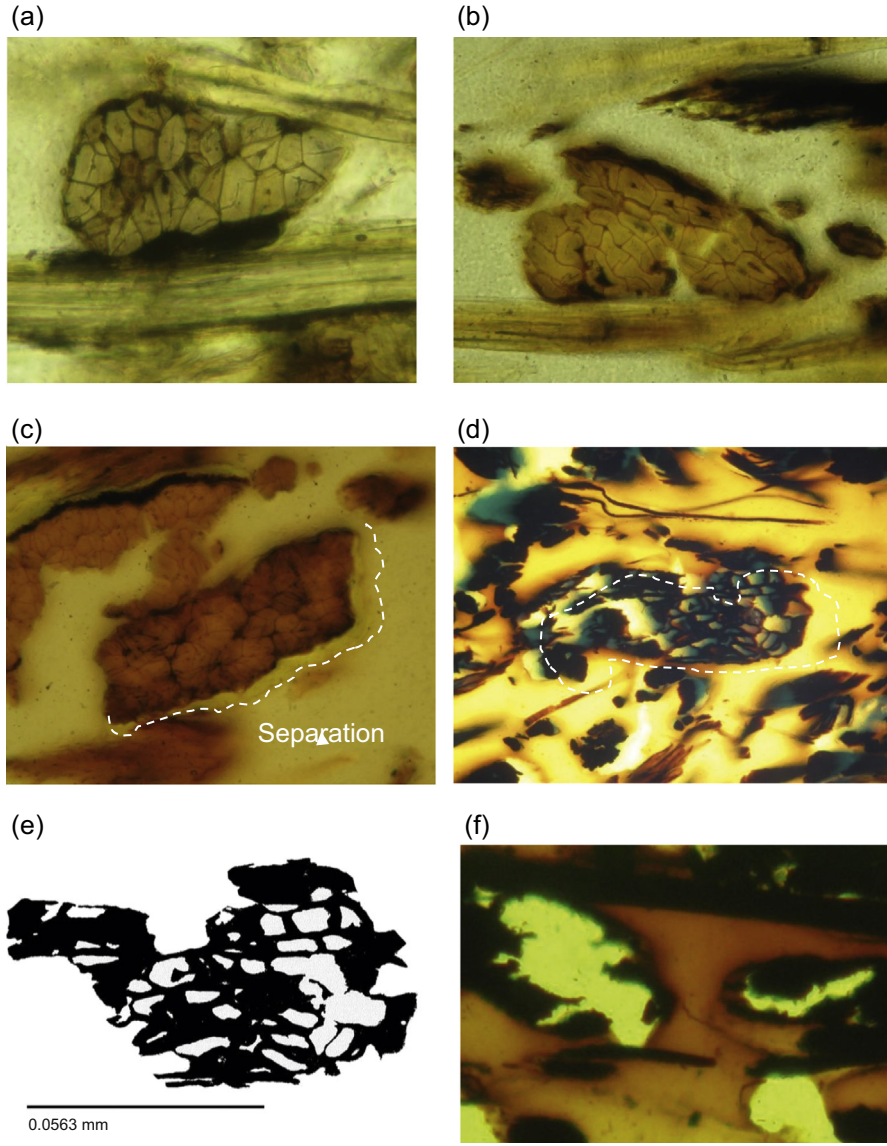

Figure 14.2 Thermal decomposition of natural fibres (a) virgin hemp, (b) discoloured hemp, (c) deeply discoloured hemp with interfacial separation, (d) deeply blackened hemp with decomposition of secondary cell wall, (e) completely decomposed fibre, and (f) decomposition of fibre bundle with voids in secondary cell walls of elementary fibres.

are deeply blackened but intact. The volume of voids can be calculated using the analysis in Adobe Photoshop by creating a silhouette of decomposed fibres (Fig. 14.2(e)). The average void volume was measured as 35.33%. Finally, at the pyrolysis front, the fibre has almost completely decomposed, leaving a char residue (Fig. 14.2(f)).

The mechanism by which such a fibre can appear in the cross section is by the conduction of heat and subsequent convective transport of mass through a fibre.

14.4 Thermal process in the manufacture of natural fibre composites

14.4.1 Material selection

The selection of appropriate fibres for specific applications is dictated by the desired properties of the composite and the performance requirements in use. However, the generic terms for fibre choice are primarily based on:

- elongation of the fibre at failure
- elastic modulus
- tensile capacity
- thermal stability
- adhesion in the mix
- durability of the fibre
- cost of processing and manufacture
- and more recently, life cycle assessment and environmental impact

14.4.2 Manufacturing of natural fibre composites

The manufacture of NFCs is based on the manufacturing processes of petrochemical-based composites such as:

- pultrusion
- wet lay-up
- compression molding
- resin transfer molding
- vacuum infusion

Injection molding of NFCs is considered by some to have huge potential in industrial applications (Fowler et al., 2006). However, opportunities for NFCs are hindered by regulations for existing materials, highlighting the need for further development of characterisation methodologies and theoretical analysis.

It has been noted that at temperatures over 200°C during manufacturing processes, flax fibres can be irreversibly damaged (Bodros et al., 2007). This is primarily due to vapour evaporation and differential expansion coefficients in the cell walls of the fibres, which lead to porosity in the fibres and reduce their mechanical properties. Controlling the processes in the manufacture of NFCs is essential to preserve the mechanical properties of the fibres. The film stacking method reduces the damage to the fibres, as it requires only one heating process (Bodros et al., 2007).

Randomly oriented fibres are known to provide a good formability and are slightly cheaper to produce than highly directional fibre composites (Zampaloni et al., 2007). However, they do not display the same mechanical advantages of directional fibres.

Squeeze flow tests showed that randomly orientated fibres display directionality due to the 'by hand' manufacture process (Zampaloni et al., 2007). The optimal fabrication method was discovered to be a layered sifting of microfine polypropylene fibre and chopped kenaf fibre in a compression molding process. A 3% Epolene G3015 coupling agent was also found to aid fibre/matrix adhesion (Zampaloni et al., 2007).

NFCs can be manufactured by a sheet molding process traditionally used for glass fibre reinforced polyester composites. The process can be adapted for any kind of natural fibre. It was also proposed that bioresins could be used in the future instead of a polyester matrix and that with further optimisation, natural fibre reinforced biocomposites could be produced with similar mechanical properties to glass/polyester composites (Mehta et al., 2005).

The injection molding processing technique is the most commonly used method in the plastics industry and is suitable to produce a wide variety of products (Wan Abdul Rahman et al., 2008). However, the process requires an in depth knowledge of polymer processing and rheology of the materials to minimise the cost of production. There are commercially available software packages that can model injection moulded products such as Moldflow and Moldex3D, which help to study the flow patterns in the injection moulding process. A model was developed using commercially available software to analyse a rice husk fibre composite window frame manufactured by an injection moulding process (Wan Abdul Rahman et al., 2008). The results were encouraging, but more information is needed on the thermal properties of natural fibre composites to determine their rheology and flow rate at different temperatures.

A thermal pressing process for manufacturing flax fibre and flax mucilage has been successfully trialled (Alix et al., 2008). Glutaraldehyde was used to cross-link the matrix solution, providing moisture resistance. However, glutaraldehyde is not ideal, as it is toxic to the environment. The sorption of water by the composite was reduced when the composite was prepared with a high level of protein in the mucilage.

14.5 Fire performance of natural fibre composites

Fire is always a critical design factor, especially in lightweight structures. Fire risk is defined as the potential for any material or object to catch fire in any given situation (Morgan and Gilman, 2012). Fire in structures accounts for the highest fire risk to humans, and it is assumed that a structure will experience one fire during the course of its design life that does not destroy the structure (Bregulla, 2003). Whilst only accounting for 20% of all building fires, domestic structures account for 75% of all casualties, equating to 400–600 lives each year. Many of the casualties are a result of a lack of awareness during a fire, such as when people are asleep (Bregulla, 2003).

Structural members and framing elements have been observed in surveys to be the first materials to be ignited in 9% of all homes. They were the third most frequent items to be ignited after cooking materials and household waste. They were also found to be the third most frequent cause of death due to structural collapse (Bregulla, 2003).

During a fire the elements within a building, such as walls and wall coverings, are required to protect the inhabitants, to protect and limit damage to the structure and to provide relative safety to firefighting crews. Depending on the type of building and the function (ie, load bearing or partition), the walls are required to be fire resistant for a set period of time. The appropriately designed fire-resistant building element will perform as a barrier for a structural element during a fire. Good fire resistance restricts the size of a fire and prevents the collapse of a building (Bregulla, 2003).

Polymer composites are not normally employed as structural elements within a building. However, they are used as external and internal wall coverings and architectural features within buildings, such as furniture or door frames, window frames, etc. Consequently, they do account for a large proportion of potential fire load within a building. The maximum temperature of FRPs is governed by two main factors: the glass transition temperature (T_g) and the temperature at which the chemical decomposition starts to become significant (Halliwell and Reynolds, 2004). High temperature resins can be obtained, but they are generally more expensive. Initially, the design of FRPs for use in the construction industry mysteriously neglected to incorporate fire performance. After several disasters, the fire performance of FRPs is as important a design consideration as the modulus, yield stress and clarity (Halliwell and Reynolds, 2004). The main emphasis on fire performance is in adding fire retardants into the resin mixture. The use of fire retardant additives has a detrimental effect on the weathering of FRPs. Therefore a highly fire retardant substrate combined with a regular gelcoat is desirable.

Full-scale fire testing can be defined as the study of products and assemblies in sizes and configurations that resemble the actual configurations in practice (Peacock and Babrauskas, 1991). A number of methods have been adopted to assess the performance of FRP composites in large-scale tests, such as ISO 9705 (full-scale room test for surface products), ISO 13784-1 and ISO 13784-2 (large- and small-room tests for sandwich panels) and ISO 13785-2 (large-scale test for façades) (BS ISO 25762). Full-scale fire tests are required to provide a certificate of fire performance for a construction material or building element. The certificate is based on the ability of the product to meet fire resistance requirements for a prescribed period of time: typically 30, 60 or 90 min. Full-scale tests are inhibitive for the research and development of new materials, as they only provide pass/fail information, and further scientific analysis of the mechanisms for failure are restricted since the product is normally destroyed.

The effect of type and volume of fibre reinforcement on the thermal properties of NFCs has been studied (Rudnik, 2007). A Hydroxypropyl starch was used for the matrix and flax and cellulose fibre for the reinforcement. In general, it was established that incorporating natural fibres into a modified starch matrix leads to an increase in the glass transition temperature (T_g), and flax and cellulose reinforcement provided an increase in thermal stability. Kim et al. (2005) found that with the increasing presence of lignin, there is an increase in the thermal stability of the composite. Contrarily, Dorez et al. (2013) found that the introduction of flax fibres into polybutylene succinate composite led to a reduction in thermal stability. Poor interfacial adhesion in NFCs contributes to thermal degradation, and the thermal stability of biodegradable

polymers is lower than in plastics (Kim et al., 2005). Natural fibres start degrading at about 150°C. Low temperature degradation is associated with hemicelluloses, whereas high temperature degradation is associated with the presence of cellulose (Kim et al., 2005).

The efficiency of intumescent additive systems to polyefin/flax composites has been confirmed (Le Bras et al., 2005). The work confirms that a Polyproylene/flax fibre composite with added ammonium polyphosphate as an ecologically friendly fire retardant produces an optimised fire resistance performance for the composite. Hemp fibre reinforced polyester composites, which were treated with a fire retardant, performed well in terms of peak heat release rates compared to other established construction products (Hapuarachchi et al., 2007). The char formation with the introduction of nanoclays improved the flame resistance of the composites. The clay layer acts as a barrier to mass transport. Differential scanning calorimetry showed an increase in the melting and crystallization temperatures of the polypropylene (Biswal et al., 2012). The chloride-based fire retardant can also improve the thermomechanical properties of hemp fibres. It was found that the ultimate tensile strength of fibres exposed to flame for 10 s increased with an increase in the volume of fire retardant magnesium chloride (Chand and Verma, 1989).

The study on the influence of natural fibres on the thermal and fire behaviour of Polybutylene succinate composites showed that although the thermal stability of composites decreased, the peak heat release rate (pHHR) decreased with an increase in the volume of natural fibres. An increase in the production of a char residue was attributed to the lower pHHR, which is in agreement with Hapuarachchi et al. (2007). The cone calorimetry tests on a natural fibre sheet molding compound in comparison with other traditional building products showed that natural fibre composites present a similar reaction to fire as timber-based products such as OSB. It was also noted that with increasing V_f in biocomposites, there was an improvement in reaction to fire. With increasing V_f there was more char produced, which insulates the substrate and protects the product from the propagation of fire and reduces the pHRR (Hapuarachchi, 2006)

The time to ignition (TTI) can be reduced with the incorporation of flax fibres, which were attributed to the flammability of gas released by lignocellulosic fibres (Dorez et al., 2013). However, it was also reported that the TTI for fire retardant and nonfire retardant hemp fibre reinforced polyester composites was greater than glass fibre reinforced composites (Hapuarachchi, 2006). The study on the fire resistance of polyester composites reinforced with jute, flax and sisal indicated that flax reinforced composites had a longer ignition time and less observable thermal degradation due to the low lignin content (Manfredi et al., 2006).

14.5.1 Reaction to fire testing

The cone calorimeter was normally used to develop a better scientific understanding of the parameters for fire performance. Cone calorimetry can be used to determine several parameters for fire performance, such as flammability, smoke production, mass loss and heat release rates. This data readily contributes to the development of a scientific understanding of the combustion and fire reaction properties of various materials.

It has been successfully used to examine the combustion properties of NFCs (Hapuarachchi, 2006) and their natural fibre reinforcement (Ceylan et al., 2012).

Several versions of the original cone calorimeter exist today. Naughton (2013) explores a bench-scale method based on the cone calorimeter to indicate the fire performance of NFCs for structural building materials (Fig. 14.3). The method was initially developed in response to the limited scientific analysis offered from full-scale fire resistance tests, which provide only pass−fail information. Although the cone calorimeter is a powerful tool to understand various fire performance parameters, it does not necessarily indicate how well a material will perform in the full-scale fire tests. The designed method can indicate the fire resistance of a material in comparison with a database of construction materials held at the building research establishment. The calorimetry data is neglected in deference to data pertaining to fire resistance, such as thermal resistance, degree of damage and residual mechanical properties.

The most common method to measure thermal decomposition is thermogravimetric analysis (TGA). Samples in a TGA experiment are subjected to a linearly increasing temperature at a predetermined rate until the desired temperature is reached. The weight of the sample is closely monitored during the course of the experiment. The dependence of the experiment on heating rate is due to the fact that thermal decomposition is a function of both the temperature and the degree of decomposition that has preceded it. Analytical thermogravimetric studies provide useful information on the decomposition process, although the relationship to actual fire behaviour is questionable (Beyler and Hirschler, 2002).

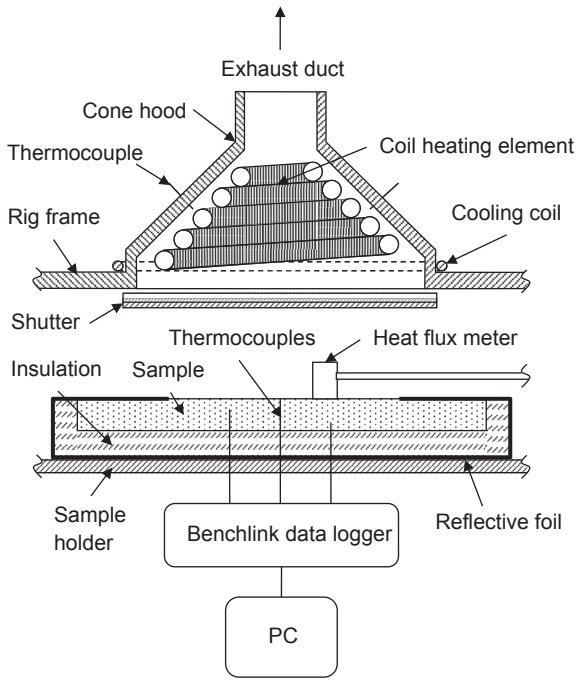

Figure 14.3 Schematic diagram of natural fibre composite fire testing.

Differential thermogravimetric analysis (DTG) provides the mass loss rate versus time, whereas TGA provides only mass loss versus time. DTG is useful in identifying at what temperatures various stages of decomposition take place. Another method for determining mass loss rate is thermal volatilization analysis. Differential thermal analysis (DTA) can examine whether the thermal decomposition of a material is endothermic (consuming energy) or exothermic (producing energy).

It is normally advisable to carry out simultaneous TGA, DTG and DTA experiments to gain an exact analysis of the thermal decomposition process. This can be done using a simultaneous thermal analyser (STA), which can determine the amounts of polymer decomposed, the rates at which these stages occur and the amount of heat evolved or absorbed in each stage. The STA can be combined with transform infrared spectrometers for chemical identification and analysis of the gases evolved at each stage.

14.5.2 Heat transfer of natural fibre composite building materials

Thermal conductivity is most easily observed when a hot object is brought in to physical contact with a cold object. The process of the hot object cooling and the cold object heating is known as heat conduction. Heat conduction is related to the heat content of an object (Q). The heat content is the property of the object subject to movement by conduction. It is expressed as the integral of the specific heat of the object at zero Kelvin to the temperature in question. It is associated with the kinetic energy of vibration in atomic particles, which vibrate about their average position at temperatures above absolute zero. Heat content is related to the movement of free electrons and phonons. Free electrons are most common in metals and can pass between the atoms that make up the object. Phonons are the product of atomic vibration within the crystal lattice and are observed as acoustic waves (Rockett, 1988).

Fourier's equation from 1812 states that the quantity of heat transferred per unit time across an area is proportional to the area and the temperature gradient (Rockett, 1988). The modern basic equation for heat conduction is a more precise version of Fourier's original equation. A steady-state solution to thermal conductivity is a relatively simple calculation. However, when a fibrous material such as an FRP is to be considered, thermal conductivity becomes a complex problem. Thermal conductivity in a fibrous material, such as a unidirectional fibre reinforced composite, is dependent on the direction of heat flow in relation to the direction of the fibres. The conductivity matrix for such orthotropic solids is a diagonal matrix, the only nonzero elements being diagonals, k_{ij} , stated as k_x, k_y and k_z. The basic equation for heat transfer within a solid material is:

$$\rho C \frac{\partial T}{\partial t} = k_x \frac{\partial^2 T}{\partial x^2} + k_y \frac{\partial^2 T}{\partial x^2} + k_z \frac{\partial^2 T}{\partial x^2} + Q \tag{14.3}$$

where, ρ is density, C is the specific heat capacity, T is temperature, t is time, x is a spacial coordinate and Q is the heat content.

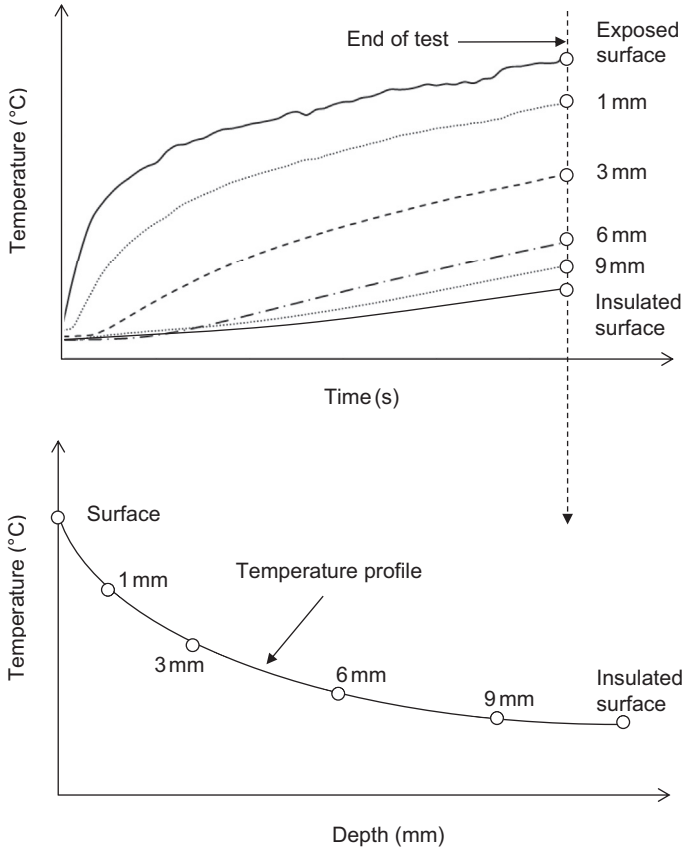

Figure 14.4 Temperature change across the thickness direction of natural fibre composites.

In order to simplify the analysis of heat transfer, many studies consider only one spacial dimension. This is a practical assumption for flat panel materials used in construction applications, as the heat contribution is generally only applied to one surface and the dimensions of the material, even though the thermal behaviour varies depending on material parameters (Fig. 14.4); in walls for example, the influence of heat transfer in other planes is often negated (Bregulla, 2003). However, the thermal properties of many materials are temperature-dependent, which complicates the heat transfer model and transient analysis is required. Additionally, for materials which decompose at high temperatures, the heat transfer model requires some additional manipulation to account for physical changes.

14.5.3 Thermal decomposition of natural fibre composites

Thermal decomposition is the process of chemical species change due to the application of heat. Thermal degradation is the loss of mechanical properties and dimensional

instability due to the application of heat. Thermal decomposition is the most important consideration in terms of fire. The thermal decomposition of a solid material generates ignitable gasses that burn above the surface of the material. If the burning gases feed back sufficient heat to propagate the further decomposition of the solid-state material, the process becomes cyclic, leading to the complete degradation of the material. A polymer is a relatively inert material. The propagation of volatile gasses requires the breakdown of large molecules into smaller ones that can vaporise. The lighter molecular fragments will vaporise immediately on their creation, thereby becoming fuel for burning. The heat created by this process leads to the decomposition of the larger molecules in the solid state, which break down into smaller molecular fragments, leading to more combustible vapour.

The degradation characteristics such as melting and charring will alter the decomposition process and burning characteristic and prevent the cyclic nature of thermal decomposition and the propagation of ignitable gases, leading to complete thermal breakdown. For example, the formation of a char layer, as in wood, can act as an intumescent layer, which provides insulation against further thermal decomposition. Inorganic residues can form a glassy surface on the solid material that can protect underlying layers from thermal breakdown.

Thermosetting and cellulosic materials do not have a fluid state and do not have a T_g phase (Beyler and Hirschler, 2002). Cellulosic materials have a semi-physical change on heating, which is the desorption of water. This occurs at just below the boiling temperature of water.

Many materials produce carbonaceous chars on thermal decomposition, which greatly affects the thermal decomposition of the material. The most important characteristics of a char layer are density, continuity, coherence, adherence, oxidisation resistance, thermal insulation properties and permeability. A good char has low density and high porosity. It prevents the flow of heat from gaseous combustion zone through to the solid phase behind it and slows the rate of thermal decomposition. The char layer can be developed from intumescent additives in the polymer matrix.

The minimum decomposition temperatures are lower in the presence of oxidants (air and oxygen). As the prediction of the level of oxidant present at the surface of the material during thermal decomposition is incredibly difficult, the problem of predicting thermal decomposition is very complicated. Most studies on the thermal decomposition of materials have been conducted in inert atmospheres, despite oxidation having a distinct effect on the decomposition process.

Flat panel composites that have been uniformly heated on one surface present a clear distribution of damage through the depth of the material (Fig. 14.5). There are several types of observable postfire induced damages that are associated with thermal decomposition and degradation of a composite material, such as charring, overheating of matrix phase, cracking and delamination. By examining a cross section of the damaged material, it is possible to identify and define different degrees of damage and the depth at which they occur. The type and degree of damage can be identified in ‘regions’ through the depth of the sample.

It is apparent that the pyrolysis front is the boundary between the pyrolysis region and the char region. As such, there is a modest transition between pyrolysis

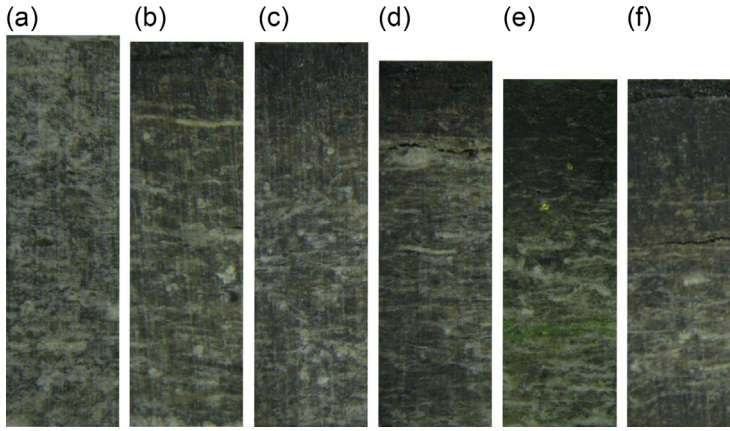

Figure 14.5 Damage profile of natural fibre composites: (a) virgin material, (b) 5 min exposure, (c) 7.5 min, (d) 10 min, (e) 12.5 min, and (f) 15 min.

phenomena and char phenomena. The char region contains a combination of decomposed fibre, mass loss of polyester, charred fibres, deeply discoloured polyester and evidence of the degradation of the fibre/matrix interface. In general, thermally damaged polyester in the char region is characterised by a dark red colour, becoming a pale orange colour with the direction of heat transfer until it resembles the undamaged pale grey colour of virgin material. The fibre in the char region is characterised as a deep black colour, becoming a dark ochre red with the direction of heat transfer until it becomes an orange/red.

There is a differential colour transition between the fibres and polyester in the char region. The transition from discoloured red to pale grey in the polyester is more rapid than the transition from black to orange in the fibres. The polyester begins to decompose at a higher temperature than hemp fibre, which could explain the differential colour transition between the two. It should be noted that the material in the char region is not strictly char but is a combination of overheated polyester and fibres in an extreme state of decomposition.

The degradation region is characterised by pale grey polyester, with red fibres becoming orange and pale with the direction of heat transfer, and the occurrence of thermal voids as observed in the char region and evidence of delamination. The colour of the fibres suggests that they have undergone some thermal damage but are not charred. The red colour of the fibres is more indicative of extreme dehydration and the onset of decomposition.

Mouritz et al. (2004) considered a partly burnt composite to consist of two layers defined as a thermally degraded region and an unburnt region. The thermally degraded region in this case is defined as the region where organic compounds have decomposed to form volatiles and a carbonatious char.

Burchill et al. (2005) identified and defined three regions within the partially burnt composite. As with Mouritz et al. (2004), the regions included a char region and a region of undamaged material. However, a third region of discoloured material was

also identified between the char region and the undamaged region. The discoloured region could be assumed to consist of partially thermally decomposed polymer.

Gibson et al. (2003) also identified this discoloured region. It was also observed that the discoloured region included delaminations. The boundary between the charred region and the discoloured region can be described as the combustion front, while the boundary between the discoloured region and the undamaged region could be considered to be the pyrolysis front.

A study into the mechanical properties of fire damaged glass fibre reinforced phenolic composites showed that the flaming ignition did not contribute significantly to the reduction of postfire mechanical properties, and it was the process of charring that most dictated the reduction in strength (Mouritz and Mathys, 2000). However, a process of degradation prior to visible charring of the material was observed. Despite showing no visible evidence of degradation, the mechanical properties of phenolic glass fibre reinforced composites exposed to a relatively low heat flux of 25 kW/m^2 may be reduced by as much as 30%. This was in part due to the partial chemical decomposition of the resin matrix.

A study into the fire properties of glass fibre reinforced polymers found that with an increase in fibre volume fraction, there was a decrease in overall flammability (Morgan et al., 2009). However, the decrease in flammability came at the expense of the mechanical durability of the resultant char, with many samples disintegrating prior to mechanical testing. There is no correlation between decreased flammability and mechanical durability. Flaming ignition is insignificant when compared with the depth and production of charred material.

Combined fire and mechanical testing has shown that the failure time for compressive failure is shorter than that of tensile failure (Mouritz et al., 2011). Compressive failure is preceded by viscous softening of the matrix, which results in delamination and plastic kinking of fibre tows while tensile failure depends on the softening of the fibres, which occurs at a higher temperature for glass fibres. In the case of NFCs the tensile failure time should be shorter due to the poor fire resistance of natural fibres, which begin to decompose at relatively low temperatures.

14.5.4 Fire resistance of natural fibre composites

Flammability of a material can often limit its use, and smoke generation properties of composite materials are important factors that dictate the end use of the products. The flammability of a composite is often found to be different from the flammability of the constituent materials. Fire retardant resins can improve the fire performance of NFCs. However, the additives used to improve fire resistance can have a detrimental effect on the processing techniques and on mechanical performance. Fire resistance can be achieved with flame retardant additives, flame retardant polyester components and flame retardant vinyl monomers (Fink, 2005). The incorporation of fluorine into a polymer's backbone can increase the fire resistance (Koo et al., 2000). Flame retardant systems consisting of cellulosic charring agents can improve the postfire mechanical properties of polymer composites (Kandare et al., 2011). Nanoparticles, even in small quantities within a polymer composite, can improve fire resistance performance

(Bahramian and Kokabi, 2011). Upon pyrolysis, composites with nanoparticles form a uniform ceramic layer, leading to a higher resistance to oxidation and mechanical degradation.

Structural tests on composite materials reveal that weakening due to thermal loading is a primary mechanism for failure (Feih et al., 2007). The tensile strength of carbon fibre reinforced composites can be reduced by as much as 50% with exposure to temperature in the range from 400−700°C. The stiffness loss of carbon composites is sensitive to the oxidisation of the surface of the material. However, the reduction in tensile strength is more sensitive to an increase in temperature. This was attributed to small flaws and the removal of sizing caused by high temperatures (Feih and Mouritz, 2012). An increase in the volume of glass fibres was also found effective in reducing flammability but at the expense of residual mechanical properties (Morgan et al., 2009).

14.6 Modelling fire performance of natural fibre composites

The decomposition of polymers in numerical models is generally described as a first order Arrhenius relationship to relate mass loss to the heat of a reaction. Char formation and the depth of char can be similarly evaluated from the reaction kinetics, but charring of polymer composites is more normally described as a simple two-phase structure: char and solid materials.

Mass loss prior to ignition may be negligible, and charring occurs post ignition. The char formation is initially dependent on heat flux and does not increase at a constant rate. It was found that there is an initial steady increase in char, which corresponds with the peak rate of mass loss. The rate of charring decreases after this point due to the insulating effect of the developed char layer. With further burning, mass loss continues and char formation proceeds at a higher rate. An equation for char thickness (d_c) was derived from the results (Burchill et al., 2005):

$$d_c = \frac{1}{\alpha - \beta}\left(\frac{M}{V_r \rho_r} - d(1-\alpha)\right) \tag{14.4}$$

where, M is the mass loss per unit area of the material, V_m is the volume fraction of the polyester, ρ_m is the density of the polyester, h_o is the original thickness, a is the average density of polyester beyond the char front relative to the original density of polyester and b is the average density of polyester residue in the pyrolysis region relative to the density of polyester.

The delamination of composites due to internal vapour pressure at temperatures above 100°C was successfully modelled by Davies et al. (1998). The discontinuity in the thermal properties in the matrix and the local decrease in thermal conductivity was modelled as a small air gap between two infinitely large surfaces (Davies and Wang, 1998).

Moisture content is a consideration for hygroscopic materials such as polymers and natural fibres. Water molecules, which are free to move through microvoids and holes, are defined as free moisture, and water molecules attached to polar groups are defined as bound moisture. The heat transfer in a hygroscopic material is influenced by the evaporation of physically and chemically bound moisture. A simple and effective method to describe the evaporation, chemical dislocation and diffusion of moisture within a solid is to convert these energies into an additional specific heat capacity (Davies and Wang, 1998).

Wang (1995) developed a heat transfer model to include terms for the transport of volatile gases, mass transport and decomposition with a good accordance with experimental data:

$$\frac{\partial}{\partial t}(\rho h) = \frac{\partial}{\partial x}\left(k\frac{\partial T}{\partial x}\right) - \frac{\partial}{\partial x}(m_g h_g) - Q\frac{\partial \rho}{\partial t} \tag{14.5}$$

where, h is enthalpy, h_g is the enthalpy of gas, m_g is the mass flux of gas and Q is the heat of decomposition.

Dodds et al. (2000) developed a similar model, which includes terms for endothermic decomposition assuming equilibrium between decomposing material and the resultant gases:

$$\rho C\frac{\partial T}{\partial t} = k_x\frac{\partial^2 T}{\partial x^2} - \dot{M}_g\frac{\partial}{\partial x}h_g - \rho A e^{(-E/RT)}(Q + h - h_g) \tag{14.6}$$

where, $\dot{M}_g$ is the mass flux, A is the rate constant, E is the activation energy and R is the gas constant.

Lattimer and Ouellette (2006) ignored the convective contribution of the gas term to simplify the decomposition model and found a good agreement with experimental results:

$$\left[\rho C + (h + Q)\frac{\partial \rho}{\partial T}\right]\frac{\partial T}{\partial t} = k\left(\frac{\partial^2 T}{\partial x^2}\right) \tag{14.7}$$

The heat transfer equations can be solved as finite difference of finite element equations and are relatively simple. Complications arise in the designation of appropriate thermal properties at high temperatures. Lattimer et al. (2009) used the decomposition model as an inverse technique to derive the temperature-dependent material properties such as conductivity and specific heat capacity.

Feih et al. (2007) developed a model for the tensile strength of glass fibre reinforced polymer composites in fire. The model is based on a combination of Gibson's (Gibson et al., 1995) one-dimensional heat transfer model and the tensile strength of a polymer matrix with respect to temperature. The one-dimensional thermal model is similar to Dodds's equation (Eq. (14.6)) and is applicable to hydrocarbon fires. The thermal model predicts the temperature in order that the tensile strength of the matrix and

the fibres can be calculated with respect to temperature at different locations through depth. The model can predict the tensile strength and estimate failure time of glass fibre reinforced polymer composites exposed to a constant heat flux.

14.6.1 Residual mechanical properties

Many thermomechanical models have been developed to analyse the residual strength of composites at ambient temperature after exposure to elevated temperatures or fire on one face, some more complex than others. For this investigation, it is considered that thermal decomposition of hemp fibres is the dominant mechanism for the loss of tensile strength. Therefore more complex thermomechanical models, which include terms for softening of the matrix phase, are not considered in this review.

Mouritz et al. (2004) developed simple models to predict the residual mechanical properties of composite materials. As discussed earlier, it was found that the most significant influence on residual mechanical properties of fire damaged composites is the char depth. The models developed were based on this premise, and a good correlation with experimental data was achieved. The only data necessary to calculate the residual mechanical properties was therefore the char depth of the material and the original mechanical properties.

A two-layer model for fire damaged polymer composites was also proposed (Gibson et al., 2003). The model ignores the decomposition region and combines an undamaged laminate with a damaged char layer to characterise the residual behaviour of the composite after fire. Although a good correlation between the model and experimental results was found, it was acknowledged that the model must be considered as an approximation only, as it does not include the transition zone. With respect to the findings of Mouritz and Mathys (2000), the transition zone should be considered to have a quantifiable effect on the residual mechanical properties of the composite. Given that partial chemical decomposition of the polymer has been shown to contribute to a reduction in tensile strength of approximately 30%, a proportion of apparently undamaged material should be considered part of the transition zone. Therefore the transition zone is expected to be composed of a combination of charred material and material that is apparently undamaged. A method to model the transition zone is recommended.

The residual tensile strength of NFCs with respect to temperature has been modelled from input parameters derived from the thermal model (Model 1) and from parameters derived from experimental data (Model 2). A reasonable correlation has been found between the two models and experimental results with respect to fibre volume fraction (Fig. 14.6).

14.6.2 Thermophysical properties of natural fibre composites

In general, the transverse thermal conductivity of NFCs is lower than the in-plane conductivity. Transverse thermal conductivity decreases with an increase in V_f, and in-plane conductivity increases with an increase in V_f, which is in line with the accepted theory for thermal conductivity of FRPs. Many researchers have found a good correlation with thermal conductivity models for FRPs. The simplest form is

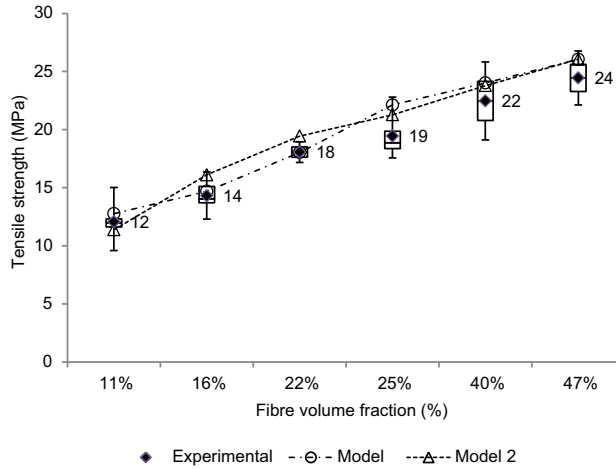

Figure 14.6 Residual tensile strength of natural fibre composites with respect to fibre volume fraction.

the rule of mixture (ROM) equations for in-plane and transverse thermal conductivity. In-plane conductivity is given as the parallel rule of mixtures equation:

$$k_{\parallel} = V_{\mathrm{f}} k_{\mathrm{f}\parallel} + (1 - V_{\mathrm{f}} k_{\mathrm{m}}) \tag{14.8}$$

where, k_{f} is the in plane fibre conductivity and k_{m} is the matrix conductivity. Behzad and Sain (2007) found a good correlation between unidirectional hemp fibre reinforced polyester and the parallel ROM equation. The transverse conductivity is given as the series rule of mixtures equation:

$$\frac{1}{k_{\perp}} = \frac{V_{\mathrm{f}}}{k_{\mathrm{f}\perp}} + \frac{(1 - V_{\mathrm{f}})}{k_{\mathrm{m}}} \tag{14.9}$$

where, $k_{\mathrm{f}\perp}$ is the transverse thermal conductivity of the fibre. Idicula et al. (2006) found a good correlation with the series model for NFRPs. The parallel and series rule of mixture equations act as the theoretical upper and lower bounds for thermal conductivity, respectively. In practice the thermal conductivity of NFCs generally lies between the two. A good correlation between experimental values for hemp fibre reinforce polyester composites and the Springer-Tsai equation (Springer and Tsai, 1967) can be found:

$$k_{\mathrm{c}} = k_{\parallel} \sin^2 \theta + k_{\perp} \cos^2 \theta \tag{14.10}$$

where, k_{c} is the conductivity of the composite and θ is the fibre angle to the direction of heat transfer. When $\theta = 90^{\circ}$ the equation reduces to the parallel ROM and when $\theta = 0^{\circ}$, it reduces to the series ROM.

Liu et al. (2011) found a good correlation between experimental results for manila hemp fibre (banana fibre) reinforced polyester and the Hasselman-Johnson model:

$$k_c = k_m\left[\left(\frac{k_f}{k_m} - 1 - \frac{k_f}{ah_c}\right)V_f + \left(1 + \frac{k_f}{k_m} + \frac{k_f}{ah_c}\right)\right] \times \left[\left(1 - \frac{k_f}{k_m} - \frac{k_f}{ah_c}\right)V_f + \left(1 + \frac{k_f}{k_m} + \frac{k_f}{ah_c}\right)\right]^{-1} \tag{14.11}$$

Other models, which have been corroborated with natural fibre composites (Li et al., 2008) are the Maxwell and Russell models. Maxwell (1954) developed a relationship for the conductivity of distributed noninteracting homogeneous spheres in a homogeneous medium:

$$k_c = k_m\frac{k_f + 2k_m + 2V_f(k_f - k_m)}{k_f + 2k_m - V_f(k_f - k_m)} \tag{14.12}$$

Russell (1935) developed an electrical analogy assuming that the fibres are cubes of the same size dispersed in the matrix:

$$k_c = k_m\left[\frac{V_f^{2/3} + \frac{k_m}{k_f}\left(1 - V_f^{2/3}\right)}{V_f^{2/3} - V_f + \frac{k_m}{k_f}\left(1 + V_f - V_f^{2/3}\right)}\right] \tag{14.13}$$

Using a transient plane source technique, thermal diffusivity, conductivity and specific heat of banana fibre polyester composites were tested at ambient temperature (Agarwal, 2006). The thermal conductivity was found to increase with some fibre surface treatments. Treatment with 1% NaOH was found to produce the greatest increase in thermal conductivity. It was concluded that the improved interfacial bond was the mechanism for an increase in conductivity. Chemical treatment of fibres reduces the thermal contact resistance (Idicula et al., 2006).

The specific heat capacity of hemp fibre reinforced polyester composites has been shown to increase linearly with an increase in temperature between 20°C and 100°C (Behzad and Sain, 2007). Specific heat and thermal diffusivity have been shown to increase with an increase in V_f for flax fibre composites (Li et al., 2008). The influence of temperature on the thermal conductivity of flax fibre composites was shown to be minimal in the range of 170–200°C.

Liu et al. (2011) found a good correlation between experimental results and the Hasselman-Johnson model for transverse thermal conductivity of hemp fibres (0.1847 W/mK). Behzad and Sain (2008) found a parallel conductivity of 1.48 W/mK and a transverse conductivity of 0.115 W/mK. Theoretically the thermal conductivity of fibre reduces with an increase in the volume of lumen.

A series of hemp fibre composites have been examined, and the thermal conductivity was verified (Fig. 14.7).

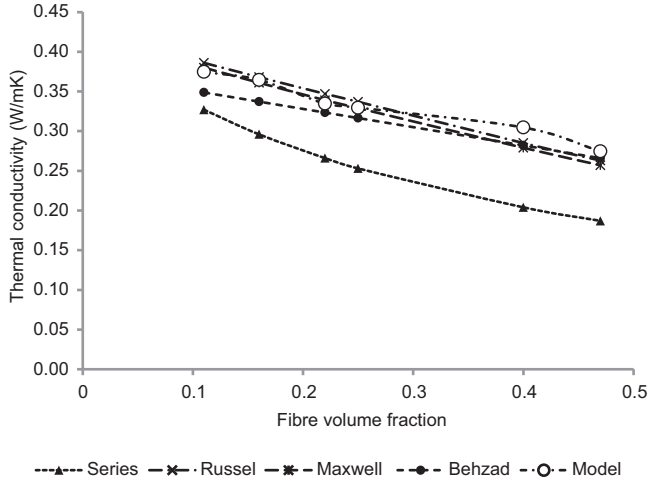

Figure 14.7 Transverse thermal conductivity of hemp natural fibre composites.

14.7 Conclusions and future trends

Most studies on the fire performance of NFCs are based on cone calorimetry experiments and do not account for actual fire resistance. There appears to be some disparity between different researchers on the thermal and fire performance of NFCs. The disparity suggests that the fibre type, matrix type and interaction between the two have a significant influence on the mechanisms of thermal decomposition. It also suggests that these mechanisms are not yet fully understood.

With an increase in the volume content of natural fibres, there is a delay in ignition, an increase in the thermal resistance of the material, which is manifested as a reduction in temperature increase through depth with respect to time, a reduction in pyrolysis depth and a reduction in char thickness. The ignition is arrested by the increase in the volume of less ignitable gases at the surface of the material. This mechanism is associated with the decomposition of hemicellulose in hemp fibres.

The char region may mainly be composed of charred fibres with little evidence of the decomposition of polyester. The char temperature may be constant with respect to the volume of fibres and increases with an increase in exposure time. This mechanism is associated with the production of monomers, which requires higher temperatures for further decomposition to occur.

The degradation of mechanical properties in the char region of NFCs is characterised as a loss of fibre strength, and the degradation of mechanical properties in the degradation region is characterised as a combination of the degradation of the interfacial bond and a reduction in fibre strength.

There is a potential avenue for further research to develop a thermomechanical model that can describe the fibre−matrix interaction. If this can be achieved, the model could be applied in principle to any material where the decomposition kinetics of the fibres is known. Further mechanical testing is recommended including flexural and

compressive tests. There is a large scope for potential work in this area. Additionally, mechanical testing at high temperatures is recommended to investigate the structural integrity of the material during a fire. The heat transfer model could be used as a powerful analysis tool for further research to account for moisture diffusion.

The mechanical degradation has been characterised as a degradation of the interfacial bond due to the decomposition of lignin. Fibre treatment methods, which reduce the volume of lignin and hemicellulose, could improve the residual mechanical properties of fire damaged NFCs by eliminating the mechanism for the degradation of the interfacial bond. It will be interesting and potentially very important to investigate how fibre surface treatment will change the dynamics of decomposition and residual mechanical properties. It is an especially important parameter to investigate given the volume of research dedicated to this field of study.

References

Agarwal, R., 2006. Thermal conduction and diffusion through polyester composites. Indian Journal of Pure and Applied Physics 44, 746.

Alix, S., Marais, S., Morvan, C., Lebrun, L., 2008. Biocomposite materials from flax plants: preparation and properties. Composites Part A: Applied Science and Manufacturing 39 (12), 1793−1801.

Bahramian, A.R., Kokabi, M., 2011. Numerical and experimental evaluations of the flammability and pyrolysis of a resole-based nanocomposite by cone calorimeter. Iranian Polymer Journal 20 (5), 399−411.

Behzad, T., Sain, M., 2008. Measurement and prediction of thermal conductivity of hemp fibre reinforced composites. Polymer Engineering and Science 47 (7), 977−983.

Behzad, T., Sain, M., 2007. Measurement and prediction of thermal conductivity for hemp fiber reinforced composites. Polymer Engineering & Science 47 (7), 977−983.

Beyler, C.L., Hirschler, M.M., 2002. Thermal Decomposition of Polymers. SFPE Handbook of Fire Protection Engineering. NFPA, Quincy.

Biswal, M., Mohanty, S., Nayak, S.K., 2012. Thermal stability and flammability of banana-fiber-reinforced polypropylene nanocomposites. Journal of Applied Polymer Science 125 (S2), E432−E443.

Bodros, E., Pillin, I., Montrelay, N., Baley, C., 2007. Could biopolymers reinforced by randomly scattered flax fibre be used in structural applications? Composites Science and Technology 67 (3−4), 462−470.

Braun, E., Levin, B.C., 1986. Polyesters: a review of the literature on products of combustion and toxicity. Fire and Materials 10, 107−123.

Bregulla, J., 2003. Investigation into the Fire and Racking Behaviour of Structural Sandwich Panel Walls. University of Surrey.

Burchill, P.J., Mathys, Z., Gardiner, C.P., 2005. An analysis of the burning of polyester and vinylester fibre glass composites. Fire and Materials 29 (4), 249−264.

Ceylan, Ö., Alongi, J., Van Landuyt, L., Frache, A., De Clerck, K., 2012. Combustion characteristics of cellulosic loose fibres. Fire and Materials 37 (6), 482−490.

Chand, N., Verma, S., 1989. Effect of chloride-based fire retardant on the physico-mechanical characteristics of sunhemp fibre. Journal of Materials Science Letters 8 (8), 891−892.

Chapple, S., Anandjiwala, R., 2010. Flammability of natural fiber-reinforced composites and strategies for fire retardancy: a review. Journal of Thermoplastic Composite Materials 23 (6), 871−893.

Cripps, A., Handyside, R., Dewar, L., Fovargue, J., 2004. Crops in Construction Handbook. CIRIA, London.

Dai, D., Fan, M., 2010. Characteristic and performance of elementary hemp fibre. Materials Sciences and Applications 1, 336−342.

Davies, J.M., Wang, H.B., 1998. Glass reinforced phenolic laminates subject to hydrocarbon fire test. FRC'98, Seven International Conference on Fibre Reinforced Composites, 1998. University of Newcastle Upon Tyne.

Dodds, N., Gibson, A.G., Dewhurst, D., Davies, J.M., 2000. Fire behaviour of composite laminates. Composites Part A: Applied Science and Manufacturing 31, 689−702.

Dorez, G., Taguet, A., Ferry, L., Lopez-Cuesta, J.M., 2013. Thermal and fire behavior of natural fibers/PBS biocomposites. Polymer Degradation and Stability 98 (1), 87−95.

Fan, M., 2010. Characterisation and performance of elementary hemp fibre: factors influencing tensile strength. Bio Resources 5 (4), 2307.

Feih, S., Mouritz, A.P., 2012. Tensile properties of carbon fibres and carbon fibre−polymer composites in fire. Composites Part A: Applied Science and Manufacturing 43 (5), 765−772.

Feih, S., Mouritz, A.P., Mathys, Z., Gibson, A.G., 2007. Tensile strength modeling of glass fiber—polymer composites in fire. Journal of Composite Materials 41 (19), 2387−2410.

Feng, X., Chen, J., Zhang, H., 2008. Effect of high temperature alkali cooking on the constituents, structure and thermal degradation of hemp fiber. Journal of Applied Polymer Science 108 (6), 4058−4064.

Fink, J.K., 2005. Reactive Polymers. Fundamentals and Applications. A Concise Guide to Industrial Polymers. William Andrew, Inc, Norwich NY, USA.

Fowler, P.A., Hughes, J.M., Elias, R.M., 2006. Biocomposites: technology, environmental credentials and market forces. Journal of the Science of Food and Agriculture 86 (12), 1781−1789.

Gibson, A.G., Wu, Y.-S, Chandler, H.W., Wilcox, J.A.D., Bettes, P., 1995. A model for the thermal performance of thick composite laminates in hydrocarbon fires. Revue de L'Institut Francais du Petrole 50 (1), 69−74.

Gibson, A.G., Wright, P.N.H., Wu, Y.-S, Mouritz, A.P., Mathys, Z., Gardiner, C.P., 2003. Modelling residual mechanical properties of polymer composites after fire. Plastics, Rubber & Composites 32 (2), 81−90.

Halliwell, S., Reynolds, T., 2003. Fibre Rienforced Polymers in Construction: Long-term Performance in Use. BRE Bookshop, London.

Halliwell, S., Reynolds, T., 2004. Fibre Reinforced Polymer Materials in Construction. BRE Bookshop, Watford.

Hapuarachchi, D., 2006. The Feasability of Natural Fibre Sheet Molding Compound for Application in Construction- Reaction to Fire Investigations. Queen Mary University, London.

Hapuarachchi, T.D., Ren, G., Fan, M., Hogg, P.J., Peijs, T., 2007. Fire retardancy of natural fibre reinforced sheet moulding compound. Applied Composite Materials 14 (4), 251−264.

Idicula, M., Boudenne, A., Umadevi, L., Ibos, L., Candau, Y., Thomas, S., 2006. Thermophysical properties of natural fibre reinforced polyester composites. Composites Science and Technology 66 (15), 2719−2725.

Kaczmar, J.W., Pach, J., Burgstaller, C., 2011. The chemically treated hemp fibres to reinforce polymers. Polimery 56 (11−12), 817.

Kandare, E., Kandola, B.K., Mccarthy, E.D., Myler, P., Edwards, G., Jifeng, Y., Wang, Y.C., 2011. Fiber-reinforced epoxy composites exposed to high temperature environments. Part II: modeling mechanical property degradation. Journal of Composite Materials 45 (14), 1511−1521.

Kim, H.-S., Yang, H.-S., Kim, H.-J., Lee, B.-J., Hwang, T.-S., 2005. Thermal properties of agro-flour-filled biodegradable polymer bio-composites. Journal of Thermal Analysis & Calorimetry 81 (2), 299−306.

Koo, J.H., Venumbaka, S., Cassidy, P.E., Fitch, J.W., Grand, A.F., Bundick, J., 2000. Flammability studies of thermally resistant polymers using cone calorimetry. Fire and Materials 24 (5), 209−218.

Kozlowski, R., Wladyka-Przybylak, M., 2008. Flammability and fire resistance of composites reinforced by natural fibers. Polymers for Advanced Technologies 19 (6), 446−453.

Kozlowski, R., Mieleniak, B., Muzyczek, M., Kubacki, A., 2002. Flexible fire barriers based on natural nonwoven textiles. Fire and Materials 26 (4−5), 243−246.

Kymalainen, H., Sjoberg, A., 2008. Flax and hemp fibres as raw material for thermal insulations. Building and Environment 43, 1261.

Lattimer, B.Y., Goodrich, T.W., Chodak, J., Cain, C., 2009. Properties of composite materials for high temperature response. In: The 17th International Conference on Composite Materials 2009.

Lattimer, B.Y., Ouellette, J., 2006. Properties of composite materials for thermal analysis involving fires. Composites Part A: Applied Science and Manufacturing 37 (7), 1068−1081.

Le Bras, M., Duquesne, S., Fois, M., Grisel, M., Poutch, F., 2005. Intumescent polypropylene/flax blends: a preliminary study. Polymer Degradation and Stability 88 (1), 80−84.

Li, X., Tabil, L.G., Oguocha, I.N., Panigrahi, S., 2008. Thermal diffusivity, thermal conductivity, and specific heat of flax fiber−HDPE biocomposites at processing temperatures. Composites Science and Technology 68 (7−8), 1753−1758.

Liu, K., Takagi, H., Yang, Z., 2011. Evaluation of transverse thermal conductivity of Manila hemp fiber in solid region using theoretical method and finite element method. Materials & Design 32 (8−9), 4586−4589.

Madsen, B., Hoffmeyer, P., Lilholt, H., 2007. Hemp Yarn reinforced composites-II. Tensile properties. Composites Part A: Applied Science and Manufacturing 38 (10), 2204−2215.

Manfredi, L.B., Rodríguez, E.S., Wladyka-Przybylak, M., Vázquez, A., 2006. Thermal degradation and fire resistance of unsaturated polyester, modified acrylic resins and their composites with natural fibres. Polymer Degradation and Stability 91 (2), 255−261.

Maxwell, J.C., 1954. A Treatise on Electricity & Magnetism, fourth ed. General Publishing Company, Canada.

Mehta, G., Mohanty, A.K., Thayer, K., Misra, M., Drzal, L.T., 2005. Novel biocomposites sheet molding compounds for low cost housing panel applications. Journal of Polymers and the Environment 13 (2), 169−175.

Ming, G., Qui-Ju, D., 2006. Studies on the thermal degradation of cellulosic fibers treated with flame retardants. The Chinese Journal of Process Engineering 6 (2).

Mohanty, A., 2009. Natural Fibres, Biopolymers and Their Biocomposites, 15/12/09.

Morgan, A.B., Gagliardi, N.A., Price, W.A., Galaska, M.L., 2009. Cone calorimeter testing of S2 glass reinforced polymer composites. Fire and Materials 33 (7), 323−344.

Morgan, A.B., Gilman, J.W., 2012. An overview of flame retardancy of polymeric materials: application, technology, and future directions. Fire and Materials 37 (4), 259−279.

Mouritz, A.P., Mathys, Z., 2000. Mechanical properties of fire-damaged glass-reinforced phenolic composites. Fire and Materials 24 (2), 67−75.

Mouritz, A.P., Feih, S., Mathys, Z., Gibson, A.G., 2011. Mechanical property degradation of naval composite materials. Fire Technology 47 (4), 913−939.

Mouritz, A.P., Mathys, Z., Gibson, A.G., 2006. Heat resistance of polymer composites in fire. Composites Part A: Applied Science and Manufacturing 37 (6), 1040−1054.

Mouritz, A.P., Mathys, Z., Gardiner, C.P., 2004. Thermomechanical modelling the fire properties of fibre−polymer composites. Composites Part B: Engineering 35 (6−8), 467−474.

Naughton, A., 2013. Fire characterization of natural fibre composites for building construction. University of London.

Nechwatal, A., Mieck, K., Reussmann, T., 2003. Developments in the characterization of natural fibre properties and in the use of natural fibres for composites. Composites Science and Technology 63 (9), 1273−1279.

Naughton, A., Fan, M., Bregulla, J., 2014. Fire resistance characterisation of hemp fibre reinforced polyester composites for use in the construction industry. Composite Part B Engineering 60, 546−554.

Patten, G.A., 1961. Ignition temperatures of plastics. Modern Plastics 38 (11), 119.

Peacock, R.D., Babrauskas, V., 1991. Analysis of large-scale fire test data. Fire Safety Journal 17 (5), 387−414.

Pejic, B.M., Kostic, M.M., Skundric, P.D., Praskalo, J.Z., 2008. The effects of hemicelluloses and lignin removal on water uptake behavior of hemp fibers. Bioresource Technology 99 (15), 7152−7159.

Pickering, K.L., Beckermann, G.W., Alam, S.N., Foreman, N.J., 2007. Optimising industrial hemp fibre for composites. Composites Part A: Applied Science and Manufacturing 38 (2), 461−468.

Placet, V., 2006. Characterization of the Thermo-mechanical Behaviour of Hemp Fibres Intended for the Manufacturing of High Performance Composites. http://arxiv.org/ftp/arxiv/papers/0906/0906.3597.pdf edn.

Placet, V., Trivaudey, F., Cisse, O., Gucheret-retel, V., Boubakar, M.L., 2012. Diameter dependence of the apparent tensile modulus of hemp fibres. A morphological, structural and ultrastructural effect? Composite Part A. Applied Science and Manufacturing 43 (2), 275−282.

Rockett, A., 1988. Conduction of heat in solids. In: NFPA (Ed.), The SFPA Handbook of Fire Protection Engineering, first ed. NFPA, Quincy, MA, pp. 1−49.

Roulac, J.W., 1997. Hemp Horizons: The Comeback of the World's Most Promising Plant. Chelsea Green Publishing Co, White River Junction.

Rudin, A., 1999. The Elements of Polymer Science and Engineering, second ed. Academic Press, London.

Rudnik, E., 2007. Thermal properties of biocomposites. Journal of Thermal Analysis & Calorimetry 88 (2), 495−498.

Russell, H.W., 1935. Principles of heat flow in porous insulators. Journal of the American Ceramic Society 18 (1−12), 1−5.

Silva, F.D.A., Chawla, N., Filho, R.D.D.T., 2008. Tensile behavior of high performance natural (sisal) fibers. Composites Science and Technology 68 (15−16), 3438−3443.

Springer, S.G., Tsai, S.W., 1967. Thermal conductivity of unidirectional materials. Journal of Composite Materials. 1 (2), 166−173.

Stafford, P.G., Bigwood, J., 1992. Psychedelics Encyclopedia. Ronin Publishing Inc., Oakland.

Thygesen, A., 2006. Properties of Hemp Fibre Polymer Composites- An Optimisation of Fibre Properties Using Novel Defibration Methods and Fibre Characterisation. Royal Veterinary and Agricultural University, Denmark.

Virk, A.S., 2010. Numerical Models for Natural Fibre Composites With Stochastic Properties (Ph.D. edn). University of Plymouth, Plymouth.

Wan Abdul Rahman, W.A., Sin, L.T., Rahmat, A.R., 2008. Injection moulding simulation analysis of natural fiber composite window frame. Journal of Materials Processing Technology 197 (1−3), 22−30.

Wang, H.B., 1995. Heat Transfer Analysis of Components of Construction Exposed to Fire- A Theoretical, Numerical and Experimental Approach (Ph.D. edn). University of Salford, Manchester.

Zampaloni, M., Pourboghrat, F., Yankovich, S.A., Rodgers, B.N., Moore, J., Drzal, L.T., Mohanty, A.K., Misra, M., 2007. Kenaf natural fiber reinforced polypropylene composites: a discussion on manufacturing problems and solutions. Composites Part A: Applied Science and Manufacturing 38 (6), 1569−1580.

Temperature sensitive colour-changed composites

15

F. Fu, L. Hu
Research Institute of Wood Industry, Chinese Academy of Forestry, Beijing, China

15.1 Introduction

The colour-changed material is a new type of functional material, which changes its colour under the external stimuli, belonging to the category of smart materials (Seeboth et al., 2007). According to the type of stimuli sources including temperature, light, electricity, pressure and magnetic, the colour-changed materials are divided into various categories (Ferrara and Bengisu, 2014). In recent years, temperature sensitive colour-changed materials, which are also termed "thermochromic" materials, have aroused much interest in the field of functional materials. The thermochromic material refers to materials that appear colour change phenomenon within a specific temperature range due to the change of their structures (White and LeBlanc, 1999), and has been widely used in the field of smart textile, security printing, temperature indicator and daily decoration.

With the rapid development of functional and intelligent wood products, thermochromic materials combine with wood to form a novel functional material: thermochromic wood composite. The unique colour-changed properties would greatly enrich the visual characteristics of wood products and thus increase their value-in-use. A variety of inorganic, mesomorphic and organic thermochromic materials provide much room to choose colour categories and colour-changed behaviours, and to meet the needs for different occasions. Nevertheless, current research and development has been mainly focussing on reversible thermochromic wood composites. These products are able to present repeated colour changes between two different colours, and have broad application prospects in the field of floor, furniture and building wall (Jiang et al., 2013; Liu et al., 2011, 2012). The development and application of smart wood materials such as thermochromic wood composites would inevitably promote the intelligentization of modern home.

15.2 Temperature sensitive colour-changed compounds

15.2.1 Classification

Numerous thermochromic materials have been developed and applied to many industrial sectors since 1960s. They are classified based on their colour-changed features or chemical composition. According to the reversibility of the colour-changed process,

Advanced High Strength Natural Fibre Composites in Construction. http://dx.doi.org/10.1016/B978-0-08-100411-1.00015-7

they are divided into reversible and irreversible groups. The colour of the former can repeatedly change between A and B during heating and cooling, while the colour of the later alters only once. On the basis of colour-changed temperature, they are classified into high-temperature (>100°C) and low-temperature (<100°C) groups. In terms of the chemical composition, they are categorized into inorganic, liquid crystal and organic compounds. This classification is most commonly used by researchers and such adopted in the following discussions.

Inorganic thermochromic compounds generally contain iodide, coordination compound and double salt of Ag, Cu and Hg, as well as chemical compound generated from the reaction between cobalt and nickel salt and methenamine. In addition, chromate, vanadate and tungstate have also become important sources of inorganic thermochromic materials. Thermochromic liquid crystals mainly include cholesteric liquid crystal and cyano biphenyl liquid crystal. Organic thermochromic compounds can be further divided into two categories. One group consists of single component (such as Schiff bases, spiro and double anthracene ketone chemicals), and its colour-changed properties are ascribed to changes in the composition or structure after heating. Another group is the mixture of some compounds which individually show no colour-changed phenomenon under heating. The typical mixture is the combination of crystal violet lactone, bisphenol A and polyol compound.

The basic performance of inorganic, liquid crystal and organic thermochromic compounds is presented in Table 15.1. The inorganic type shows advantages of simple

Table 15.1 Property comparison between three categories of thermochromic materials

Property		Inorganic thermochromic material	Organic thermochromic material	Liquid crystal thermochromic material
Colour-changed temperature (°C)	−100 ~ −50	No	Yes	No
	−50−0	No	Yes	Few
	0−50	No	Yes	Yes
	50−100	Few	Yes	Yes
	100−200	Yes	Yes	Yes
Colour change	Colour to colourless	No	Yes	No
	Colour A to colour B	Yes	Yes	Yes
Colour-changed sensitivity		Moderate	High	High
Photo stability		High	Moderate	Moderate
Toxicity		High	Low	Low
Cost		Moderate	Low	High

synthesis process, low cost and excellent light fastness, but its application areas are limited due to its narrow range of colour-changed temperature, high toxicity and poor colour-changed sensitivity. The thermochromic liquid crystal has a relatively wide range of colour-changed temperature and high colour-changed sensitivity; nevertheless it is difficult to fully commercialize it at the moment for its shortcomings of light colour, few colour categories and expensive price. Compared with inorganic and liquid crystal types, the organic thermochromic compounds have more advantages in terms of more colour categories, wider range of colour-changed temperature and lower cost. Therefore, the development and application of organic thermochromic materials have become the research focus in the field of thermochromic materials.

15.2.2 Application

15.2.2.1 Textile industry

Along with growing demands for high-grade and personalized products, as well as the maturation of thermochromic technologies, many temperature sensitive colour-changed fibres and clothing have appeared in the textile industry (Chowdhury et al., 2014). In 1980s, the American Del Sol Company began to use the thermochromic dyes to produce shirts with special colour characteristics. Thermochromic fibres developed by the Japanese Toray company were able to display eight different colours in the temperature range from −40 to 80°C, and were welcomed by its industry peers. Thermochromic materials enable the colour or pattern of textiles to change with temperature, showing a "dynamic change" effect. Hence these particular products are in line with the modern consumer demand for fashions, and have been widely used in T-shirts, pants, swimming suit, leisure sports clothing, work clothes, children's clothing, curtains, wall cloth and toys. In addition, the thermochromic textiles, which can simulate the variation of surrounding environmental colours, could be used as military protective clothing.

15.2.2.2 Anti-counterfeiting field

Reversible thermochromic materials characterized by repeatedly colour changes are very suitable for anti-counterfeiting treatment, and have been successfully utilized in the production of anti-counterfeiting inks and papers (Dong et al., 2011). The thermochromic anti-forgery inks originated in the late 1950s and have shown their wide applications in the printing industry. They present features of simple-manufacturing process, easy-identification and low cost, and have unique advantages in technical security and anti-fake effectiveness. In 1993, the American Del Sol Company firstly introduced reversible thermochromic materials into paper industry, and developed reversible thermochromic anti-counterfeit paper with the merit of rapid, convenient and accurate identification. Following the advancement of technologies, thermochromic materials have been successfully used in anti-counterfeiting of money, securities, credentials and packages. The organic thermochromic material is the favourite type in anti-fake field, not only for its free selectivity of colour and colour-changed temperature, but also for its high colour-changed sensitivity.

15.2.2.3 Industrial temperature indicator

Thermochromic materials are mainly used as temperature indicators in many industrial sectors, to determine the temperature variation and reaction heat in chemical reactions, to measure temperature distribution of chemical heating apparatus such as heat exchangers and reactors, and to indicate the temperature variation in containers for chemicals and dangerous goods and storage vaults (Smith et al., 2001; Vanderroost et al., 2014). For example, the addition of thermochromic materials to plastic extruder in feeding process could be helpful in judging if the feeding temperature fulfils the processing requirement. At the same time, a wide variety of temperature-sensitive paints can be easily applied for the indication, monitoring and warning of temperature in industrial production.

15.2.2.4 Daily supplies field

At present, the temperature sensitive colour-change material has also entered people's daily life. As an effective temperature indicator, it is utilized to indicate suitable service temperature for the home appliance, as well as proper storage temperature of frozen foods, vegetables and fruits. In addition, baby spoons containing thermochromic materials would change colour rapidly when the food is very hot, warning that the food is not edible for babies. Furthermore, thermochromic materials can also be used in ceramic and plastic products, to make their colour altering with the variation of ambient temperature. The unique decorative effects of these thermochromic daily supplies are expected to greatly enrich people's lives.

15.2.2.5 Other applications

In the medical field, thermochromic materials can be used as temperature indicators in therapeutic process. In the transportation field, they can be used for making road signboard to warm freezing, as well as for warning explosion dangers of overheated tyres. Besides, thermochromic paints can be used as energy-saving coating in architectures (Gobakis et al., 2015). They would reflect the sun light and cool the building in hot summer, while they could absorb solar energy and warm the building when it comes to cold winter. In conclusion, as a new type of high-tech material, the thermochromic material with high added-value and benefit has broad application prospects both in industry fields and in daily life.

15.3 Temperature sensitive colour-changed composites by mixtures impregnation

15.3.1 Colour-changed mechanisms

The organic thermochromic compound is most suitable for wood composites, in consideration of its outstanding advantages: the colour category is rich and it can be selected freely; the colour-changed temperature is low and controllable; the production

cost is relatively low. The organic thermochromic compound, which shows a reversible colour change, is usually composed of the dye (electron donor), the colour developer (electron acceptor) and the solvent. The dye and colour developer determine the colour and colour shade of the mixture respectively, while the temperature range of colour change depends on the solvent (Zhu and Wu, 2005). The thermochromism for the system can be explained by the "electron transfer theory". The oxidation-reduction potential of the electron donor is close to that of the electron accepter. However, when the temperature changes, the variation of oxidation-reduction potential is different for each, which prompt the changes of the redox reaction direction with the variation of temperature. During the oxidation-reduction reactions, the electron transfers between the electron donor and the electron accepter, leading to the structure changes of the dye and thus the reversible changes in the colour of the compound. The red thermochromic mixture, which consists of heat sensitive rose red (TF-R1), bisphenol A and tetradecanol, is taken as a representative to specify the thermochromic mechanism.

The red thermochromic mixture is prepared by stirring the hybrid of TF-R1, bisphenol A and tetradecanol (with a mass ratio of 1:4:40) at temperature of 70°C for 1 h, and the product is red in room temperature but colourless while temperature beyond 38°C. Fig. 15.1 shows spectra of red thermochromic mixture in status of red and colourless. It is found that the chemical structure of the mixture has not changed much during the colour-changed process. The main variation is that a new characteristic peak of 1759 cm^{-1} appears in the spectrum of red mixture. The peak could be ascribed to the stretching vibration of C═O of carboxylic acid. In combination with analysis of other characteristic peaks, it can be concluded that the ester carbonyl (1681 cm^{-1}) of the dye turns into carbonyl of carboxylic acid, which could account for the colour-changed phenomenon of the red mixture (MacLaren and White, 2003).

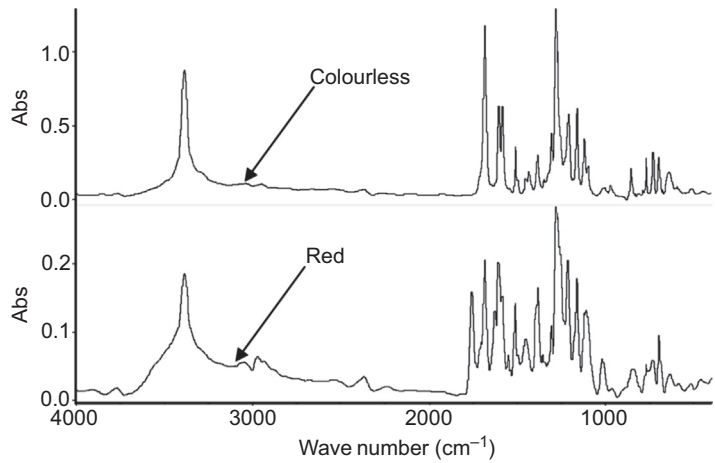

Figure 15.1 FT-IR spectra of red thermochromic mixture in colour-changed process.

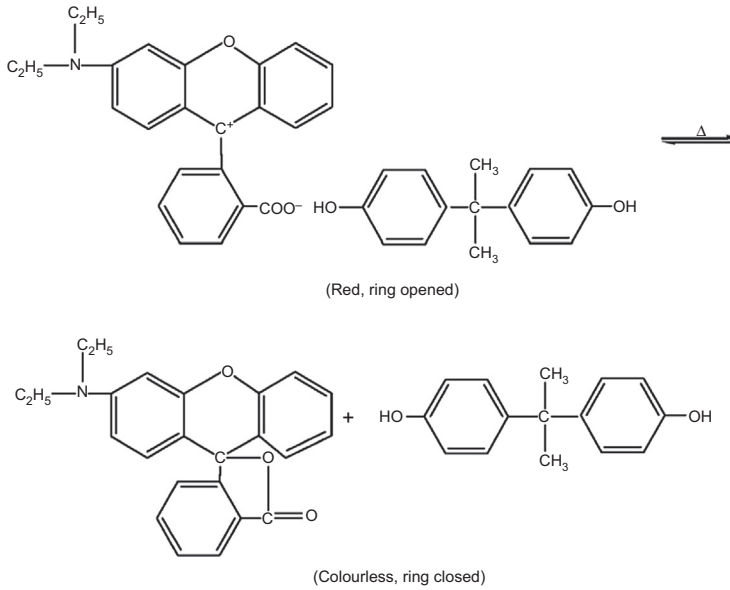

Figure 15.2 Reaction formula of red thermochromic mixture in colour-changed process (Zhu and Wu, 2005).

According to the above analysis, the lactonic ring of TF-R1 opens at low temperature but closes at high temperature with the action of bisphenol A, accompanied by electron transfers between each other (Zhu and Wu, 2005). TF-R1 with an opened lactonic ring presents red colour, while the mixture containing TF-R1 with a closed lactonic ring turns into colourless. Therefore, the colour of the mixture can repeatedly vary between red and colourless following the change of temperature. The possible reaction formulation for the red thermochromic mixture in colour-changed process is shown in Fig. 15.2.

15.3.2 Impregnation methods and performance

Impregnating treatment, which is a common method for wood modification, has become a convenient way to prepare thermochromic wood composites. The wood units for impregnation could be block lumbers or laminar veneers. During the treatment, temperature must be kept above the melting point of the solvent in order to avoid the solidification of the mixture. Rising temperature or ultrasonic assistant treatment during impregnating process would contribute to a more uniform distribution of the mixture in wood materials (Liu et al., 2011). The permeability of the thermochromic materials in wood is anisotropic, as shown in Table 15.2. The rates of weight gain in tangential and radial directions are about half that of in the longitudinal direction. The red compound shows the best permeability than others, which suggests that the permeability for different categories of thermochromic compounds varies due to their different surface tension and polarity. Generally, the colour-changed effect is mainly

Table 15.2 The permeability anisotropy of thermochromic agent in *Populus tomentosa*

Thermochromic agent	Impregnating parameters			Growth rate of weigh (%)		
	Temperature (°C)	Time (h)	Ultrasonic power (W)	Longitudinal	Radial	Tangential
Black-red	55	4	140	30.34	16.66	15.79
Orange-yellow	75	4	120	18.67	7.65	7.01
Blue	75	4	120	20.39	13.13	12.12

Note: Sample size 15 × 15 × 15 mm, moisture content 7%, air-dry density 0.40 g/cm^3; when one section of the samples is tested, other sections are sealed with polyvinyl acetate.

determined by the surface property of wood composite, and hence the excessive internal penetration of compound is unnecessary. Above all, impregnation treatment is an effective way to prepare thermochromic wood materials.

Thermochromic property is the most important performance of temperature sensitive colour-changed wood composites, which will be mainly used as interior decoration material, including colour-changed temperature, colour-changed sensitivity and colourimetry parameters. Currently, the performance based evaluation of colour-changed materials remains as the main theme, although these materials have been used in many fields. Usually, colour-changed temperature and sensitivity are tested in simulated environment with climatic cabinet, temperature and humidity chamber, glass water-bath, electrical heating plate and thermocouple facilities. Both potable and online metres have been used to measure colourimetry parameters. Fig. 15.3 shows the surface colours of black-red, orange-yellow and blue thermochromic wood before and after colour-changed process. All of them change colours in the temperature range of 26−32°C, and show high colour-changed sensitivity. Their colourimetry parameters are shown in Table 15.3. The colour difference is more than 35, which suggests that people will have a very strong sense of colour change while observing the thermochromic process of the composite, according to the relationship between colour difference and visual perception (Table 15.4).

As shown in Fig. 15.4, the colour change of reversible thermochromic veneers includes decolourization process and colourization process, and the corresponding variation of colour difference is continuous and finally forms a closed loop. As for decolourization (heating) process, the colour difference of veneers firstly remains stable below 19°C. It then gradually decreases following the temperature rises, and enters in another steady state in 35°C. Conversely, the colour difference gradually increases in colourization (cooling) process. It is worth to note that the colourization temperature (25°C) is lower than the decolourization temperature (31°C), which indicates that the colour change of thermochromic veneers depends not only on the temperature but also the thermal history. This particular phenomenon is named "colour hysteresis" (Kulvcar et al., 2010; Vikov and Vik, 2005). Fig. 15.5 is a good interpretation of this phenomenon, since the decolourization

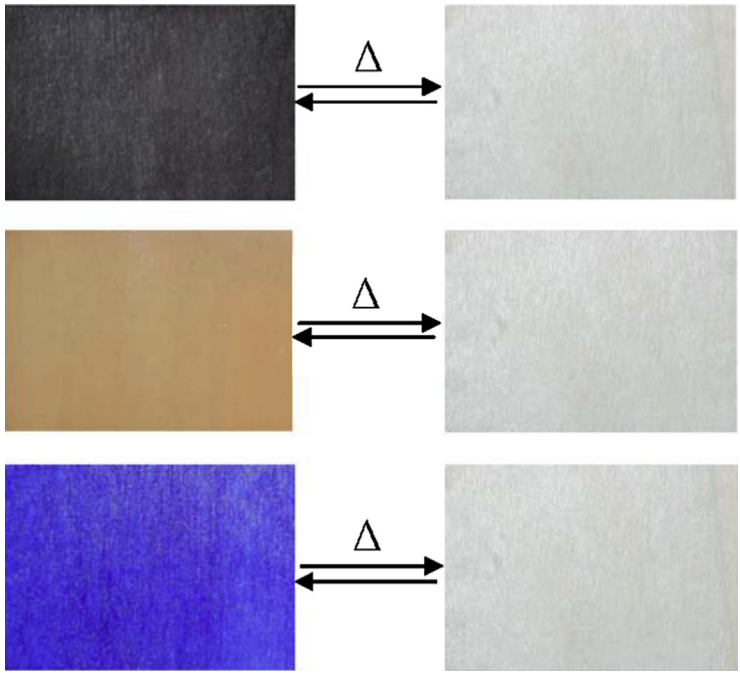

Figure 15.3 The changes of surface colour for thermochromic bleached wood (left = 26°C, right = 32°C).

Table 15.3 The changes of colourimetry parameters of thermochromic bleached wood

Thermochromic agent	Rightness index ΔL	Red-green index Δa	Yellow-blue index Δb	Colour difference ΔE
Black-red	46.72	−7.08	15.66	49.78
Orange-yellow	13.83	−24.15	−22.27	35.64
Blue	65.81	−7.28	20.48	69.31

process is not identical with the colourization process. Therefore, reversible thermochromic veneers belong to physical systems with hysteresis feature.

In addition to thermochromic properties, the colour-changed effectiveness of the thermochromic wood composites is another issue for consumers. Hence, the colour-changed properties of products should be maintained within the service period, especially for reversible thermochromic composites. The organic thermochromic materials generally have a long service life. It is also confirmed that the loss of colour difference for reversible thermochromic veneers was only three to six after 40 cycles of alternate

Table 15.4 The relationship between colour differences (ΔE) and vision

Colour difference ΔE	Visual perception	Variation of the colour
0−0.5	Trace	Unnoticeable change
0.5−1.5	Slight	Slight change
1.5−3.0	Noticeable	Perceivable change
3.0−6.0	Appreciable	Marked change
6.0−12.0	Strong	Extremely marked change
Over 12.0	Very strong	Change to another colour

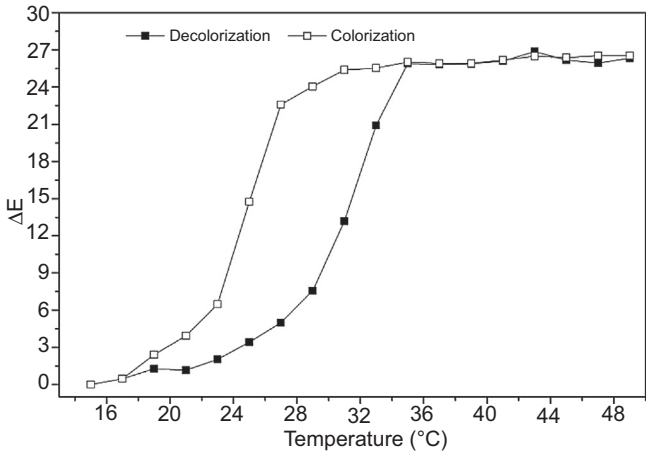

Figure 15.4 Relationship between colour differences (ΔE) and temperature for thermochromic veneers in decolourization and colourization process.

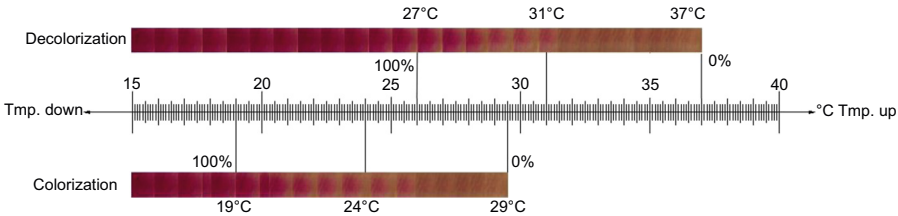

Figure 15.5 Diagram of reversible colour-changed process of thermochromic wood.

cooling and heating treatment. In conclusion, the organic reversible thermochromic materials are able to meet the requirement of long-term use.

Meanwhile, the thermochromic wood composites in use may be affected by light and other climatic conditions, and thus their durability comes to be an important

performance as well. In consideration of the test time and cost, artificial accelerated ageing test methods are preferred for durability evaluation. The common equipment covers metal halide ageing test box, ultraviolet light (UV) ageing chamber, xenon arc lamp ageing chamber and carbon arc lamp ageing chamber. The spectral distribution of the xenon arc lamp ageing chamber is closest to the solar spectrum distribution, and has been recognized as the best simulative light source. The commonly used phenol colour developers have poor light stability (especially UV stability). In order to extend the service life of these thermochromic systems, light stabilizers such as ultraviolet absorber are usually added while applying to wood composites (Fu et al., 2013).

15.3.3 Bonding mechanisms

Thermochromic wood is formed by the infusion of thermochromic materials (as functional fluid) into wood substrate. The series and parallel connections of cell lumens, intercellular spaces and micro capillaries, vessels and pits in the cell wall constitute a complex capillary system. The interconnected structure provides impregnation approach and storage space for thermochromic materials. By impregnating treatment, the thermochromic material can effectively combine with wood substrates in a physical adsorption way.

Moreover, chemical bonding also exists between thermochromic materials and wood substrates. The hydroxyl groups in thermochromic materials are easy to combine with free hydroxyl in wood to form hydrogen bond. Besides, the substitution reaction between thermochromic material and wood could also form chemical bond. In summary, the bonding mechanism for thermochromic wood composites is the combination of physical adsorption and chemical bonding.

Overall, impregnating treatment of wood with organic thermochromic mixture has successfully opened a new chapter of the application of thermochromic materials in wood field. However, the solvent which determines the colour-changed temperature would appear solid−liquid phase transition during colour-changed process, prone to flowing and leaching. Consequently, the performance of the thermochromic wood shows poor stability, which give rise to great inconvenience in its practical application. In order to improve the durability of thermochromic wood products, it is very necessary to develop effective protection technologies for thermochromic systems.

15.4 Temperature sensitive colour-changed composites fabricated by microcapsules

15.4.1 Microencapsulation mechanisms

Microencapsulation is the protective technology of encapsulating solid, liquid or gas materials into micro particles with a diameter of 1−1000 μm, and has been widely used in fields of medicine, cosmetics, food, textile and advanced materials (Campos

et al., 2013; Dubey et al., 2009). The unique advantage of microencapsulation lies in that the core material is completely coated and isolated from external environment. More importantly, microencapsulation would not affect the properties of core materials, provided that proper shell material and preparing method are chosen. Therefore, microencapsulation is very suitable for improving the stability of thermochromic mixtures. After being encapsulated, the thermal stability and the resistances to leaching, acid and solvent for thermochromic materials would be significantly enhanced, which obviously extends their application fields. As a result, the majority of commercial thermochromic materials are produced in the form of microcapsule powders or microcapsule suspensions.

The essence of microencapsulation is that a uniform and stable layer of shell material covers the core material by physical or chemical reactions. The production of microcapsules began in 1930s and boomed in 1970s. According to the forming mechanism and condition of shell, microencapsulation methods can be divided into three categories, namely physical, chemical and physicochemical methods (Jyothi et al., 2010) (Table 15.5). As for physical method, the microencapsulation is based on physical and mechanical principles, and the formation of shell depends on solid−liquid phase transition under heating or solubility reduction due to solvent evaporation. The chemical method is based on chemical reactions, in which the monomers with small molecules polymerize to form the polymer shell. In physicochemical microencapsulation process, the pre-dissolved shell-forming materials precipitate from the solution following the variation of temperature, pH value or electrolyte concentration, and gradually deposit on the surface of core material to form the shell. The ultimate morphology of microcapsules mainly depends on the morphology of core materials. Generally, solid core remains its morphologies during microencapsulation, while microcapsules with liquid core are usually spherical resulting from the process of mechanical dispersion or emulsion.

Currently, complex coacervation and in situ polymerization are usually used to prepare thermochromic microcapsule. The complex coacervation belongs to physicochemical microencapsulation method. Two or more oppositely charged polymeric materials combine together by electrostatic interaction under appropriate conditions

Table 15.5 Classification of microencapsulating methods

Category	Specific methods
Physical method	Spray drying, spray cooling, air suspension, envelop-combination, extrusion, supercritical solution, porous centrifugal, electrostatic binding, solvent evaporation, rotary separation
Chemical method	Interfacial polymerization, in situ polymerization, piercing-solidifying
Physical-chemical method	Simple coacervation, complex coacervation, phase separation, drying bath, powder bed grinding, melting-dispersion-condensation, capsule-core exchange

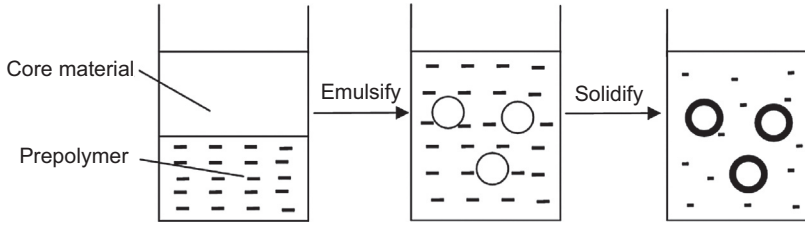

Figure 15.6 Diagram of the in situ polymerization for liquid core materials.

(such as changes in pH or temperature), and gradually deposit on the surface of core materials to form the shell with the decrease of solubility. The typical shell group is the combination of gelatin and gum arabic. During the microencapsulation, the charge number of the two oppositely charged polymers must be identical, and the reaction parameters such as pH and temperature should be accurately controlled.

In situ polymerization is generally carried out in two steps (Fig. 15.6). The first process is the formation of emulsion for liquid core or suspension for solid core. Then, reactive monomers (or soluble prepolymers) slowly precipitate on the core particles under the action of heat and catalysts. The chemical reaction for melamine-formaldehyde resin (a typical shell material for in situ polymerization) during microencapsulation is shown in Fig. 15.7, mainly including the hydroxymethylation between melamine and formaldehyde under alkaline condition and the condensation of prepolymers catalysed by acid and heat. The performance of microcapsules generally depends on synthetic technology of pre-polymer, concentration of shell material, core/shell ratio, emulsifying technology and curing condition.

15.4.2 Production and performance

15.4.2.1 Production and performance of thermochromic microcapsules

The shell material used in coacervation methods such as gelatin-acacia shows relatively low mechanical strength and easily degrades in natural environment. The thermosetting resin used for in situ polymerization has better mechanical strength, thermal stability and durability. During production and application, wood materials would suffer friction, press and even impact. Therefore, microcapsules applied to wood materials should have excellent mechanical performance. Moreover, the shell material for encapsulating thermochromic mixtures should have high transparency, low light absorbance and low refractive index, so as to bring less adverse influences on colour-changed sensitivity and colour shade of core materials. In general, amino resins such as urea-formaldehyde and melamine-formaldehyde, which have excellent mechanical properties, high transparency and low cost, are selected as shell materials to produce thermochromic microcapsules according to the in situ polymerization principle.

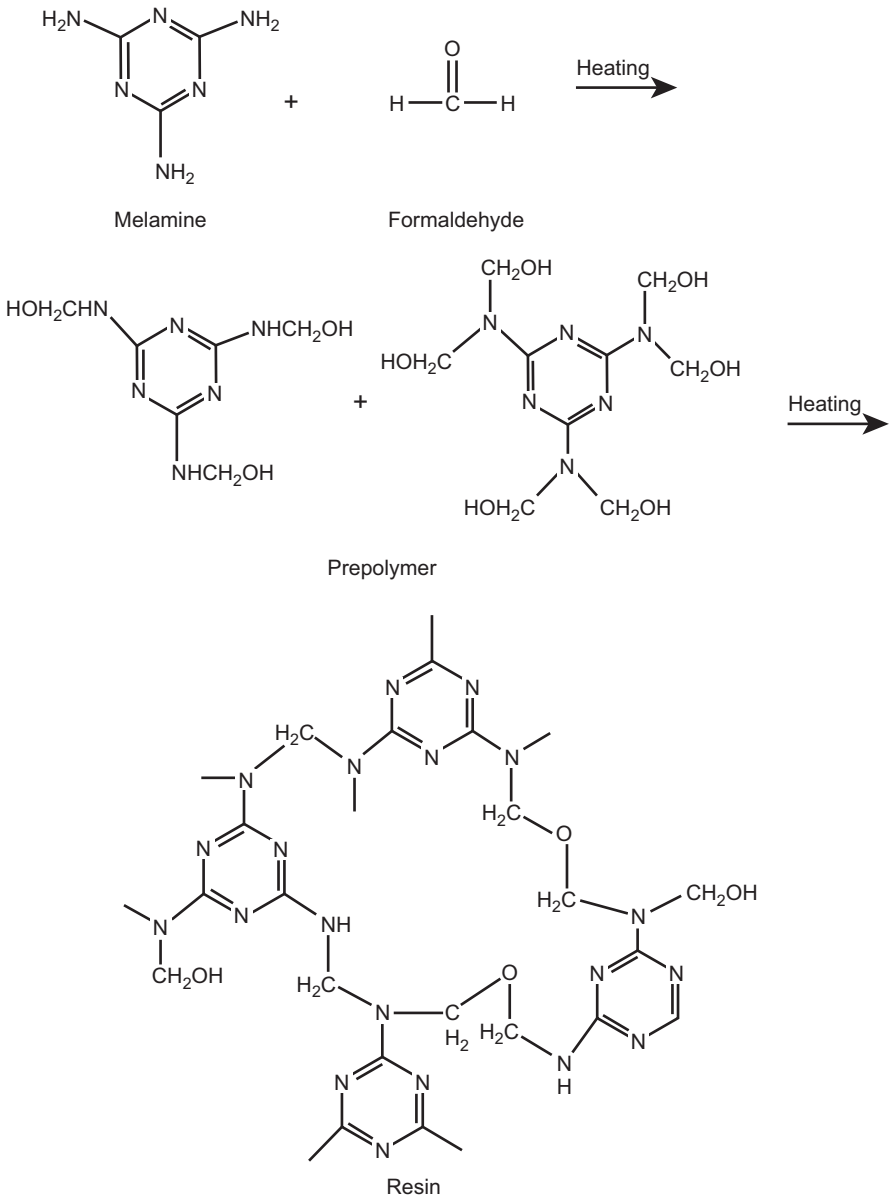

Figure 15.7 Reaction scheme of the formation of melamine-formaldehyde resin (Wu et al., 2009).

Synthesis of the pre-polymer is the first step to prepare microcapsules with amino resin as the shell. The appropriate processes are pH of 8.0−9.0, temperature of 60−80°C and reaction time of 30−90 min. In the subsequent emulsification, oil in water (O/W) emulsifiers should be chosen because the organic thermochromic material

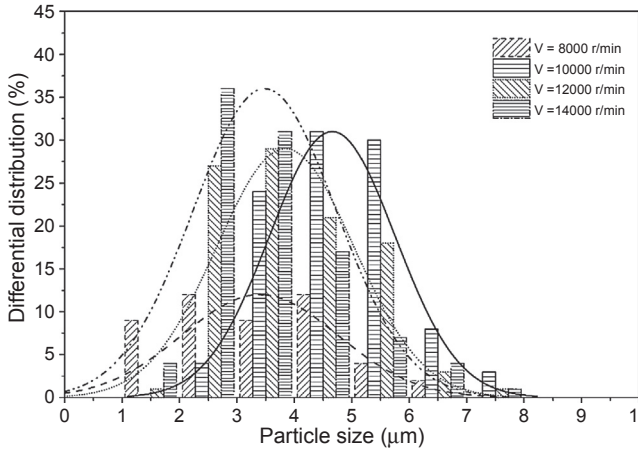

Figure 15.8 Effect of the stirring rate (v) on particle size of microcapsules.

is hydrophobic and lipophilic substance. To be specific, non-ionic surfactants (such as polyvinyl alcohol and gum arabic) and anionic surfactants (such as maleic anhydride copolymer) are preferable emulsifiers. The microcapsule size is mainly determined by the emulsification process, and usually decreases with the increase of stirring rate or dosage of emulsifiers. Generally, the size of microcapsules could be controlled below 10 μm, with a stirring rate beyond 10,000 r/min (Fig. 15.8). The proper dosage of emulsifies is closely related to the species, typically 1−5% by mass of the reaction system. Emulsification time is usually 30−60 min, to ensure the uniform dispersion of emulsion droplets. In the final polymerization stage, optimum process conditions are shell material concentration of 5−10%, core/shell ratio of 3:1 to 1:1, pH of 4−6, reaction temperature of 60−75°C and reaction time of 2−4 h.

The evaluation of thermochromic microcapsules mainly refers to their morphology, particle size distribution, thermal stability and thermochromic properties. Optical microscope and scanning electron microscope (SEM) are commonly used to observe the morphology (Fig. 15.9) of microcapsules, and the ideal condition comes to be that microcapsules are all spherical and show no aggregation. The particle size distribution

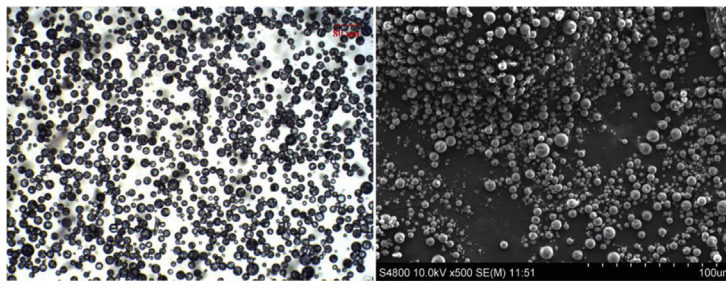

Figure 15.9 Morphologies of thermochromic microcapsules (*left*-optical micrograph, *right*-SEM image).

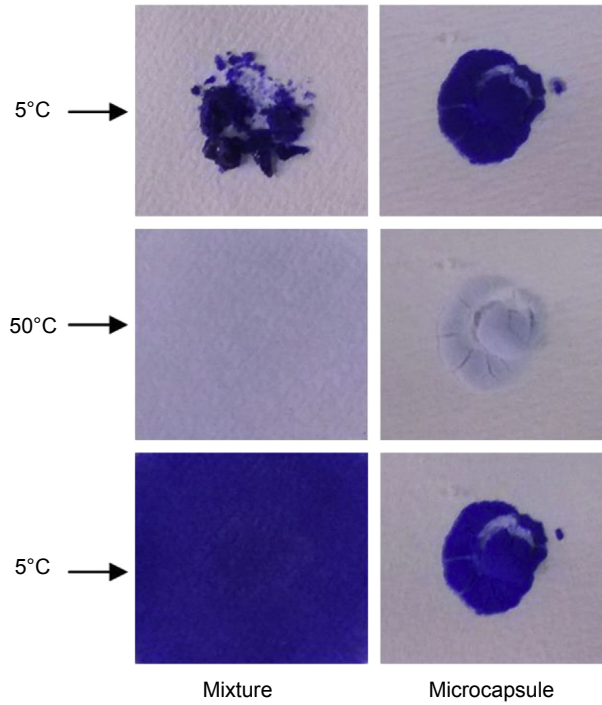

Figure 15.10 Appearance of thermochromic mixture and microcapsule in reversible colour-changed process.

is usually directly obtained from laser particle size analyser, and can also be evaluated by the combination of microscope with dimension testing software. Thermochromic microcapsules with smaller size have larger specific surface area for heat transfer and thus show higher colour-changed sensitivity, but the synthesis and separation will be relatively difficult for smaller particles. The thermal stability of microcapsules is usually measured by thermal gravimetric analyser. The microcapsules applied to wood composites should maintain the morphology and performance during heating processes such as hot pressing. The thermochromic properties of microcapsules mainly depend on the core materials. Nevertheless, it is worth noting that some chemicals used in microencapsulation may damage the colour shade or stability of the thermochromic mixture. As can be seen from Fig. 15.10, unprotected thermochromic agent will melt and flow in colour-changed process, while the microcapsules can retain their morphology. The microencapsulation is an effective way to improve the stability of thermochromic mixture.

15.4.2.2 Production and evaluation of thermochromic wood composites

Adding the thermochromic microcapsules into wood coating is a convenient way to prepare thermochromic wood composite. The performance of the thermochromic film

should meet the requirements regulated in standards of furniture, flooring and other wood products. It is not suitable to add microcapsules into top coat, because the microcapsules may be damaged under long-term wear if they stay in the surface of composites. Adding the microcapsules into base coat may weaken the bonding strength between film and substrate, and is also not recommended. Furthermore, the thermochromic microcapsules should be evenly distributed in the film, in order to obtain uniform colours. The content of microcapsules in coatings should be moderate, since less addition would be cost-effective and reduce the negative impact on coating performance.

Another way to fabricate thermochromic wood materials is to impregnate the wood with microcapsule suspension. During the treatment, microcapsules fill with pores on the wood surface, endowing the wood with colour-changed function. Compared with the above coating method, impregnation process will consume more microcapsules and thus increases the cost. Meanwhile, bonding strength between microcapsules and wood is weak, which may adversely affect the following finish process. However, the thermochromic wood composites fabricated by impregnating method can retain part of the natural texture of wood, and thereby display a particular decorative effect.

Thermochromic microcapsules can also be added into adhesives to prepare thermochromic wood-based composites, according to conventional production process. Thermochromic wood/plastic composites (WPC) could be prepared by mixing the microcapsules with wood and plastic during moulding process. The thermochromic composites should be as thin as possible to reduce production cost. Thermochromic sheet with good mechanical strength would bring new vitality into interior decoration industry.

15.4.3 Incorporating mechanisms

As described in the previous section, thermochromic microcapsules can be incorporated into wood composites by three methods, depending on the structural characteristics of wood composite (Fig. 15.11). Wood consists of micro-to-nano natural pores, which provides enough space for thermochromic microcapsules. Hayward et al. (2014) pointed out that pressure treatment is an effective way to prepare preservative-treated wood if the diameter of microcapsules was less than 20 μm. As for larger microcapsules, bigger pores can be obtained by pre-treatment technologies such as microwave puffing to realize effective incorporation (He et al., 2014).

With regard to wood-based panels, the microcapsules can be incorporated into wood materials by simply blending them with adhesives. In this case, microcapsules size can vary in a large scope, but microcapsules must be strong enough to maintain their morphology and function under heat and pressure. Furthermore, wood materials often require finishing treatment before use, and thus adding the microcapsules into coating is a convenient way to combine the wood materials with microcapsules. The thickness of the coating layer is typically tens to hundreds micrometres. Meanwhile, finishing technology generally contains several painting processes, leading to that the layer painted once is obviously thinner than the final film. Therefore, it is recommended that the diameter of microcapsules should be smaller than 10 μm, to reduce the adverse effect of microcapsules on coating performance.

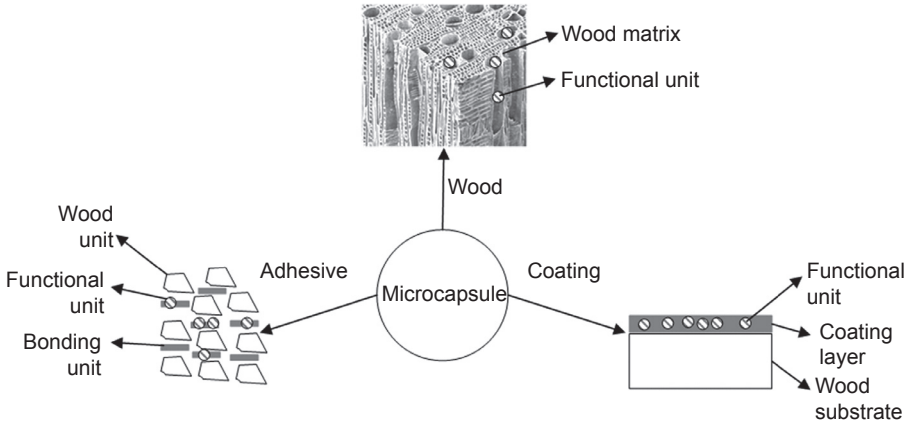

Figure 15.11 Schematic diagram for incorporation methods of microcapsules into wood materials.

15.5 Future trends

As a new emerging wood functional composite product, thermochromic wood composites have injected much vitality into the diversification and intelligence of home furnishing products. Thermochromic wood composites are suitable for uses as indoor refurbishing materials, such as shutter (Fig. 15.12), floor and wallboard. The unique colour-changed features will bring new experience to consumers. Meanwhile, temperature sensitive colour-changed wood composite (Fig. 15.13) is a novel raw material for industries of craft, furniture and architecture. In addition to the refurbishing applications, thermochromic materials also have the potential to become temperature indicators for wood composites. A thermochromic wood baby tub, which turns into

Figure 15.12 Temperature sensitive colour-changed shutters.

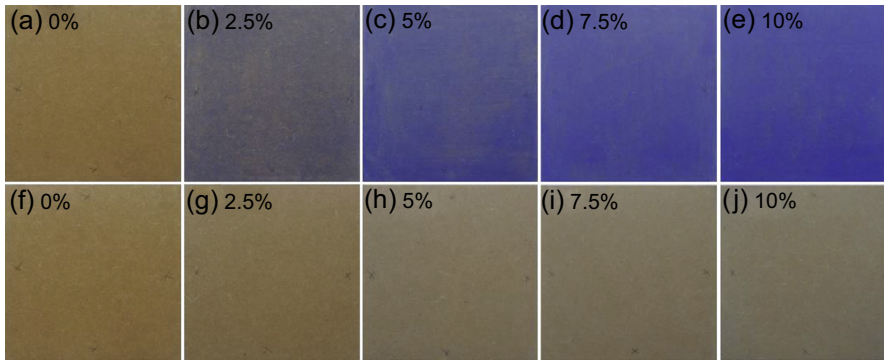

Figure 15.13 Appearance of thermochromic MDF at 10°C (a–e) and 50°C (f–j) with various microcapsule concentrations (Hu et al., 2016).

different colours with the variation of temperature, will enable parents to know the water temperature as well as water level in tub and thus to avoid uncomforted to the baby.

Although many mature products of thermochromic compounds are available in the current market, it is still necessary to further reduce the production cost and develop new compounds with multiple colours and excellent durability. Meanwhile, the bonding mechanism between microcapsules and wood substrate should be studied in-depth, and the effects of specific production processes (such as hot press and finishing) and external environment (such as heat and light) on the properties of thermochromic wood composites still needs systematic investigation, in order to provide more theoretical basis for their production and application. At the same time, the standardized assessment system for thermochromic wood products remains to be build, building up from evaluation systems available for wood products and thermochromic materials. A standardized evaluation system is expected to effectively guide production and application of thermochromic wood composites, which will be beneficial to the healthy and sustainable development of this burgeoning industry.

Acknowledgements

This work was financially funded by the National High Technology Research and Development Program of China (863. Programme) (No. 2010AA101704).

References

Campos, E., Branquinho, J., Carreira, A.S., Carvalho, A., Coimbra, P., Ferreira, P., Gil, M.H., 2013. Designing polymeric microparticles for biomedical and industrial applications. European Polymer Journal 49 (8), 2005–2021.

Chowdhury, M.A., Joshi, M., Butola, B.S., 2014. Photochromic and thermochromic colourants in textile applications. Journal of Engineered Fibers and Fabrics 9, 107–123.

Dong, C.H., Liu, Y., Long, Z., Pang, Z.Q., Luo, Y.H., Li, X.Z., 2011. Effect of papermaking conditions on the retention of reversible thermochromic microcapsule in paper. BioResources 7 (1), 66−77.

Dubey, R., Shami, T.C., Rao, K.U., 2009. Microencapsulation technology and applications. Defence Science Journal 59 (1), 82−95.

Ferrara, M., Bengisu, M., 2014. Materials That Change Colour: Smart Materials, Intelligent Design. Springer.

Fu, F., Jiang, H.C., Lu, K.Y., 2013. Effect of ultraviolet absorber on light fastness of thermochromic wood. China Wood Industry 27 (6), 9−12.

Gobakis, K., Kolokotsa, D., Maravelaki-Kalaitzaki, N., Perdikatsis, V., Santamouris, M., 2015. Development and analysis of advanced inorganic coatings for buildings and urban structures. Energy and Buildings 89, 196−205.

Hayward, P.J., Rae, W.J., Black, J.M., 2014. Encapsulated Wood Preservatives. US 20140057095, pp. 1−6.

He, S., Lin, L.Y., Fu, F., Zhou, Y.D., Fan, M.Z., 2014. Microwave treatment for enhancing the liquid permeability of Chinese fir. BioResources 9 (2), 1924−1938.

Hu, L., Lv, S.Y., Fu, F., Huang, J.D., Wang, S.Q., 2016. Preparation and properties of multifunctional thermochromic energy-storage wood materials. Journal of Materials Science 51 (5), 2716−2726.

Jiang, H.C., Fu, F., Lu, K.Y., 2013. Development of thermochromic wood material. China Wood Industry 27 (4), 9−12, 45.

Jyothi, N.V.N., Prasanna, P.M., Sakarkar, S.N., Prabha, K.S., Ramaiah, P.S., Srawan, G.Y., 2010. Microencapsulation techniques, factors influencing encapsulation efficiency. Journal of Microencapsulation 27 (3), 187−197.

Kulvcar, R., Frivskovec, M., Hauptman, N., Vesel, A., Gunde, M.K., 2010. Colourimetric properties of reversible thermochromic printing inks. Dyes and Pigments 86 (3), 271−277.

Liu, Z.J., Bao, F.C., Fu, F., 2011. Study of manufacturing thermochromic wood. Wood and Fiber Science 43 (3), 239−243.

Liu, Z.J., Bao, F.C., Fu, F., 2012. Impregnation process of thermochromic functional poplar veneer. Scientia Silvae Sinicae 48 (1), 143−147.

MacLaren, D.C., White, M.A., 2003. Dye-developer interactions in the crystal violet lactone−lauryl gallate binary system: implications for thermochromism. Journal of Materials Chemistry 13 (7), 1695−1700.

Seeboth, A., Klukowska, A., Ruhmann, R., Lotzsch, D., 2007. Thermochromic polymer materials. Chinese Journal of Polymer Science 25 (2), 123−135.

Smith, C.R., Sabatino, D.R., Praisner, T.J., 2001. Temperature sensing with thermochromic liquid crystals. Experiments in Fluids 30 (2), 190−201.

Vanderroost, M., Ragaert, P., Devlieghere, F., De Meulenaer, B., 2014. Intelligent food packaging: the next generation. Trends in Food Science & Technology 39 (1), 47−62.

Vikov, A.M., Vik, M., 2005. Colour shift photochromic pigments in colour space CIE L*a*b*. Molecular Crystals and Liquid Crystals 431 (1), 403−415.

White, M.A., LeBlanc, M., 1999. Thermochromism in commercial products. Journal of Chemical Education 76 (9), 1201−1205.

Wu, K., Song, L., Wang, Z.Z., Hu, Y., Kandare, E., Kandola, B.K., 2009. Preparation and characterization of core/shell-like intumescent flame retardant and its application in polypropylene. Journal of Macromolecular Science, Part A: Pure and Applied Chemistry 46 (1), 837−846.

Zhu, C.F., Wu, A.B., 2005. Studies on the synthesis and thermochromic properties of crystal violet lactone and its reversible thermochromic complexes. Thermochimica Acta 425 (1), 7−12.

Architectural (decorative) natural fiber composites for construction

16

P. Cao, X. Guo, R. Li
Nanjing Forestry University, Nanjing, Jiangsu, China

16.1 Introduction

Fiberboard, as a kind of natural fiber composite, is made from wood or some nonwood fiber materials. These natural fiber composites with various outstanding performances are widely used for construction. Unfortunately, these unprocessed composites cannot be applied directly in construction due to some defects, such as poor aesthetics, low water resistance, and poor corrosion resistance. Various decorative methods were developed to improve the surface quality and performance of natural fiber composites and extend their application fields (Budakci et al., 2007). After decorative processing, many improved qualities, such as appearance, water, corrosion and abrasive resistance, and mechanical property of the natural composites, will be achieved.

In the modern manufacturing industry, the commonly used surface decorative methods for natural fiber composites include surface laminating and finishing. Among the various processes, surface laminating can be divided into flat laminating and foil laminating, and the surface finishing involves coating and printing (Suxia, 2007).

In this chapter, different decorative methods are presented. The principles, materials, technological processes, and applications of different methods are discussed.

16.2 Flat lamination

Flat lamination is a commonly used technique for the surface overlaying of fiberboard composites. Depending on the overlaying materials, it can be divided into two types: veneer flat lamination and impregnated paper flat lamination.

16.2.1 The form of veneer flat lamination

Veneer flat lamination of the main form is shown in Fig. 16.1. The process proceeds as follows: coating the surface of the base material with adhesive, then laying the paper on the surface of the glue, and landscaping for a period of time after the paper surface coating, finally gluing the veneer on the paper surface. Usually a board or paper is glued on the back of the base material as the balancing layer to ensure the structural symmetry of veneer-faced artificial board.

Advanced High Strength Natural Fibre Composites in Construction. http://dx.doi.org/10.1016/B978-0-08-100411-1.00016-9

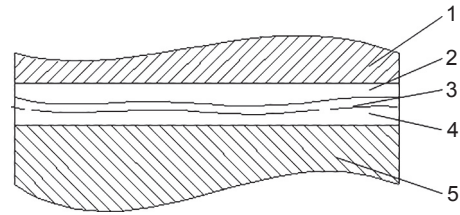

1. Veneer 2,4. Adhesive layer 3. Paper 5. Base material

Figure 16.1 The main form of veneer flat lamination.

16.2.2 The principle of impregnated paper flat lamination

The common forms of impregnated paper flat lamination are shown in Fig. 16.2; there are five main types. The most common form attaches a melamine resin impregnated paper on the base material and pastes the back with a balance paper.

16.2.3 The flat lamination materials

16.2.3.1 Veneer flat lamination materials

The materials for veneer flat lamination include plywood, particleboard, fiberboard, and other wood-based composites. The wood species suitable for making overlaying veneer are fraxinus mandshurica, basswood, crataegus pinnatifida, camphorwood, and some other species (Chun-li et al., 2014).

The glue applied for veneer flat lamination is normally related to the compression technologies. Dry press is normally used for hot melt adhesive, and the wet press method is normally used for thermosetting resin adhesive.

16.2.3.2 Impregnated paper flat lamination materials

The materials for impregnated paper flat lamination include particleboard, fiberboard, and other wood-based composites. The surface decoration material is usually

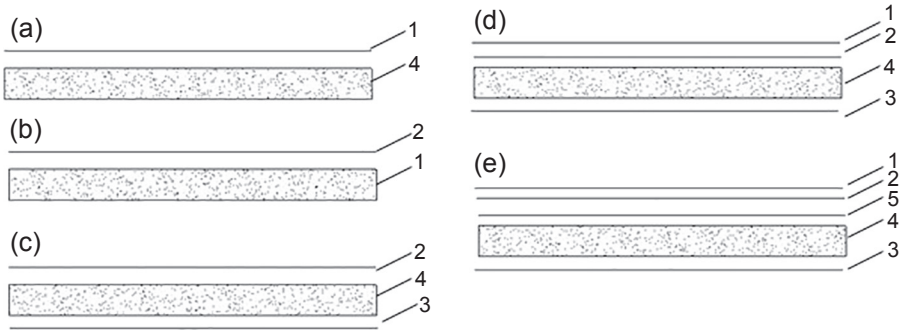

1. Surface paper 2. Decorative paper 3. Underlying paper 4. Base material 5. Cover paper

Figure 16.2 The main form of impregnated paper flat lamination.

melamine impregnated paper. The glues applied for veneer flat lamination are normally methylated trimethylol melamine and urea-formaldehyde resin.

16.2.4 The technological process of flat lamination

16.2.4.1 The technological process of veneer flat lamination

The veneer flat lamination process is changed by the arrangement of the lamination production lines. There is a brief introduction of the process with the typical structure, which is shown in Fig. 16.3.

Using the trolley, load the stack of boards, which need to be stuck on the hydraulic lift platform (10). The pneumatic feeder (11) automatically feeds the boards to the duster (9) to clean the surface of the boards. The stack of boards is transported from the conveying roller table (1) and the coater (8) to the tray conveyor (2). The operator groups decorative veneer and boards on the grope (4), and the boards should have been gummed. After the grouping, the conveyor puts the grouped boards into the short-cycle overlaying press (7) to pressure. Finally, the finished boards will be conveyed by the lift (5) into the roller table (6) to stack.

16.2.4.2 The technological process of impregnated paper flat lamination

A typical production line of impregnated paper flat lamination is shown in Fig. 16.4.

The stack of boards is transported on the table roller conveyor (1) to ensure continuous feeding. The melamine impregnated paper is put on the stock table (16); one of them is for the top surface decoration and the other for bottom surface decoration. The stack transports from the conveying roller table (1) to the lift (3), and the lift then raises a thick distance of boards. The pusher (2) puts the last piece of the stack of boards into duster (4) to remove any dust. After that, the lift returns to the initial position to carry the next stack from the conveying roller table (1). The boards transport from duster (4) and the intermediate conveyor (5, 6) into the transfer station (7). The impregnated paper storage trolley (18) sends it to the vacuum conveyor (17).

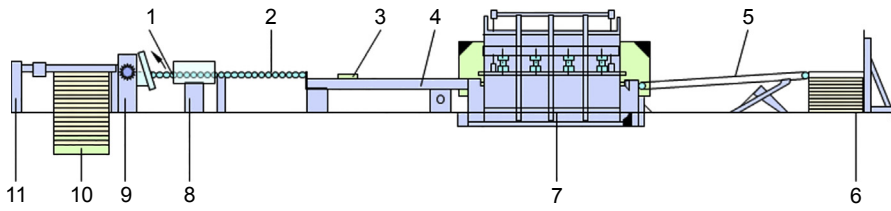

1. Conveying roller table 2. Tray conveyor 3,4. Group table 5. Lift 6. Roller table
7. Short-cycle overlaying press 8. Coater 9. Duster 10. Hydraulic lift platform 11. Feeder

Figure 16.3 The typical production lines of veneer flat lamination.

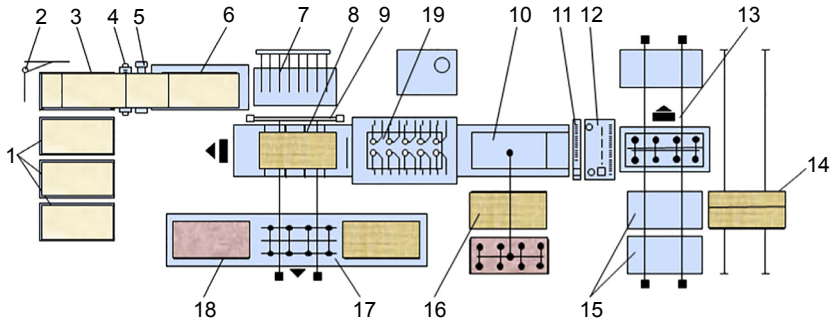

1. Conveying roller table 2. Pusher 3. Lifts 4. Duster 5,6. Intermediate conveyor
7. Transfer platform 8. Group table 9. Loading device 10,13. Conveyor 11. Saw 12. Trimmer
14,18. Trolley 15. Roller table 16. Stock table 17. Vacuum conveyor 19. Press

Figure 16.4 The typical production line of impregnated paper flat lamination.

The vacuum conveyor carries the impregnated paper to the group table (8) by vacuum cups. The transfer platform (7) puts the board on the bottom surface decorative paper, then the vacuum conveyor (17) places the upper surface decorative paper on it.

After the grouping is completed, the package is sent into the press (19) by the loading device (9). After pressing, the loading device removes the workpiece out of the press and puts it on the conveyor (10). The board is cut into a smaller format by the saw (11) and is trimmed by the trimmer (12). The boards are inspected on the conveyor (13) for the surface quality, then according to quality classification, they are put into the corresponding roller table (15). When the finished boards reach a certain quantity, the trolley (14) sends the stack into the storage room.

16.2.5 Technical parameters of flat lamination

16.2.5.1 The technical parameters of veneer flat lamination

The thickness of veneer is normally 0.15−0.4 mm, and the most commonly used thickness is 0.2 mm; the base material should not only meet the quality requirements, but also should control the moisture content within 8−16%.

The veneer lamination commonly uses single spread gluing, and the amount of spread depends on the kind of base material and the thickness of veneer. When using plywood as the base material and the veneer thickness$\leq$0.4 mm, the single spread is 110−120 g/m^2; when veneer thickness>0.4 mm, the single spread is 145−170 g/m^2. When using particleboard as the base material, the single spread is 170−200 g/m^2. When using fiberboard, the single spread is 150 g/m^2.

The veneer flat lamination machine is generally used in the short-cycle overlaying press, the normally used pressing pressure is 0.7−1 MPa, temperature is 90−110°C, and press time is 1−2 min.

16.2.5.2 The technical parameters of impregnated paper flat lamination

Commonly, the spread (adhesives) used for impregnated paper is 52−58%, and volatile content is 6−7%; the base material should not only meet the quality requirements, but also should control the moisture content within 6−8.5%.

Melamine-formaldehyde resin adhesive must be modified to enable it to have a good flow and malleable and fast curing properties at the working environment of 150°C and pressure of 2 Mpa, while the board should not crack at 160−200°C after relieving pressure.

Currently, the main device for the production of impregnated paper overlaying is the short-cycle overlaying press, and the most commonly used is low-pressure short-cycle overlaying press. Its hot-pressing process conditions are the pressing temperature 190−220°C, the unit pressure 2−3 MPa, and curing time of 25−50 s. Nowadays, the advanced short-cycle overlaying press is available in the market for producing the laminate flooring, and its maximum pressure can be up to 10 MPa. The fastest press cycle can be 180 times/h.

16.2.6 The application of flat lamination

Veneer flat lamination and impregnated paper flat lamination has been widely used in furniture and woodwork production, especially in panel furniture, flooring, wood doors and windows, and decorative building materials. Veneer overlay materials tend to be advanced materials for furniture manufacturing and interior decoration. Melamine impregnated paper overlaying in laminate flooring and the panel furniture industry is an irreplaceable role.

16.3 Roll flat laminating with polyurethane reactive hot melt

Fiberboard composites, with the raw surface for the industrial application, are restricted to a certain extent. With the foil decoration as a secondary processing, the value and application range can be increased due to the improvement of surface quality and physical and mechanical properties. This section introduced the technology of roll flat laminating with PUR hot melt, including the features of polyurethane reactive hot melt (PUR), the working principle and engineering of roll flat laminating, and the factors influencing the quality and solutions.

16.3.1 Feature of polyurethane reactive hot melt

Polyurethane reactive hot melt (PUR) provides specific bonding characteristics that are not offered by any other single adhesive. PUR bonds well to a variety of substrates and forms effective bonds between similar or dissimilar materials.

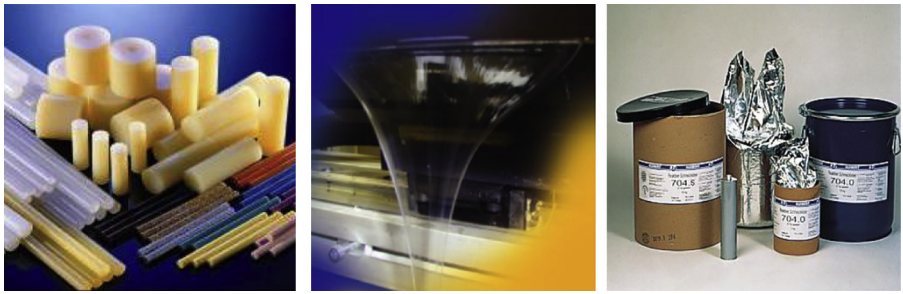

Figure 16.5 Polyurethane reactive hot melt.

It is a meltable polymer with 100% content, without solvent and water. The solid polymer will be melted into liquid at processing temperature. The initial bonding results principally from the hardening, which occurs during the cooling of the adhesive. A reaction then occurs with the moisture of the ambient air and the permanent hardening of the adhesive bonding. The reaction is dependent on moisture from ambient vapor, but not water, and it is reversible. Therefore the PUR hot melt should be protected against moisture and supplied in sealed plastic foil, a barrel, or a bag (Fig. 16.5).

The PUR hot melt has the following features:

- Low processing temperature. Especially for thin and thermoplastic surface foils.
- No Solvent. No drying process for the solvent, avoiding risk of explosion and being environmentally friendly.
- No water. No change on surface morphology when the adhesive penetrates into the substrate.
- No heat required during the bonding and curing process. This will ensure the flatness of the substrate surface.
- Easy to handle. It is a single component, moisture-reactive glue, and the parts after press can soon go to the operation downstream.
- 100% solid content. No shrinkage after curing to ensure the surface quality.
- Once cured, it presents excellent temperature resistance, high water and creep resistance, and high chemical resistance, as well as high bond strength.

Working principles and conditions require the following:

- The heated roller can apply the PUR hot melt onto the treated substrate, and the melting of solid PUR can take place in specially designed melting systems or, for smaller amounts, directly in the roller gap of the applying unit.
- The amount to be applied is determined by the roller gap setting and speed of the doctor roller.
- The surface material is then processed in sheets cut to size or from the roll via the lay-up unit.
- The calender, which creates its contact pressure pneumatically, presses the individual layers to a compound or sandwich, then moisture curing takes place and is followed by further processing.

See the procedure flow in Fig. 16.6.

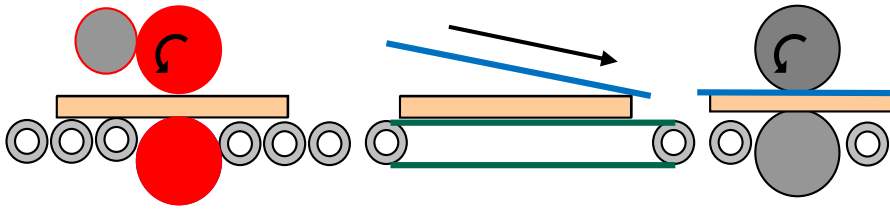

Figure 16.6 Procedure flow of polyurethane reactive hot melt lamination.

The working environment is required as follows:

- Ambient temperature $T > 18°C$.
- Ambient relative humidity RH > 40%.
- The operation area should be clean and dust free, especially when having the high-gloss laminating.
- The stacking condition after laminating should have a temperature $T > 18°C$, and relative humidity RH > 40%.

To the fiberboard/substrate, it is required for:

- Board temperature $T > 18°C$.
- Board quality must be suited for the lamination process, ie, it must have a smooth surface without dirt, particles, and raised fibers.
- The board has to be calibrated and fine-sanded for high-requirement laminating, especially high-gloss application with thin foils.

The foils to be laminated with fiberboard can be plastic foils, such as PVC, PP, PMMA, ABS, and PET, fire-proof laminates, such as HPL and CPL, and paper foil and thin veneer (<1.0 mm). The surface material also requires the following:

- Some materials (eg, PVC or Al sheet) have to be corona-treated or coated with a bonding agent (primer).
- High-gloss surface materials have to be protected by protective foil, and the reverse side must be clean.
- The foil temperature should be suited and so elastic that no splintering will occur during trimming.

16.3.2 Typical production line

A typical roll flat laminating line with PUR consists of a conveyor, a roller coating machine, a lay-up table that can be adapted in length, the calender press, and another conveying element for taking over the finished parts. Due to different requirements, it can be optionally equipped with a sward brushing unit for board cleaning, an IR unit for board preheating, a drum melting unit for glue premelting and automatic feeding, a UV black light for checking the glue applied, and an unwinding station for feeding surface materials from the roll.

Thermal oil-heated rollers (up to 160°C) apply the glue onto the substrates. A key advantage is the accurate uniform temperature for keeping the viscosity and applying quantities. Material layers are then assembled.

The glue applying quantity is 30−100 g/m^2. Optionally, a mobile rack for laminating materials to the lay-up table can be added. The press calender consists of a solid, welded machine frame with chromium-plated or rubber-covered calender rollers. These calender systems are absolutely necessary for premium products such as high-gloss surfaces. A precise lifting gear adjusts the upper roller according to the workpiece thickness.

For increasing the capacity and the quality, additional loading and stacking systems, as well as automated lay-up systems for material sheets cut to size or from the roll, are available. Companies can upgrade their existing machines by an automation system for reaching a fully automated line.

16.3.3 Main factors influencing the quality of lamination

16.3.3.1 Substrate sanding

The substrate has to be double-sided and calibrated to a precision ±0.1 mm, which is essential for the following processes, like glue application and calender press, to have an even pressure on the substrate surface. Then, depending on the gloss degree of the final surface and thickness of the foil, the substrate should be fine-sanded via a sander, with sanding belt grit 320#/400#/600#, and equipped cross-belt if necessary to have a smooth and reactive surface. A good sanding means better outcomes, and the smoother the surface, the smoother the final foil surface will be, but the adhesion problem should be considered.

16.3.3.2 Substrate cleaning

The substrate after sanding should be cleaned thoroughly to avoid the negative effects of any particles on the laminated surface, which will decrease the degree of quality of the final board. A sward brushing unit with patented cleaning method is recommended.

16.3.3.3 Substrate preheating

In order to have a warm surface, so that the glue will not be cooled soon after being spread on the substrate, a preheating unit with short wavelength IR lamps is required. The suitable temperature after heating is around 30°C, to prolong the flowing properties of the glue and improve the compatibility between the substrate and the glue. As a result, less orange peels will appear on the surface of the final board.

16.3.3.4 Glue application

Glue application is the key factor influencing the quality of laminating. A consistent, accurate quantity of resin leads to a good result after foil laminating. As a result, the roller coating machine for PUR should have an even temperature distribution on the

surface when applying the roller and doctor roller in order to keep the viscosity at the same level. A design of heating system (it means one kind of heating system) for the application and doctor rollers is with double heated design (up to 160°C), with thermal oil spirally circulated inside both rollers. In this case the temperature deviation on the roller surface is within ±1°C. For high-gloss foil laminating, a thin and even glue firmly applied on the substrate surface is a precondition to have a good quality degree.

16.3.3.5 Calender press

For foil laminating the roller press will be designed for sheet goods cut to size and roll goods. For the latter, the roller press should be equipped with an unwinding station so that it can have a continuous feeding of the roll goods. The roller press contains two rubber covered rollers, 70 shore, and pneumatic-loaded upper rollers (max 4500 N/side). Optionally, hard chromium-plated, polished for the upper roller for high-gloss lamination (no walking effect), can be used.

16.4 Thermal forming

16.4.1 The principle of thermal forming

Thermal forming is a kind of technology with a molding machine, which can implement a three-dimensional (3-D) overlay for wood-based composites. The main schematic of thermal forming is shown in Fig. 16.7. During the hot-pressing, the air cushion chamber is pressurized and the lower platen vacuumed. The air cushion and wrapping film then overlay on the workpiece surface with the same press. Any special-shaped workpiece surface can be realized with this overlaying process.

16.4.2 The thermal forming materials

The materials for thermal forming include particleboard, fiberboard, and other wood-based composites. The surface decoration materials are mainly thermoplastic foils such as PVC and PET. Veneer, linoleum, or Kydex can also be processed. In recent years, the glue applied for thermal forming process is PE (need to add the curing agent).

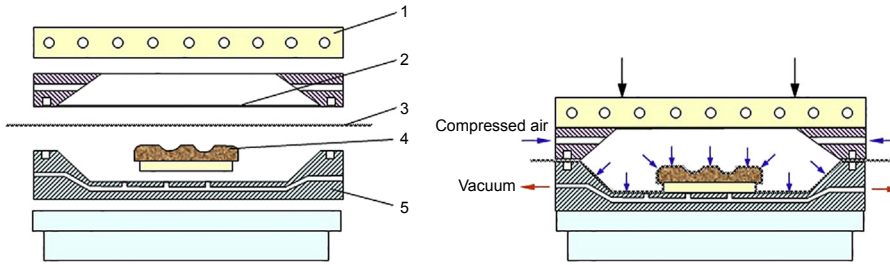

Figure 16.7 The main schematic of thermal forming process.

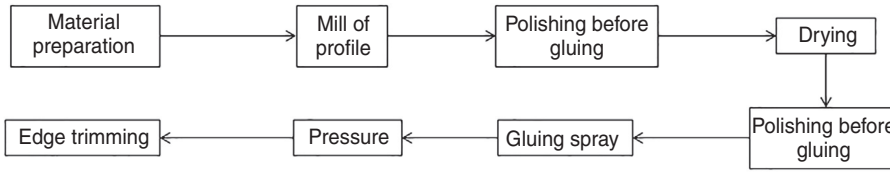

Figure 16.8 The technological process of thermal forming.

16.4.3 The technological process of thermal forming

The technological process of thermal forming is shown in Fig. 16.8.

- Material preparation: the main steps are to cut composites into the size of required thermal forms.
- Mill of profile: generally, produces composites by efficient CNC. Before milling, the profile of the workpiece should be noticed. Not every profile could be efficiently thermally formed, such as too narrow lines, the forming of which could lead to the film in the wrong place. Sharp edges and angles should not be allowed either; the 90 degree angle should especially be avoided.
- Polishing before gluing: The best effect can normally be achieved by repeating the polish three times with different sand papers, which are 120, 240, and 400 mesh, respectively. On every cutting surface, engraving and milling surfaces should also be polished. After polishing, the surface of parts should be smooth, and it is best to match the board surface.
- Gluing spray: high-quality special glue should be chosen. Glue should have little flow and be highly atomized. As to the high-gloss PVC, the cutting and milling surfaces should be sprayed twice. After the first spray is dry, gently sweep the surfaces that are not milled, and then carry out the second spray. The amount of adhesive spread is 25−30 g/m^2 and 100−120 g/m^2 on the surface and on the around, respectively.
- Drying: glue dries automatically in the summer, but dry the glue in a 35°C conditioning room in the winter. When the glue on the boards is dry, the boards should be used to produce within four hours to ensure the glue has a good adhesive strength and temperature-tolerance performance.
- Polishing after gluing: use more than 800 mesh sand paper to polish the sprayed surface and meanwhile remove the plastic head.
- Pressure: mainly use molding press to make the films form on the wooden materials such as fiberboards.

The process of the molding machine can be summarized as follows (PVC material thermal forming as an example) (Fig. 16.9):

- The molding machine opens. The workpiece (5) enters the machine by a feeding device, and an air pipe (8) vacuums the air cushion chamber (3). Vacuum I makes the air cushion (2) close to the upper hot platen (1) for heating.
- The molding machine is closing. Thermal air circulates in the air cushion chamber (3), a multifuction frame (4) vacuums, and vacuum II makes the air cushion heat the PVC film (6) to plasticize it. Meanwhile the vacuum II can make the film not contact the cold workpiece, to ensure the film will not be plicated. For hot-pressing, thermal compressed air circulates in the air cushion chamber (3), and vacuum III makes the PVC film (6) cling over the surface of the workpiece (5) to avoid producing bubbles. The hot compressed air makes the adhesive cured fully.

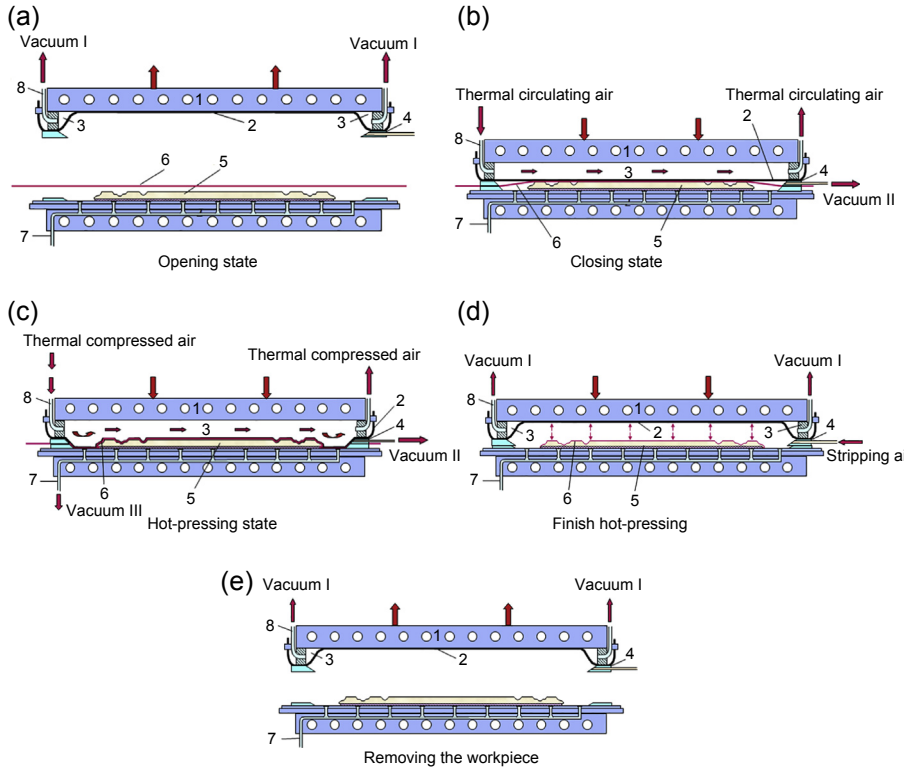

Figure 16.9 The typical working process of the molding machine. (a) Opennig state, (b) Closing state, (c) Hot-pressing state, (d) Finish hot-pressing, (e) Removing the workpiece.

- To finish hot-pressing, the air cushion chamber (3) vacuums, and meanwhile, cold air fills from the multifunction frame to separate the air cushion from the PVC film. In order to avoid the film strip from the workpiece when the molding machine opens and the pressure releases simultaneously, a certain pressure must be maintained.
- To removing the workpiece, open the molding machine, and the air cushion chamber (3) vacuums. Vacuum I makes the air cushion (2) close to the upper hot-platen (1) preheat, then removes the workpieces and starts the next cycle.
- When edge trimming, once the finished workpiece is removed from the molding machine, wait until the glue is fully cured and the PVC film is no longer shrinking, and then trim the edges. It is better to trim the workpiece after 24 h.

16.4.4 Technical parameters of thermal forming

Commonly used working parameters of molding machines:

- upper hot-platen temperature: 110−150°C;
- airbag (silica gel plate) temperature: 85−115°C;

- pressure: 0.3−0.6 Mpa;
- preheating time: 15−60 s;
- pressure on time: 20−60 s;
- in/out mechanical time: 20 s; and
- pressure cycle: 90−120 s.

The different parameters for PVC and veneer thermal forming:

- When using the veneer as the film for thermal forming, only workpieces with the flat range and smooth curve can be overlaid. Thermal forming on special shapes with veneer may damage the workpieces.
- When thermal forming on veneer, it is not necessary to vacuum from the bottom of the workpieces, as the veneer is porous and the vacuum is not effective. The veneer is pressed by the silica gel film.
- While thermal forming the veneer, it better to spray water mist on the veneer. Meanwhile, place a layer of insulating film, such as a nonwoven fabric, between the veneer and the silica gel film to avoid the veneer being damaged by high temperatures.
- Compared with PVC thermal forming, the veneer forming needs a molding machine to provide a higher temperature and pressure.

16.5 Wrapping

16.5.1 The principle of wrapping

Wrapping is a process to protect and enhance furniture and is usually expensive. The profile-wrapping method has been developed to apply thin wood veneer and some other cover materials to substrate materials such as low-cost particleboard composites (Jun, 2004). The profile-wrapping technique involves attaching cover materials to substrates to provide a decorative or aesthetically pleasing appearance to some furniture or other wood products. The principle of profile wrapping is shown as follows: the profile is fed into a wrapping machine that applies an adhesive substance and attaches the cover materials to the surface of substrate materials via a variety of pressure rollers to simulate the manual veneering process. The set-up process, which includes adjusting a number of profile holders along the track of the wrapping machine, will be needed to adjust the wrapping of different profiles. The schematic diagram of the wrapping technique is shown in Fig. 16.10. The technical process includes the cleaning of substrate materials, preheating of substrate materials, gluing, and pressing.

16.5.2 The wrapping materials

The substrate materials for wrapping involve fiberboard, particleboard, lumber, or other composites. The cover materials for wrapping include veneer, decorative paper, PVC, CPL, and leather. The cover materials may be provided in roll form and applied to a substrate in a continuous process until the entire roll is depleted. In recent years, the adhesive applied for the wrapping process is PUR and EVA.

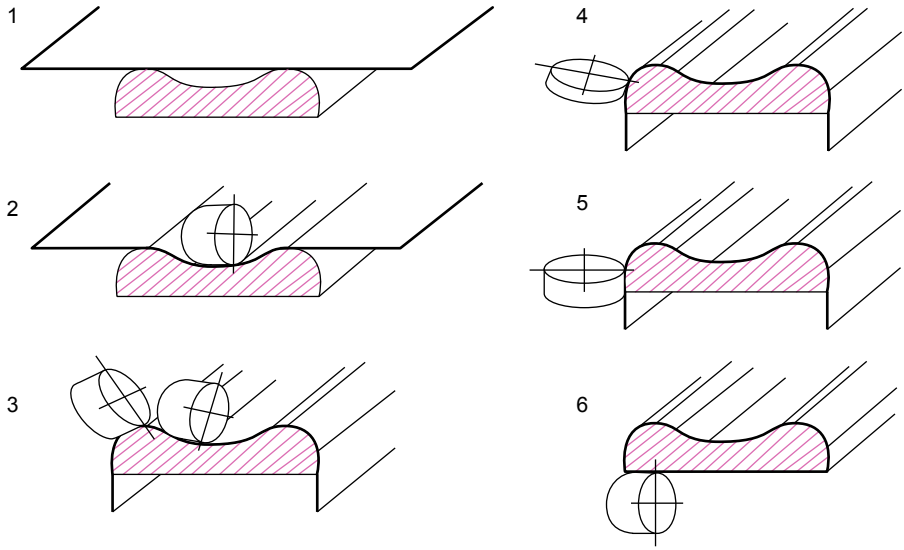

Figure 16.10 The schematic diagram of the wrapping technique.

16.5.3 The technological process of wrapping

The technological process of wrapping includes the cleaning of substrate materials, preheating of substrate materials, gluing of cover materials, and pressing.

16.5.3.1 Cleaning of substrate materials

Prior to wrapping, the substrate material should be cleaned because the dust on the wrapping surface will have a negative effect on the performance of wrapping.

16.5.3.2 Preheating of substrate materials

Before applying the cover materials, the substrate material needs to be heated by infrared preheating lamps on all sides. The preheating system is shown in Fig. 16.11. The temperature difference between substrate materials and cover materials will be reduced by preheating to achieve a better wrapping performance. To a certain extent, the preheating is also a benefit for the adhesive curing and the reduction of the curing time.

16.5.3.3 Gluing cover materials

The adhesive-spreading device varies from different cover materials. Ink rollers normally can be used for discrete glue adhesion and solvent adhesive, and the wrapping material can be thermoplastic film and veneer. The glue should be dried with fans. The

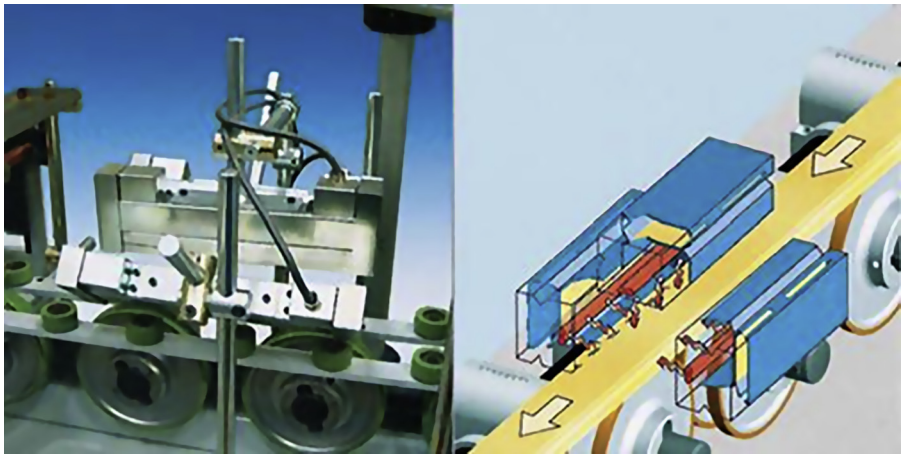

Figure 16.11 Preheating system for wrapping.

adhesive spreading device can be rotated. It can be set up and adjusted to operate with each operating track (Fig. 16.12).

16.5.3.4 Pressing

After gluing the cover material, the rubber rollers apply pressure and the heat guns apply processing heat, which rapidly bonds the cover materials to the substrate material. The applied pressure is about 0.6 Mpa. In the pressing process, there are two kinds of rollers, one for pressing and the other for guiding. These rollers are shown in Fig. 16.13.

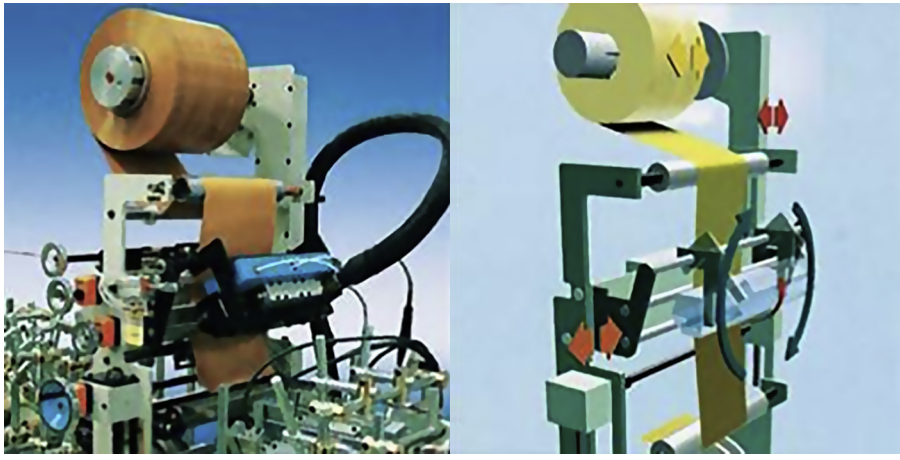

Figure 16.12 The gluing system for wrapping.

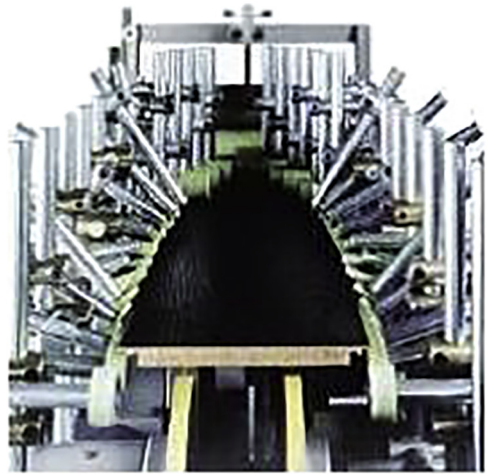

Figure 16.13 The pressing device.

16.5.4 Technical parameters of wrapping

The debugging process is a key process of wrapping, because the uniform pressure will be achieved by the set-up process. To a certain extent, the quality of the wrapping process depends on the accuracy of the set-up process. The set-up process, which includes adjusting a lot of profile holders along the track of the profile-wrapping machine, might take up to 90% of the operational time. In order to reduce the time of the set-up process, the following methods were proposed: using the machine with high adaptability, using coiled cover materials to keep the machine working continuously, and using programmable equipment to reduce the time of resetting. It is better to use unitization technology when manufacturing the wrapping products.

16.5.5 The application of wrapping

The ready to assembly (RTA) furniture is a kind of panel furniture. The RTA furniture with a high accuracy and large production is most suitable to be manufactured by wrapping. The decorated panel can be cut into many pieces in a lengthwise direction.

The wrapping process is also frequently used for making cabinets and bathroom furniture to improve their performance (such as waterproofing) (Fig. 16.14).

16.6 Surface finishing and printing

This section discusses the technology of roller coating with a UV lacquer and indirect printing system, including the feature of applications, working principles, and processing, as well as the possible lacquering results.

Figure 16.14 Wrapping products.

16.6.1 Roller coating with ultraviolet lacquer

The features of UV roller coating are shown as follows:

16.6.1.1 Introduction of UV lacquer

Under the exposure of UV rays, the liquid binder components of the UV coating material react within a fraction of a second to form a dry, solid film. This process is known as polymerization. The polymerization process is activated by means of photo initiators. On absorption of the high-energy UV rays, the photo initiator breaks down into various constituents. These elements activate the reactive molecules of the binder.

UV rays are produced by mercury gas discharge lamps. The mercury gas discharge lamp consists of a quartz tube with an insert gas filling and metal electrodes melted into the ends of the tube. The application of a high-ignition voltage produces an electric arc and the UV lamp heats up. The mercury evaporates and the surface of the UV lamp heats up to approx. 800−900°C, emitting UV rays.

Depending on the applications, mercury or gallium lamps are used. The former (pure mercury gas discharge lamp HG) is suitable for clear lacquer and the latter (eg, mercury gas discharge lamp GA with added metal halogenide gallium) is suitable for the pigmented lacquer. Gallium lamps achieve higher penetration due to their radiation characteristics.

UV lacquer has a number of advantages:

- It is environmentally friendly. No solvent is released during the curing process.
- It is fast curing, which leads to a high production capacity.
- It has a low finishing cost, which saves energy and resources.
- It is easy to handle, has a single component, and no limitation in lifetime.
- The coating film has a good performance.

16.6.1.2 Introduction of roller coating

The roller coating machine in principle consists of an applying roller, doctor roller, as well as a transport system. The applying roller will be coated with a thick film of material after the roller gap. This film is rolled onto the surface of the workpiece, passing through the roller gap by applying the roller against the workpiece. As a result, the coating process finishes in a few seconds without any overcoat and waste.

The application dosage can be influenced by the contact pressure of the doctor roller onto the applying roller, speed difference between the applying roller and doctor roller (turning direction of doctor roller as to applying roller), and the viscosity of coating materials and type of applying roller used.

The high efficiency of production, loss free of materials, and environmentally friendly and excellent finishing performance have made the roller coating with UV lacquer widely used in the finishing of wood products.

A typical finishing process is normally composed by several phases defined according to raw materials and required finishing. Generally, as to the finishing of fiberboard, the technological cycle can be divided into the substrate calibrating and fine sanding; filler and base coat application and curing; base coating fine sanding; and topcoat application and curing.

The configuration of a typical UV roller coating line for the pigmented finishing of fiberboard is shown in Fig. 16.15.

Legend: 1, 3, 8, 10, 22-Belt conveyors; 2-Calibrating and fine sanding machine for substrate; 4, 6-Filler coating machines; 5, 12, 14, 16-UV units with one lamp; 7-UV unit with two lamps; 9-Sanding machine for UV lacquer; 11, 13, 15-Roller coating machines for base coat; 18, 19-Roller coating machines for top coat; 20-Flow leveling machine; 21-UV unit with three lamps.

Substrate sanding

Natural fiber composites, eg, fiberboard, are made of wood or other natural fibers, due to the long-term transportation and storage, and the dimension, especially thickness, may change. It is important to have a calibrating process before finishing to achieve an even

Figure 16.15 Line layout.

thickness reference. The workpiece will be fed into a sanding machine configured with three roll sanding units, with sanding belt grits normally 80#/120#/150# to ensure the calibration. As a result, a workpiece thickness with a tolerance ±0.1 mm is achieved.

Then, in order to have a fine surface and make the filler coating process easy, the workpiece will be fed into a sanding machine for finer sanding, normally with a sanding unit with two piano keys and sanding belt 180#/240#, length/length. As a result, a workpiece with a fine and active surface is achieved.

Filler application

The natural fiber composite is a porous structure material, and there are lots of holes exposed after sanding. Before the application of a base coat, filler coating is applied in order to seal the holes and make an even and rigid base.

A filler coating machine is used. Applying the roller, which rotates in the same direction as the workpiece feed, applies a certain amount of liquid UV filler onto the surface of the workpiece, then a smoothing roller, with rotating direction in reverse as to the workpiece feeding, fills the UV filler into the exposed holes and cracks. After UV curing with the required radiation energy, the filling process is finished. Normally two fillers are required, as shown in Fig. 16.15.

Filler sanding

After the filler coating, the workpiece should have an even and rigid surface without any holes and unevenness on it. Due to the composition of UV filler, after curing, there will be some burrs left, so it is required for a sanding machine to make the surface smooth and flat, so that the base coat afterward has no function in filling just to save material.

A sanding machine after filler curing is required, which configures a sanding unit with two piano keys, with a sanding belt 320#/400#, length/length. This should achieve a thorough sanding for a flat and fully sanded surface, but without any oversanding.

Base coat application

The base coat, as an intermediate layer of the lacquer film, provides not only physical and chemical performance, but also a critical part to combine the filler and top coat and contribute in flatness, adhesion, hardness, and wear resistance.

For pigmented lacquering for fiberboard, due to the curing, flatness, and coverage consideration, three coats are advised. Each time, an application amount of 10−15 g/m^2 should be applied, but the latter one should be thinner. As described, a Gallium lamp UV unit is required for the curing.

Top coat application

The top coat is the last coat, and the quality of top coat is directly related with the final result. Two coated rollers are used for top coat application. The first coated roller has a normal, smooth rubber roller and applies 6−8 g/m^2 onto the surface, which has a wet film base. The second coater, with an optiroller (80 grooves per inch on the rubber roller surface), applies more than 20 g/m^2 onto the wet film, due to the line created by the

grooves of the roller, together with the flow leveling machine with IR heating afterward. The certain amount of top coat flows to a level to achieve a flat but full surface after the UV full curing. At last, after cooling, the final board with finishing is obtained.

UV curing

After the coating, curing is a necessary part, no matter for filler, base coat, or top coat. It can be judged by UV energy checking in mJ/cm^2 or by finger touch with experience when in real production. Between the coats, semicuring is required. UV energy is UVA_80−100 mJ/cm^2 for transparent filler or UVV_150−200 mJ/cm^2 for pigmented base coat. When touching the surface, it is slightly sticky. Between coating and sanding, surface curing is required for the pigmented base coat, and the UV energy is UVA_150−200 mJ/cm^2 + UVV_250−300 mJ/cm^2, which is easy for sanding but does not effect adhesion. After the top coat, the full curing is required and UV energy is UVA_250−300 mJ/cm^2 + UVV_450−500 mJ/cm^2.

16.6.2 Indirect printing combining with roller coating

Indirect printing is a decoration to make a composite, such as fiberboard, into a high-value decorative board, via sanding, filler application and curing, base coat application and curing, indirect printing, and a top coat on the surface. For the fiberboard, usually the print is wood grains, so the indirect printing for fiberboard is also called grain printing (Krystofiak et al., 2010).

The grain printing has the following features:

- no need for the decorative papers, plastic foils, or wood veneers
- provides the fiberboard surface with different and vivid grains
- no need for a press machine/line to apply the decorative layer on to the fiberboard
- continuous production line for producing the grain-printed boards
- less loss required and more simple production procedures

For the typical configuration of the production line, it is the same as the finishing aforementioned, except between the final base coat and top coat, a grain printing unit will be added. The print is applied between “coloring” and “top coat.” The grain of most different species of wood can be imitated. Decorative surfaces with different patterns or structures can be produced. Single or multicolor printing of patterns are possible.

A grain print machine is shown in Fig. 16.16. It is, in principle, composed of a transport unit with a rubber-covered counter-pressing roller and guiding rollers and an applying unit with an engraved cylinder and rubber-covered applying roller.

The workpieces are fed to the transport unit by a precedent machine in the feed direction, and after activating the material circulation system, the coating material circulates continuously between the material container and the applying unit. The material feed rate must be set so as to ensure a continuous supply of coating material between the roller and the scraper (material feed rate > material consumption when coating the workpieces). When bringing the engraving roller into contact with the applying roller, the printing pattern is applied to the applying roller. This pattern is rolled onto the surface of the workpiece, passing through the applying roller pressed against the workpiece.

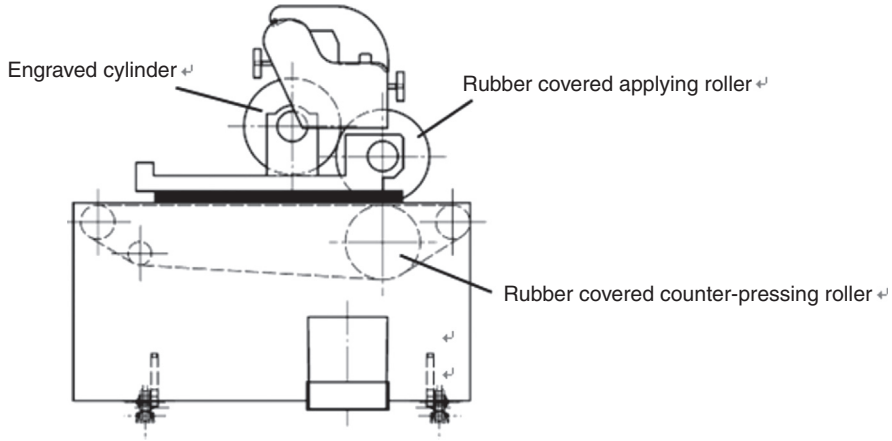

Figure 16.16 Grain print machine.

With the different combinations of grain printing, single or multicolored printing of patterns are applied to the workpiece surface to realize different print results.

16.6.3 Possible lacquering results and causes

The surface of the workpiece is not completely lacquered, and free spots are visible in the lacquer coat or the print.

Cause: the pressure of the applying roller onto the workpiece is not sufficient. The passing height should be at least 0.5 mm less than the thickness of the workpieces. The basic adjustment of the machine must be checked.

The workpieces have a crosswise shadow/marking to the direction of feed, always at the same distance.

Cause: the applying roller has a pressure mark and needs to be reground or replaced.

The workpieces have several crosswise shadows or marks to the direction of feed at irregular distances.

Cause: the applying roller has several pressure marks on the surface of the rubber covering, and possibly the speed of the applying roller is not synchronous with the feed speed.

A continuous curved mark is visible on the surface.

Cause: the scraper blade of the applying roller or the doctor roller is dirty or damaged and draws a line. The wave form of the marking is caused by the oscillation of the scraper blade.

A continuous straight mark is visible on the surface.

Cause: the oscillation of the scraper blade is not active and possibly defective. This causes accumulation of dirt or solids behind the scraper blade and produces stripes.

At the outfeed side, there is an accumulation of lacquer on the edge of the workpiece.

Cause: the speed of the applying roller is lower than the speed of the transport system. Either the speed of the transport system is too fast or the speed of the applying roller is too slow.

At the infeed side, there is an accumulation of lacquer on the edge of the workpiece.

Cause: the speed of the applying roller is faster than the speed of the transport system.

After one run of the applying roller, the thickness of the coat and consequently the intensity of color are decreasing when applying colored lacquers and paints.

Cause: the scraper blade of the applying roller is either not in operation or correctly adjusted.

16.7 Conclusions

Nowadays, flat lamination, thermal forming, wrapping, surface finishing, and printing are widely used for natural fiber composite decorating. In this chapter, different decorative methods for natural fiber composites were discussed. The principles, technological processes, technological parameters, and typical production lines were proposed.

References

Budakci, M., et al., 2007. Effect of wood finishing and planing on surface smoothness of finished wood. Journal of Applied Sciences 16.

Chun-li, L.U.O., Zhi-gang, Z., July 2014. Furniture veneer overlaying equipment and processing performance. Forestry Machinery & Woodworking Equipment 42, P45−P48.

Jun, L., 2004. Modern decorative technology for wooden furniture. Furniture 6, P24−P26.

Krystofiak, T., et al., 2010. "Some aspects of finishing of wood based materials in digital printing technology." Wood is good: transfer of knowledge in practice as a way out of the crisis. In: Proceedings of the 21st International Scientific Conference, Zagreb, Croatia, 15th October 2010.

Suxia, W., 2007. The surface processing technology of modern wood furniture. Woodworking Machinery 3, P21−P22.

Short term and long-term properties of natural fibre composites

17

J.S. Machado [1], *S. Knapic* [2]
[1]Laboratório Nacional de Engenharia Civil, Lisboa, Portugal; [2]Centro de Estudos Florestais, Instituto Superior de Agronomia, Universidade de Lisboa, Lisboa, Portugal

17.1 Introduction

Natural fibre composites (NFCs) include a large range of materials consisting in plant, animal or mineral fibres embedded into a polymer matrix (natural or synthetic). These materials offer a total or partial possibility of recyclability, showing a lower environmental impact compared with traditional glass fibre reinforced composites (Joshi et al., 2004). The large stock of natural fibres available worldwide constitutes an opportunity to produce attractive alternative composites. Also, natural fibres represent, in comparison to traditional composites, the possibility of obtaining a lower cost and lower density composites, biodegradable composites, less equipment abrasion, less skin and respiratory irritation and enhanced energy recovery, consuming on average 60% less energy than glass fibres (Azwa et al., 2013; Faruk et al., 2012; Herrera-Franco and Valadez-González, 2005; Sgriccia et al., 2008; Wambua et al., 2003). New regulations and directives opened new market opportunities for recyclable materials. The EU recyclability regulation in vehicle industries (in accordance with Directive, 2005/64/EC) mandates that vehicles may be put on the market only if they are reusable and/or recyclable to a minimum of 85% by mass or are reusable and/or recoverable to a minimum of 95% by mass. As a result the interior parts of the vehicle industries are one of the dominant applications of sustainable materials as NFCs.

However, NFCs' durability behaviour is often a barrier to a much broader use. The increased use of NFCs is confronted by the critical need to adjust the short and long-term performance of these composites to the end-use requirements. Two major risks are related to fire safety and resistance to moisture. Most natural fibres show low degradation temperatures (chemical and physical deterioration below 280°C), contributing significantly to the flammability and deterioration of the composites when exposed to fire. The hydrophilic nature of natural fibres implies the need to consider coupling agents to enhance the adhesion to hydrophobic matrices. Other challenges lay on the large variability of the mechanical properties, lower ultimate strength, lower elongation and poor resistance to weathering (Sgriccia et al., 2008). Overall, NFCs face a higher risk of degradation when subjected to outdoor applications, compared to composites with synthetic fibres.

Advanced High Strength Natural Fibre Composites in Construction. http://dx.doi.org/10.1016/B978-0-08-100411-1.00017-0

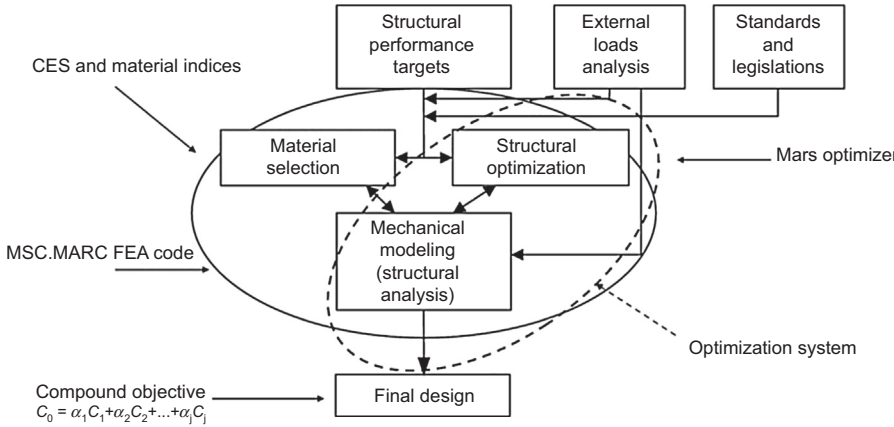

Figure 17.1 Natural fibre composite development process (Ermolaeva et al., 2002).

NFCs show more or less substantial differences when compared to the properties of their constituent phases. By manipulation of the fibre (type, amount and surface treatment), the type of matrix and additives (namely for reaction to fire and against weathering agents) and production process (wetting degree, moisture content of the fibres and extrusion process), the final design of the product can be reached. The development and production of NFCs should be oriented by limiting states of performance defined considering external factors (eg, load regime, temperature and humidity) and restrictions imposed by existing standardization or regulations. Such a decision scheme is suggested by (Ermolaeva et al., 2002) for the development of a sustainable car replacing conventional and nonconventional fibre composites by NFCs, shown in Fig. 17.1.

17.2 Physical properties

NFCs are generally developed with, as benchmark materials, solid wood or current wood-based panels (inferior performance limit and low cost) and glass or carbon fibre reinforcement products (superior performance limit and high cost). Compared to the latter, NFCs bring concerns regarding dimensional stability and reaction to fire due to the incorporation of natural fibres.

The number of studies dedicated to physical properties of NFCs and how the exposure to environment conditions affects them is scarce when compared to the number of publications covering the mechanical performance of NFCs.

17.2.1 Dimensional stability

Seen as a potential alternative material to more expensive and less recyclable composites, NFCs are nevertheless expected to reach a high dimensional stability for high-tech applications as aircraft, spacecraft or even for some components of the automobile sector. A lower level of dimensional stability is accepted by the construction industry.

Dimensional changes due to water adsorption or absorption are very low compared to traditional wood-based panels but higher when compared to reinforced glass fibres (Sgriccia et al., 2008; Assarar et al., 2011).

The response of material (dimensional changes) when exposed to water or relative humidity and/or temperature changes due to the surrounding environment is closely linked with existing hydrophilic free radicals in natural fibres. The consequent dimensional changes are generally evaluated following an immersion in water method. Few studies analyze the variations from a standard (65% relative humidity) to a higher (85%) or lower (30%) relative humidity environment. In this type of experiment, Madsen et al. (2012) observed, for a hemp/polyethyleneterephthalate (PET) composite (fibre weight fraction $w_f = 0.43$), a very small hygral strain between -0.0035 and 0.0005 determined with respect to the reference condition of 65% relative humidity and for a variation of relative humidity between 33% and 85%. As aforementioned the majority of studies have been done following a water immersion procedure, as seen in Table 17.1.

The hydrophilic nature of plant fibres, existence of microcracks in the matrix or lack of adhesion between fibres and matrix are responsible for the absorption/sorption capacity and consequent dimensional changes. Therefore fibre loading and fibre surface treatments for enhancing the adhesion to the matrix are important factors to define the hygroscopic capacity of a particular NFC (Azwa et al., 2013; Herrera-Franco and Valadez-González, 2005). The link between water absorption and fibre loading can easily be observed when compared to a composite consisting of the same matrix but reinforced with glass fibres (Assarar et al., 2011). Production variables, such as thermal shrinkage of the matrix during the cooling period after the curing reaction, temperature and time of exposure to a high moisture environment, also influence that capacity. Moisture intake shows a standard pattern consisting of a steady increase of moisture content until a saturation condition is reached (maximum value). When subjected to cycling and wetting/drying phases a separation of fibres from the polymer matrix occurs, originating voids that enhances the water absorption capacity of the composite (Cheng et al., 2010).

NFCs show a similar sorption hysteresis behaviour (difference between the sorption and desorption curve at the same air relative humidity condition) observed in wood when exposed to a cycling environment (low and high relative humidity) (Madsen et al., 2012). The sorption and diffusion coefficients increase with the temperature of water and fibre loading (Josepha et al., 2002).

Dimensional stability has been found to improve after treatment with chemicals, such as maleic anhydride, acetic anhydride and silanes (Wambua et al., 2003; Lu et al., 2000), or fibre modification, such as heat treatment (Kaboorani and Englund, 2011).

The equilibrium moisture content (α_c) can be predicted using a weight-based mixture equation dependent upon the weight fraction of the fibres (w_f) and the moisture content uptake by the net matrix and the net fibres (α_m and α_m, respectively) (Madsen et al., 2012; Ansari et al., 2014).

$$\alpha_c = \alpha_f w_f + \alpha_m (1 - w_f)$$

Table 17.1 Dimensional stability properties/indicators

	Dimensional changes	Moisture dynamic	
	Water immersion - thickness swelling (%)	Water absorption (%)	Diffusion coefficient (m^2/s)
Flax/epoxy (w_f) = 0.51) (Assarar et al., 2011)	–	13.5 (room temperature)	10.51×10^{-6}
Wood fibres/ unsaturated polyester (w_f) = 0.30) (Carvalho et al., 2013)	–	14.04 to 16.81 (dependent upon composite thickness and water temperature)	2.2 to 21.0 $\times 10^{-12}$
Wood flour/HDPE (w_f = 0.40)	4.86 (23°C)	11.6 (23°C)	3.95×10^{-12}
Wood flour/PP (w_f = 0.40) (Adhikary et al., 2008)	7.32 (23°C)	15.81 (23°C)	4.45×10^{-12}
Saw dust/PET (w_f = 0.40) (Rahman et al., 2013)	5.7 (25°C) 7.29 (75°C)	13.8 (25°C) 23.2 (75°C)	–
Ramie fibre fabric// phenolic resin (w_f = 40.4%) (Wang and Xian, 2014)		8.4 (20°C) 10.5 (40°C)	2.28×10^{-12} 3.28×10^{-12}

HDPE, high-density polyethylene; *PP*, polypropylene.

The moisture sorption capacity of fibres seems not to be strongly affected by being embedded in the matrix (Madsen et al., 2012). However, chemical interaction between fibre's hydroxyl radicals and the matrix or fibre treatment can be responsible for some lag between the predicted moisture content (rule of mixtures) and the real moisture content (Madsen et al., 2012). All these variables sustain the need to comprehend the structural design of an NFC in order to be able to assume a model and predict its properties reliably.

Water interaction with NFC affects not only its dimensional stability but also other fundamental properties as mechanical performance and durability when exposed to high humidity conditions or outdoor exposure.

17.2.2 Reaction to fire

Many uses of NFCs (eg, building, transportation) imply the need to comply with different fire safety regulations. Regarding reaction to fire (the response of a material in contributing by its own decomposition to a fire to which it is exposed under specified conditions) the European standard EN 13501-1 includes three types of classes for defining the reaction to fire class. The main class is related to the measured critical heat flow (A1 to F), a second class indicates the smoke level and finally a third class indicates the generation of flaming droplets or particles.

Reaction to fire behaviour of NFC composites is dependent upon the thermal decomposition kinetics of fibres and polymers used in its composition. Thermal stability decreases with the increase of fibre loading (El-Shekeil et al., 2012). Polymers such as polyester and polyamide do not ignite easily, whereas poly(acrylic) polymers are easy to ignite. Melamine and its derivatives were successfully tested as fire-retardant products incorporated into wood−plastic composites. However, the results are very dependent upon the composition of the melamine films.

As opposed to nonvegetable fibres (eg, glass, carbon and aramid), natural plant fibres can contribute to the fire propagation. Composites tend to show a shorter time-to-ignition (TTI) than the matrix alone due to the presence of fibres (Borysiak, 2015). However, the matrix generally burns quickly after ignition, whereas composites show a similar behaviour to lignocellulose materials. Therefore flammability of composites is largely determined by the type of lignocellulose fillers and by the quality of the interface matrix and filler (Borysiak, 2015).

The thermal stability limit of NFCs seems to be in the range of 240−355°C (Monteiro et al., 2012).

The majority of studies conducted use the Cone calorimeter test. The facility of the test and the possible extrapolation to the results obtained following the Single Burning Item test made this method suitable for a development phase (Van, 2007). The comparison of composites using the same matrix but varying the type of fibres shows that there is no significant difference according to the type of fibre used (Table 17.2).

Table 17.2 Cone calorimeter test results for different fibres and PBS matrix (radiant heat flux of 35 kW/m^2) (Dorez et al., 2013)

NFC	TTI (s)	THR (kJ)	HRR kW/m^2)
Sugarcane/PBS ($w_f = 0.3$)	74	862	313
Cellulose/PBS ($w_f = 0.3$)	96	984	385
Hemp/PBS ($w_f = 0.3$)	67	818	332
Bamboo/PBS ($w_f = 0.3$)	43	884	339
Flax/PBS ($w_f = 0.3$)	61	934	270
Flax/PBS/APP ($w_f = 0.3$)	55	-	208

APP, ammonium polyphosphate; *PBS*, polybutylene succinate.

The addition of Ammonium polyphosphate (APP) in Table 17.2 shows a noticeable decrease of the TTI, leading to the formation of a strong char barrier. This implies a decrease of Heat Release Rate (HRR).

Fibre modification can improve reaction to the fire behaviour of NFCs (Borysiak, 2015; Pan et al., 2012).

17.3 Mechanical properties

Fibres are responsible for enhancing the mechanical properties of the polymeric matrices. This is based on the superior mechanical properties, namely tensile properties, showed by fibres when compared to the matrix properties (Fig. 17.2) (Ku et al., 2011; Hossain et al., 2013).

A study on the influence of natural fibres in ecocomposites showed that the addition of natural fibres such as kenaf, rice husks or wood to polymeric matrices improves the mechanical performance of the composites remarkably, regardless of the nature of the polymer (García et al., 2007). Pickering et al. (2015) presents a summary of the variation of the mechanical properties obtained for a variety of NFCs and showed that tensile strength and tensile modulus vary from 410 to 40 MPa and from 39 to 6 GPa, respectively. Fig. 17.2 intends to show the variation that could be expected for the same mechanical properties.

However, this enhanced performance is dependent upon the load capacity of its components (fibres and matrix) and the capacity of fibres to transmit stress to the matrix (quality of the interface fibre/matrix and fibre volume fraction). When a perfect adhesion between fibres and matrix is ensured a linear increase of Young modulus

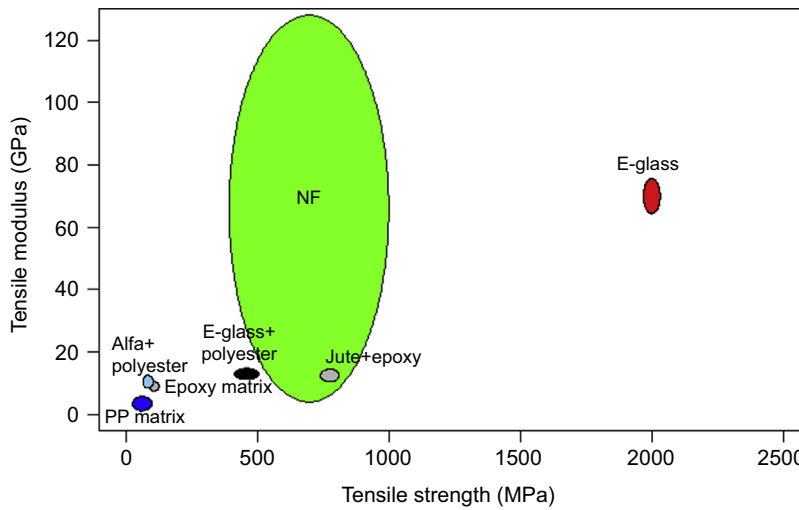

Figure 17.2 Tensile properties of different fibres, matrices and fibre reinforced composites.

of the composite ($E_{t,c}$) is expected with the increment of fibres according to the following equation (Brahim and Cheikh, 2007):

$$E_{t,c} = w_f\left(E_{t,f} - E_{t,m}\right) + E_{t,m}$$

Where $E_{t,f}$ and $E_{t,m}$ are the Young modulus of the fibre and matrix, respectively.

The addition of fibres can improve some of the properties but lead to a decrease of other properties, or even the mere addition can deteriorate the composite's mechanical performance (Shalwan and Yousif, 2013). The presence of voids (in the matrix from a weak connection between fibre and matrix) can bring a severe deterioration to the expected load capacity and stiffness. The presence of voids increases with fibre loading and explains why composites made from PP and kenaf and jute fibres with different w_f ratios showed a decrease of tensile strength as fibre loading increases, whereas the modulus showed a steady increase until a w_f around 23% and then a decrease (Lee et al., 2009). For kenaf/TPU (thermoplastic polyurethane) composites, increasing fibre loading has a different outcome depending on the type of stress (El-Shekeil et al., 2012). Therefore the following is observed: an increase of tension strength until a 0.30 w_f factor and then a steady decrease; an increase of tension modulus of elasticity, bending strength and modulus; no noticeable effect on impact strength until a loading level of 0.26 and then a considerable drop as loading increases.

Optimal fibre loading is therefore difficult to predict and varies with the type of fibre and matrix, being however generally between 5% and 50%.

The possible anisotropy of the composites should be considered. The mechanical properties of NFCs are strongly affected by the angle between fibre orientation and load direction. As opposed to randomly oriented fibre composites, monoaxial fibre orientation composites show a strong anisotropic mechanical behaviour. When the load is applied along the fibres, there is a strong contribution of fibres for the final mechanical performance, and in the opposite direction, it is the matrix that controls the final mechanical performance. Alfa/Polyester composites show a decreasing around 59%, 59% and 88% of the Young modulus, poisson ratio and tensile strength, respectively, with an increasing angle between 0 and 90 degree (Brahim and Cheikh, 2007).

Another factor that affects the mechanical behaviour seems to be the geometry of the fibre (length and diameter). Generally it can be assumed that long and slim fibres have positive effects on the mechanical properties of NFCs. This difference in critical length is mainly due to the differences in the interfacial adhesion of the fibre with the matrix that in turn controls tension and shear strength between the fibre and the matrix (Kalaprasad et al., 1997).

Modelling of the mechanical properties of NFCs uses micromechanical models considering the volume fraction of fibres and properties of each individual component. These models assume a perfect interface adhesion between fibres and matrix (which is critical in most cases of NFCs) and also a uniform strain condition.

The following models can be applied to rigid reinforcement in a rigid matrix (Kalaprasad et al., 1997).

Models	
Parallel model (rule of mixture) $M_c = M_f V_f + M_m V_m$; $T_t = T_f V_f + T_m V_m$ **Series model (inverse rule of mixture)** $M_c = \frac{M_m M_f}{M_m V_f + M_f V_m}$; $T_c = \frac{T_m T_f}{T_m V_f + T_f V_m}$	T − Tensile strength M − Young moduli c, f, m − composite, matrix and fibre, respectively
Hirsch's model $M_c = x(M_m V_m + M_f V_f) + 1(1-x)\frac{M_f M_m}{M_m V_f + M_f V_m}$ $T_c = x(T_m V_m + T_f V_f) + 1(1-x)\frac{T_f T_m}{T_m V_f + T_f V_m}$	x − parameter, which determines the stress transfer between fibre and matrix
Halpin−Tsai model $M_c = M_m\left(\frac{1 + A\eta V_f}{1 - \eta V_f}\right)$; $\eta = \frac{M_f/M_m - 1}{M_f/M_m + A}$ $T_c = T_m\left(\frac{1 + A\eta V_f}{1 - \eta V_f}\right)$; $\eta = \frac{T_f/T_m - 1}{T_f/T_m + A}$	A − fibre geometry, distribution and loading conditions
Modified Halpin−Tsai model $M_c = M_m\left(\frac{1 + A\eta V_f}{1 - \eta\psi V_f}\right)$; $T_c = T_m\left(\frac{1 + A\eta V_f}{1 - \eta\psi V_f}\right)\psi = 1 + \left(\frac{1-\phi_{max}}{\phi_{max}^2}\right)$; $A = K - 1$; $K = 1 + 2\,L/d$	ψ − parameter dependent upon particle packing fraction A − determined from the Einstein coefficient, K, reported in Shalwan and Yousif (2013) ϕ_{max} − maximum packing fraction
Cox model $M_c = M_f V_f\left(1 - \frac{\tanh \beta 1/2}{\beta 1/2}\right) + M_m V_m$ $T_c = T_f V_f\left(1 - \frac{\tanh \beta 1/2}{\beta 1/2}\right) + T_m V_m$ $\beta = \left[\frac{2\pi G_m}{M_f A_f \ln(R/r)}\right]^{1/2}$; $R = r\left(\frac{\pi}{4V_f}\right)^{1/2}$; square packed fibres $R = \left(\frac{2\pi r^2}{3^{1/2} V_f}\right)^{1/2}$ hexagonal packed fibres	L − average fibre length A_f − fibre cross-sectional area R − radius of the representative volume element R − fibre radius G_m − matrix shear modulus

The Hirsch model and the modified Bowyer and Bader equations provided a good correlation between the theoretically and experimentally determined tensile strength of Sisal/low-density polyethylene composites (fibre length around 6 mm), showing longitudinal oriented fibre prepared through a solution mixing technique (Kalaprasad et al., 1997).

Halpin−Tsai was the model that shows a higher capacity to predict the Young modulus of natural fibres (hemp, hardwood, rice hulls) and E-glass using HDPE (high density polyethylene) as the matrix (Ku et al., 2011). The Halpin−Tsai model was also more adjusted to an E-glass/HDPE composite, whereas the inverse rule of mixture was the best model for NFC (hemp, hardwood flour (20 mesh), hardwood flour (40 mesh) and rice hulls in an HDPE matrix) (Facca et al., 2006).

An empirical model ($E_{\text{random}} = 3/8E_{\text{L}} + 5/8E_{\text{T}}$) was successfully used along with Halpin−Tsai equations for longitudinal and transversal modulus to predict the Young modulus of PP polymer composite containing randomly oriented kenaf or jute fibres (Lee et al., 2009).

Fibre treatment can modify the mechanical properties of NFCs. The increase or decrease effect is dependent upon the type of treatment and stress load (Seki, 2009). The modification of jute fibres (bleached) used in a PP matrix composite show a decrease of 12% and 28% of the tensile strength and modulus, respectively, and an increase of 26% and 40% of the flexural strength and modulus, respectively (Dash et al., 2007).

Also, the production process can have a considerable effect on the final properties of biocomposites (Pickering et al., 2015; Mohanty et al., 2004). The production of hemp/cellulose acetic plastic biocomposite by powder impregnation through compression molding shows much lower flexural strength and modulus than the same composite made by conventional extrusion followed by injection molding (Mohanty et al., 2004).

17.4 Influence of service conditions in durability

The application of biocomposites is not only dependent upon their short-term properties but also on their long-term behaviour under different load and environmental conditions. Regarding outdoor exposure, two factors can affect the short-term properties shown by NFCs; UV radiation and water absorption.

Water intake can induce structural deterioration in NFCs, affecting their mechanical performance. Water immersion leads to a significant loss of tensile strength and modulus of flax/epoxy composites and, for those same properties, a slight decrease for a glass-fibre/epoxy composite (Assarar et al., 2011). Increasing moisture content affects the adhesion between fibres and matrices and thus leads to lower interfacial shear and tensile strength (Assarar et al., 2011; Josepha et al., 2002).

NFC properties are also affected by UV radiation. Photooxidation results in the decrease of the mechanical properties. PP polymer shows a decrease of tensile strength of 92.57% after a three-month exposure to UV radiation, whereas a composite sisal/PP shows, in the same period of time, only a loss of 58% (Josepha et al., 2002).

Fatigue, load duration and creep behaviour of NFCs have been studied in a very small extent. Mechanical performance is time-dependent, showing a viscoelastic and

microdamage evolution (Marklund et al., 2008). Kenaf/epoxy showed that fatigue life increases along with fibre volume ratios (0%, 15% and 45%), independent of the stress level applied (Abdullah, 2012). The same study also indicates that the effect of fibre loading is considerably higher at a low fatigue regime, rather than at a high fatigue regime. The comparison between three models (Mandel, Manson-Coffin and Hai Tang) showed that none could predict fatigue life satisfactorily (Abdullah, 2012).

A comparison study between flax and glass fibres embedded in an epoxy matrix showed, for flax/epoxy composites, a more stable fatigue performance in regards to strength. For both composites the stiffness degradation seems to be independent from the loading level (Liang et al., 2012).

A model for accounting to nonlinear viscoelasticity, viscoplasticity and damage shown by a hemp/lignin composite is proposed by Marklund et al. (2008). This composite showed different behaviours, depending on the level of stress and strain applied. Depending on the load, threshold nonlinear viscoelasticity is observed for lower load levels, and a nonlinear viscoelastic and viscoplastic behaviour is observed for higher load levels. In all cases, microdamage evolution was observed for strain levels higher that 0.3%.

The creep behaviour of a wood-filled polystyrene/high density polyethylene composite was successfully described by an empirical three-parameter power model (Xu et al., 2001). The comparison between a wood−plastic composite and solid wood showed a more pronounced effect load duration for the former material (Brandt and Fridley, 2003).

17.5 Final remarks

The increasing use of NFCs is promoted by its recognized contribution toward 100% renewability and biodegradability products. However, challenges such as low degradation temperatures and hydrophilicity have to be resolved in order to ensure the minimum working life expected for each end-use.

If perfect adhesion conditions can be guaranteed, then the addition of natural fibres improves the mechanical, weathering and durability performance of the composites. UV radiation and water absorption are factors that affect the short and long-term properties of the NFCs by causing low interfacial shear and affecting their tensile strength, fatigue and creep behaviour.

It is possible to enhance the natural fibre properties by fibre modification and chemical treatments and thus improve the adhesion to the matrix, dimensional stability and reaction to fire.

References

Azwa, Z.N., Yousif, B.F., Manalo, A.C., Karunasena, W., 2013. A review on the degradability of polymeric composites based on natural fibers. Materials and Design 47, 424−442.

Assarar, M., Scida, D., El, M.A., Poilâne, C., Ayad, R., 2011. Influence of water ageing on mechanical properties and damage events of two reinforced composite materials: flax−fibres and glass−fibres. Materials and Design 32, 788−795.

Adhikary, K.B., Pang, S., Staiger, M.P., 2008. Long-term moisture absorption and thickness swelling behaviour of recycled thermoplastics reinforced with Pinus radiata sawdust. Chemical Engineering Journal 142, 190−198.

Ansari, F., Galland, S., Johansson, M., Christopher, J.G., Plummer, C.J.G., Berglund, L.A., 2014. Cellulose nanofiber network for moisture stable, strong and ductile biocomposites and increased epoxy curing rate. Composites: Part A 63, 35−44.

Abdullah, A.H., Alias, S.K., Jenal, N., Abdan, K., Ali, A., 2012. Fatigue behavior of kenaf fibre reinforced epoxy composites. Engineering Journal 16, 105−113.

Borysiak, S., 2015. The thermo-oxidative stability and flammability of wood/polypropylene composites. Journal of Thermal Analysis and Calorimetry 119, 1955−1962.

Brahim, S.B., Cheikh, R.B., 2007. Influence of fibre orientation and volume fraction on the tensile properties of unidirectional Alfa-polyester composite. Composites Science and Technology 67, 140−147.

Brandt, C.W., Fridley, K.J., 2003. Load-duration behavior of wood-plastic composites. Journal of Materials in Civil Engineering 15, 524−536.

Carvalho, L.H., Canedo, E.L., Neto, S.R.F., Lima, A.G.B., Silva, C.J., 2013. Moisture transport process in vegetable fiber composites: theory and analysis for technological applications. Industrial and Technological Applications of Transport in Porous Materials Advanced Structured Materials 36, 37−62.

Cheng, Q., Muszynski, L., Shaler, S., Wang, J., 2010. Microstructural changes in wood plastic composites due to wetting and re-drying evaluated by X-ray microtomography. Journal of Nondestructive Evaluation 29, 207−213.

Dorez, G., Taguet, A., Ferry, L., Lopez-Cuesta, J.M., 2013. Thermal and fire behavior of natural fibers/PBS biocomposites. Polymer Degradation and Stability 98, 87−95.

Dash, B.N., Rana, A.K., Mishra, S.C., Mishra, H.K., Nayak, S.K., Tripathy, S.S., 2007. Novel low-cost jute−polyester composite. II. SEM observation of the fractured surfaces. Polymers-Plastic Technology and Engineering 39, 333−350.

Ermolaeva, A.S., Kaveline, K.G., Spoormaker, J.L., 2002. Materials selection combined with optimal structural design: concept and some results. Materials and Design 23, 459−470.

El-Shekeil, Y.A., Sapuan, S.M., Abdan, K., Zainudin, E.S., 2012. Influence of fiber content on the mechanical and thermal properties of kenaf fiber reinforced thermoplastic polyurethane composites. Materials and Design 40, 299−303.

Faruk, O., Bledzki, A.K., Fink, H.-P., Sain, M., 2012. Biocomposites reinforced with natural fibers: 2000−2010. Progress in Polymer Science 37, 1552−1596.

Facca, A.G., Kortschot, M.T., Yan, N., 2006. Predicting the elastic modulus of natural fibre reinforced thermoplastics. Composites: Part A 37, 1660−1671.

García, M., Garmendia, I., García, J., 2007. Influence of natural fiber type in eco-composites. Journal of Applied Polymer Science 107, 2994−3003.

Herrera-Franco, P.J., Valadez-González, A., 2005. A study of the mechanical properties of short natural fiber-reinforced composites. Composites: Part B 36, 597−608.

Hossain, R., Aminul Islam, A., Van, V.A., Verpoest, I., 2013. Tensile behavior of environment friendly jute epoxy laminated composite. Procedia Engineering 56, 782−788.

Joshi, S.V., Drzal, L.T., Mohanty, A.K., Arora, S., 2004. Are natural fiber composites environmentally superior to glass fiber reinforced composites? Composites: Part A 35, 371−376.

Josepha, P.V., Rabello, M.S., Mattoso, L.H.C., Joseph, K., Thomas, S., 2002. Environmental effects on the degradation behaviour of sisal fibre reinforced polypropylene composites. Composites Science and Technology 62, 1357−1372.

Kaboorani, A., Englund, K.R., 2011. Water sorption and mechanical performance of preheated wood/thermoplastic composites. Journal of Composite Materials 45, 1423−1433.

Ku, H., Wang, H., Pattarachaiyakoop, N., Trada, M., 2011. A review on the tensile properties of natural fiber reinforced polymer composites. Composites: Part B 42, 856−873.

Kalaprasad, G., Joseph, K., Thomas, S., Pavithran, C., 1997. Theoretical modelling of tensile properties of short sisal fibre-reinforced low-density polyethylene composites. Journal of Materials Science 32, 4261−4267.

Lu, J.Z., Wu, Q., McNabb Jr., H., 2000. Chemical coupling in wood fiber and polymer composites: a review of coupling agents and treatments. Wood and Fiber Science 32, 88−104.

Lee, B., Kim, H., Yu, W., 2009. Fabrication of long and discontinuous natural fiber reinforced polypropylene biocomposites and their mechanical properties. Fibers and Polymers 10, 83−90.

Liang, S., Gning, P.B., Guillaumat, L., 2012. A comparative study of fatigue behaviour of flax/epoxy and glass/epoxy composites. A review. Composites Science and Technology 72, 535−543.

Madsen, B., Hoffmeyer, P., Lilholt, H., 2012. Hemp yarn reinforced composites − III. Moisture content and dimensional changes. Composites: Part A 43, 2151−2160.

Monteiro, S.N., Calado, V., Rodriguez, R.J.S., Margem, F.M., 2012. Thermogravimetric stability of polymer composites reinforced with less common lignocellulosic fibers − an overview. Journal of Materials Research and Technology 1, 117−126.

Mohanty, A.K., Wibowo, A., Misra, M., Drzal, L.T., 2004. Effect of process engineering on the performance of natural fiber reinforced cellulose acetate biocomposites. Composites: Part A 35, 363−370.

Marklund, E., Eitzenberger, J., Varna, J., 2008. Nonlinear viscoelastic viscoplastic material model including stiffness degradation for hemp/lignin composites. Composites Science and Technology 68, 2156−2162.

Pan, M., Mei, C., Song, Y., 2012. A novel fire retardant affects fire performance nad mechancial properties of wood flour-high density polyethylene composites. Bioresources 7, 1760−1770.

Pickering, K.L., Aruan Efendy, M.G., Le, T.M., 2015. A review of recent developments in natural fibre composites and their mechanical performance. Composites: Part A. http://dx.doi.org/10.1016/j.compositesa.2015.08.038.

Rahman, K.S., Islam, N., Rahman, M., Md Hannan, O., Dungani, R., Khalil, A., 2013. Flat-pressed wood plastic composites from sawdust and recycled polyethylene terephthalate (PET): physical and mechanical properties. SpringerPlus 2, 629.

Sgriccia, N., Hawley, M.C., Misra, M., 2008. Characterization of natural fiber surfaces and natural fiber composites. Composites: Part A 39, 1632−1637.

Shalwan, A., Yousif, B.F., 2013. In state of art: mechanical and tribological behaviour of polymeric composites based on natural fibres. Materials and Design 48, 14−24.

Seki, Y., 2009. Innovative multifunctional siloxane treatment of jute fiber surface and its effect on the mechanical properties of jute/thermoset composites. Materials Science and Engineering A 508, 247−252.

Van, H.P., Axelsson, J., 2007. Modelling of euroclass test results by means of the cone calorimeter. In: Multifunctional Barriers for Flexible Structure. Materials Science, vol. 97, pp. 215−226.

Wambua, P., Ivens, J., Verpoest, I., 2003. Natural fibers: can they replace glass in fibre reinforced plastics? Composites Science and Technology 63, 1259−1264.

Wang, H., Xian, G., Li, H., Sui, L., 2014. Durability of a ramie-fiber reinforced phenolic composite subjected to water immersion. Fibers and Polymers 15, 1029−1034.

Xu, B., Simonsen, J., Rochefort (Skip), W.E., 2001. Creep resistance of wood-filled polystyrene/high density polyethylene blends. Journal of Applied Polymer Science 79, 418−425.

Creep behaviour of plant fibre composites

18

C. Santulli
Università degli Studi di Camerino, Ascoli Piceno, Italy

18.1 Introduction: perspectives and applications of plant fibre composites

Most polymer matrices in composites experience creep behaviour, even at ambient temperatures or slightly above. In particular, when the matrix is stressed, its free energy is raised, then the polymer segments gradually reorient, coming back to a lower energy rate. For polymers where glass transition temperature is above ambient temperature, therefore operating in the rubbery state (which is the case for polyolefins), the viscous resistance to reorientation of chain segments is normally easily overcome (Raghavan and Meshii, 1998). In contrast, for polymers operating at the glassy state, the viscous resistance to the reorientation of chain segments will be very high, with the polymer matrix behaving like a brittle solid. The latter is usually the case of lignocellulosic fibres. For example, a study on flax and nettle fibres subjected to tensile loading demonstrated the measurable effect of environmental humidity over the progression of their creep behaviour (Davies and Bruce, 1998).

This combined presence of two polymers as the matrix and the fibre (cellulose itself is a polymer), which is the case for plant fibre composites (PFCs), acting differently if not with contrasting modes as regards dynamical behaviour, hence creep, is inherent to the nature of these matrix and fibre materials. This is particularly significant in most recent studies, where, due to sustainability reasons, the traditional thermoplastic matrices, such as polyolefins (polypropylene and polyethylene) and the biodegradable/compostable ones, such as polylactic acid (PLA) or polycaprolactone (PCL), have been considered for the production of plant fibre composites. An early yet comprehensive review on this topic is available in Bogoeva-Gaceva et al. (2007). More precisely, plant fibres can be considered as hierarchical cellular composites, according to the definition by Lakes (1993). In practical terms, a reasonably clear example of the arrangement of a technical lignocellulosic fibre is offered in Fig. 18.1, referred to as sisal (Oksman et al., 2002). In the specific case, they are formed by cellulose, hemicellulose and lignin, all of which are polysaccharides, though with very different structural arrangements and properties. For this reason, they include in themselves softer and harder parts, which can be again schematized as acting as matrix and fibres, respectively, therefore ideally forming a suitable bonding of uniform strength, in other words an interface. A consequence of this is that, as stated earlier, a plant fibre is itself a polymer and therefore subject to viscoelastic behaviour. To summarize these first observations, it can be

Advanced High Strength Natural Fibre Composites in Construction. http://dx.doi.org/10.1016/B978-0-08-100411-1.00018-2

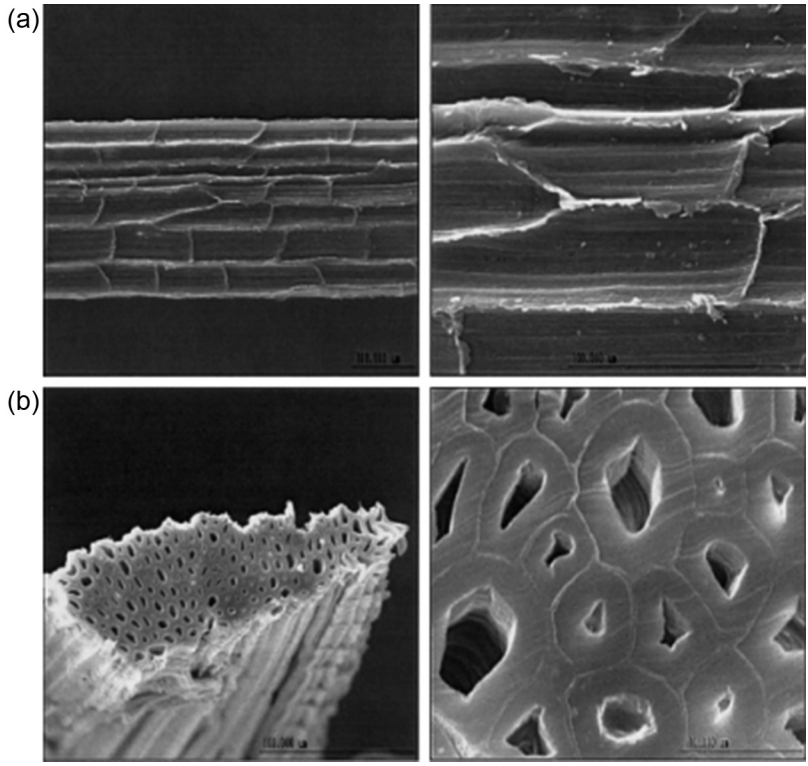

Figure 18.1 Technical fibre of sisal (sisal bundle): (a) longitudinal section and (b) cross section.

reasonable to assume that in fabricating PFCs, both the matrix (a polymer) and the reinforcement (a hierarchical natural fibre) would present viscoelastic behaviour. It will be not obvious therefore to lead to a reasonable prediction of the sum of the different effects (from plant fibres and from the matrix polymer) over the behaviour of the PFCs in service, hence over a suitably long period of time. These considerations justify the study of this topic for the practical application of plant fibre composites, also to enhance their profile of use, which has been so far in semistructural components (Mwaikambo, 2006). On the other hand, only a limited number of investigations have been carried out on the subject of viscoelasticity of PFCs, which mainly cover only the most frequently used plant fibres.

Going into slightly greater detail, an influence of temperature and applied stress is obviously present on stress behaviour, as it was clarified in the case of hemp and sisal fibre reinforced composites. In general, it is very important to determine creep compliance of the material, as measurable in terms of time-dependent strain per unit stress in the range of temperatures intended for material service. In practice, creep measurement in PFCs is influenced by a very large number of factors interacting among them, so that it is fair to say that data so far are still insufficient for a complete creep assessment of a large range of materials in the domain of PFCs, so that these could reliably be used in

engineering applications. In particular, it is noteworthy that most studies concern flexural creep: this fact both derives from the main uses envisaged for PFC laminates, hence as semistructural panels, and proved easily to be consistently measured, considering the inherent scattering of properties obtained in these materials. Another significant phenomenon, which appears to be very important, is the growing occurrence of creep both in terms of increasing strains and in terms of reduced ultimate stresses after loading and unloading cycles. It needs to be considered, though fatigue testing has had a limited coverage in the literature on PFCs. This is a necessary step in a view to improve their range of applications to also include structural uses. Most studies from which useful indications in this regard can be obtained concern dynamical mechanical analysis of PFC, especially in the proximity of critical temperatures, such as glass transition and softening temperature. The possible ways of reducing creep sensitivity of PFC, for example, through blending with ceramic fillers and/or modifying the production process, using methods that have been widely validated on traditional composites, such as pultrusion, are worth consideration and have been investigated in the literature.

18.2 Some indications on viscoelasticity of polymers

Viscoelasticity of polymers involves the presence of a complex relationship between time, temperature and stress: concerning their behaviour over time, it is possible to distinguish between a linear and a nonlinear viscoelasticity (Zaslavsky, 1963). Without going into very specific details, which are out of scope with respect to the present work, this appears of crucial importance, as far as polymer processing for the production of components is concerned. Dealing with PFCs, an aspect that is particularly significant is that the use of linear polymers is rare not only as the fibre, where hierarchization arranges microfibrils in the form of helices, but also as the matrix, where the need for suitable flow for injection moulding and hence the introduction of additives, creates variable levels of entanglement of the polymer chains. This is particularly true in the case biodegradable and/or compostable polymers are used as the matrix, as these phenomena have been thoroughly investigated in the case of natural biopolymers, such as gluten in its interaction with glycerol (Redl et al., 1999) or starch-fatty acid systems in their interaction with sorbitol (Mantzari et al., 2010).

In this situation, where rheological behaviour is determined by a number of factors, including temperature, plasticizer content and mixing speed, all of which contribute to the determination of storage modulus and loss modulus in the polymer, arrangements can often be complex. This is also the case for synthetic biopolymers. For example, when considering the most commonly used polymer, polylactic acid (PLA), one of the most suitable forms of PLA can be modelled as a star-shaped chain, which presents enhanced melt stability (Biela et al., 2006). By contrast, the melt stability of common forms of PLA and other synthetic biopolymers and blends is considerably lower; in other words, variability is very significant at processing temperatures (Signori et al., 2009).

This proves to be an even more realistic scenario when using thermoplastic starch-based polymers, due to the considerable variety of agromaterials (in practice, granules of starch from different crops) from which these are obtained. For example, differences in mechanical properties with different blends of corn and wheat starch with PLA are discussed by Ke and Sun (2000). Other possibilities include potato or barley starch (Eliasson, 1986) or even pea starch (Ma et al., 2009). As a consequence, the study of entangled polymers, which has been often carried out, appears particularly to obtain realistic information on the flow behaviour of PFCs. The differences in the viscoelastic properties between linear and branched polymers indicate the importance of chain end mobility: in the specific case of blends (as usually bio-based polymers are), the component molecular weights and compositions significantly affect the entanglement lifetime (Watanabe, 1999).

18.3 Creep behaviour of biopolymers and possible improvement

Some studies are available that are more specific on the differences between the viscoelastic behaviour of oil-derived polymers and biopolymers in terms of performance. Limited study is present so far on creep during service of biopolymers, some of which will be discussed in the next sections, with most studies instead concentrating on rheology during processing (Picout and Ross-Murphy, 2003). This aspect of course bears considerable similarities with creep for the presence of temperature effects, but does not include considerations of polymer ageing and subsequent degradation. In particular, since creep is much more significant in biopolymers with respect to traditional thermoplastic polymers, such as polyethylene and polypropylene, some emphasis is put on the possibility to reduce creep by the use of adapted additives and/or plasticizers. Some plasticizers are particularly effective in modifying the rheology of thermoplastic starch (TPS), hence the results of their addition to TPS have been widely investigated, especially glycerol and sorbitol. It has been proven that the effect of glycerol on the reduction of viscosity is far from being linearly growing with the amount introduced. Instead there are regions in which a kind of transition occurs, so that even the addition of a small amount of glycerol produces very notable effects on easing the polymer flow: this has been revealed to be around 40% of glycerol in TPS (Rodriguez-Gonzalez et al., 2004). The effects of glycerol and sorbitol have been compared in typical TPS/PLA blends, which are used in a number of applications for consumables (eg, shopping biobags). The glycerol/sorbitol ratio in the blend played a very significant role in affecting the rheology, especially due to the different actions of the two plasticizers: it was suggested that glycerol was generally more prone to transfer from the TPS to the PLA phase than sorbitol (Li and Huneault, 2011). Another blend of PLA that has been investigated, also with respect to its rheology and effect on melt processing, is the one with poly(butylene adipate-co-terephtalate) (PBAT), on which different processing conditions were adopted for temperature (ranging from 150−200°C) and other parameters,

such as moisture removal and processing in the nitrogen atmosphere. Analysis of PLA/PBAT blends indicated that intermolecular chain reactions took place under strong degradative conditions of PLA, yielding PLA/PBAT mixed chains (copolymers). Increasing amounts of copolymers resulted in improved phase dispersion and increased ductility, as SEM and mechanical tests indicated. Conversely, reduced PLA degradation with less copolymer formation afforded the production of higher modulus materials, owing to poorer dispersion of the soft phase (PBAT) into the PLA matrix (Signori et al., 2009).

An additive that is proven to be most effective in reducing creep in PLA and polyhydroxyalkanoates was thiodiphenol, which formed hydrogen bonds at the interface of polymer and fibre, while also tributyl citrate, a plasticizer, produced some, yet less obvious, effects (Wong and Shanks, 2008).

As exposed earlier, starch rheology is not always suitable for the use as a matrix in composites, especially for their very high sensitivity to creep and scattering of properties. Modifications have been proposed, particularly in blending with clay, especially in nanometric form. Results suggested that during gelatinization, the structural part of starch, ie, amylose, interacted with a nanoclay interlayer and consequently improved reinforcement and modulus values; this was particularly effective with wheat and corn starch, less so with potato and waxy corn, since the latter had modulus values rapidly decreasing at higher temperatures (Chiou et al., 2005). Other biopolymers available on the market, such as polycaprolactone (PCL), have been employed in blending with starch, in order to modify the rheology of the latter: it has been noticed that creep compliance increased with the increase of temperature, even if PCL has obvious limitations from its melting temperature of around 60°C, although the fragmentation of the polymer macromolecules showed a notable influence on creep behaviour (Cyras et al., 2002).

18.4 Relaxation of polymers forming plant fibres: effect of temperature, load and humidity

It is well known that for fibres, such as glass or carbon, scaling laws exist, which suggest that above a critical load the deformation of the creeping system monotonically increases in time, resulting in global failure, while below the critical load the system suffers only partial failure, and the deformation tends to a constant value, giving rise to an infinite lifetime (Kun et al., 2003). This presence of a ‘safety load’ can be considered true whenever the occurrence of defects is limited and the geometry of the fibre can be supposed to be regular and uniform, which is mainly the case for carbon, glass and aramidic (Kevlar) fibres.

By contrast, plant fibres, often more precisely referred to as ‘lignocellulosic’, are complex structures made of variable amounts of polysaccharides and therefore are highly sensitive to relative displacements over time of the different parts they are formed of. In general terms, plant tissues suffer as an effect of tensile loading and unloading during life internal ‘microstructural’ prestresses, which result in

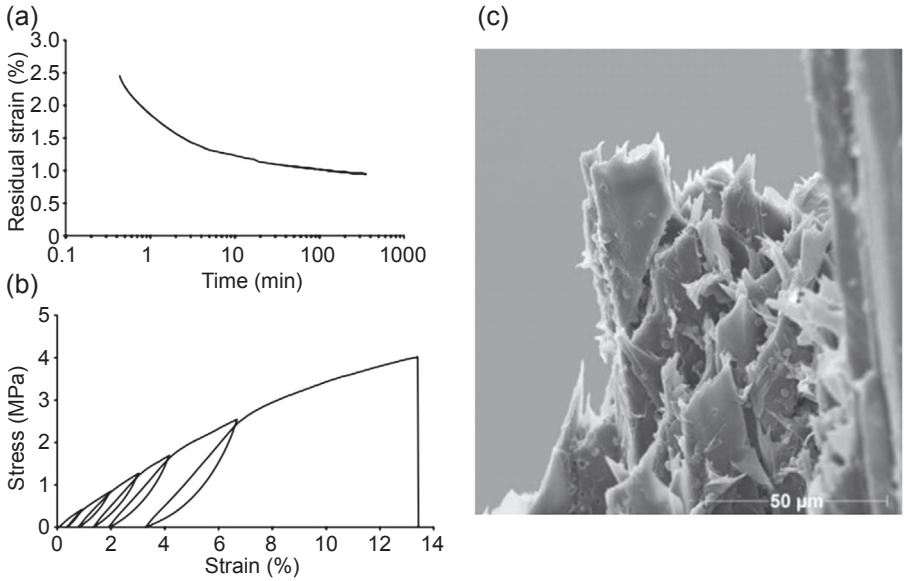

Figure 18.2 (a) Creep curve after loading sclerenchyma *of Aristolochia macrophylla* to 5.1% extension and unloading to 0% stress, showing that the residual deformation remains finite even after 6 h. (b) An ontogenetically young axis of *Aristolochia macrophylla* subjected to successively larger cycles of loading and unloading. The stress−strain relationship shows that the yield point is shifted towards increasingly higher values of the overall stress. Up to this point, the loading curves are nearly linear from the second cycle on. (c) SEM image of a strip of strengthening tissue from *Aristolochia macrophylla* after tensile fracture.

viscoelastic and viscoplastic behaviour (Spatz et al., 1999), as reported in greater detail in Fig. 18.2, for the loading and unloading behaviour of a specific case of *Aristolochia macrophylla*. This is particularly evident, considering that fibres present large amounts of defects due to their hierarchical structure, which leaves voids or geometrical mismatches, also referred to as dislocations. These tend to show creep over time, leading to a mechanical flow of the whole structure. The need to reduce, as much as possible, creep of lignocellulosic fibres, arranged in structures such as nets, mats or woven tissues, is of paramount importance for applications such as structural upgradation of soil, in which case they need to be self-sustaining and promote self-reliance, characteristics that are also useful for the production of composites. It has been noticed for upgradation that the combined use of more fibres would promote a synergistic effect (Sen and Jagannatha Reddy, 2011). However, this is not frequent in composites, where normally a single fibre is used to be introduced in the polymer matrix.

More precisely, dislocations are areas of the cell wall where the local microfibril angle differs from the microfibril angle of the surrounding cell wall (Thygesen et al., 2006). In the particular case of hemp fibres, it has been indicated that the straining of dislocations does not lead to a new stable, but rather dislocations creep in long-term behaviour (Thygesen et al., 2007). This evidence can be of variable intensity

in different lignocellulosic fibres; in particular, creep was observed in nettle fibres, but not in flax ones (Davies and Bruce, 1998). As a matter of fact, under repeated loading and unloading cycles, the tensile stiffness of flax fibres proved to increase with unrecoverable strain; this was attributed to a progressive phenomenon of reorientation of the fibrils in the direction of loading (Baley, 2002). It is also worth noting that fibre becomes more prone to possible strain with the absorption of moisture. This was particularly observed on hemp (Placet et al., 2012). In this case, absorption and desorption cycles lead to substantial rotation of the fibre about its axis, due to the modification of adhesion between cellulose microfibrils and the amorphous matrix, leading to the rearrangement of the former in the latter constituent under cyclic loading.

18.5 Interfacial strength in plant fibre composites: effect of fibre treatment

Over the years, a number of treatments have been applied on lignocellulosic fibres: a basic distinction can be made between different types of treatments according to their effect on the fibre surface. In particular, primary treatments, such as alkali (typically with sodium hydroxide), are aimed at nonstructural matter removal from the fibre surface, which results in a shrinkage process of the fibres and hence comes some mechanical effect, which was firstly demonstrated on the static properties of jute fibre composites, combined with the effect of alkali concentration (Gassan and Bledzki, 1999a) (Fig. 18.3). By contrast, secondary treatments, such as silane, provide some coverage of the surface to make it smoother and more regular. There are then grafting treatments, typically maleic anhydride, which are able to provide a substantial interface strength by chemical reaction to some matrices, specifically polypropylene (MAPP) and polyethylene (a quite comprehensive review on the effect of maleation on the interface strength between plant fibres and polyolefin matrices is offered by Keener et al., 2004). However, the evolution of silane treatments towards multifunctionality, typically with oligomeric siloxane, also resulted in a substantial increase of tensile, flexural and interlaminar shear strength (eg, on jute fibre reinforced composites, as from Seki, 2009). This improvement of interface strength may also result in a variation of dynamical properties under continuous loading, such as the case for creep. This may occur as the consequence of some evidences; in particular, the modification of chemical removal of cementing materials facilitates the exposure of reactive hydroxyl (OH) groups on the fibre surfaces, thus enabling better bonding between the fibre and the polymer matrix or coupling agent. A comprehensive review on fibre treatments is offered by Li et al. (2007).

The elementary fibres may also be separated from their fibre bundles, thus increasing the effective surface area for bonding with a matrix material and improving the fibre dispersion within the composite, all factors which improve mechanical interlocking. An increase in fibre thermal stability and fibre crystallinity index as effects of treatments have also been documented. The consequence, from the point of view of mechanical properties, is definitely for fibres; once inserted in PFCs, there is an

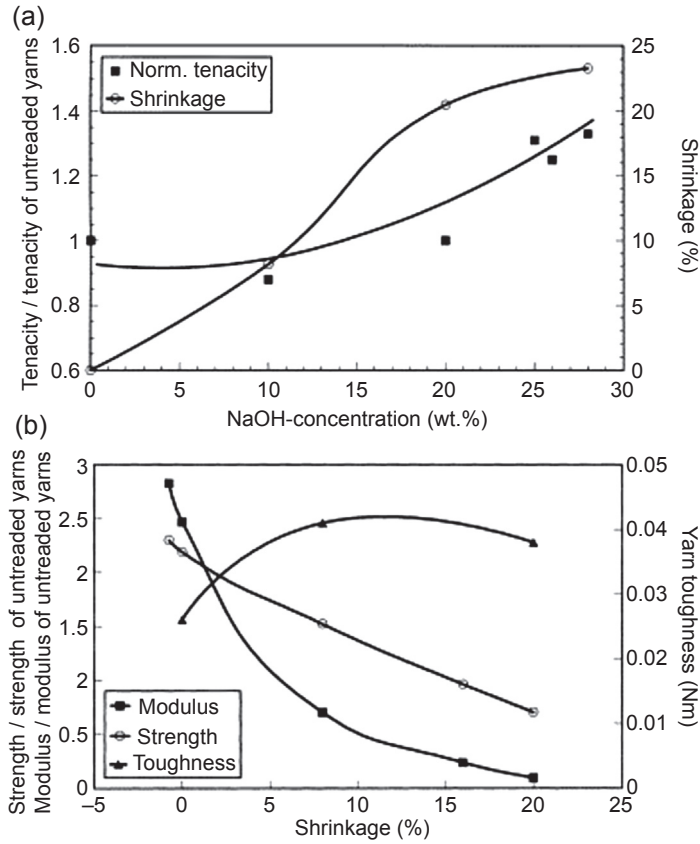

Figure 18.3 (a) Influence of NaOH concentration on normalized tenacity (isometric conditions) and shrinkage of jute fibre yarns (treatment time = 20 min, treatment temperature = 20°C). (b) Influence of shrinkage during alkalinization process on the change of modulus, strength and toughness of jute fibre yarns (25 wt% NaOH, treatment time = 20 min, treatment temperature = 20°C).

increase of tensile, flexural and impact properties. A large number of studies exist that demonstrate the effect of the aforementioned treatment. These studies are particularly representative whenever a new treatment is proposed and its effects would be assessed; for example, this is the case on jute of siloxane treatment, which has been discussed by Seki (2009), or shellac treatment of yarns, proposed by Ray et al. (2006). Most studies, as the two mentioned earlier, have been performed for the introduction of fibres in thermosetting matrices.

In the case of the effect of chemical treatment of thermoplastic matrix composites, especially biodegradable ones such as PLA, literature coverage is much more limited. For example, a significant study is offered by Sawpan et al. (2011). In this case, it was demonstrated that alkali and silane treatments applied on hemp fibre inserted in a PLA matrix improved tensile and Charpy impact properties as the result of good

fibre/matrix adhesion and increased matrix crystallinity. This increase of crystallinity is also effective as reducing the sensitivity of PFCs to creep: this was particularly noticed in jute fibre reinforced composites, due to the closer packing of cellulose fibres, consequent to the removal of nonstructural matter (Ray et al., 2009). More specific treatments, aimed to the reduction of creep, have also been attempted; in the case of cyanoethylation, composites prepared from cyanoethylated jute showed better creep resistance at comparatively lower temperatures, whilst the reverse was observed at higher temperatures, such as 120°C and above (Saha et al., 1999). A limited amount of works exist comparing different treatments on plant fibres, regarding their creep performance; in particular, on bagasse fibre reinforced composites, it has been suggested that an alkali treatment, also referred to as mercerization, leads to the highest creep activation energy (Vazquez et al., 1999).

18.6 Dynamical and creep behaviour of composites including plant fibres

A limited number of studies on the dynamical and creep behaviour of PFCs exist. This aspect is particularly important if these materials are to be subjected to the application of repeated loading during service. This is the case of their application in construction, in which case a ceramic, typically clay-based matrix is used, or in the automotive sector, where instead a traditional, nonbiodegradable thermoplastic polymer matrix is more typically used. In both cases, loading and unloading cycles are typically produced mainly by the effect of vibration and by the junction with other parts of the structure. In the following part of this chapter, studies that are suggestive of creep behaviour in composites are reported and commented on.

18.6.1 Hemp

Early studies on tension−tension fatigue behaviour of woven hemp polyester composites elucidated the fact that there is no substantial difference in qualitative terms with what has been observed on fibreglass, as far as the three-stage evolution of fatigue damage (steep slope, plateau and then again steep slope) is concerned, with the last stage being related to fractures of fibre strands (De Vasconcellos et al., 2014) (Fig. 18.4). Hemp fibres were demonstrated to be particularly suitable for the industrial production of plant fibre composites; in particular, when the resin transfer moulding process was used, the laminates were demonstrated to be virtually free from defects, although when subjected to flexural creep loading, the deformation was proved to be substantial and of some concern (Rouison et al., 2006), as indicated in Fig. 18.5. This might as well apply to creep behaviour of hemp fibre reinforced composites, on which limited studies exist (though even less exist on thermoplastic matrix composites). It was pointed out on hemp fibre reinforced unsaturated polyester composites containing different fibre (10, 15, 21 and 26 vol.%) percentages that the process of flexural creep behaviour is greatly influenced by both stress level and temperature,

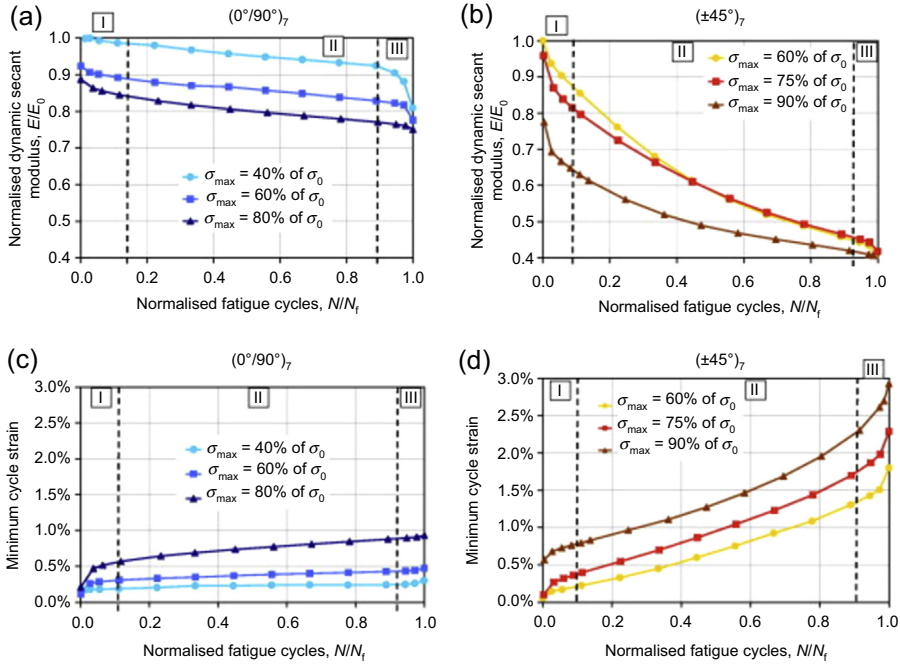

Figure 18.4 (a and b) Evolution of dynamic modulus versus fatigue lifetime for (a) $[0°/90°]_7$ and (b) $[\pm45°]_7$ hemp/epoxy laminates. (c and d) Evolution of minimum cycle strain versus fatigue lifetime for (c) $[0°/90°]_7$ and (d) $[\pm45°]_7$ hemp/epoxy laminates.

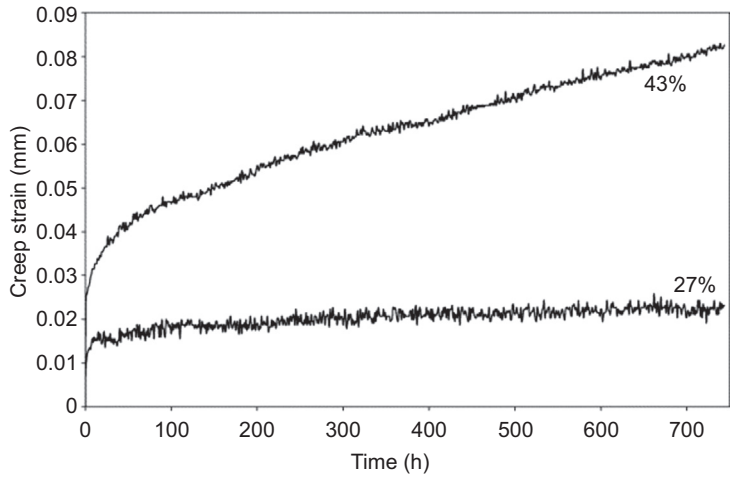

Figure 18.5 Creep strain of 21 vol.% hemp fibre composites with an applied load of 27% and 43% of the breaking load.

with the best performance offered at ambient temperature (Dhakal et al., 2009). In case a starchy matrix is used with hemp fibres, it was proven that the improvement of interfacial properties clearly allows a better control of damage onset (Hbib et al., 2011).

18.6.2 Flax

In terms of fatigue performance, flax has been suggested as having properties not very far from glass fibre composites: a thorough comparative review was carried out by Liang et al. (2012), which concentrates on epoxy resin composites. Results as far as S−N curves are concerned are reported in Fig. 18.6. Marked nonlinearity in tension has been observed on PLA−flax composites, which was attributed to microdamage and viscoelastic and viscoplastic response (Varna et al., 2012). In particular, two models have been suggested for this behaviour, namely, Schapery's type of model for viscoelasticity and Zapas' model for viscoplasticity: both models that have been originally developed for oil-based thermoplastics, such as polyethylene (Schapery, 1969; Crissman and Zapas, 1985). Another study pointed out the effect of additives

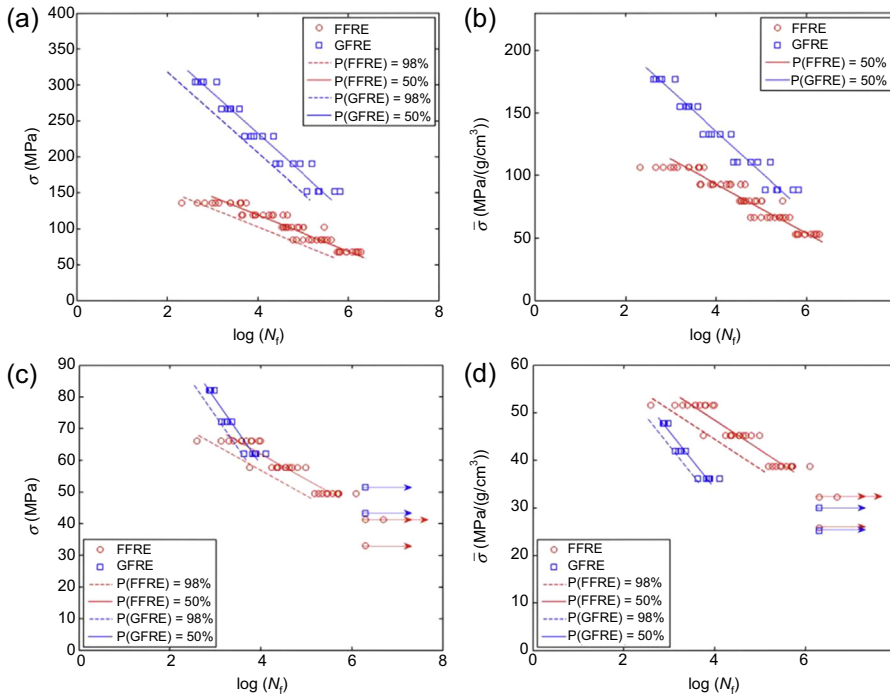

Figure 18.6 P−S−N (probability of failure-stress-number of cycles) (a) and specific S−N (b) behaviour of $[0/90]_{3S}$ flax fibre reinforced epoxy (FFRE) and glass fibre reinforced epoxy (GFRE) specimens; S−N (c) and specific S−N (d) behaviour of $[\pm 45]_{3S}$ FFRE and GFRE specimens.

to PLA on creep properties, which was revealed to be more pronounced at low frequencies (Siengchin and Dangtungee, 2013).

18.6.3 Sisal

A study on short-term flexural creep on sisal fibre composites in a MaterBi TPS matrix demonstrated that even an addition of a limited amount (5−15 wt%) of fibres had a positive influence on the creep resistance of the composite (Alvarez et al., 2004) (Fig. 18.7). However, at this low level of reinforcement, a particular attention needs to be paid to fibre length. Large differences were noticed in terms of the rheological properties of sisal fibres/PLA composites when passing from 4 to 12 mm sisal fibre length at levels as low as 10 wt%, whereas at higher levels of reinforcement the effect of the amount of fibres introduced becomes predominant (Da-Wei et al., 2011). In other words, a possible assumption of continuity for the fibres is crucial when only a small quantity of them is introduced.

18.6.4 Jute

In the case of jute fibre reinforced polypropylene composites, the use of maleic anhydride grafting on the matrix drastically improved creep behaviour. In contrast, as far as the reinforcement is concerned, creep deformation decreases as jute content increases, although only marginally when fibre concentrations larger than 25 wt% are used, which might be the result of the very large number of defects present in the fibres (Acha et al., 2007) (Fig. 18.8). Another work demonstrated that MAPP was able, through the improvement of fibre-matrix interface and the subsequent reduction of fibre pull-out, to produce lower creep strain in the outer fibres (Gassan and Bledzki, 1999b).

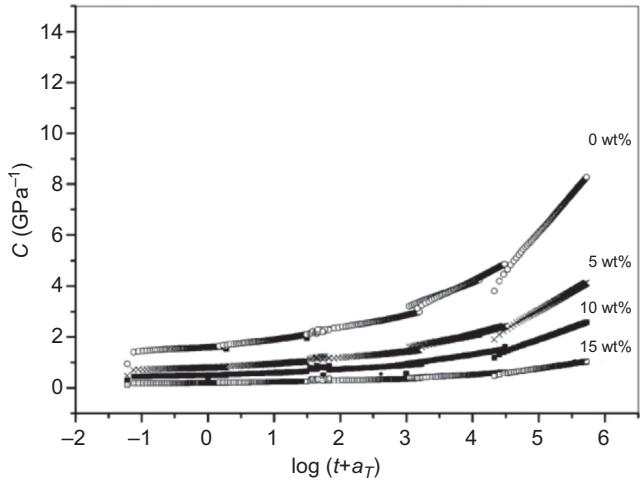

Figure 18.7 Master compliance curve (results of time−temperature superposition) for the cellulose derivatives/starch blend with different sisal fibre contents.

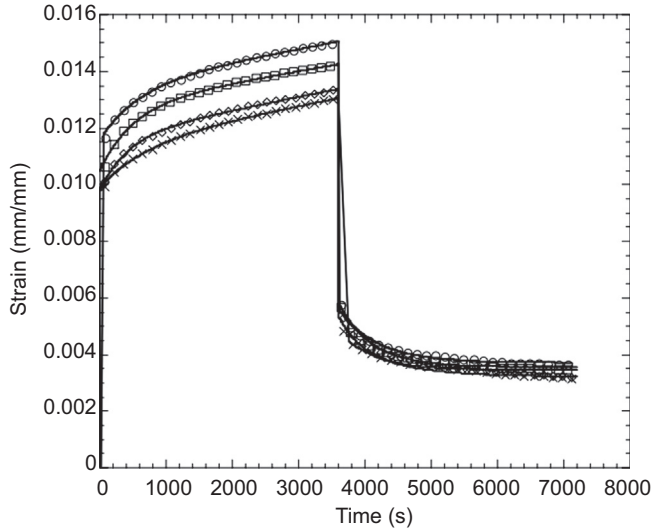

Figure 18.8 Experimental creep−recovery curves (symbols) and fitting with the four elements model (lines) for polypropylene-jute (PPJ) composites. Jute content (wt%): ○, 9; □, 17; ◇, 25; ×, 30.

18.6.5 Other fibres

Also on kenaf fibre reinforced polypropylene composites, the positive influence of the addition of maleic anhydride on creep properties is confirmed. However, other elements are also added, in the sense that MAPP has an influence on crystallization properties, which leads to the fact that melting temperature is somehow reduced (Feng et al., 2001). A subsequent study on a similar material, including 50 wt% of kenaf fibres into a compatibilized polyethylene matrix, tried quite ambitiously to model creep behaviour from a 24 h creep test. Extrapolation did indicate that the composite was thermorheologically complex, so that in the end the model proved not adequate to predict the long-term performance of the material (Tajvidi et al., 2005). Kenaf fibres of different lengths were also introduced as the reinforcement of a soy-based matrix in an extruded, then compression or injection moulded, laminate. Here, creep studies were performed to measure the heat deflection temperature: the differences between the different laminates were very considerable, which suggest a very large influence of processing parameters and of fibre length on creep behaviour (Liu et al., 2007). Some details are given in Fig. 18.9.

An interesting study was also carried out by introducing fique mats in a low-density polyethylene matrix with aluminium films, obtained from the recycling of the nonpaper part of Tetra Pak. In particular, the creep strains decrease as fique content increases; it is also notable that fibre−matrix interactions attributed to treatment with silane and subsequent covalent bonds result in much lower creep (Hidalgo-Salazar et al., 2013).

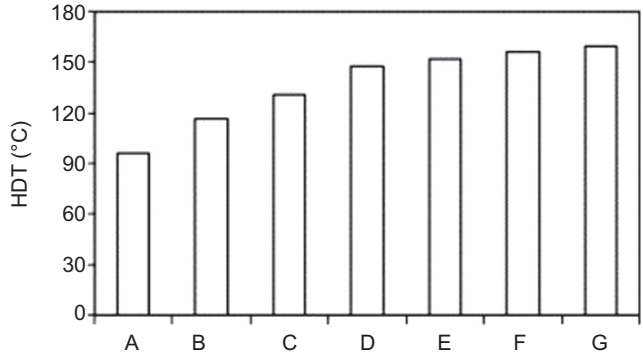

Figure 18.9 Heat deflection temperature of kenaf fibre reinforced soy-based biocomposites for (A) 30 wt% kenaf fibre injection moulded composite; (B) 33 wt% 6 mm kenaf fibre compression moulded composite; (C) 55 wt% 2 mm kenaf fibre compression moulded composite; (D) 56 wt% 6 mm kenaf fibre compression moulded composite; (E) 57 wt% 25 mm kenaf fibre compression moulded composite; (F) 53 wt% 50 mm kenaf fibre compression moulded composite; (G) 54 wt% long kenaf fibre compression moulded composite.

18.7 Prospective application of plant fibre composites in the construction sector with reference to their creep behaviour: cement matrix plant fibre composites

Along with ancient traditions, it has been considered suitable to use lignocellulosic fibres as fillers for building materials. Of course, a more up-to-date approach needs to be aware of the fact that processing is no longer manual, and some related issues need to be taken into account in trying a mass production of cement matrix plant fibre composites. In particular, an aspect that was elucidated was that the introduction of hemp fibres (but this is supposed to be quite general) in Portland cement pastes results in some delay on the setting time. This appears to be due to the pectin contained in the fibres forming complex molecules with calcium ions (Sedan et al., 2008).

One of the fibres that is particularly adapted for this use is sisal (Swift and Smith, 1979), whose use has been proposed in the form of short fibres or even pulp. In this case, small amounts of the natural materials are introduced, which tend to stop creep and particularly have an enormous effect on improving toughness; as an example, an addition of 8 wt% pulp led to a 50- to 60-fold increase in fracture toughness (Coutts and Warden, 1992). The more general effect of improving soil consolidation has been fully demonstrated, particularly in the specific case of sisal and coir fibres around 50 mm in length, allowing the prevention of the shrinkage cracks due to the soil drying process (Ghavami et al., 1999). Early attempts also included the possible introduction of jute fibres in different lengths and amounts into cement mortar and then tested in direct tension, flexure, axial compression and impact (Mansur and Aziz, 1982). In a more industrially aware context, it proved also useful and beneficial for mechanical

performance to insert mercerized jute fibres in a concrete mix on which interface was provided by polymer latex and tannin, so that concrete pipes could be fabricated (Kundu et al., 2012). It was also indicated that a possible addition of coir or bamboo (or others) offers an improvement in ductility and reduced shrinkage to enhance the impact and fracture toughness of vegetable fibre reinforced concrete (Ramaswamy et al., 1983).

18.8 Conclusions

When trying to apply vegetable fibres as the reinforcement for polymers, one has to face the evidence that these fibres have hierarchical structures, which are purposely extracted from the plant at a level that applies loading, especially tensile and torque, on them (the elongated stretches of material that are obtained in that way are normally defined as 'technical fibres'). This hierarchical arrangement has a number of mechanical consequences. The structure obtained is cellular and hence porous and irregular; in addition, defects are not uniformly concentrated in it. In addition, it is a polymer variably constituted by some amounts of polysaccharides, such as (mainly) cellulose and lignin, with some less structural ones, such as hemicellulose and pectin, which are variably removed from the fibre as the effect of treatments, such as mercerization, typically with sodium hydroxide. All the aforementioned considerations result in the fact that the fibres are suffering from the persistence of strain after load is removed.

Investigations on creep are still quite scarce, nevertheless indicating that a number of factors are heavily involved in the variation of properties, eg, the geometrical aspects and the density of the fibres. Some fibres have been found more suitable for creep-resisting applications, in particular hemp, sisal and flax. The application of treatments, in particular those applied for coverage and protection of the fibres, such as silanization, or aimed at compatibilization with polyolefin matrices, such as maleinization, could make a significant difference to the creep behaviour.

The ultimate objective of these investigations on creep of plant fibres is particularly to tend towards the production of fully sustainable composites with biopolymers, eg, starch-based, or the introduction of these fibres into cementitious matrices. In both cases the unpredictable synergistic effect between the two different creep-prone materials would lead to a design of the components aimed at use in the construction industry.

References

Acha, B.A., Reboredo, M.M., Marcovich, N.E., 2007. Creep and dynamic mechanical behavior of PP–jute composites: effect of the interfacial adhesion. Composites Part A 38 (6), 1507–1516.

Alvarez, V.A., Kenny, J.M., Vázquez, A., 2004. Creep behavior of biocomposites based on sisal fiber reinforced cellulose derivatives/starch blends. Polymer Composites 25 (3), 280–288.

Baley, C., 2002. Analysis of the flax fibres tensile behaviour and analysis of the tensile stiffness increase. Composites Part A 33 (7), 939–948.

Biela, T., Duda, A., Penczek, S., 2006. Enhanced melt stability of star-shaped stereocomplexes as compared with linear stereocomplexes. Macromolecules 39 (11), 3710–3713.

Bogoeva-Gaceva, G., Avella, M., Malinconico, M., Buzarowska, A., Grozdanov, A., Gentile, G., Errico, M.E., 2007. Natural fiber eco-composites. Polymer Composites 28 (1), 98–107.

Chiou, B.-S., Yee, E., Glenn, G.M., Orts, W.J., 2005. Rheology of starch–clay nanocomposites. Carbohydrate Polymers 59 (4), 467–475.

Coutts, R.S.P., Warden, P.G., 1992. Sisal pulp reinforced cement mortar. Cement and Concrete Composites 14 (1), 17–21.

Crissman, J.M., Zapas, L.J., 1985. On the mechanical preconditioning of ultrahigh-molecular-weight polyethylene at small uniaxial deformations. Journal of Polymer Science Part B 23 (12), 2599–2610.

Cyras, V.P., Martucci, J.F., Iannace, S., Vazquez, A., 2002. Influence of the fiber content and the processing conditions on the flexural creep behavior of sisal-PCL-starch composites. Journal of Thermoplastic Composite Materials 15 (3), 253–265.

Davies, G.C., Bruce, D.M., 1998. Effect of environmental relative humidity and damage on the tensile properties of flax and nettle fibers. Textile Research Journal 68 (9), 623–629.

Da-Wei, Z., Yi-Jie, L., Yan-Hong, F., Jin-Ping, Q., He-Zhi, H., Bai-Ping, X., 2011. Effect of initial fiber length on the rheological properties of sisal fiber/polylactic acid composites. Polymer Composites 32 (8), 1218–1224.

De Vasconcellos, D.S., Touchard, F., Chocinski-Arnault, L., 2014. Tension–tension fatigue behaviour of woven hemp fibre reinforced epoxy composite: a multi-instrumented damage analysis. International Journal of Fatigue 59, 159–169.

Dhakal, H.N., Zhang, Z.Y., Richardson, M.O.W., 2009. Creep behaviour of natural fibre reinforced unsaturated polyester composites. Journal of Biobased Materials and Bioenergy 3 (3), 232–237.

Eliasson, A.C., 1986. Viscoelastic behaviour during the gelatinization of starch. I. comparison of wheat, maize, potato and waxy-barley starches. Journal of Texture Studies 17 (3), 253–265.

Feng, D., Caulfield, D.F., Sanadi, A.R., 2001. Effect of compatibilizer on the structure-property relationships of kenaf-fiber/polypropylene composites. Polymer Composites 22 (4), 506–517.

Gassan, J., Bledzki, A.K., 1999a. Possibilities for improving the mechanical properties of jute/epoxy composites by alkali treatment of fibres. Composites Science and Technology 59 (9), 1303–1309.

Gassan, J., Bledzki, A.K., 1999b. Influence of fiber surface treatment on the creep behavior of jute fiber-reinforced polypropylene. Journal of Thermoplastic Composite Materials 12 (5), 388–398.

Ghavami, K., Toledo Filho, R.D., Barbosa, N.P., 1999. Behaviour of composite soil reinforced with natural fibres. Cement and Concrete Composites 21 (1), 39–48.

Hbib, M., Guessasma, S., Bassir, D., Benseddiq, N., 2011. Interfacial damage in biopolymer composites reinforced using hemp fibres: finite element simulation and experimental investigation. Composites Science and Technology 71 (11), 1419–1426.

Hidalgo-Salazar, M.A., Mina, J.H., Herrera-Franco, P.J., 2013. The effect of interfacial adhesion on the creep behaviour of LDPE–Al–Fique composite materials. Composites Part B 55, 345–351.

Ke, T., Sun, X., 2000. Physical properties of poly(lactic acid) and starch composites with various blending ratios. Cereal Chemistry 77 (6), 761−768.

Keener, T.J., Stuart, R.K., Brown, T.K., 2004. Maleated coupling agents for natural fibre composites. Composites Part A 35 (3), 357−362.

Kun, F., Hidalgo, R.C., Herrmann, H.J., Pál, K.F., 2003. Scaling laws of creep rupture of fiber bundles. Physical Review E 67 (6), 061802.

Kundu, S.P., Chakraborty, S., Roy, A., Adhikari, B., Majumde, S.B., 2012. Chemically modified jute fibre reinforced non-pressure (NP) concrete pipes with improved mechanical properties. Construction and Building Materials 37, 841−850.

Lakes, R., 1993. Materials with structural hierarchy. Nature 361 (6412), 511−515.

Li, H., Huneault, M.A., 2011. Comparison of sorbitol and glycerol as plasticizers for thermoplastic starch in TPS/PLA blends. Journal of Applied Polymer Science 119 (4), 1439−1448.

Li, X., Tabil, L.G., Panigrahi, S., 2007. Chemical treatments of natural fiber for use in natural fiber-reinforced composites: a review. Journal of Polymers and the Environment 15 (1), 25−33.

Liang, S., Gning, P.B., Guillaumat, L., 2012. A comparative study of fatigue behaviour of flax/epoxy and glass/epoxy composites. Composites Science and Technology 72 (5), 535−543.

Liu, W., Drzal, L.T., Mohanty, A.K., Misra, M., 2007. Influence of processing methods and fiber length on physical properties of kenaf fiber reinforced soy based biocomposites. Composites Part B 38 (3), 352−359.

Ma, X., Chang, P.R., Yu, J., Stumborg, M., 2009. Properties of biodegradable citric acid-modified granular starch/thermoplastic pea starch composites. Carbohydrate Polymers 75 (1), 1−8.

Mansur, M.A., Aziz, M.A., 1982. A study of jute fibre reinforced cement composites. International Journal of Cement Composites and Lightweight Concrete 4 (2), 75−82.

Mantzari, G., Raphaelides, S.N., Exarhopoulos, S., 2010. Effect of sorbitol addition on the physicochemical characteristics of starch−fatty acid systems. Carbohydrate Polymers 79 (5), 154−163.

Mwaikambo, L.Y., 2006. Review of the history, properties and application of plant fibres. African Journal of Science and Technology 7 (2), 120−133.

Oksman, K., Wallstrom, L., Berglund, L.A., Toledo Filho, R.D., 2002. Morphology and mechanical properties of unidirectional sisal−epoxy composites. Journal of Applied Polymer Science 84 (13), 2358−2365.

Picout, R.D., Ross-Murphy, S.B., 2003. Rheology of biopolymer solutions and gels. The Scientific World Journal 3, 105−121.

Placet, V., Cisse, O., Boubakar, M.L., 2012. Influence of environmental relative humidity on the tensile and rotational behaviour of hemp fibres. Journal of Materials Science 47 (7), 3435−3446.

Raghavan, J., Meshii, M., 1998. Creep of polymer composites. Composites Science and Technology 57 (12), 1673−1688.

Ramaswamy, H.S., Ahuja, B.M., Krishnamoorthy, S., 1983. Behaviour of concrete reinforced with jute, coir and bamboo fibres. International Journal of Cement Composites and Lightweight Concrete 5 (1), 3−13.

Ray, D., Sengupta, S.P., Rana, A.K., Bose, N.R., 2006. Static and dynamic mechanical properties of vinylester resin matrix composites reinforced with shellac-treated jute yarns. Industrial and Engineering Chemistry Research 45 (8), 2722−2727.

Ray, D., Das, M., Mitra, D., 2009. Influence of alkali treatment on creep properties and crystallinity of jute fibres. Bioresources 4 (2), 730−739.

Redl, A., Morel, M.H., Bonicel, J., Guilbert, S., Vergnes, B., 1999. Rheological properties of gluten plasticized with glycerol: dependence on temperature, glycerol content and mixing conditions. Rheologica Acta 38 (4), 311–320.

Rodriguez-Gonzalez, F.J., Ramsay, B.A., Favis, B.D., 2004. Rheological and thermal properties of thermoplastic starch with high glycerol content. Carbohydrate Polymers 58 (2), 139–147.

Rouison, D., Sain, M., Couturier, M., 2006. Resin transfer molding of hemp fiber composites: optimization of the process and mechanical properties of the materials. Composites Science and Technology 66 (7–8), 895–906.

Saha, A.K., Das, S., Bhatta, D., Mitra, B.C., 1999. Study of jute fiber reinforced polyester composites by dynamic mechanical analysis. Journal of Applied Polymer Science 71 (9), 1505–1513.

Sawpan, M.A., Pickering, K.L., Fernyhough, A., 2011. Improvement of mechanical performance of industrial hemp fibre reinforced polylactide biocomposites. Composites: Part A 42 (3), 310–319.

Schapery, R.A., 1969. On the characterization of nonlinear viscoelastic materials. Polymer Engineering & Science 9 (4), 295–310.

Sedan, D., Pagnoux, C., Smith, A., Chotard, T., 2008. Mechanical properties of hemp fibre reinforced cement: influence of the fibre/matrix interaction. Journal of the European Ceramic Society 28 (1), 183–192.

Seki, Y., 2009. Innovative multifunctional siloxane treatment of jute fiber surface and its effect on the mechanical properties of jute/thermoset composites. Materials Science and Engineering A 508 (1–2), 247–252.

Sen, T., Jagannatha Reddy, H.N., 2011. Application of sisal, bamboo, coir and jute natural composites in structural upgradation. International Journal of Innovation, Management and Technology 2 (3), 186–191.

Siengchin, S., Dangtungee, R., 2013. Effect of woven flax structures on morphology and properties of reinforced modified polylactide composites. Journal of Thermoplastic Composite Materials 26 (10), 1424–1440.

Signori, F., Coltelli, M.B., Bronco, S., 2009. Thermal degradation of poly(lactic acid) (PLA) and poly(butylene adipate-co-terephthalate) (PBAT) and their blends upon melt processing. Polymer Degradation and Stability 94 (1), 74–82.

Spatz, H., Kohler, L., Niklas, K.J., 1999. Mechanical behaviour of plant tissues: composite materials or structures? Journal of Experimental Biology 202, 3269–3272.

Swift, D.G., Smith, R.B.L., 1979. The flexural strength of cement-based composites using low modulus (sisal) fibres. Composites 10 (3), 145–148.

Tajvidi, M., Falk, R.H., Hermanson, J.C., 2005. Time-temperature superposition principle applied to a kenaf fiber/high density polyethylene composite. Journal of Applied Polymer Science 97 (5), 1995–2004.

Thygesen, L.G., Bilde-Sørensen, J.B., Vázquez, P.H., 2006. Visualisation of dislocations in hemp fibres: a comparison between scanning electron microscopy (SEM) and polarized light microscopy (PLM). Industrial Crops and Products 24 (2), 181–185.

Thygesen, L.G., Eder, M., Burgert, I., 2007. Dislocations in single hemp fibres—investigations into the relationship of structural distortions and tensile properties at the cell wall level. Journal of Materials Science 42 (2), 558–564.

Varna, J., Rozite, L., Joffe, R., Pupurs, A., 2012. Non-linear behaviour of PLA based flax composites. Plastic, Rubber and Composites 41 (2), 49–60.

Vazquez, A., Domínguez, V.A., Kenny, J.M., 1999. Bagasse fiber-polypropylene based composites. Journal of Thermoplastic Composite Materials 12 (6), 477–497.

Watanabe, H., 1999. Viscoelasticity and dynamics of entangled polymers. Progress in Polymer Science 24, 1253−1403.

Wong, S., Shanks, R., 2008. Creep behaviour of biopolymers and modified flax fibre composites. Composite Interfaces 15 (2−3), 131−145.

Zaslawsky, M., February 1963. Viscoelasticity of Polymers. California Univ Livermore Radiation Lab report no. ADA307528.

Thermal and flame retardancy properties of thermoplastics/ natural fiber biocomposites

19

S. Fu, P. Song, X. Liu
Zhejiang A & F University, Linan, Hangzhou, China

19.1 Introduction

Growing environmental issues, such as global scale pollution and climate change, have dramatically stimulated the interest in the utilization of natural materials all over the world. Natural fibers, especially cellulose-rich fibers, are considered eco-friendly alternatives to synthetic fibers, such as glass fibers, as popular reinforcement fillers for polymeric materials because of their low cost and renewable and biodegradable features (Chen et al., 2005; Holbery and Houston, 2006; Monteiro et al., 2009; Nam et al., 2012a). Most significantly, utilizing them makes a great contribution to reducing the carbon footprints of human beings on the planet. Meanwhile, natural fiber reinforced polymer composites have been widely used in many fields including automobile, airplane, household, and construction industries, due to their lightweight and high specific strength and stiffness compared with glass fiber reinforced polymer composites, gradually replacing traditional materials such as steel and wood (Chen et al., 2005; Holbery and Houston, 2006; Monteiro et al., 2009).

For the polymer matrix, most commercially available petroleum-based polymers like polypropylene (PP), polyethylene (PE), and polystyrene (PS) are adding a burden to the environment since they are basically not recyclable and biodegradable (Khedari et al., 2003). As a result, much research is currently focusing on fully biodegradable composites, also called "biocomposites" or "green composites" based on natural fibers and bioderived polymers including poly (lactic acid) (PLA) and polyhydroxybutyrate (PHB), polycaprolactone (PCL), poly(1,4-butanediol succinate) (PBS), and thermoplastic starch. Biocomposites have been attracting great interest due to the eco-friendliness and biodegradability and thus at the end of life, they can be disposed without generating any impact to our environment (Luo and Netravali, 1999).

However, besides some drawbacks, including moisture absorption, low durability, and variable quality (Nam et al., 2012a), natural fibers are thermally unstable due to the poor thermal stability of noncrystalline hemicellulose and cellulose, thus leading to restricted processing temperature and the types of polymers available as the matrix. Thermal instability makes these natural fibers extremely flammable because of their chemical structure characteristics. Meanwhile, the majority of the thermoplastic polymer matrix, such as PLA and PHB, are also inherently flammable and thermally unstable, especially in the presence of oxygen (Bledzki and Gassan, 1999; Chapple

Advanced High Strength Natural Fibre Composites in Construction. http://dx.doi.org/10.1016/B978-0-08-100411-1.00019-4

and Anandjiwala, 2010; Hapuarachchi et al., 2007; Kozłowski and Władyka-Przybylak, 2008; Matkó et al., 2005; Netravali and Chabba, 2003). With biocomposites increasingly finding many new applications, such as building, transport, automobile, and aerospace, enhancing their thermal stability and flame retardancy performances is becoming a necessary requirement for protecting people's lives and properties (Hapuarachchi et al., 2007; Kozłowski and Władyka-Przybylak, 2008; Matkó et al., 2005).

19.2 Types of natural fibers

19.2.1 Classification of natural fibers

Until now, a variety of commercial natural fibers have been employed to create polymer biocomposites, and natural fibers can be simply classified according to their sources, as listed in Fig. 19.1.

19.2.2 Structural organization of plant fibers

Among all these kinds of natural fibers, plant fibers are used most widely for polymeric biomaterial fabrication because of their renewable and abundant features. Actually, plant-based natural fibers are lignocellulosic ones and are made up of cellulose, hemicellulose, lignin, pectin, and waxy substances. The schematic structure, the model of structural organization, and the chemical structure of three main components of natural fibers are presented in Fig. 19.2 (Kabir et al., 2012; Madsen et al., 2004). As presented

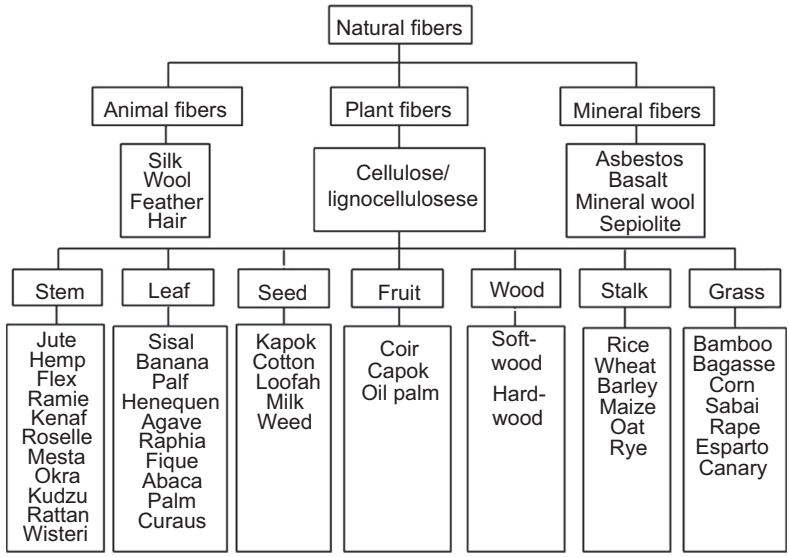

Figure 19.1 Classification of natural fibers (Bajpai et al., 2012; Sathishkumar et al., 2014).

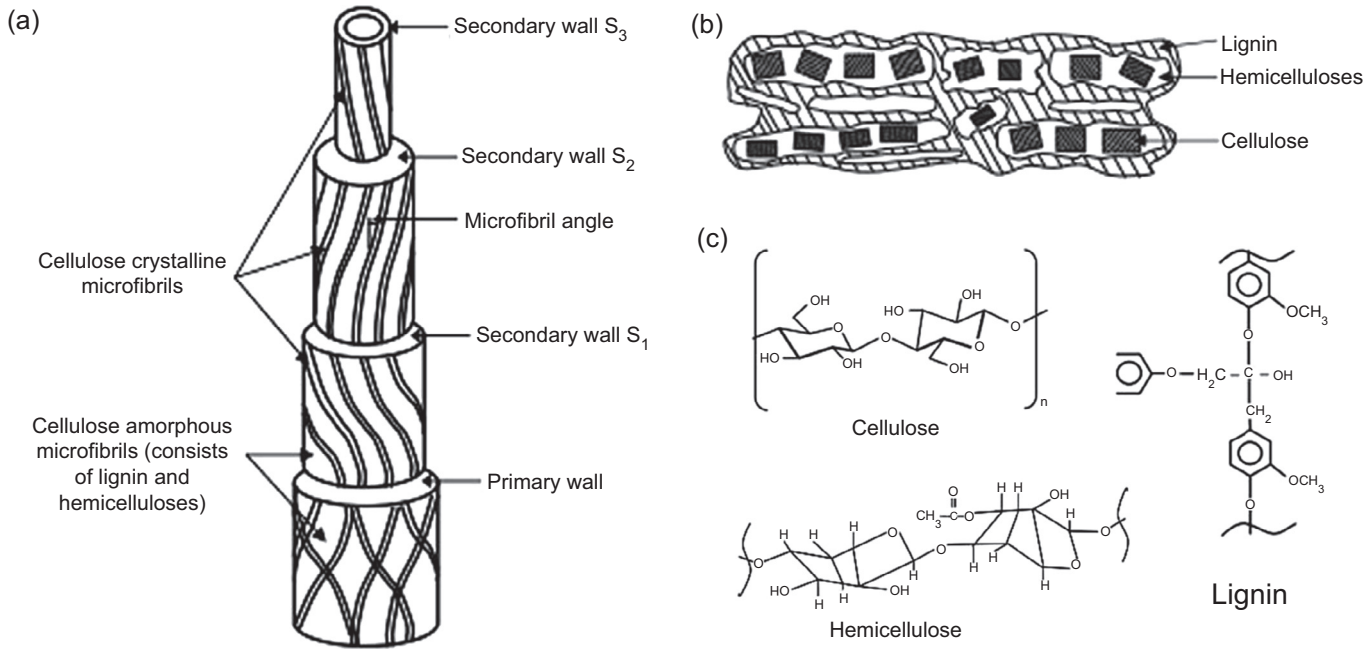

Figure 19.2 (a) Microstructure of plant fibers, (b) the model of structural organization of three main components in the fiber cell wall, and (c) chemical structures of cellulose, lignin, and hemicellulose.
Reproduced from Kabir, M., Wang, H., Lau, K., Cardona, F., 2012. Chemical treatments on plant-based natural fibre reinforced polymer composites: an overview. Composites Part B: Engineering 43, 2883−2892, with permission.

in Fig. 19.2(a), for a specific kind of fiber, cellulose microfibrils generally have their own cell geometry, which is responsible for the mechanical properties of fiber (Bledzki and Gassan, 1999; Kabir et al., 2012). Each fiber cell wall contains primary and secondary layers of microfibrils. The secondary thick layer (s_2) determines the mechanical performance of the fiber, and thus the fiber with a higher content of cellulose and lower microfibrial angle usually displays better mechanical properties. The structure of fibers forms in the primary cell wall and then deposits with growing. The second wall is comprised of three layers, with each layer holding a long chain of helical cellulose microfibrils (John and Anandjiwala, 2008). The content of cellulose increases gradually, and the amount of lignin decreases from primary layer to secondary layer, while the amount of hemicellulose is similar in each layer. Hemicellulose are bonded with hydrogen bonding interactions to form cementing components for the fiber structure, while the lignin and pectin are coupled with the cellulose and hemicellulose network and act as adhesives to hold the macromolecules together (see Fig. 19.2(b)) (Kabir et al., 2012).

As shown in Fig. 19.2(c), cellulose is the major framework component, and there are abundant hydroxyl groups (eOH) on the repeating glucose unit, forming wide inter/intramolecular hydrogen bonding interactions responsible for the stiffness, strength, and structural stability of the fiber. Branched hemicellulose primarily exists in the cell wall of fibers, containing five and six carbon sugars of various chemical structures, while amorphous lignin mainly has three aromatic structures depending on the types of plants (Saheb and Jog, 1999).

19.3 Types of flame retardants

Based on flame retardant elements and chemical structure, flame retardants (FRs) largely include phosphorus, halogen, metal compounds, silicon, and nanoparticle-based flame retardants. Phosphorus-based flame retardants contain red phosphorus and organic, inorganic, and intumescent flame retardant systems. Most of the halogen-based flame retardants have been prohibited because of the potential environmental toxicity. Inorganic mineral flame retardants are metal hydroxides and borates. The silicon-based flame retardants primarily contain silica and silicones, while nanoscale flame retardants mainly consist of nanoclay, carbon nanotubes, layered double hydroxides, and grapheme (Bourbigot and Duquesne, 2007; Bourbigot and Fontaine, 2010; Faruk et al., 2012; Jang et al., 2012; Jimenez et al., 2006; Laoutid et al. 2006, 2009; Mngomezulu et al., 2014; Morgan and Gilman, 2013; Zhang and Horrocks, 2003).

19.3.1 Phosphorus-containing flame retardants

For phosphorus-based FRs, their structures vary from inorganic to organic forms, and the phosphorus element mainly has three oxidation states of 0, +3, and +5. Phosphorus-based FRs mainly contain phosphates, phosphonates, phosphinates, phosphine oxides, and red phosphorus (Chapple and Anandjiwala, 2010; Faruk et al., 2012;

Jang et al., 2012; Mngomezulu et al., 2014; Morgan and Gilman, 2013; Zhang and Horrocks, 2003).

19.3.1.1 Organic phosphorus

On the basis of functional groups, organic phosphorus flame retardants can be categorized as phosphate esters, phosphonates, and phosphinates. According to the molecular weight, they can be classified into two major classifications, namely, monomers and oligomers. Monomeric organic phosphorus is mainly alkyl-substituted triaryl phosphates like triphenyl phosphophosphate, tertbutylphenyl diphenyl phosphate, or tricresyl phosphate, and this type of flame retardant has restricted applications in engineering plastics due to its high volatility and relatively low fire retardancy effectiveness. Commercially available oligomomeric phosphates are mainly resorcinol bis (diphenyl phosphate) and bisphenol A bis (diphenyl phosphate). They are normally used in some engineering thermoplastics like PA-6 and ABS because of much higher thermal stability and lower volatility as compared with the monomeric type. Additionally, combining volatile and nonvolatile phosphate flame retardants results in a synergistic flame-retardancy effect, probably because of the combination role of them played in both condensed and vapor phases. Most importantly, reactive phosphorus flame retardants can be directly incorporated into polymer main chains by copolymerizing phosphorus-containing monomers with main monomers or chemically grafting phosphorus-containing vinyl monomers or oligomers onto the polymer matrix to create phosphate polymeric materials. In this way the volatilization of flame retardants during processing and migration of them toward the polymer surface can be effectively avoided (Faruk et al., 2012; Jang et al., 2012; Mngomezulu et al., 2014; Morgan and Gilman, 2013; Zhang and Horrocks, 2003).

19.3.1.2 Inorganic phosphorus

Ammonium polyphosphate (APP) and melamine polyphosphate (MPP) are two typical inorganic phosphorus flame retardants. APP is a branched or linear polymeric compound with a variable degree of polymerization (n). Generally, APP of a low degree of polymerization ($n \leq 100$, crystalline form I) is water soluble or water sensitive, while APP with longer chains ($n \geq 1000$, crystalline form II) displays a very low water solubility (<0.1 g/100 mL). Compared with APP, MPP holds higher thermal stability and lower water sensitivity. In general, long-chain APP starts to degrade at a temperature of above 300°C, generating ammonia and polyphosphoric acid, while the short-chain one begins decomposing at 150°C. Thus choosing APP as the flame retardant strongly depends on the processing temperature of materials. When APP is added into a polymeric material containing oxygen and/or nitrogen elements, the char may form. At high temperature, APP degrades to create free acidic hydroxyl groups and form ultraphosphate and polyphosphoric acid, which can catalyze the dehydration reaction of polymers to yield char residues. However, in nonself-charring polymeric materials, APP only alters the degradation mechanism of the polymer (Bourbigot and Fontaine, 2010; Chapple and Anandjiwala, 2010; Jang et al., 2012; Mngomezulu et al., 2014).

19.3.1.3 Intumescent flame retardants

Intumescent flame retardants (IFRs) have been considered to be one of the most promising eco-friendly flame retardants because of their advantages of relatively high efficiency, low smoke, and low toxicity. Typical IFRs are comprised of three major components: an acid source, a carbonizing source, and a foaming or blowing source. For IFRs, they should decompose at a temperature lower than the thermal degradation temperature of the polymer matrix. The acid source can be one of phosphoric acid, sulphuric acid, boric acid, and halides, as well as their derivatives; the carbonizing source mainly includes pentaerythritol (monomer, dimer, trimer), sorbitol, mannitol, dextrins, starch, phenol-formaldehyde resins, and char-forming polymers like PA-6, PU, and PC. The blowing source (agent) is primarily nitrogen-containing compounds, such as urea, urea-formaldehyde resin, melamine, dicyandiamide, and polyamides. At an elevated temperature, the acid source decomposes and generates inorganic strong acid, which can promote the dehydration of the carbonizing agent to produce the carbonaceous layer. And the quality of the carbon layer is dependent on the number of carbon atoms, while the reactive hydroxyl groups (OH) determine the rate of dehydration reaction. Meanwhile, the blowing agent degrades and releases inflammable gases, which can expand the carbonaceous layer and make it form a swollen multicellular layer. Thus the blowing agent should decompose during the dehydration reaction of the carbonizing source in order to promote the expansion of the carbonaceous layer. This layer can insulate underlying polymers from the heat, flames, and oxygen, thus leading to improved flame retardancy (Bourbigot and Duquesne, 2007; Jimenez et al., 2006; Laoutid et al., 2009; Morgan and Gilman, 2013).

19.3.1.4 Red phosphorus

Red phosphorus is the most concentrated source of phosphorus and has the highest content of phosphorus among phosphorus-based flame retardants; thus its loading level is normally below 10 wt%. It is highly active in both condensed and gas phases, and the created PO· radicals can trap the free radicals in the vapor phase and reduce the heat of oxidation and quench the free radicals in the condensed phase. As a flame retardant, it is effective for both oxygen-containing polymers, such as polyesters, polyamides, and polyurethanes, and nonoxygenated polymers, such as polypropylene and polyethylene (Faruk et al., 2012; Laoutid et al. 2006, 2009). Unfortunately, red phosphorus will release toxic phosphine (PH_3) via a reaction with moisture because of poor thermal stability. Therefore to avoid the formation of PH_3, the microencapsulation treatment is normally required, and another approach is adding some metallic salts, including $AgNO_3$, MoS_2, CuO, and $FeCl_3 \cdot H_2O$ to trap PH_3 via high reaction activity between them (Laoutid et al., 2009).

19.3.2 Metal hydroxides and oxide flame retardants

Metal hydroxide flame retardants offer an attractive alternative to traditional halogenated formulations for flame-retarding polymeric materials because of their low

toxicity, corrosion, and emission of smoke during processing and combustion. Typical metal hydroxide flame retardants are $Al(OH)_3$ (ATH), $Mg(OH)_2$ (MDH), and basic magnesium carbonate (BMC). They normally decompose endothermically and generate H_2O molecules upon heating and thus reduce the heat flow and lower the temperature of the substrate. ATH and BMC start to decompose in the temperature range of 180−340°C, with a peak at about 320°C. BMC also exhibits a peak decomposition temperature at about 410°C. Among these three metal hydroxides, MDH is the most endothermic upon decomposition occurring above 300°C, BMC the least, and ATH is between them. However, a very high loading level of metal hydroxides is usually required to achieve an acceptable degree of flame retardancy and tend to lead the polymer matrix to poor mechanical properties (Focke et al., 2009; Hollingbery and Hull, 2010; Laoutid et al., 2009). Apart from them, other metal oxides, such as SnO_2 and SbO_3, are primarily used as synergists for halogen-contained flame retardants to enhance the fire performance (Hirschler, 1984; Jha et al., 1986).

19.3.3 Silicon-containing flame retardants

Silicon-based flame retardants are silicones, silicas, organosilicates, silsesquixanes, and silicates. Silicone flame retardants are considered to be "eco-friendly" additives because they hardly lead to harmful impacts on the environment (Zhang and Horrocks, 2003). Typical silicones are polydimethysiloxane polymers that have excellent thermal stability, high heat release, and very low release of toxic gases like CO during thermal degradation. Their superior flame retardancy is primarily attributed to the excellent dispersion in polymer matrices and migration toward the material surface during combustion followed by the formation of a highly flame retardant char layer. Silica or silicon dioxide (SiO_2) also have various types, such as silica gel, fumed silica, and fused silica. Its effectiveness mainly depends on several factors, such as pore size, particle size, surface silanol concentration, surface area, density, and viscosity (Mngomezulu et al., 2014). The silica flame retardants show a significantly reduced heat release rate and mass loss rate due to the physical action of the silica in the condensed phase (Mngomezulu et al., 2014; Zhang and Horrocks, 2003).

19.3.4 Nanoscale flame retardants

The formation of nanocomposites has been considered to one of the most promising approaches to create flame-retardant polymeric materials because both mechanical and flame retardancy performances can be significantly improved by adding a very low loading level of nanoparticles (usually $\leq$2.0 wt%). Based on the chemical structure and geometry, nanoscale flame retardants can be classified as particulate (zero-dimensional), fibrous (one-dimensional), and layered (two-dimensional) additives. Particulate nanoflame retardants mainly include polyhedral oligosilsesquioxane (POSS) and its derivatives, such as aluminumisobutyl silsesquioxane (Al-POSS) and zinc isobutyl silsesquioxane (Zn-POSS), spherical nanosilica, nanoscale MDH, titanium oxide (TiO_2), ferric oxide (Fe_2O_3), aluminum oxide (Al_2O_3), and antimony oxide (Sb_2O_3). One-dimensional nanoflame retardants contain single/multiwalled

carbon nanotubes, halloysite, and sepiolite, etc., and two-dimensional nanoflame retardants include inorganic nanoclay (eg, montmorilonite), layered double hydroxides, expanded graphite, and graphene. Adding POSS can enhance both the thermal stability and fire performance by reducing heat release rate upon combustion, during which POSS acts like a precursor forming a thermally stable ceramic material at elevated temperatures. For nanoscale metal oxides, their flame retardancy properties strongly depend on the filler content, particle size, and surface area, and they are normally used as flame-retardant synergistic agents because of their high thermal stability and large specific area. As for one-dimensional CNTs, the formation of a three-dimensional physical network can not only increase the molten viscosity of polymers but also form a compact layer. This layer can act as thermal insulation barrier and thus effectively protect the underlying polymer matrix. The presence of a small amount of two-dimensional flame retardants like nanoclay and graphene can reduce the flammability and slow down the release of polymeric materials, mainly because of their physical barrier effects (Franchini et al., 2009; Gallo et al., 2011; Gao et al., 2005; Mngomezulu et al., 2014; Zhang and Horrocks, 2003).

19.4 Biocomposites fabrication

19.4.1 Chemical modification of natural fibers

The surface-abundant hydroxyl groups make natural plants fibers (mainly containing cellulose, hemicellulose, and lignin) show strong polarity and thus rather easily absorb moisture from the environment. In addition, the large polarity difference between fibers and the polymer matrix, especially for the polymer with weak polarity, presents a huge challenge for creating high-performance biocomposites because of poor interfacial compatibilities. Also the presence of pectin and waxy substances on the fiber surface may act as an interfacial barrier to prevent the interfacial adhesion. Therefore the chemical surface modification of fibers and the addition of interfacial compatibilizer are usually required to ensure the homogeneous dispersion of natural fibers in the polymeric matrix and the good interface strength (Dash et al., 2000; Kabir et al., 2012; Wang et al., 2007).

Until now, to improve the interfacial adhesion of fibers with the polymeric matrix, varied chemical methods have been developed, such as the alkaline treatment, silane modification, acetylation, benzoylation, oxidation, maleated coupling modification, sodium chlorite treatment, acrylation and acrylontrile grafting, isocynate treatment, stearic acid treatment, permanganate treatment, triazine treatment, fatty acid derivative treatment, and fungal treatment. Among these treatment approaches, alkaline and silane treatments are two of the most effective methods so far (Kabir et al., 2012). They are able to change the surface structure and morphology of natural fibers, and at the same time the hydrophilic hydroxyl groups can be changed into other groups with weak polarity. The treatments can facilitate the interfacial compatibility of natural fibers with the polymer matrix via in situ chemical reactions, thus leading to improved dispersion and mechanical properties. Figs. 19.3 and 19.4 presents the possible reaction between siliane coupling agent-modified banana fibers with PLA.

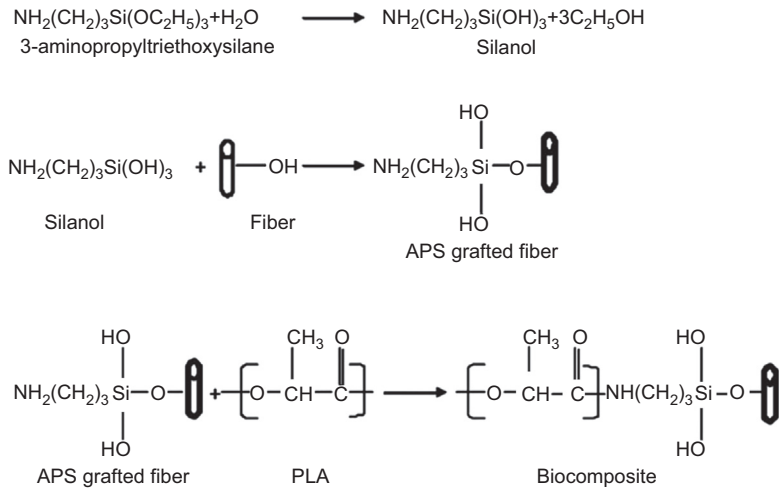

Figure 19.3 Hypothetical reactions between the silane coupling agent-modified fibers and poly (lactic acid).
Reprinted from Sajna, V., Mohanty, S., Nayak, S.K., 2014. Hybrid green nanocomposites of poly (lactic acid) reinforced with banana fibre and nanoclay. Journal of Reinforced Plastics and Composites 33, 1717−1732, copyright 2014, with permission from SAGE.

19.4.2 Fabrication approaches

Natural fibers are mechanically anisotropic materials, thus various manufacturing methodologies have been adopted to create advanced fiber reinforced polymeric biocomposites. These preparation approaches primarily include the injection molding, hydraulic press, and hand lay-up method followed by compression molding, technological process, screw extrusion process, screw extrusion process followed by compression molding, resin transfer molding, stirring, drying and compression molding process, mixing and compression molding, hand lay-up and cold press, and vacuum-assisted resin infusion method. Four typical fabrication process is shown in Fig. 19.4. Among these processing methods, screw extruding is the most facile and widely used one to create biocomposites; however, for different natural fibers and different applications of composites, one specific fabrication method will be chosen. Table 19.1 lists some of the manufacturing methods of natural fiber reinforced thermoplastic biocomposites.

19.5 Thermal properties

Thermal stability of natural fiber reinforced thermoplastic biocomposites is very significant because it may restrict their processing temperatures and applications in some fields where the atmosphere temperature may cause thermal degradation of the reinforcing fibers, the polymer matrix, and composites, leading to reduced

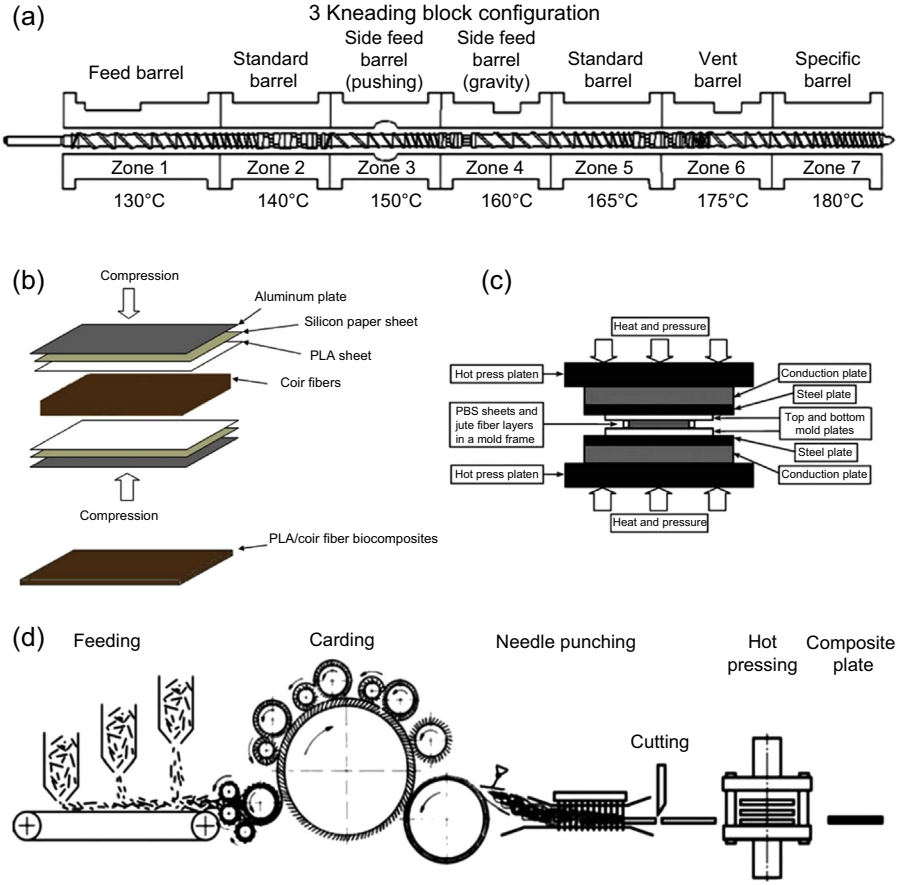

Figure 19.4 Schematic representation of four typical fabrication processes for thermoplastic/natural fibers biocomposites. (a) typical twin-screw extrusion (Woo and Cho, 2013), (b) hand layout and hot press (Dong et al., 2014), (c) hot pressing (Nam et al., 2012b), and (d) multicylinder carding machine (Sajna et al., 2014).
Reproduced from Chen, Y., Chiparus, O., Sun, L., Negulescu, I., Parikh, D.V., Calamari, T.A., 2005. Natural fibers for automotive nonwoven composites. Journal of Industrial Textiles 35, 47−62, Holbery, J., Houston, D., 2006. Natural-fiber-reinforced polymer composites in automotive applications. JOM 58, 80−86, Monteiro, S., Lopes, F., Ferreira, A., Nascimento, D., 2009. Natural-fiber polymer-matrix composites: cheaper, tougher, and environmentally friendly. JOM 61, 17−22, Nam, T.H., Ogihara, S., Kobayashi, S., 2012a. Interfacial, mechanical and thermal properties of coir fiber-reinforced poly(lactic acid) biodegradable composites. Advanced Composite Materials 21, 103−122.

mechanical properties of composites. Generally, the thermal stability of biocomposites strongly depends on the thermal stability of the polymer matrix and natural fibers, the reinforcing agent, since the biocomposites are primarily made of these two major components.

Table 19.1 Typical preparation methods of thermoplastic/natural fiber biocomposites

Natural fibers	Resin	Fabrication methods	References
Flax	Polybutylene succinate (PBS)	Melt blending + compression molding	Dorez et al. (2014)
Cellulose	Polycaprolactone (PCL)	Manually blending	Jiménez and Ruseckaite (2006)
OPEFB	Poly-hydroxybutyrate/hydroxy-valerate (PHBV)	Melt blending	Salim et al. (2011)
Bamboo/cellulose	Polylactic acid (PLA)	Injection molding	Okubo et al. (2009)
Kenaf	PLA	Wet impregnation	Gomes et al. (2007)
Hemp	PLA	Roller carding + compression molding	Graupner et al. (2009)
Banana	PLA	Melt blending + injection molding	Sajna et al. (2014)
Durian skin	PLA	Screw extrusion + injection molding	Manshor et al. (2014)
Coir	PLA	Hand lay-up + hydraulic press	Nam et al. (2012a)
Kenaf	PLA	Carding, punching + hot pressing	Lee et al. (2009)
Ramie	PLA	Two-roll plastics mill + hot pressing	Huda et al. (2008)

OPEFB refers to the oil palm empty fruit punch.

19.5.1 Thermal properties of natural fibers

As is well known, natural fibers consist of cellulose, hemicellulose, and lignin, all of which exhibit different thermal stability and further determine the thermal stability of fibers. It has been demonstrated that cellulose starts to decompose at 210−260°C via the dehydration reaction followed by depolymerization with maximum weight loss peaks varying from 310 to about 450°C. Hemicellulose displays a maximum mass loss temperature of 290°C with activation energy of 150 kJ/mol while the lignin begins to decompose with decomposition peaks from 280 to 520°C and activation energy of up to 229 kJ/mol. (Nabi Sahed et al., 1999) mentioned that the extrusion temperature of some thermoplastic matrices, especially for some engineering plastics, may limit the use of some types of natural fibers because thermal degradation of fibers generates volatile products during melt processing above 200°C. These volatile products will make polymeric composites porous and display inferior mechanical properties. Therefore

Table 19.2 Thermal degradation parameters of four types of common natural fibers (Nguyen et al., 1981; Satyanarayana et al., 2007)

Natural fibers	1st stage		2nd stage					3rd stage
	Mass loss (%)	DTG peak (°C)	T_{onset} (°C)	Mass loss (%)	DTG peaks			Mass loss (%)
					Shoulder (°C)	Main (°C)	Tail (°C)	
Jute	8	60	260	89	290	340	470	3
Sisal	9	52	250	76	275	345	465	15
Cotton	4	55	265	91	280	330	410	5
Wood	2	107	290	85	270	367	400	13

DTG, derivative thermogravimetry; T_{onset}, the onset of the thermal degradation.

some work has been done to enhance the thermal stability of jute and sisal fibers by chemically grafting acrylonitrile onto the surface of fibers (Sabaa, 1991; Yap et al., 1991).

Additionally, different natural fibers may display slightly different thermal stability due to different chemical constituents. Table 19.2 lists thermal stability properties of four types of natural fibers. Obviously, four fibers share similar thermal degradation behaviors to each other, except that the wood fiber exhibits a much higher DTG peak in the first decomposition stage than the other three fibers. According to Nguyen et al., both the weight loss and DTG (derivative thermogravimetry) peak in the first stage probably arise from the loss of absorbed water, and the thermal degradation of three major components of the fiber initially takes place at the onset of the second stage. The DTG shoulder and main DTG peak in the second stage are attributed to the degradation of cellulose and hemicellulose, and the tail peak belongs to the end of lignin degradation.

Moreover, different atmospheres also affect thermal stability of fibers (Monteiro et al., 2012). In general, two atmospheres, namely inert (helium and nitrogen) and oxidative (air and oxygen), are widely used to determine the thermal stability of fibers and their composites. Under inert conditions, the thermal degradation of cellulose displays a main DTG peak probably associated with the generation of macromolecular rings bearing double bonds (Nguyen et al., 1981). In comparison, this degradation peak may overlap with the exothermic peak attributed to the reaction of oxygen with cellulose in an oxidative atmosphere, and consequently main DTG peaks shift to lower temperature. For example, the maximum mass loss temperature of wood flour takes place at 320−330°C in air while at 350−370°C in nitrogen atmosphere.

19.5.2 Thermal properties of biocomposites

19.5.2.1 Thermal degradation of poly (lactic acid)/natural fibers biocomposites

Among all the biodegradable polymers used as the matrix of green composites, PLA is the most widely used polymer matrix with growing commercial interest because of its

good stiffness, high strength, and extensive applications in medical, automotive, food, and packaging fields. Therefore thermal properties of PLA/natural fiber biocomposites are also intensively investigated. Tao et al. (2009) added 50 wt% of untreated jute fibers into PLA and found that composites show lower degradation temperatures than the PLA matrix in nitrogen. Meanwhile, the author also observed that PLA reinforced with 30 wt% ramie fibers displayed an initial degradation temperature of about 220°C, far lower than about 310°C of the PLA matrix. Additionally, the composite also exhibits a lower maximum mass loss temperature than the PLA matrix, and the author attributed this to the decrease of relative molecular mass of PLA during melt processing. Lee and Wang (2006) investigated thermogravimetric behavior of 30 wt% bamboo fiber (BF)-filled PLA biocomposites in nitrogen and observed a two-stage degradation behavior with one degradation stage in the range of 280−340°C ascribed to the degradation of fibers and a small shoulder peak at 350°C owing to the degradation of PLA, to different extents lower than 376°C (one main loss peak) of pure PLA. The author also indicated that the cross-linking reaction between fibers and PLA by adding lysine-based diisocyanate could increase the thermal stability of composites. Manshor et al. (2014) observed that PLA biocomposites filled with 30 wt% of durian skin fibers (DSF) displayed two degradation regions, and the first region was due to the degradation of DSF and the second associated with depolymerization of PLA. Moreover, alkali-treated DSF improved the thermal stability of PLA but reduced the char residue relative to untreated DSF, which was attributed to the better interfacial bonding between DSF and PLA. However, Dong et al. (2014) found that adding 30 wt% of alkali-treated coir fibers resulted in poorer thermal stability than equal amounts of untreated coir fibers. This phenomenon is probably due to the types of natural fibers and different fabrication methods. Interestingly, unlike DSF and coir fibers, Sajna et al. (2014) found that incorporating both untreated or silane-treated banana fibers (BF) resulted in enhanced thermal stability and higher char residue. In addition, adding C30B clay further improved the thermal stability of PLA/BF composites because of the barrier effect of clay.

Oza et al. (2014) investigated effects of surface treatment on the thermal stability of hemp-PLA biocomposites and found that adding acetic-anhydride-treated hemp resulted in higher activation energy and thermal stability than alkali or silane-treated fibers, probably because acetic-anhydride treatment can significantly reduce the hygroscopic nature of the fibers. Meanwhile, Battegazzore et al. (2014) systematically studied effects of six kinds of natural fibers or waste (cellulose fibers, wood sawdust, hazelnut shells, flax fibers, corn cob, and starch) on the thermal stability of PLA and observed that the presence of these fillers led to a slight reduction in the thermal stability of PLA in nitrogen, especially for wood sawdust.

19.5.2.2 *Thermal degradation of polyhydroxybutyrate-co-hydroxyvaerate /natural fiber biocomposites*

Polyhydroxybutyrate is another important biodegradable polymer matrix for creating natural fiber reinforced polymer green composites. Bhardwaj et al. (2006) found that the onset of thermal degradation of polyhydroxybutyrate-co-hydroxyvaerate

(PHBV)/recycled cellulose fiber (RCF) composites was comparable to that of PP-based composites. Unfortunately, the decomposition rate of the former was far more dramatic after 250°C, probably due to the lower thermal stability of fibers in RCF and PHBV. Luo and Netravali (1999) observed that adding 28 wt% of pineapple leaf fibers hardly affected thermal stability of PHBV, and the composites displayed two major degradation regions, with the main decomposition peak associated with the PHBV matrix, respectively at 268°C in air and 273°C in nitrogen and the second peak belonging to the degradation of the fiber at 327°C in air and 334°C in nitrogen. In addition, Singh et al. (2008) found that unlike one major peak for PHBV, PHBV/30 wt% bamboo fiber composites also exhibited two main stages of degradation, showing the main peak around 320°C corresponding to the polymer matrix followed by a small peak at about 375°C associated with bamboo fibers.

19.5.2.3 *Thermal degradation of poly(1,4-butanediol succinate)/natural fiber biocomposites*

Dorez et al. (2014) investigated effects of the flame-retardant modified flax on PBS and found that the macromolecular phosphorus-containing modifier made PBS composites show much higher thermal decomposition temperatures than small molecular modifier (dihydrogen ammonium phosphate, DAP) but lower char residues. For instance, PBS/Tfl-10DAP displayed decomposition temperatures of 284.5 and 399.3°C, while 344.2 and 413.3°C for PBS/Tfl-10P (MAPC1 $(OH)_2$), compared with only one degradation peak of 401.2°C for PBS/Tfl composite. The chemical structure of flame retardants was shown in Fig. 19.5. Nam et al. (2012b) reported that the surface modification of jute fibers had little effect on thermal stability of PBS, and the composites basically showed two main degradation stages, with the first peak associated with the thermal degradation of fibers and the second for the PBS matrix. Dorez et al. (2013) investigated effects of five kinds of natural fibers (cellulose, flax, hemp, sugar cane, and bamboo) on thermal stability of PBS and found the presence of all fibers reduced to a different extent the thermal degradation temperature of the polymer matrix, but led to higher char residues. The detailed thermal degradation parameters are listed in Table 19.3. Moreover, for all composites the experimental values of char residues were much higher than theoretical values, probably because of strong interactions between fibers and the polymer matrix.

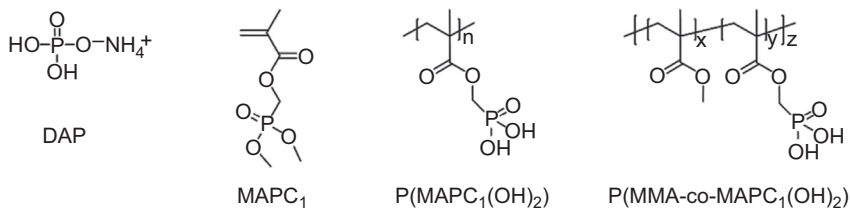

Figure 19.5 Chemical structure of four kinds of flame retardants (Dorez et al., 2014).

Table 19.3 Thermal degradation parameters for poly(1,4-butanediol succinate), fibers, and their composites

Run	$T_{20\%}$ (°C)	Mass residues at 700°C (%)	
		Experimental	Theoretical
PBS	370	0.75	0
Cellulose	353	10	
Flax	335	21	
Hemp	312	27	
Sugar cane	309	18	
Bamboo	307	23	
PBS/30 wt% cellulose	360	4.9	3.5
PBS/30 wt% flax	358	8.2	6.8
PBS/30 wt% hemp	352	10.4	8.6
PBS/30 wt% sugar cane	358	8.9	5.9
PBS/30 wt% bamboo	356	10.6	7.4

Reproduced from Dorez, G., Taguet, A., Ferry, L., Lopez-Cuesta, J., 2013. Thermal and fire behavior of natural fibers/PBS biocomposites. Polymer Degradation and Stability 98, 87–95.

19.5.2.4 *Thermal degradation of other natural fiber-based biocomposites*

Besides PLA, PHBV, and PBS-based biocomposites, thermal properties of other biopolymer-based composites are also extensively studied. For instance, Julkapli and Akil (2010) reinforced chitosan with 28 wt% of kenaf fibers, and the results showed that the presence of kenaf fibers hardly led to changes in the thermal stability of the biocomposites. Like most biocomposites, chitosan-based composites also displayed two DTG peaks. Kim and Netravali (2010) investigated thermal degradation of sisal fiber-filled soy protein/gelatin (SG) resin blends, and results demonstrated that the thermal degradation profiles were basically identical with three-stage decomposition for both types of matrices: SG-0 (no gelatin) and SG-20 (with 20 wt% gelatin). Moreover, the SG-20 composite showed an improvement in thermal stability because of better interactions between fibers and the blend matrix.

19.6 Flame retardancy properties

19.6.1 Flammability of natural fibers

Actually, natural plant fibers are a source of fuel and are thus highly flammable and susceptible to ignition and combustion. As for natural fibers, unlike protein fibers,

plant fibers have poor fire retardancy, and cotton, for example, only has a low limited oxygen index (LOI) of 18−20, while an LOI of 25 for wool (Mark et al., 1975). Consequently, the flammability property of plant fibers, as promising green reinforcing agents, is widely investigated. Generally, the thermal degradation of natural plant fibers involves a series of reactions including the desorption of absorbed water, cross-linking of cellulose chains with the evolution of water to generate dehydrocellulose that continues to decompose to yield char and volatiles, formation of levoglucosan and its decomposition to generate flammable and nonflammable volatiles and gases, tar, and char (Biagiotti et al., 2004; Chapple and Anandjiwala, 2010).

For the flammability of plant fibers, it has been reported that many factors including the chemical composition, crystallinity, degree of polymerization, and fibrillar orientation determine the flammability. Table 19.4 presents chemical compositions and cone calorimeter data for several natural fibers, and Fig. 19.6 shows heat release rate curves of several plant fibers. In general, fibers tend to be more flammable with an increasing content of cellulose (see Table 19.4 and Fig. 19.6), while hemicellulose decomposes at lower temperatures than cellulose and thus a relatively high content of hemicellulose renders fibers easier to undergo thermal degradation and ignite. The decomposition of lignin contributes to the char formation more than cellulose and hemicellulose, but lignin starts degrading at a lower temperature, from about 160 to 400°C. Therefore for plant fibers, the higher the content of lignin, the more flammable, for example, sugar cane and bamboo.

19.6.2 Flammability of polymeric biocomposites

The flammability of a biocomposite depends on the matrix polymer, the type of fibers, and the interactions between them. Because the majority of biopolymers, including PLA, PHBV, and PBS, and plant fibers are inherently flammable, they present a threat to human beings' lives and properties during their service. Normally, modifying fibers with flame retardants or directly incorporating flame retardants into biocomposites are two main strategies to enhance the flame retardancy of natural fiber-based biocomposites. The flammability property of several typical biocomposites is summarized in the following sections.

19.6.2.1 Flammability of poly (lactic acid)-based biocomposites

Shumao et al. (2010) prepared three flame-retardant PLA/ramie fiber biocomposites via three approaches: (1) PLA was first blended with APP and then with ramie fibers; (2) ramie fibers were pretreated with APP and then blended with PLA; (3) both PLA and ramie fibers were treated with APP and blended together. Results showed that the composite fabricated with the third method displayed the best fire retardancy property, achieving a V-0 rating in the UL-94 test and an LOI value of 35.6 relative to no rating in the UL-94 test and only an LOI of 19.1 for the PLA/ramie composite. Digital images of composites prepared with the three methods after burning tests strongly confirm the biocomposite prepared with the third strategy holds better flame retardancy performance, as shown in Fig. 19.7.

Table 19.4 Chemical compositions and cone calorimeter data for several natural fibers

Natural fibers	Cellulose (%)	Hemicellulose (%)	Lignin (%)	Ash (%)	TTI (s)	PHRR (kW/m^2)	THR (kJ)	Residue (%)
Cellulose	100	0	0	0	50	144	234	12
Flax	80	13	2	1	16	112	130	47
Hemp	70–77	17.9–22.4	3.7–5.7	0.8	9	114	32	65
Sugar cane	32–34	27–32	19–24	1.5–5	13	143	143	25
Bamboo	26–49	15–27.7	21–31	1.3–2	17	155	205	26

TTI, PHRR, THR, and *mass residue*, respectively, refer to the time to ignition, peak of heat release rate, total heat release, and mass residue after burning.
Reproduced from Dorez, G., Taguet, A., Ferry, L., Lopez-Cuesta, J., 2013. Thermal and fire behavior of natural fibers/PBS biocomposites. Polymer Degradation and Stability 98, 87–95, copyright 2013, with permission from Elsevier Press.

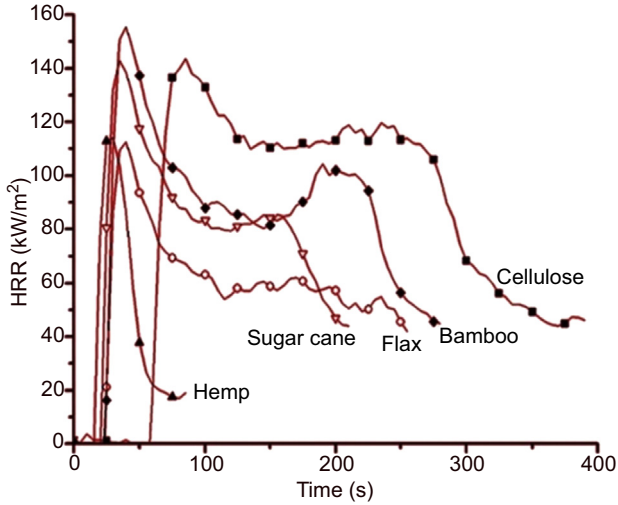

Figure 19.6 Heat release rate curves for several natural fibers at a radiant heat flux of 35 kW/m^2. Reproduced from Dorez, G., Taguet, A., Ferry, L., Lopez-Cuesta, J., 2013. Thermal and fire behavior of natural fibers/PBS biocomposites. Polymer Degradation and Stability 98, 87−95.

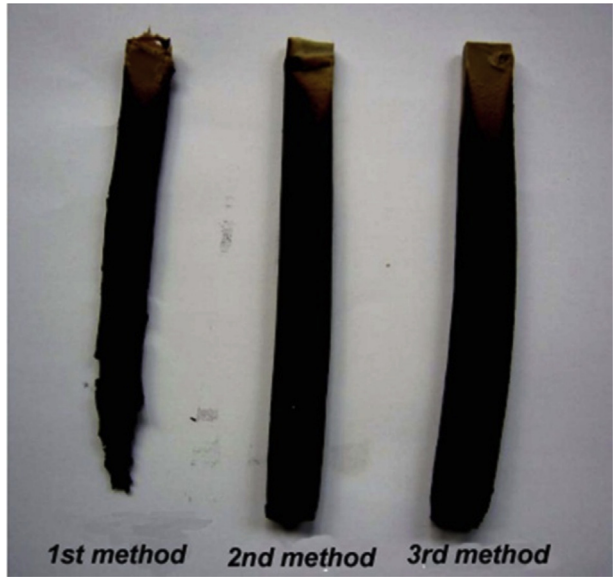

Figure 19.7 Digital photos of composites prepared with three methods after burning tests. Reprinted from Shumao, L., Jie, R., Hua, Y., Tao, Y., Weizhong, Y., 2010. Influence of ammonium polyphosphate on the flame retardancy and mechanical properties of ramie fiber-reinforced poly (lactic acid) biocomposites. Polymer International 59, 242−248, copyright 2009, with permission from the Society of Chemical Industry.

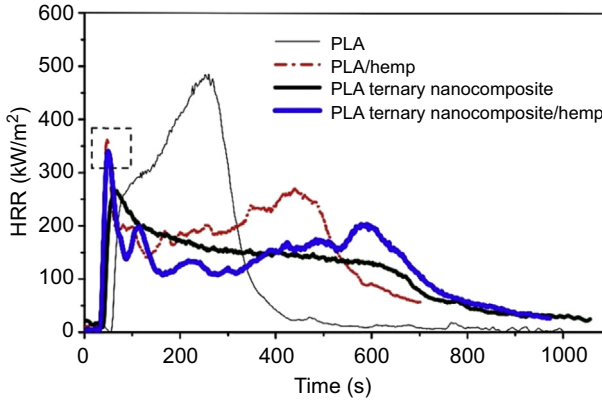

Figure 19.8 Heat release rate profiles for four specimens tested on cone calorimeter. Reprint from Hapuarachchi, T.D., Peijs, T., 2010. Multiwalled carbon nanotubes and sepiolite nanoclays as flame retardants for polylactide and its natural fibre reinforced composites. Composites Part A: Applied Science and Manufacturing 41, 954–963, copyright 2010, with permission from Elsevier Press.

Hapuarachchi and Peijs (2010) developed fully bio-based flame-retardant PLA/hemp fiber composites with multiwalled carbon nanotubes (MWNTs) and sepilolite nanoclay (Sep) as flame retardants. A cone calorimeter test results showed that compared with the PLA matrix, the peak heat release rate (PHRR) was reduced from 485 to 265 kW/m^2 for the PLA/MWNTs/Sep ternanocomposite; however, incorporating hemp fibers into the PLA ternanocomposites increased the PHRR value to 340 kW/m^2, indicating slightly better flame retardancy than PLA/hemp composites, showing a PHRR of 361 kW/m^2. Fig. 19.8 gives the heat release rate curves for four composites tested on cone calorimeter.

In addition, Woo and Cho (2013) investigated effects of aluminum trihydroxide (ATH) on the flame retardancy of kenaf/PLA green composites. The PLA/40 wt% kenaf composite exhibits an LOI value of 23.9, and the LOI was increased up to 39.7 after adding 50 wt% of ATH as flame retardants. The digital photos of PLA/kenaf composite without and with ATH after LOI tests clearly show that the latter holds better flame retardancy than the former (see Fig. 19.9).

19.6.2.2 Flammability of polyhydroxybutyrate-co-hydroxyvaerate -based biocomposites

Gallo et al. (2013) tailored the flame retardant property of kenaf fibers reinforced PHBV/PBAT (30/70, w/ww) composites by preparing multicomponent laminates, shown in Fig. 19.10(a) Results showed that the introduction of fibers and flame retardants composed of aluminum diethyphosphinate (AlPi) and antimony oxide (Sb_2O_3) only slightly prolonged the time to ignition, as shown in Fig. 19.10(b). After ignition, the E-PHBV burned violently immediately, and the HRR curve exhibited two heat release peaks with the first small peak of 724 kW/m^2 and a second large peak of

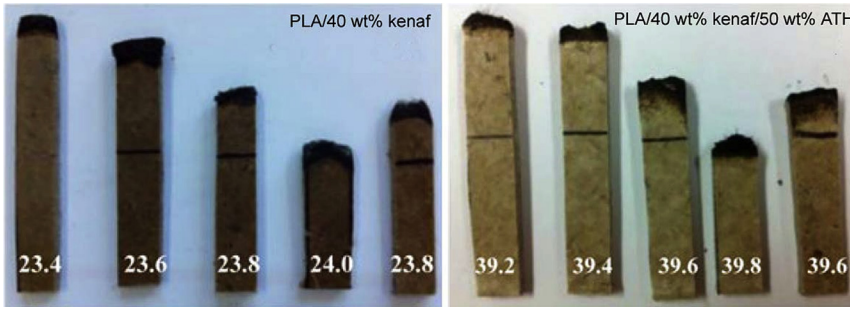

Figure 19.9 Digital photos for poly (lactic acid)-based green composites after LOI tests. Reproduced from Woo, Y., Cho, D., 2013. Effect of aluminum trihydroxide on flame retardancy and dynamic mechanical and tensile properties of kenaf/poly (lactic acid) green composites. Advanced Composite Materials 22, 451−464, copyright 2013, with permission from Talor and Francis Group.

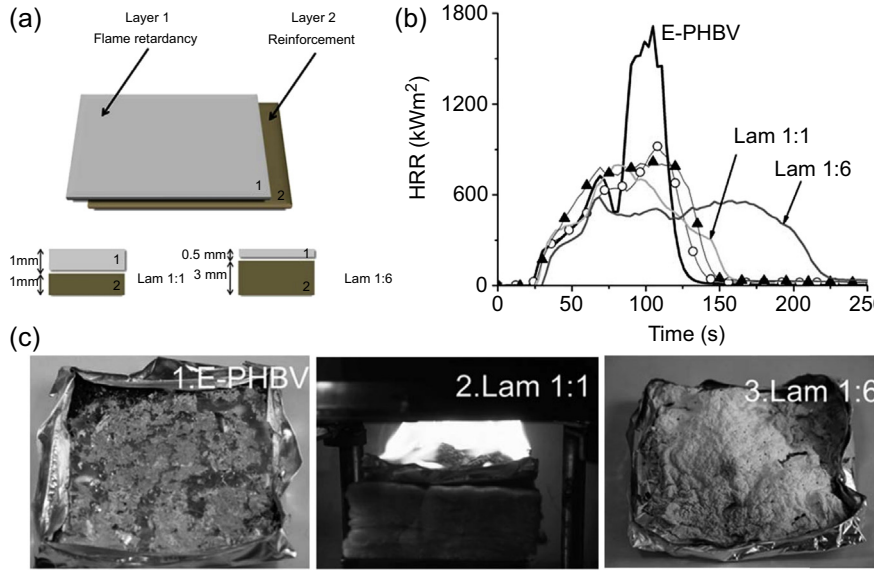

Figure 19.10 (a) structure and laminate thickness of prepared biocomposites, (b) heat release rate curves, and (c) photographs of E-PHBV, Lam 1:1, and Lam 1:6.
Reproduced from Gallo, E., Schartel, B., Acierno, D., Cimino, F., Russo, P., 2013. Tailoring the flame retardant and mechanical performances of natural fiber-reinforced biopolymer by multi-component laminate. Composites Part B: Engineering 44, 112−119, copyright 2013, with permission from Elsevier Press.

1713 kW/m^2. The polymer matrix combusts quickly without any char residue left at last. The HRR curves for Layers 1 and 2 did not change much but the second PHRR was suppressed. Compared with E-PHBV, the PHRR value was reduced by 47%, while the kenaf fiber in Layer 2 resulted in a further decrease by 50%. Compared

with E-PHBV, the HRR curve of Lam 1:1 was not changed remarkably relative to those of Layer 1 and Layer 2, producing a PHRR of 764 kW/m^2, about 55% lower than that of E-PHBV, and Lam 1:6 displayed a much longer burning time of 200 s as compared with 150 s for other materials. Moreover, for Lam 1:6 the HRR exhibited a plateau after reaching a peak of 586 kW/m^2 (about 66% reduction), indicating the formation of a protective thermal stable layer, suppressing the fire progression during combustion (see Fig. 19.10(c)).

19.6.2.3 Flammability of poly(1,4-butanediol succinate)-based biocomposites

In addition to the thermal stability properties, Dorez et al. (2014) also investigated effects of three kinds of flame retardant-treated flax fibers on flame retardancy of PBS, and detailed data obtained from cone calorimeter tests are listed in Table 19.5. Flame retardant biocomposites based on grafted fibers with DAP, P(MAPC$_1$(OH)$_2$), and P(MMA-*co*-MAPC$_1$(OH)$_2$) (see their chemical structure in Fig. 19.5) showed, to different degrees, shorter time to ignition and lower PHRR values than PBS/Tfl as a result of the formation of a thick char layer on the surface of underlying composites, limiting pyrolysis gas transfer from the sample to the flame. The insulating barrier layer resulted in a remarkable reduction in PHRR and a dramatic increase in char residues. For three types of different flame retardant-treated flax fibers, there are not big differences between composite-based flax fibers treated with P(MAPC$_1$(OH)$_2$) and

Table 19.5 Detailed parameters obtained from cone calorimeter tests of PBS-FTfl

Samples	TTI (s)	PHRR (kW/m^2)	THR (kJ/g)	EHC (kJ/g)	Xchar (%)
PBS + Tfl	68	379.5	17.7	18.4	4.2
PBS + Tfl-5DAP	56	321.8	17.3	18.4	6.1
PBS + Tfl-10DAP	64	314.5	16.1	17.7	9.2
PBS + Tfl-5P(MAPC$_1$(OH)$_2$)	70	323.5	17.4	18.7	7.0
PBS + Tfl-10P(MAPC$_1$(OH)$_2$)	57	292.6	16.6	18.3	9.4
PBS + Tfl-15P(MAPC$_1$(OH)$_2$)	52	291.4	17.0	18.7	9.2
PBS + Tfl-23.5P(MMA-*co*-MAPC$_1$(OH)$_2$)	36	289.1	18.1	19.3	6.2

TTI, PHRR, THR, and Xchar respectively refer to the time to ignition, peak of heat release rate, total heat release, and char residue after burning. *Tfl* means treated flax fibers with ethanol.
Reproduced from Dorez, G., Otazaghine, B., Taguet, A., Ferry, L., Lopez-Cuesta, J.M., 2014. Improvement of the fire behavior of poly (1, 4-butanediol succinate)/flax biocomposites by fiber surface modification with phosphorus compounds: molecular versus macromolecular strategy. Polymer International 63, 1665−1673, copyright 2013, with permission from Elsevier Press.

DAP. In comparison, P(MMA-*co*-MAPC$_1$(OH)$_2$)-treated fiber-based composites led to the biggest reduction in PHRR value (289.1 kW/m^2), only 76% of PHRR value (379.5 kW/m^2) for PBS/Tfl biocomposite. The authors concluded that phosphorus covalently bonded to flax is more effective in favoring dehydration and thus increasing char yield of the lignocellulosic fibers than phosphorus in the composite bulk. However, the total heat release value was slightly higher than the former two, probably due to the presence of MMA in the flame retardant (Dorez et al., 2014).

Dorez et al. (2013) systematically investigated five kinds of natural fibers including the flame retardancy of PBS, and detailed data obtained cone calorimeter tests are shown in Fig. 19.11 and Table 19.6.

As shown in Fig. 19.11 and Table 19.6, the heat release rate (HRR) curve of PBS is typical of a pure polymer since the TTI is relatively long (about 150 s) because of a relatively high degradation temperature. Upon ignition, the combustion of flammable volatiles results in a drastic increase of HRR reaching a peak of 485 kJ/m^2 followed by rapid decrease in HRR due to the rapid consumption of the fuel decomposed from the polymer. In comparison, although all reinforced biocomposites considerably shorten the TTI, they show significantly lower PHRR than the PBS matrix, especially for PBS composite filled with bamboo fibers, showing a TTI of 43 s and a PHRR of 339 kJ/m^2. The authors believed that the presence of natural fibers led to an early ignition, mainly because the fiber starts degrading at a lower temperature (350−380°C)

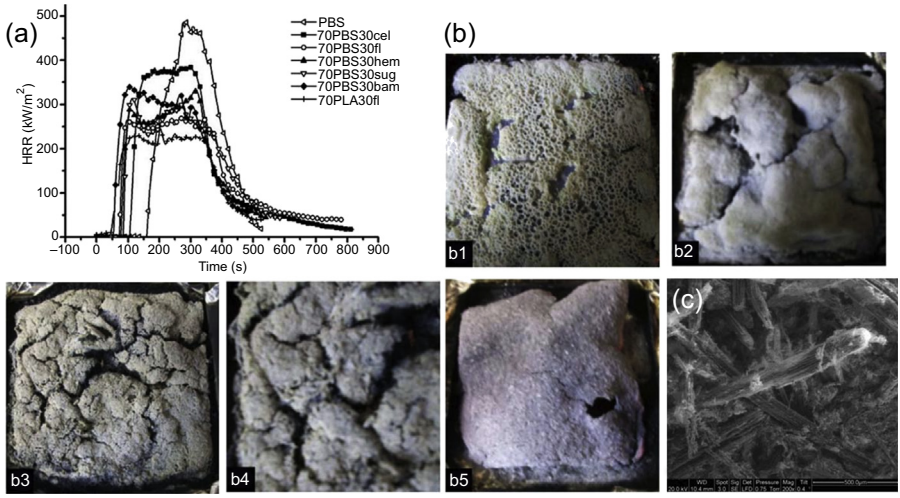

Figure 19.11 (a) HRR curves of PBS and its natural fiber-reinforced PBS biocomposites, (b) digital photos of char residues for (b1) 70PBS30cellulose, (b2) 70PBS30flax fibers, (b3) 70PBS30hemp, (b4) 70PBS30sugar cane, and (b5) 70PBS30bamboo fibers, and (c) micromorphology of the core of 70PBS30bamboo after cone calorimeter test. Reproduced from Julkapli, N.M., Akil, H.M., 2010. Thermal properties of kenaf-filled chitosan biocomposites. Polymer-plastics Technology and Engineering 49, 147−153, copyright 2013, with permission from Elsevier Press.

Table 19.6 Detailed data obtained from cone calorimeter tests of poly(1,4-butanediol succinate) biocomposites with various natural fibers (Julkapli and Akil, 2010)

Biocomposites	TTI (s)	PHRR (kW/m^2)	THR (kJ/g)	EHC (kJ/g)	Residue (%)
PBS	150	485	873	21.0	0
70PBS30cellulose	96	385	984	19.8	1.7
70PBS30flax	61	270	884	19.5	5.5
70PBS30hemp	67	332	818	18.1	10.0
70PBS30sugar cane	74	313	862	19.3	5.4
70PBS30bamboo	43	339	884	19.6	4.6

TTI, PHRR, THR, EHC, and residue respectively refer to the time to ignition, peak of heat release rate, total heat release, effective hear capacity and char residue after burning.

than 390°C of pure PBS. As shown in Fig. 19.11(a), after ignition, a first heat release rate peak is observed, due to the rapid decomposition of natural fibers, and then the HRR levels off due to the formation of a protective char layer, as evidenced by Fig. 19.11(b). The degradation of fibers contributed to the formation of a thermal insulting layer acting as a barrier for heat and mass transport, thus reducing the HHR value and flammability of the polymer matrix. Micromorphology of char residues for the PBS/bamboo composite (see Fig. 19.11(c)) clearly indicated that the protective layer is mainly composed of natural fiber residue, and the authors attributed the char to the role of lignin played in the process of char formation.

Subsequently, the second HRR peak appeared (see Fig. 19.11(a)), which was believed to be ascribed to the char cracking, as evidenced by Fig. 19.11(b). It is worth noting that the PBS/cellulose composite only shows an intermediate curve between PBS and cellulose mainly because it hardly forms a protective layer during burning. As listed in Table 19.6, no cohesion is observed for the residue of 70PBS/30cellulose (1.7%) relative to those of 70PBS/30hemp (10%), 70PBS30flax (5.5%), 70PBS30sugar cane (5.4%), and 70PBS30bamboo (9.7%), which basically displayed a cohesive char layer in spite of some cracks on the surface. The author considered that 70PBS30flax composite exhibits the lowest PHRR, EHC, and THR, probably due to the highest char residue (10%), leading to the best barrier effect and fire retardancy (Table 19.6).

19.7 Flame retardancy mechanism

Although the flammability properties of natural fiber reinforced thermoplastic biocomposites are crucial for their applications, only phosphorus-based flame retardant

APP and DAP, inorganic aluminium diethyphosphinate (AlPi) combined with antimony oxide (Sb_2O_3), and nanoscale MWNTs and nanoclay have been introduced to reduce their flammability. The proposed flame-retardancy mechanism is investigated in detail.

19.7.1 Flame retardancy mechanism of phosphorus-based flame retardants

As already investigated by Shumao et al. (2010), for the PLA/ramie fiber composite without flame retardants the formation of char residues is not effective enough to protect the matrix. The ramie fibers simply experience dehydration of both hemicellulose and cellulose followed by yielding a small amount of char residue and other small gas products like H_2O, CO, and CO_2, most of which is mainly from the degradation of lignin during combustion (see Fig. 19.12(a)).

After introducing APP, the presence of APP could help enhance the formation of a coherent carbonaceous char layer as a protective shield and thermal barrier. Moreover, with APP as both acid source and gas source, ramie fibers that are rich in polyhydric compound could act as a char-forming agent to form an intumescent flame-retardant system. Generally, when exposed to temperature, APP releases phosphoric acid and polyphosphoric acid, and the resulting acid can catalyze the intramolecular or intermolecular dehydration of ramie fibers and/or the polymer matrix to form the condensed carbonaceous layer. The resultant cross-linked or carbonized structures can significantly limit the volatilization of fuel and the diffusion of oxygen. This process is also accompanied by the release of water and nonflammable NH_3 and H_2O gases and the dehydrogenizing, charring, and breaking of chemical bonds (see Fig. 19.12(a) and (b)). In addition, phosphorus leads to flame inhibition through a radical trapping mechanism in the gaseous phase, and the nonflammable gases can dilute the fuel concentration in the flame and thus reduce or quench the flame. Therefore these physical and chemical actions in both the condensed phase and gas phase play a combined role in improving flame retardancy.

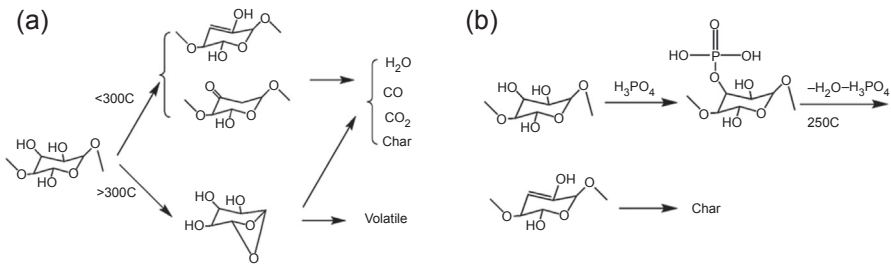

Figure 19.12 Hypothetical char-forming process of (a) ramie fibers and (b) phosphate ramie. Reproduced from Shumao, L., Jie, R., Hua, Y., Tao, Y., Weizhong, Y., 2010. Influence of ammonium polyphosphate on the flame retardancy and mechanical properties of ramie fiber-reinforced poly (lactic acid) biocomposites. Polymer International 59, 242−248, copyright 2009, with permission from the Society of Chemical Industry.

19.7.2 Flame retardancy mechanism of inorganic flame retardants

To uncover the flame retardancy mechanism of AlPi/Sb_2O_3 in the PHBV/kenaf biocomposites, Gallo et al. (2013) investigated the micromorphology and structure of char residues. Fig. 19.13 presents the SEM images of char residue for Layer 2 and Lam 1:6. Besides observing the fibers in the char, the char structure for Layer 2 was porous and inhomogeneous, featured by holes and cavities of different sizes that hardly effectively prevent the transfer of heat and volatiles from the decomposing polymer into the flame zone (see Fig. 19.13(a)). Therefore the char layer leads to limited improvement in PHRR value and flame retardancy. After introducing the flame retardant of AlPi/Sb_2O_3, for instance, Lam 1:6, the cross section of char was a homogeneous, compact, and close surface, covering a dense hollow structure, thus making

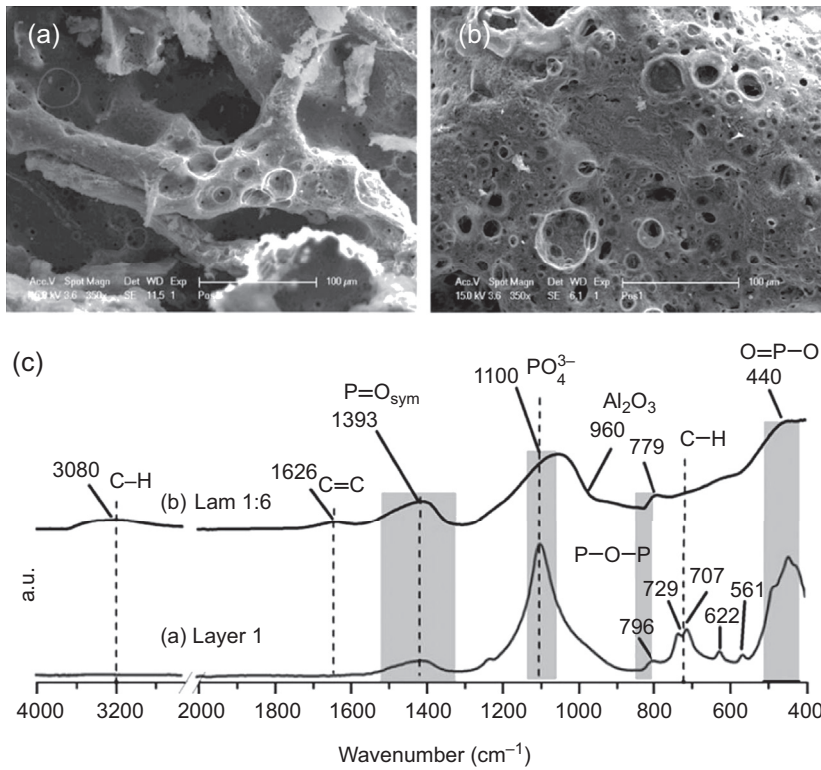

Figure 19.13 SEM images of char residues for (a) Layer 2 (PHBV composites containing 30 wt% kenaf) and (b) Lam 1:6 (1 mm thick Layer 1 + 6mm thick Layer 2); (c) FTIR spectra of char residues for Layer 1 (PHBV composites containing 8 wt% AlPi and 2 wt% Sb_2O_3). Reproduced from Gallo, E., Schartel, B., Acierno, D., Cimino, F., Russo, P., 2013. Tailoring the flame retardant and mechanical performances of natural fiber-reinforced biopolymer by multicomponent laminate. Composites Part B: Engineering 44, 112−119, copyright 2013, with permission from Elsevier Press.

fibers unobserved in the char structure. Moreover, both holes and cavities are to some degree connected to each other (see Fig. 19.13(b)), creating an even and dense texture. This cohesive char structure can obstruct the release of volatile degradation products from the burning polymer. The trapping of pyrolysis gases made the char layer swell during combustion, producing a dense and porous structure and further interfering and blocking the release of fuel into the flame. Therefore the flame retardancy was improved significantly with remarkable reduction in PHRR.

Additionally, to elucidate the chemical composition of char residue, authors also studied the IR spectra of residues of Layer 1 and Lam 1:6, as shown in Fig. 19.13(c). For Layer 1 the char residue was dominated by the formation of inorganic phosphates, as evidenced by the appearance of absorption peaks at 1393 cm^{-1} (P═O), 1100 cm^{-1} (PO_4^{3-}), 796 cm^{-1} (P−O−P), and 440 cm^{-1} (O═P−O). Moreover, other absorption bands at 729, 707, 622, and 561 cm^{-1} were attributed to the characteristic peaks of aluminum phosphates. In comparison, the IR spectrum of Lam 1:6 displayed broad absorption peaks centered at 1393, 1100, and 440 cm^{-1}, indicating the formation of inorganic phosphates. In addition, peaks at 3080, 1626 cm^{-1}, and the broad absorption band in the range of 750−700 cm^{-1} were ascribed to aromatic hydrocarbons. The results indicated that the char residue was a mixture of inorganic phosphates, aluminum trioxides, and carbonaceous char. Moreover, the presence of natural fibers was responsible for changing the char-forming mechanism of the phosphorus-based layer (Gallo et al., 2013).

19.8 Summary and outlook

This chapter reviewed the thermal stability and flame retardancy of natural plant fiber reinforced thermoplastic biocomposites. Because of the growing environmental awareness on global warming and weather change, various natural plant fibers including jute, hemp, flax, coir, ramie, bamboo, etc. have been widely employed to create biodegradable green composites due to their high strength-weight ratio and recyclability characteristics. Despite improved mechanical properties for these composites, low thermal stability and inherent flammability extremely restrict the wide applications of plant fibers and their biocomposites. Therefore improving the thermal stability and flame retardancy is extremely crucial to ensure their safe applications during their services. Until now, phosphorus-based flame retardants, especially intumescent flame retardants, inorganic metal compounds, and nanoscale particles have been incorporated to different extents to improve thermal stability and flame retardancy properties of natural fiber reinforced biocomposites. Although thermal stability and flame retardancy properties have been improved to some extent, incorporating flame retardants usually leads to poorer mechanical properties relative to the biocomposites because of weak interfacial adhesion and strong polarity of flame retardants.

Great advances have been made on the thermal stability and flame retardancy properties of plant fiber reinforced biocomposites; however, there are still some challenges to be addressed: (1) magnitudes of improvement in flame retardancy remains limited;

(2) more effective flame retardants need to be developed; and (3) much work needs to done to achieve natural fiber reinforced thermoplastic biocomposites with excellent flame retardancy and mechanical properties.

Acknowledgments

This work was financially funded by the National Science Foundation of China (Grant 51303162) and the Nonprofit Project of Science and Technology Agency of Zhejiang Province of China (2013C32073 and 2012C22077) and the Program for Key Science and Technology Team of Zhejiang Province (2013TD17).

References

Bajpai, P.K., Singh, I., Madaan, J., 2012. Development and characterization of PLA-based green composites: a review. Journal of Thermoplastic Composite Materials 27, 52−81.

Battegazzore, D., Alongi, J., Frache, A., 2014. Poly (lactic acid)-based composites containing natural fillers: thermal, mechanical and barrier properties. Journal of Polymers and the Environment 22, 88−98.

Bhardwaj, R., Mohanty, A.K., Drzal, L., Pourboghrat, F., Misra, M., 2006. Renewable resource-based green composites from recycled cellulose fiber and poly (3-hydroxybutyrate-co-3-hydroxyvalerate) bioplastic. Biomacromolecules 7, 2044−2051.

Biagiotti, J., Puglia, D., Kenny, J.M., 2004. A review on natural fibre-based composites-part I: structure, processing and properties of vegetable fibres. Journal of Natural Fibers 1, 37−68.

Bledzki, A.K., Gassan, J., 1999. Composites reinforced with cellulose based fibres. Progress in Polymer Science 24, 221−274.

Bourbigot, S., Duquesne, S., 2007. Fire retardant polymers: recent developments and opportunities. Journal of Materials Chemistry 17, 2283−2300.

Bourbigot, S., Fontaine, G., 2010. Flame retardancy of polylactide: an overview. Polymer Chemistry 1, 1413−1422.

Chapple, S., Anandjiwala, R., 2010. Flammability of natural fiber-reinforced composites and strategies for fire retardancy: a review. Journal of Thermoplastic Composite Materials 23, 871−893.

Chen, Y., Chiparus, O., Sun, L., Negulescu, I., Parikh, D.V., Calamari, T.A., 2005. Natural fibers for automotive nonwoven composites. Journal of Industrial Textiles 35, 47−62.

Dash, B., Rana, A., Mishra, S., Mishra, H., Nayak, S., Tripathy, S., 2000. Novel low-cost jute−polyester composite. II. SEM observation of the fractured surfaces. Polymer-plastics Technology and Engineering 39, 333−350.

Dong, Y., Ghataura, A., Takagi, H., Haroosh, H.J., Nakagaito, A.N., Lau, K.-T., 2014. Poly-lactic acid (PLA) biocomposites reinforced with coir fibres: evaluation of mechanical performance and multifunctional properties. Composites Part A: Applied Science and Manufacturing 63, 76−84.

Dorez, G., Otazaghine, B., Taguet, A., Ferry, L., Lopez-Cuesta, J.M., 2014. Improvement of the fire behavior of poly(1,4-butanediol succinate)/flax biocomposites by fiber surface modification with phosphorus compounds: molecular versus macromolecular strategy. Polymer International 63, 1665−1673.

Dorez, G., Taguet, A., Ferry, L., Lopez-Cuesta, J., 2013. Thermal and fire behavior of natural fibers/PBS biocomposites. Polymer Degradation and Stability 98, 87−95.

Faruk, O., Bledzki, A.K., Fink, H.-P., Sain, M., 2012. Biocomposites reinforced with natural fibers: 2000−2010. Progress in Polymer Science 37, 1552−1596.

Focke, W.W., Molefe, D., Labuschagne, F., Ramjee, S., 2009. The influence of stearic acid coating on the properties of magnesium hydroxide, hydromagnesite, and hydrotalcite powders. Journal of Materials Science 44, 6100−6109.

Franchini, E., Galy, J., Gérard, J.-F., Tabuani, D., Medici, A., 2009. Influence of POSS structure on the fire retardant properties of epoxy hybrid networks. Polymer Degradation and Stability 94, 1728−1736.

Gallo, E., Schartel, B., Acierno, D., Cimino, F., Russo, P., 2013. Tailoring the flame retardant and mechanical performances of natural fiber-reinforced biopolymer by multi-component laminate. Composites Part B: Engineering 44, 112−119.

Gallo, E., Schartel, B., Acierno, D., Russo, P., 2011. Flame retardant biocomposites: synergism between phosphinate and nanometric metal oxides. European Polymer Journal 47, 1390−1401.

Gao, F., Beyer, G., Yuan, Q., 2005. A mechanistic study of fire retardancy of carbon nanotube/ethylene vinyl acetate copolymers and their clay composites. Polymer Degradation and Stability 89, 559−564.

Gomes, A., Matsuo, T., Goda, K., Ohgi, J., 2007. Development and effect of alkali treatment on tensile properties of curaua fiber green composites. Composites Part A: Applied Science and Manufacturing 38, 1811−1820.

Graupner, N., Herrmann, A.S., Müssig, J., 2009. Natural and man-made cellulose fibre-reinforced poly (lactic acid)(PLA) composites: an overview about mechanical characteristics and application areas. Composites Part A: Applied Science and Manufacturing 40, 810−821.

Hapuarachchi, T.D., Peijs, T., 2010. Multiwalled carbon nanotubes and sepiolite nanoclays as flame retardants for polylactide and its natural fibre reinforced composites. Composites Part A: Applied Science and Manufacturing 41, 954−963.

Hapuarachchi, T.D., Ren, G., Fan, M., Hogg, P.J., Peijs, T., 2007. Fire retardancy of natural fibre reinforced sheet moulding compound. Applied Composite Materials 14, 251−264.

Hirschler, M., 1984. Reduction of smoke formation from and flammability of thermoplastic polymers by metal oxides. Polymer 25, 405−411.

Holbery, J., Houston, D., 2006. Natural-fiber-reinforced polymer composites in automotive applications. JOM 58, 80−86.

Hollingbery, L., Hull, T., 2010. The thermal decomposition of huntite and hydromagnesite—a review. Thermochimica Acta 509, 1−11.

Huda, M.S., Drzal, L.T., Mohanty, A.K., Misra, M., 2008. Effect of fiber surface-treatments on the properties of laminated biocomposites from poly (lactic acid)(PLA) and kenaf fibers. Composites Science and Technology 68, 424−432.

Jang, J.Y., Jeong, T.K., Oh, H.J., Youn, J.R., Song, Y.S., 2012. Thermal stability and flammability of coconut fiber reinforced poly (lactic acid) composites. Composites Part B: Engineering 43, 2434−2438.

Jha, N., Bajaj, P., Misra, A., Maurya, P., 1986. Flame retardation of polypropylene: effect of organoantimony compounds on the flammability and thermal behavior. Journal of Applied Polymer Science 32, 4393−4403.

Jiménez, A., Ruseckaite, R., 2006. Binary mixtures based on polycaprolactone and cellulose derivatives: thermal degradation and pyrolysis. Journal of Thermal Analysis and Calorimetry 88, 851−856.

Jimenez, M., Duquesne, S., Bourbigot, S., 2006. Intumescent fire protective coating: toward a better understanding of their mechanism of action. Thermochimica Acta 449, 16−26.

John, M.J., Anandjiwala, R.D., 2008. Recent developments in chemical modification and characterization of natural fiber-reinforced composites. Polymer Composites 29, 187.

Julkapli, N.M., Akil, H.M., 2010. Thermal properties of kenaf-filled chitosan biocomposites. Polymer-plastics Technology and Engineering 49, 147−153.

Kabir, M., Wang, H., Lau, K., Cardona, F., 2012. Chemical treatments on plant-based natural fibre reinforced polymer composites: an overview. Composites Part B: Engineering 43, 2883−2892.

Khedari, J., Charoenvai, S., Hirunlabh, J., 2003. New insulating particleboards from durian peel and coconut coir. Building and Environment 38, 435−441.

Kim, J.T., Netravali, A.N., 2010. Mechanical and thermal properties of sisal fiber-reinforced green composites with soy protein/gelatin resins. Journal of Biobased Materials and Bioenergy 4, 338−345.

Kozłowski, R., Władyka-Przybylak, M., 2008. Flammability and fire resistance of composites reinforced by natural fibers. Polymers for Advanced Technologies 19, 446−453.

Laoutid, F., Bonnaud, L., Alexandre, M., Lopez-Cuesta, J.-M., Dubois, P., 2009. New prospects in flame retardant polymer materials: from fundamentals to nanocomposites. Materials Science and Engineering: R: Reports 63, 100−125.

Laoutid, F., Gaudon, P., Taulemesse, J.-M., Cuesta, J.L., Velasco, J., Piechaczyk, A., 2006. Study of hydromagnesite and magnesium hydroxide based fire retardant systems for ethylene−vinyl acetate containing organo-modified montmorillonite. Polymer Degradation and Stability 91, 3074−3082.

Lee, B.-H., Kim, H.-S., Lee, S., Kim, H.-J., Dorgan, J.R., 2009. Bio-composites of kenaf fibers in polylactide: role of improved interfacial adhesion in the carding process. Composites Science and Technology 69, 2573−2579.

Lee, S.-H., Wang, S., 2006. Biodegradable polymers/bamboo fiber biocomposite with bio-based coupling agent. Composites Part A: Applied Science and Manufacturing 37, 80−91.

Luo, S., Netravali, A., 1999. Interfacial and mechanical properties of environment-friendly "green" composites made from pineapple fibers and poly (hydroxybutyrate-co-valerate) resin. Journal of Materials Science 34, 3709−3719.

Madsen, B., Lilholt, H., Damkilde, L., Hoffmeyer, P., Thomsen, A.B., 2004. Properties of Plant Fiber Yarn Polymer Composites: An Experimental Study. Technical University of DenmarkDanmarks Tekniske Universitet, Administration Administration, Office for Study Programmes and Student Affairs Afdelingen for Uddannelse og Studerende.

Manshor, M., Anuar, H., Aimi, M.N., Fitrie, M.A., Nazri, W.W., Sapuan, S., El-Shekeil, Y., Wahit, M., 2014. Mechanical, thermal and morphological properties of durian skin fibre reinforced PLA biocomposites. Materials & Design 59, 279−286.

Mark, H., Atlas, S., Shalaby, S., Pearce, E., 1975. 'Combustion of Polymers and its Retardation', Flame-retardant Polymeric Materials. Springer, pp. 1−17.

Matkó, S., Toldy, A., Keszei, S., Anna, P., Bertalan, G., Marosi, G., 2005. Flame retardancy of biodegradable polymers and biocomposites. Polymer Degradation and Stability 88, 138−145.

Mngomezulu, M.E., John, M.J., Jacobs, V., Luyt, A.S., 2014. Review on flammability of biofibres and biocomposites. Carbohydrate Polymers 111, 149−182.

Monteiro, S., Lopes, F., Ferreira, A., Nascimento, D., 2009. Natural-fiber polymer-matrix composites: cheaper, tougher, and environmentally friendly. JOM 61, 17−22.

Monteiro, S.N., Calado, V., Rodriguez, R.J.S., Margem, F.M., 2012. Thermogravimetric behavior of natural fibers reinforced polymer composites—an overview. Materials Science and Engineering: A 557, 17−28.

Morgan, A.B., Gilman, J.W., 2013. An overview of flame retardancy of polymeric materials: application, technology, and future directions. Fire and Materials 37, 259−279.

Nabi Sahed, D., Jog, J.P., 1999. Natural fiber polymer composites: a review. Advances in Polymer Technology 18, 221−274.

Nam, T.H., Ogihara, S., Kobayashi, S., 2012a. Interfacial, mechanical and thermal properties of coir fiber-reinforced poly(lactic acid) biodegradable composites. Advanced Composite Materials 21, 103−122.

Nam, T.H., Ogihara, S., Nakatani, H., Kobayashi, S., Song, J.I., 2012b. Mechanical and thermal properties and water absorption of jute fiber reinforced poly (butylene succinate) biodegradable composites. Advanced Composite Materials 21, 241−258.

Netravali, A.N., Chabba, S., 2003. Composites get greener. Materials Today 6, 22−29.

Nguyen, T., Zavarin, E., Barrall, E.M., 1981. Thermal Analysis of lignocellulosic materials: Part I. Unmodified materials. Journal of Macromolecular Science—Reviews in Macromolecular Chemistry vol. 20, 1−65.

Okubo, K., Fujii, T., Thostenson, E.T., 2009. Multi-scale hybrid biocomposite: processing and mechanical characterization of bamboo fiber reinforced PLA with microfibrillated cellulose. Composites Part A: Applied Science and Manufacturing 40, 469−475.

Oza, S., Ning, H., Ferguson, I., Lu, N., 2014. Effect of surface treatment on thermal stability of the hemp-PLA composites: correlation of activation energy with thermal degradation. Composites Part B: Engineering 67, 227−232.

Sabaa, M.W., 1991. Thermal degradation behaviour of sisal fibers grafted with various vinyl monomers. Polymer Degradation and Stability 32, 209−217.

Saheb, D.N., Jog, J., 1999. Natural fiber polymer composites: a review. Advances in Polymer Technology 18, 351−363.

Sajna, V., Mohanty, S., Nayak, S.K., 2014. Hybrid green nanocomposites of poly (lactic acid) reinforced with banana fibre and nanoclay. Journal of Reinforced Plastics and Composites 33, 1717−1732.

Salim, Y.S., Abdullah, A.A.-A., Sipaut, C.S., Nasri, M., Ibrahim, M.N.M., 2011. Biosynthesis of poly (3-hydroxybutyrate-co-3-hydroxyvalerate) and characterisation of its blend with oil palm empty fruit bunch fibers. Bioresource Technology 102, 3626−3628.

Sathishkumar, T., Naveen, J., Satheeshkumar, S., 2014. Hybrid fiber reinforced polymer composites−a review. Journal of Reinforced Plastics and Composites 33, 454−471.

Satyanarayana, K., Guimarães, J., Wypych, F., 2007. Studies on lignocellulosic fibers of Brazil. Part I: source, production, morphology, properties and applications. Composites Part A: Applied Science and Manufacturing 38, 1694−1709.

Shumao, L., Jie, R., Hua, Y., Tao, Y., Weizhong, Y., 2010. Influence of ammonium polyphosphate on the flame retardancy and mechanical properties of ramie fiber-reinforced poly (lactic acid) biocomposites. Polymer International 59, 242−248.

Singh, S., Mohanty, A.K., Sugie, T., Takai, Y., Hamada, H., 2008. Renewable resource based biocomposites from natural fiber and polyhydroxybutyrate-co-valerate (PHBV) bioplastic. Composites Part A: Applied Science and Manufacturing 39, 875−886.

Tao, Y., Yan, L., Jie, R., 2009. Preparation and properties of short natural fiber reinforced poly (lactic acid) composites. Transactions of Nonferrous Metals Society of China 19, 651−655.

Wang, B., Panigrahi, S., Tabil, L., Crerar, W., 2007. Pre-treatment of flax fibers for use in rotationally molded biocomposites. Journal of Reinforced Plastics and Composites 26, 447−463.

Woo, Y., Cho, D., 2013. Effect of aluminum trihydroxide on flame retardancy and dynamic mechanical and tensile properties of kenaf/poly (lactic acid) green composites. Advanced Composite Materials 22, 451−464.

Yap, M., Que, Y., Chia, L., Chan, H., 1991. Thermal properties of tropical wood−polymer composites. Journal of Applied Polymer Science 43, 2057−2065.

Zhang, S., Horrocks, A.R., 2003. A review of flame retardant polypropylene fibres. Progress in Polymer Science 28, 1517−1538.

Design characteristics, codes and standards of natural fibre composites

20

M.A. Alam[1], *S.M. Sapuan*[2], *M.R. Mansor*[3]
[1]Universiti Tenaga Nasional, Kajang, Selangor, Malaysia; [2]Universiti Putra Malaysia, Serdang, Selangor, Malaysia; [3]Universiti Teknikal Malaysia Melaka, Durian Tunggal, Malacca, Malaysia

20.1 Introduction

Nowadays, there is an emerging demand to upgrade the existing infrastructures all over the world. These are due to upgrade of design codes, mistakes in design calculation, improper detailing of shear reinforcement, construction errors or poor construction practices, insufficient shear reinforcement or reduction in steel area due to corrosion in the service environment. Since replacement for such deficient structures requires a huge amount of money and time, strengthening is the most acceptable way to rehabilitate those structures to increase their load carrying capacity and extend their service life.

Another drive towards upgrading the building and construction infrastructure is to improve the existing sustainability performances. Du Plessis (2007) stated that sustainable construction relates to the development and proper management of a healthy built environment with efficient use of resources based on ecological principles. Based on the LafargeHolcim (2016) Foundation report, as the total urban world population growth is nearing one million inhabitants per week, sustainable performance in the construction industry needs to be quickly addressed to cater for the increasing demand. Among the areas highlighted in a similar report for a greater sustainability effort in the construction industry included the design and management of buildings, material performance, construction technology and processes, energy and resource efficiency in building and operation and maintenance.

Apart from increasing demand due to the boost in the world population, the building and construction industry also plays a major stake in the total world energy usage. It is reported that the building lifecycle in the United Kingdom, which covers construction, operation and demolition consumed approximately 40% of the nation total energy use, which in consequence causes high emission pollution (Alwan et al., 2016). Elsewhere, the construction industry in China is reported to consume nearly 793.74 million tons of coal in 2007 alone, which contributes to approximately 29.6% of the nation's total energy consumption. The value significantly showed that the construction industry is an energy-intensive industry, which plays a vital role towards the need for a more efficient and sustainable use of energy (Hong et al., 2016).

Advanced High Strength Natural Fibre Composites in Construction. http://dx.doi.org/10.1016/B978-0-08-100411-1.00020-0

In conjunction to the material performance area, traditional engineering materials such as concrete and steel are often applied in the building and construction industry due to good mechanical properties and high reliability performances. However, due to the increasing environmental awareness by consumers, new alternative materials, which have higher recyclability, biodegradability and renewability impacts are introduced to substitute, either partially or entirely, the conventional materials. The use of steel as the reinforcement agent for structural applications is also being reduced in order to cater the depleting raw material source and high energy consumption during product manufacturing and waste management processes, which affect the stability of the raw material cost in the market and consequently impact the overall building and construction cost (Yahya et al., 2016).

Based on the aforementioned scenarios, many efforts have been made to increase the sustainability performance of current building and construction operations. One of the efforts is in term design of new construction structures using renewable and recyclable raw materials as a substitution to the current conventional construction materials. Within the pool of alternative materials being explored, natural fibre composites (NFCs) are among the candidate materials, which have sparked a high potential for many construction applications such as for the design of beams, door panels, decking, railing and window frames. Several notable advantages of NFCs for construction application is low raw material cost, low energy intensity requirement during manufacturing and high environmental friendly characteristics (such as renewable, recyclable and biodegradable) (Dittenber and GangaRao, 2012). In addition, the use of NFCs also offers additional low health side effects during use as compared to glass fibre, which is often linked with skin irritations and respiratory complications (Ardente et al., 2008).

Moreover the push towards improving the sustainability performance of buildings is also in action through the application of environmental conscious design methods. This can be observed through the introduction of many design guidelines and assessment methodologies for green buildings, such as the United States Leadership in Energy and Environmental Design (LEED) method, Canadian Building and Environmental Performance Assessment Criteria and Japanese Comprehensive Assessment System for Building Environmental Efficiency (Franzoni, 2011). In addition, new design methodologies, which resulted in the integration of conventional design guidelines and assessment methodologies, were also formed to further enhance the design process of green buildings throughout the planning, analysis and execution phases. Among the examples is the development of integrated Building Information Modeling (BIM) and LEED framework, which enabled design assistance and certification management processes to be performed concurrently (Wu and Issa, 2010). Furthermore, enhancement of the BIM-LEED method was also proposed through the integration of the cost estimation function to the existing design model, which is reportedly able to provide a more holistic approach in the conceptual design of the green building to designers and clients. The cost estimation function allowed the prediction of cost to obtain the green building certification, in addition to the information of the planned building rating performance prior to the actual construction process (Jalaei and Jrade, 2015).

Thus in this chapter, focus is given towards realizing a higher sustainability performance of current building and construction industry practices through design practices. Among the topics included are an overview of NFC design practices for sustainable construction and a new design model for shear strengthening of reinforced concrete (RC) beams using NFC. In addition, to demonstrate the applicability of the new proposed design model, a case study on the design of kenaf fibre reinforced polymer composites (KFRP) is also included at the end of this chapter for the shear strengthening of RC beams.

20.2 Overview of natural fibre composite applications for sustainable construction

The application of NFCs for sustainable construction was dated since 4000 BC by the Egyptian civilization through the use of straw as a reinforcement agent in clay bricks for housing development purposes. The combination of straw and clay to form the brick demonstrates the early application of composite materials made from natural resources, which was reportedly able to lower the building material cost as well as increase the structural performance of the material (Mansour et al., 2007). The use of natural fibre for mud brick building materials such as straw and coconut coir were also reportedly able to increase the initial conventional mud brick compressive strength and thermal insulation properties, as well as reduce the conventional mud brick weight (Khedari et al., 2005; Binici et al., 2005).

A good thermal insulation property using NFCs was also reported by Khedari et al. (2004). In their study, three types of NFCs were applied to produce low thermal conductivity particleboard products using durian peel fibres, coconut coir fibres and hybrid durian peel/coconut fibres. The feasibility of using the NFC materials was able to conserve energy usage when applied as insulating materials for wall and ceiling sections inside the building. Furthermore, they also point out that the NFC particleboards can also be used as furniture material, which increases the diversity of application of the NFCs towards higher usage of agricultural waste. Elsewhere, Binici et al. (2014) reported similar thermal insulation building material applications using NFCs. In their report, two types of natural fibres were used, which are sunflower stalks and cotton textile waste, to form the NFC materials, while epoxy resin was applied as the matrix material. Both NFC insulation materials showed acceptable mechanical and thermal performance, which successfully satisfied the Turkish TS 805 EN 601 insulation material application standard. The NFC developed also reportedly contributed to reducing agrowaste scenarios for the country.

Besides that, feasibility on the application of NFCs for building and residential structural flooring materials was also investigated. Burgueño et al. (2004) reported the production of cellular beams and panels made from hemp/unsaturated polyester composites and flex/unsaturated polyester composites. Their study revealed that both NFC materials showed equal performance in terms of allowable pressure load for flooring applications compared to commercial grade flooring materials. Moreover,

Burgueño et al. (2005), in another report, showed that the use of hybrid NFCs was also able to further enhance the structural properties of cellular plate products for housing panel applications. The hybrid NFC cellular plate was fabricated from short hemp fibres as sandwich plate core material, while jute fibres in a mat form as the outer and inner skin of the sandwich plate structure. Mechanical characterization results showed that the hybrid natural fibre reinforced unsaturated polyester composite cellular plate has a higher modulus of elasticity value as compared to E-glass fibre reinforced unsaturated polyester composites. In addition to that, Li and Xian (2012) also reported on the application of unidirectional hemp reinforced epoxy composites for civil structural beam products. In their report, an NFC beam prepared using a prior mercerization process to the hemp fibres was able to increase the flexural strength and flexural modulus of the composite materials.

Among the many applications of NFC for building and construction, based on a literature review, concrete is the type of product most heavily associated with NFC. In general, concrete is the most applied building material in the construction industry due to its superior mechanical and physical properties, which enable it to handle very high compressive loads, while at the same time offer advantages such as great flexibility to be manufactured in many geometrical shapes, incombustible, affordable and highly available source of material (Aprianti et al., 2015). Concrete is produced through the combination of three main constituents, which are cement, water and aggregates (in both fine and coarse forms). Despite the advantages, conventional concrete materials also have significant drawbacks in terms of negative environmental impacts, such as high carbon dioxide (CO_2) emission release during the manufacturing stage and high energy consumption (Mo et al., 2016). Therefore in order to cater the limitation, many studies have been made to incorporate natural fibres as a filler material to the cement, a replacement for the aggregates and as a reinforcement to the concrete. The role of natural fibres as supplementary cementitious materials is to reduce the Portland cement volume in forming the concrete, which helps to reduce the overall concrete cost and decrease CO_2 emissions. On the other hand, the use of natural fibres also improved the ductility, toughness and impact resistance of the concrete when used as reinforcement materials through reducing the brittleness of the cement (Onuaguluchi and Banthia, 2016). Various sources of natural fibres are investigated as alternative materials in concrete formulation, which can be grouped into two categories: those from farming or agriculture waste and those from commodity crops. Examples of the agriculture waste type of natural fibres, which have been applied to formulate green concretes and other building materials, are coconut coir, rice husk, palm oil fuel ash, bagasse, wood chips, bamboo leaf ash, banana, wheat straw, barley straw and sisal; while natural fibre resources from commodity crops used in similar green concrete applications are kenaf, jute and hemp plants (Pacheco-Torgal and Jalali, 2011; Senaratne et al., 2016; Yan et al., 2016).

As shown in earlier examples, there are many utilizations of NFCs in sustainable construction applications. It should be noted that the process of converting the raw material into a successful product in not a trivial task and involves various stages along the whole product development process. Based on the Pugh Total Design method, the development process of any product can be summarized into six main stages, which

are market analysis, development of design requirements in the form of product design specifications, conceptual design, detail design, product manufacturing and finally sales of the finished product (Pugh, 1991). During the conceptual design stage of the product, the material selection process is performed to define the appropriate type of material which can be used to construct the product. In a sustainable construction point of view, decision making on the best type of material need to be systematically and scientifically conducted for specific building and applications, so the final candidate material will be able to deliver the expected performance in term of product functionality and safety, while at the same time providing the best environmental performance in terms of lower greenhouse gas emissions and energy usage (González and Navarro, 2006).

The direct linkage between material selection and sustainable construction can be observed through the inclusion of material selection activity as one of the six key areas involved in the LEED green building rating and certification system (Gurgun et al., 2015). The use of renewable, recyclable and biodegradable raw material resources such as NFCs can provide a higher score in the green building assessment process and finally contribute to a higher total rating for the desired building. The positive impact in the green building certification process is also one of the driving factors why designers and building owners are increasing the presence of NFC materials in the construction industry (Castro-Lacouture et al., 2009).

Material selection involves the consideration of many criteria from various stakeholders and the presence of multiple material alternatives for an intended product, which need to be considered by the decision makers. Kibert (2008) stated that among the challenges faced in the sustainable material selection process are a high variety of products and materials which need to be evaluated individually and assembled as building components, varying assessment of product parameters and inadequate information of the manufacturing process. In another report, Akadiri (2015) revealed that other challenges in material selection for construction also included factors such as perception of extra costs being incurred by utilizing the green materials, lack of material information for the selection process and perception of extra time incurred by using green materials. On the other hand, the assessment of selection criteria also involved many considerations. Akadiri and Olomolaiye (2012) stated that among the selection consideration in sustainable material selection in a building project are utilization of less resources, the use of renewable and recyclable resources, and materials with the lowest environmental impact throughout the whole product life cycle.

Despite the process complexity, there are several methods to assists designers in performing the material selection process in sustainable building and construction applications. Govindan et al. (2016) demonstrated the use of a hybrid multicriteria decision making (MCDM) method in performing brick material selection for the UAE construction industry. The hybrid MCDM method is comprised of the Decision Making Trial and Evaluation Laboratory method, the Analytic Network Process method and the Technique for Order Preference by Similarity to an Ideal Solution method to analyse and rank the best candidate material among the given alternatives for the desired application. Besides that, a new approach in the building material selection process involving economic, social and environmental aspects was also

applied using the Analytic Hierarchy Process (AHP) method by Cuadrado et al. (2016). The use of the AHP tool in the new Integrated Value Model for Sustainable Assessment method proposed in their study also included additional sustainability criteria such as employee safety, product functionality and corporate image. Furthermore, the Simple Additive Weighing and AHP methods were also applied for the material selection for dwelling house construction. Three main selection criteria were included in the analyses, which are cost, environmental impacts and qualitative aspects (such as project duration) (Medineckiene et al., 2010). Apart from that, a new model of decision making framework was also developed to assist decision makers in similar material selection process. Zavadskas et al. (2005) developed a web-based decision support system for construction material selection, which incorporated various selection criteria such as price, product geometry, availability, supplier information and delivery methods. Among the reported advantages of the decision support system is the integration of a search mode for information as well as a web-based selection tool.

The outcome of the material process also gave a direct impact to the end-of-life stage of the product. Various disposal options during the product's end-of-life stage will contribute to varying environmental performance such as emission type and amount generated, as well as the energy use during the disposal process (Dodoo et al., 2009; Silvestre et al., 2014). For example, the selection of wood as the construction material in the conceptual design stage will open for two disposal options for the wood-based product, which are either incinerated or land filled. In consequence, the disposal option made for the product, if the type of materials used are not carefully taken into consideration, will give effect to either positive or balanced greenhouse gas performance to the environment (Ortiz et al., 2009).

20.3 Design of natural fibre composites for shear strengthening of reinforced concrete beams

In general, reinforced concrete (RC) beams fail in flexure or shear. In order to take full advantage of the potential ductility of the RC members, it is desirable to ensure the flexural failure rather than shear since shear failure is sudden, brittle and catastrophic in nature, which occurs with no advance warning of distress. Thus shear strengthening of an RC beam is crucial to increase the shear capacity of the shear-deficient beams. There have been a series of studies in the past for the shear strengthening of RC beams using externally bonded carbon fibre reinforced polymer (CFRP) laminates (Alam et al., 2016; Alsayed and Siddiqui, 2013; Bae et al., 2013; Barros and Dias, 2006; Belarbi and Acun, 2013; Costa and Barros, 2010; Dias and Barros, 2011; Dong et al., 2013; Jumaat and Alam, 2009; Koutas and Triantafillou, 2013). However, CFRP laminates were found to be less effective for shear as compared to flexure in strengthening of RC structures. As per the ACI design guideline, the maximum CFRP strain of 0.004 could be used in the design for the shear strengthening of an RC beam, which is 30% of its ultimate capacity. However, the actual design strain

of CFRP laminate could be lower, as compared to 0.004, to avoid premature debonding failure based on the proposed guideline of ACI (2002).

It is noted that the effective strain of CFRP laminate is found to be 0.0013, which is almost 10% of the ultimate strain of CFRP laminate. Alam et al. (2016) also investigated that the design strain of CFRP laminate could be used around 0.0017, which is almost 14% of the ultimate capacity of CFRP laminate to prevent the debonding of laminate. Thus the strengthening of a reinforced concrete beam for shear using CFRP laminate would not be the economical choice. Hence low strength NFC materials such as kenaf fibre reinforced polymer (KFRP) laminate could be used for shear strengthening of reinforced concrete beams.

Kenaf fibre has been used in a composite plate for nonstructural applications over the last decade (Elsaid et al., 2011; Rassmann, 2010; Shibata et al., 2006; Bernard et al., 2011; Rassmann et al., 2011; Huda et al., 2008; Ghani et al., 2012). Most of the research works were found to be on the development of a biodegradable kenaf fibre composite plate with low strength. In general, the tensile strength of kenaf fibre composite plates was found to be lower as compared to CFRP laminate. However, the position and amount of fibres in the composite plate would have a significant effect to enhance the tensile strength of the laminate. Recently, development of NFC plates for potential application in shear strengthening of an RC structure has been carried out by Alam et al. (2015a,b, 2016). Thus a systematic guideline to design an RC beam for shear strengthening using a KFRP plate is vital. The subsequent sections in this chapter will mainly focus on the design parameters of a KFRP plate for shear strengthening of an RC beam based on Euro Code-2 (EC2, 2004).

20.4 Proposed design model for shear strengthening of reinforced beam using kenaf fibre reinforced polymer laminate

In general, an externally bonded shear strengthened beam failed due to the debonding of laminate with lower strain as compared to yield strength of shear reinforcement (Alam et al., 2016). However, because of lower stiffness, the debonding strain of KFRP laminate could be higher as compared to yield strain of shear reinforcement. Thus the dimension of KFRP laminate for shear strengthening of a reinforced concrete beam could be obtained through the new proposed guideline as shown in the following section.

20.4.1 Design strain of kenaf fibre reinforced polymer laminate

The debonding strain of an externally bonded plate could be obtained based on the proposed guideline of Alam et al. (2015a), as shown in Eq. (20.1):

$$\varepsilon_{\mathrm{KFRP,debonding}} = \frac{(d-d')w_{\mathrm{KFRP}}F_{\mathrm{bu}}}{A_{\mathrm{KFRP}}E_{\mathrm{KFRP}}} = \frac{F_{\mathrm{bu}}(d-d')}{t_{\mathrm{KFRP}}E_{\mathrm{KFRP}}} \tag{20.1}$$

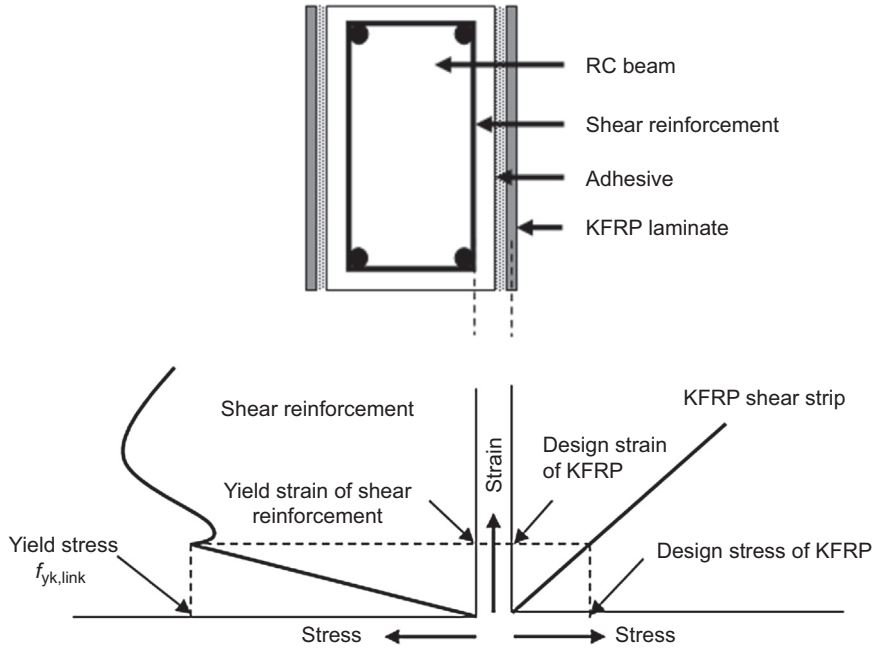

Figure 20.1 Strain compatibility between shear link and kenaf fibre reinforced polymer laminate.

The shear reinforcement of the beam will start to yield if the debonding strain of the externally bonded plate is higher than the yield strain of shear reinforcement. In that case the design strain of KFRP laminate would be the yield strain of shear reinforcement because of strain compatibility nature between shear reinforcement and KFRP laminate, as shown in Fig. 20.1. Thus the design strain of KFRP laminate would be Eq. (20.2):

$$\varepsilon_{\mathrm{KFRP,design}} = \varepsilon_{\mathrm{y,link}} = \frac{f_{\mathrm{y,link}}}{E_{\mathrm{s}}}; \quad \text{when } \varepsilon_{\mathrm{KFRP,debonding}} \geq \varepsilon_{\mathrm{y,link}} \tag{20.2}$$

20.4.2 Design shear force of kenaf fibre reinforced polymer laminate strengthened beam

The maximum flexural capacities of all beam specimens could be theoretically predicted using Eqs. (20.3)–(20.5), based on EC2 (2004):

$$M = \mathrm{Tz} = 0.87 A_{\mathrm{s}} f_{\mathrm{yk}} \left[d - \frac{0.45 A_{\mathrm{s}} f_{\mathrm{yk}}}{f_{\mathrm{ck}} b} \right] \tag{20.3}$$

where,

$$x = \frac{A_s f_{yk}}{0.567 f_{ck}(0.8)b} = \frac{A_s f_{yk}}{0.45 f_{ck} b} \tag{20.4}$$

$$z = d - 0.4x = \left[d - \frac{0.45 A_s f_{yk}}{f_{ck} b} \right] \tag{20.5}$$

Thus the maximum design shear force of the beam can be calculated using Eq. (20.6):

$$V_d = V = \frac{M}{\text{Shearspan}}; \quad \text{if } V_d > V, \text{the beam will fail by flexure} \tag{20.6}$$

if $V_d < V$,

Shear strengthening is not possible without the enhancement of the flexural capacity of the beam

20.4.3 Required dimension of kenaf fibre reinforced polymer laminate for shear strengthening of reinforced concrete beam

Shear force resisted by shear link is first calculated using Eq. (20.7) as:

$$V_{y,link} = 0.87 A_{s,link} f_{y,link} N \tag{20.7}$$

where N is the number of shear link that could be obtained using Eq. (20.8) (shown in Fig. 20.2

$$N = \frac{[d - d']\cot\theta}{s} \tag{20.8}$$

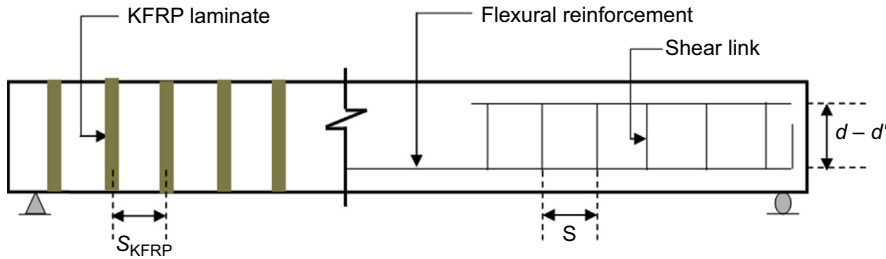

Figure 20.2 Details of a shear strengthened beam.

As per EC2 requirements, at the failure stage, concrete is ignored to resist the shear force. Only shear links resist the shear force. Thus the shear resisting capacity of the unstrengthened beam is calculated using Eq. (20.9). Eqs. (20.10) and (20.11):

$$V_{\mathrm{y,link}} = 0.87A_{\mathrm{s,link}}f_{\mathrm{y,link}}\left[\frac{(d-d')\cot\theta}{s}\right] \tag{20.9}$$

Shear force needs to be resisted by KFRP laminate,

$$V_{\mathrm{KFRP}} = V_d - V_{\mathrm{link}} \tag{20.10}$$

$$\text{Shear force resisted by KFRP strip} = 0.67A_{\mathrm{KFRP}}E_{\mathrm{KFRP}}\varepsilon_{\mathrm{KFRP,design}} \tag{20.11}$$

Assuming the safety factor of KFRP laminate is 1.5, which is similar with concrete. Further research is required to develop a safety factor of KFRP laminate using Eqs. (20.12)–(20.14):

$$\begin{aligned}&\text{Shear force resisted by two sided laminate}\\ &= 2(0.67)A_{\mathrm{KFRP}}E_{\mathrm{KFRP}}\varepsilon_{\mathrm{KFRP,design}} = \frac{1.34A_{\mathrm{KFRP}}E_{\mathrm{KFRP}}f_{\mathrm{y,link}}}{E_{\mathrm{s}}}\end{aligned} \tag{20.12}$$

$$V_{\mathrm{KFRP}} = V_d - V_{\mathrm{link}} = \frac{1.34A_{\mathrm{KFRP}}E_{\mathrm{KFRP}}f_{\mathrm{y,link}}}{E_s}N_{\mathrm{KFRP}} \tag{20.13}$$

where,

$$N_{\mathrm{KFRP}} = \frac{[d-d']\cot\theta}{s_{\mathrm{KFRP}}} \tag{20.14}$$

Thus the required cross-sectional area of a single KFRP shear strip can be calculated using Eq. (20.15):

$$A_{\mathrm{KFRP}} = \frac{E_{\mathrm{s}}s_{\mathrm{KFRP}}(V_d - V_{\mathrm{link}})}{1.34E_{\mathrm{KFRP}}f_{\mathrm{y,link}}(d-d')\cot\theta} \tag{20.15}$$

20.4.4 Theoretical model to predict the shear capacities of beam specimens

The shear capacities of control and KFRP laminate strengthened beams could be predicted using the proposed Eqs. (20.16) and (20.17), respectively:

$$V_{\mathrm{CB}} = A_{\mathrm{s,link}}f_{\mathrm{t,link}}\left[\frac{(d-d')\cot 45}{s}\right] \tag{20.16}$$

$$V_{SB,KFRP} = A_{s,link} f_{t,link} \left[\frac{(d-d')\cot 45}{s}\right] + 2A_{KFRP} E_{KFRP} \varepsilon_{KFRP,design} \left[\frac{(d-d')\cot 45}{s_{KFRP}}\right] \quad (20.17)$$

20.5 Design example: case study on shear strengthening of kenaf fibre composite reinforced concrete beam

20.5.1 Design descriptions

A 150 × 300 × 2300 mm full-scale reinforced concrete beam was fabricated with 2−16 mm flexural reinforcement and 6 mm shear reinforcement of 110 mm spacing. The beam was supported using a roller with the span of 2 m. It was tested for two-point load with the shear span of 650 mm. The properties of materials are shown in Table 20.1. The beams need to be strengthened for shear using KFRP laminate for its maximum capacities.

20.5.1.1 Flexural capacities of beams

Using Eq. (20.2), as stated in the previous section, the flexural capacities of beams is calculated as:

$$M = \mathrm{Tz} = 0.87 A_s f_{yk} z = (0.87)(402)(550)\left[261 - \frac{0.45(402)(550)}{(25.6)(150)}\right]$$

$$= 45.23 \text{ kN.m}$$

Total failure load,

$$P = 2V_d = \frac{2M}{L_s} = \frac{2(45.23)}{0.65} = 140 \text{ kN}$$

Table 20.1 Design parameters

Beam	Concrete strength	Shear link	Flexural reinforcement	KFRP laminate
$b = 150$ mm $h = 300$ mm $d = 261$ mm $d' = 39$ mm	$f_{cu} = 32$ MPa $f_{ck} = 25.6$ MPa $\beta = 0.28$	$f_{t,link} = 556$ MPa $s = 110$ mm $f_{y,link} = 520$ MPa $A_{s,link} = 47.5$ mm^2 $E_s = 200$ GPa	$f_{yk} = 550$ MPa $f_{tk} = 654$ MPa $A_s = 402$ mm^2	$t_{KFRP} = 6$ mm $E_{KFRP} = 11.4$ GPa $S_{KFRP} = 110$ mm

Design shear force,

$$V_d = \frac{140}{2} = 70 \text{ kN}$$

20.5.1.2 Design strain of kenaf fibre reinforced polymer laminate

The design strain is first calculated by determining the yield strain of the shear reinforcement and the debonding strain of the KFRP laminate:

Yield strain of shear reinforcement,

$$\varepsilon_{\text{y,link}} = \frac{f_{\text{y,link}}}{E_{\text{s}}} = \frac{520}{200000} = 0.0026$$

Debonding strain of KFRP laminate,

$$\varepsilon_{\text{KFRP,debonding}} = \frac{F_{\text{bu}}(d - d')}{t_{\text{KFRP}} E_{\text{KFRP}}} = \frac{1.58(261 - 39)}{(6)(11400)} = 0.00512 > \varepsilon_{\text{y,link}}$$

Finally, the design strain of KFRP laminate is calculated as the following:

$$\varepsilon_{\text{KFRP(design)}} = \varepsilon_{\text{y,link}} = 0.0026$$

20.5.1.3 Required cross sectional area of kenaf fibre reinforced polymer laminate for shear strengthening of reinforced concrete beam

As per the proposed guideline, the cross-sectional area of CFRP laminate can be calculated based on Eq. (20.12) stated in the previous section. For conservative design, the shear crack inclination of the beam could be considered as 45°.

$$V_{\text{y,link(45)}} = 0.87 A_{\text{s,link}} f_{\text{y,link}} \left[\frac{(d - d')\cot 45}{\text{s}}\right]$$

$$= 0.87(47.5)(520)\left[\frac{(261 - 39)\cot 45}{110}\right]$$

$$= 43360 \text{ N}$$

$$= 43.36 \text{ kN}$$

$$A_{\mathrm{KFRP}} = \frac{E_{\mathrm{s}} s_{\mathrm{KFRP}} (V_d - V_{\mathrm{link}})}{1.34 E_{\mathrm{KFRP}} f_{\mathrm{y,link}} (d - d') \cot\theta} = \frac{(200000)(110)(70000 - 43360)}{1.34(11000)(520)(261 - 39)\cot 45}$$

$$= 345 \ \mathrm{mm}^2$$

$$= 6\ \mathrm{mm} \times 57\ \mathrm{mm} \approx 6\ \mathrm{mm} \times 60\ \mathrm{mm}$$

Thus from the earlier results of the analysis, the provided KFRP laminate was 6 mm × 60 mm × 300 mm with 110 mm spacing for shear strengthening of the beam.

20.5.1.4 Theoretical shear capacity of kenaf fibre reinforced polymer laminate strengthened beam

The theoretical shear capacity of the KFRP laminate for strengthened beam is calculated as:

$$V_{\mathrm{t,link}} = A_{\mathrm{s,link}} f_{\mathrm{t,link}} \left[\frac{(d - d')\cot 45}{\mathrm{s}}\right] = (47.5)(556)\left[\frac{(261 - 39)\cot 45}{110}\right]$$

$$= 53.3\ \mathrm{kN}$$

$$V_{\mathrm{KFRP}} = 2A_{\mathrm{KFRP}} E_{\mathrm{KFRP}} \varepsilon_{\mathrm{KFRP,design}} \left[\frac{(d - d')\cot 45}{s_{\mathrm{KFRP}}}\right]$$

$$= 2(300)(11400)(0.0026)\left[\frac{(261 - 39)\cot 45}{110}\right] = 35.89\ \mathrm{kN}$$

Hence the total shear force of the KFRP laminate shear strengthened beam is calculated as:

$$V_{\mathrm{SB}} = V_{\mathrm{y,link}} + V_{\mathrm{KFRP}} = 53.3 + 35.89 = 89.2\ \mathrm{kN}$$

while the shear failure load is 178.4 kN.

20.6 Conclusion

This chapter has revealed the design practices of NFCs towards achieving sustainable construction performance. It can be observed that the use of NFC can highly contribute to improve the sustainability of building and construction materials through its renewable, recyclable and biodegradable properties as compared to conventional materials for similar applications. The use of NFCs in structural building applications can be made feasible through a systematic design process, which encompassed areas of materials selection and design development. In addition, the proposed shear strengthening

design model of an RC beam using an NFC model, as explained in this chapter, showcased a systematic design guideline for designers to apply it for future applications. Moreover, the practicability of the design model using KFRP laminate in the case study also provided a hands-on guideline for easy understanding to practitioners. Finally, the use of the proposed design model can also be expanded for various types of natural fibres to help designers explore the potential of other sources of reinforcement materials, such as agricultural waste materials, which could bring greater benefits for similar applications.

Nomenclature

$\varepsilon_{KFRP,debonding}$	Debonding strain of KFRP laminate
d	Effective depth of beam
d'	Depth of compression reinforcement (top bar)
w_{KFRP}	Width of KFRP shear strip
F_{bu}	Bond strength of concrete
t_{KFRP}	Thickness of KFRP laminate
A_{KFRP}	Cross-sectional area of KFRP laminate
E_{KFRP}	Modulus of elasticity of KFRP laminate
$\varepsilon_{KFRP,design}$	Design strain of KFRP laminate
$\varepsilon_{y,link}$	Yield strain of shear reinforcement
$f_{y,link}$	Yield strength of shear reinforcement
E_s	Modulus of elasticity of steel bar
M	Moment resisting capacity of beam
T	Tensile force of flexural reinforcement
Z	Moment arm
A_s	Cross-sectional area of flexural reinforcement
f_{tk}	Tensile strength of flexural reinforcement
f_{yk}	Yield strength of flexural reinforcement
f_{ck}	Concrete compressive strength based on cylinder test
b	Width of beam
x	Depth of neutral axis
V_d	Design shear force
L_s	Shear span
N	Number of shear links that resist shear
θ	Inclination of shear crack
s	Spacing of shear link
$V_{y,link}$	Shear force of beam due to yielding of shear reinforcement
$A_{s,link}$	Cross-sectional area of shear link
V_{KFRP}	Shear force resisted by KFRP laminate
N_{KFRP}	Number of KFRP laminate to resist shear (from one side of beam)
s_{KFRP}	Spacing of KFRP laminate
V_{CB}	Shear capacity of control beam
V_{SB}	Shear capacity of KFRP laminate strengthened beam
$f_{t,link}$	Tensile strength of shear reinforcement
$V_{SB,KFRP}$	Shear capacity of KFRP laminate strengthened beam

References

ACI Committee 440, 2002. Guide for the Design and Construction of Externally Bonded FRP Systems for Strengthening Concrete Structures. ACI 440 (2R-02).

Akadiri, P.O., 2015. Understanding barriers affecting the selection of sustainable materials in building projects. Journal of Building Engineering 4, 86−93.

Akadiri, P.O., Olomolaiye, P.O., 2012. Development of sustainable assessment criteria for building materials selection. Engineering Construction Architecture Management 19 (6), 666−687.

Alam, M.A., Hassan, A., Muda, Z.C., 2015a. Development of kenaf fibre reinforced polymer laminate for shear strengthening of reinforced concrete beam. Materials and Structures 49 (3), 795−811.

Alam, M.A., Alriyami, K., Jumaat, M.Z., Zakaria, C.M., 2015b. Development of high strength natural fibre based composite plates for potential application in retrofitting of RC structure. Indian Journal of Science and Technology 8 (15), 1−7.

Alam, M.A., Alriyami, K., Muda, Z.C., Jumaat, M.Z., 2016. Hybrid kenaf fibre composite plates for potential application in shear strengthening of reinforced concrete structure. Indian Journal of Science and Technology 9 (6), 1−7.

Alsayed, S.H., Siddiqui, N.A., 2013. Reliability of shear-deficient RC beams strengthened with CFRP-strips. Construction and Building Materials 42, 238−247.

Alwan, Z., Jones, P., Holgate, P., 2016. Strategic sustainable development in the UK construction industry, through the framework for strategic sustainable development, using building information modelling. Journal of Cleaner Production. http://dx.doi.org/10.1016/j.jclepro.2015.12.085 (in press).

Aprianti, E., Shafigh, P., Bahri, S., Farahani, J.N., 2015. Supplementary cementitious materials origin from agricultural wastes − a review. Construction and Building Materials 74, 176−187.

Ardente, F., Beccali, M., Cellura, M., Mistretta, M., 2008. Building energy performance: a LCA case study of kenaf-fibres insulation board. Energy and Buildings 40 (1), 1−10.

Bae, S.W., Murphy, M., Mirmiran, A., Belarbi, A., 2013. Behavior of RC T-beams strengthened in shear with CFRP under cyclic loading. Journal of Bridge Engineering 18 (2), 99−109.

Barros, J.A.O., Dias, S.J.E., 2006. Near surface mounted CFRP laminates for shear strengthening of concrete beams. Cement and Concrete Composites 28 (3), 276−292.

Belarbi, A., Acun, B., 2013. FRP systems in shear strengthening of reinforced concrete structures. Procedia Engineering 57, 2−8.

Bernard, M., Khalina, A., Ali, A., 2011. The effect of processing parameters on the mechanical properties of kenaf fibre plastic composite. Materials and Design 32, 1039−1043.

Binici, H., Eken, M., Dolaz, M., Aksogan, O., Kara, M., 2014. An environmentally friendly thermal insulation material from sunflower stalk, textile waste and stubble fibres. Construction and Building Materials 51, 24−33.

Binici, H., Aksogan, O., Shah, T., 2005. Investigation of fibre reinforced mud brick as a building material. Construction and Building Materials 19 (4), 313−318.

Burgueño, R., Quagliata, M.J., Mohanty, A.K., Mehta, G., Drzal, L.T., Misra, M., 2004. Load-bearing natural fiber composite cellular beams and panels. Composites Part A: Applied Science and Manufacturing 35 (6), 645−656.

Burgueno, R., Quagliata, M.J., Mehta, G.M., Mohanty, A.K., Misra, M., Drzal, L.T., 2005. Sustainable cellular biocomposites from natural fibers and unsaturated polyester resin for housing panel applications. Journal of Polymers and the Environment 13 (2), 139−149.

Castro-Lacouture, D., Sefair, J.A., Flórez, L., Medaglia, A.L., 2009. Optimization model for the selection of materials using a LEED-based green building rating system in Colombia. Building and Environment 44 (6), 1162−1170.

Costa, I.G., Barros, J.A.O., 2010. Flexural and shear strengthening of RC beams with composite materials − the influence of cutting steel stirrups to install CFRP strips. Cement and Concrete Composites 32 (7), 544−553.

Cuadrado, J., Zubizarreta, M., Rojí, E., Larrauri, M., Álvarez, I., 2016. Sustainability assessment methodology for industrial buildings: three case studies. Civil Engineering and Environmental Systems 33 (2), 1−19.

Dias, S.J.E., Barros, J.A.O., 2011. Shear strengthening of RC T-section beams with low strength concrete using NSM CFRP laminates. Cement and Concrete Composites 33 (2), 334−345.

Dittenber, D.B., GangaRao, H.V., 2012. Critical review of recent publications on use of natural composites in infrastructure. Composites Part A: Applied Science and Manufacturing 43 (8), 1419−1429.

Dodoo, A., Gustavsson, L., Sathre, R., 2009. Carbon implications of end-of-life management of building materials. Resources, Conservation and Recycling 53 (5), 276−286.

Dong, J., Wang, Q., Guan, Z., 2013. Structural behaviour of RC beams with external flexural and flexural−shear strengthening by FRP sheets. Composites Part B: Engineering 44 (1), 604−612.

EC2, 2004. General Rules and Rules for Building Eurocode 2: Design of Concrete Structures Part 1−1 1992-1-1.

Elsaid, A., Dawood, M., Seracino, R., Bobko, C., 2011. Mechanical properties of kenaf fiber reinforced concrete. Construction and Building Materials 25 (4), 1991−2001.

Franzoni, E., 2011. Materials selection for green buildings: which tools for engineers and architects? Procedia Engineering 21, 883−890.

Ghani, M.A.A., Salleh, Z., Hyie, K.M., 2012. Mechanical properties of kenaf/fiberglass polyester hybrid composite. Procedia Engineering 41, 1654−1659.

González, M.J., Navarro, J.G., 2006. Assessment of the decrease of CO_2 emissions in the construction field through the selection of materials: practical case study of three houses of low environmental impact. Building and Environment 41 (7), 902−909.

Govindan, K., Shankar, K.M., Kannan, D., 2016. Sustainable material selection for construction industry−a hybrid multi criteria decision making approach. Renewable and Sustainable Energy Reviews 55 (0), 1274−1288.

Gurgun, A.P., Komurlu, R., Arditi, D., 2015. Review of the LEED category in materials and resources for developing countries. Procedia Engineering 118, 1145−1152.

Hong, J., Shen, G.Q., Guo, S., Xue, F., Zheng, W., 2016. Energy use embodied in China's construction industry: a multi-regional input−output analysis. Renewable and Sustainable Energy Reviews 53, 1303−1312.

Huda, M.S., Drzal, L.T., Mohanty, A.K., Misra, M., 2008. Effect of fiber surface-treatments on the properties of laminated biocomposites from poly(lactic acid) (PLA) and kenaf fibers. Composites Science and Technology 68 (2), 424−432.

Jalaei, F., Jrade, A., 2015. Integrating building information modeling (BIM) and LEED system at the conceptual design stage of sustainable buildings. Sustainable Cities and Society 18 (0), 95−107.

Jumaat, M.Z., Alam, M.A., 2009. Effects of intermediate anchors on end anchored CFRP laminate flexurally strengthened reinforced concrete beams. Journal of Applied Sciences 9 (1), 142−148.

Khedari, J., Nankongnab, N., Hirunlabh, J., Teekasap, S., 2004. New low-cost insulation particleboards from mixture of durian peel and coconut coir. Building and Environment 39 (1), 59−65.

Khedari, J., Watsanasathaporn, P., Hirunlabh, J., 2005. Development of fibre-based soil−cement block with low thermal conductivity. Cement and Concrete Composites 27 (1), 111−116.

Kibert, C.J., 2008. Sustainable Construction: Green Building Design and Delivery, second ed. John Wiley & Sons, New Jersey.

Koutas, L., Triantafillou, T.C., 2013. Use of anchors in shear strengthening of reinforced concrete T-beams with FRP. Journal of Composites for Construction 17 (1), 101−107.

LafargeHolcim, 2016. Understanding Sustainable Construction. Retrieved on February 17, 2016 from: https://www.lafargeholcim-foundation.org/AboutPages/what-is-sustainable-construction.

Li, H., Xian, G., 2012. Mechanical property enhancement of flax fibre-based green composites for civil structural application. International Journal of Sustainable Materials and Structural Systems 1 (1), 95−103.

Mansour, A., Srebric, J., Burley, B.J., 2007. Development of straw-cement composite sustainable building material for low-cost housing in Egypt. Journal of Applied Sciences Research 3 (11), 1571−1580.

Medineckiene, M., Turskis, Z., Zavadskas, E.K., 2010. Sustainable construction taking into account the building impact on the environment. Journal of Environmental Engineering and Landscape Management 18 (2), 118−127.

Mo, K.H., Alengaram, U.J., Jumaat, M.Z., Yap, S.P., Lee, S.C., 2016. Green concrete partially comprised of farming waste residues: a review. Journal of Cleaner Production 117, 122−138.

Onuaguluchi, O., Banthia, N., 2016. Plant-based natural fibre reinforced cement composites: a review. Cement and Concrete Composites 68, 96−108.

Ortiz, O., Castells, F., Sonnemann, G., 2009. Sustainability in the construction industry: a review of recent developments based on LCA. Construction and Building Materials 23 (1), 28−39.

Du Plessis, C., 2007. A strategic framework for sustainable construction in developing countries. Construction Management and Economics 25 (1), 67−76.

Pacheco-Torgal, F., Jalali, S., 2011. Cementitious building materials reinforced with vegetable fibres: a review. Construction and Building Materials 25 (2), 575−581.

Pugh, S., 1991. Total Design: Integrated Methods for Successful Product Engineering, Wokingham. Addison-Wesley Publishing, England.

Rassmann, S., Paskaramoorthy, R., Reid, R.G., 2011. Effect of resin system on the mechanical properties and water absorption of kenaf fibre reinforced laminates. Materials and Design 32, 1399−1406.

Rassmann, S., Reid, R.G., Paskaramoorthy, R., 2010. Effects of processing conditions on the mechanical and water absorption properties of resin transfer moulded kenaf fibre reinforced polyester composite laminates. Composites Part A: Applied Science and Manufacturing 41 (11), 1612−1619.

Shibata, S., Cao, Y., Fukumoto, I., 2006. Lightweight laminate composites made from kenaf and polypropylene fibres. Polymer Testing 25 (2), 142−148.

Senaratne, S., Gerace, D., Mirza, O., Tam, V.W., Kang, W.H., 2016. The costs and benefits of combining recycled aggregate with steel fibres as a sustainable, structural material. Journal of Cleaner Production 112 (4), 2318−2327.

Silvestre, J.D., de Brito, J., Pinheiro, M.D., 2014. Environmental impacts and benefits of the end-of-life of building materials−calculation rules, results and contribution to a "cradle to cradle" life cycle. Journal of Cleaner Production 66, 37−45.

Wu, W., Issa, R.R., 2010. Application of VDC in LEED projects: framework and implementation strategy. In: Proc. CIB W-78 27th International Conference on IT in Construction, 15−19 November 2010. Cairo, Egypt.

Yahya, K., Boussabaine, H., Alzaed, A., 2016. Using life cycle assessment for estimating environmental impacts and eco-costs from the metal waste in the construction industry. Management of Environmental Quality: An International Journal 27 (2), 227−244.

Yan, L., Kasal, B., Huang, L., 2016. A review of recent research on the use of cellulosic fibres, their fibre fabric reinforced cementitious, geo-polymer and polymer composites in civil engineering. Composites Part B: Engineering 92, 94−132.

Zavadskas, E.K., Kaklauskas, A., Banaitis, A., Trinkūnas, V., 2005. System for real time support in construction materials selection. International Journal of Strategic Property Management 9 (2), 99−109.

Sustainability and life assessment of high strength natural fibre composites in construction

21

C. Cao
Green Crane Consulting, Watford, Hertfordshire, United Kingdom

21.1 Introduction

Sustainability and sustainable development are developed from concerns to our economic obligations, providing products and services to sustain the growth of communities and businesses, which are at a speed to undermine the earth's capacity to meet the need for resources, absorb waste and support the incredibly diverse life that it does – including people. Providing society all the benefits that economic growth can offer is undermining the ecosystem integrity, social fabric and health of all. Therefore sustainability is about maintaining our environmental resources with the quality of life over time. It also refers to being tolerant and overcoming the deprivation of natural environmental services and the reduced productivity due to man's interaction with the planet. Hence resilience is a fundamental element to sustainability.

People from different disciplines, for example, environmental science and advocacy, land and economic development, health, safety and social justice, began to use the concept to tackle the interdependence between these issue areas and apply it to the wide range of development activities: industry, construction, planning, transportation, agriculture and resource management.

Therefore what is sustainable material? The following questions can help assess the sustainability of any material:

- What is its function in its whole life cycle?
- Does it meet the optimal performance requirement for its application?
- How widely is it available?
- Do they regenerate and how quickly?
- What is the process to make it into a usable form and what are the environmental impacts of the process?
- How much energy and water does it take for its production?
- How much waste material does it generate?
- What does it need to operate (maintenance inputs, operating energy)?
- Are the people involved in producing, delivering and installing it fairly compensated and are they provided with safe and healthy working conditions?
- How long will it last and what will happen at the end of its service life?

When selecting materials, it is very likely that the information to these questions is not available. Even if all the answers can be obtained, it is hard to make judgements, as

Advanced High Strength Natural Fibre Composites in Construction. http://dx.doi.org/10.1016/B978-0-08-100411-1.00021-2

the trade-offs vary between materials that excel in different areas and within a particular material category and corporate practices. Additionally, new technologies and innovations change the answer over time. An assessment technology is needed to help people quantify the answers.

Life cycle assessment (LCA) is a technology to assess the environmental aspects and potential impacts associated with a product, process or service, by:

- compiling an inventory of relevant energy and material inputs and environmental releases;
- evaluating the potential environmental impacts associated with identified inputs and releases; and
- interpreting the results to help you make a more informed decision.

In order to carry out an LCA analysis of high strength natural fibre composites, four basic stages of conducting an LCA, as for any other products, services and systems, may be followed:

- goal and scope definition
- inventory analysis
- impact assessment
- interpretation

The high strength natural fibre composite industry encompasses a range of products and processes. High strength natural fibre composites are made from natural plants, primarily heated and combined with bonding agents under pressure. The basic components are water, natural fibres and bonding agents. Natural fibres are grown, usually quite close to their point of use. The high strength natural fibre composites may be formed in factories into a wide range of structures and structural components, including houses, floors and walls. High strength natural fibre composites contribute to sustainable development on two levels: as an industry and as a widely used component of built environments.

21.2 A brief history of sustainability and life cycle assessment for construction products

The first well-known environmental study was conducted in 1969 by Coca-Cola (Table 21.1). The study focused on beverage containers and showed that all container materials had a real environmental impact and some materials had a greater impact than others. In response to this discovery, Coca-Cola acted not by removing the worst-performing materials from their products but by working with local authorities to develop a take-back scheme and a recycling infrastructure to collect aluminium cans. In doing so, the company realized a 90% reduction in the energy used throughout the can's lifetime.

Since then, embodied impact studies have evolved from a focus on reducing manufacturing waste and packaging, and after the first oil crisis in 1973, the LCA studies shifted to concentrate on energy and then on the recognition of a broad range of impacts throughout the life of a product from its manufacture through use to disposal.

Table 21.1 Timeline of life cycle assessment event

Year	Event
1969	First study for Coca Cola in US
1973	First Oil Crisis-OPEC oil embargo
1975	LCA type studies shift to concentrate on energy
1988	WMP and UNEP established International Panel on Climate Change
1990	First BGaBi Software launched
1990	First BREEAM Schemes launched
1997	Kyoto Protocol
1997	ISO 14040: LCA: Principles and Framework
1998	Green Guide to Specification 2nd Edition published and linked credits in BREEAM
1998	ISO 14041: LCA: Goal and Scope
1999	BRE Environmental Profiles Methodology and Generic Environmental Profiles published
1999	Envest Building LCA tool launched
2000	ISO 14042: LCA: Impact Assessment
2000	ISO 14043: LCA: Interpretation
2001	ISO 14020: Labels General Principles
2004	CEN/TC 350 Standardisation Mandate issued
2004	NEN 8006: Dutch PCR for construction products
2004	NF P-01-010: French PCR for construction products
2006	ISO 14025: Labels: Type 3 EPDs
2006	ISO 14040: LCA Principles and Framework updated
2006	ISO 14044: LCA: Requirements and Guidelines updated
2006	IBU PCR for construction products in Germany
2007	ISO 21930: EPDs for Construction Products
2007	UKGBC launched
2008	PAS 2050: Assessment of Greenhouse Gas emissions of goods and services
2009	LCADesign LCA tool launched in Australia
2010	CEN TR 15941: Generic Data
2010	EN 15643-1: General Framework
2010	BPIC PCR Methodology launched in Australia
2010	RICS Ska tool for Fit Out launched
2011	EN 15643-2: Environmental Framework
2011	EN 15878: Building level Calculation methods
2011	EN 15942: EPD B2B Communication Formats
2011	Construction Products Regulations
2011	PAS 2050 updated
2012	EN 15643-3: Social Framework
2012	EN 15643-4: Economic Framework
2012	EN 15804 Core Rules for the Product Category Construction products
2013	Release of IMPACT specification by BRE

Key environmental events
European and International Standards
Construction product focus
Building level focus

After 'The embodied impacts of construction products'

During the 1970s and 1980s, many approaches to reducing environmental harm included the regulatory control of point-source waste releases. Because these approaches were based on a single stage of a product's life, such as production, or a single issue, such as wastewater, they were not particularly effective in achieving net environmental benefits. What they did achieve was a change in the way people thought about business and environmental management.

In 1979, the Society of Environmental Toxicology and Chemistry (SETAC) was founded to serve as a nonprofit professional society to promote multidisciplinary approaches to the study of environmental issues. SETAC's other founding principles include multidisciplinary approaches to solving environmental problems; tripartite balance among academia, business and government; and science-based objectivity.

Hence in the late 1980s, LCA emerged as a tool to better understand the risks, opportunities and trade-offs of product systems as well as the nature of environmental impacts. PE International's GaBi software, released in 1989, was one of the first commercial software tools that emerged and has since evolved into the market-leading LCA tool and database.

At 1988, World Missionary Press and United Nations Environment Programme (UNEP) have established the International Panel on Climate Change. The establishment of this panel has improved the awareness of environment issues, and it also leads to various researches to solve environmental issues.

At the first SETAC-sponsored international workshop in 1990, the term 'life cycle assessment' (LCA) was coined. The advantage of LCA over point-source regulations is that it avoids shifting a product's environmental burden to other life cycle stages or to other parts of the product system.

To tackle environmental issues in a built environment, the Building Research Establishment (BRE) launched the world's very first environment assessment method (BREEAM) for buildings in 1990. This method is a holist environmental assessment method, assessing nine categories of environmental issues, including materials. In 1996, BRE released the first edition of the *Green Guide* series, aimed to provide a simple 'green guide' to the environmental impacts of building materials, which was easy to use and soundly based on numerical data. In 1998, the *Green Guide to Specification 2nd Edition* published, and it was linked with credits in BREEAM.

Beginning in 1993, the International Organization for Standardization (ISO) tasked a small group of SETAC LCA experts with making a recommendation regarding the need to standardize LCA. The recommendation from the group was to proceed with standardization, and by 1997 the ISO14040 standard for life cycle assessment − principles and framework was completed. A number of additional standards were developed and ultimately reviewed and compiled in 2006 in the form of ISO 14044 life cycle assessment − requirements and guidelines.

In 2002, the UNEP, SETAC and partners from the government, academia, civil society, business and industry joined forces to promote life cycle approaches worldwide.

A number of LCA-based guidelines and standards have subsequently been developed, including the PAS 2050:2011 specification for the assessment of the life cycle greenhouse gas emissions of goods and services issued by the World Resource Institute and World Business Council for Sustainable Development. In 2012, the Institute

for Environment and Sustainability of the European Commission Joint Research Centre released the International Reference Life Cycle Data System Handbook as part of the European life cycle push and further specified the broader provisions of the ISO 14040 and 14044 standards. During 2011 and 2012, a series of ISO/EN standards have been released, including EN 15643-1 about General Framework, EN 15643-2 about Environmental Framework, EN 15878 about Building Level Calculation Methods and EN 15804 about Core Rules for the Product Category Construction products. PAS 2050 was updated in 2011.

According to Jim Fava, one of the fathers of LCA, 'life cycle assessment has become a recognized instrument to assess the ecological burdens and human health impacts connected with the complete life cycle of products, processes and activities, enabling the practitioner to model the entire system from which products are derived or in which processes and activities operate'.

LCA continues to expand and is now being heavily integrated into green building schemes around the world. BREEAM was the first environmental assessment method to link assessment credits to materials. Especially, in 2013, BRE released IMPACT, the specification and database for software developers to incorporate their tools to enable consistent LCA for buildings. IMPACT compliant tools work by allowing users to attribute environmental impacts to draw or schedule items in the Building Information modelling (BIM) 3-D models, in other words, the IMPACT takes quantity information from the BIM 3-D models and multiplies this by environmental impact to produce an overall impact for the whole (or a selected part) of a building design. The results generated by IMPACT allow the user to analyze the design to environmental impacts and compare whole-building results to a suitable benchmark to assess performance, which can be linked to building assessment schemes, for example, BREEAM.

21.3 The environmental impacts measured in life cycle assessment

LCA is a 'cradle-to-grave' approach for assessing industrial systems and products. This approach begins with the gathering of raw materials from the earth to create the product and ends at the point when all materials are returned to the earth (Life Cycle Assessment (LCA) Overview), or it measures the environmental impacts from the extraction of raw materials through processing, manufacture and refurbishment to the eventual end of life and disposal.

The assessed environmental impacts can change, and their importance can increase or decrease over time as the concerns and priorities of society change. In the 1960s/1970s, the biggest environmental concern in Europe was acid rain caused by the sulphur emissions from power stations; this was followed in the 1980s by concerns over CFCs from aerosols and other sources, which were associated with the depletion of the protective ozone layer in the upper atmosphere. Today, in the early 21st century, the concern is about climate change believed to be caused by increasing carbon

emissions caused by human activity. The environmental impacts most commonly considered in an LCA of a construction product are listed here:

- climate change
- acidification
- eutrophication
- stratospheric ozone depletion
- photochemical ozone creation

Other indicators commonly provided in an LCA include:

- renewable and nonrenewable primary energy
- water consumption
- waste for disposal
- toxicity to ecosystems and humans
- resource depletion (covering various minerals and scarce chemical elements)
- radioactivity

21.4 Life cycle assessment

Two types of LCA, namely generic and manufacturer-specific or proprietary LCA, can be evaluated in LCA studies, resulting in two types of data. Generic LCAs are comprised of data gathered from several manufacturers of the same product, which very often is collected by trade associations. As a means of verification the data are compared to each other or to existing datasets. The datasets are combined to create an industry average, ie, a generic LCA for that product. Proprietary LCAs are made up of data provided by a company, and the LCA is specific to that product. The LCA data can be combined to create LCAs not only for building products, but also for building components, systems and the whole building.

21.4.1 The life cycle of a construction product in life cycle assessment

The scope of different LCA studies can vary, but the manufacture of the construction product will always be included (cradle-to-gate). Cradle-to-grave is the full life cycle assessment from resource extraction (‘cradle’) to the use phase and disposal phase (‘grave’). Cradle-to-gate is an assessment of a *partial* product life cycle from resource extraction (*cradle*) to the factory gate (ie, before it is transported to the consumer). Cradle-to-gate assessments are sometimes the basis for environmental product declarations (EPD) termed business-to-business EDPs. Cradle-to-cradle is a specific kind of cradle-to-grave assessment, where the end-of-life disposal step for the product is a recycling process. It is a method used to minimize the environmental impact of products by employing sustainable production, operation and disposal practices, and it aims to incorporate social responsibility into product development (Cradle-to-cradle definition, 2010). Gate-to-gate is a partial LCA method, looking at only one

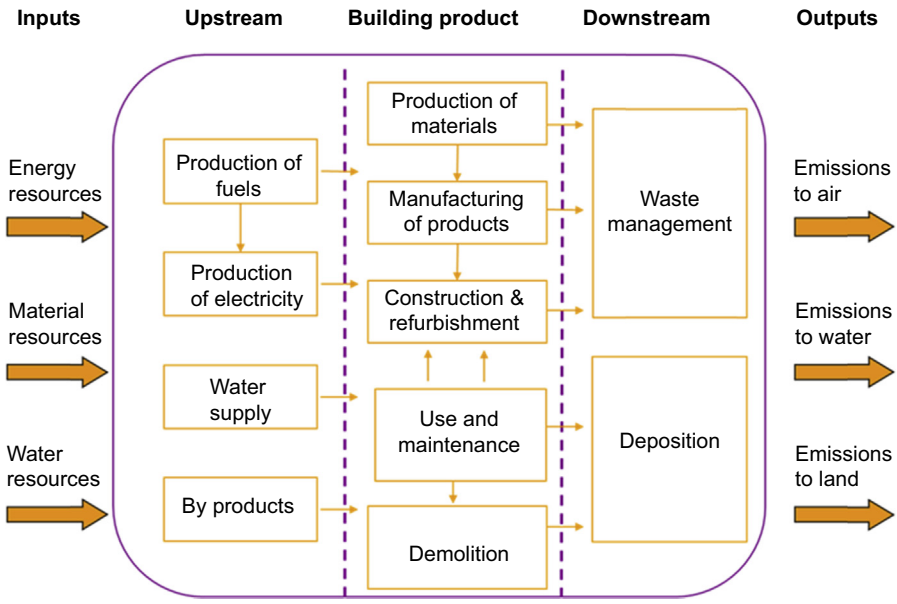

Figure 21.1 Illustration of the life cycle of a product (BRE internal report prepared for TSB NATCOM project by Brunel University, 2011).

value-added process in the entire production chain. Gate-to-gate modules may also later be linked in their appropriate production chain to form a complete cradle-to-gate evaluation (Jiménez-González et al., 2000).

Construction products, because of their use in a wide range of raw materials and the very different forms of processing used to produce final products and the different ways that they are used, can be responsible for many environmental impacts at different stages in the life cycle, as in Fig. 21.1. For example:

Production of materials: for materials such as aggregates, raw material extraction will be one of the principal impacts, but for more highly processed materials the production impacts are likely to dominate.

Manufacturing of products: the impact of manufacturing can be the major environmental impact, especially if large amounts of energy are required in the production of metals or cement.

Construction and refurbishment: during construction and refurbishment, energy and water are used. The IGT (BIS, 2010) Final Report states that 10−15% of materials sent to a building site end up as waste; the impacts of producing these materials, that are then wasted, are a considerable impact associated with the construction and refurbishment.

Use and maintenance: these activities are estimated to be 45% of contractor output (ie, annual turnover), so a significant proportion of extraction and manufacturing impacts are likely to occur for materials used during maintenance.

Demolition: some products are unable to be reused or recycled and therefore end up as waste in landfills. The emphasis is now beginning to turn to consider the end-of-life

issues at the very start of the manufacture of a product so that it can be deconstructed and reused or recycled easily at the end of life.

21.4.2 Stages of the life cycle assessment (LCA)

According to the ISO 14040 (2006) and ISO 14044 (2006) standards, a life cycle assessment is carried out in four distinct phases, as illustrated in Fig. 21.2. The phases are often interdependent in that the results of one phase will inform how other phases are completed.

21.4.2.1 Goal and scope

An LCA starts with an explicit statement of the goal and scope of the study, which sets out the context of the study and explains how and to whom the results are to be communicated. This is a key step, and the ISO standards require that the goal and scope of an LCA be clearly defined and consistent with the intended application. The goal and scope document therefore includes technical details that guide subsequent work:

- the functional unit, which defines what precisely is being studied and quantifies the service delivered by the product system, providing a reference to which the inputs and outputs can be related. Further, the functional unit is an important basis that enables alternative goods, or services, to be compared and analyzed (Rebitzer et al., 2004);
- any assumptions and limitations;
- the allocation methods used to partition the environmental load of a process when several products or functions share the same process; and
- the impact categories chosen.

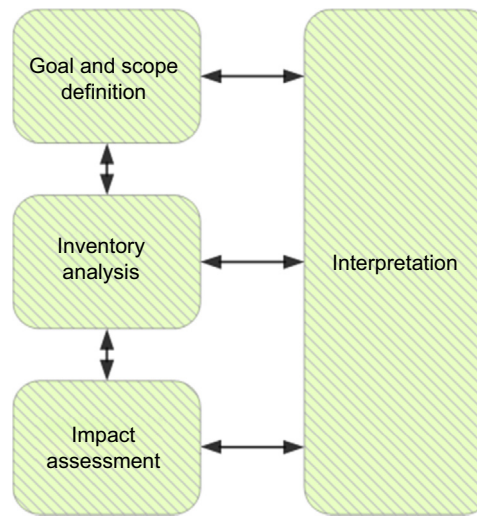

Figure 21.2 Illustration of life cycle assessment phases.
From the web.

21.4.2.2 Life cycle inventory

Life cycle inventory (LCI) analysis involves creating an inventory of flows from and to nature for a product system. Inventory flows include inputs of water, energy and raw materials, and releases to air, land and water. To develop the inventory, a flow model of the technical system is constructed using data on inputs and outputs. The flow model is typically illustrated with a flow chart that includes the activities that are going to be assessed in the relevant supply chain and gives a clear picture of the technical system boundaries. The input and output data needed for the construction of the model are collected for all activities within the system boundary, including from the supply chain (referred to as inputs from the technosphere).

The data must be related to the functional unit defined in the goal and scope definition. Data can be presented in tables, and some interpretations can be made already at this stage. The results of the inventory is an LCI that provides information about all inputs and outputs in the form of elementary flow to and from the environment from all the unit processes involved in the study.

21.4.2.3 Life cycle impact assessment

Inventory analysis is followed by impact assessment. This phase of LCA is aimed at evaluating the significance of potential environmental impacts based on the LCI flow results. Classical life cycle impact assessment (LCIA) consists of the following mandatory elements:

- selection of impact categories, category indicators and characterization models;
- the classification stage, where the inventory parameters are sorted and assigned to specific impact categories; and
- impact measurement, where the categorized LCI flows are characterized, using one of many possible LCIA methodologies, into common equivalence units that are then summed to provide an overall impact category total.

In many LCAs, characterization concludes the LCIA analysis; this is also the last compulsory stage according to ISO 14044:2006. However, in addition to the earlier mandatory LCIA steps, other optional LCIA elements – normalization, grouping and weighting – may be conducted depending on the goal and scope of the LCA study. In normalization, the results of the impact categories from the study are usually compared with the total impacts in the region of interest.

21.4.2.4 Interpretation

Life cycle interpretation is a systematic technique to identify, quantify, check and evaluate information from the results of the life cycle inventory and/or the life cycle impact assessment. The results from the inventory analysis and impact assessment are summarized during the interpretation phase. The outcome of the interpretation phase is a set of

conclusions and recommendations for the study. According to ISO 14040:2006, the interpretation should include:

- identification of significant issues based on the results of the LCI and LCIA phases of an LCA;
- evaluation of the study, considering completeness, sensitivity and consistency checks; and
- conclusions, limitations and recommendations.

A key purpose of performing life cycle interpretation is to determine the level of confidence in the final results and communicate them in a fair, complete and accurate manner.

21.4.3 Data generated from life cycle assessments

The data measured in an LCA are summarized to give a more detailed description of the environmental impact. The importance and impact of the data are explained and also illustrate how it is measured and what the metric of measurement is.

21.4.3.1 Embodied carbon

Embodied carbon is the carbon dioxide (CO_2) or greenhouse gas (GHG) emissions associated with the manufacture and use of a product or service. For construction products, this means the CO_2 or GHG emission associated with extraction, manufacturing, transporting, installing, maintaining and disposing of construction materials and products. The majority of embodied carbon for a construction product is CO_2 emitted from the use of fossil fuels in extraction and manufacturing of construction materials and as a result of process emissions from manufacturing.

21.4.3.2 Acidification

Acidic gases such as sulphur dioxide (SO_2) react with water in the atmosphere to form 'acid rain', a process known as acid deposition. When this rain falls, often a considerable distance from the original source of the gas, it causes ecosystem damage of varying degrees, depending upon the nature of the landscape ecosystems.

21.4.3.3 Eutrophication

Nitrates and phosphates are essential for life, but the increased concentrations in water can encourage excessive growth of algae and reduce the oxygen within the water. Eutrophication can therefore be classified as the overenrichment of water courses. Its occurrence can lead to the damage of ecosystems, increasing mortality of aquatic fauna and flora and to loss of species dependent on low-nutrient environments. This leads to an overall reduction in the biodiversity of these environments and has knock-on effects on nonaquatic animals and humans who rely on these ecosystems.

21.4.3.4 Stratospheric ozone depletion

Ozone-depleting gases cause damage to stratospheric ozone or the 'ozone layer' by releasing free radical molecules, which breakdown ozone (O_3). Damage to the ozone

layer reduces its ability to prevent ultraviolet (UV) light entering the earth's atmosphere and increases the amount of carcinogenic UVB light hitting the earth's surface. This in turn results in health problems in humans such as skin cancer or cataracts and sun-related damage to animals and crops. The major ozone depleting gases are CFCs, HCFCs and halons. Growing concern in the 1980s led to worldwide efforts to curb the destruction of the ozone layer, culminating in the Montreal protocol, which banned many of the most potent ozone-depleting gases.

21.4.3.5 Photochemical ozone creation

In atmospheres containing nitrogen oxides (NO_x), a common pollutant, and volatile organic compounds (VOCs), ozone and other air pollutants can be created in the presence of sunlight. Although ozone is critical in the high atmosphere to protect against UV radiation, low-level ozone is implicated in impacts as diverse as crop damage and increased incidence of asthma and other respiratory complaints.

21.4.3.6 Abiotic depletion

Abiotic depletion indicators aim to capture the decreasing availability of nonrenewable resources as a result of their extraction and underlying scarcity. As implied in the earlier titles, there are several different versions of abiotic depletion covering either all nonrenewable resources or more particular resources such as scarce elements/ores or nonrenewable fuels.

21.4.3.7 Raw material use/mineral extraction

'Raw material use' takes account of the use of all renewable and nonrenewable resources, while 'mineral extraction' accounts for all virgin mineral material consumed in a process/product/project, eg, the extraction of aggregates, metal ores and minerals.

21.4.3.8 Toxicity

Toxicity indicators aim to quantify the degree to which a particular substance causes damage to living organisms. There are a number of different indicators that indicate toxicity to different groups of organisms in different ecosystems. Assessments of toxicity are based on guidelines for tolerable concentrations in air and water, tolerable daily intake and acceptable daily intake for human toxicity. Substances that generally have the highest impacts in toxicity categories include heavy metals such as mercury or chromium and aromatic hydrocarbons (substances with a benzene ring). It should be noted that indoor air quality and its effect on human health is not covered by this category, but they are sometimes accounted for in a separate 'indoor air quality' category.

21.4.3.9 Land use

The way that land is used and the way that land use changes over time have significant implications on ecosystems, landscapes and the environment. Changes in the qualities of the soil in terms of nutrient content, pH, soil depth (ie, due to erosion) or water

filtration have knock-on effects on biodiversity, food production and land values. Therefore land use is a true sustainability issue as it covers social, economic and environmental issues.

21.4.3.10 Embodied water

Fresh water resources are coming under increasing pressure from population growth, rising per capita water use, urbanization and increased industrial activity and the effects of climate change. Embodied water begins to consider the effect of man's activities on water, for example, in reducing availability.

21.4.4 Environmental product declarations

The particular type of LCA known as an Environmental Product Declaration (EPD) has been developed to provide environmental information from LCA studies in a common format, based on common rules, known as Product Category Rules (PCR). PCR for construction products have been developed in the United Kingdom, France, the Netherlands, Scandinavia, Germany and Australia, amongst others.

EPD have been used for construction products since the first environmental assessment schemes were developed in the 1990s, and an ISO standard for EPD, ISO 14425: 2006, sets out standards they should meet.

EPD are published by a programme operator such as BRE Global, EPD Norge or IBU using ISO 14025 compliant PCR. EPD from a common programme can therefore be used alongside each other to make comparisons and evaluations at a building level.

For compliant EPD, an independent verifier must be used to critically review the LCA and ensure it has followed the PCR. The verifier will see a full LCA report, known as the background report and the EPD, to undertake this task, but only the EPD needs to be published, so the detailed and often confidential data provided in the background report need not be publicly disclosed. Construction product EPD are normally modular, so that an EPD for cement can be used with an EPD for aggregate to produce an EPD for concrete. The construction product industry was actively involved in the development of the international standards for LCA and EPD.

21.5 Regulations and standards

TC 207 of ISO is responsible for the 'standardization in the field of environmental management systems and tools in support of sustainable development'. TC 207 explicitly excludes 'test methods of pollutants, setting limit values and levels of environmental performance, and standardization of products' from its remit. The subcommittee TC 207/SC 5 'life cycle assessment' is responsible for standards relating to LCA studies. CEN Technical Committee 350 in Europe has also developed some standards to suit development needs and environmental initiatives in Europe. In the

meantime, some ISO standards had been taken over as European standards by this committee, for example ISO 14020.

The following section sets out relevant standards categorized into product and building levels.

21.5.1 Regulations and standards for products

ISO 14041 1998 life cycle assessment − LCA − goal and scope
ISO 14041:1998 is intended to provide special requirements and guidelines for the preparation of, conduct of and critical review of life cycle inventory analysis, the phase of LCA that involves the compilation and quantification of environmental relevant inputs and outputs of a product system. It was replaced in 2006 by updated 14040.
ISO 14042 2000 life cycle assessment − LCA − impact assessment
ISO 14042:2000 is intended to provide guidance on the impact assessment phase of LCA, the phase of LCA aimed at evaluating the significance of potential environmental impacts using the results of the life cycle inventory analysis. It was replaced in 2006 by updated 14040.
ISO 14043 2000 life cycle assessment − LCA − interpretation
ISO 14043:2000 is intended to provide guidance on the interpretation of LCA results in relation to the goal definition phase of the LCA study, involving review of the scope of the LCA, as well as the nature and quality of the data collected. It was replaced in 2006 by updated 14040.
ISO 14020:2001 life cycle assessment − LCA − labels general principles
ISO 14020:2001 provides guidance on the goals and principles that should frame all environmental labelling programs and efforts, including practitioner programs and self-declaration.
ISO 14040 2006 environmental management − LCA − principles and framework
ISO 14040:2006 describes the principles and framework for life cycle assessment (LCA) including: definition of the goal and scope of the LCA, the life cycle inventory analysis (LCI) phase, the life cycle impact assessment (LCIA) phase, the life cycle interpretation phase, reporting and critical review of the LCA, limitations of the LCA, the relationship between the LCA phases and conditions for use of value choices and optional elements.
ISO 14044 2006 environmental management − LCA − requirements and guidelines
ISO 14044:2006 specifies requirements and provides guidelines for life cycle assessment (LCA) including: definition of the goal and scope of the LCA, the life cycle inventory analysis (LCI) phase, the life cycle impact assessment (LCIA) phase, the life cycle interpretation phase, reporting and critical review of the LCA, limitations of the LCA, relationship between the LCA phases and conditions for use of value choices and optional elements.
ISO 21930 2007 sustainability in building construction − EPD for building products
ISO 21930:2007 provides a framework for and the basic requirements for product category rules for type III environmental declarations of building products. Type III environmental declarations for building products are primarily intended for use in business-to-business communication.
EN 15804 2012 core rules for the product category construction products
EN 15804:2012 gives core product category rules (PCR) for Type III environmental declarations for any construction product and construction service. It supersedes BS ISO 21930: 2007. The PCR of BRE EPD schemes is in line with these standards.

21.5.2 Regulations and standards for the building level

Following a mandate by the European Commission, CEN Technical Committee 350 has developed the following building level standards in Europe covering environmental impacts.

EN 15643-1:2010 sustainability of construction works − sustainability assessment of buildings − part 1: general framework
EN 15643-2:2011 sustainability of construction works − assessment of buildings − part 2: framework for the assessment of environmental performance
EN 15978:2011 sustainability of construction works − assessment of environmental performance of buildings − calculation method

These standards provide guidance on implementing the consistent evaluation of building-level environmental impacts, both embodied and operational, for all types of buildings across Europe. The standards use a life cycle assessment approach to evaluate a common set of environmental indicators over a series of defined life cycle stages. Impacts from materials used in the building fabric, structure, and services and fit out will be included, as will maintenance, repair, refurbishment and demolition, with the impacts of disposal and the benefits of any resulting reuse, recycling or energy recovery. Impacts from operational energy use are also included in the same matrix, so this will emphasize that the carbon emissions from material use and building operation are really indistinguishable.

21.6 Life cycle assessment applied to high strength natural fibre composites

A full LCA study requires the verified datasets for inputs (materials and energy), see Fig. 21.1, for the life cycle of composites as a product and outputs (products, waste and emissions). Data should be collected from the beginning of a life cycle (growing and harvesting). It is essential to understand the process. Background information on the techniques to manufacture the high strength natural fibre composites are also critical to carry out quality analysis. A small scale of information or derivation of data from similar processes does not provide a high-level quality input date, and full scale production data analysis may have different results.

First of all, it is necessary to analyze the composite profile, and then different sources will be analyzed. If there is no basic data for any fibres, work has to be carried out to generate relevant data.

21.6.1 Create environmental profiles

To carry out the LCA analysis, an environmental profile shall be created. Ideally, the profile should be a standardized method of identifying and assessing the environmental effects associated with high strength natural fibre composites, and it should have been peer reviewed and compiled with ISO standards 14040, an internationally established

approach for analyzing the environmental impact of products and processes. The data can be normalized if it is needed.

Environmental profiles can be created for high strength natural fibre composites and are presented at discrete life cycle stages. Reporting is commonly made on a unit mass (1 tonne of composites). Manufacturers have the discretion to publish any or all of the profile models they develop in the UK database. Common profile models include:

- extraction of raw materials and transport (cradle-to-factory gate)
- production (factory gate to factory gate)
- transport, installation and end-of-life (cradle-to-grave)
- cradle to end-of-life

21.6.2 Data set from the analysis

The data collected during the life cycle of high strength natural fibre composite products are then analyzed against the created environment profiles. Take BRE environmental methodology as an example: data assessed against to it can include 13 impact categories.

1. global warming (GWP100)
2. water extraction
3. mineral resource extraction
4. ozone depletion
5. human toxicity
6. freshwater aquatic toxicity
7. nuclear waste
8. terrestrial ecotoxicity
9. waste disposal
10. fossil fuel depletion
11. eutrophication
12. photochemical oxidation
13. acid deposition

There might be some variances if products are assessed against other profiles.

References

BIS, 2010. Low Carbon Construction IGT Final Report. www.bis.gov.uk/assets/biscore/business-sectors/docs/l/10-1266-low-carbonconstruction-igt-final-report.pdf.

BRE internal report prepared for TSB NATCOM project by Brunel University, 22nd March 2011. BIS, government response to IGT final.

Cradle-to-Cradle Definition. Ecomii. 19 October 2010. http://www.ecomii.com/ecopedia/cradle-to-cradle.

ISO 14040, 2006. Environmental Management – Life Cycle Assessment – Principles and Framework. International Organisation for Standardisation (ISO), Geneve.

ISO 14044, 2006. Environmental Management – Life Cycle Assessment – Requirements and Guidelines. International Organisation for Standardisation (ISO), Geneve.

Jiménez-González, C., Kim, S., Overcash, M., 2000. Methodology for developing gate-to-gate life cycle inventory information. The International Journal of Life Cycle Assessment 5, 153−159.

Life Cycle Assessment (LCA) Overview. sftool.gov. Retrieved 1 July 2014.

Life-cycle_assessment. https://en.wikipedia.org/wiki/Life-cycle_assessment#cite_note-3.

Rebitzer, G., et al., 2004. Life cycle assessment Part 1: framework, goal and scope definition, inventory analysis, and applications. Environment International 30 (5), 701−720.

The embodied impacts of construction products, construction products association, ISBN:978-0-9567726-6-4.

Future scope and intelligence of natural fibre based construction composites

22

M. Fan
Brunel University London, London, United Kingdom

22.1 Introduction

As construction activity continues to increase across the world, so does the demand for building materials and raw materials as a result. The construction industry is considered one of the most significant emitters of global greenhouse gas. Around 36% of all CO_2 emissions and 40% of all energy are related to building construction and building uses. The construction industry could therefore play a key role in meeting the global target for a low carbon economy. To make the transition towards the bioeconomy in the construction industry, the focus should be on the use of renewable raw materials, such as natural fibre composites. The use of plant fibre enables CO_2 to be captured in materials. This is also consistent with the European strategy, and also a global target, aiming at converting an oil-based economy into a bio-based economy, which shall inevitably adopt a strategy aimed at increasing the use of renewable resources in the economy and using them in a more sustainable manner, such as more efficient production and high value-added applications. The development of advanced natural fibre composites and exploitation of their intelligence with inherent characteristics of natural fibres would be of vital importance.

22.2 Future scope and challenges

Advanced natural fibre composites, in common with other engineering materials, have evolved through empiric findings and the understanding of physical and structural mechanisms and their modelling. In parallel, various attempts have been made to advance natural fibre composites and utilise abundantly available natural fibre resources as building materials, for example, the construction of an inexpensive primary building school using jute fibre reinforced polyester in Bangladesh under the auspices of the Cooperative of American Relief Everywhere and the United Nations Industrial Development Organisation (Singh and Gupta, 2005), building panels and roofing sheets made from bagasse phenolic combination in Jamaica, Ghana and the Philippines (Salyer and Usmani, 1982), wall panels and roofing sheets made from jute-polyester-epoxy-polyurethane for temporary shelters, bunker houses, storage silos, post office

Advanced High Strength Natural Fibre Composites in Construction. http://dx.doi.org/10.1016/B978-0-08-100411-1.00022-4

boxes and helmets (Satyanarayana et al., 1984). However, these early developed composites failed to sustain wet conditions either through surface roughening caused by fibre swelling or delamination. Further investigations have indicated that natural fibre composites could be manufactured to be sufficiently strong and durable for structural applications in construction (Fan and Bonfield, 2007; Fan, 2008). A complex research programme, 'NATCOM', led technically by Fan (2007) has demonstrated that the fit-for-purpose, low carbon and low energy sustainable construction products could be made by using natural resources for various matrix and mat designs of construction products.

On the other hand, the construction industry has advanced technologies and practices of modern methods of construction, allowing the innovations to make use of innovative materials even in conjunction with traditional materials and original structural design. Building construction is now encouraged to employ construction materials which are environmentally friendly, competitive in terms of initial cost and superior in terms of life cycle cost, durability, light weight and well-being in use. Natural fibre composites are demonstrating these merits superior to conventional strong materials, eg, concrete and steel.

The advanced natural fibre composite contributes to enhancing the development of biocomposites in terms of performance and sustainability. Biocomposites have created substantial commercial markets for value-added products, especially in the automotive sector. The market and commercialisation of the advanced natural fibre composites in construction are growing and are anticipated to expand in the future with the increase of economic, social and environmental awareness among consumers and producers and the development of efficient processing technology and further innovation in products. New generations of natural fibre composites are expected to be used in a wide range of applications in mass-produced consumer products for short-term uses, as well as for long-term indoor applications (Fig. 22.1). Natural fibre composites exhibit good specific properties, and if a proper matrix is used, they could be 100% biodegradable.

New advanced technologies, as discussed in many chapters of this book, have been of great interest for a new generation of natural fibre composites to achieve high-quality performance, serviceability, durability and reliability standards, especially the major advancement that lies within the establishment of nanotechnology of both reinforcing and producing nanocrystalline cellulose from natural fibres for advanced natural fibre composites. Natural fibres consist of approximately 30−40% cellulose and about half of that is crystalline cellulose. The nanocrystalline cellulose may be only one-tenth as strong as carbon nanotubes but costs 50−1000 times less to produce. Nano-/microfibrils cannot only be produced from wood pulp but are also extracted from diverse nonwood sources including hemp, jute, flax, sisal, bamboo, bagasse, wheat straw, pea hull, banana rachis, pineapple leaf, sugar beet, potato, swede root and algae. The use of nanocrystalline cellulose is being explored for a variety of uses, since it is stronger than steel and stiffer than aluminium. Nanocrystalline cellulose reinforced composites could soon provide advanced performance, durability, value, service life and utility, while at the same time being a fully sustainable technology. By the time advanced natural fibre composites and associated design methods are

Figure 22.1 Advanced natural fibre composites in building construction.

sufficiently mature to allow their widespread use, issues arise related to construction materials. The development of methods, systems and standards could see advanced natural fibre composite materials at a distinct advantage over traditional materials. In the future, these biocomposites will see increased uses in structural applications. Various other applications depend on their continuing developments. There is a significant research effort underway to address and resolve the bottlenecks in the whole supply chain of natural fibre composites and explore their use as construction materials, especially for load-bearing applications (Fan, 2015).

Natural fibre composites could offer a number of advantages over the traditional materials used in construction. However, the challenges remain in replacing conventional construction materials with those that exhibit comparable structure and functionalities, long-term durability, cost and design.

22.2.1 Challenge 1: variability of mechanical property and stiffness

Advanced natural fibre composites exhibit good specific properties, but there are two drawbacks: one of them is the variabilities in their properties. Plants from which the

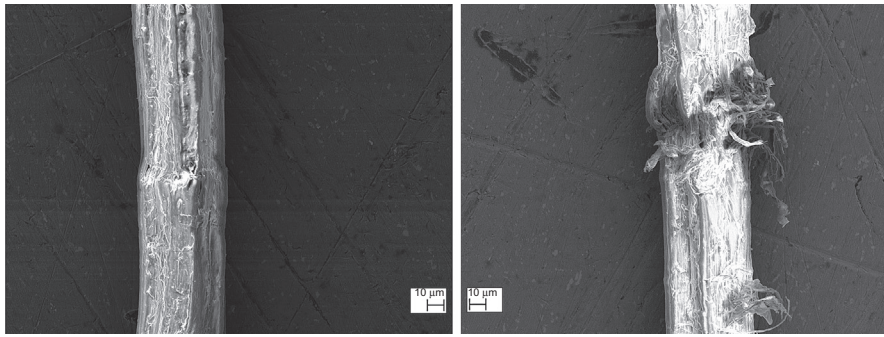

Figure 22.2 Inherent dislocation (left) and its possible damage (right) of natural fibres.

natural fibres are extracted subject the natural environment with variable surrounding conditions, which endow natural fibres with a number of inherent characteristics, eg, defects (dislocation) (Fig. 22.2) and changing properties among species, location of trees and processing technologies (Fan, 2010; Dai and Fan, 2011). Advanced natural fibre composites from such resources inevitably exhibit some variation in properties. These weaknesses have been studied and will be overcome with the development of more advanced processing of natural fibres and their composites.

However, natural fibre composites (NFCs) offer a greater versatility to engineer than traditional materials by varying the type of fibres, resin and other additives, the orientation and location of reinforcing fibres and processing parameters to produce structures with a combination of performance characteristics for a particular application, although this normally requires a process which allows localised variations of laminate composition. This tends to preclude the use of some automated procedures. For example, the pultrusion process only allows some variations in reinforcing fibre type on a ply-by-ply basis but does not allow a variation in resin composition or localised changes in laminate lay-up.

Another drawback is the stiffness of composites. Construction designs of civil structures are normally governed by stiffness performance. Natural fibre composites may relatively have low stiffness in comparison with their strength. Structures with fibre reinforced polymer composites may become significantly overdesigned for strength and consequently are less economically competitive. Synthetic stiffening may be carried out (eg, carbon fibres) with the sacrifice of raw material costs. New materials and designs of composite structures are to be sought after in order to take advantage of the composites.

22.2.2 Challenge 2: long-term durability

Natural fibre composites could be 100% biodegradable. Biological and environmental durability is often cited as a key advantage of natural fibre composites over traditional materials. However, the biodegradation is difficult to control. The uses of natural fibre composites in construction applications are also relatively new, and a full understanding of their durability is yet to be achieved. The research gap

for long-term durability data, eg, moisture effect, alkaline solution, fatigue, creep and physical degradation has been recognised in the community, eg, a lack of long-term data relevant to civil structures with a service life of 75−100 years, the major detrimental effect of the combined temperature, humidity and UV radiation are in particular vital to property deterioration, discolouring and deformation. Significant research is currently underway around the world to address and overcome the obstacles, and the effort to develop NFCs with improved performance for global applications is an ongoing process.

22.2.3 Challenge 3: reduction of costs

NFCs are currently expensive when compared to conventional construction materials. The cost of NFCs must be brought down by a better exploitation of mass-production manufacturing if the transition from conventional materials to NFCs is to continue. Pultrusion is precisely such a method. Continuous pultrusion of linear sections achieves far better cost competitiveness for NFCs compared with labour-intensive hand lay-up techniques.

Techniques used to price civil infrastructure projects can vary considerably from one project to another, depending on individual circumstance. The scale of costs for NFCs could be very difficult to determine since the costs are related to the level of importance of various costs for different applications and requirements. There are short-term (eg, design, construction and installation) and long-term (eg, maintenance, update, deconstruction and disposal) or direct (eg, materials and production) and indirect (eg, interruption, depreciation, resale and impact on environment) costs. The costs of building projects are often based on the initial cost of the structure because of the tendency for the owner to be more concerned with obtaining the best structure possible for their money and less concerned with its long-term performance. Therefore current low volume production of NFCs is a major disadvantage for their market and further commercialisation.

22.2.4 Challenge 4: codes and standards

The provision of objective information on the performance (and guarantee of performance) of available bio-based technologies by product certifications can boost customers' acceptance and accelerate deployment. Harmonised and standardised national/international testing and evaluation procedures for specific bio-based products and technologies increases understanding among developers, architects and installers and accelerates the maturity of the industry more broadly. Standards, specifications and codes of practice are yet to be developed to facilitate the design and construction applications of natural fibre composites. NFCs are very difficult to design compared to some conventional construction materials due to their anisotropy. The vitally important items of reliability and performance are difficult to address without fully understanding the characteristics of materials or guideline databases; on the other hand, it is a daunting task for some engineers to undertake analyses and designs utilising the advanced composites.

22.2.5 Challenge 5: market acceptance

One of the major hurdles for the commercialisation of natural fibre composites, until recently, is the nonrecognition of research and development, especially in developing countries with abundant natural fibre resources. Often the public is not aware of the existence of bio-based materials, such as those based on flax and hemp. Nevertheless, material scientists have been dealt with challenges regarding the acceptance criteria, particularly from many industrialised countries, eg, European countries. Awareness through examples promoted by experienced people is encouraging and could be served as foundations for further development and support. More active marketing, communication and promotion of sustainable building materials are a prerequisite, as it is an essential step towards a growing market. By informing consumers and users of renewable resources about intrinsic qualities and environmental advantages, hesitations for purchasing these products can be minimised. Architects and entrepreneurs have an openness towards working with renewable building products, but the fact that these are unknown slows their market success.

The performance and costs have been the prime driving forces for the use of natural fibre composites, despite the renewability and recyclability of the matrix, and reinforcements are attractive. In addition to appropriate product standards to support the performance of the products, NFCs designed for a structural purpose should also meet regulations regarding the management of huge volumes of waste.

22.3 New technologies and intelligence of natural fibre composites

Enormous effort and resources are invested to migrate natural fibre composites to construction applications. These not only optimise the potential capability of NFCs, but also explore the intelligence of NFCs with their specific characteristics.

22.3.1 Inherent intelligence of natural fibre composites

The inherent complex microstructure of natural fibres has recently been recognised as invaluable remit for bio-based construction materials, despite the traditional perception of the sorption behaviour of natural fibres as a problematic parameter. The sorption characteristic inherited from the live tree could potentially endow natural fibre composites with the characteristic of breathing air either moisture or pollutants for building construction. Three key things characterise the issue of breathing construction: (1) vapour permeability, ie, the movement of water vapour through building components and constructions; (2) hygroscopicity, ie, the ability of building materials to absorb, store and release vapour; and (3) capillarity, ie, the ability of building materials to absorb, store and release water as liquid. The microstructure and intelligent network systems of natural fibres have demonstrated their capacity of capillary, convection, micro- or nanoworking mechanisms of air/moisture and have the capacity to process and transfer water vapours in a natural way (Fig. 22.3).

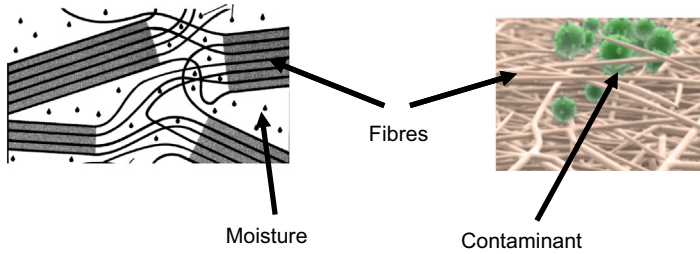

Figure 22.3 Moisture moves in and out of the natural fibres (left) and filtration of contaminant (right).

Another exploration of using this characteristic is to improve the indoor environment of construction. There is currently a great interest in developing a process which can degrade and remove volatile organic compounds (VOCs), formaldehyde (HCHO) and NO_2 in air. Natural fibre composites could also be a filter for the removal of microparticulates (Fig. 22.2). The breathable walling composites would have heterogenic structures and soft microchannels that would allow the infiltration of air and adsorption of pollutants such as NO_x, CO, HCHO and VOCs, where these can be degraded by embedded catalyst dopants. The cellulose chemistry may allow the attachment of functional groups and metal oxides of the dopants with strong base sites to donate electrons to electrophilics such as NO_x and HCHO for degradation, since a large number of VOCs are oxidisable. The mechanisms of photocatalystic oxidation of VOCs involves three stages: (1) transfer of contaminants from bulk to the surface, (2) adsorption on the catalyst surface and formation of reactive ions and (3) degradation by the ions formed on the surface. For example, the capacity of TiO_2-based photocatalyst to degrade indoor air contamination has been studied and considered promising for the development of modified titania with metal dopants with high activity under visible light to enable degradation of pollutants in sunlight as well as interior lighting.

Modern breathing walls, using timber frames, natural fibre boards and natural insulations, are now available in many developed countries, eg, in the United Kingdom. Breathing components for building construction would lead to more environmentally benign buildings, providing not only significantly 'greener' construction, but also better durability, much less risk of damage, better air quality, greater comfort, greatly reduced waste in the long term and a host of other incidental benefits which give rise, in short, to a far higher performance.

22.3.2 Smart natural fibre composites

Much effort has been spent on the functionalisation of natural fibre composites for their intelligence. The microstructure of natural fibres provides a unique platform for realising the functionalisation of composites for specific characteristics. One of these is the colour-changed smart wood-based composites, which change their colour under the external stimuli. Three groups of compound, inorganic, liquid crystal and organic compounds have been used for the production of natural fibre composites

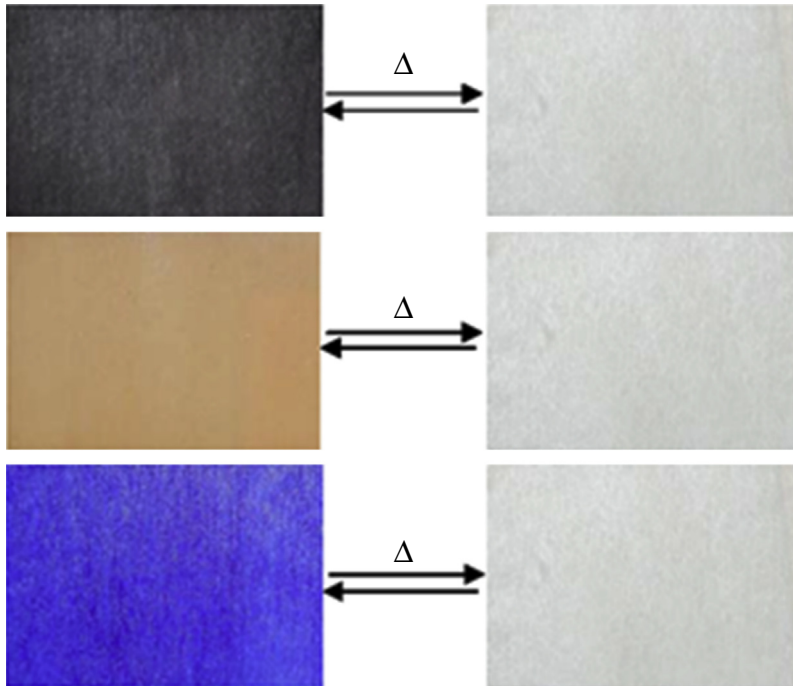

Figure 22.4 Colour change with the temperature for thermochromic bleached wood (left = −26°C, right = −32°C) (Fu and Hun, 2016).

(Fu and Hun, 2016), and the intelligence temperature-sensitive colour-changed composites have been manufactured by mixture impregnation (Fig. 22.4) and fabricated by microcapsules (Fig. 22.5). The development and application of smart wood materials such as thermochromic wood composites would inevitably promote the intelligence characteristics of modern homes.

Textile engineering and modelling technologies have been used in composite fabrication with a view to develop multifunctionalised composites (Fan and Weclawski, 2016). Textile engineering has provided an opportunity for producing hybrid composites with the flexibility of fibre content, fibre orientation and roving texture of hybrid fabrics and the options of weave styles, such as plain, twill, satin and leno, to prepare the required form of reinforcements. The addition of textile engineering technologies could significantly extend the content of intelligence of natural fibre composites, for example, the weaving of super-tough carbon nanotubes with natural fibre could result in a nanocomposite with a special strength and electronic characteristics for making electronic devices such as sensors, connectors and antennas. The electrospinning of polymeric fibres to produce nanopolymer fibres could give rise to a large surface area useful for various improvements of nanocomposites; the textile engineering can also facilitate the doping of various functional agents for the development of various intelligent composites.

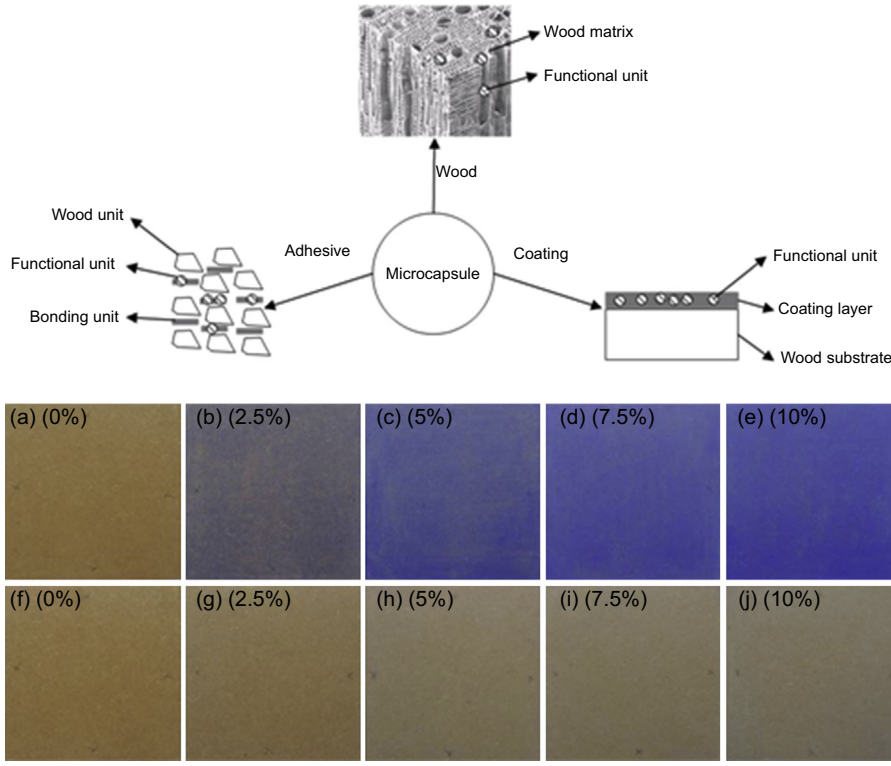

Figure 22.5 Incorporation of colour-sensitive microcapsules in natural fibres (top) and colour change of MDF with a temperature at 10°C (a–e) and 50°C (f–j) with various microcapsule concentrations (Fu and Hun, 2016) (bottom).

22.3.3 Nanocoating

Nanotechnology shows numerous opportunities for improving biocomposite products by providing nanotechnology-based coatings to increase water uptake and reduce biodegradation and volatile organic compounds and even flame resistance. As soon as the performance coating product is applied on the substrate to treat, the transport material brings the nanoparticles into and onto the substrate, where a chemical reaction with the pores and capillaries or the surface takes place. The transport material evaporates, leaving only the nanoparticles that are 'welded together' with the substrate, creating an incredibly intelligent design, such as self-cleaning construction materials (Fig. 22.6), which may not only provide protection to damage, discolouration and rotting, but also provide an antibacterial hygienic protective surface, resisting salt and UV damage, fouling and contamination.

Novel treatment agents such as nanodye and nanopreservatives have been investigated for the natural fibre composites industry. Advancing nanotechnology research for such multifunctional products requires cross-disciplinary teams of material

Figure 22.6 Nanocoating construction materials in uses.

scientists, biological scientists, polymer scientists, wood and plant scientists and chemical engineers, as well as close partnerships in order to capture synergies.

22.3.4 Nanocellulose composites

Nanotechnology is considered to be one of the most important drivers of this century. Research and development in nanotechnology is critically important for the new generation process and products of NFCs. New or enhanced composites with unique properties can be developed by using nanotechnology. Nanotechnologies may also reduce energy consumption and could improve economic competitiveness. Traditional manufacturing processes use materials from the top to down, while nanotechnology uses materials from down to up by improving or altering existing materials.

Nanocellulose composites mainly consist of two major categories: one using nanocellulose for the modification of reinforcement and the other for the modification of the matrix. Nanocellulose was used to modify natural fibres by using two-step nanomodification (Dai and Fan, 2013). This nanomodification technology increased the mechanical properties and interfacial property significantly. Tensile testing results showed that under the optimised condition the nanomodification could increase the modulus, tensile stress and tensile strain of hemp fibres by 36%, 73% and 68%, respectively. FEG-SEM micrograph showed that nanocellulose covered the surface of fibres in two ways: namely, (1) nanocellulose filling in the stria and (2) bonding the interfibril on the gap between two fibrils (Fig. 22.7). X-ray Powder Diffraction (XRD) results showed the nanomodification increased the crystallinity index of natural fibres up to 38%. Resin absorption results showed that the nanomodification can increase the absorption 39%.

Nanocellulose is also able to catalyse the composite mix to develop stronger composites. Using 10% cellulose nanofibres obtained from various sources, such as hemp fibres and kraft pulp to reinforced poly(vinyl alcohol), showed that both tensile strength and Young's modulus of the nanofibre reinforced composite were

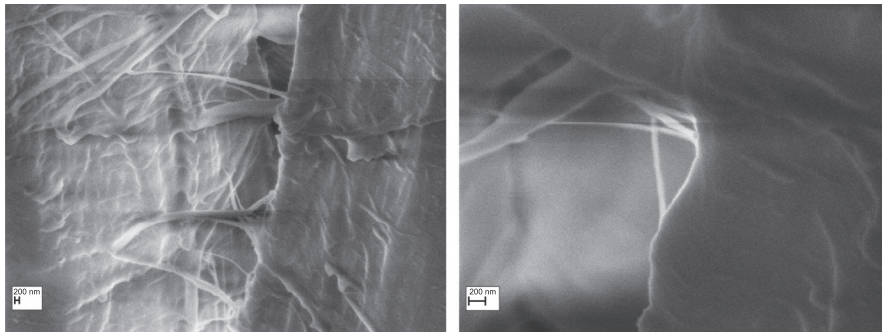

Figure 22.7 The surface of hemp fibres modified with nanocellulose (left = before modification; right = after nanocellulsoe modification).

improved by a pronounced four to five folds (Dai et al., 2013). With a higher loading of microfibrillated cellulose, the relative enhancement of mechanical properties was even more remarkable.

Full biocomposites have also been developed with the use of natural polymers and lignocellulosic. It is expected that by 2050, about 50% of the basic chemical building blocks will come from renewable plant resources as hurdles to their use are reduced. Work on biodegradable composites started nearly three decades ago. Different processing techniques and their effect on properties of biopolymer blends are investigated, of particular interest is the blending of poly(hydroxybutyrate) and poly(hydroxybutyrateco-valerate) through miscibility, poly(lactic acid), poly(glycolic acid) and poly(-caprolactone).

References

Dai, D., Fan, M., 2013. Green modification of natural fibres with nanocellulose. RSC Advances 3 (14), 4659−4665.

Dai, D., Fan, M., Collins, P., 2013. Fabrication of nanocelluloses from hemp fibers and their application for the reinforcement of hemp fibers. Industrial Crops and Products 44, 192−199.

Dai, D., Fan, M., 2011. Investigation of the dislocation of natural fibres by fourier transform infrared spectroscopy. Vibrational Spectroscopy 55, 300−306.

Fan, M., 2010. Characterization and performance of elementary hemp fibres: factors influencing tensile strength. BioResources 5 (4), 2307−2322.

Fan, M., Weclawski., 2016. Fire performance of natural fibre composites in construction. Advanced High Strength Natural Fibre Composites in Construction 15.

Fan, M., 2015. Grow2Build, European Centre of Excellence. Brunel University London.

Fan, M., Bonfield, P., 2007. Process for Making Composite Products. International Patent, WO2007110660.

Fan, M., 2008. High strength natural fibre composites for construction: development of strong natural fibres. In: Proc. 16th Int. Conf. on Composite and Nano-Engineering, (Kunming, China).

Fan, M., 2007. 'NATCOM' Optically Efficient Production of High Strength Natural Fibre Composites. Technology Programme, TSB Reference TP/5/SUS/6/I/H0565L.

Fu, F., Hun, L., 2016. Temperature sensitive colour-changed composites. In: Fan, M., Fu, F. (Eds.), Advanced Natural Fibre Composites for Construction. Woodhead Publishing.

Salyer, I.O., Usmani, A.M., 1982. Utilization of bagasse in new composite building materials. Industrial & Engineering Chemistry Product Research and Development 21 (1), 17−23.

Satyanarayana, K.G., Sukumaran, K., Ravikumar, K.K., Brahmakumar, M., Pillai, S.G.K., Pavithran, C., Mukherjee, S., Pai, B.C., 1984. Possibility of Using Natural Fibre Polymer Composites as Building Materials in Low Cost Housing. CBRI, Roorkee.

Singh, B., Gupta, M., 2005. Performance of pultruded jute fibre reinforced phenolic composites as building materials for door frame. Journal of Polymers and the Environment 3 (2), 127−137.

Index

'*Note*: Page numbers followed by "f" indicate figures, "t" indicate tables.'